



University
of Glasgow

Adams, Steven Henry (2014) *The impact of changing climate on tree growth and wood quality of Sitka spruce*. PhD thesis.

<http://theses.gla.ac.uk/5121/>

Copyright and moral rights for this thesis are retained by the author

A copy can be downloaded for personal non-commercial research or study, without prior permission or charge

This thesis cannot be reproduced or quoted extensively from without first obtaining permission in writing from the Author

The content must not be changed in any way or sold commercially in any format or medium without the formal permission of the Author

When referring to this work, full bibliographic details including the author, title, awarding institution and date of the thesis must be given

The Impact of Changing Climate on Tree Growth and Wood Quality of Sitka spruce

Steven Henry Adams
BSc Honours

Submitted in fulfilment of the requirements for the Degree
of Doctor of Philosophy

Environmental Chemistry
School of Chemistry
College of Science and Engineering
University of Glasgow

January 2014

Abstract

The recent trend in climate has shown that UK temperatures are increasing, summers are getting drier and winters are getting wetter. It is thought that this trend is set to continue for the foreseeable future and that this will have an impact on the growth and quality of timber in the UK. Sitka spruce (*Picea sitchensis* (Bong.) Carr) is one of the most widely planted and important commercial tree species in the UK but our knowledge of tree growth and wood properties is based on tree growth in the climate of the past 40 - 80 years. The rotation time for Sitka spruce is approximately 40 years so trees planted now will mature in the 2050s, when the climate could be different from today leading to impacts on the quality and quantity of the wood being produced. This project aims to predict the effect that changes in climate will have on Sitka spruce, by looking not only at growth but also at different properties of the wood and their susceptibility to any change in climate. This information could then be used to help make decisions as to whether Sitka spruce is the best tree to be planting now, at any specific site in the UK, to obtain the best quality wood in the future.

The effect of seasonally changing weather on growth was measured at two sites by the use of LVDT point dendrometers to record changes in the radius of the tree stems. The data were compared to meteorological data collected from the site and from local weather stations, to determine how weather affected the growth of the trees. Data collection from the site at Griffin Forest near Aberfeldy was initiated in 2008 as part of a long term project at that site. Measurements taken during 2008 and 2009 were used as part of a previous PhD study and continued as part of the present study from 2010. The second site was newly established at Harwood Forest in Northumberland, northern England. At both sites the onset of growth at the beginning of the season was found to correspond to temperature $>5^{\circ}\text{C}$. Deficit of soil moisture was found to decrease the growth rate during the peak growth period.

Radial density, radial growth and the radial profile of longitudinal stiffness were investigated by analysing increment core samples taken from sites covering the full latitudinal range that Sitka spruce grows in Great Britain, with the aim of

quantifying the effect of site factors such as latitude, longitude, initial spacing and elevation. The cores were measured from density and ring width using an ITRAX x-ray densitometer and analysed using Windendro software. Stiffness was investigated using acoustic velocity measurements taken directly on the increment cores using an ultrasonic scanner, modified to measure cores.

A wide range of published radial growth models and a smaller number of radial density models were explored to see which were able to describe the data and compared to simpler linear segmented models. The sample population was found to be highly variable and the ability of the models to predict ring width or density from ring number alone was limited. Improved prediction of density was possible when ring width was included along with ring number as a predictor. The linear segmented models were found to be able to predict growth and density from ring number alone and this provides a useful and powerful tool. In practice ring width may not always be available and so there is a need for models which can predict density from ring number alone. Ring width was found to be negatively correlated with density, although the nature of the relationship was different between juvenile and mature wood.

Most of the variation in both density and growth was between trees at the same site. Initial spacing was found to be the only significant effect on growth and then only by having a positive effect on the growth rate of the juvenile wood, which had a knock on effect on the size of the trees at the end of the juvenile phase. Both spacing and latitude were found to have significant effects on the mean density of the juvenile wood with spacing having a negative effect and latitude a positive effect. In the mature wood, cambial age was found to be the only significant effect on radial density.

Table of Contents

Abstract	2
List of Tables	8
List of Figures	11
Acknowledgement	22
Author's Declaration	24
Definitions/Abbreviations	25
1 Introduction	26
1.1 Sitka Spruce	27
1.2 Climate	28
1.3 UK climate predictions	29
1.3.1 Climate Change to Date	30
1.3.2 Climate Change in the Future	31
1.3.3 Emission Scenarios	31
1.3.4 Temperature	34
1.3.5 Precipitation	36
1.3.6 Thermal Growing Season	38
1.3.7 Storminess	39
1.3.8 Windiness	39
1.4 Relationship between climate and tree growth	40
1.4.1 Management	47
1.4.2 Provenance	48
1.5 Aims	50
2 Variation in Wood Properties	52
2.1 Resource Evaluation Study	52
2.2 Extension of Resource Evaluation Study	53
2.2.1 Extension Sites	54
2.3 Method	57
2.3.1 Site Selection	57
2.3.2 Field Work	58
2.3.3 Density and Ring Width Analysis	60
2.4 Climate Data	66
2.4.1 Weather Station Data	66
2.4.2 Ecological Site Classification	66
2.5 Categorical Groups	72
2.5.1 Longitude and Latitude as Categorical Variables	72
2.5.2 Elevation Groups	74

2.5.3	Spacing Groups.....	75
3	Modelling Radial Growth of Sitka Spruce	76
3.1	Introduction	76
3.1.1	Definitions	76
3.1.2	Outline	76
3.1.3	Aim	77
3.2	Radial Variation in Growth	78
3.3	Fitting Models to Radial Growth.....	82
3.3.1	Model Parameters	85
3.4	Comparing Models of Radial Growth.....	87
3.4.1	Hossfeld4 Model.....	87
3.4.2	Other Growth Models	94
3.4.3	Exponential Model.....	95
3.4.4	Segmented Model - Split between Juvenile and Mature Growth ...	100
3.4.5	Segmented Model - Juvenile and Mature Growth	108
3.4.6	Linear Mixed Effects Models	121
3.4.7	Discussion on Growth Models	127
3.5	Factors Affecting Growth.....	129
3.5.1	Regression Analysis	129
3.5.2	Mixed Effects Model Structure.....	129
3.5.3	Factors Affecting Juvenile Growth.....	130
3.5.4	Factors Affecting Mature Growth	133
3.5.5	Effect on Mature Growth When Spacing is taken into Account	135
4	Modelling Ring Density of Sitka Spruce	141
4.1	Introduction	141
4.1.1	Definitions	141
4.1.2	Outline	141
4.1.3	Aim	142
4.2	Radial Variation in Density	143
4.3	Fitting Models to Ring Density	147
4.3.1	Density Model Parameters.....	149
4.3.2	Gardiner3 Model	152
4.3.3	Lindstrom Model	159
4.3.4	Exponential Model.....	161
4.3.5	Linear Segmented Model - Split Point between Juvenile and Mature Phase of Density.....	163
4.3.6	Density Segmented Model - Juvenile and Mature Segments.....	170
4.4	Factors Affecting the Density Radial Profile.....	171
4.4.1	Juvenile Density Segment	171

4.4.2	Mature Segment	181
4.4.3	Mixed Effects Model Structure	190
4.4.4	Regression Analysis - Juvenile Segment	191
4.4.5	Factors Affecting the Juvenile Density Profile	193
4.4.6	Regression Analysis - Mature Segment.....	194
4.4.7	Factors Affecting the Mature Density Profile	195
4.5	Discussion	197
4.5.1	Discussion of Density Models	197
4.5.2	Discussion of Modelling Factors Affecting Ring Density	199
5	Radial Profiles of Longitudinal Acoustic Velocity.....	201
5.1	Introduction	201
5.2	Materials and Method	202
5.2.1	Description of Work	203
5.3	Method Testing.....	206
5.3.1	Measurement Resolution	206
5.3.2	Effect of Grain Orientation on Acoustic Velocity	207
5.3.3	Effect of the Physical Condition of the Cores	210
5.4	Discussion of Method for Measuring Acoustic Velocity on Cores	222
6	Modelling Radial Profiles of Longitudinal Acoustic Velocity	224
6.1	Introduction	224
6.1.1	Definitions	224
6.1.2	Outline	224
6.1.3	Aim	225
6.2	Radial Variation in Acoustic Velocity	226
6.3	Modulus of Elasticity (MoE).....	230
6.4	Fitting Models to Acoustic Velocity	233
6.5	Comparing Models Fitted to Acoustic Velocity	234
6.5.1	Model Parameters	234
6.5.2	Segmented Model - Split Point between Juvenile and Mature Phases in Acoustic Velocity.....	236
6.5.3	Segmented Model - Juvenile and Mature Segments	242
6.5.4	Juvenile Segment of Acoustic Velocity	243
6.5.5	Mature Segment of Acoustic Velocity.....	253
6.5.6	Exponential Model of Acoustic Velocity	253
6.6	Discussion of Acoustic Velocity models.....	262
7	Within Season Variation in Tree Radial Expansion	265
7.1	Griffin Site.....	267
7.1.1	Tree Selection.....	268
7.1.2	Methods	269

7.1.3	Results.....	271
7.2	: Harwood Site	314
7.2.1	Site Selection.....	314
7.2.2	Tree Selection.....	315
7.2.3	Method	315
7.2.4	Results.....	317
7.3	Variation in Stem Width - Diurnal / Seasonal Changes / Amplitude	326
7.3.1	Analysis.....	327
7.3.2	Results.....	328
7.4	Discussion on Tree Growth at Griffin and Harwood	334
8	Discussion	343
8.1	Discussion of Method	343
8.1.1	Resource Evaluation Study	343
8.1.2	Acoustic Velocity Method.....	345
8.2	Discussion of Tree Growth and Wood Properties	347
8.2.1	Radial Growth	348
8.2.2	Radial Density	350
8.2.3	Radial Profile of Longitudinal Acoustic Velocity	354
8.2.4	Comparing Growth and Wood Properties.....	354
8.3	Discussion on Seasonal Variation in Tree Growth	358
8.4	How will projected climate affect Sitka spruce	361
8.5	Conclusion	363
	Appendices	365
	List of References	367

List of Tables

Table 1-1: Data taken from UKCP09 showing key finding in observed trends in climate in the recent past. © UK Climate Projections 2009 (Jenkins et al., 2009b).....	30
Table 1-2: Projected mean change in summer temperature for regions of the UK for the decades of the 2020's, 2050's and 2080's. Showing the range between 10% - unlikely to be lower than, to 90% - unlikely to be higher than, as well as the central estimate (50%). © UK Climate Projections 2009.....	35
Table 1-3: Projected mean change in winter temperature for regions of the UK for the decades of the 2020's, 2050's and 2080's. Showing the range between 10% - unlikely to be lower than, to 90% - unlikely to be higher than, as well as the central estimate (50%). © UK Climate Projections 2009.....	35
Table 1-4: Projected mean change in spring temperature for regions of the UK for the decades of the 2020's, 2050's and 2080's. Showing the range between 10% - unlikely to be lower than, to 90% - unlikely to be higher than, as well as the central estimate (50%). © UK Climate Projections 2009.....	35
Table 1-5: Observed and modelled changes, for control period (1961-1990) and future period (2080), of number of frost days across various sites in the UK. © UK Climate Projections 2009.....	36
Table 1-6: Projected mean change in summer precipitation for regions of the UK for the decades of the 2020's, 2050's and 2080's. Showing the range between 10% - unlikely to be lower than, to 90% - unlikely to be higher than, as well as the central estimate (50%). © UK Climate Projections 2009.....	37
Table 1-7: Projected mean change in winter precipitation for regions of the UK for the decades of the 2020's, 2050's and 2080's. Showing the range between 10% - unlikely to be lower than, to 90% - unlikely to be higher than, as well as the central estimate (50%). © UK Climate Projections 2009.....	37
Table 1-8: Projected mean change in spring precipitation for regions of the UK for the decades of the 2020's, 2050's and 2080's. Showing the range between 10% - unlikely to be lower than, to 90% - unlikely to be higher than, as well as the central estimate (50%). © UK Climate Projections 2009.....	38
Table 2-1: Details of the sites sampled in the extension of the resource evaluation study.....	54
Table 2-2: Sites from the original study chosen to be analysed as part of this study.....	55
Table 2-3: Conditions and levels of the experimental factorial design.....	57
Table 2-4: Combination class for each site, listed by region, along with the experimental design conditions.....	58
Table 2-5: The number of sites along with the site name sorted into the relevant Easting group.....	73
Table 2-6: The number of sites along with the site name sorted into the relevant Northing group.....	73
Table 2-7: The number of sites along with the site name sorted into the relevant elevation group.....	74
Table 2-8: The number of sites along with the site name sorted into the relevant spacing group.....	75
Table 3-1: Number of samples per site.....	77
Table 3-2: The number of trees being analysed decreases as ring number increases.....	79
Table 3-3: The number of samples and sites per group.....	81

Table 3-4: Growth equations for statistical models from (Zeide, 1993), where RG = radial growth, t is cambial age. a , b , c and d are parameters estimated from the data.....	82
Table 3-5: Equations for the three statistical models describing curves and the two segmented model, where RG = radial growth, t is cambial age. a , b and c are parameters estimated from the data.....	83
Table 3-6: Parameter estimates along with Standard Errors, residual standard error and R-squared value for the statistical model equations. Also shows the number of trees and the percent of the total that the model was unable to fit.	86
Table 3-7: The nine highest coefficients that the Exp model fitted to the samples, where b_1 is the rate parameter, b_0 and b_2 are constants estimated from the data.....	98
Table 3-8: Result of linear mixed effects model testing the effect of northing, easting, spacing and elevation on the juvenile segment of growth.....	130
Table 3-9: Result of linear mixed effects model on juvenile growth with the non-significant terms of northing and easting removed	130
Table 3-10: Summary of linear mixed effects model on juvenile growth with all non-significant terms removed.....	131
Table 3-11: Effect of a linear model on the juvenile growth	131
Table 3-12: ANOVA of lme model testing the effect of northing, easting, spacing and elevation on the mature segment of growth.....	133
Table 3-13: ANOVA of lme model on mature growth with the non-significant terms of northing, easting and elevation removed.....	133
Table 3-14: ANOVA of lme model on mature growth with all non-significant terms removed.	133
Table 3-15: Pearson correlation coefficients between growth at ring numbers 1, 12, 25, 30 and 35 which all had significant p -values (<0.0001)	135
Table 3-16: Anova of lme model on mature growth at 2m initial spacing showing no significant effects	136
Table 3-17: Summary of mixed effects model which includes accumulated temperature, Moisture Deficit, Summer rainfall, continentality, DAMS, soil moisture regime and soil nitrogen regime.....	139
Table 4-1: The number of samples per site measured for density	142
Table 4-2: The number of samples and sites for each group when measured for density. Northing groups are based on the 100km OS grid square, where 0 is south and 9 is furthest north. Easting is also based on the 100km OS grid square with 1 being west and 4 being east. Spacing is based on the initial spacing in metres and Elevation is grouped in 50 metre increments from 50 to 500 metres above sea level. A total of 47 sites were tested covering a combination of these factors.....	146
Table 4-3: Parameter estimates for the density models along with Standard Errors, residual standard error and R-squared values.....	149
Table 4-4: Parameter estimates for the density models from Gardiner et al. (2011) along with Standard Errors, residual standard error and R-squared values. Where rd is ring density, rn is ring number from the pith, rw is the ring width of each ring and a_i , b_i and c_i are the parameters estimated from the data when converted to basic specific gravity.	155
Table 4-5: Result of linear mixed effects model testing the effect of northing, easting, spacing and elevation on the juvenile segment of the density profile. Age is cambial age.....	193
Table 4-6: Result of the linear mixed effect model on juvenile density profile with the non-significant interaction terms removed. Age is cambial age.	193

Table 4-7: Result of linear mixed effects model testing the effect of northing, easting, spacing and elevation on the mature segment of density.	196
Table 4-8: Result of linear mixed effects model on the mature segment of density once the non-significant terms have been removed.....	196
Table 5-1: Number of sites and cores used in the acoustic velocity measurements	202
Table 6-1: Number of samples per site.....	227
Table 6-2:: The number of samples and sites per group	228
Table 6-3: Parameter estimates along with Standard Errors, residual standard error and R-squared value for the four model equations. Also shown is the number of trees and the percent of the total that the model wouldn't fit to. .	234
Table 7-1: Tree and dendrometer (LVDT) number, diameter at breast height (DBH) and height of the trees selected at Griffin forest in April 2008 (Vihermaa, 2010) and the DBH of the same trees measured in July 2012 towards the end of the current experiment.....	268
Table 7-2: Comparison between manual DBH measurements and the radial expansion measurements taken by the dendrometers.....	278
Table 7-3: Amount of radial expansion achieved by each tree each year measured by point dendrometers.	281
Table 7-4: Comparison of characteristics of Griffin and Harwood sites.....	314
Table 7-5: Number, diameter at breast height (DBH) and height of the trees selected at Harwood forest in April 2010	315
Table 7-6: Comparison between Griffin and Harwood sites of the days when radial expansion started and stopped.	320
Table 7-7: Comparison between Griffin and Harwood sites of total radial expansion for each tree during 2012	321
Table 7-8: The number of days during the preceding winter that the mean temperature was below 5 ⁰ C before the growing season at Griffin started.	336

List of Figures

Figure 1-1: Predicted range of changes in summer temperature in the UK, using 10%, 50% and 90% probability levels for low, medium and high emission scenario. © UK Climate Projections 2009.....	32
Figure 1-2: Predicted range of changes in winter temperature in the UK, using 10%, 50% and 90% probability levels for low, medium and high emission scenario. © UK Climate Projections 2009.....	33
Figure 1-3: Predicted range of changes in summer precipitation in the UK, using 10%, 50% and 90% probability levels for low, medium and high emission scenario. © UK Climate Projections 2009.....	33
Figure 1-4: Predicted range of changes in winter precipitation in the UK, using 10%, 50% and 90% probability levels for low, medium and high emission scenario. © UK Climate Projections 2009.....	34
Figure 1-5: Locations of sites for Weather Generator projected change analysis. © UK Climate Projections 2009.....	36
Figure 2-1: Location of the sites sampled in the extension study (red) and the original study (green). The sites from the original study which were used to examine wood properties in the current study are shown in blue.	56
Figure 2-2: Taking a 12mm increment core from a tree in Site 303 on North Wales using a Tanaka increment corer.....	60
Figure 2-3: 12 mm increment core taken at site 303 in North Wales. A standard sized pen is added for scale.	60
Figure 2-4: Sample core glued to an MDF holder.	61
Figure 2-5: MDF and core clamped in position in the mill.	61
Figure 2-6: The sample core after milling with the 2 mm strip along the centre of the core.....	61
Figure 2-7: Sample strips ready for analysis on the ITRAX.	61
Figure 2-8: Sample strips in position in the ITRAX densitometer.....	62
Figure 2-9: Grey scale image of the calibration wedge which was calibrated for each run of samples.....	64
Figure 2-10: Greyscale image of a sample with path and density profile calculated by Windendro.....	64
Figure 2-11: The grey scale image of sample 2723-31 along with the corresponding density and ring width output calculated using Windendro.....	65
Figure 2-12: Accumulated temperature, rainfall, moisture deficit and DAMS score from ESC plotted against latitude shown as an OS grid reference and fitted with a linear trendline.....	67
Figure 2-13: Accumulated temperature, rainfall, moisture deficit and DAMS score from ESC plotted against longitude shown as an OS grid reference and fitted with a linear trendline.....	68
Figure 2-14: Accumulated temperature, rainfall, moisture deficit and DAMS score from ESC plotted against elevation shown as an OS grid reference and fitted with a linear trendline.....	68
Figure 2-15: Continentality of sites from ESC plotted by longitude and latitude fitted with a linear trendline.....	69
Figure 2-16: ESC data on current accumulated temperature, along with the accumulated temperature predicted by the low scenario after 50 and 80 years of UKCP09 (2009a) for the sites used within this study to measure ring growth and ring density.....	70

Figure 2-17: Current ESC moisture deficit data, along with the moisture deficit predicted by the low scenario after 50 and 80 years of UKCP09 (2009) for the sites used within this study to measure ring growth and ring density.	71
Figure 2-18: The Ordnance Survey British National Grid. Each 100 km x 100 km grid is described by a pair of letters which have been translated into numbers based on columns and rows. Also shown is the location of the sites used in this study in relation to the grid squares.....	72
Figure 3-1: Radial growth plotted by cambial age with a LOWESS trend line	78
Figure 3-2: Distribution of sample length measured from pith to bark (radius) on the core samples	79
Figure 3-3: Boxplot showing the radius of the samples at cambial age 25 plotted by site running sequentially from furthest south (left) to furthest north (right).	80
Figure 3-4: Radius of samples at cambial age 25 plotted against longitude, latitude, spacing and altitude	81
Figure 3-5: The fitted line for each of the growth models (red) plotted against the mean of the observed data (blue) by ring number from the pith.	84
Figure 3-6: Observed V Predicted for the Hossfeld4 model on the global data. .	87
Figure 3-7: Residuals plotted against cambial age for the Hossfeld4 model on the global data.	87
Figure 3-8: Observed Vs Predicted for the Hossfeld4 model when fitted to individual tree.	88
Figure 3-9: Residuals of Hossfeld4 model when fitted to individual trees, plotted against cambial age with LOWESS trend line (red).	89
Figure 3-10: Residuals of Hossfeld4 model when fitted to individual trees, plotted against growth with LOWESS trend line (red).	89
Figure 3-11: Coefficients of the Hossfeld4 model plotted by northing group, easting group, spacing and elevation group.	90
Figure 3-12: Growth rates of the 9 trees that the Hossfeld4 model couldn't fit.	91
Figure 3-13: Histogram showing the large range in the coefficients a and b for the Hossfeld4 model.	92
Figure 3-14: The growth rate and fitted line for the three samples which the Hossfeld4 model predicts the highest values for coefficient a (top row) and lowest values (bottom row).	93
Figure 3-15: The growth rate and fitted line for the three samples which the Hossfeld4 model predicts the highest values for coefficient b (top row) and lowest values (bottom row).	94
Figure 3-16: Observed Vs Predicted for Log model on the global data. Red line shows the line of equality.....	95
Figure 3-17: Residuals plotted against cambial age for the Log model on the global data. Also showing the LOWESS trend line in red	95
Figure 3-18: Growth rate of 27 trees which the Exp model could not fit.	96
Figure 3-19: Histogram showing the frequency of the fitted coefficients for the Exponential Model.....	97
Figure 3-20: The 9 trees for which the Exponential model fitted the highest coefficients.....	97
Figure 3-21: Observed Vs Predicted for Exp model when fitted to individual tree. R squared 0.9961	98
Figure 3-22: Residuals of Exp model when fitted to individual trees plotted against cambial age	99
Figure 3-23: Residuals of Exp model when fitted to individual trees plotted against growth	99

Figure 3-24: Coefficients of the Exp model plotted by northing, easting spacing and elevation groups.....	100
Figure 3-25: The split point between juvenile and mature growth segments plotted by Northing, Easting Spacing and Elevation. The dashed line shows the value (11.6 years) when modelled against the global data.	101
Figure 3-26: The split point between juvenile and mature slopes plotted by Site and radius. The dashed line shows the value (11.6 years) when modelled against the global data.....	102
Figure 3-27: Observed growth and breakpoint fitted by the segmented model on a selection of benchmark trees	103
Figure 3-28: Growth rates for trees which the segmented model couldn't fit a split point.....	104
Figure 3-29: Growth of trees where the segmented model fitted the mature growth rate to be greater than the juvenile growth rate	104
Figure 3-30: Observed Vs Predicted for the two segment model when fitted individual trees.	105
Figure 3-31: Histogram showing the distribution of split points between the juvenile and mature growth segments fitted by the segmented model on growth.	106
Figure 3-32: Growth of the nine trees with the lowest split points fitted by the segmented model.....	106
Figure 3-33: Growth of the nine trees with the highest split points fitted by the segmented model.....	107
Figure 3-34: All benchmark growth data with red line showing where segmented model fitted the split between juvenile and mature wood (cambial age 11.6) and the upper limit of ring 25 (blue).	108
Figure 3-35: Growth up to year 11 (juvenile growth) with LOWESS trend line..	109
Figure 3-36: Growth from year 12 to year 25 (mature growth) with LOWESS trend line	109
Figure 3-37: Intercept coefficients of the juvenile growth section plotted by northing, easting spacing and elevation groups.....	110
Figure 3-38: Slope coefficients of the juvenile growth section plotted by northing, easting spacing and elevation groups.....	110
Figure 3-39: Residuals for the linear model of rings 1 to 11	111
Figure 3-40: Observed Vs predicted growth for the juvenile segment of the linear model. Red line shows the line of equality	112
Figure 3-41: Intercept and Slope coefficients fitted by a linear model to growth between cambial age 0 to 11 years old for each sample.	112
Figure 3-42: Residuals of linear model when fitted to the juvenile growth of each tree with LOWESS trend line (red).	113
Figure 3-43: Observed Vs predicted for the juvenile linear model giving an R-squared of 0.99	113
Figure 3-44: Intercept coefficients of the mature growth section plotted by northing, easting spacing and elevation groups.....	114
Figure 3-45: Slope coefficients of the mature growth section plotted by northing, easting spacing and elevation groups.	115
Figure 3-46: Residuals for the linear model of rings 12 to 25.	116
Figure 3-47: Observed Vs predicted growth for the mature segment of the linear model. Red line shows the line of equality, R squared = 0.1856	117
Figure 3-48: Intercept and Slope coefficients fitted by a linear model to growth between cambial age 12 to 25 years old for each sample.....	118

Figure 3-49: Residuals for the mature growth section when linear model is fitted to each tree individually.	119
Figure 3-50: Observed Vs predicted for the mature linear model fitted to individual trees, giving an R-squared of 0.99	119
Figure 3-51: Residuals for linear model on the juvenile and mature segments combined	120
Figure 3-52: Residuals of mixed effects model on the juvenile segment with random intercept only	122
Figure 3-53: Residuals of mixed effects model on the juvenile segment with random intercept and slope	122
Figure 3-54: The relationship between the predicted values and observed growth values for the mixed effects model on the juvenile segment of growth. The red line represents the line of equality.	123
Figure 3-55: Residuals of mixed effects model on the mature growth segment with only random intercept.	125
Figure 3-56: Residuals of mixed effects model on the mature growth with random intercept and slope.	125
Figure 3-57: Observed Vs Predicted for Mixed Effects Model on the mature segment of growth, showing line of equality (red).	126
Figure 3-58: Linear model on juvenile growth showing the effect of 1.5m, 2.0m and 2.5m spacing	132
Figure 3-59: Scatterplot showing the correlation between accumulated growth at ring 12 versus accumulated growth at rings 1, 25, 30 and 35.	134
Figure 3-60: The effect of Northing (A), Easting (B) and Elevation (C) on the intercept coefficients when fitted to each tree	136
Figure 3-61: The effect of Northing (A), Easting (B) and Elevation (C) on the slope coefficients when fitted to each tree	137
Figure 3-62: Correlation between winter and summer rainfall taken from ESC Data	138
Figure 4-1: Radial profile of mean ring density plotted by cambial age with a LOWESS trend line	143
Figure 4-2: Histogram of mean ring density	144
Figure 4-3: Observed density of each tree plotted by site. Showing the LOWESS trend by site (red line) compared to the LOWESS trend for the full data set (blue line)	145
Figure 4-4: Boxplot showing the spread of density when grouped by longitude, latitude, spacing and altitude	147
Figure 4-5: The form of the density models plotted along with the mean density for each ring.	150
Figure 4-6: Ring width by cambial age (as measured by ring number from the pith) with the mean value for each ring plotted	151
Figure 4-7: The relationship between density and early wood percentage. Pearson correlation coefficient for juvenile wood (i.e. less than or equal to ring 7) is -0.597 and for mature wood (i.e. greater than ring 7) is -0.671.	151
Figure 4-8: Relationship between density and ring width showing these are different between juvenile and mature wood	152
Figure 4-9: Relationship between specific gravity measured as calculated from the ITRAX density data and basic specific gravity. The dashed line shows the line of equality.	154
Figure 4-10: Fitted lines for the three models from Gardiner et al. (2011), using the parameters which were derived from the original data and the parameters derived from the data in this study converted at 4% moisture content.	155

Figure 4-11: Observed Vs Predicted for the Gardiner3 model on all of the density data. Red line shows the line of equality.	157
Figure 4-12: Residuals for the Gardiner3 model plotted against cambial age on all of the density data. Red line shows the LOWESS trend line.	157
Figure 4-13: Residuals for the Gardiner3 model plotted against observed values on all of the density data. Red line shows the LOWESS trend line.	158
Figure 4-14: Residuals for the Gardiner3 model plotted against ring width on all of the density data. Red line shows the LOWESS trend line.	158
Figure 4-15: Observed Vs Predicted for the Lindstrom model on all of the density data. Red line shows the line of equality.	159
Figure 4-16: Residuals for the Lindstrom model plotted against cambial age on all of the density data. Red line shows the LOWESS trend line.....	160
Figure 4-17: Residuals for the Lindstrom model plotted against the observed values on all of the density data. Red line shows the LOWESS trend line.	160
Figure 4-18: Residuals for the Lindstrom model plotted against ring width on all of the density data. Red line shows the LOWESS trend line.	161
Figure 4-19: Observed Vs Predicted for the Exponential model on all of the density data. Red line shows the line of equality.	162
Figure 4-20: Residuals for the Exponential model on all of the density data. Red line shows the LOWESS trend line.....	162
Figure 4-21: Example of the observed density profiles for a selection of trees with the split point fitted by the segmented model	164
Figure 4-22: Histogram showing the distribution of split points for the density segmented model. The minimum split point was 3.0 years, the maximum was 23.9 years and the mean was 8.7 years.	165
Figure 4-23: The density profile of the 7 trees that the segmented model could not fit	165
Figure 4-24: Observed Vs Predicted for the density segmented model when fitted to individual trees. R-squared = 0.83.....	166
Figure 4-25: The effect of the different variables on the density profile split point, with the black line showing the regression fitted to the data for each. Ring number is measured from the pith.....	167
Figure 4-26: The segmented model split plotted by site in order from south (left) to north (right) with ring number measured from the pith.	169
Figure 4-27: Density data showing the mean line (green), the LOWESS trend line (red), the line where the segmented model fitted the split (cambial age 7.4 years) and the upper age limit (25 years) used in this analysis.....	170
Figure 4-28: Residual plots for the density juvenile segment linear model	172
Figure 4-29: Observed versus predicted density values for the juvenile segment linear model. The red line shows the line of equality.	172
Figure 4-30: Slope and intercept coefficients fitted by the linear model to the density profile up to year 7 for each sample.....	173
Figure 4-31: The density profiles from rings 2 to 7 of the samples which the linear model predicted a positive slope for density in the juvenile phase.	174
Figure 4-32: Residuals of linear model when fitted to the density profile of the juvenile segment of each tree, with LOWESS trend line (red)	175
Figure 4-33: Observed Vs predicted for the juvenile density linear model giving an R-Squared of 0.91.....	175
Figure 4-34: The effect of northing, easting, spacing and elevation on the juvenile segment linear model slope coefficient.	176
Figure 4-35: The effect of northing, easting, spacing and elevation on the juvenile segment linear model intercept coefficient.	177

Figure 4-36: Residuals of mixed effects model on juvenile density segment with random intercept only.	179
Figure 4-37: Residuals of mixed effects model on density segment with random intercept and slope.	179
Figure 4-38: The relationship between the observed density and the predicted values for the juvenile density linear mixed effects model giving an R-Squared of 0.91.....	180
Figure 4-39: Residual plots for the density mature segment linear model	181
Figure 4-40: Observed versus predicted density values for the mature segment linear model. The red line shows the line of equality.	182
Figure 4-41: Slope and intercept coefficients fitted by the linear model to the density profile of years 8 to 25 for each sample.....	183
Figure 4-42: The density profiles from year 2 to 25 of the samples which the linear model fitted a negative slope for density in the mature phase. The blue dashed line indicates the split point of 7.4 years showing the cut off between the juvenile and mature phases calculated on the full data set.	183
Figure 4-43: Residuals of linear model when fitted to the density profile of the mature segment of each tree, with LOWESS trend line (red).....	184
Figure 4-44: Observed Vs predicted for the mature density linear model giving an R-Squared of 0.7675.....	185
Figure 4-45: Residuals for linear models of the juvenile and mature segments together.....	185
Figure 4-46: The effect of northing, easting, spacing and elevation on the mature segment linear model slope coefficient.	186
Figure 4-47: The effect of northing, easting, spacing and elevation on the mature segment linear model intercept coefficient.	187
Figure 4-48: Residuals of mixed effects model on density velocity segment with random intercept only.	188
Figure 4-49: Residuals of mixed effects model on mature density segment with random intercept and slope.	189
Figure 4-50: The relationship between the observed density and the predicted values for the juvenile density linear mixed effects model giving an R-squared of 0.7647	190
Figure 4-51: Correlation between the linear model slope of the juvenile density segment and northing, easting, spacing and altitude. Only northing was found to have a significant correlation.....	191
Figure 4-52: Correlation between the linear model intercept of the juvenile density segment and northing, easting, spacing and altitude. Northing and spacing were found to have a significant correlation.	192
Figure 4-53: Correlation between the linear model slope of the mature density segment and northing, easting, spacing and altitude. Spacing and elevation were found to have a significant correlation.	194
Figure 4-54: Correlation between the linear model intercept of the mature density segment and northing, easting, spacing and altitude. Only spacing was found to have a significant correlation.	195
Figure 4-55: Correlation between density measured on different ring numbers where rings are counted from the pith.....	197
Figure 5-1: Map showing the location of the sites used in this study (red) and the sites from a previous evaluation study (green).	203
Figure 5-2: Ultrasonic Scanner at University of Canterbury, Christchurch, New Zealand	204

Figure 5-3: 12mm Sitka spruce increment core clamped into the ultrasonic scanner.....	204
Figure 5-4: Computer photographic output showing position of pith (red dot), the start and end points (yellow dots) and scan pattern (blue line)	205
Figure 5-5: Computer output showing the core thickness (top) and the acoustic velocity (bottom) produced by the ultrasonic scanner.	205
Figure 5-6 - The effect of different step sizes on acoustic velocity. Velocity was measured at 2mm, 3mm, and 4mm to determine if this would have an effect.	206
Figure 5-7: Schematic showing the change in grain angle from vertical.	207
Figure 5-8 - The effect of turning the core by 10° and 20° clockwise and anticlockwise on the acoustic velocity on three separate tree cores	208
Figure 5-9: Examples of cores taken as part of this study.....	209
Figure 5-10: Schematic showing direction from which the cores were taken. ..	209
Figure 5-11: Older cores from the original study showing the rough surface which in some cases has crumbled into powder	210
Figure 5-12: Examples showing the rough surface of the core (bottom) and a smoothed surface once sanded (top).....	211
Figure 5-13: Acoustic velocity measurements on the full data set showing a LOWESS trendline for the unsanded and sanded data	212
Figure 5-14: Acoustic velocity of the 72 samples where acoustic velocity was measured unsanded and then sanded.	213
Figure 5-15: Histogram showing the frequency and range of acoustic velocity measurements on the 72 cores which were measured unsanded (red) and then sanded (black).	213
Figure 5-16: Acoustic velocity for the 72 samples which were measured both unsanded and sanded.	215
Figure 5-17: Scatterplot of acoustic velocity measured on the same cores unsanded and then sanded. Also shown is the line of equality (black). R-squared =0.34	216
Figure 5-18: The relationship between unsanded and sanded acoustic velocity on the same cores.	217
Figure 5-19: Schematic showing how the distance measured could be affected by the shape of the core.	218
Figure 5-20: The variation in the thickness of the increment cores measured by the acoustic scanner.	219
Figure 5-21: Thickness measured by the acoustic scanner for each 2mm increment plotted against the acoustic velocity.....	220
Figure 5-22: The variation in the thickness of the 72 increment cores which were measured by the acoustic scanner both unsanded and sanded.	221
Figure 5-23: Distance measured by the acoustic scanner plotted against the acoustic velocity for the 72 increment cores which were measured by the acoustic scanner both unsanded and sanded.	221
Figure 6-1: Acoustic velocity of all data plotted by ring number with a LOWESS trend line	226
Figure 6-2: Acoustic velocity and LOWESS trend line plotted by site in order from south (bottom left) to north (top right).....	229
Figure 6-3: Dynamic MoE by ring for the set of data that was measured for acoustic velocity and density.	230
Figure 6-4: Dynamic MoE by ring for a selection of trees	232
Figure 6-5: The fitted line for each of the statistical models plotted against the LOWESS trend line.....	235

Figure 6-6: Observed acoustic velocity and the split point fitted by the segmented model on a selection of trees.....	237
Figure 6-7: Histogram showing the distribution of split points between the two segments fitted by the segmented model.	238
Figure 6-8: Acoustic velocity measurements of the 4 trees that the segmented model couldn't fit to.....	238
Figure 6-9: Acoustic velocity curves for 6 of the 59 trees that the segmented model couldn't fit a split point.	239
Figure 6-10: Observed Vs predicted for the two segmented model on acoustic velocity when fitted to individual trees. R-squared =0.9389	239
Figure 6-11: Split point between the two phases of the acoustic velocity curve plotted by northing, easting, spacing and elevation groups. Dashed line shows the value (13.3 years) that the model fitted to the global data.	240
Figure 6-12: The split point between the juvenile and mature phases of acoustic velocity plotted by Site organised from south (left) to north (right). The dashed line shows the value (13.3 years) when modelled against the global data.	241
Figure 6-13: Acoustic Velocity data with blue lines showing where the segmented model fitted the split (age 13.2) and the upper limit of ring 25. Also shown is the LOWESS trend line (red line).....	242
Figure 6-14: Acoustic velocity up to year 13, with LOWESS trend line	243
Figure 6-15: Acoustic velocity year 14 to 25, with LOWESS trend line	243
Figure 6-16: Residual plots for the linear model of rings 2 to 13	244
Figure 6-17: Observed Vs Predicted acoustic velocity for the juvenile segment of the linear model. The line of equality is shown in red	244
Figure 6-18: Slope and Intercept coefficients fitted by a linear model to the acoustic velocity up to cambial age 13 year for each sample	245
Figure 6-19: Samples with a negative juvenile slope (top row) compared to those with the highest positive slope (bottom row).	246
Figure 6-20: Residuals of linear model when fitted to the acoustic velocity of the juvenile segment of each tree, with LOWESS trend line (red)	247
Figure 6-21: Observed Vs predicted for the juvenile linear model giving an R-Squared of 0.91.	247
Figure 6-22: Slope coefficients for the juvenile segment of acoustic velocity plotted by northing, easting, spacing and elevation groups. Also shown is the overall mean (red line).	248
Figure 6-23: Intercept coefficients for the juvenile segment of acoustic velocity plotted by northing, easting, spacing and elevation groups. Also shown is the overall mean (red line).	249
Figure 6-24: Residuals of mixed effects model on juvenile acoustic velocity segment with random intercept only.....	251
Figure 6-25: Residuals of mixed effects model on juvenile acoustic velocity segment with random intercept and slope.	251
Figure 6-26: Observed Vs predicted for the juvenile mixed effects model giving an R-Squared of 0.91.....	252
Figure 6-27: Observed Vs Predicted for the Exponential model on all of the acoustic data. Red line shows the line of equality.	254
Figure 6-28: Residuals for the Exponential model on all of the acoustic data. Red line shows the LOWESS trend line.....	254
Figure 6-29: Observed vs predicted for exponential model of acoustic velocity when fitted to individual trees. R-Squared = 0.9127.....	255
Figure 6-30: Residuals of Exponential model of acoustic velocity when fitted to individual trees, plotted against cambial age.....	256

Figure 6-31: Residuals of Exponential model of acoustic velocity when fitted to individual trees, plotted against acoustic velocity.	256
Figure 6-32: Acoustic velocity of 15 of the 43 trees (15% of the total) which the Exponential model couldn't fit.	257
Figure 6-33: Coefficients for the exponential model for acoustic velocity when fitted to individual trees.	258
Figure 6-34: Top row shows trees which the Exponential model fitted the highest b_0 and b_2 coefficients. These also correspond to the lowest b_1 coefficients. Also shown are the samples with the lowest b_0 coefficient (2 nd top row), the samples with the lowest b_2 coefficients (3 rd row) and the samples with the highest b_1 coefficient (bottom row).	259
Figure 6-35: Coefficients of the Exponential model plotted by latitude, longitude, spacing and altitude groups.	260
Figure 6-36: Correlation between the Exponential model coefficients, calculated by site, and latitude. Showing a significant correlation between latitude and b_0 , but no significant correlation between either b_1 or b_2 and latitude.	261
Figure 6-37: Correlation between the Exponential model coefficients, calculated by site, and longitude. Showing a significant correlation between longitude and b_1 , but no significant correlation between either b_0 or b_2 and longitude.	261
Figure 7-1: Map of Scotland and Northern England showing locations of the Griffin and Harwood sites.	267
Figure 7-2: Plan of the experimental site within Griffin Forest. Showing the position of the trees used within the experiment along with the position of the other trees and where trees have been thinned. This plan is an approximation and not to scale.	269
Figure 7-3: Picture of an LVDT dendrometer and insulated steal beam supports measuring tree growth on Tree 8 at Griffin Forest.	270
Figure 7-4: Picture of an LVDT dendrometer and spirit level attached to Tree 8 at Griffin Forest.	271
Figure 7-5: Comparison of soil moisture probes showing how the soil moisture can change over a short distance on one site.	272
Figure 7-6: Comparison of soil moisture measured at Griffin site during 2010 with rainfall measured at Aberfeldy, Dull weather station.	273
Figure 7-7: Comparison of minimum daily temperature measured at Griffin site during 2010 with that measured at Aberfeldy Dull weather station.	274
Figure 7-8: Comparison of mean daily temperature measured at Griffin site during 2010 with that measured at Aberfeldy Dull weather station.	274
Figure 7-9: Comparison of daily mean air temperature by year measured at the Griffin site.	275
Figure 7-10: Comparison of the daily mean soil moisture by year measured at the Griffin site.	276
Figure 7-11: Griffin site measurements from June 2008 to October 2012. The top panel of the graph shows air temperature ($^{\circ}\text{C}$, black) and relative humidity (% , blue), soil moisture (%) is shown in the middle and radial expansion of the five trees, as measured by LVDT dendrometers in the bottom panel.	277
Figure 7-12: Measurements for tree 48 during the winter of (a) 2009/2010 and (b) 2010/2011 showing a big dip in readings corresponding to extreme cold events.	278
Figure 7-13: Comparison by year of the radial expansion curves of the 5 trees at Griffin when radial expansion is reset to zero each year.	280

Figure 7-14: Example of calculating the radial expansion rate for tree 48 during the growing season of 2011. The rate value was calculated by subtracting each daily value from the following daily value.....	282
Figure 7-15: The effect of soil moisture and temperature on the rate of expansion of Tree 48 at Griffin during 2008.	284
Figure 7-16: The effect of soil moisture and temperature on the radial expansion rate of Trees 43, 8, 15 and 66 at Griffin during 2008.	286
Figure 7-17: The effect of soil moisture and temperature on the radial expansion rate of Tree 48 at Griffin during 2009.	287
Figure 7-18: The effect of soil moisture and temperature on the rate of radial expansion of Trees 43, 8, 15 and 66 at Griffin during 2009.	289
Figure 7-19: The effect of soil moisture and temperature on the radial expansion rate of Tree 48 at Griffin during 2010.	290
Figure 7-20: The effect of soil moisture and temperature on the rate of radial expansion of Trees 43, 15 and 66 at Griffin during 2010.	292
Figure 7-21: The effect of soil moisture and temperature on the radial expansion rate of Tree 48 at Griffin during 2011.	293
Figure 7-22: The effect of soil moisture and temperature on the radial expansion rate of Trees 43, 15 and 66 at Griffin during 2011.	295
Figure 7-23: The effect of soil moisture and temperature on the radial expansion rate of Tree 48 at Griffin during 2012.	296
Figure 7-24: The effect of soil moisture and temperature on the radial expansion rate of Trees 43, 8, and 66 at Griffin during 2012.	298
Figure 7-25: Shows the day of the year that the radial expansion rate starts to rapidly increase along with when temperature is greater than 5 °C.....	299
Figure 7-26: Shows the day of the year that the slow expansion of the trees starts and when the mean temperature is greater than 3°C.....	300
Figure 7-27: Shows the day of the year that the radial expansion stops along with the days that the mean temperature is consistently below 5°C.....	300
Figure 7-28: Shows the day of each year that the radial expansion rate of the trees at Griffin starts to decrease.	301
Figure 7-29: Example of detrending the radial expansion curve for tree 48 in during the growing season of 2011. The detrended value was calculated by subtracting the 30 day moving average smoothed radial expansion value from the radial expansion value for the same day.....	302
Figure 7-30: The detrended maximum daily expansion measured for each tree plotted against the mean daily soil moisture value for the period where growth was occurring during 2008.	303
Figure 7-31: Soil moisture measured at Griffin plotted against rainfall at Aberfeldy for year 2008. A period of low soil moisture at approximately day 210 corresponds to a period relatively low rainfall.	304
Figure 7-32: Rainfall measured at Aberfeldy weather station compared to the maximum daily expansion of trees for the same period during 2008.....	305
Figure 7-33: The detrended maximum daily expansion measured for each tree plotted against the mean daily soil moisture value for 2009.	306
Figure 7-34: Rainfall measured at Aberfeldy weather station compared to the maximum daily expansion of trees for the same period during 2009.	307
Figure 7-35: The detrended daily maximum expansion measured for each tree plotted against the mean daily soil moisture value for 2010.	308
Figure 7-36: Rainfall measured at Aberfeldy weather station compared to the maximum daily expansion of trees for the same period during 2010.	309

Figure 7-37: The detrended daily maximum expansion measured for each tree plotted against the mean daily soil moisture value for 2011.	310
Figure 7-38: Rainfall measured at Aberfeldy weather station compared to the maximum daily expansion of trees for the same period during 2011.	311
Figure 7-39: The detrended daily maximum expansion measured for each tree plotted against the mean daily soil moisture value for 2012.	312
Figure 7-40: Rainfall measured at Aberfeldy weather station compared to the maximum daily expansion of trees for the same period during 2012.	313
Figure 7-41: Schematic of Harwood field site showing position of trees, tower, soil moisture probes and air temperature/ relative humidity probes and the associated dataloggers.....	317
Figure 7-42: Comparison of temperatures measured at Griffin and Harwood during 2012.	318
Figure 7-43: Comparison of soil moisture measured at Griffin and Harwood during 2012.	319
Figure 7-44: Harwood site radial expansion measurements from February 2012 showing radial growth of the five trees, as measured by LVDT dendrometers..	320
Figure 7-45: The effect of soil moisture and temperature on the radial expansion rate of Tree 48 at Harwood during 2012.	322
Figure 7-46: The effect of soil moisture and temperature on the radial expansion rate of Trees 28, 41, and 19 at Harwood during 2012.	323
Figure 7-47: The detrended daily maximum expansion measured for each tree at Harwood plotted against the mean daily soil moisture value for 2012.	325
Figure 7-48: The daily expansion and contraction of the tree trunk along with the radial increment (red). Here the radial expansion curve has also been detrended (blue) to take account of the seasonal increase in size allowing the amplitude of the diurnal variation to be measured.	327
Figure 7-49: Dendrometer data collected from Griffin in June 2010 showing the raw data (a) showing the upward trend and the detrended data (b) showing the daily variation in readings and so the diurnal variation in stem width	328
Figure 7-50: Air temperature, soil moisture and detrended radial expansion logged at Griffin in June 2009.	329
Figure 7-51: Air temperature, soil moisture and detrended radial expansion logged at Griffin in July and August 2010.....	330
Figure 7-52: Air temperature, soil moisture and detrended radial expansion logged at Griffin in June and July 2011.	331
Figure 7-53: Air temperature, soil moisture and detrended radial expansion logged at Griffin in November and December 2009.	332
Figure 7-54: The amplitude of the daily changes in radius of the trees at Griffin site from April 2008 to October 2012.....	333
Figure 7-55: The daily hours of daylight changes throughout the year, peaking at approximately 17.5 hours on 21 st June.....	339
Figure 8-1: Correlation between the intercept coefficient of the juvenile linear models of growth and density	355
Figure 8-2: Correlation between the intercept coefficient of the mature linear models of growth and density	356
Figure 8-3: The transition point between the juvenile and mature phases when fitted by density, growth and acoustic velocity	357
Figure 8-4: Relationship in the transition points between juvenile and mature phases when modelled by density, growth and acoustic velocity.....	358

Acknowledgement

I would like to say a big thank you to the following people who have helped me throughout my PhD.

Firstly I would like to thank WestChem and Forest Research for their funding which has enabled me to undertake this project. I would like to thank my supervisors; Dr. Mike Jarvis of Glasgow University for his help and support throughout the project, Prof. Barry Gardiner for his initial help from Forest Research and continued support from France and Dr. Mike Perks of Forest Research for his taking over supervision half way through.

I would like to say a big thank Dr. Leena Vihermaa for input and suggestions during the early stages and help throughout my PhD. For showing me how to use equipment and help with field work at Griffin Forest where she began and collected data for the long term monitoring project used in this study...thank you. I would also like to thank Dr. Axel Wellpott for his help processing Griffin data and Dr. Kate Beauchamp and Dr. Rob Clement for getting me to Griffin through the snow.

I would also like to thank Michael Beglan for all his invaluable technical support at Glasgow University and Carina Convey for hers at NRS and in the field. I am also indebted to Dr Kevin Scott for his help with setting up and programming the dendrometer system at Harwood, to Dave Auty for helping source all the parts and to John Strachan for helping build the equipment.

I would like to thank Dr. Paul McLean for his help analysing the data and trying to get me to understand modelling and R.

Thank you to Dr. Clemens Altaner for his help arranging my STSM to the University of Canterbury in New Zealand, Nigel Pink and Lachlan Kirk for their assistance, and coffee, while there and to COST Action FP0802 who funded the trip.

I would like to thank Dr. Kate Beauchamp and Andy Price for their help setting up the Benchmark field work and them along with Stefan Lehneke for helping

carry out the field work and making it such an interesting and enjoyable experience.

I would like to thank everyone at NRS who has helped me with this project including Elspeth MacDonald for her vast knowledge, as well as Stephen Bathgate and Louis Sing for their help with ESC data.

Finally I would like to say a huge thank you to Allison Ford for being there when needed and without whose support this project would not have been impossible.

Author's Declaration

This work is entirely my own, except where help received has been acknowledged. Work that has been done by other people has been reported in the relevant chapters.

Definitions/Abbreviations

Acoustic Velocity: refers to the speed that sound travels through a piece of wood. The velocity at which sound travels through wood is dependent on its modulus of elasticity, i.e. stiffness, and its density.

DBH: Diameter at breast height (1.3 m).

ESC: Ecological Site Classification.

GYC: General Yield Class. The measure of forest growth used in Britain, expressed as $\text{m}^3 \text{ha}^{-1} \text{yr}^{-1}$

LVDT: Linear Variable Displacement Transducer. The type of probe used by point dendrometers to measure radial growth.

MFA: Micro fibril angle. The angle of the cellulose microfibril helix in the S2 layer of the wood cell wall.

MoE: Modulus of Elasticity. A measure of wood stiffness.

Ring density: refers to the average ring density measured as kilograms of mass per cubic metre (kg m^{-3}) at 4% moisture content.

Radial growth: refers to secondary growth, that is, radial growth from the vascular cambium. All measurements of secondary growth were at breast height (approximately 1.3 m).

QCI: Queen Charlotte Island. A source of Sitka spruce seed imported into the UK.

UKCP09: the working name given to the UK Climate Projections website, user interface and reports.

1 Introduction

The climate of the UK is projected to change in the future (UKCP09, 2009a) and although there is huge uncertainty about the manner and scale of this change it is predicted that in the UK there could be warmer, drier and longer growing seasons during the summer, and wetter, warmer winters (UKCP09, 2009a, Murphy et al., 2009a) and although this is likely to have an effect on both tree growth and timber quality (Broadmeadow, 2002b, Ray, 2008b, UKCP09, 2009a), the nature of this effect is still largely unknown in the UK.

According to (Broadmeadow, 2002b) and (Ray, 2008b) possible effects could include:

- Higher temperatures during the growing season would increase productivity if water is not limited, which in turn could lead to a decrease in construction grade timber due to a decrease in density.
- Longer growing seasons could lead to early bud burst and later dormancy, which could lead to higher risks of frost damage. However there is evidence that tree species with a high chilling requirement that was no longer met would be subject to a delay in bud burst and so may not benefit from a longer growing season (Cannell and Smith, 1983, Murray et al., 1989).
- Milder winters could lead to trees not entering full dormancy resulting in damage due to the cold and also the trees not reaching their chilling requirement. Increased temperatures during winter could also mean a decrease in mortality of disease and pests during winter which could lead to an increase in damage to the trees (Proe et al., 1996).
- Lower precipitation in summer, especially in the east, could lead to drought conditions that can cause stem cracking in susceptible conifers
- Wetter winters could lead to a higher water table damaging and killing roots.

- Trees could be left vulnerable to pathogens due to being weakened by these effects of climate

As well as having an effect on the amount of wood produced, a change in climate could also have an effect on the quality of wood produced (Zobel and Buijtenen, 1989). To qualify as construction grade timber the main quality criteria looked at are stiffness, strength, and dimensional stability. There are various properties of wood that affect these including: knots, grain angle, density, tracheid length, microfibril angle, juvenile wood and compression wood (MacDonald and Hubert, 2002, MacDonald et al., 2010). In addition stem straightness affects the out-turn of construction-grade timber. Silviculture, i.e. the way a forest is managed, can have a big influence on these properties (MacDonald and Hubert, 2002) as competition between trees for sunlight, water and nutrients can have an effect on tree growth. For example the initial spacing (planting distance) can have an effect on the number of knots, the amount of juvenile wood, stem straightness and to a lesser extent density (Brazier and Mobbs, 1993), and these can also be influenced by the practice of thinning (Kilpatrick et al., 1981, Savill and Sandels, 1983). Genetics can also have an effect on wood properties (Lee, 1999, McLean, 2008, Moore et al., 2009b) with lower density generally being found in faster growing trees (Brazier, 1967) as shown by a negative correlation between ring width and density (Dutilleul et al., 1998, Saranpaa, 1994). This correlation has been explained by an increase in the amount of earlywood and a reduction in the density of the earlywood (Brazier, 1970). Selecting and breeding the fastest growing trees may therefore have an adverse effect on the properties that are being looked for in the quality of timber and this is a major challenge for future breeding programs (Lee and Connolly, 2010). As well as silviculture and genetics, characteristics of the stand can have an influence on the amount and quality of wood produced including soil type, elevation, latitude and differences in climate between sites (Moore et al., 2009a, Vihermaa, 2010).

1.1 Sitka Spruce

Sitka spruce (*Picea sitchensis* (Bong.)Carr) is one of the most commercially important tree species in the UK.

The Forestry Commission in the UK carries out woodland surveys at 10 to 15 year intervals to compile forest inventories, with the next cycle due for completion in 2014. The most recent report on the volume of coniferous timber in Britain (Forestry Commission, 2011) estimated that conifer trees covered approximately 1.4 million hectares (ha) of which almost half (682,100 ha) consisted of Sitka spruce and approximately 523,300 ha was in Scotland. Other notable conifer species in Britain are Scots pine (*Pinus sylvestris*) (241,000 ha), Larches (133,300 ha), lodgepole pine (*Pinus contorta*) (106,400 ha), Norway spruce (*Picea abies* [L.] Karst.) (61,600 ha), Corsican pine (*Pinus nigra*) (48600 ha) and Douglas fir (*Pseudotsuga menziesii*) (45,400 ha) with a further 39,400 ha made up of other conifers (Forestry Commission, 2011). Sitka spruce originates from the west coast of North America where it grows in a mild, moist climate. It was first introduced to the UK in the 19th century where it found the climate and conditions favourable. Following the setting up of the Forestry Commission after World War I, Sitka spruce quickly became popular as it not only out-grew the native UK conifer species Scots pine but also the European species Norway spruce and European larch (*Larix decidua*) (Cannell, 1984). The rotation time for Sitka spruce is approximately 40 years so trees being planted now will mature in the 2050s/2060s when the climate could be different from what it is currently (UKCP09, 2009a). This could have an impact on the quality and quantity of the wood being produced.

1.2 Climate

Tree growth is influenced by climate, site factors and competition in a complex way. Therefore in a given location the limiting factors may vary. The effects of climate change in UK are foreseen to influence tree growth (Read et al., 2009, Ray, 2008a, Ray, 2008c, Ray et al., 2008, Broadmeadow, 2002a). Alteration in growth is expected to have implications for timber properties as these are strongly linked (Makinen et al., 2007, Guilley et al., 2004, Berges et al., 2008). It has been predicted that rising CO₂ and increasing temperatures in the future will increase the average yield class of Sitka spruce from YC 14 to YC 16 (Ray et al., 2008). Since 1930s there has been an increase in General Yield Class (GYC), which in percent terms corresponds to 20-40 % increase (Cannell et al., 1998). Approximately half of this increase was thought to be due to combined effects of increases in N deposition, CO₂ and temperature (Cannell et al., 1998).

1.3 UK climate predictions

UKCP09 is the working name given to the UK Climate Projections website, user interface and reports which have been created, based on data from the Met Office, to help people who want to consider possible impacts of a changing climate (UKCP09, 2009b). It gives details on projected climate changes for the whole of the UK as well as on the level of administrative regions. It provides projections of changes in different climate variables for 30-year periods until the year 2099. These variables include projected changes in precipitation and temperature at yearly, seasonal or monthly timescales.

UKCP09 projections are based on Low, Medium or High greenhouse gas emission scenarios that in turn are based on the Special Report on Emissions Scenarios (SRE) from the Intergovernmental Panel on Climate Change, IPCC, (Nakicenovic and Swart, 2000). These scenarios take into account changes in global population, economy, amount of energy use, and type of energy use (e.g. the proportion from fossil fuels compared to nuclear). It also states that there is considerable uncertainty about future emissions, which has an effect on the uncertainty of predicting climate change. A recent study published in 2014 states that estimates for future warming using current climate models vary from approximately 1.5°C to 5°C if carbon dioxide concentration in the atmosphere is doubled (Sherwood et al., 2014). They were able to show that about half of the variance is due to differences in the feedback effect from clouds which changes as temperature rises and their observations implied a temperature rise of more than 3°C for a doubling of carbon dioxide concentration in the atmosphere.

UKCP09 provides predictions on different levels of certainty. For example a probability level of 10% means that there is a 10% chance that the change will be less than that predicted (i.e. unlikely to be less). A probability level of 90% yields a value where there is a 90% chance that the change will be less than that predicted (i.e. unlikely to be higher than). The 50% value presents the central estimate within the prediction range.

1.3.1 Climate Change to Date

As part of UKCP09 historical data was analysed and a report was published on the recent trends in UK climate (Jenkins et al., 2009b). Table 1-1 below shows a summary of the key findings with regards to recent changes in climate.

Table 1-1: Data taken from UKCP09 showing key finding in observed trends in climate in the recent past. © UK Climate Projections 2009 (Jenkins et al., 2009b).

Global average temperatures having risen by nearly 0.8 °C since the late 19th century, and rising at about 0.2 °C/decade over the past 25 years.
Central England Temperature has risen by about a degree Celsius since the 1970s, with 2006 being the warmest on record. It is likely (>66% probability, IPCC) that there has been a significant influence from human activity on the recent warming.
Temperatures in Scotland and Northern Ireland have risen by about 0.8 °C since about 1980, but this rise has not been attributed to specific causes.
Annual mean precipitation over England and Wales has not changed significantly since records began in 1766. Seasonal rainfall is highly variable, but appears to have decreased in summer and increased in winter, although with little change in the latter over the last 50 years.
All regions of the UK have experienced an increase over the past 45 years in the contribution to winter rainfall from heavy precipitation events; in summer all regions except NE England and N Scotland show decreases.
Severe windstorms around the UK have become more frequent in the past few decades, though not above that seen in the 1920s.
All regions of the UK have experienced an increase in average temperatures between 1961 and 2006 annually and for all seasons. Increases in annual average temperature are typically between 1.0 and 1.7 °C, tending to be largest in the south and east of England and smallest in Scotland.
The annual number of days with air frost has reduced in all regions of the UK between 1961 and 2006. There are now typically between 20 and 30 fewer days of air frost per year, compared to the 1960s, with the largest reductions in northern England and Scotland.
There has been a slight increase in average annual precipitation in all regions of the UK between 1961 and 2006, however this trend is only statistically significant above background natural variation in Scotland where an increase of around 20% has been observed.
There has been an increase in average winter precipitation in all regions of the UK between 1961 and 2006, however this trend is only statistically significant above background natural variation in Northern England and Scotland where increases of 30 to 65% have been experienced.
There has been a slight decrease in average summer precipitation in most regions of the UK between 1961 and 2006, however this trend is not statistically significant above background natural variation.
Average annual and seasonal relative humidity has decreased in all regions of the UK, except Northern Ireland, between 1961 and 2006, by up to 5%.
There are no statistically significant trends in the average number of rain days or mean sea level air pressure for any region of the UK between 1961 and 2006.

1.3.2 Climate Change in the Future

The UKCP09 user interface is a tool that allows predictions of projected future climate change using a number of scenarios, probability levels and climate variable as well as being able to split the UK into administrative regions. The tool produces output data based on the IPCC (Nakicenovic and Swart, 2000) low, medium or high emission scenarios.

Figure 1-1 to Figure 1-4 show the difference between the ranges for each of these scenarios for summer and winter temperature and precipitation in the UK as a whole with each figure showing the 10%, 50% and 90% probability level for each emission scenario, i.e. it is unlikely that any future change will be less than the 10% value and unlikely that it will be higher than the 90% value, with 50% being the central estimate.

The time periods shown represent a thirty-year average where the decade shown is the centre. For example 2020 is the decade centred on the period of 2010 to 2039, 2050 is the decade centred on the period of 2040 to 2069 and 2080 is the decade centred on the period of 2070 to 2099. The period from 1961 to 1990 was used by UKCP09 as the baseline period, with projections of changes reported relative to the average climate of this period.

1.3.3 Emission Scenarios

UKCP09 is based around three projected scenarios involving low, medium and high emission of greenhouse gases. It states that due to the uncertainty of future emissions, projections used should include all three scenarios. This section compares the difference in the projected change for both winter and summer temperature and precipitation for the UK as a whole.

Both summer and winter temperature are projected to rise no matter which emission scenario is used, with summer temperatures projected to rise by approximately 0.5 °C - 3°C by 2020 and between 1°C and 8°C by 2080 (Figure 1-1). Winter temperatures are projected to rise by between approximately 0.2 °C and 2.2°C by 2020 and between approximately 1°C and 4.7°C by 2080 (Figure 1-2).

The projected data for precipitation show that there is more uncertainty, especially with summer precipitation (Figure 1-3), where the output ranges from an increase of approximately 25% to a decrease of up to approximately 60%. Winter precipitation (Figure 1-4) is mostly projected to increase especially by the year 2080 but again there is a wide range in the projected change within each scenario. These graphs show that there is a general trend for decreased precipitation in the summer and increased precipitation in the winter.

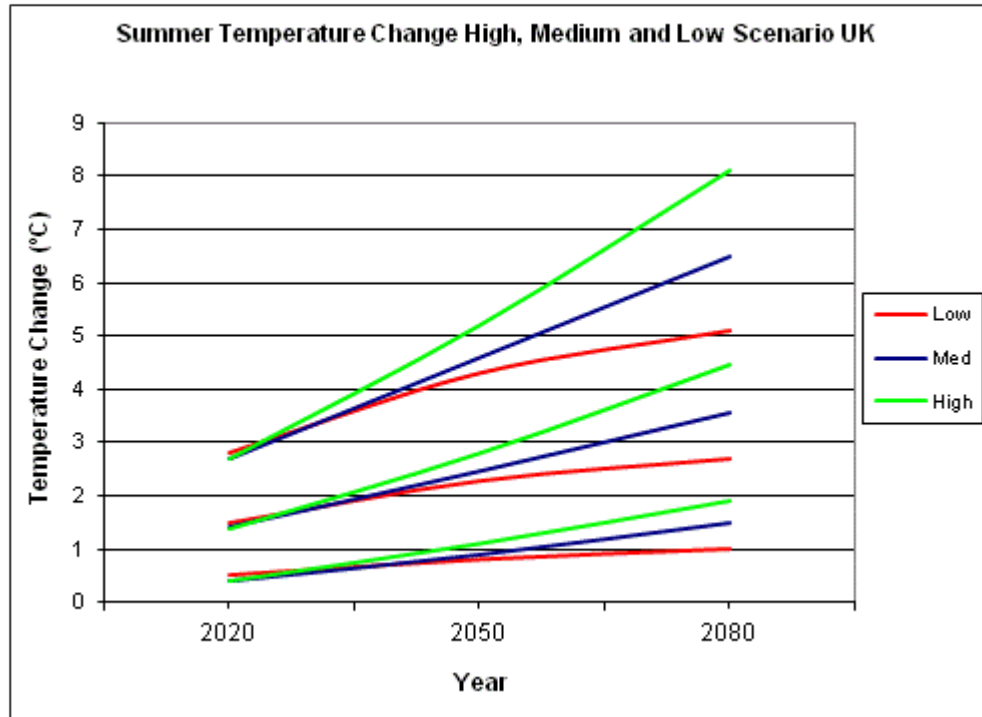


Figure 1-1: Predicted range of changes in summer temperature in the UK, using 10%, 50% and 90% probability levels for low, medium and high emission scenario. © UK Climate Projections 2009

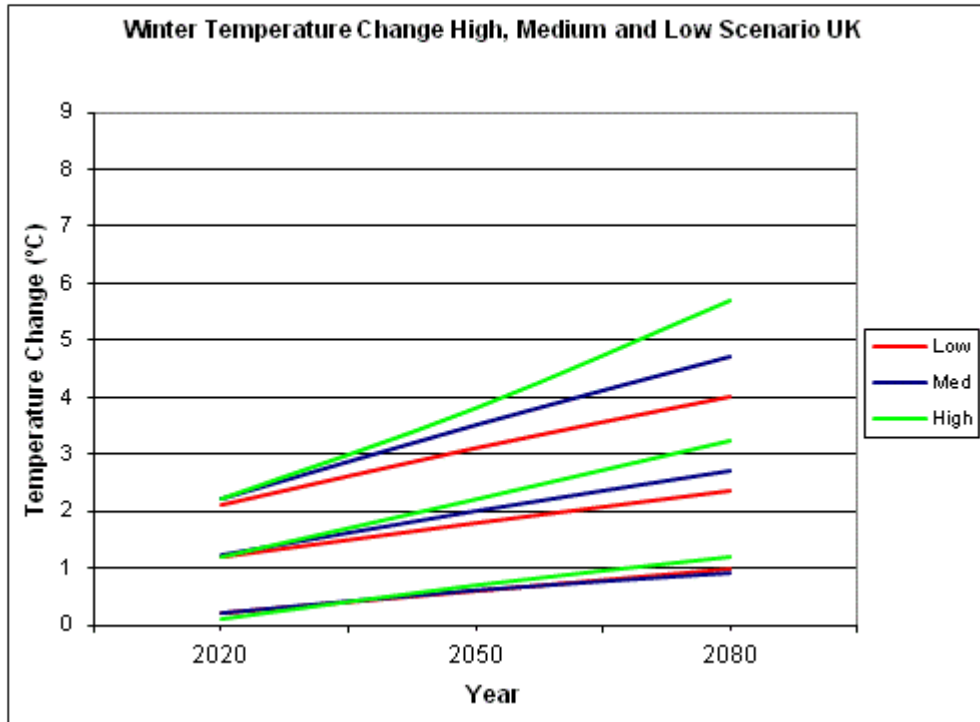


Figure 1-2: Predicted range of changes in winter temperature in the UK, using 10%, 50% and 90% probability levels for low, medium and high emission scenario. © UK Climate Projections 2009.

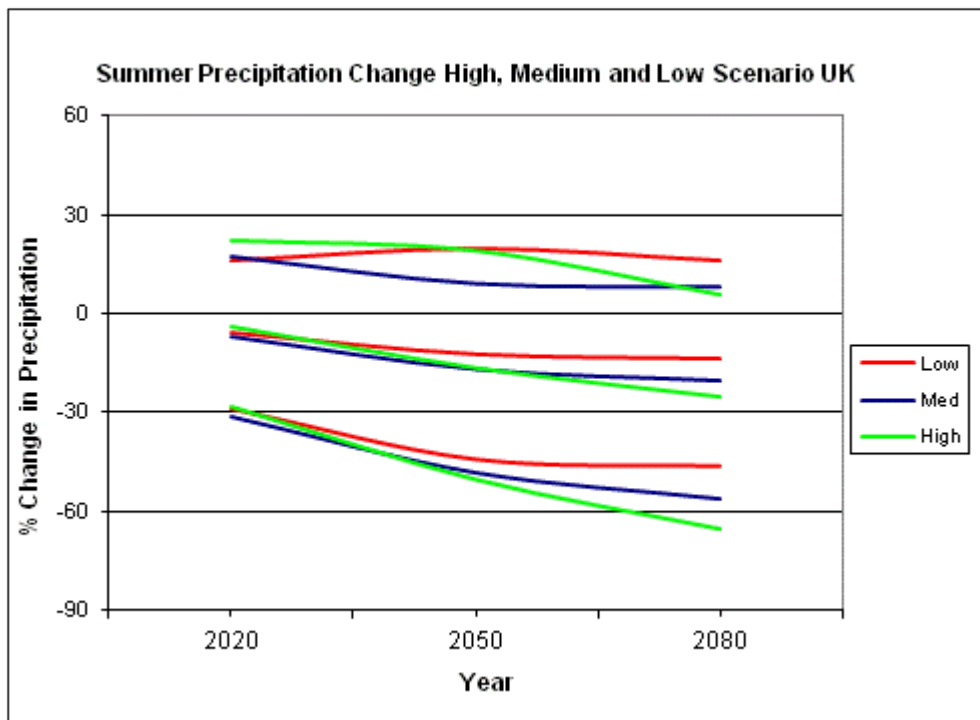


Figure 1-3: Predicted range of changes in summer precipitation in the UK, using 10%, 50% and 90% probability levels for low, medium and high emission scenario. © UK Climate Projections 2009

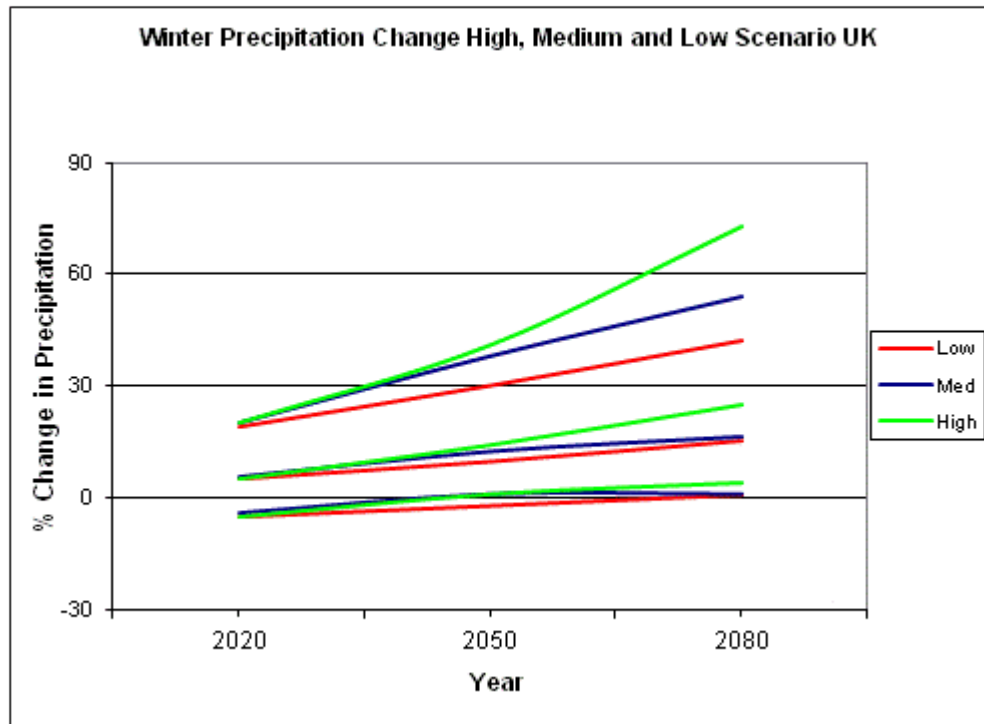


Figure 1-4: Predicted range of changes in winter precipitation in the UK, using 10%, 50% and 90% probability levels for low, medium and high emission scenario. © UK Climate Projections 2009

1.3.4 Temperature

Figure 1-1 to Figure 1-4 show that while there is uncertainty about future changes in climate due to the wide range shown within each emission scenario, there are similar trends under the different scenarios. To look at each area within the UK separately, the output for only the medium emission scenario is used in Table 1-2 to Table 1-5, to show the range of the projected change in climate broken down into different areas. These tables show that the projections for each region of the UK follow a similar pattern, with temperatures in all regions for all seasons projected to increase, although there is a slight north south difference.

As can be seen in Table 1-2 each region shows a similar range in the projected increase in summer temperature with the south of England showing the largest projected rise, and Northern Ireland showing the smallest rise. Whilst higher than the increases for Northern Ireland, the projected increases in temperature in Scotland are consistently lower than that of North England and Wales, which in turn are lower than that projected for South England. This pattern is repeated

in Table 1-3 and Table 1-4, which show the projected change in temperature for winter and spring respectively.

Table 1-2: Projected mean change in summer temperature for regions of the UK for the decades of the 2020's, 2050's and 2080's. Showing the range between 10% - unlikely to be lower than, to 90% - unlikely to be higher than, as well as the central estimate (50%). © UK Climate Projections 2009

Medium Scenario Change in mean summer temperature (°C)									
Region	2020			2050			2080		
	10%	50%	90%	10%	50%	90%	10%	50%	90%
UK	0.4	1.4	2.7	0.9	2.5	4.6	1.5	3.6	6.5
Scotland	0.5	1.3	2.4	0.9	2.2	3.9	1.5	3.3	5.7
North England	0.5	1.4	2.5	1.1	2.5	4.1	1.7	3.6	5.9
South England	0.5	1.5	2.7	1.2	2.6	4.6	1.8	3.8	6.5
Wales	0.5	1.4	2.5	1.2	2.5	4.1	1.9	3.5	5.8
Northern Ireland	0.4	1.3	2.2	1.0	2.2	3.5	1.7	3.2	5.0

Table 1-3: Projected mean change in winter temperature for regions of the UK for the decades of the 2020's, 2050's and 2080's. Showing the range between 10% - unlikely to be lower than, to 90% - unlikely to be higher than, as well as the central estimate (50%). © UK Climate Projections 2009

Medium Scenario Change in mean winter temperature (°C)									
Region	2020			2050			2080		
	10%	50%	90%	10%	50%	90%	10%	50%	90%
UK	0.2	1.2	2.2	0.6	2.0	3.5	0.9	2.7	4.7
Scotland	0.2	1.1	2.0	0.6	1.8	3.0	0.9	2.3	4.0
North England	0.5	1.2	2.1	1.1	2.0	3.4	1.4	2.7	4.6
South England	0.6	1.3	2.2	1.1	2.2	3.5	1.6	3.0	4.7
Wales	0.6	1.3	2.0	1.1	2.0	3.1	1.6	2.8	4.2
Northern Ireland	0.5	1.1	1.8	0.9	1.7	2.7	1.3	2.3	3.6

Table 1-4: Projected mean change in spring temperature for regions of the UK for the decades of the 2020's, 2050's and 2080's. Showing the range between 10% - unlikely to be lower than, to 90% - unlikely to be higher than, as well as the central estimate (50%). © UK Climate Projections 2009

Medium Scenario Change in mean spring temperature (°C)									
Region	2020			2050			2080		
	10%	50%	90%	10%	50%	90%	10%	50%	90%
UK	0.5	1.2	2.0	0.8	2.0	3.3	1.0	2.8	4.5
Scotland	0.5	1.2	1.9	0.8	1.8	3.2	1.0	2.5	4.4
North England	0.7	1.3	2.0	1.2	2.1	3.2	1.7	2.9	4.5
South England	0.7	1.3	1.9	1.2	2.1	3.3	1.8	3.0	4.5
Wales	0.7	1.2	1.9	1.2	2.0	3.1	1.8	2.9	4.4
Northern Ireland	0.7	1.2	1.7	1.2	1.9	2.9	1.8	2.8	4.1

As part of the Weather Generator report for UKCP09 (Jones et al., 2009) models were run to analyse statistically what might happen to certain variables in a particular climate across various locations (Figure 1-5) in the UK. Table 1-5 shows the results from this report for observed and future projected number of frost days using the medium emission scenario. As a control the number of frost

days was predicted for the period of 1961 to 1990 and this was compared to the mean observed data for the same period. The projections for the 2080s show that there are large decreases in the number of frost days across all of the UK with the greatest reductions in absolute terms being where the number of frost days is currently highest.

Table 1-5: Observed and modelled changes, for control period (1961-1990) and future period (2080), of number of frost days across various sites in the UK. © UK Climate Projections 2009.

	Observed	1961-1990			2080s Medium Scenario		
	50%	10%	50%	90%	10%	50%	90%
Heathrow	39	26	41	56	3	11	26
Yeovilton	54	30	44	59	3	12	27
Coltishall	49	33	49	65	3	13	29
Dale Fort	11	6	14	23	0	2	9
Ringway	43	31	44	60	4	13	28
Aldergrove	44	30	43	57	4	13	28
Eskdalemuir	94	80	98	115	16	38	64
Wick	52	33	47	62	6	18	35

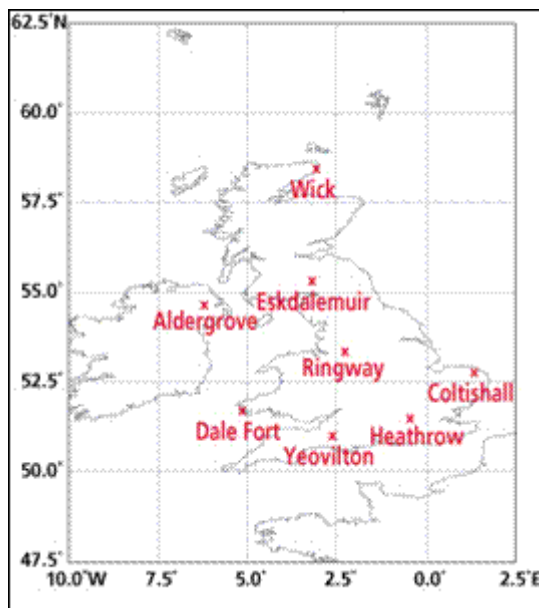


Figure 1-5: Locations of sites for Weather Generator projected change analysis. © UK Climate Projections 2009.

1.3.5 Precipitation

There was uncertainty about the changes in precipitation (Jones et al., 2009) with the projections ranging from a decrease in precipitation to an increase, for all seasons. The projected change in precipitation is shown as a percent change from the baseline so any change is relative to the amount of precipitation each

region currently receives. Although there is uncertainty within the wide range of projections, Table 1-6 shows that the projected change in summer precipitation is centred on a decrease in precipitation, with the range showing a downward trend over the periods shown. As with temperature, there seems to be a north - south difference in the projected change with the data showing that the projected change in summer precipitation is lowest in Scotland and highest in the south of England. Conversely, Table 1-7 shows that there is a projected increase in winter precipitation over the periods shown with the south of England again having the biggest change. The projected change in spring precipitation is less certain (Table 1-8) with the range neither showing a strong bias towards increasing or decreasing precipitation throughout all of the time periods.

Table 1-6: Projected mean change in summer precipitation for regions of the UK for the decades of the 2020's, 2050's and 2080's. Showing the range between 10% - unlikely to be lower than, to 90% - unlikely to be higher than, as well as the central estimate (50%).%. © UK Climate Projections 2009

Medium Scenario Change in mean summer precipitation (%)									
Region	2020			2050			2080		
	10%	50%	90%	10%	50%	90%	10%	50%	90%
UK	-31.0	-6.8	17.0	-48.0	-16.6	9.0	-56.0	-20.1	8.0
Scotland	-17.0	-5.3	7.0	-27.0	-12.3	2.0	-33.0	-15.0	4.0
North England	-24.0	-7.3	10.0	-36.0	-17.3	1.0	-44.0	-21.0	1.0
South England	-27.0	-7.2	14.0	-42.0	-18.0	7.0	-50.0	-21.8	7.0
Wales	-23.0	-7.0	11.0	-36.0	-17.0	6.0	-43.0	-20.0	5.0
Northern Ireland	-17.0	-5.0	7.0	-27.0	-13.0	3.0	-33.0	-15.0	3.0

Table 1-7: Projected mean change in winter precipitation for regions of the UK for the decades of the 2020's, 2050's and 2080's. Showing the range between 10% - unlikely to be lower than, to 90% - unlikely to be higher than, as well as the central estimate (50%).%. © UK Climate Projections 2009

Medium Scenario Change in mean winter precipitation (%)									
Region	2020			2050			2080		
	10%	50%	90%	10%	50%	90%	10%	50%	90%
UK	-4.0	5.7	20.0	1.0	13.4	38.0	1.0	18.0	54.0
Scotland	-2.0	5.7	16.0	1.0	12.7	29.0	1.0	16.7	42.0
North England	-4.0	4.7	14.0	1.0	11.7	26.0	2.0	15.0	34.0
South England	-4.0	5.8	20.0	2.0	14.8	38.0	3.0	20.0	54.0
Wales	-1.0	7.0	17.0	2.0	14.0	30.0	4.0	19.0	42.0
Northern Ireland	-2.0	4.0	10.0	2.0	9.0	19.0	2.0	11.0	24.0

Table 1-8: Projected mean change in spring precipitation for regions of the UK for the decades of the 2020's, 2050's and 2080's. Showing the range between 10% - unlikely to be lower than, to 90% - unlikely to be higher than, as well as the central estimate (50%).%. © UK Climate Projections 2009

Medium Scenario Change in mean spring precipitation (%)									
Region	2020			2050			2080		
	10%	50%	90%	10%	50%	90%	10%	50%	90%
UK	-8.5	1.0	10.1	-8.8	0.8	13.1	-8.4	1.9	14.6
Scotland	-4.8	2.1	9.9	-6.3	2.5	13.1	-8.4	2.5	14.6
North England	-7.1	1.1	9.1	-7.4	0.9	10.2	-6.7	1.7	9.9
South England	-7.3	0.4	8.7	-7.5	-0.1	7.9	-6.1	1.2	9.8
Wales	-6.3	0.1	6.9	-6.5	-0.5	5.9	-4.8	1.7	8.6
Northern Ireland	-4.1	1.7	7.8	-4.8	2.2	9.7	-3.2	2.9	9.4

1.3.6 Thermal Growing Season

In 2002 a set of climate change scenarios were released under UKCIP02 (Hulme et al., 2002) which has now been superseded by the projections made in UKCP09. The study in 2002 did, however, use observed data to report on changes to the length of the thermal growing season that have happened in the recent past and also attempted to give projections on changes in the future. They described the thermal growing season as:

“The longest period within a year that satisfies the twin requirements of: (i) beginning at the start of a period when daily-average temperature is greater than 5.5°C for five consecutive days; and (ii) ending on the day prior to the first subsequent period when daily-average temperature is less than 5.5°C for five consecutive days” (Hulme et al., 2002).

This therefore is only dependant on temperature and does not take into account water availability or day length. The report concluded that the thermal growing season in Central England had increased by about one month during the 20th century. This had taken place in two phases; 1920 to 1960 there was an average of 0.7 days increase per year due to both an earlier onset of spring and later onset of winter; and in 1980 to 2000 which had an average increase of 1.7 days per year, mostly attributed to an earlier onset of spring (Hulme et al., 2002). Using models they projected that by the year 2080 the length of the thermal growing season in Scotland could have increased by 20-60 days and in England by 40-100 days. They also projected that by 2080 the south of England may experience years with year round thermal growing seasons.

1.3.7 Storminess

Projections made by running models for UKCIP02 suggested that winter depressions would become more frequent due to the depression tracks moving further south (but reversed in summer when there would be less depressions). It also suggested that the North Atlantic Oscillation (NAO) would become more positive which would result into wetter, windier, but milder winters (Hulme et al., 2002). This differs from the models for UKCP09 which project that while the storm tracks will move south, this will occur south west of the UK and hence have little effect on the frequency and intensity of storms in the UK (Murphy et al., 2009b).

Due to these discrepancies and the differences between individual models run for UKCP09 and the observed data, there is a great deal of uncertainty about future projections on storms and robust projections were not currently possible (Jenkins et al., 2009a). Similarly, model projections for anticyclones, which are often associated with low wind and clear skies, do not give clear results of a particular direction of change (Jenkins et al., 2009a).

1.3.8 Windiness

There were attempts made in UKCIP02 to try and model projected changes in wind and while results were obtained it was also stated that due to lack of consistency between different models the authors were unable to give any level of confidence to the results and they should only be used with extreme caution (Hulme et al., 2002).

UKCP09 did not attempt to project changes to wind speed, as this was not available from the multi-model system used for the other variables such as temperature and precipitation. When different models were compared there was a great deal of variation in the projected changes to wind with little evidence of a systematic change (Murphy et al., 2009b). A separate study was done to evaluate alternative sources to model changes in wind, which reported that the most suitable data may be obtained from “*an 11-member ensemble of variants of the Met Office regional climate model*” (Brown et al., 2009).

1.4 Relationship between climate and tree growth

When no other factors are limiting, in a temperate climate, tree growth usually responds positively to an increase in temperature. However, if summer temperatures increase, the rate of evaporation and transpiration will also increase, which in turn will decrease the amount of water available to plants at a time when the requirement for water is increasing. In areas where summer rainfall is forecast to decrease drought conditions may result and this can damage trees either directly or by making them more at risk from diseases (Green and Ray, 2009). In eastern Scotland, where there are soils with poor water holding capacity, the conditions may become unfavourable to drought sensitive species such as Sitka spruce (Ray, 2008a).

Any increase in the frequency of extreme winds may also lead to more damage (Ray, 2008a, Broadmeadow, 2002a). However, since the trees are thought to be better anchored in the autumn rather than after repeated wind exposure in late winter the timing of the occurrence of the high winds is important (Broadmeadow, 2002a). In Scandinavia, milder conditions during the winter might make trees more susceptible to windthrow during winter and spring as they lose additional support provided by frozen ground (Peltola et al., 1999) and a study in Finland suggested the risk of trees being uprooted is increased by strong winds occurring during times when the soil is unfrozen (Vitasse et al., 2011). The climate predictions discussed in this section did not include wind but generally extreme weather events are expected to increase in frequency (Broadmeadow, 2002a). Large parts of the Sitka spruce plantations in the UK are located in the Scottish highlands where strong winds are common and plantations on higher ground are already subjected to windthrow, so if strong winds become more common the problems are likely to increase both in frequency and in severity. Wind could influence timber properties in less extreme events as well, by inducing compression wood formation.

Using a process model analysis of Sitka spruce grown at different UK sites Waring (2000) concluded that whilst poor soil nutrition was an issue in limiting growth at several sites, drought and vapour pressure deficit were not imposing major limitations to growth. However, variation in solar radiation was found to be the most influential factor governing growth. An earlier study by Ford et al. (1978)

also found a significant positive correlation between earlywood cell production and daily solar radiation. However, it has also been reported that Sitka spruce is very sensitive to vapour pressure deficit and may close its stomata even before soil water availability becomes limiting (Read et al., 2009). According to Jarvis et al. (1983) in Sitka spruce the net photosynthesis is only reduced by vapour pressure deficit after 1.2 kPa. Drought conditions may alter the allocation patterns with more carbon used for root growth which can affect the stem wood production (Jarvis et al., 1983).

Care has to be taken when investigating the effect of site factors on tree growth as a number of factors can interact to give a different effect. For example both elevation and latitude are correlated with factors which affect tree growth such as accumulated temperature and rainfall, and so the relationship between yield class and elevation of Sitka spruce in Britain is not constant and varies between different meteorological regions (Mayhead, 1973). Investigating the effect of site factors on dynamic modulus of elasticity (MOE) of standing Sitka spruce trees Moore et al. (2009a) found a negative relationship with elevation and with latitude, but no effect of accumulated temperature or soil moisture, which may have been due to the relatively limited range in the study. A study into the effect of Norway spruce growing at an altitude of 580m and 1260m in Austria found that timber grown at lower elevation had thicker cell walls and wider growth rings (Gindl et al., 2001). Rossi et al. (2007) investigated growth of different species of conifers (Norway spruce, larch and Stone pine (*Pinus pinea*)) at high altitudes and found that xylogenesis occurred for all three species only when air temperatures reached 5.6 to 8.5°C suggesting that temperature at high altitude limits growth. Low temperatures were found to be the limiting factor at high altitude sites and more northern sites in a study on Norway spruce in Finland, while precipitation was important at more southern and lower altitude sites (Makinen et al., 2002). General Yield Class (GYC) has been found to decrease with elevation at the rate of 3.2-4.0 m³ ha⁻¹ yr⁻¹ per 100 m and at the same time productivity was found to be highly correlated with temperature and windiness (Worrell and Malcolm, 1990a). Proe et al. (1996) predicted that GYC would increase by 2.8 m³ ha⁻¹ yr⁻¹ for each degree of rise in temperature if the increase was uniform over the year. However, if greater warming took place during the winter months, the growth increase would only amount to 2.4 m³ ha⁻¹

yr⁻¹ due to a negative correlation between winter temperature and growth rate (Proe et al., 1996). Allison et al. (1994) analysed the distribution of yield classes across Scotland and reported that an increase in summer rainfall would have a positive influence on the GYC unless it was accompanied with a decrease in temperature, and that high winter temperatures had a negative effect. They concluded that GYC estimates were more sensitive to temperature than rainfall. No effect of increased temperature was detected on radial growth in a whole tree chamber experiment on Norway spruce in Sweden (Kostiainen et al., 2009), but they found that elevated temperature led to an increase in earlywood cell wall thickness and wood density and also observed an increasing trend in microfibril angle under elevated temperature, although this was not found to be statistically significant (Kostiainen et al., 2009). Larger earlywood cells were found in Norway spruce from a cool-humid site in Germany compared with trees from warm-dry site which had a higher number of latewood cells and thicker cell walls (Park and Spiecker, 2005).

An increase in mean temperature could potentially increase the length of growing season in Britain; however, there is evidence that Sitka spruce has a high chilling requirement which may negate the effect of any increase in temperature. Sitka requires 140 days at temperatures less than 5°C during the winter preceding the growing season in order to fulfil the chilling requirement (Cannell and Smith, 1983, Murray et al., 1989). When this requirement was met, growth would start when the lowest temperature sum was reached, but when chilling requirement was only partially fulfilled a higher temperature sum was required for bud burst (Cannell and Smith, 1983). In Britain, these conditions may currently only be met at high altitude and during particularly cold winters. Due to the high chilling requirement increased temperature might only shift bud burst a few days earlier or might even lead to a delay in bud burst (Cannell and Smith, 1986). This would protect Sitka against spring frosts but it also means that Sitka would not benefit from any increase in the length of the growing season (Murray et al., 1989). Among provenances of Sitka spruce that all come from fairly maritime climates, the southern origins flushed early and all Island provenances (except one from Prince of Wales Island) flushed later (Burley, 1966).

A study investigating the effect of a changing climate on Cajander larch (*Larix cajanderi* Mayr) and Scots Pine found that over the past 120 years the date when mean daily temperature rises above 0°C has moved approximately 10 days earlier and the onset of growth in both species has moved by a similar amount (Nikolaev et al., 2011). However this study was of trees growing in Eastern Siberia where winter temperatures are colder for a longer period than in Great Britain and so any winter chilling requirement was easily met. Using microcores taken from different provenances of Norway spruce in a trial in southern Finland (Kalliokoski et al., 2012) found that while there were large differences between the onset of tracheid formation between years there was no significant difference between the provenances. The thermal growing season is widely accepted as when temperatures are above a 5°C threshold (Sarvas, 1972), but Kalliokoski et al. (2012) found that mean air temperatures had been above 5°C for a number of weeks before tracheid formation begun, although cambial activity was detected earlier. The same study found that highest tracheid formation rates were around the time of the summer solstice, coinciding with the period of highest temperatures and that a mid-summer drought slowed down and stopped tracheid formation earlier compared with years where there was no drought. There was no difference found in cessation date between the provenances (Kalliokoski et al., 2012). Investigating Black spruce (*Picea mariana* (Mill.) BSP) at two locations in Quebec, Canada, Lupi et al. (2010) found no causal link between the onset and cessation of xylem formation. They found that cambial reactivation in spring was influenced by temperature, but also that growth did not start until snow had melted and the soil had thawed which occurred at different times between the two sites investigated. Strimbeck and Kjellsen (2010) investigated the hypothesis that single freezing events late in the growing season can be the trigger by which Norway spruce trees begin the process of acclimatising to low temperature. However, no effect was found and even after repeated and prolonged freezing events there were no consistent effects. They suggested that for this species decreasing day length or temperature was the driver for low temperature acclimation.

Macdonald (1979) recommended that in areas of Southern Scotland where annual rainfall is less than 900 mm Sitka spruce should not be planted. However, annual total is not always sufficient guidance for suitability in the future since

sites with impeded drainage are more vulnerable to the forecasted wet winters and dry summers regime (Hendry, 2009). Currently drought may cause cracking and ring shake in Sitka spruce mainly in eastern Scotland but in the future the risk area may spread to southern Scotland as well (Ray et al., 2008). The sites types predisposing Sitka to drought cracking vary geographically. In the east cracking typically occurs at sites with impeded drainage where under normal conditions water is present in surface layers of the soil and the rooting depth is restricted (Hendry, 2009). In the west cracking occurs in freely draining soils where prolonged drought leads to drying of the entire soil profile (Hendry, 2009). Vigorously growing trees that have high water demand and produce low density earlywood are particularly susceptible (Brazier, 1970). Cherubini et al. (1997) studied drought cracks in Norway spruce in the Italian Alps. They concluded that the drought cracks had been formed when the cambium had been inactive because there was no increase in the frequency of traumatic resin canals connected with the cracks. They postulated that transpiration losses combined with inadequate water supply from very cold roots in the spring caused the cracking. In contrast Grabner et al. (2006) concluded on Larch that the drought cracks are usually initiated during the growing season but typically occur in rings formed 1 to 2 years earlier since newly tracheids in the newly formed ring tend to be more elastic and hence protected against cracking. Larch, as a deciduous species, is not subjected to spring transpiration losses and the cracking in older rings would explain the absence of traumatic resin channels (Grabner et al., 2006).

In Deeside in eastern Scotland a drought in 2003 caused on average approximately 20% mortality in 420 studied trees across 3 sites (Hendry, 2009, Green et al., 2008), but within these sites there were areas where the mortality locally reached 60-70%. Green et al. (2008) investigated damage in Sitka spruce after the drought year, 2003, and concluded that all the lesions occurred after the end of the 2003 growing season. Traumatic resin canals were observed around the entire circumference of the 2004 tree ring. These resin canals had formed early in the season 2004 and in some cases they were still formed in 2005. Xylem cells in these damaged rings contained almost solely latewood type cells with thickened walls and very small lumens (Green et al., 2008).

In Norway spruce growing in France it was observed that wood density was strongly positively correlated with soil water deficit, which the authors attributed to reduction in tracheid enlargement (Bouriaud et al., 2005). Therefore in less extreme conditions decreased water availability might increase density; as the ring width of Sitka increases this mainly occurs as an increase in earlywood width and hence leads to larger earlywood proportion and lower density (Brazier, 1970). Aakala and Kuuluvainen (2011) also found a relationship between radial growth and moisture deficit during the summer in Norway spruce in northwest Russia, with periods of low soil moisture having a negative impact on growth. Comparing properties of Norway spruce rings with climate in Germany, Wimmer and Grabner (2000), found that ring width had no relationship with monthly climate but latewood density and maximum density were highly correlated with temperature and precipitation.

In a study investigating the effect of temperature on latewood formation in Momi fir (*Abies firma*) in its native Japan, Begum et al. (2012) found that artificially heating the stems could induce growth. Stopping the artificial heat led to a rapid decrease in temperature which resulted in cells being produced which had latewood characteristics, i.e. smaller diameter with thicker walls. Investigating the relationship between cell characteristics and climate in both black spruce and balsam fir (*Abies balsamea*) in Canada, Krause et al. (2010) found that temperature was an important factor on the cell size of earlywood, with less effect on latewood. However in this part of Canada temperatures during the earlywood phase can still be cold and often below 0°C, whereas during the latewood phase (August-September) temperatures are generally warmer with less freezing events.

In an experiment in Canada on Black spruce Lupi et al. (2012) found that artificially heating the soil had no effect on xylem production and concluded that air temperature was the limiting factor for the formation of wood. However a study on Scots pine growing in southern Finland found that air temperature was the limiting factor in autumn, winter and early spring but that soil temperature was the limiting factor in late spring (Wu et al., 2012), especially during warm springs where low soil temperature could affect moisture availability.

In northern Arizona Kerhoulas and Kane (2012) investigated the effect of climate on wood properties at different heights in the stem of Ponderosa pine (*Pinus ponderosa* Dougl.) and found that correlations between climate and radial growth increased with height suggesting that higher positions in the tree are more sensitive to stresses caused by climate.

Studies into growth and the effect that climate has on it have often been focussed on dominant trees as this minimizes any effect that competition from larger trees may have. However, forests are made up of dominant, co-dominant and sub-dominant trees and how these different groups react to climate is important as the dominant trees may not be fully representative of the site. By splitting trees within a stand into different size classes, Merian and Lebourgeois (2011) studied the effect of climate and size on tree growth at sites throughout France. They found that there was no difference in the sensitivity to either temperature or water availability between the size classes for species which are shade intolerant or moderately shade tolerant, such as Norway spruce, Scots pine and Sessile oak (*Quercus petraea* Liebl.). However, larger trees of shade tolerant species such as silver fir (*Abies alba*) and European beech (*Fagus sylvatica*) were more sensitive to drought during the summer than smaller trees. From this they recommended that to study the relationship between growth and climate it would be sufficient to sample only the larger trees of species which are shade intolerant or moderately shade tolerant, whereas sampling of only larger trees of shade tolerant species could result in the sensitivity to climate being over estimated (Merian and Lebourgeois, 2011). Sitka spruce is described as a moderately shade tolerant species which is able to grow in partial shade (Cannell, 1984). Conversely, a study in Germany into the response to summer drought by trees of different sizes found that larger Norway spruce trees were limited more by hot dry summers than smaller trees (Zang et al., 2012). In contrast they found that smaller Scots Pine trees were more limited by high temperatures and low moisture than larger trees. Similarly, in Spain growth of dominant Aleppo pine (*Pinus halepensis*) trees showed less sensitivity to environmental conditions than suppressed trees with lack of precipitation being the biggest influence in line with other Mediterranean species (Olivar et al., 2012)

Due to its high chilling requirement Sitka spruce of the provenances currently planted may fail to benefit from earlier onset of growth (Cannell and Smith, 1983, Cannell and Smith, 1986). However, in terms of growth rate Sitka will benefit from higher temperatures during the growing season, which has been forecast to increase the GYC from 16 to 18 (Ray et al., 2008). Faster growth may be accompanied with reduction in density (Brazier, 1970, Makinen et al., 2007). Any increase in windiness (Broadmeadow, 2002a) may particularly influence Sitka spruce as large areas in the exposed areas on Scottish Highlands have been planted with Sitka spruce (Worrell and Malcolm, 1990b). Also increasing vapour pressure deficit may influence growth of Sitka spruce (Read et al., 2009) and drought cracking may increase in drier areas.

1.4.1 Management

Silviculture practices are well known to have an impact on Sitka spruce growth, with factors such as initial spacing and thinning having major effects. A recent review summarized the effects that these factors can have on tree growth and wood properties (MacDonald and Hubert, 2002). A recent study has found that the initial spacing at which a Sitka spruce site is planted can have an effect on the spiral grain angle, which can lead to increased distortion in the wood produced (Fonweban et al., 2013). This study found that sites planted at wider spacings as well as those which had received heavy thinning or are exposed to strong winds can increase the grain angle significantly. They recommended that closer spacing, delayed or less thinning and planting on less exposed sites may help to reduce spiral grain.

Thinning is also a forest management tool that can have an impact on growth and quality. A 2002 review into the practice in Britain suggested that a decline in selective thinning may have had an impact on the quality of logs in recent years (Cameron, 2002). More recently there has been a trend to move towards continuous cover forests which would have more irregular and diverse structures and this would have an impact on the quality of the wood produced (MacDonald et al., 2010).

By heavily thinning a Norway spruce forest in Belgium Herman et al. (1998) showed that increasing the radial growth rate by 1.7 to 2.7 cm per year had a

limited negative effect on density. Similarly, again in Belgium, Dutilleul et al. (1998), investigating whether thinning affected the correlation between ring width and density, found that when the growth rate of Norway spruce was more than 2.2 cm per year the negative correlation between ring width and density disappeared. Sohn et al. (2012) investigated the impact of drought on growth under different thinning regimes and at different heights in the stem. They found that the response to drought was similar at different heights in trees that had been heavily thinned but was different in trees that had only been moderately thinned. They also found that moderately thinned trees were more sensitive to variations in climate and took longer to recover after drought events than trees on heavily thinned sites. This may be due to the increased competition for both sunlight and moisture.

A recent study into the effect of rotation length on wood properties found that longer rotation lengths could result in timber with improved properties since timber taken from the outer section of the tree had higher stiffness and bending strength than that near the pith (Moore et al., 2012) however they also point out that longer rotation lengths can increase the risk of windthrow and may not be of economic benefit.

1.4.2 Provenance

Growth and the quality of the wood produced depend on how well trees are adapted to their local environmental conditions, and trees originating from different provenances can react in different ways. Originating from the west coast of North America, when Sitka spruce seeds were brought to Britain in the 1920s at the start of the period of widespread afforestation, the seed was from the Queen Charlotte Islands, which by chance rather than design had a very similar climate to upland western Britain, and so seed of this provenance was well suited to grow here (Cannell, 1984). Since the last ice age Sitka spruce has expanded its range (Mimura and Aitken, 2010) running south to north along a narrow band of the east coast of North America. This almost linear range makes it an ideal species in which to study the change in genetic structure and different phenotypic traits among populations and to understand how it has adapted to local changes in the environment. Mimura and Aitken (2007) observed large differences in the way populations have adapted to environmental

conditions along this distribution. For example, they found that while southern populations grew taller, those from the north grew faster per day, which seems to be a strategy adapted to a shorter growing season. Investigating the genetic structure, the same study suggested that there was a large amount of adaptive divergence amongst all populations and that the local adaptation can occur over just a few generations (Mimura and Aitken, 2007). A more recent study found that Sitka spruce has adapted locally throughout its natural range in response to the current local climate conditions (Mimura and Aitken, 2010). Whilst they found differences within populations, bud break was earlier in southern populations and was later with progress north, due to differences in heat sum accumulation. Conversely bud set occurred earlier in northern populations and later in the southern ones, leading to a shorter growing period for more northern trees (Mimura and Aitken, 2010). Holliday et al. (2010) were able to study the phenotype and genotype on the same range of trees and found 28 candidate genes which explained 28% of the variance in cold hardiness and 34% of the variation in bud set, among which were 5 genes involved in the pathway regulating the end of growth in autumn.

Since a changing climate is likely to have some impact on other plantation tree species, recent studies in Europe have also been carried out investigating the effect of climate on different provenances of species such as Norway spruce (Kapeller et al., 2012) and Scots pine (Taeger et al., 2013). Selecting the right provenance for the right environment may become important in the future with any change in climate. Both of these studies found that the response to climate was different between provenances. Norway spruce populations from areas in Austria which are currently warm and dry were seen as being already better adapted to these conditions, and so may be better suited elsewhere if conditions are to get drier and warmer (Kapeller et al., 2012). Similarly, in Germany differences were found between provenances of Scots pine in their response and recovery to drought conditions. Choosing these provenances for future forests may help if, as projected in that area, the climate were to get warmer and drier (Taeger et al., 2013). McLane et al. (2011) investigated the climate effect on different provenances of lodgepole pine growing in western Canada. They found that in general growth was positively correlated with temperature and negatively with moisture deficit, although this differed between the different

provenances. The biggest effects were seen in trees from populations originating from warmer provenances growing in colder sites, and vice versa. This indicates that sensitivity to climate can be genetically controlled and that the provenance of the trees is important when planting them elsewhere. Using trees grown in a trial in Kershope Forest in northern England, McLean (2008) investigated the variation in wood properties between three selectively bred progeny of Sitka spruce and compared this to control trees of a Queen Charlotte Island (QCI) seed origin. The QCI control was found to have significantly higher stiffness than the other genotypes and while in general it seemed to have higher density, this was not significant. The same study found a relationship between density and growth though suggested that this relationship may be different between the progeny.

1.5 Aims

The overall aim of this study is to predict the future impacts of climate change on growth and timber quality of Sitka spruce. This was approached in two ways; Firstly using data collected as part of a resource evaluation study which looked at the broad geographic variation in wood properties spanning the full latitudinal range of Britain and secondly through dendrometer experiments where the variation was coming from year-to-year changes in weather.

One of the aims of the resource evaluation study is to explore a number of new and existing models which describe radial growth and wood density in Sitka spruce and to examine the linkage between these two parameters. Using a more complete dataset than has hitherto been available, this study aims to investigate which empirical models best describe radial growth with age as well as the radial profile of ring density, to examine whether these parameters can be modelled using a segmented linear approach, and to compare this approach to other empirical models describing the radial profile of growth with age within the sampled trees. These models were then used to investigate differences in growth rate and wood density due to altitude, latitude and longitude, which all can be linked to climate, and due to management effects such as initial spacing.

A further aim of the resource evaluation study is to investigate a method of measuring the radial profile of longitudinal stiffness directly on 12mm increment cores using acoustic velocity, by making use of a purpose built acoustic scanner

at The University of Canterbury, Christchurch, New Zealand, and to model the pith to bark radial profile.

This study also aims to investigate seasonal variation in tree growth and to examine how climate effects such as temperature and soil moisture influence the growth of Sitka spruce. By using LVDT point dendrometers to record changes in the radius of the tree stem, growth was investigated at two Sitka spruce plantation sites; at Griffin Forest near Aberfeldy where measurements were initiated in 2008 as part of a long term project and continued as part of this study, and at a newly established at Harwood Forest in Northumberland, northern England. The dendrometer data were compared to meteorological data collected from the site and from local weather stations, to determine how weather affected the growth of the trees.

2 Variation in Wood Properties

In order to investigate the national range of variation in wood properties such as radial growth, radial density and the radial profiles of longitudinal stiffness, samples were collected from a number of sites throughout Great Britain. This section describes the method of collecting and preparing the samples which were used for this analysis.

2.1 Resource Evaluation Study

The “Benchmarking Study” was a resource evaluation survey started in 2006, and led by John Moore of Napier University, in collaboration with Forest Research and the University of Glasgow, to look at the variation in wood properties of Sitka spruce (specifically bending strength, stem straightness and form, stiffness and density) and to try to identify the site and stand factors which could be the source of this variation (Moore et al., 2009a). The initial study investigated 64 sites across Scotland and in Northern England which were selected on the basis of yield class (i.e. productivity), elevation, latitude, longitude, initial spacing and thinning history. A portable acoustic tool was used to measure modulus of elasticity (MOE), i.e. stiffness on standing trees and sample cores were taken for detailed analysis. Data from this study have been published by Moore et al. (2009a) and also looked at in further detail by Vihermaa (2010) as part of a Ph.D. thesis. Moore et al. (2009a) found that 55% of the variation in standing-tree MOE was due to differences between individual trees within a site and 36% was due to differences between sites, with elevation and yield class being the most important site factors for MOE.

The sample cores were analysed by Vihermaa (2010), with the aim of using the tree ring data to carry out climatic analysis; however, due to problems with the sampling technique (the outer rings were often missing or damaged) accurate dating and ring identification was not always possible. The analysis was able to show a negative correlation between ring width and density, which was stronger in mature wood than juvenile wood showing that an increase in growth is often accompanied by a reduction in density in Sitka spruce.

2.2 Extension of Resource Evaluation Study

The study by Moore et al. (2009a) did not find a significant relationship between latitude and stiffness whereas previous studies had found a relationship between latitude and density (Bryan and Pearson, 1955). Stiffness and density are not always linked, but this observation was explained by the relatively small range in latitude covered in the study. To determine if latitude does have an effect on wood properties, a wider range of latitude would have to be covered, such as sites in northern Scotland, Wales, and southwest of England. Also, the study by Vihermaa (2010) was unable to come to any conclusions regarding the variation in density due to the problems encountered with the samples.

The objectives of this study were to examine radial density, the radial variation in longitudinal stiffness and detailed radial growth by extending the evaluation study to cover areas of Scotland, England and Wales which were not included in the original survey. It is hoped that this 'Benchmarking Extension' study will give further information on the variation in wood properties covering the whole latitudinal range of Sitka spruce in Great Britain. At the same time it would also provide valuable information on how growth and wood properties could change in a changing climate, by the detailed analysis of cores for density, ring width and stiffness considered alongside with the varying climatic data covering the whole latitudinal range of the UK.

2.2.1 Extension Sites

Table 2-1: Details of the sites sampled in the extension of the resource evaluation study

Site	Region	Elevation (m)	Yield Class	Spacing (m)	Age (Years)	Easting	Northing
4301	England (NE)	196	14	2.0	35	488364	852801
7643	England (NE)	240	16	2.0	36	488167	494894
9004	England (NE)	350	12	2.0	41	461550	499113
9008	England (NE)	340	16	1.7	44	461860	499401
2013	England (NW)	320	22	1.7	38	320670	524315
2042	England (NW)	280	12	2.0	47	318585	524934
2304	England (NW)	200	14	1.7	45	316766	531911
86	England (NW)	250	22	1.7	43	374912	458152
FERN	England (SW)	425	18	2.0	40	266004	082670
5234	England (SW)	225	12	2.0	41	322227	133764
EXM7	England (SW)	183	18	2.0	41	269680	133212
QUA6	England (SW)	285	14	2.0	40	316574	135751
2723	Mid Wales	495	14	1.8	43	278407	259628
3237	Mid Wales	467.5	18	2.0	39	274058	255893
1390	N Wales	337.4	18	2.0	43	284047	230734
1600	N Wales	278	20	2.0	45	285688	329686
303	N Wales	411	14	2.0	43	300342	352019
54	N Wales	291	10	2.0	40	273287	329315
2142	S Wales	484.3	10	1.7	43	290043	198669
2185	S Wales	280.7	16	2.0	39	280759	188300
2436	S Wales	484.3	14	1.7	45	283204	208079
2559	S Wales	102	24	2.0	41	247662	229775
2789	S Wales	190.5	14	2.0	40	272116	224383
2191	S Wales	312.4	18	2.0	40	298434	191990
461	Kintyre	78	14	2.0	47	172576	651283
6619	Kintyre	191	12	2.0	46	175038	666632
6630	Kintyre	137	18	2.4	40	172430	613881
6874	Kintyre	278	16	1.9	40	171198	615589
278	Sutherland	99	18	2.4	49	256817	902996
279	Sutherland	155	14	1.8	48	257262	914870
280	Sutherland	155	12	2.5	36	252241	923791
281	Sutherland	139	20	2.0	39	268494	936248

In the original study there were a number of areas of Scotland that did not get covered; these included Northern Scotland, and the Kintyre peninsula. As part of the extension to the study four sites each on the Kintyre peninsula and in Sutherland were sampled during spring 2010 by Napier University. Sample cores were collected and passed to Glasgow University to be analysed as part of the current study. A further 12 sites were selected in Wales and 12 in England and these were visited during the summer and autumn of 2011 (Table 2-1).

Table 2-2: Sites from the original study chosen to be analysed as part of this study

Site	Region	Elevation (m)	Yield Class	Spacing (m)	Age (Years)	Easting	Northing
226	NE England	232	14	1.6	36	373769	583997
64	NE England	316	16	2.5	40	365546	577797
155	SE Scotland	300	18	2.5	35	346800	656100
243	SE Scotland	225	16	1.8	37	372359	614649
23	SW Scotland	344	14	1.8	39	251212	595342
55	SW Scotland	142	22	2.5	37	229592	551367
63	SW Scotland	151	12	2.0	37	229701	568442
72	SW Scotland	156	14	1.8	45	245997	570481
80	SW Scotland	125	18	2.1	45	237781	578876
5565	NC Scotland	338	20	1.8	43	294407	754285
5945	NC Scotland	410	14	2.0	40	309477	753584
1211	NE Scotland	444	12	1.5	45	342422	831547
1251	NE Scotland	394	12	1.6	45	337580	807464
3323	NE Scotland	290	10	2.0	46	370839	785121
339	NE Scotland	356	18	2.0	37	353213	810020

As well as the 32 sites selected for the extension study, for the purposes of measuring wood properties a selection of 15 sites were chosen from the original study which would give further coverage of areas within the UK such as North East Scotland, South West Scotland, South East Scotland and North East England. These sites are detailed in Table 2-2 and the location of all the sites used in this study can be seen in Figure 2-1 along with the location of the sites used in the original study.

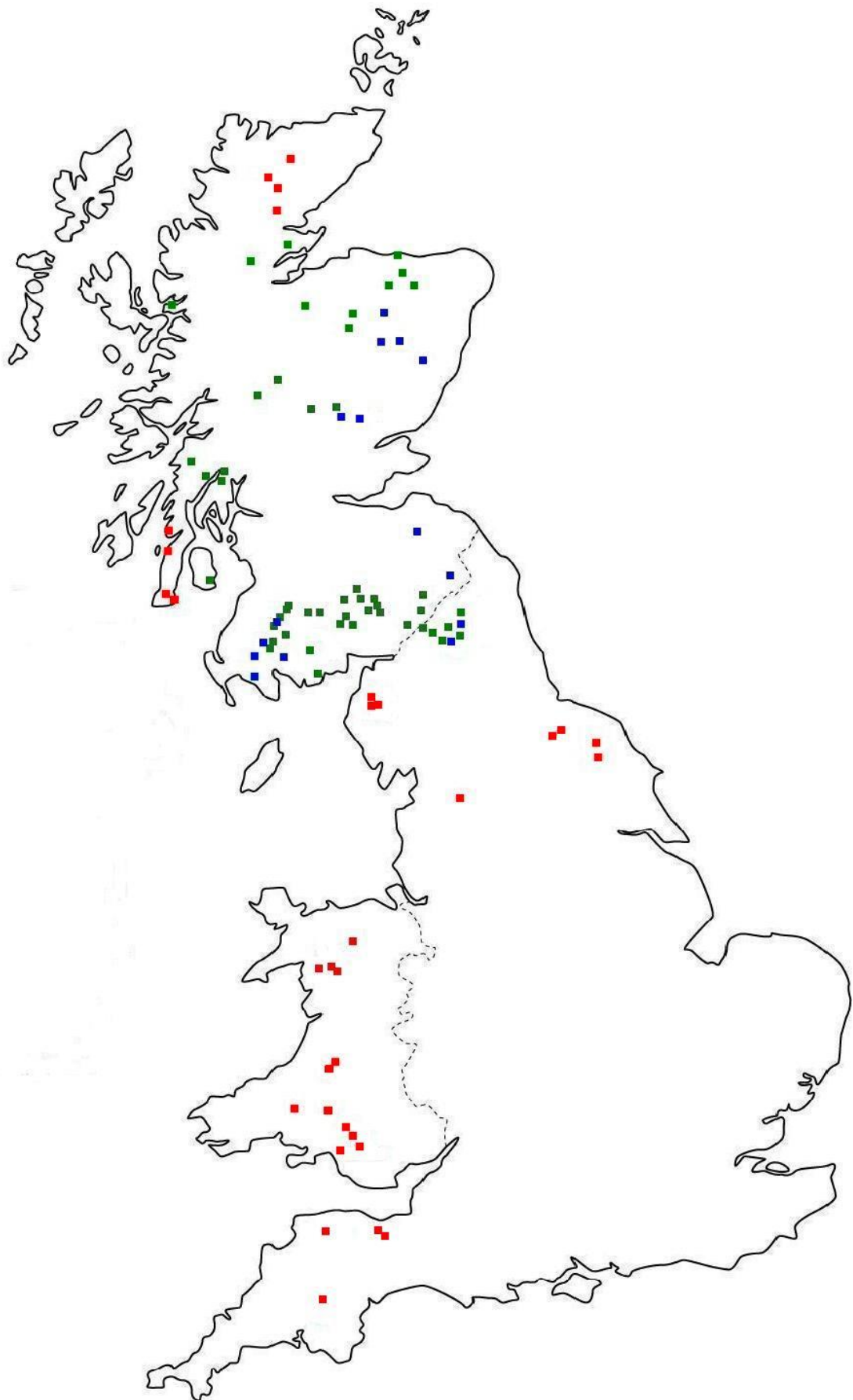


Figure 2-1: Location of the sites sampled in the extension study (red) and the original study (green). The sites from the original study which were used to examine wood properties in the current study are shown in blue.

2.3 Method

2.3.1 Site Selection

The sites chosen for this study were selected at random from a list of suitable sites, from the Forestry Commission's sub-compartment database, which were close to felling age of around 35 to 45 years old. In order to get a representative sample three factors were used (Yield Class, Elevation and Latitude) and these were divided into low or high level. The combinations of these can be classified into 8 categories in a factorial design with three conditions and two levels as shown in Table 2-3.

Table 2-3: Conditions and levels of the experimental factorial design

Factor	Low Level	High Level
Yield Class	<=14	>14
Elevation	<=280	>280
Latitude	>300	<=300

The combination category of the chosen sites along with the level of each condition is shown in Table 2-4 along with the site location.

Table 2-4: Combination class for each site, listed by region, along with the experimental design conditions.

Combination	Latitude	Yield Class	Elevation	Wales	England (SW)	England (NW)	England (NE)	Scotland
1	HIGH	LOW	LOW	54	-	2304	4301	279 280 6619 461
2	HIGH	LOW	HIGH	303	-	2042	9004	-
3	HIGH	HIGH	LOW	1600	-	86	7643	278 281 6630 6874
4	HIGH	HIGH	HIGH	1390	-	2013	9008	-
5	LOW	LOW	LOW	2436 2789	5234	-	-	-
6	LOW	LOW	HIGH	2142 2723	5223	-	-	-
7	LOW	HIGH	LOW	2185 2559	4117	-	-	-
8	LOW	HIGH	HIGH	2191 3237	8027	-	-	-

As part of the desk study, once the sites had been selected a 0.2 hectare (ha) plot within each site was randomly selected from Forestry Commission maps using GPS co-ordinates avoiding features such as streams and rock formations.

2.3.2 Field Work

At each site a circular sample plot of 0.02 ha (radius 8 metres) was set up in accordance with the pre-determined GPS location again avoiding features such as forest edges, streams and other geological features which may not have been seen on a map when determining the GPS location. The trees within the plot were assessed for stem straightness and stem form (which included other physical attributes such as forks, ramicorn branches, broken tops and stem scarring) using a scoring system described by MacDonald et al. (2000). The height of ten trees within the site was measured using a Vertex III Hypsometer and Transponder T3 (Haglöf Sweden AB) to give an average height for the plot. The diameter at breast height (DBH) of every tree over 7 cm diameter within the plot was measured. DBH is a measure of tree size and to standardize it across different sites the measurement is taken around the trunk at a height of 1.3

metres in accordance with Forestry Commission standard operating procedure SOP 094.

At each site ten experimental trees were randomly selected using randomly generated number sequences and tested for Modulus of Elasticity (MOE) on both the north and south side of each standing tree using the portable IML Electronic Hammer, (Instrumenta Mechanik Labor GmbH) which measures the velocity of a stress wave between two probes inserted into the tree at a vertical distance of 1 metre and centred on breast height.

The output from the standing tree acoustic measurements along with the site measurements of stem straightness and form were published as part of an internal report for the Strategic Integrated Research in Timber group (SIRT) and Forest Research (McLean, 2012).

Using a Tanaka TED-250RS, (Tanaka Kogyo Co., Ltd.) increment corer (Figure 2-2) 12 mm increment cores (Figure 2-3) were taken bark to bark, as near as possible through the pith at breast height starting from the north side each of the ten experimental trees. The 10 cores from each site were taken to the University of Glasgow and the bark to pith section of the northern part of the core were analysed for ring width and density as part of this study. Starting the coring from the north side of the tree and analysing the northern part of the core solved the problem of missing outer rings and bark encountered by Vihermaa (2010). A quirk of using the increment corer meant that the bark on the side of the tree where the corer entered (north side) was left intact and in good condition. However when the corer was pushed through the tree and exited on the south side, often the bark and some wood would become detached from the core and remain attached to the tree. Visually it was impossible to tell how many rings were lost from the core. Unlike Vihermaa (2010) who analysed the south section of the cores, with missing bark, this study analysed the northern section where the bark was still intact.



Figure 2-2: Taking a 12mm increment core from a tree in Site 303 on North Wales using a Tanaka increment corer.



Figure 2-3: 12 mm increment core taken at site 303 in North Wales. A standard sized pen is added for scale.

2.3.3 Density and Ring Width Analysis

2.3.3.1 Preparation of Sample strips

The ITRAX requires the samples to be in the form of thin (approx 2mm) radial strips. To prepare the cores for analysis, they were first glued on to pre-prepared sections of MDF board; care was taken to ensure that the core samples were glued to the MDF board with the grain running horizontal (Figure 2-4). This is to ensure that the grain is perpendicular to the direction of the saw as

density measurements are made on the ITRAX in the same direction as the grain. The consequences of misalignment were explored by Vihermaa (2010). The purpose of the MDF board is to be able to clamp the sample in place during milling without damaging the sample (Figure 2-5). The sample was then milled to 2mm thick strips taken in the radial direction along the centre of the core (Figure 2-6 and Figure 2-7).

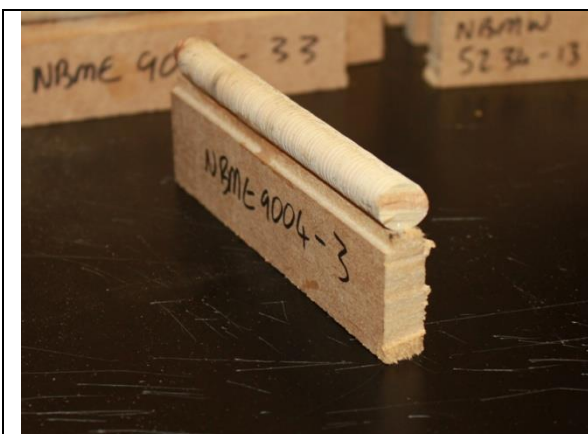


Figure 2-4: Sample core glued to an MDF holder.

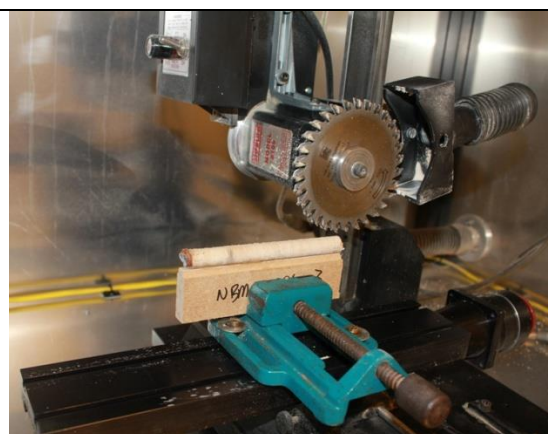


Figure 2-5: MDF and core clamped in position in the mill.



Figure 2-6: The sample core after milling with the 2 mm strip along the centre of the core.

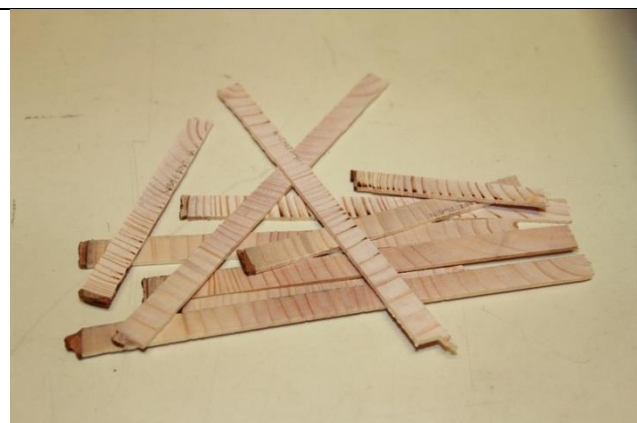


Figure 2-7: Sample strips ready for analysis on the ITRAX.

2.3.3.2 Analysis of Samples Using the ITRAX Densitometer

The sample strips were analysed for density and ring width by x-ray densitometry using an ITRAX Density Scanner built by Cox Analytical System, Gothenburg which uses a Cu source to produce an x-ray beam which is focussed,

using a slit system, to 22 mm wide and 25 μm high. The optimal settings used for the analysis for these type of samples has previously been developed by (McLean, 2008) and subsequently used by (Vihermaa, 2010): 10 mA, 20kV, 40 second exposure time and a step size of 50 μm and run alongside a Walesch Electronics cellulose propionate calibration wedge of known density.

A digital micrometer (Powerfix Profi Digital Caliper) was used to measure the thickness of the strips, to 0.001 mm, at four points along the strip and averaged to give a value that is input as the sample thickness when analysing the images using Windendro to calculate density (Section 2.3.3.3). The strips were fixed to mounting needles using double sided sticky tape along one edge and then mounted onto the movable rack within the ITRAX densitometer ready for analysis (Figure 2-8). Each run of samples on the Itrax also included a cellulose propionate calibration wedge (Section 2.3.3.3).

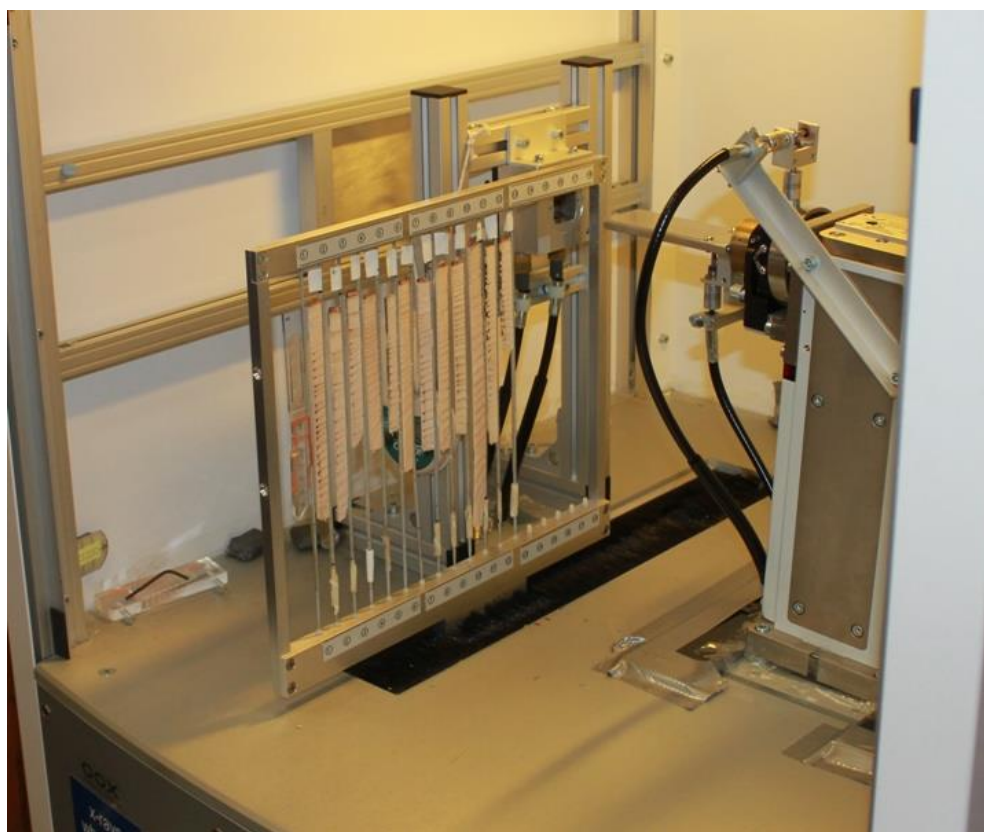


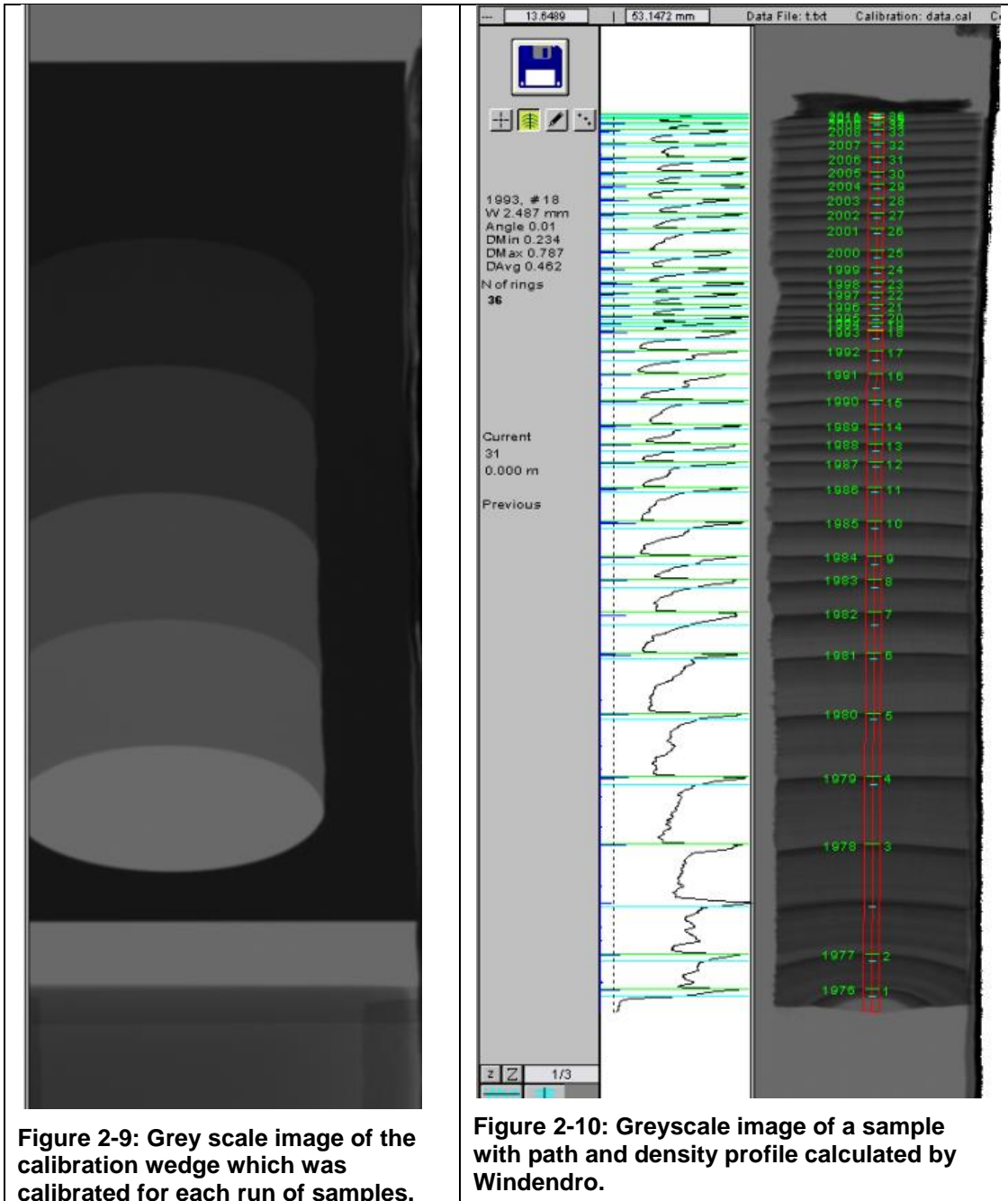
Figure 2-8: Sample strips in position in the ITRAX densitometer

It is known that extractives can influence density and some species such as Scots pine have to have these extracted before they can be analysed by densitometry (McLean, 2008). However, Sitka spruce has a low extractives content (<2%) (Caron-Decloquement, 2010) therefore extraction of these prior to analysis was deemed unnecessary.

Wood density can be affected by moisture content and so humidity within the ITRAX instrument should be kept to below 30% (Bergsten et al., 2001) and here was kept between 5% and 15%. Vihermaa, 2010 found that while humidity had an effect on density at 28% it had little effect below 15% and below this gave a sample moisture content of 4%. The ITRAX chamber was brought to 15% relative humidity by pumping in dry air using a Jun Air 2000 compressor which had been dried using an attached Dominick Hunter CO₂ R280 drier unit. The sample strips were placed within the conditioned ITRAX chamber and allowed to stabilise for 24 hours before starting the scan.

2.3.3.3 Windendro

Grey scale images are produced by the ITRAX densitometer and these were analysed using Windendro software, produced by Regent Instruments Quebec, in which the shades of grey from light to dark correspond to increasing levels of density. Calibration was carried out for each sample run using a stepped calibration wedge made of cellulose propionate, manufactured by Walesch Electronics. The thickness of each step of this calibration wedge is input by the operator and thickness of the wedge is divided by the density of the wedge (1.240 g cm^{-3}), by the software, to produce a density value in per mm of thickness along with the corresponding grey scale image (Figure 2-9). The software relates the grey scale image of the samples to density by measuring the grey scale image of the calibration wedge of known thickness. The calibration was done for each run of samples on the ITRAX. The Windendro software allows a path to be drawn onto the sample image (Figure 2-10) in which it calculates the corresponding density value for each pixel along the path which is then divided by the thickness of the sample strip as input by the operator to give a radiographic density profile.



There are differences in the way that different materials absorb x-rays therefore a conversion has to be made to correct the density measured by the ITRAX (the radiographic density described above) in kg m^{-3} to gravimetric density (oven dry wood density) also in kg m^{-3} . The process for this correction was discussed by both (McLean, 2008) and (Vihermaa, 2010) and similar values were derived empirically by both with slight differences seen due to moisture content during the scans. Since the method used in this study was based on that described by Vihermaa, 2010 the conversion factor used in this study was also that derived by Vihermaa, 2010, and was of the form:

$$\rho_{\text{wood}} = 0.7739 * \rho_{\text{rad}} + 40.9949$$

Where ρ_{wood} is the gravimetric density of the wood in kg m^{-3} and ρ_{rad} is the radiographic density as measured by the ITRAX also in kg m^{-3}

Windendro identifies the ring boundaries by variation in the intensity of the grey scale. In this experiment to ensure that a representative sample of the density was taken, three paths of 2 mm width were drawn with the average taken of the resulting output. An example of the ring width and density output from Windendro is shown in Figure 2-11. Here the ring width and the radiographic density are plotted alongside the ITRAX grey scale image of the corresponding sample. Windendro also calculates an average ring density value as well as supplying output values for earlywood width, latewood width, early and latewood width percentage, earlywood density, latewood density, maximum density and minimum density. Within this study the boundary between early wood and latewood was defined as 50% of the maximum density value.

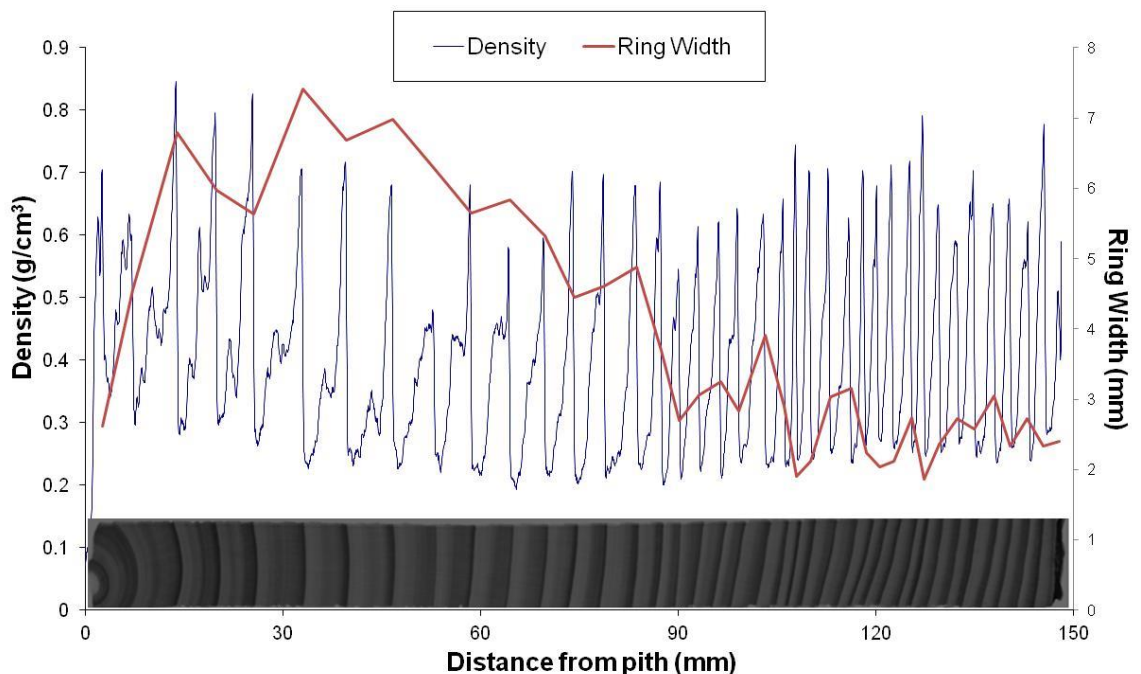


Figure 2-11: The grey scale image of sample 2723-31 along with the corresponding density and ring width output calculated using Windendro

2.4 Climate Data

2.4.1 Weather Station Data

The Weather station data used in this study was from the UK Meteorological Office downloaded from the “Met Office Integrated Data Archive System (MIDAS) Land and Marine Surface Stations Data (1853-current)” database obtained from the British Atmospheric Data Centre (BADC) website which is the Natural Environment Research Council's (NERC) Designated Data Centre for the Atmospheric Sciences (UK Meteorological Office, 2012). The data were obtained from the weather station positioned closest to the Griffin site (Aberfeldy, Dull) using the ordnance survey grid references as a guide.

2.4.2 Ecological Site Classification

The Ecological Site Classification (ESC) is a tool developed by Forest Research and described in Forestry Commission Bulletin 124 by (Pyatt et al., 2001) which allows the user to get climate and soil data for sites by inputting a six figure Ordnance Survey grid reference (i.e. 100m resolution). Climate data for ESC was obtained from the UK Meteorological Office and is based on climate recorded during the period of 1961 to 1990. The purpose of this tool is to help forest practitioners in make planning decisions regarding planting of tree species in specific locations such that the species could cope with the location's climate and soils. This system is based around two soil properties (soil moisture regime - SMR and soil nutrient regime - SNR) and four main climatic variables: Accumulated temperature which describes the warmth of a site and is measured in day degrees above 5⁰C; Moisture deficit describes the dryness of a site with higher values indicating drier sites and considers potential precipitation and evaporation; DAMS (Detailed Aspect of Scoring) looks at the exposure of a site and is a measure of windiness with higher scores being more exposed; Continentality is a score given to a site which is a measure of the climatic seasonal variability based on distance from the sea along with northing and easting (oceanic climates which have precipitation evenly spread throughout the year, have low continentality scores).

Plotting the sites used in this study against the climate variables in ESC shows some interesting patterns of climate variation in Britain and shows how there are

numerous interactions which can govern the climate of each site. That is, accumulated temperature, measuring the number of day degrees above 5°C, decreases with increasing latitude (Figure 2-12), and although not significant there may be a slight tendency to decrease with increasing longitude (Figure 2-13) and decreases with increasing altitude (Figure 2-14). The same pattern is seen for rainfall with latitude and longitude (i.e. decreases northwards and eastwards). Moisture deficit which links potential evaporation and rainfall during the growing season decreases with altitude higher sites are generally wetter. Even though rainfall decreases in these directions increasing moisture deficit may be due to lower evaporation due to lower temperatures. Rainfall decreases in an eastwardly direction showing that more eastwardly sites are generally drier.

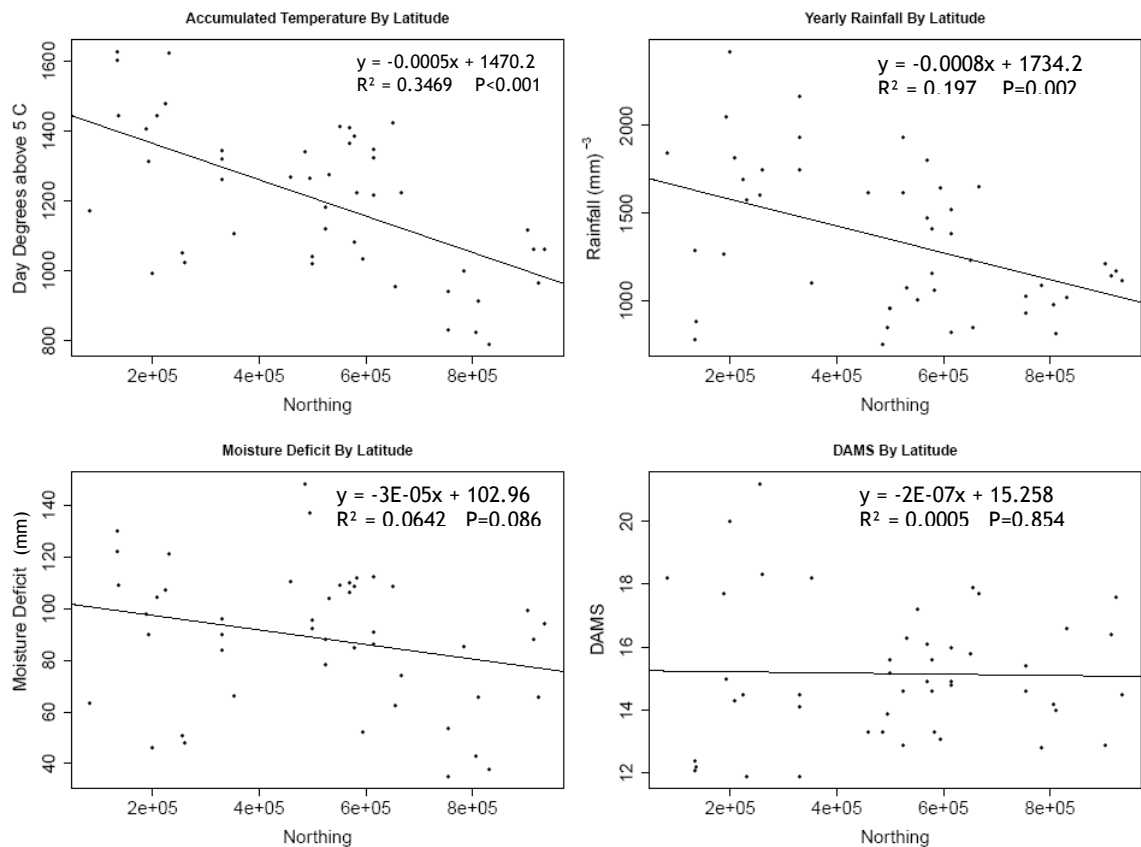


Figure 2-12: Accumulated temperature, rainfall, moisture deficit and DAMS score from ESC plotted against latitude shown as an OS grid reference and fitted with a linear trendline.

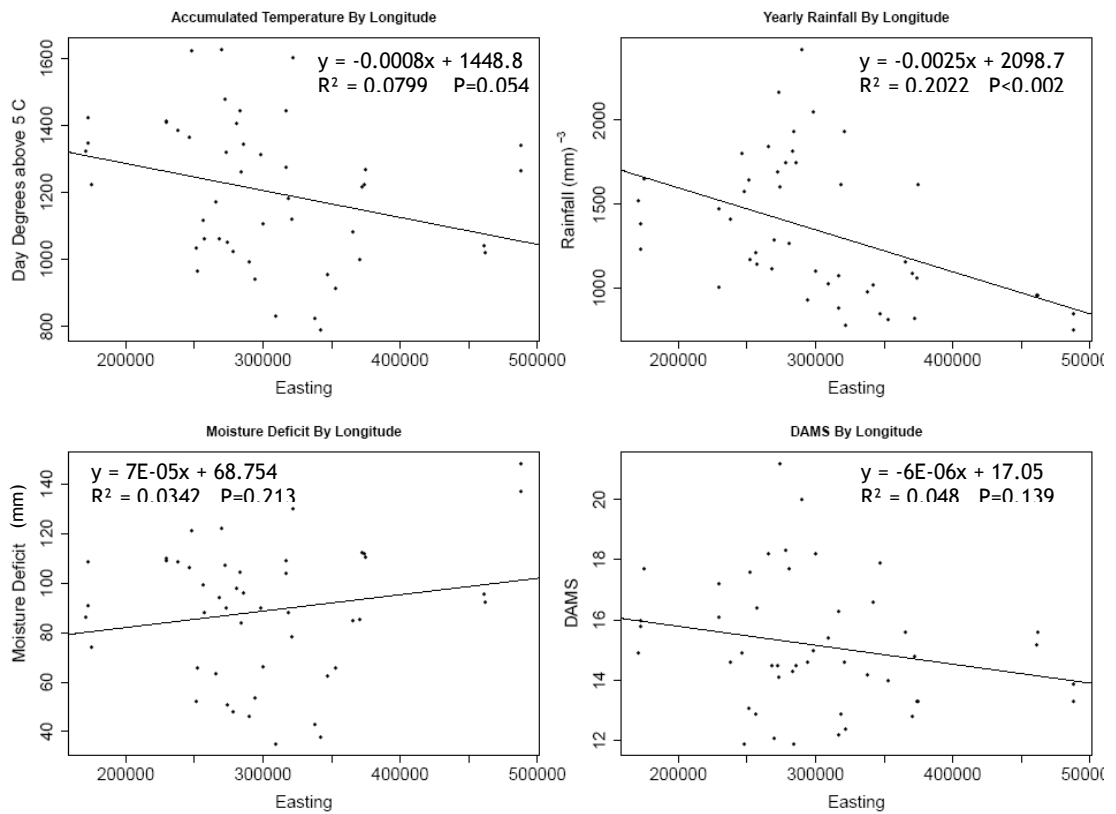


Figure 2-13: Accumulated temperature, rainfall, moisture deficit and DAMS score from ESC plotted against longitude shown as an OS grid reference and fitted with a linear trendline.

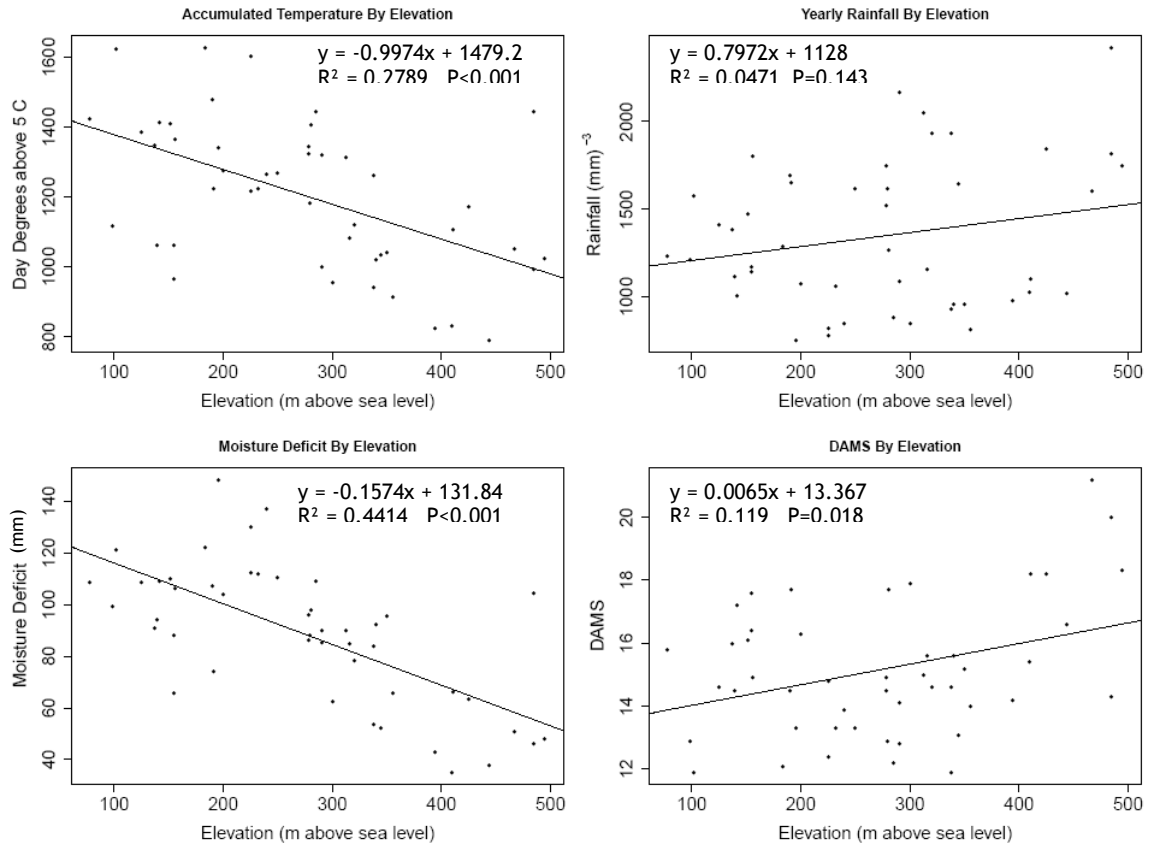


Figure 2-14: Accumulated temperature, rainfall, moisture deficit and DAMS score from ESC plotted against elevation shown as an OS grid reference and fitted with a linear trendline.

Continentality is a score given which measures how evenly precipitation is distributed throughout the year where sites with low continentality values have more evenly distributed rainfall than high score sites. Figure 2-15 shows that more southern and eastern sites have higher continentality scores meaning that they have less evenly distributed rainfall throughout the year i.e. colder, wetter winters and warmer, drier summers.

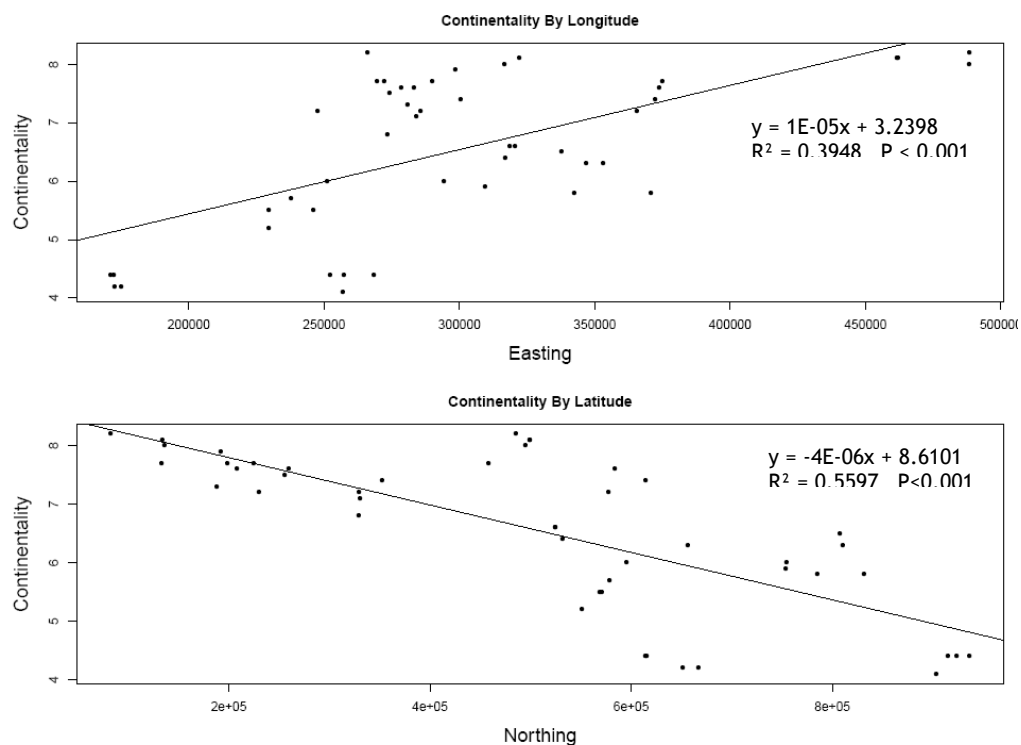


Figure 2-15: Continentality of sites from ESC plotted by longitude and latitude fitted with a linear trendline.

The ESC tool is also able to be used to generate future accumulated temperature and moisture deficit predictions based around the climate scenarios (UKCP09, 2009a), described in Chapter 1. Using the “Low Scenario” Figure 2-16 shows the current accumulated temperature compared with that predicted in 50 and 80 years. In most cases accumulated temperatures are predicted to rise with sites in the north of Scotland getting close to those currently being experienced by sites in southern England and Wales. Whilst the difference in moisture deficit (Figure 2-17) between now and what is predicted in 50 and 80 years looks more variable than accumulated temperature there does seem to be an effect whereby the more westerly sites are predicted to get wetter (lower moisture deficit) while those in the east are predicted to get drier (higher moisture deficit)

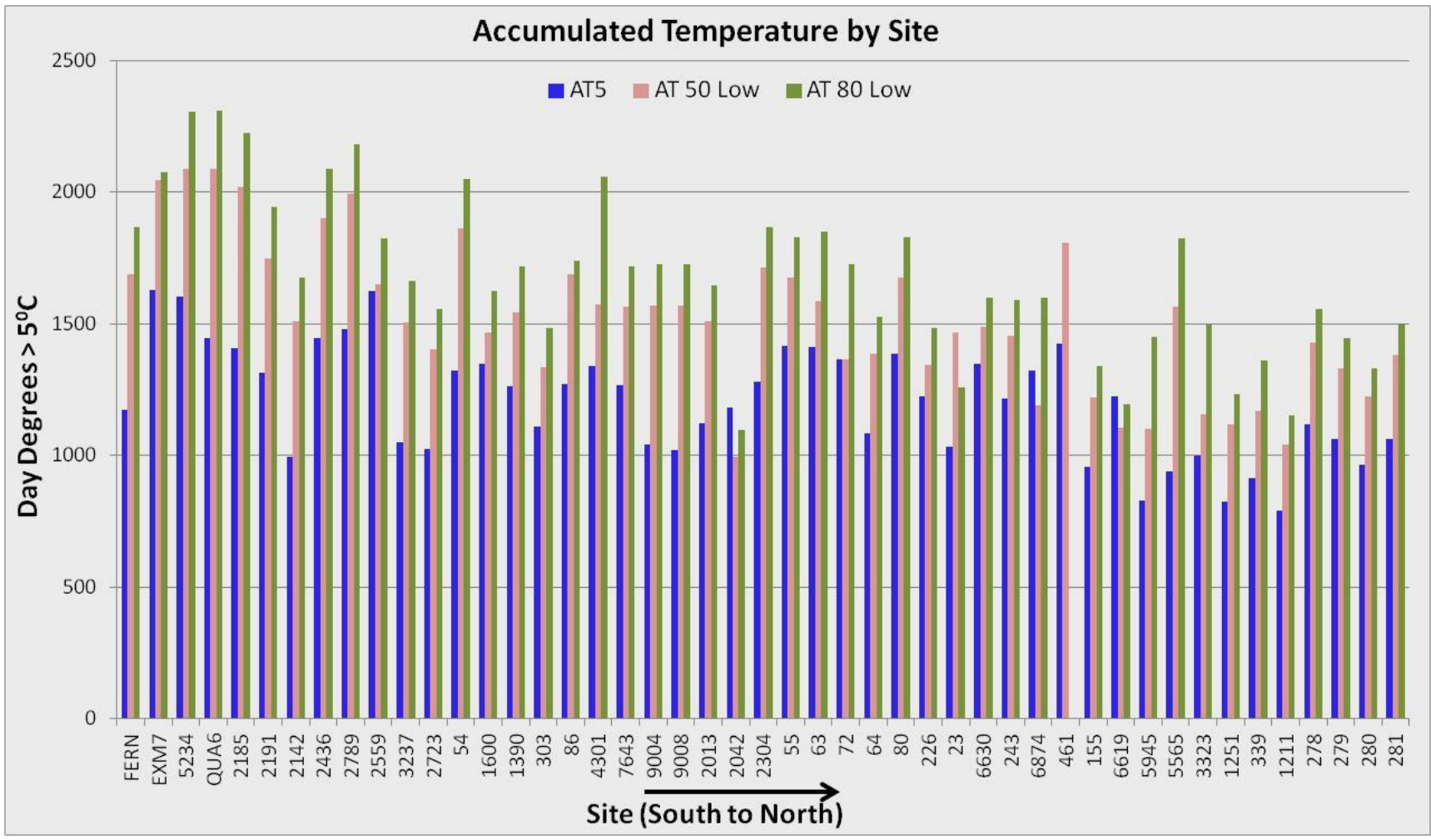


Figure 2-16: ESC data on current accumulated temperature, along with the accumulated temperature predicted by the low scenario after 50 and 80 years of UKCP09 (2009a) for the sites used within this study to measure ring growth and ring density.

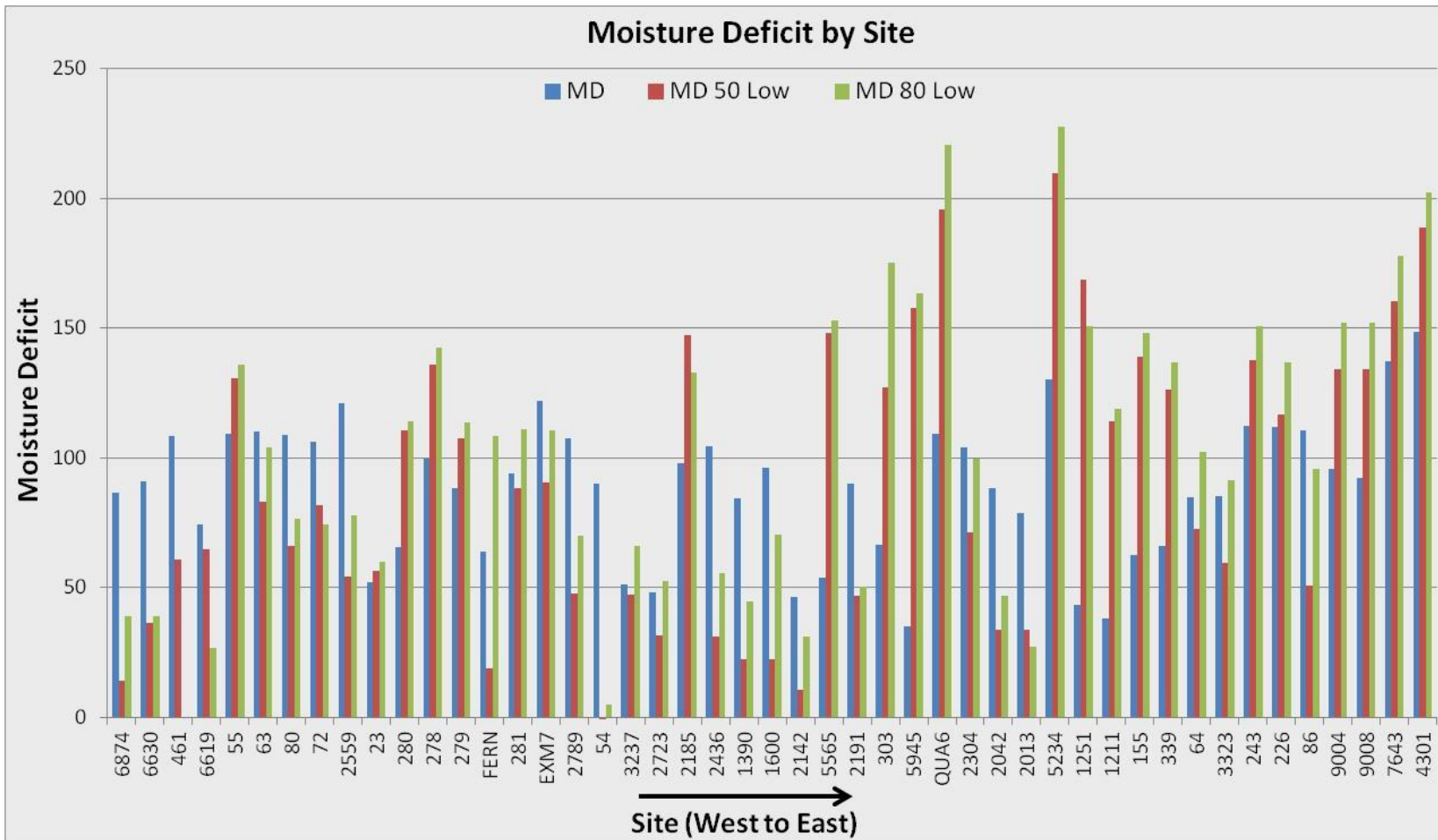


Figure 2-17: Current ESC moisture deficit data, along with the moisture deficit predicted by the low scenario after 50 and 80 years of UKCP09 (2009) for the sites used within this study to measure ring growth and ring density.

2.5 Categorical Groups

As discussed in Section 2.3.1, in the initial design of this experiment the sites were chosen according to criteria of latitude, elevation and yield class and from within these groupings it is also possible to get the longitude and initial spacing of the sites. Although the nature of these means that they are capable of being expressed as continuous variables, in order to get a sense of how wood properties varied throughout Great Britain they were also investigated as categorical variables. The following section describes how these groups were constructed.

2.5.1 Longitude and Latitude as Categorical Variables

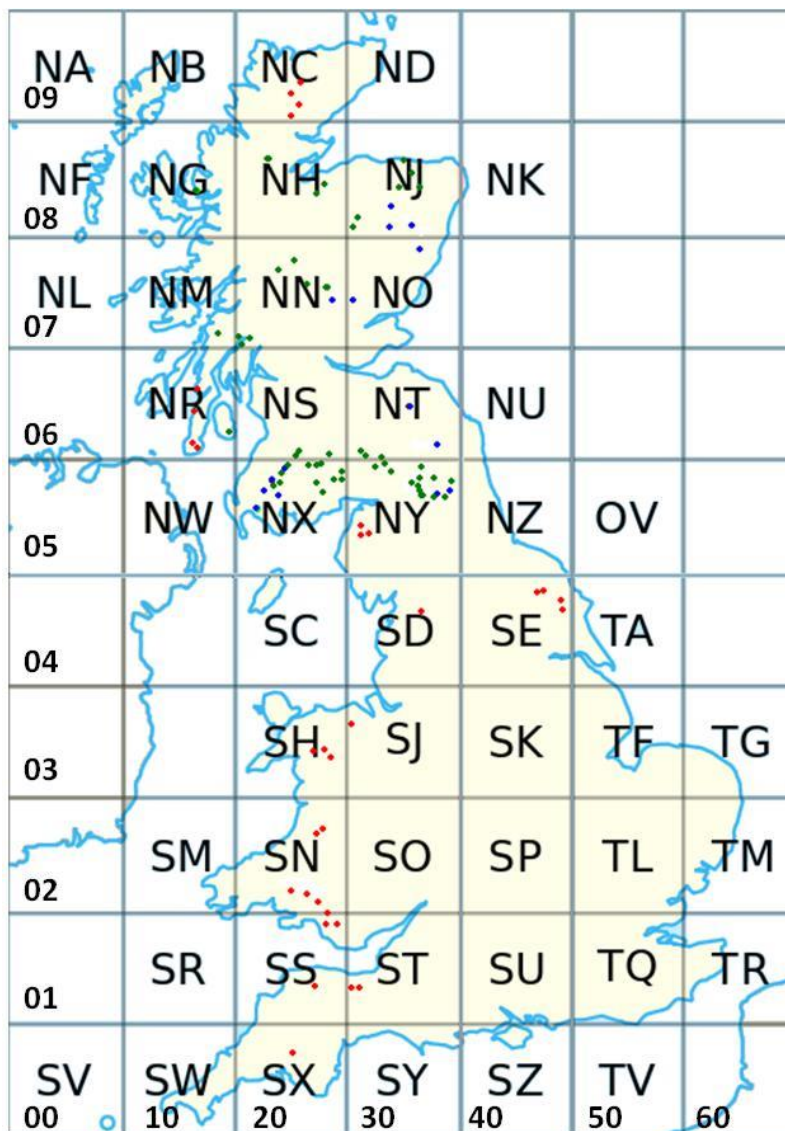


Figure 2-18: The Ordnance Survey British National Grid. Each 100 km x 100 km grid is described by a pair of letters which have been translated into numbers based on columns and rows. Also shown is the location of the sites used in this study in relation to the grid squares.

Latitude and longitude were measured using the Ordnance Survey National Grid Reference system. This uses alphanumeric references based on a grid system within the British Isles whereby the first two letters indicate a 100 x 100 km grid square within the UK (Figure 2-18) followed by a grid reference denoting the location within the grid square. This system allows for the first two letters to be substituted by numbers based on rows (or eastings) and columns (or northings). For example grid square SH becomes 23, where 2 is the progress west to east and 3 is the progress south to north. The numbers of the columns and rows are also shown in Figure 2-18 along with the position of each site positioned within its respective grid square. These data were used in the categorical analysis within this study. Table 2-5 gives a list of sites and the categorical groups for longitude and Table 2-6 gives the groups for latitude.

Table 2-5: The number of sites along with the site name sorted into the relevant Easting group

Easting Group	No. Sites	Site
1	4	461, 6619, 6630, 6874
2	23	FERN, EXM7, 2723, 3237, 1390, 1600, 54, 2142, 2185, 2436, 2559, 2789, 2191, 278, 278, 280, 281, 23, 55, 63, 72, 80, 5565
3	16	2013, 2042, 86, 5234, QUA6, 303, 226, 64, 155, 243, 5945, 1211, 1251, 3323, 339
4	4	4301, 7643, 9004, 9008

Table 2-6: The number of sites along with the site name sorted into the relevant Northing group

Northing Group	No. Sites	Site
0	1	FERN
1	6	EXM7, 2142, 2185, 2191, 5234, QUA6,
2	6	2723, 3237, 1390, 2436, 2559, 2789
3	3	1600, 54, 303,
4	4	86, 7643, 9004, 9008
5	10	23, 55, 53, 72, 80, 2013, 2042, 2304, 226, 64
6	6	461, 6619, 6630, 6874, 155, 243
7	3	5565, 5945, 3323
8	4	1211, 1251, 339, 4301
9	4	278, 279, 280, 281

2.5.1.1 Longitude and Latitude as Continuous Variables

This numerical system also allows for the grid reference to be used as a continuous numerical parameter. Since grid references are split into an easting and northing which denotes a position within a 100 x 100 km grid, the addition of the numerical grid parameter to the beginning of each allows a continuous position within Great Britain to be calculated. For example, OS Grid Reference SH 85688 29686 becomes 285688 329686 where the first set of 5 numbers are the easting value and the second set the northing value.

2.5.2 Elevation Groups

Elevation is able to be expressed as a continuous variable as altitude above sea level in metres and these were grouped in 50 m increments from lowest (Group 1 to highest (Group 9). The number of sites per elevation group along with the site number is shown in Table 2-7.

Table 2-7: The number of sites along with the site name sorted into the relevant elevation group.

Elevation Group	Elevation (m)	No. Sites	Sites
1	50 - 100	2	461, 278
2	100 - 150	5	2559, 80, 6630, 281, 55
3	150 - 200	8	63, 279, 280, 72, EXM7, 2789, 4301, 2304
4	200 - 250	5	243, 5234, 226, 7643, 86
5	250 - 300	7	1600, 6874, 2042, 2185, QUA6, 3323, 54
6	300 - 350	8	155, 2191, 64, 2013, 1390, 5565, 9008, 23
7	350 - 400	3	9004, 339, 1251
8	400 - 450	4	5945, 303, FERN, 1211
9	450 - 500	4	3237, 2436, 2142, 2723

2.5.3 Spacing Groups

Spacing is measured in metres and is the initial distance that the trees were planted and has been the subject of many studies investigating its effect on tree properties, and was the subject of a review by MacDonald and Hubert (2002). The nature of the spacing whereby there were a limited number of spacings used meant that the groups were the same as the actual spacing. By far the most predominant spacing group in this study is 2m as shown in and a non-random distribution such as this complicates analysis of the effects of spacing on wood properties.

Table 2-8: The number of sites along with the site name sorted into the relevant spacing group.

Spacing (m)	No. Sites	Site
1.5	1	1211
1.6	2	226, 1251
1.7	6	9008, 2013, 2304, 86, 2142, 2436
1.8	6	2723, 279, 243, 23, 72, 5565
1.9	1	6874
2.0	24	4301, 7643, 9004, 2042, FERN, 5234, EXM7, QUA6, 3237, 1390, 1600, 303, 54, 2185, 2559, 2789, 2191, 431, 6619, 281, 63, 5945, 3323, 339
2.1	1	80
2.4	2	6630, 278
2.5	4	280, 64, 155, 55

3 Modelling Radial Growth of Sitka Spruce

3.1 Introduction

Using the data collected from the sample cores taken as part of the resource evaluation study described in Chapter 2, this chapter aims to investigate the radial growth of Sitka spruce across the full latitudinal and longitudinal range of Great Britain. Empirical models were used to examine radial growth by age and to investigate which parameters such as latitude, longitude, altitude and spacing are having an effect on this growth.

3.1.1 Definitions

In this section when growth is discussed it is referring only to secondary growth, that is, radial growth from the vascular cambium. All measurements of secondary growth were at breast height (approximately 1.3 m).

Ring number is counted from the pith and is a measure of cambial age in years. For the purposes of this chapter the terms “Ring Number” “Age” and “Cambial Age” are interchangeable.

3.1.2 Outline

The core samples used in the section were taken from the 32 Extension Benchmark sites which covered a range from Sutherland in the north of Scotland down to Devon in the south west of England as described in the method section of Chapter 2. As well as these, samples from a further 14 sites were selected (See Map in Figure 2-1) from the original Benchmark study to cover a larger range of the UK including north east Scotland, south east and south west Scotland and north east England. Due to time constraints it was not possible to analyse all of the original benchmark sites and a subset of 14 were chosen which increased the range within Great Britain. At each of the 46 sites it was intended to take 10 core samples but due to damage and the condition of some of the cores (e.g. knots) this number varied between 8 (4 sites), 9 (12 sites), 10 (28 sites) and 11(2 sites) (Table 3-1).

Table 3-1: Number of samples per site.

Site	23	54	55	63	64	72	80	86	155	226
No.Samples	10	10	9	10	10	10	10	10	10	10
Site	243	278	279	280	281	303	339	461	1211	1390
No.Samples	10	10	10	10	10	9	9	9	9	10
Site	1600	2013	2042	2142	2185	2191	2304	2436	2559	2723
No.Samples	10	9	11	8	9	10	9	10	8	11
Site	2789	3237	3323	4301	5234	5565	5945	6619	6630	6874
No.Samples	9	8	10	10	9	9	10	10	10	10
Site	7643	9004	9008	EXM7	FERN	QUA6				
No.Samples	10	10	10	8	9	10				

Each core was split at the pith and analysis was made from pith to bark on the core to give a radial profile.

Ring width data was produced using the Itrax densitometer along with Windendro (see methods in Chapter 2) software and a simple calculation was used to calculate accumulated growth by ring for each tree:

$$\text{Accumulated Growth}_{(i)} = \sum RW_{(1:i)} \quad \text{Equation 3.1}$$

Where RW is ring width measured by Windendro and i is the cambial age in years and the number of annual rings (counting from the pih) that correspond to that age.

3.1.3 Aim

The aim of this section is to investigate which empirical models best describe radial growth with age of the sampled trees and to examine whether the radial profile of growth can be modelled using a segmented linear approach and to compare this to other empirical models which describe the radial profile of growth with age within the sampled trees. These models can then be used to investigate any difference in growth rates by altitude, latitude, longitude and initial spacing.

3.2 Radial Variation in Growth

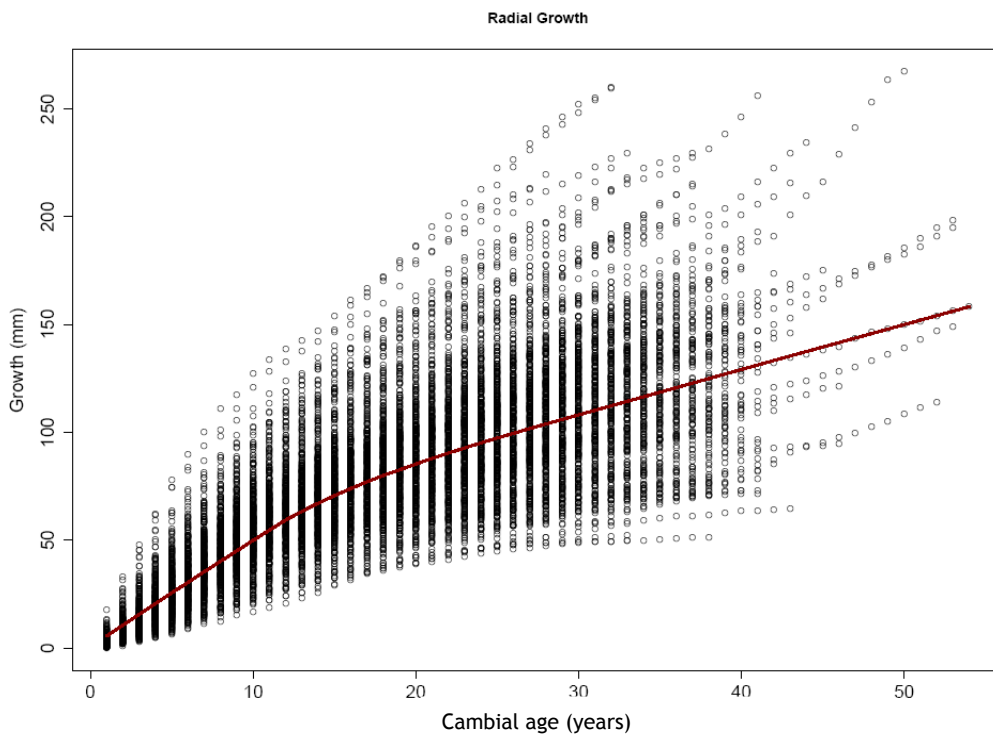


Figure 3-1: Radial growth plotted by cambial age with a LOWESS trend line

Figure 3-1 shows that there is a clear radial trend in radial growth with a greater rate near the pith which decreases between years 10 and 20. Thus growth rates were higher in the younger part of the tree (juvenile wood) compared with the older part of the tree (mature wood). This general trend in growth is similar to that described in previous literature for Sitka spruce (McLean, 2008, Moore, 2011) and may be linked to canopy closure in the forest which usually happens around 10 to 12 years depending on spacing (Kilpatrick et al., 1981, Savill and Sandels, 1983). The growth pattern also conforms to the generally accepted juvenile and mature wood periods for Sitka spruce plantations (Cameron et al., 2005, Brazier and Mobbs, 1993, Schaible and Gawn, 1989).

To ensure an even end point for each sample and since the rate of growth can be affected by silviculture practices, such as thinning (MacDonald and Hubert, 2002), it was decided that an upper limit of ring 25 (counting out from the pith) would be used in the model analysis. Typically thinning takes place sometime after age 20 (Deans and Milne, 1999) and as a result the tree will have a period of faster growth later in its lifetime (Methley, 1995) determined by when thinning took place. Setting an upper age limit therefore reduced the effect that

any thinning would have on the mature section of the growth rate. As well as this, the number of trees with rings beyond this point decreases rapidly with age (Table 3-2).

Table 3-2: The number of trees being analysed decreases as ring number increases

Ring	Number of Trees
1	442
12	442
20	438
25	428
30	342
35	192

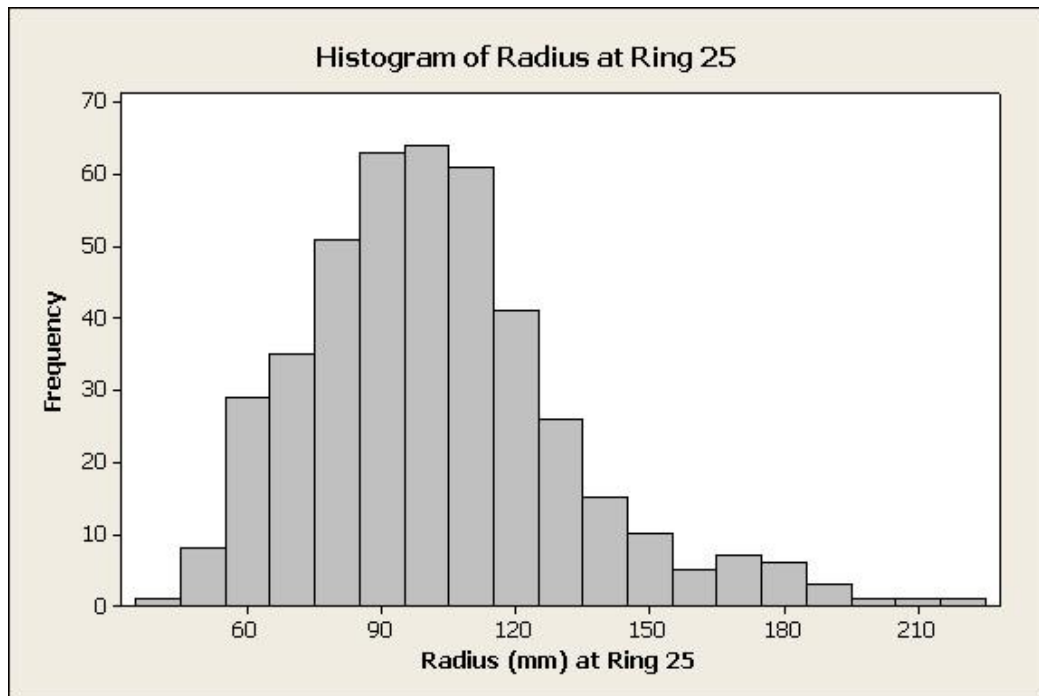


Figure 3-2: Distribution of sample length measured from pith to bark (radius) on the core samples

The length of the radial profile of each core was found to be fairly evenly distributed though there were a few larger samples (Figure 3-2). A total of 434 samples were measured and these had a mean length of 120.3 mm with a standard deviation of 37.9 mm. The largest sample was 266.7 mm in length with the shortest being just over 36.2 mm. This difference in size may reflect in the difference in age at felling as well as growth rate, and setting an upper limit of 25 years removes any age bias.

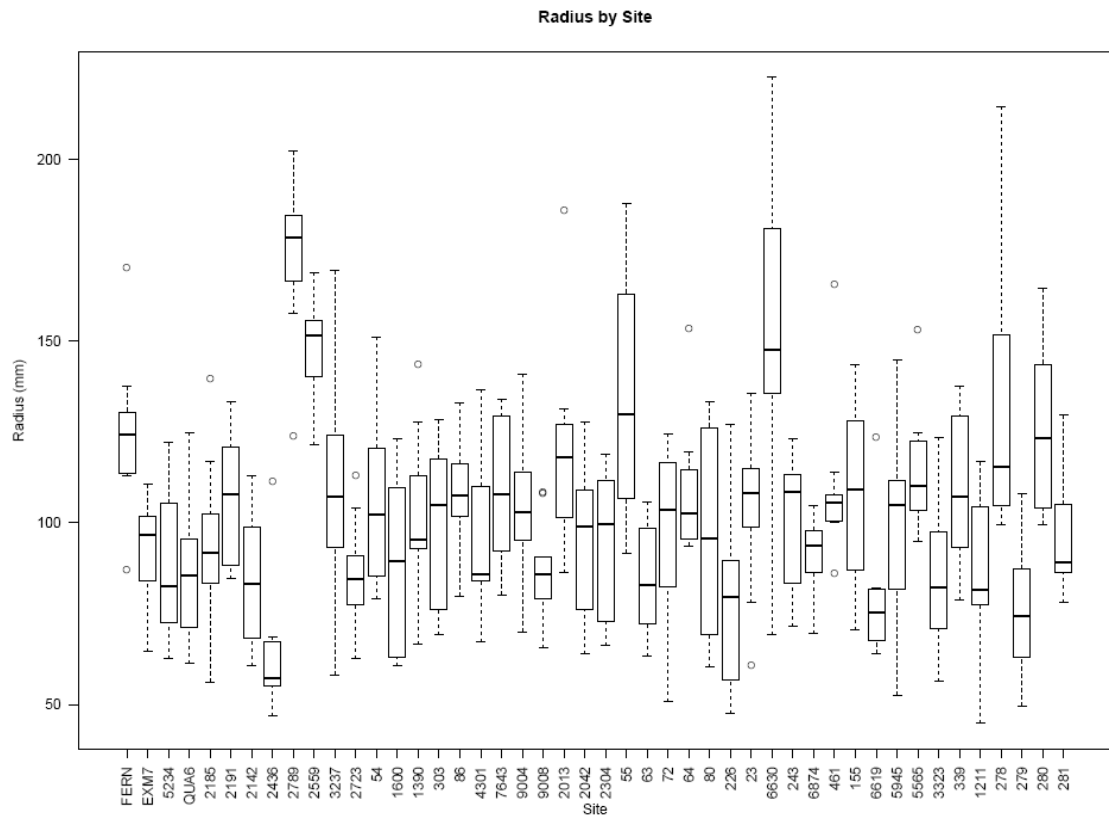


Figure 3-3: Boxplot showing the radius of the samples at cambial age 25 plotted by site running sequentially from furthest south (left) to furthest north (right).

When the length of the samples at cambial age 25 is plotted by site (Figure 3-3) it shows that whilst there would seem to be some differences between some of the sites there is also a large spread in radius within each site. The site with the lowest mean radius is site no. 2436 and the site with the highest mean radius is site 2789. Both of these sites are in South Wales showing that region alone would not be a good indicator of tree growth. Similarly sites 6619 and 6630 have very different mean radii even though both are in Kintyre in the west of Scotland.

To be able to visualize how the radius is affected by latitude, longitude, spacing and altitude these variables were split into groups as described in the method in Chapter 2. The latitude groupings progress from furthest south (Grp 0) to furthest north (Grp 9), longitude groupings run from west (Grp 1) to east (Grp 4), altitude groupings run from lowest elevation (Grp 1) to highest elevation (Grp 9) and Spacing is grouped by the measured distance in metres. The number of samples in each of these groupings is shown in Table 3-3.

Table 3-3: The number of samples and sites per group

Northing Group	0	1	2	3	4	5	6	7	8	9
No. Samples	10	54	46	39	50	98	59	29	18	40
No. Sites	1	6	5	4	5	10	6	3	2	4

Easting Group	1	2	3	4
No. Samples	39	218	145	40
No. Sites	4	23	15	4

Altitude Group	1	2	3	4	5	6	7	8	9
No. Samples	19	47	77	58	80	78	19	37	27
No. Sites	2	5	8	6	8	8	2	4	3

Spacing (m)	1.5	1.6	1.7	1.8	1.9	2	2.1	2.4	2.5
No. Samples	9	10	66	60	20	208	10	20	39
No. Sites	1	1	7	6	2	22	1	2	4

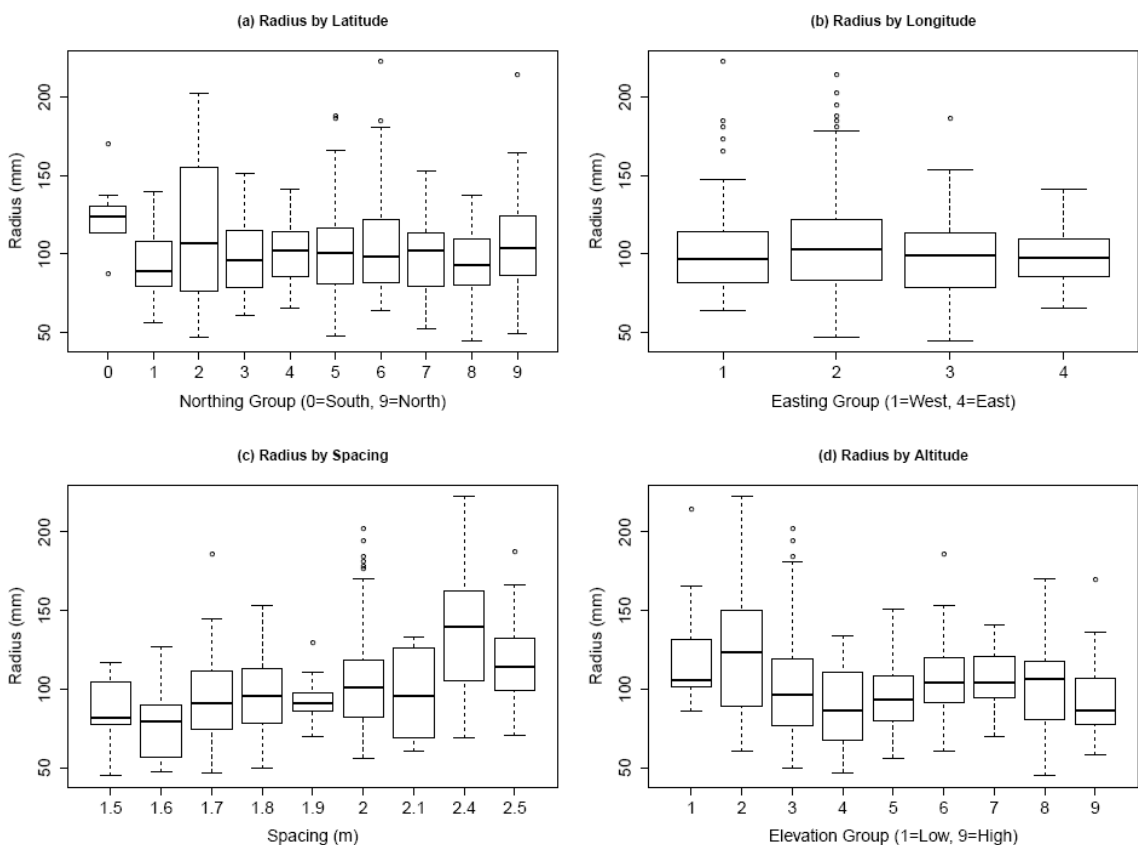
**Figure 3-4: Radius of samples at cambial age 25 plotted against longitude, latitude, spacing and altitude**

Figure 3-4 shows the radius at cambial age 25 plotted by latitude, longitude, spacing and altitude. With the exception of altitude there do not seem visually to be any obvious trends when plotted by groups. There may be a slight

tendency for the radius to decrease with increasing elevation and this was confirmed by fitting a linear model, which indicates that elevation is having a significant, negative effect on the size of the core ($p < 0.001$). A similar linear model applied to spacing indicates that it was having a positive effect on the core length ($p < 0.001$) but there was no effect of northing or easting.

3.3 Fitting Models to Radial Growth

In order to model radial growth a number of statistical models were explored to see how well they describe the growth trend of these data. A review in 1993 (Zeide, 1993) listed several statistical models that are commonly used to describe growth (Table 3-4) and these were examined to investigate which would best fit this data set.

Table 3-4: Growth equations for statistical models from (Zeide, 1993), where RG = radial growth, t is cambial age. a , b , c and d are parameters estimated from the data

Model Name	Equation	Equation No.
Hossfeld 4	$RG = t^c / (b + t^c / a)$	3.2
Gompertz	$RG = a * \exp^{-b * \exp^{-ct}}$	3.3
Logistic	$RG = a / (1 + c * \exp^{-bt})$	3.4
Monomolecular	$RG = a * (1 - c * \exp^{-bt})$	3.5
Bertalanffy	$RG = a * (1 - \exp^{-bt})^3$	3.6
Chapman-Richards	$RG = a * (1 - \exp^{-bt})^c$	3.7
Levakovic1 (Modified)	$RG = a * (t^d / (b + t^d))^c$	3.8
Levakovic3	$RG = a * (t^2 / (b + t^2))^c$	3.9
Korf	$RG = a * \exp^{-bt^c}$	3.10
Weibull	$RG = a * (1 - \exp^{-bt^c})$	3.11
Yoshida1	$RG = a * t^d / (b + t^d) + c$	3.12
Sloboda	$RG = a * \exp^{-b * \exp^{-ct^d}}$	3.13

As well as the growth models listed in Table 3-4 three separate models used to describe curves were explored to see how these compare with the growth models (Table 3-5). Along with these a segmented linear model which investigates whether there are two separate linear sections to the growth with a defined split point between the two sections using a Davies test (Davies, 1987)

to test for a significant change in gradient. Each linear section follows the form of a linear equation where there is a slope parameter and an intercept parameter. For both the juvenile and mature segments the intercept is interpreted as the value at year 0.

Table 3-5: Equations for the three statistical models describing curves and the two segmented model, where RG = radial growth, t is cambial age. a , b and c are parameters estimated from the data

Model Name	Equation	Equation No.
Segmented linear model: Juvenile Segment	$RG = a_1 * t + b_1 \quad t \leq 11$	3.14
Segmented linear model: Mature Segment	$RG = a_2 * t + b_2 \quad t > 11$	3.15
Michaelis Menten (MM)	$RG = (a * t) / (b + t)$	3.16
Exponential (Exp)	$RG = -a * \exp^{-b * t} + c$	3.17
Logarithmic (Log)	$RG = a * \log(t) + b$	3.18

To visually inspect the models they were fitted to the data in R using non linear least squares (nls) to find the best fit curve. The result of this can be seen when the fitted line for the models are plotted against the mean line (Figure 3-5)

Figure 3-5 shows visually that whilst most of these models fit quite well to the mean of the data there are a couple of exceptions (Logistics and Logarithmic) which do not fit the data as well as the others and do not need any further investigation.

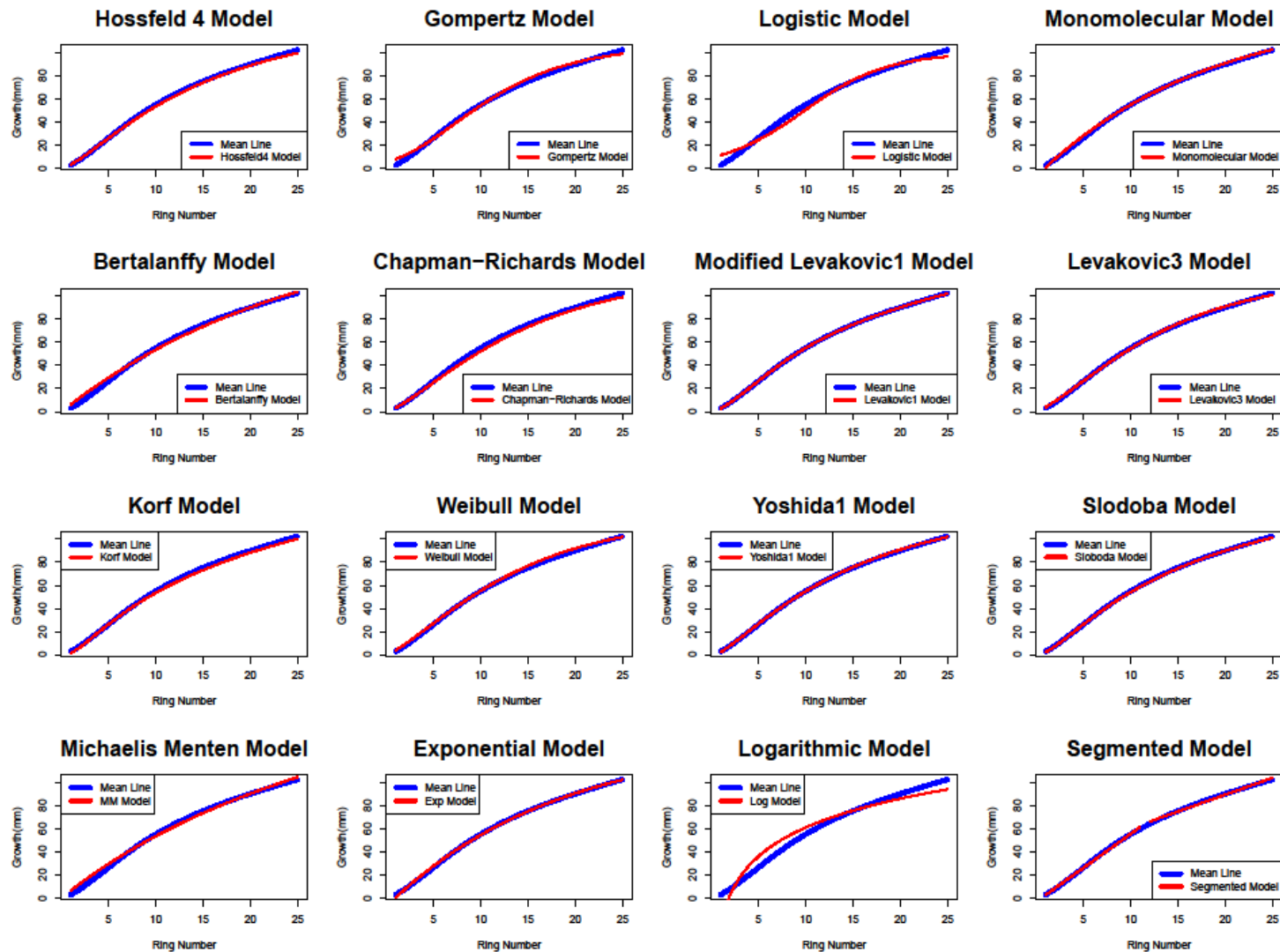


Figure 3-5: The fitted line for each of the growth models (red) plotted against the mean of the observed data (blue) by ring number from the pith.

3.3.1 Model Parameters

When each of the rest of the models are fitted to all of the data (global data), the coefficients that were estimated are presented in Table 3-6. This shows that all of the growth models plus the curve models and the segmented model are able to explain a similar amount of the variation (69% for all the models). The residual standard error is also very similar for all models at with the lowest being 20.12 mm and the highest being 20.25 mm.

Table 3-6: Parameter estimates along with Standard Errors, residual standard error and R-squared value for the statistical model equations. Also shows the number of trees and the percent of the total that the model was unable to fit.

Model Parameter	Estimate	Std Error	Residual Std Error	R-Squared	No.Trees Not Fit	% Total Not Fit
Hossfeld4						
a	149.1	4.7	20.13	0.6942	9	2
b	0.3	0.02				
c	1.4	0.04				
Gompertz						
a	106.3	39	20.22	0.6914	1	0.2
b	3.04	0.06				
c	0.15	0.003				
Monomolecular						
a	139.9	2.9	20.14	0.6938	22	5
b	0.055	0.021				
c	1.05	0.006				
Bertalanffy						
a	168	4.1	20.24	0.6921	44	10
b	0.013	0.00045				
Chapman-Richards						
a	121.8	2.44	20.13	0.6940	26	6
b	0.08	0.004				
c	1.42	0.05				
Levakovic1 Modified Equation						
a	27.9	5.4	20.12	0.6943	186	43
b	70.9	25.3				
c	0.5	0.04				
d	2.8	0.1				
Levakovic3						
a	128.96	1.99	20.14	0.6939	19	4
b	309.6	27.9				
c	0.6	0.02				
Korf						
a	294.5	26.7	20.13	0.6941	31	7
b	5.4	0.09				
c	0.5	0.03				
Weibull						
a	116.5	2.5	20.14	0.6939	10	2
b	0.033	0.0013				
c	1.27	0.027				
Yoshida1						
a	156.9	8.8	20.13	0.6942	45	10
b	39.8	4.6				
c	-1.6	1.3				
d	1.3	0.07				
Sloboda						
a	162.1	21.9	20.13	0.6943	338	78
b	18.1	13.9				
c	1.5	0.7				
d	0.3	0.1				
Segmented - Split point 11.6 years						
a1	5.87	0.09	20.14	0.6936		
b1	-3.25	0.63				
a2	2.91	0.06				
b2	31.21	0.11				
Michaelis Menten						
a	285.12	8.74	20.25	0.6915	41	9
b	43.25	1.86				
Exponential						
a	147.4	2.492	20.14	0.6938	27	6
b	0.055	0.002				
c	139.9	2.938				

When the models were fitted to individual trees, in the R statistical program (R Core Team, 2013), there were two models which were unable to fit to a high proportion of the samples, the Levakovic1 model which couldn't fit to 43% of the trees and the Sloboda model which couldn't fit to 78% of the trees. These were discounted from further investigation. The Bartalanffy (10%) model, Yoshida1 (10%) and Michaelis Menten (9%) models were also discounted as these were also unable to fit to a substantial number of trees.

3.4 Comparing Models of Radial Growth

3.4.1 Hossfeld4 Model

Although the segmented analysis may indicate that growth can be split into two separate segments with a specific change point between the two forms of growth, it is also possible that there may be a gradual change from juvenile to mature growth. This being the case models which describe juvenile and mature growth together as a curve may fit the data better. Therefore as well as looking at juvenile and mature wood as two separate segments this section looks at a selection of different curves to see which function fits the data the best and how these compare with the segmented model.

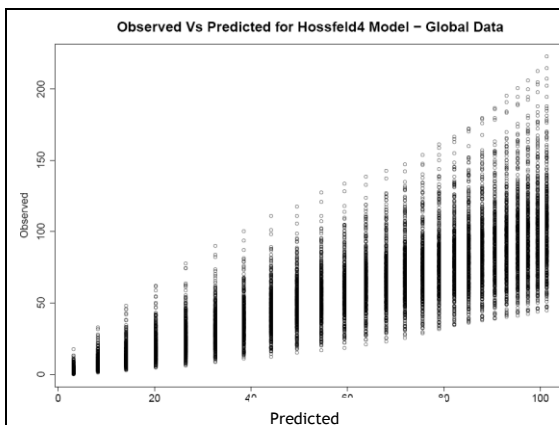


Figure 3-6: Observed V Predicted for the Hossfeld4 model on the global data.

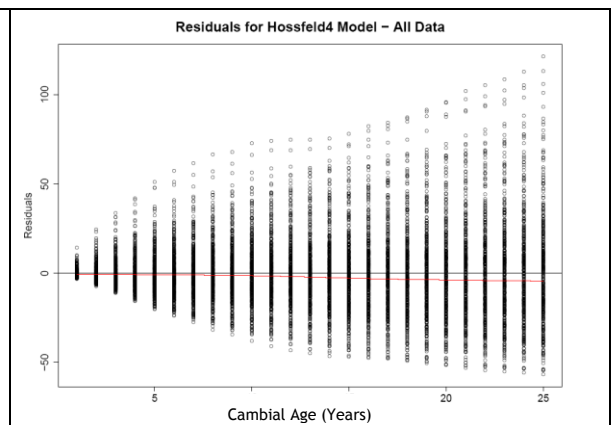


Figure 3-7: Residuals plotted against cambial age for the Hossfeld4 model on the global data.

The Hossfeld4 model was able to predict growth from cambial age, describing the age related trend in growth reasonably well (Figure 3-6). There was still variation between trees and the spread of the observations tended to increase with increasing growth. Similarly when the residuals are plotted against cambial

age they show a reasonably good fit. There is a trend for the residuals to increase with age but we should expect this as the tree growth is increasing from zero at different rates (Figure 3-7) so that the divergence tends to increase with increasing growth.

3.4.1.1 Hossfeld4 Model Fitted to Individual trees

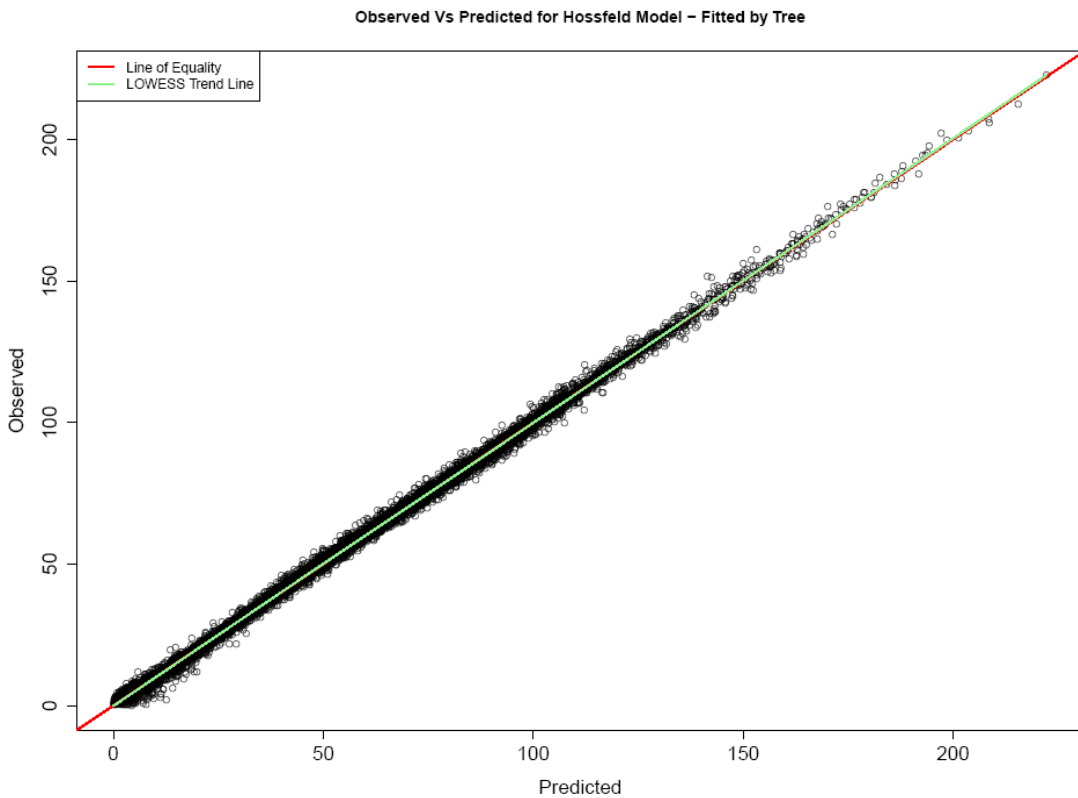


Figure 3-8: Observed Vs Predicted for the Hossfeld4 model when fitted to individual tree.

When observed versus the predicted growth values are plotted for the Hossfeld4 model fitted to individual trees (Figure 3-8), it looks to be predicting very well ($R\text{-squared} = 0.998$). There does not seem to be any curve to the data with an even spread throughout the data and the LOWESS trend line sitting almost exactly on the line of equality.

When the residuals for the Hossfeld4 model are plotted against cambial age there may be a slight curved pattern to the data (Figure 3-9) although the spread looks fairly even throughout. When the residuals are plotted against distance from the pith (Figure 3-10) they again show a fairly even spread and there does not look to be a problem at values close to the pith as seen with some of the other models.

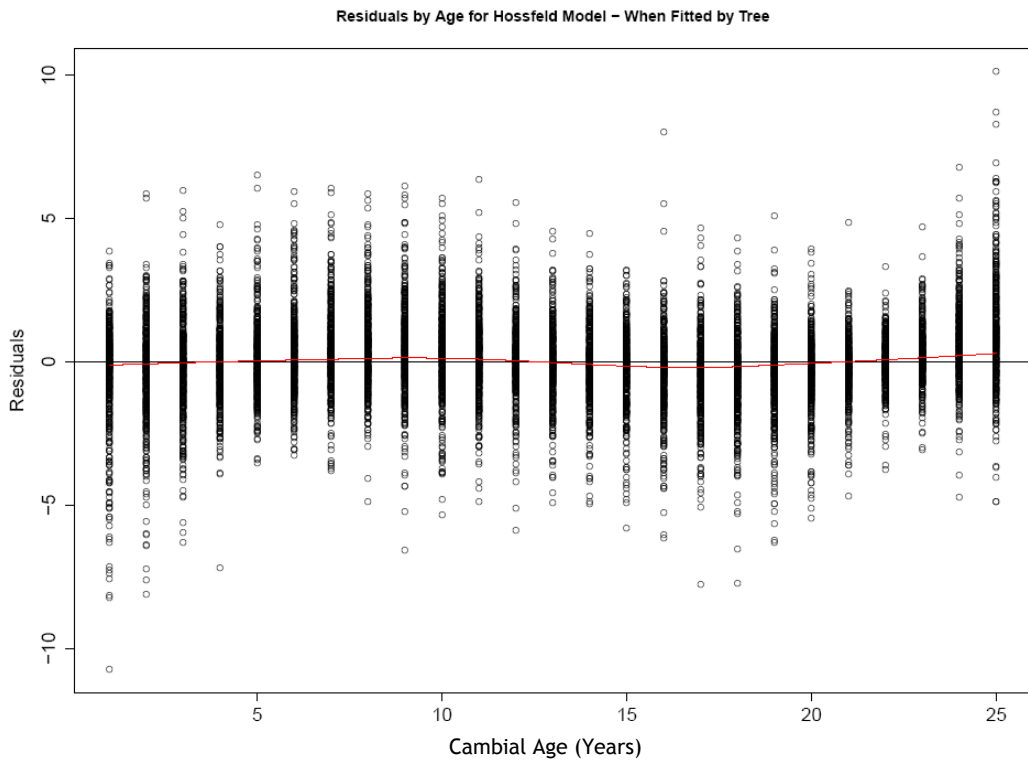


Figure 3-9: Residuals of Hossfeld4 model when fitted to individual trees, plotted against cambial age with LOWESS trend line (red).

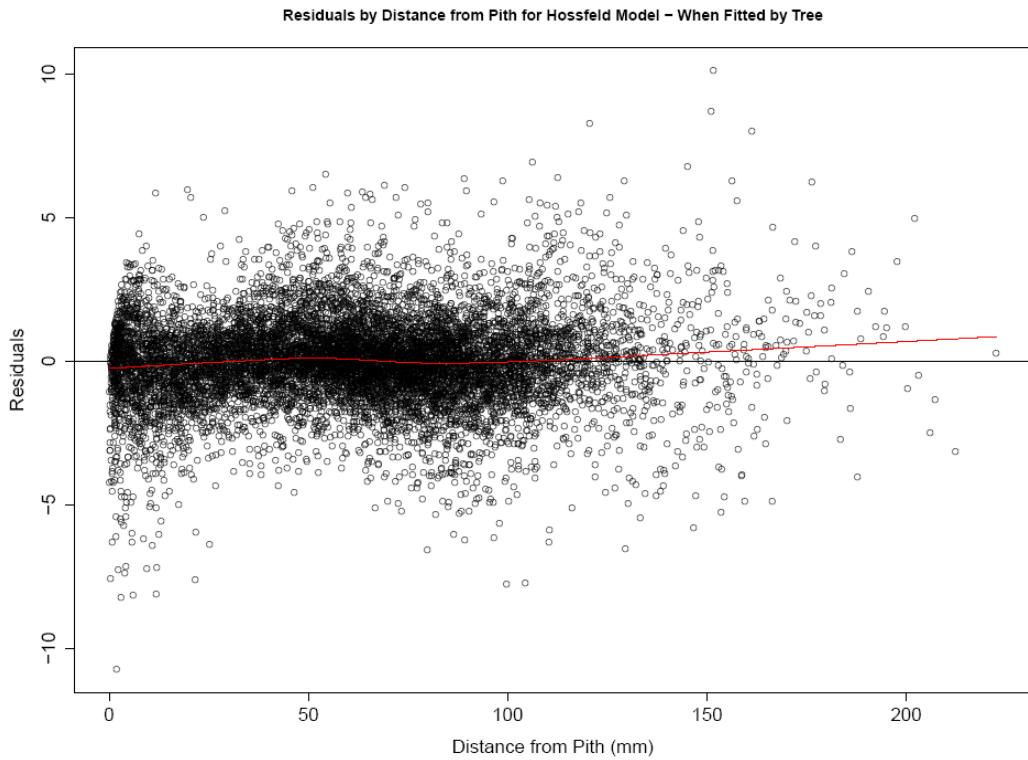


Figure 3-10: Residuals of Hossfeld4 model when fitted to individual trees, plotted against growth with LOWESS trend line (red).

While the two segment linear model was able to produce clear coefficients (slope and intercept) which could be plotted against the treatments, the other growth models produced coefficients which had an interaction between each other and it is difficult to interpret the effect that each single parameter is having on the slope. Thus it is very difficult to get a clear picture of the effect of the treatments on one of the coefficients on its own. For this reason the coefficients for each treatment were input onto the respective curved model equation and plotted. Figure 3-11 shows the effect of the different treatments, when grouped as categorical variables, on the Hossfeld4 Model. It looks as if longitude (b) had little effect but there were differences in the latitudinal groups (a) with a difference in accumulated growth at year 25 of around 30mm between the highest and lowest groups. There may be a positive effect of spacing (c) and again there is a large spread of accumulated growth at year 25 with a difference of approximately 70 mm between the highest and lowest groups. There may be a negative effect of elevation (d) with the lowest altitude groups showing the highest accumulated growth at year 25, approximately 30 - 40mm higher than the highest altitude grouping.

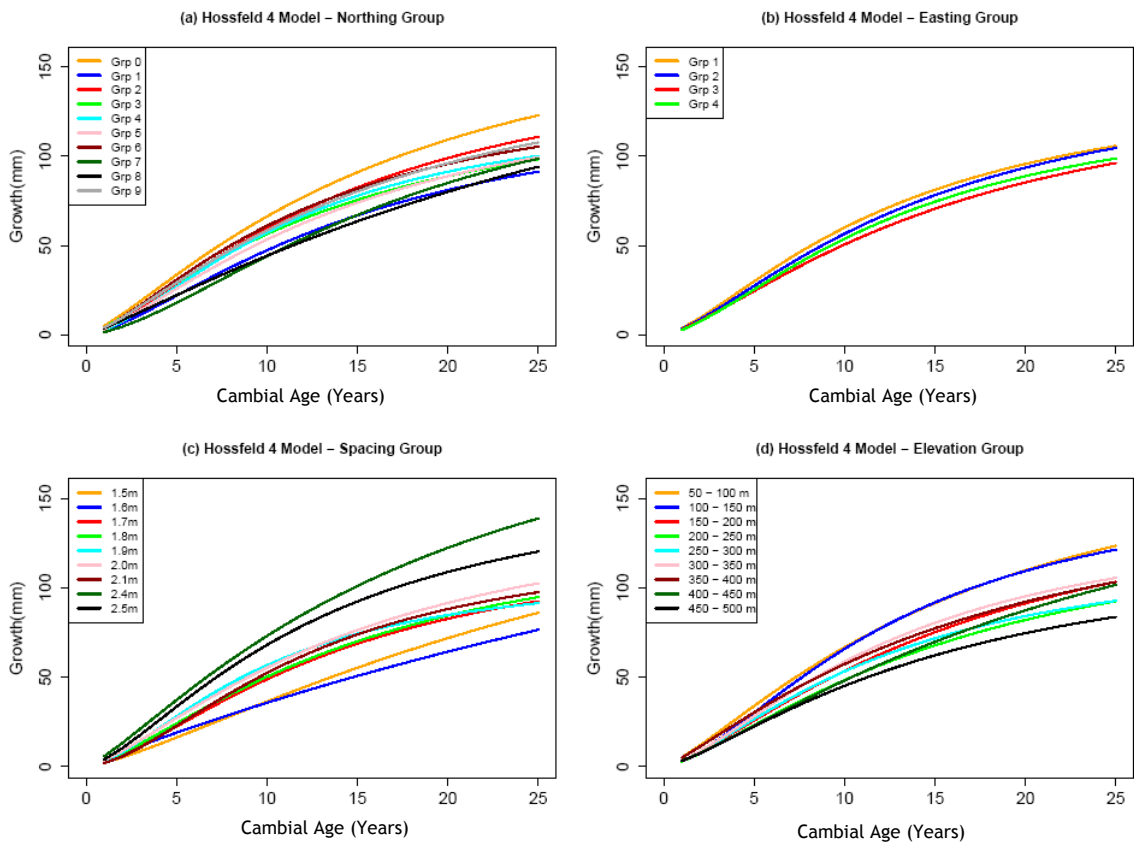


Figure 3-11: Coefficients of the Hossfeld4 model plotted by northing group, easting group, spacing and elevation group.

When the Hossfeld4 model was fitted to individual trees it was unable to fit to 9 trees (2%) and the growth rate for these are shown (Figure 3-12). Eight of the trees shown in Figure 3-12 were the same ones which both the Chapman-Richards and Levakovic3 models were unable to fit (only Tree 9008/35 is unique to the Hossfeld4 model).

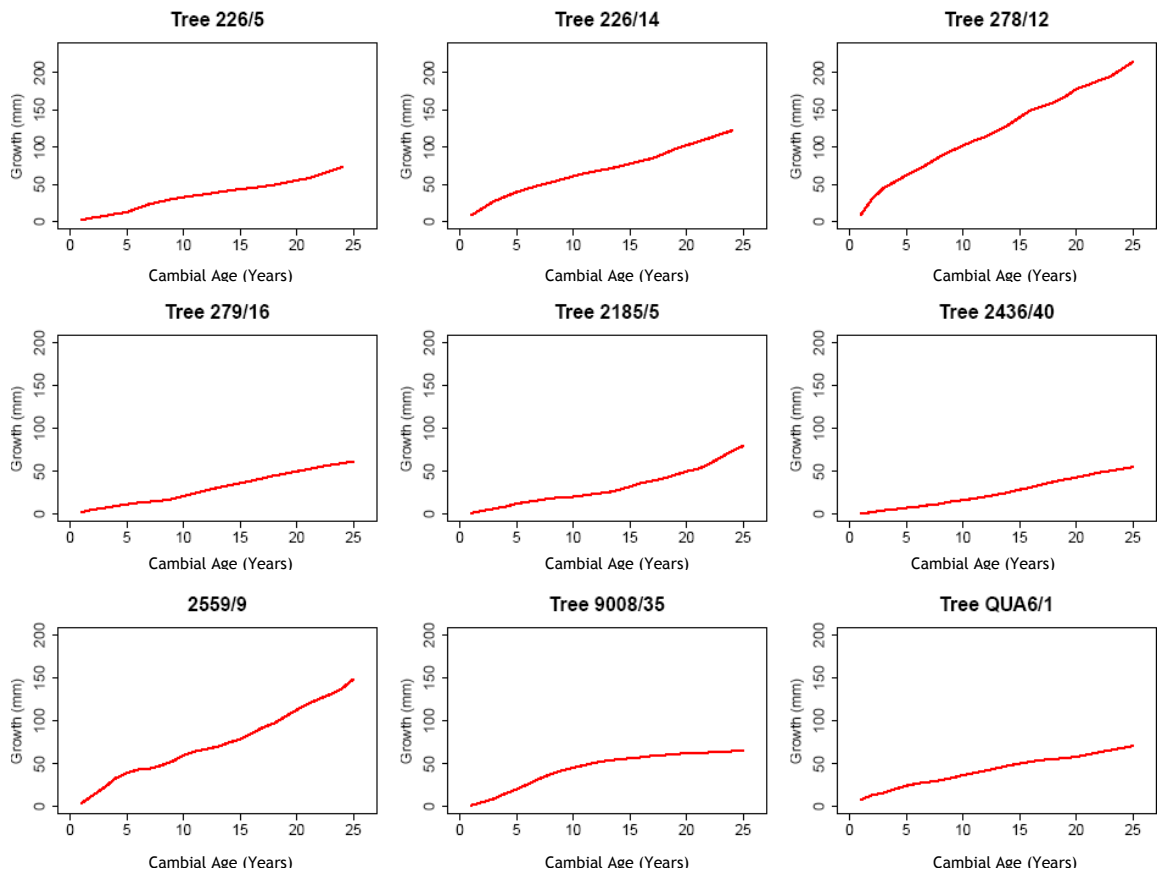


Figure 3-12: Growth rates of the 9 trees that the Hossfeld4 model couldn't fit.

The Hossfeld4 model also produced some extremely high figures (relative to the other values) for the coefficients a and b as shown in the histograms in Figure 3-13. Coefficient a ranges from a minimum value of 43 to a maximum of 10950 with the majority of values falling at the lower end of the scale (median = 139). Similarly, coefficient b has a minimum of 0.048 and a maximum of 14 but again most values fall at the lower end of the scale (median = 0.4).

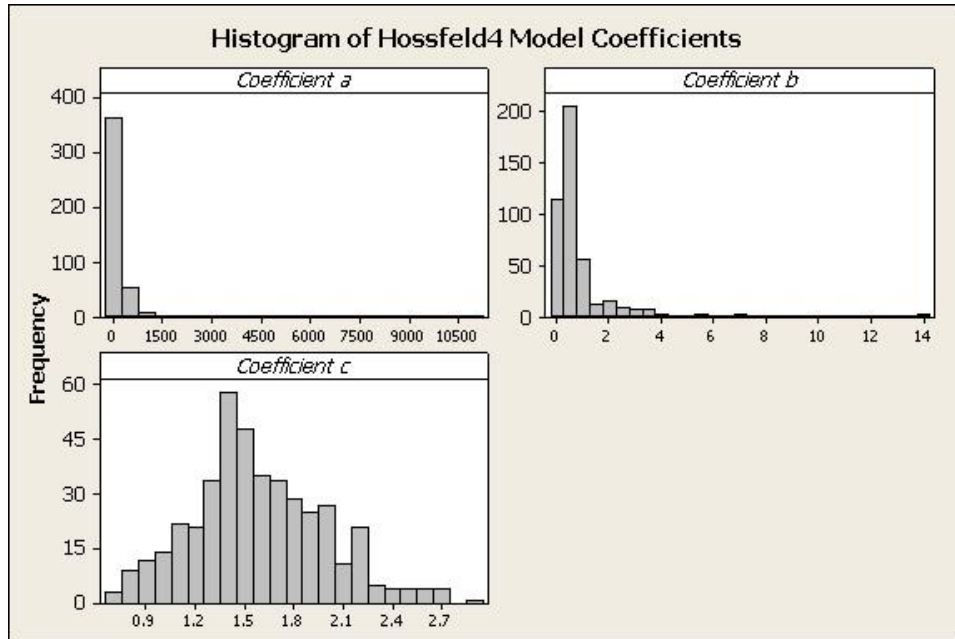


Figure 3-13: Histogram showing the large range in the coefficients *a* and *b* for the Hossfeld4 model.

When the samples which produced the highest coefficients are plotted they give a reasonably good fit to the growth of the respective tree and coefficient “a” could be described as the asymptote, i.e. maximum value. The trees with the highest coefficient “a” are plotted in Figure 3-14. This seems to be an effect of fitting to samples which have a high linear growth rate compared to those with the lowest calculated coefficient “a” which produce a slower, curved growth rate.

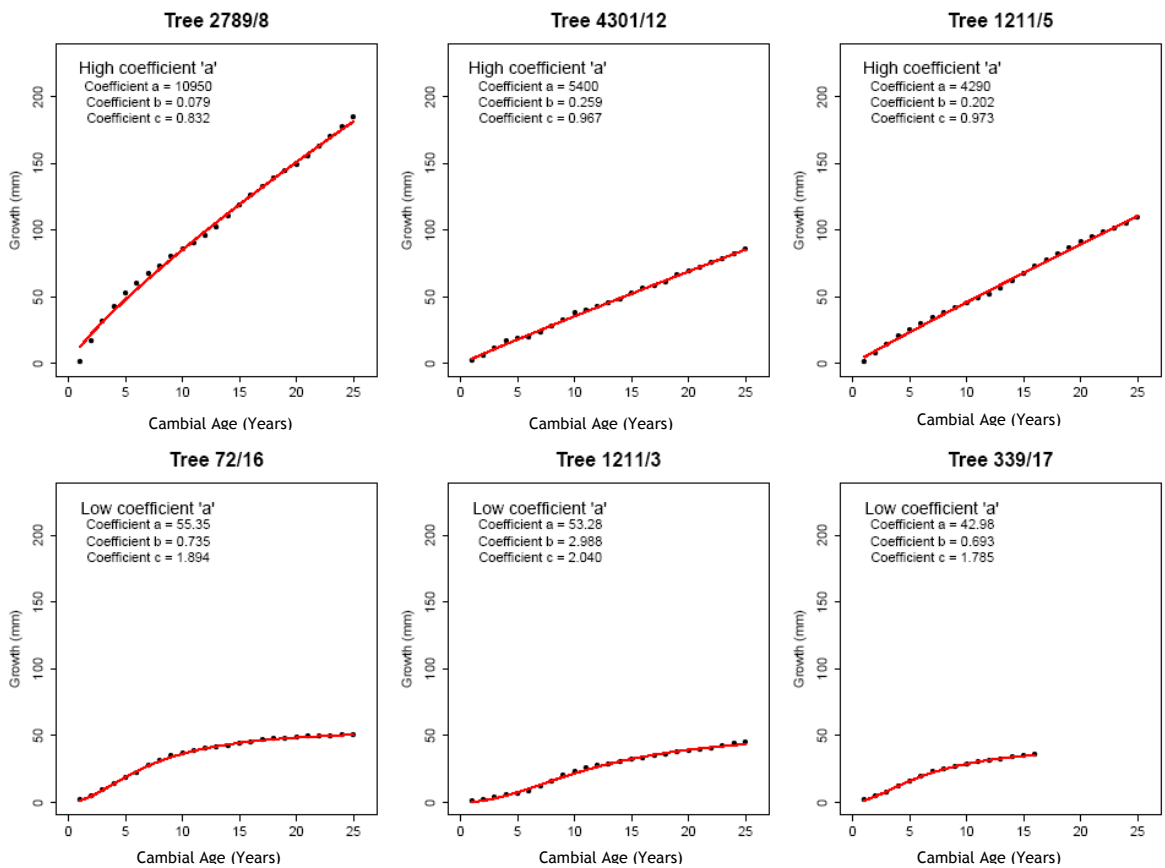


Figure 3-14: The growth rate and fitted line for the three samples which the Hossfeld4 model predicts the highest values for coefficient *a* (top row) and lowest values (bottom row).

Coefficient “*a*” from the Hossfeld4 model shows very little correlation with either coefficient “*b*” (correlation coefficient = -0.09) or coefficient “*c*” (correlation coefficient = 0.27).

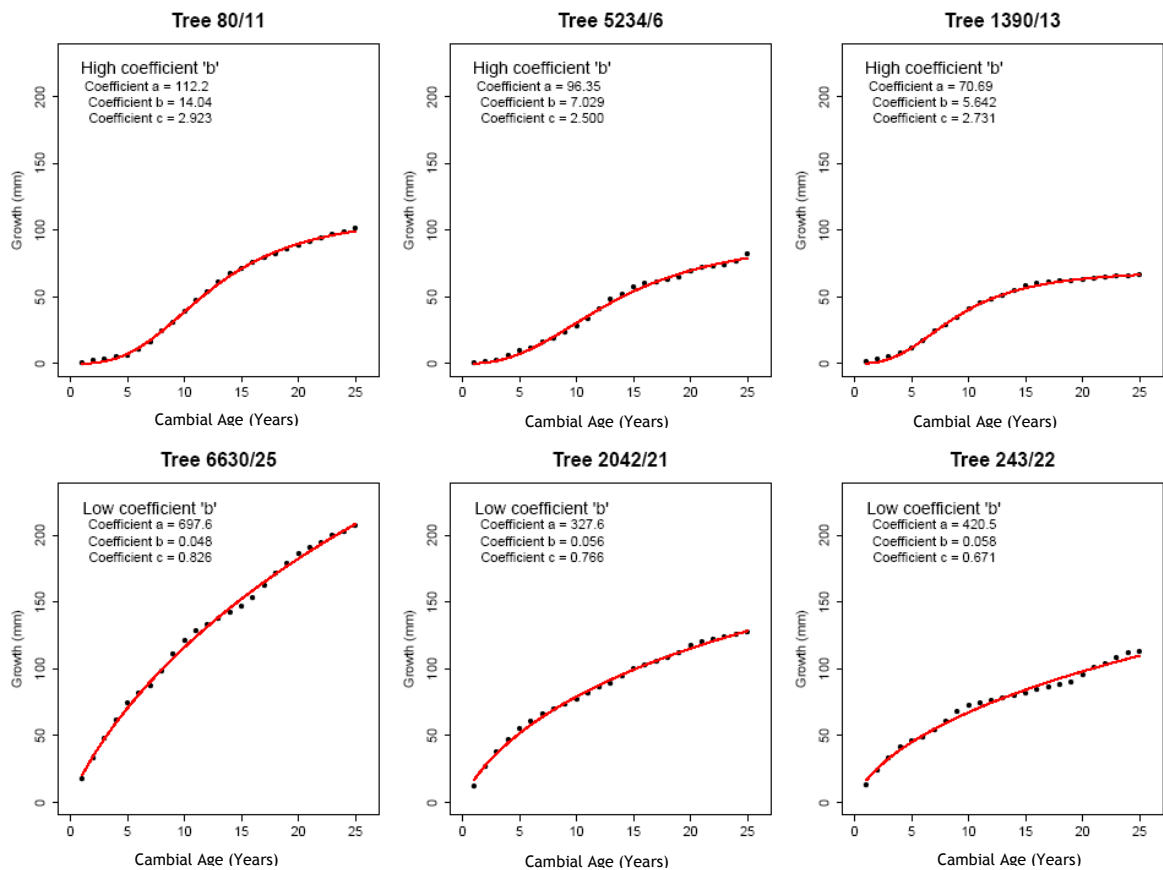


Figure 3-15: The growth rate and fitted line for the three samples which the Hossfeld4 model predicts the highest values for coefficient b (top row) and lowest values (bottom row).

The trees with the highest coefficient “ b ” are plotted in Figure 3-15 along with the samples with the lowest “ b ” coefficient. A high “ b ” coefficient seems to be associated with samples which have a sigmoid (s-shaped) growth rate. Although coefficient “ c ” does not have the same large range as the other two coefficients it was found to be relatively correlated with coefficient “ b ” (correlation coefficient = 0.66) and two of the samples with the highest “ b ” coefficient are also the two with the highest “ c ” coefficient (80/11 and 1390/13). Similarly one of the samples with the lowest “ b ” coefficient also has the lowest “ c ” coefficient (sample 243/22). This shows that both of these parameters are involved in the rate of growth and so it is difficult to determine the effect that each has individually on the slope.

3.4.2 Other Growth Models

When the remainder of the growth models shown in Table 3-4 were fitted against the global data the predicted values and the residuals were very similar

to those shown by the models in the previous section. When fitted to individual trees three of the models (Chapman-Richards, Levakovic3 and Yoshida1) showed similar residuals to the Hossfeld4 model, but these models were unable to fit to as many trees as the Hossfeld4 model as shown in Table 3-6. For this reason it was determined that the Hossfeld4 model would be most suitable out of these curvilinear models for this data set. When examined further, the remainder of the growth models all seemed to have problems when trying to fit to individual trees and so were deemed unsuitable for modelling the data.

Of the three “curve” models tested (Table 3-5), the Logarithmic Model was discounted as it did not give a good fit to the data. The Exponential model looked to give a slightly better fit to the data and was also able to fit more trees than the Michaelis Menten model.

3.4.3 Exponential Model

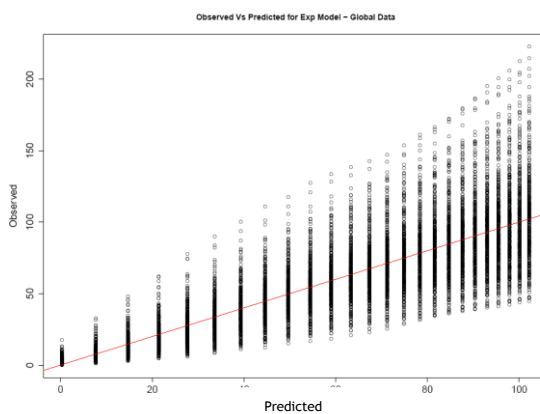


Figure 3-16: Observed Vs Predicted for Log model on the global data. Red line shows the line of equality

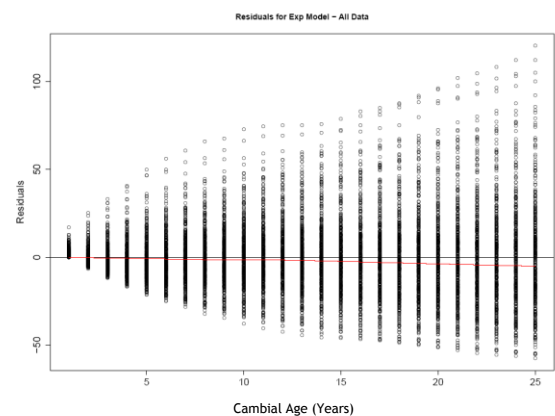


Figure 3-17: Residuals plotted against cambial age for the Log model on the global data. Also showing the LOWESS trend line in red

When the residuals and predicted growth were plotted for the Exponential (Exp) model they were shown to be very similar to that for the Hossfeld4 model. The Exp model was also able to predict growth from cambial age describing the age related trend in growth reasonably well (Figure 3-16) and when the residuals are plotted against cambial age they show a reasonably good fit (Figure 3-17). As with the other models looked at, there was a trend for the spread in predicted growth as well as the variation in residuals to increase with cambial age but again, this should be expected as the tree growth is increasing from zero at different rates causing the variance to increase with increasing cambial age.

3.4.3.1 Exponential Model Fitted To Individual Trees

When the Exp model was fitted to individual trees it was unable to fit to 27 trees (6.2%), which are shown in Figure 3-18. It also produced some extremely high figures for the coefficients “ a ” and “ c ” though not for “ b ” as shown in the histogram in (Figure 3-19). In the Exp model coefficients “ a ” and “ c ” are highly correlated (Pearson correlation = 1.0), but neither are highly correlated to b 1 (Pearson correlation of approx. 0.5 for both). When the samples which produced the highest coefficients are plotted they give a reasonably good fit to the growth of the respective tree (Figure 3-20) and, as before, seem to be an effect of fitting the curved model to the trees with no change in their growth rate.

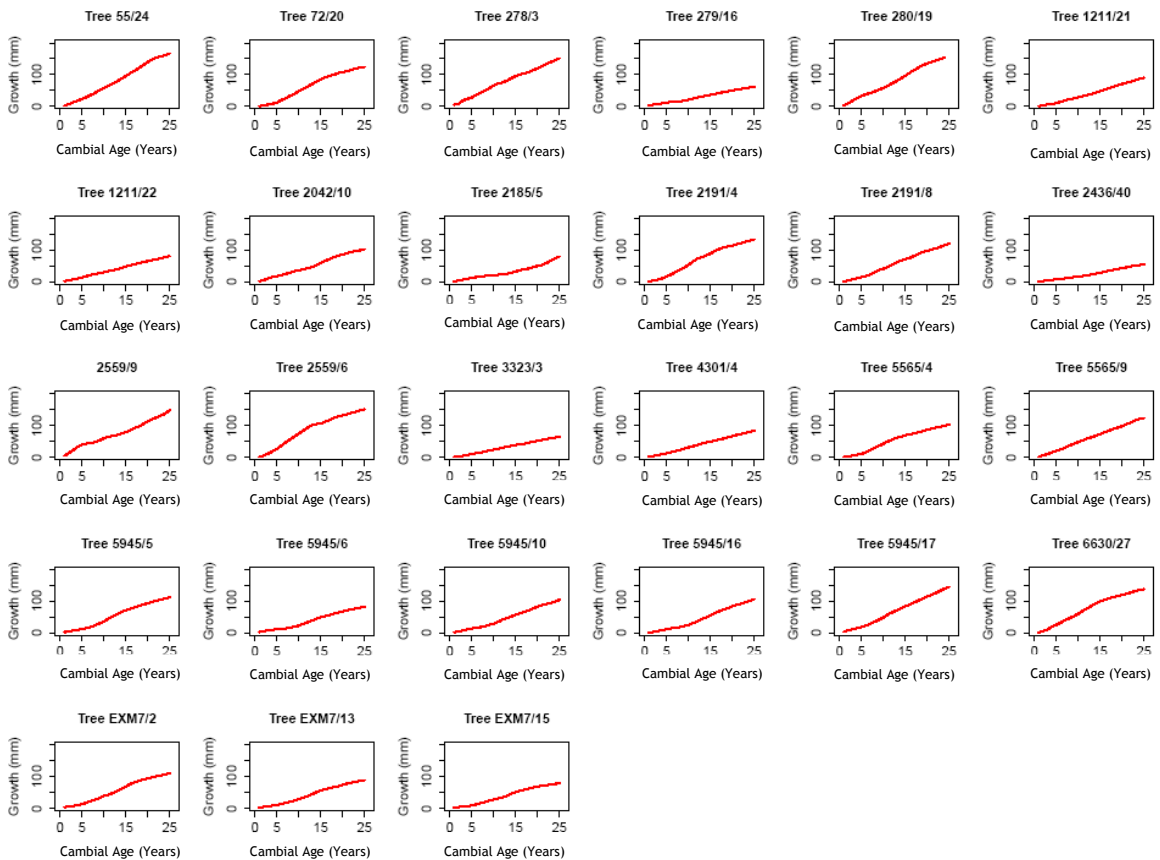


Figure 3-18: Growth rate of 27 trees which the Exp model could not fit.

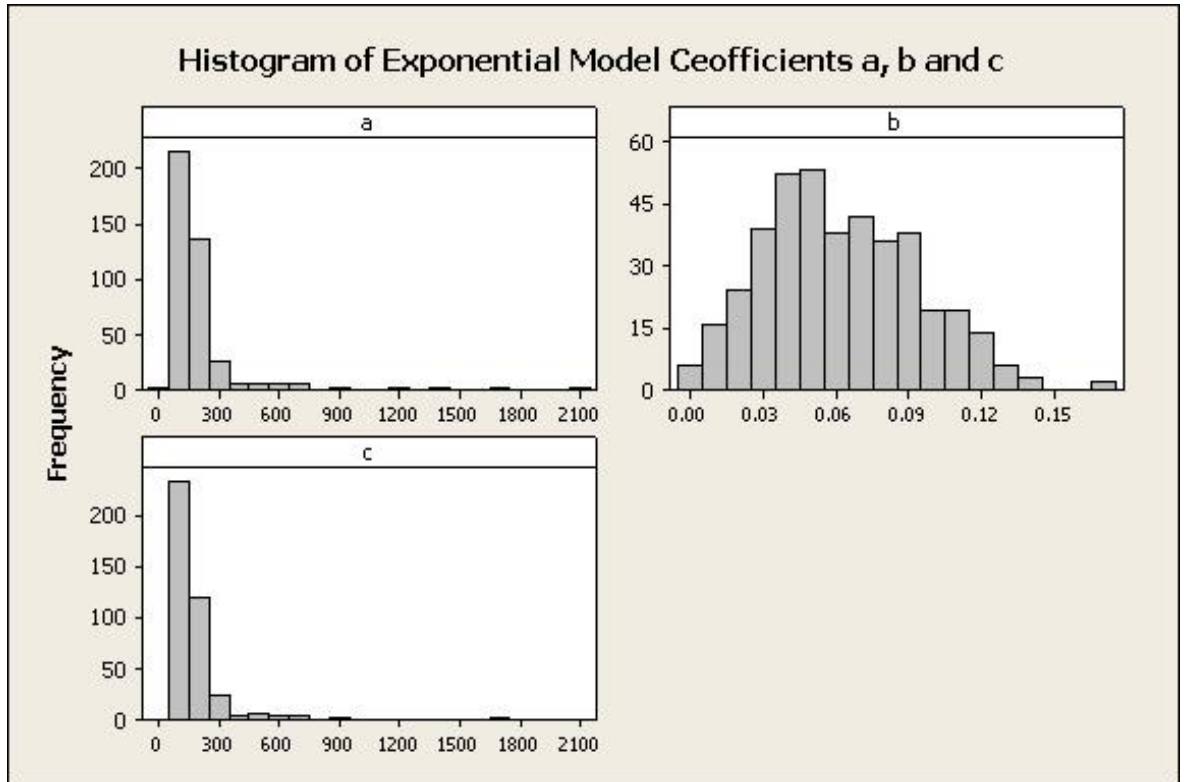


Figure 3-19: Histogram showing the frequency of the fitted coefficients for the Exponential Model

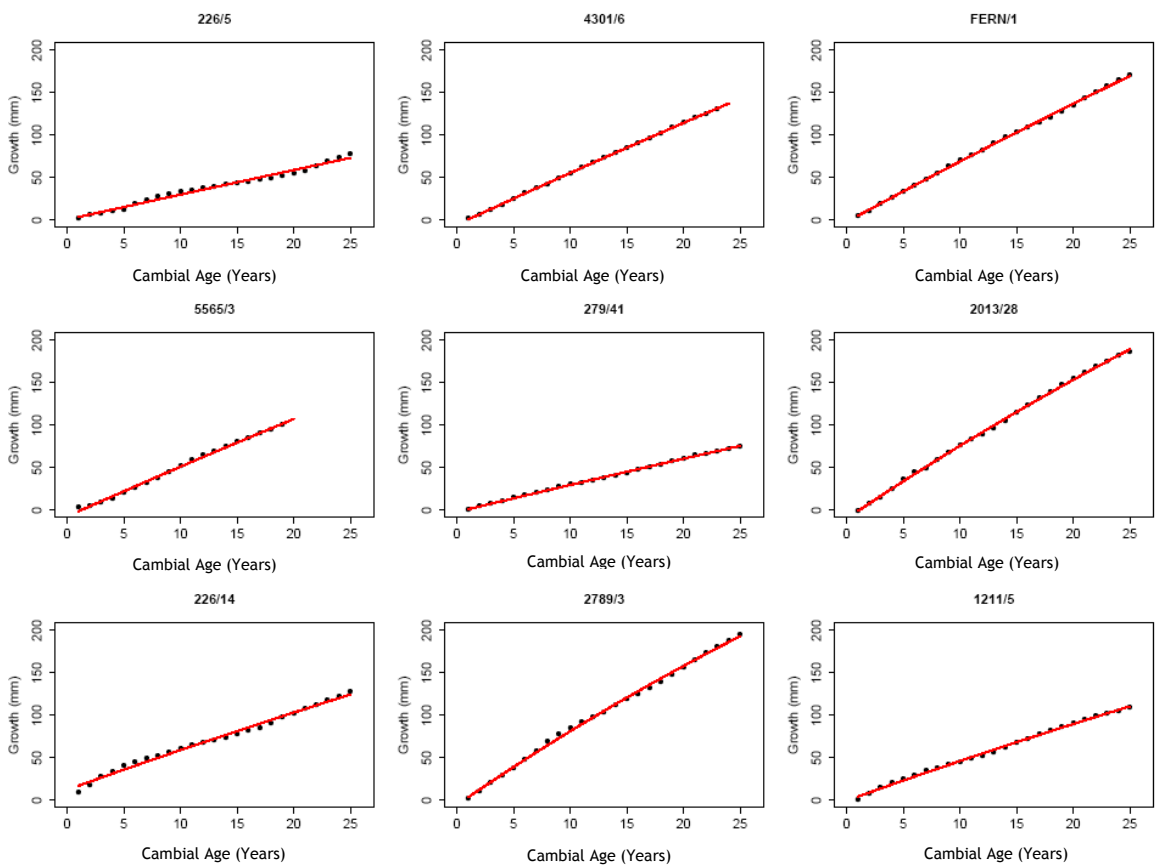


Figure 3-20: The 9 trees for which the Exponential model fitted the highest coefficients

Table 3-7: The nine highest coefficients that the Exp model fitted to the samples, where b_1 is the rate parameter, b_0 and b_2 are constants estimated from the data.

Tree ID	b_0	b_1	b_2
226/5	2069.6	0.001424	2070.4
4301/6	1743.0	0.003553	1737.7
FERN/1	1659.6	0.004356	1657.7
5565/13	1420.8	0.004193	1413.6
279/41	1202.6	0.002664	1200.7
2013/28	892.9	0.010073	883.1
226/14	886.5	0.005393	898.9
2789/3	745.8	0.012352	740.3
1211/5	740.3	0.006477	739.9

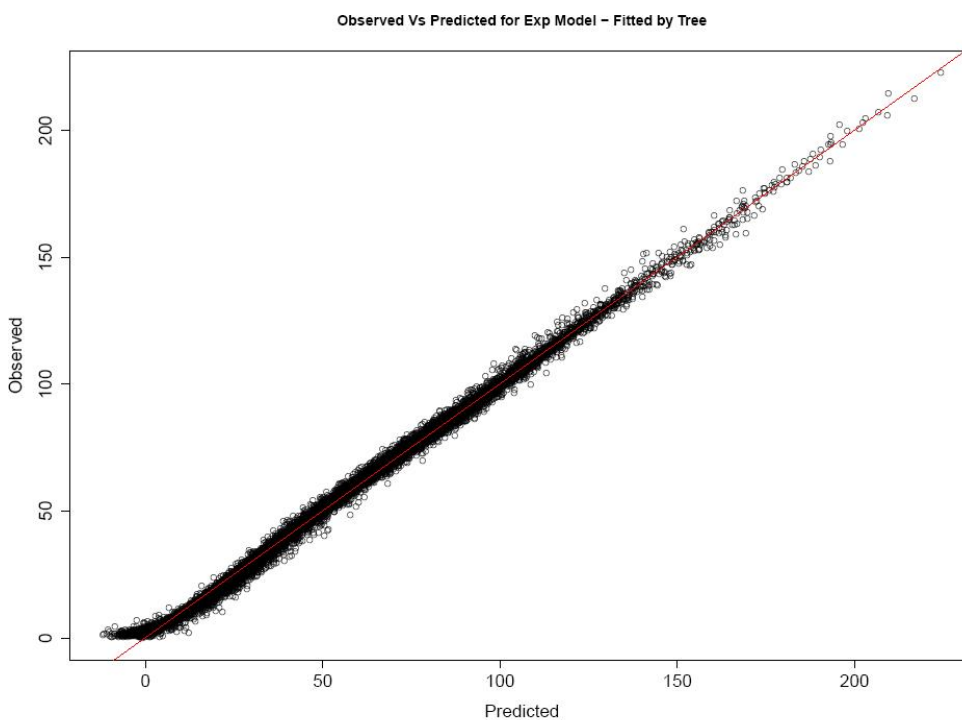


Figure 3-21: Observed Vs Predicted for Exp model when fitted to individual tree. R squared 0.9961

When observed versus the predicted growth values are plotted for the Exp model (Figure 3-21) it looks to be predicting very well (R-squared = 0.9961) when fitted against individual trees, except right at the pith (i.e. 0 mm) where it looks to be predicting negative values for growth. There may be a very slight curve to the data but this is not as pronounced as seen in both the MM and linear models.

When the residuals for the Exp model are plotted against cambial age any pattern to the data looks to have been smoothed out (Figure 3-22). When the residuals are plotted against distance from the pith it shows that there may be a

problem with this model right at the pith (Figure 3-23). As seen with the segmented models when the baseline was corrected to zero it made little difference to the residuals close to the pith (not shown).

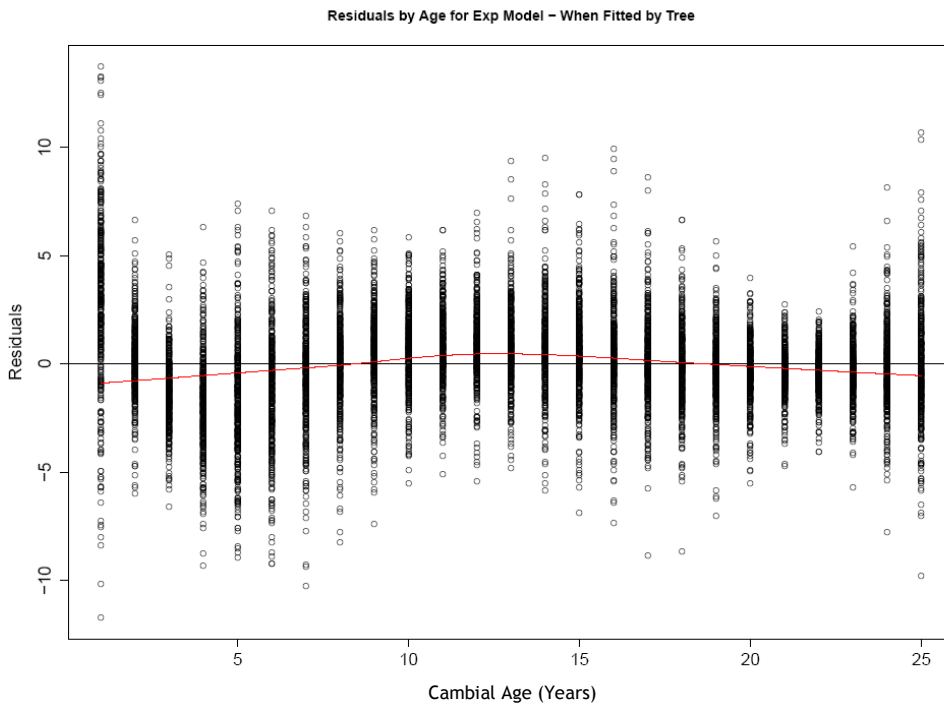


Figure 3-22: Residuals of Exp model when fitted to individual trees plotted against cambial age

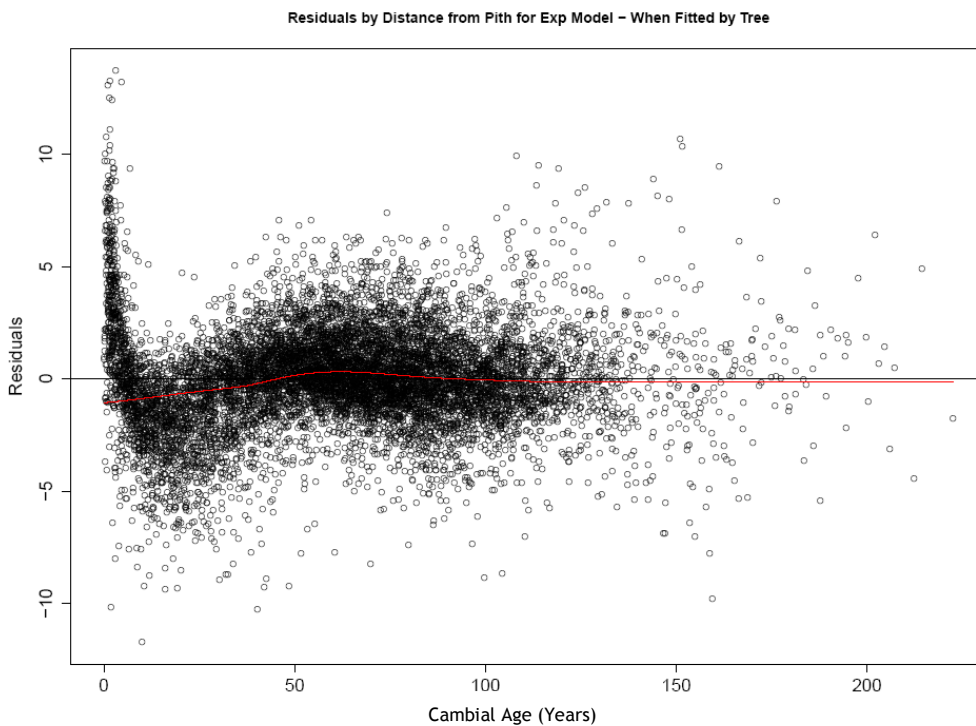


Figure 3-23: Residuals of Exp model when fitted to individual trees plotted against growth

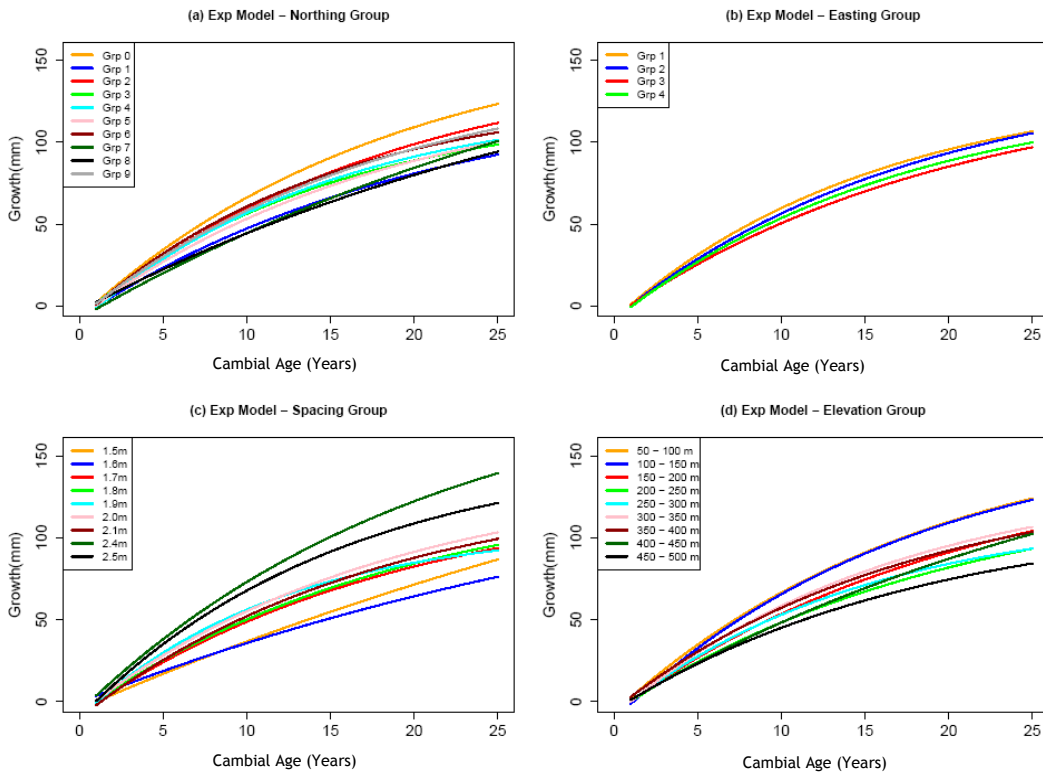


Figure 3-24: Coefficients of the Exp model plotted by northing, easting spacing and elevation groups

The graphs for the Exp model (Figure 3-24) seem to follow a very similar pattern to that of the Hossfeld4 model. Latitude may be having an effect but there does not seem to be any pattern to this effect. Longitude may be having a smaller effect. As before, spacing could be having a positive effect and elevation could be having a negative effect. Spacing looks to be having the largest effect with a difference of approximately 60 mm in growth between the highest and lowest group at year 25 which could translate to a difference of 12 cm to the diameter of the trees.

3.4.4 Segmented Model - Split between Juvenile and Mature Growth

In order to determine if there were two separate linear segments in the growth function, a Davies' test was carried out, indicating here that there was a significant change in the growth rate across the whole data set (p -value < 0.0001). Using the Segmented package in R (Muggeo, 2008) a regression model with segmented relationships was used to determine the parameters of the different slope segments (i.e. slope, intercept and break point). The result of this test gave an estimated mean split point between the juvenile and mature

growth segments at 11.6 years with a standard error of 0.26 and residual standard error of 20.14 mm.

3.4.4.1 Factors Affecting the Split Point

The effect that each treatment had on the split point between juvenile and mature growth can be seen in Figure 3-25 and Figure 3-26. Whilst there are some differences in the split point there does not seem to be any visible trend to these differences. These also show that the fits to individual trees included some high split points (>20 years) and some low split points (<5 years) which could be due to the sensitivity of the method to local fluctuations or could be indicative of the natural variation between trees in the position of the boundary between juvenile and mature growth. In a study on juvenile wood in Norway spruce Lindstrom states that juvenile (or core) wood in conifers could be anywhere between the first 3 to 32 rings (Lindstrom, 2002) so the range in split points found here could be feasible.

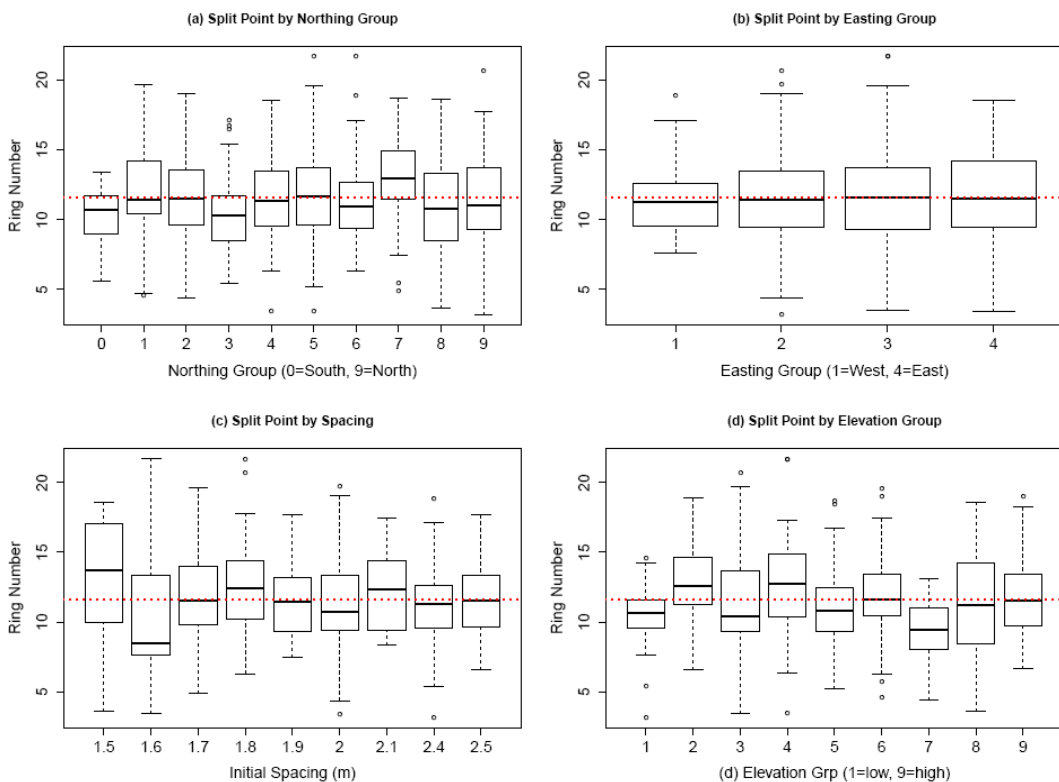


Figure 3-25: The split point between juvenile and mature growth segments plotted by Northing, Easting Spacing and Elevation. The dashed line shows the value (11.6 years) when modelled against the global data.

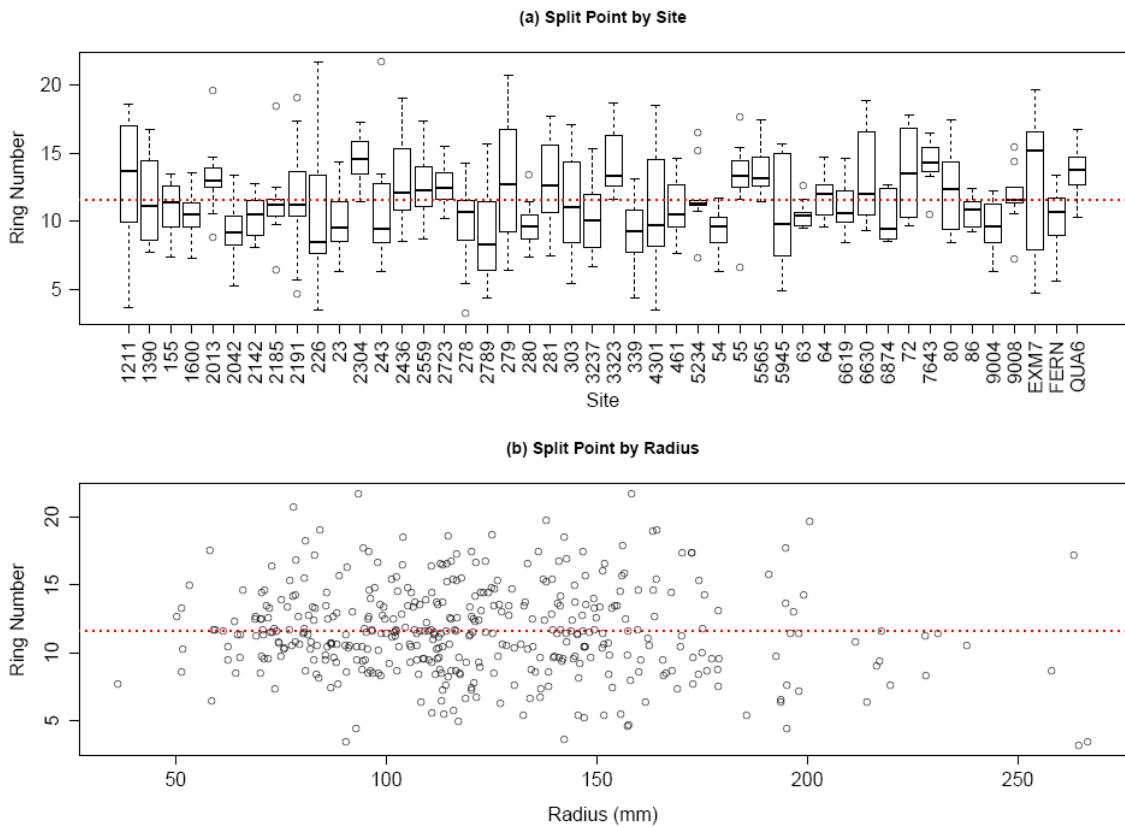


Figure 3-26: The split point between juvenile and mature slopes plotted by Site and radius. The dashed line shows the value (11.6 years) when modelled against the global data.

Figure 3-26 shows that there are visible differences in the split points between sites (a) and also a large variation within some sites. A slight decrease in split point with increasing length of samples is suggested but analysis of variance (ANOVA) shows that this was not significant ($p=0.069$) indicating that the age where there is a change from juvenile to mature growth is not dependent on the amount of growth.

3.4.4.2 Split Point Fitted to Individual Trees

A segmented model seems to work well when fitted against the global data and also when fitted against individual trees to give the growth rates, intercepts and split point for each. By calculating the Davies Test for each tree individually it was determined whether or not there was a significant change in slope. If the Davies Test was not significant then only one slope was calculated for that tree i.e. with no break point (e.g. sample 1211-22-A in Figure 3-27).

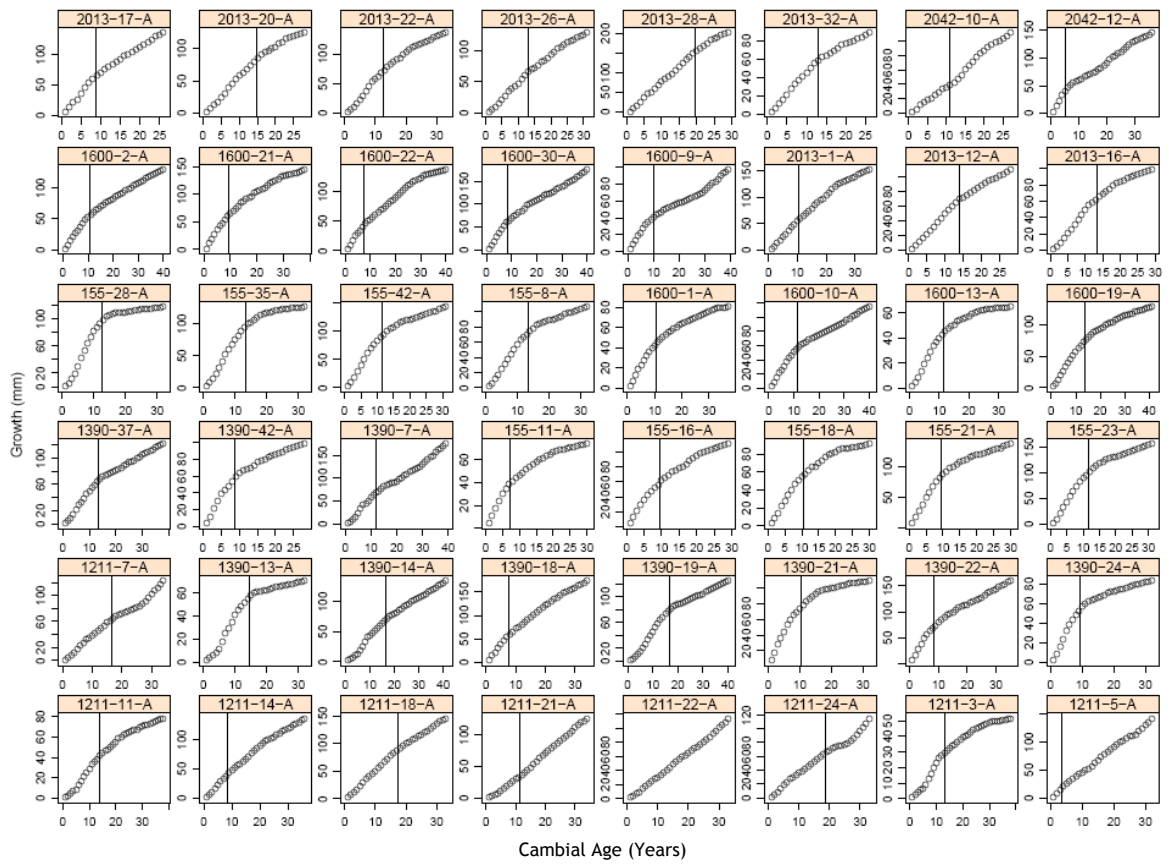


Figure 3-27: Observed growth and breakpoint fitted by the segmented model on a selection of benchmark trees

On this data set the segmented model was unable to fit a split point to 10 of the 442 samples, the growth of which are shown in Figure 3-28. There were also 16 trees where the juvenile growth rate was found to be lower than the mature growth rate (Figure 3-29) but where the difference was still found to be significant.

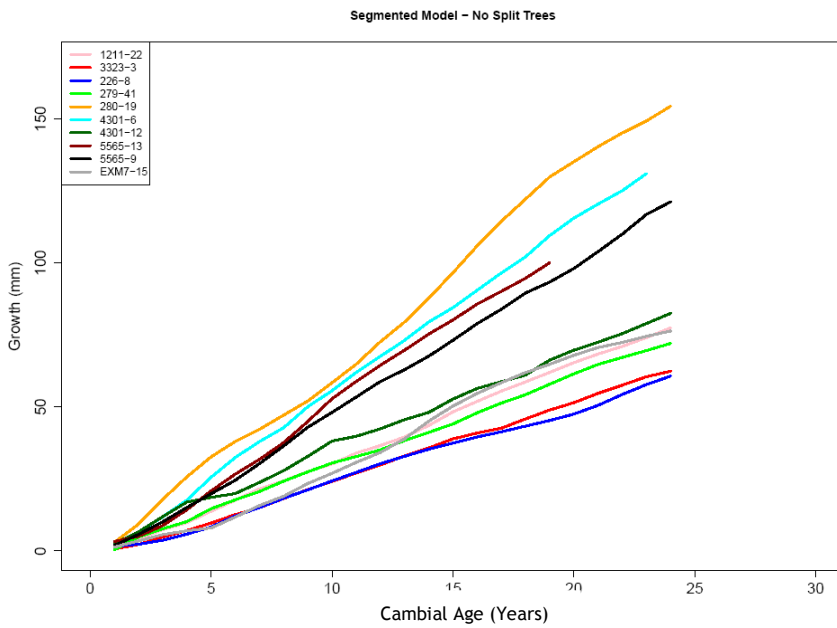


Figure 3-28: Growth rates for trees which the segmented model couldn't fit a split point.

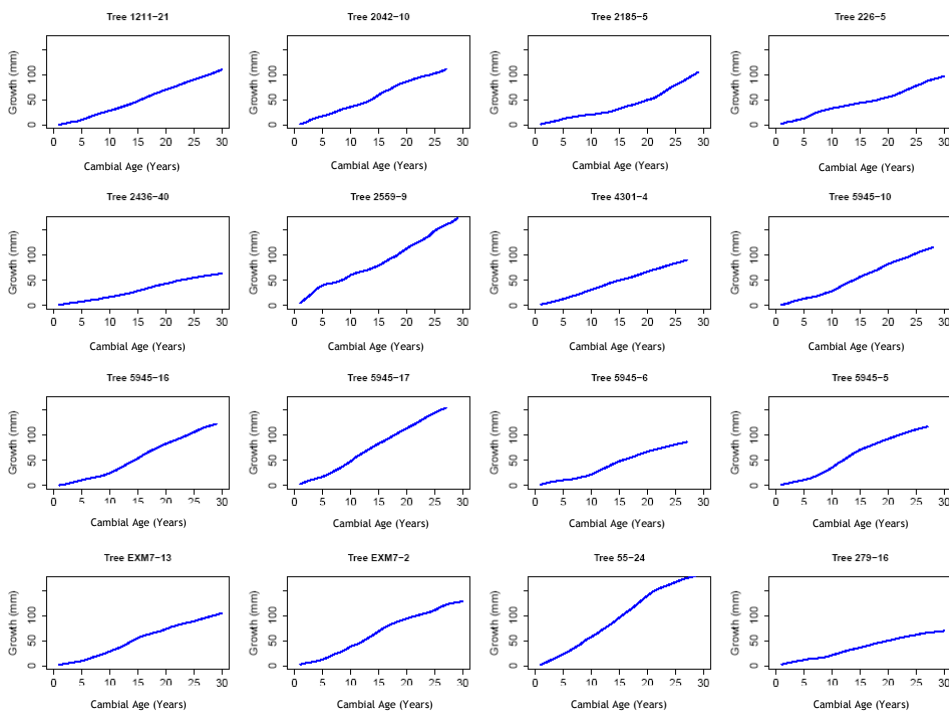


Figure 3-29: Growth of trees where the segmented model fitted the mature growth rate to be greater than the juvenile growth rate

When the observed values are plotted against the predicted values for individual trees Figure 3-30 it shows there is a very good fit with an R-Squared value of 0.99.

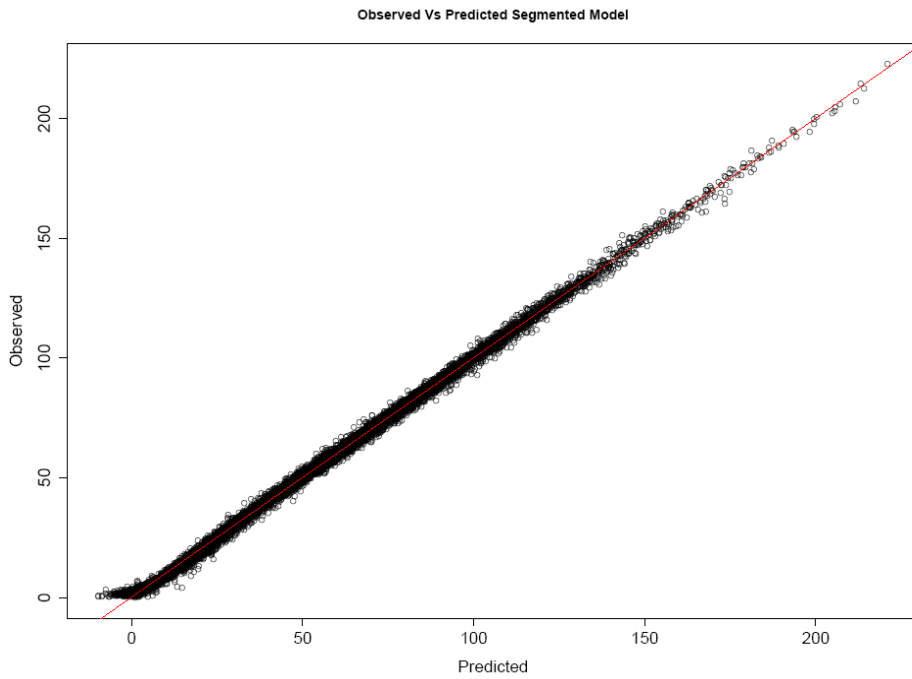


Figure 3-30: Observed Vs Predicted for the two segment model when fitted individual trees.

While the two segment model gives a good fit when modelled against the global data, the sensitivity when it is modelled against individual trees produced some very low estimates for the split point as well as some high estimates (Figure 3-31) indicating that this method of calculating the split point on individual trees may be too sensitive to local fluctuations in growth. However, further investigation would indicate that the model may in fact be fitting the lowest (Figure 3-32) and highest (Figure 3-33) split points correctly in most of the cases.

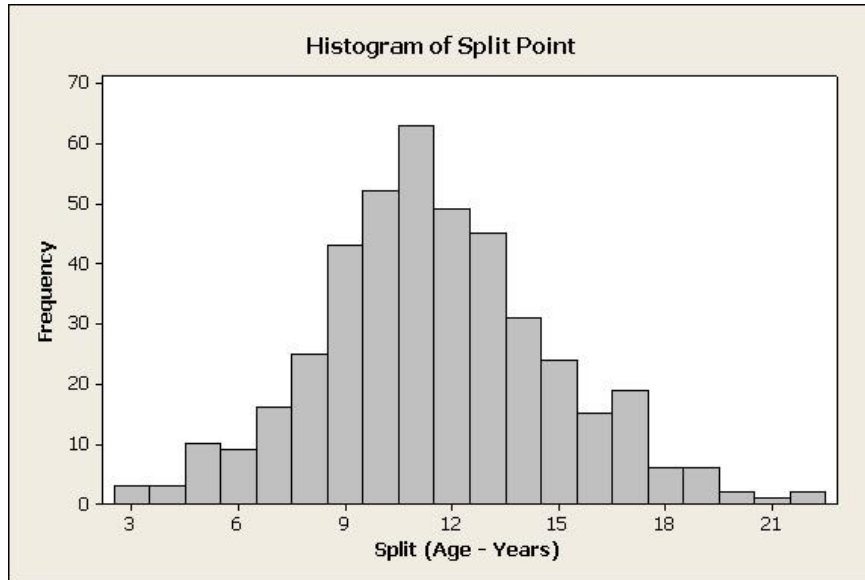


Figure 3-31: Histogram showing the distribution of split points between the juvenile and mature growth segments fitted by the segmented model on growth.

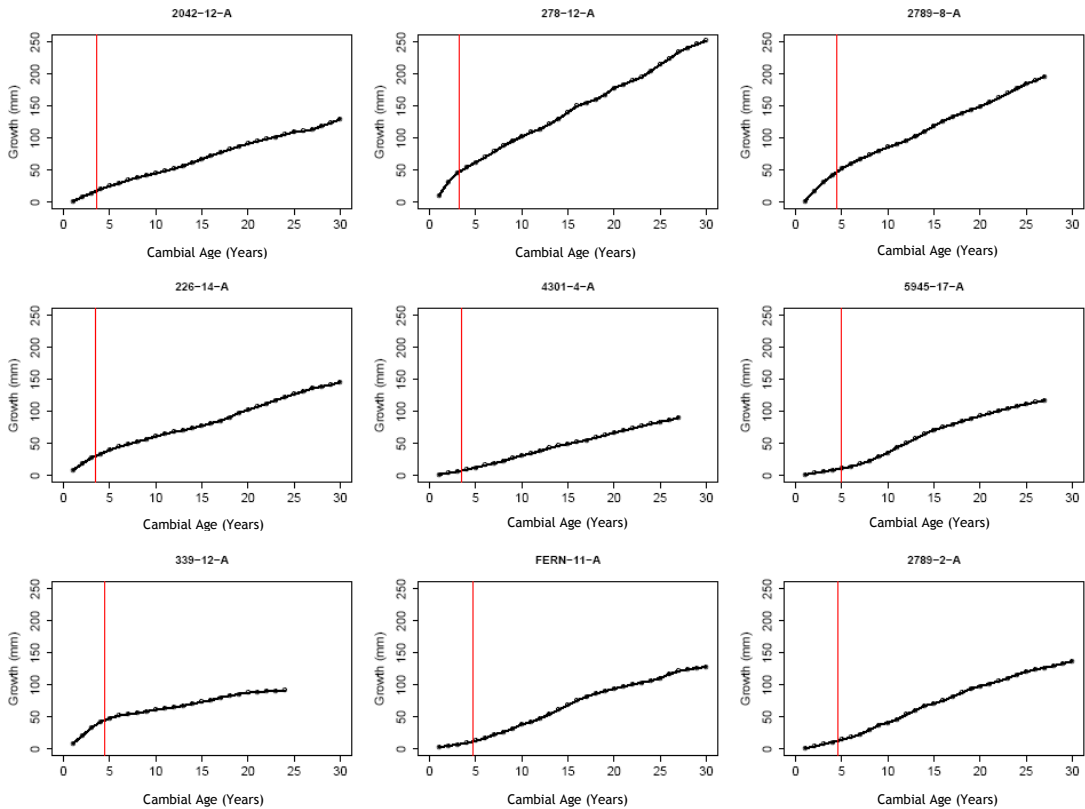


Figure 3-32: Growth of the nine trees with the lowest split points fitted by the segmented model.

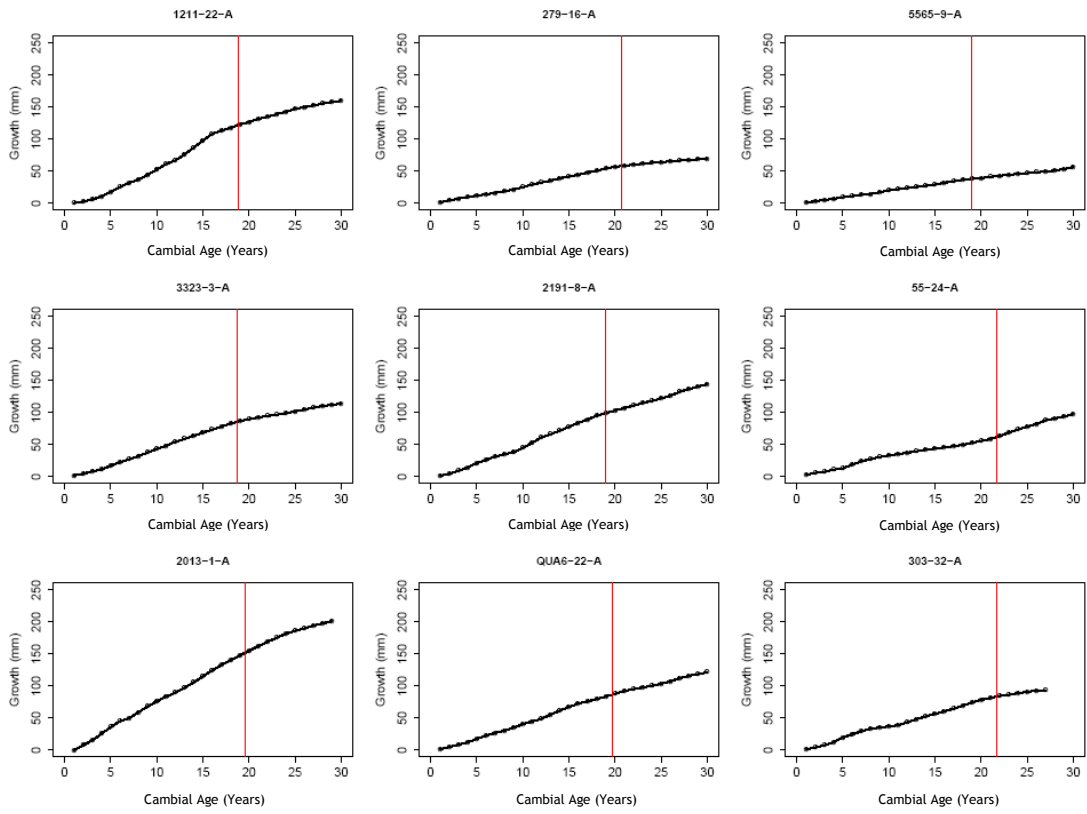


Figure 3-33: Growth of the nine trees with the highest split points fitted by the segmented model

3.4.5 Segmented Model - Juvenile and Mature Growth

Before going on to use the models to test statistically which treatments, if any, are having an effect on growth rate, this section will test how each model fits the global data and how the models fit to individual trees.

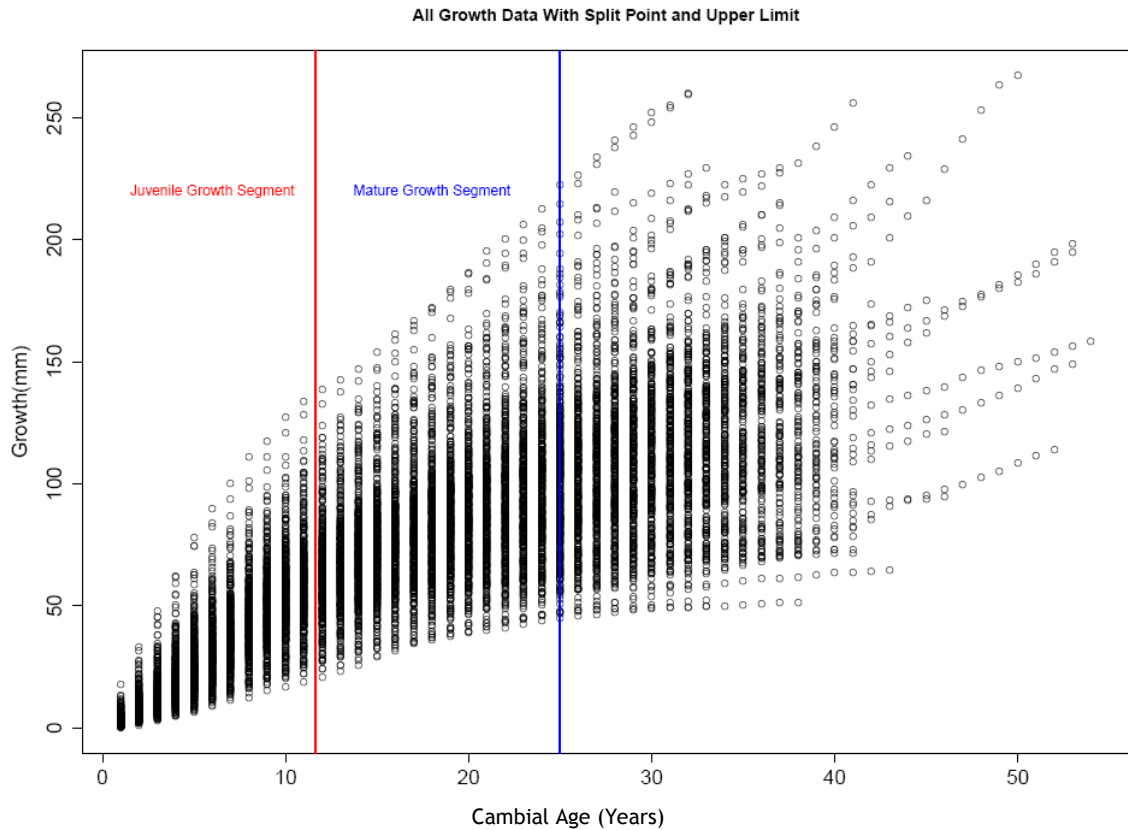


Figure 3-34: All benchmark growth data with red line showing where segmented model fitted the split between juvenile and mature wood (cambial age 11.6) and the upper limit of ring 25 (blue).

When the segmented model was fitted against the global data it gave a split between juvenile and mature growth at between year 11 and 12 with two separate linear segments: the juvenile section before the split point (cambial age 1 to 11 years) and the mature section (cambial age 12 to 25 years).

Therefore it may be possible to use a fixed split point to examine the growth of the different segments separately, i.e. the growth rate up to cambial age 11 and the growth rate over cambial age 12 but below cambial age 25 as shown in Figure 3-34. When looked at separately growth appears linear up until year 11 (Figure 3-35) and also looks relatively linear between year 12 and 25 (Figure 3-36) so it would appear reasonable to continue analysing growth under year 12 and between year 12 and 25 using two linear models.

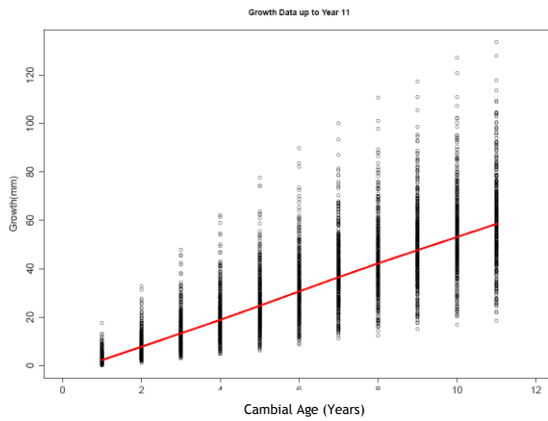


Figure 3-35: Growth up to year 11 (juvenile growth) with LOWESS trend line

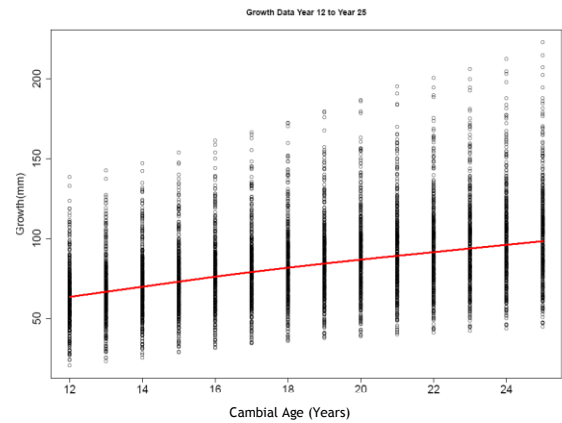


Figure 3-36: Growth from year 12 to year 25 (mature growth) with LOWESS trend line

3.4.5.1 Juvenile Growth: Site Effects

In order to get a visual impression of how the different treatment variables affect the model, the coefficients for the two segments were plotted. The intercept of the juvenile growth rate is shown in Figure 3-37 and would seem to indicate that there was not much effect of latitude (a) or longitude (b) on the intercept and analysis of variance shows that there are no significant differences due to either of these effects ($p=0.21$ and 0.54 respectively). Although there may be an increase in the spread with increasing spacing (c) there does not seem to be any increase or decrease with increasing spacing. Statistical analysis using ANOVA showed that there is no difference between the spacing groups ($p=0.47$). There may be a slight increase in the juvenile intercept with increasing elevation (d) but analysis showed that this was not significant ($p=0.079$).

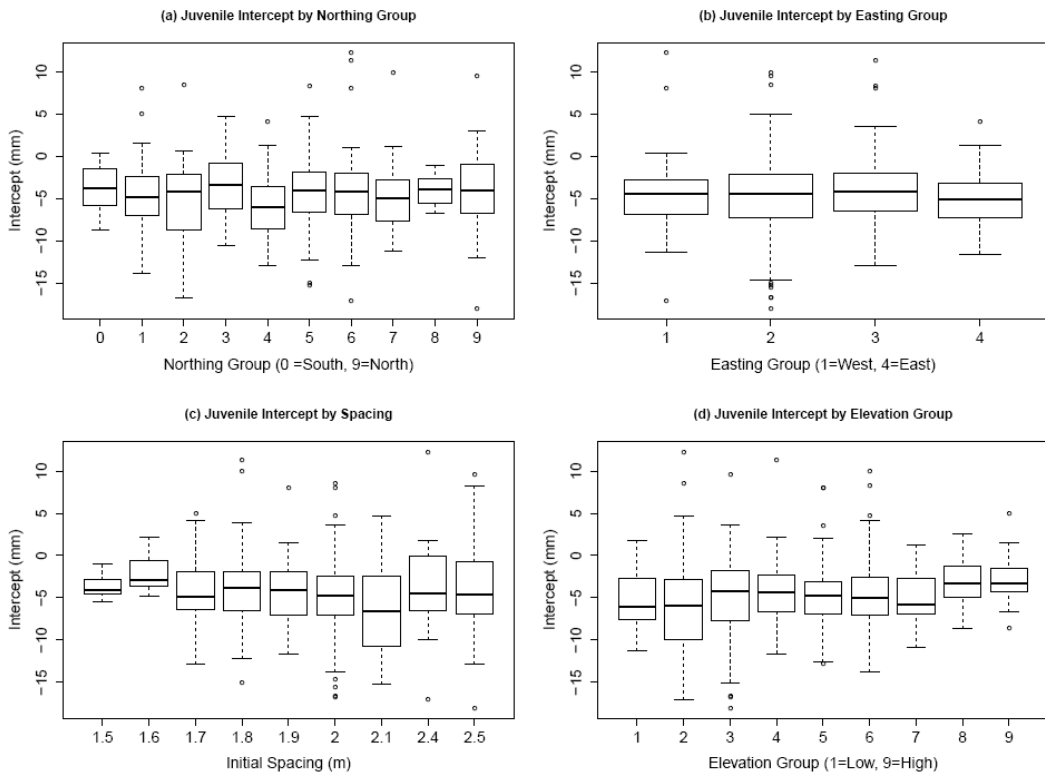


Figure 3-37: Intercept coefficients of the juvenile growth section plotted by northing, easting spacing and elevation groups

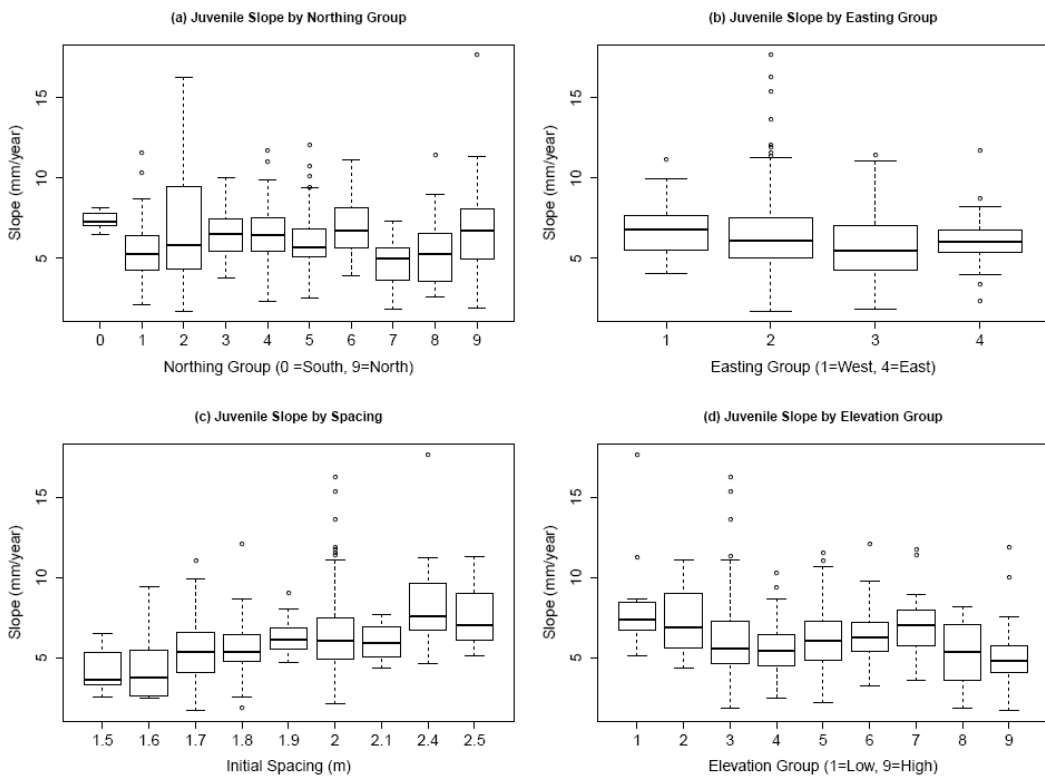


Figure 3-38: Slope coefficients of the juvenile growth section plotted by northing, easting spacing and elevation groups

Although there may be differences in the juvenile growth rate Figure 3-38 with latitude (a) ($p < 0.0001$ when tested with ANOVA) there does not seem to be any pattern to the differences. Spacing (c), however, does appear to have an effect on the juvenile growth rate with the rate increasing as spacing increases, but the very irregular distribution of sites between spacing groups means that this should be regarded with caution. The juvenile growth rate appears to decrease as elevation increases and again analysis of variance shows there are differences between the elevation groups ($p < 0.0001$).

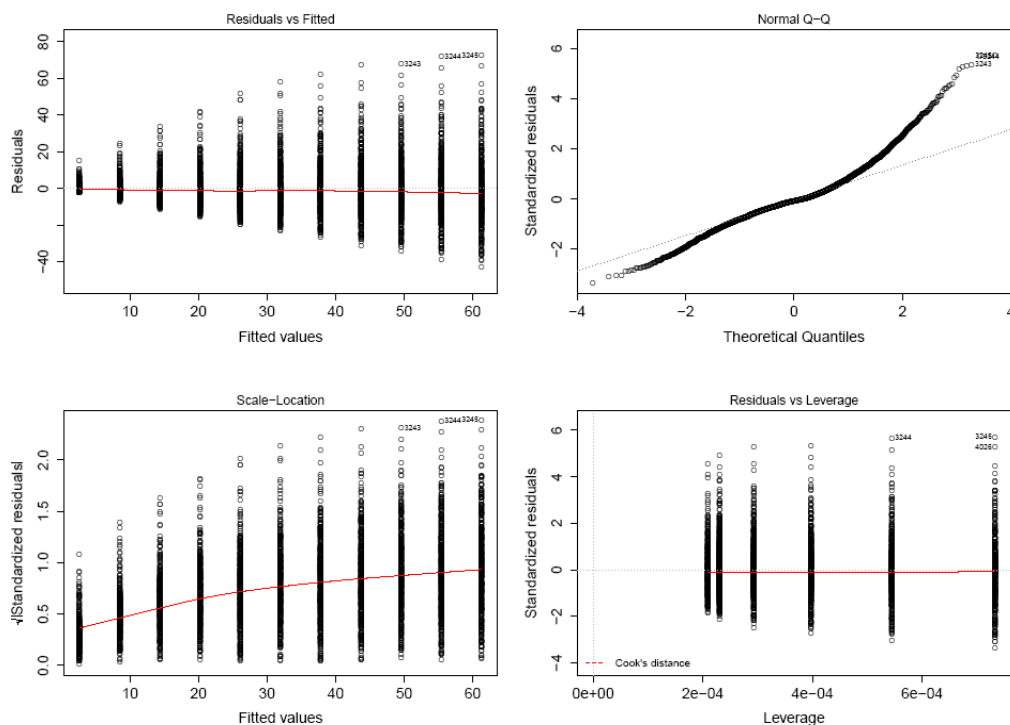


Figure 3-39: Residuals for the linear model of rings 1 to 11

When a linear model was fitted to the first 11 rings of all the data together it gave a reasonably good fit with an R-squared of 0.68. The residual plots for the linear model on the juvenile growth Figure 3-39 show there may be a problem as the variance in residuals increases as the fitted values increase. This, however, may be due to the fact that growth measurements are starting at zero and the variance is increasing as the magnitude of difference increases.

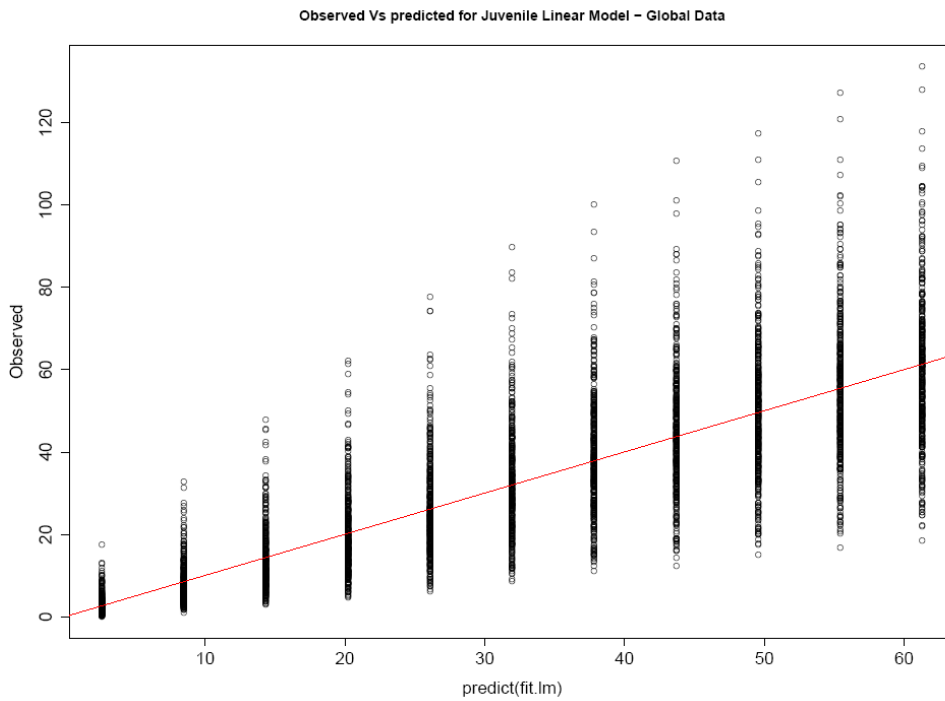


Figure 3-40: Observed Vs predicted growth for the juvenile segment of the linear model. Red line shows the line of equality

Although the linear model was able to describe the age related trend in growth for the juvenile segment reasonably well there is a lot of variation between trees when the observed values are plotted against those that the model predicts (Figure 3-40).

3.4.5.2 Linear Model Fitted to Individual Trees - Juvenile Growth

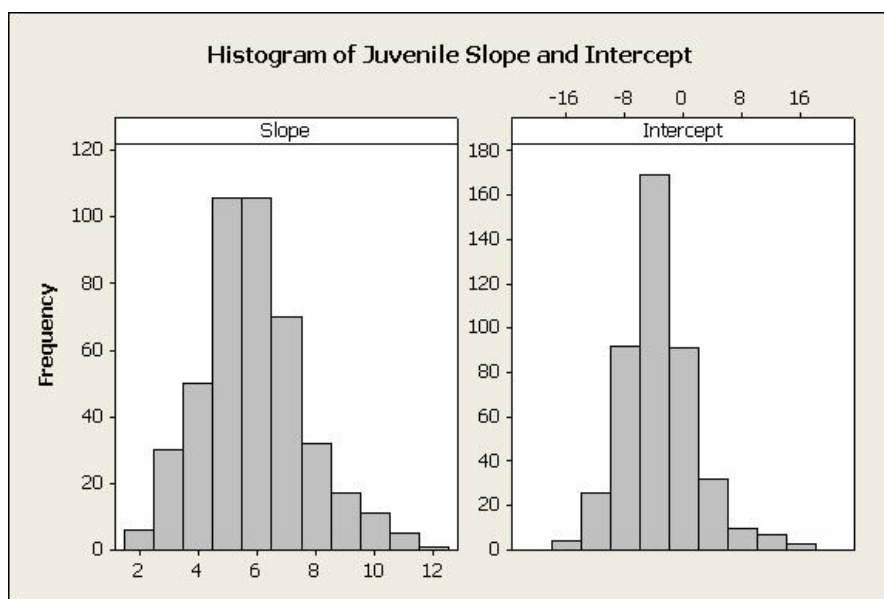


Figure 3-41: Intercept and Slope coefficients fitted by a linear model to growth between cambial age 0 to 11 years old for each sample.

When a linear model was fitted to the juvenile growth section of each tree individually the fitted coefficients, i.e. slope and intercept, showed wide variation (Figure 3-41) with the intercept ranging from approx. -16 to 16 mm and the slope (i.e. growth rate) ranging from approx. 2mm to 12mm per year. The residuals no longer had the same spread with increasing age (Figure 3-42), but it appeared that a straight line was being fitted to a curve. This is also evident when the observed data is plotted against that predicted by the linear model (Figure 3-43) where there is a slight curve from years 1 to 11.

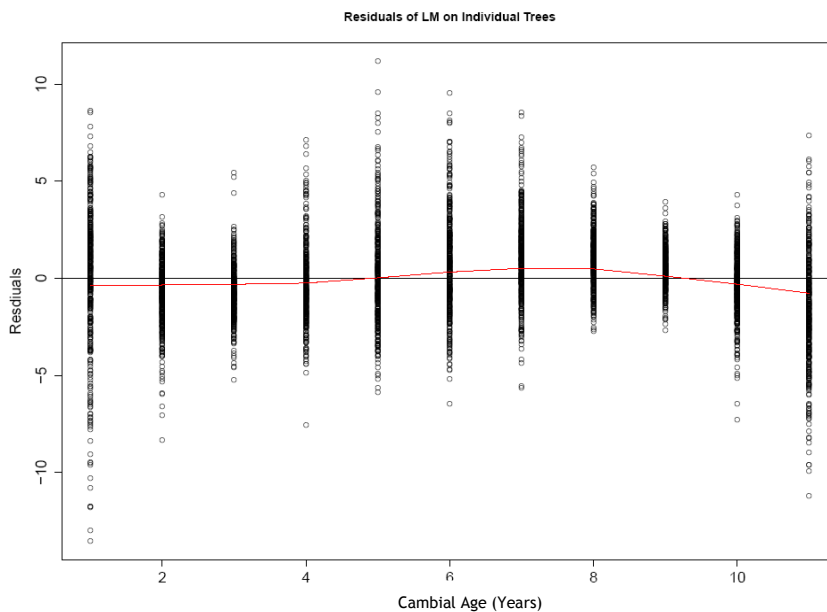


Figure 3-42: Residuals of linear model when fitted to the juvenile growth of each tree with LOWESS trend line (red).

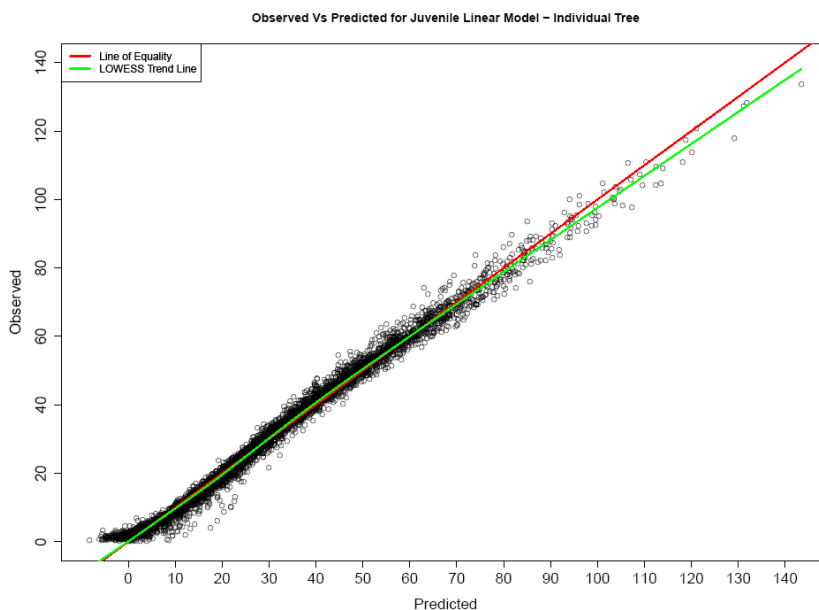


Figure 3-43: Observed Vs predicted for the juvenile linear model giving an R-squared of 0.99

3.4.5.3 Mature Growth Segment

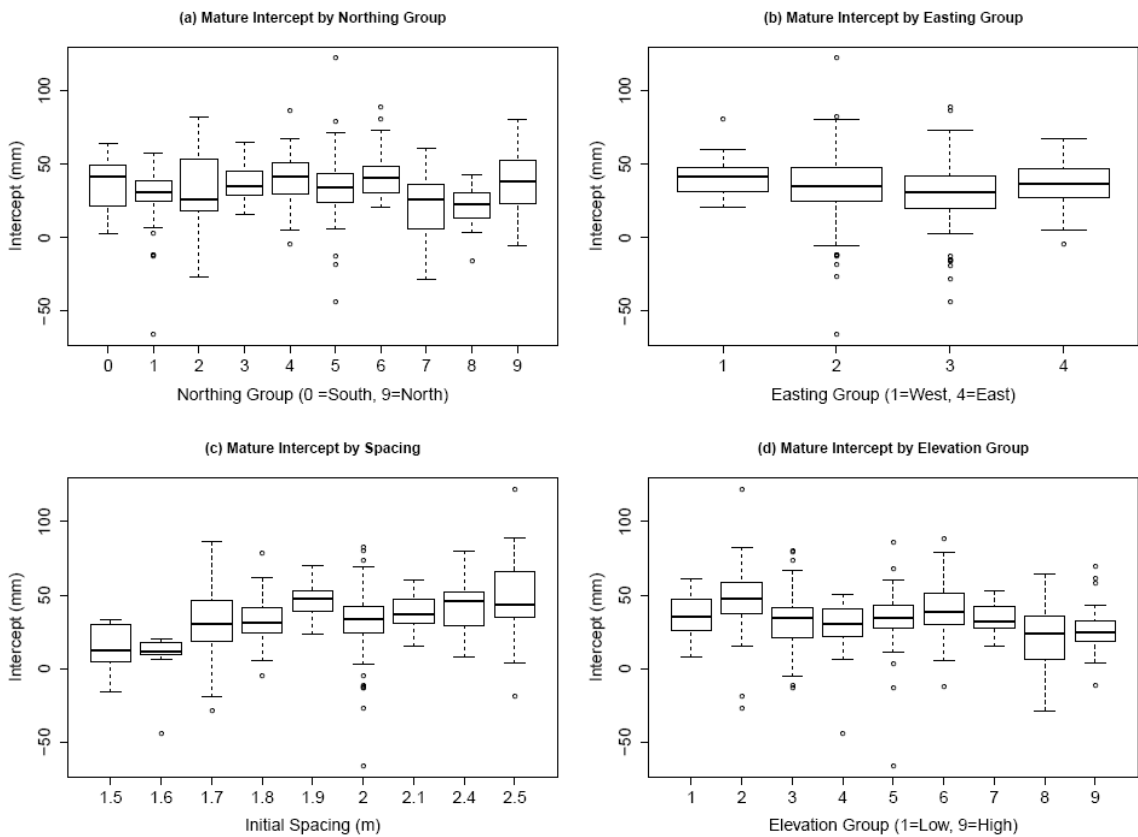


Figure 3-44: Intercept coefficients of the mature growth section plotted by northing, easting spacing and elevation groups.

Figure 3-44 shows that spacing (c) may have a positive effect on the mature intercept and statistical analysis shows that there are differences between the groups ($p < 0.0001$). This makes sense since there is a relationship between the mature intercept and the juvenile growth rate on which spacing also looked to be having an effect. While statistical analysis also shows that there are differences between the groups for latitude and elevation ($p < 0.0001$ for both) and also longitude ($p = 0.01$) it is difficult to see any logical pattern for these effects.

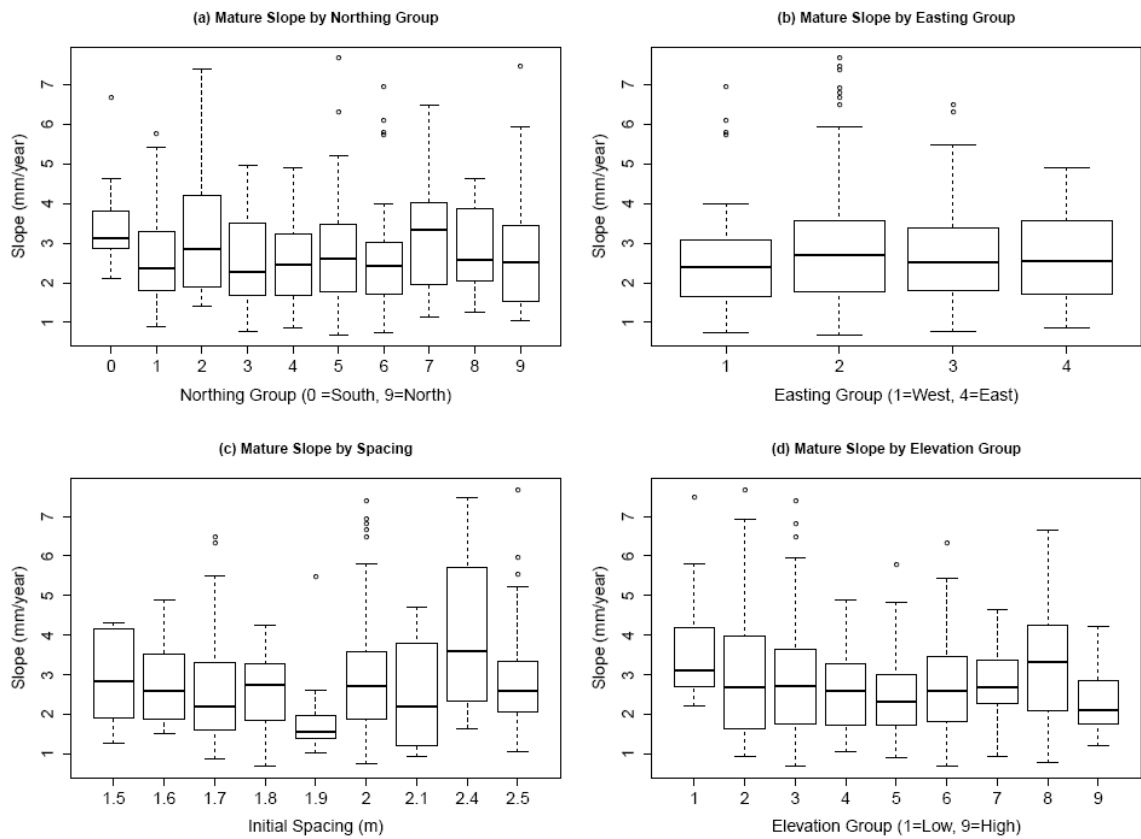


Figure 3-45: Slope coefficients of the mature growth section plotted by northing, easting spacing and elevation groups.

The plots in Figure 3-45 show that there does not seem to be any pattern to the effect of any of the treatments on the mature growth rate. There may be a slight negative effect of elevation but it is difficult to see from these graphs alone and statistical analysis using ANOVA shows that there are differences between the elevation groups ($p < 0.001$). Northing groups ($p = 0.039$) and spacing groups ($p < 0.0001$) are also significantly different but again it doesn't look like there is any pattern to the differences. The easting groups are not significantly different ($p = 0.59$).

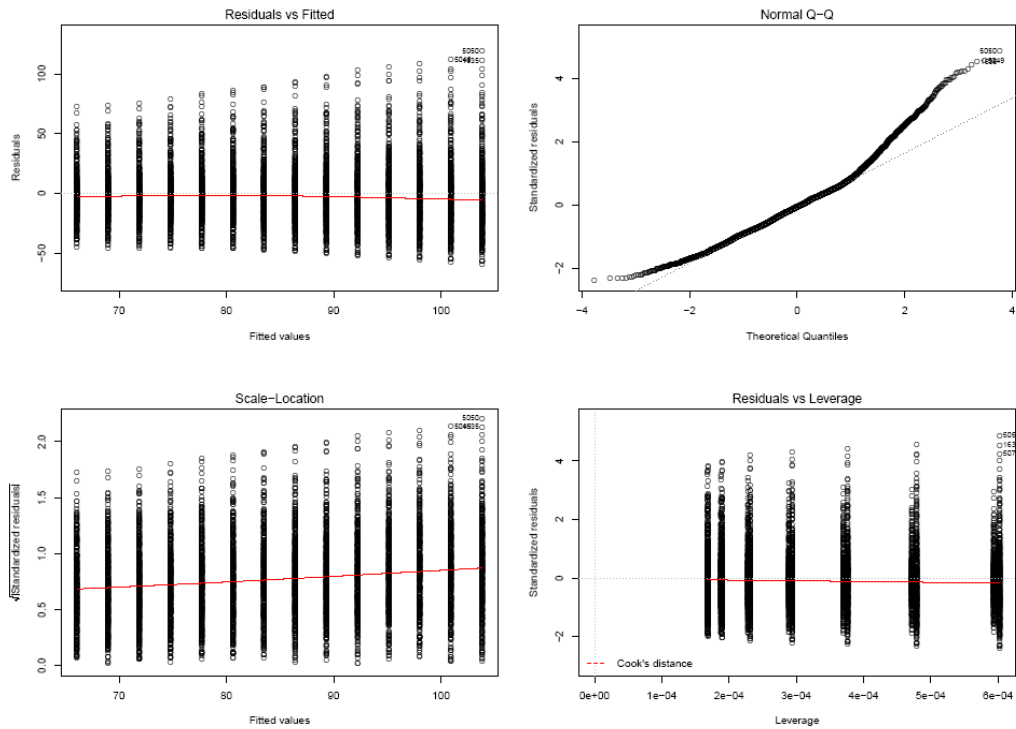


Figure 3-46: Residuals for the linear model of rings 12 to 25.

Fitting a linear model to growth of rings 12 to 25 gives an R-squared of 0.19 which may be a reflection of the large amount of variation in the intercept. The residuals for the linear model (Figure 3-46) also are showing an increase in magnitude with age which may be due to the growth rates increasing at different rates. If the intercept is set to zero (by subtracting year 11 growth from all subsequent years) the R-squared is improved to 0.47 but further analysis of this method (not shown here) showed no improvement in the overall model.

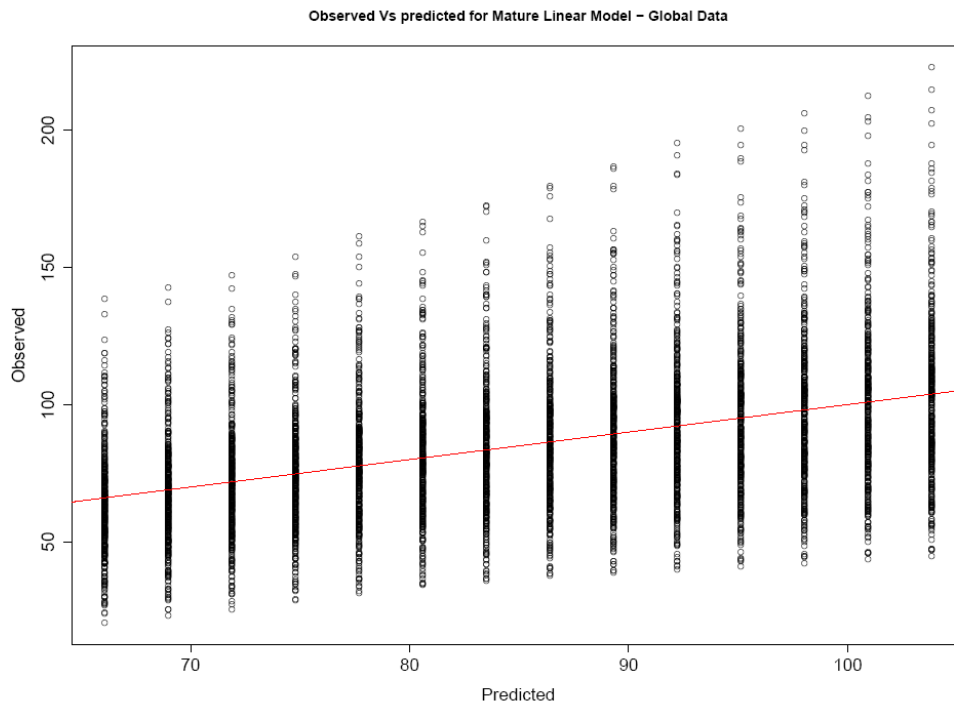


Figure 3-47: Observed Vs predicted growth for the mature segment of the linear model. Red line shows the line of equality, R squared = 0.1856

As with juvenile growth, in the mature segment the model was able to describe the age related trend reasonably well although again there is a lot of variation between trees in the observed versus predicted growth (Figure 3-47) tending to increase with increasing growth.

3.4.5.4 Linear Model Fitted to Individual Trees - Mature Growth

The coefficients derived by fitting the linear model to each individual tree in the mature section of growth show that there is considerable variation in both the intercept and the growth rate between trees. Figure 3-48 shows that the fitted intercepts varied from approx. -20mm to just over 80 mm, and the growth rate fitted by the model varied from approx. 0 mm per year to approx. 8 mm per year.

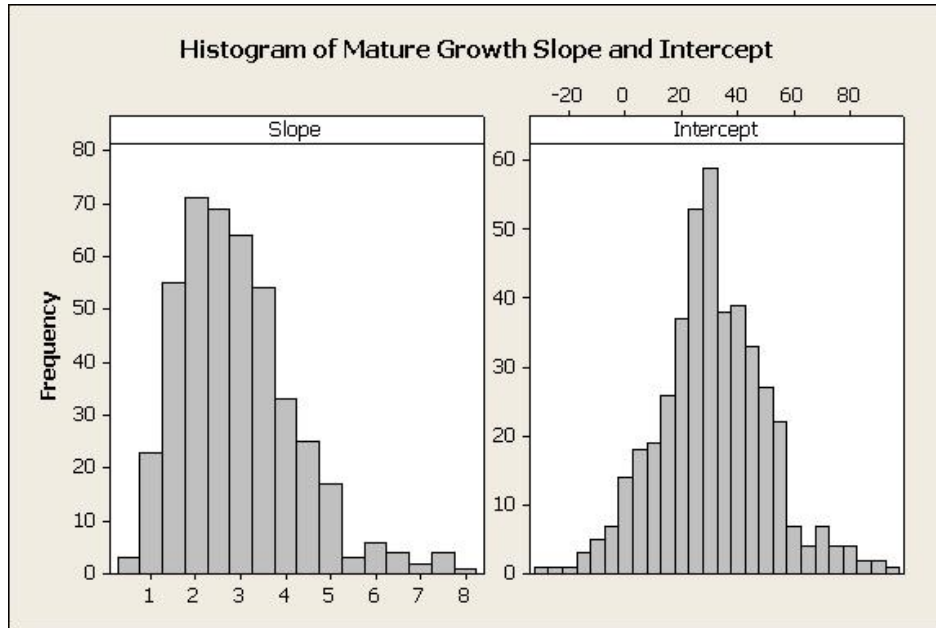


Figure 3-48: Intercept and Slope coefficients fitted by a linear model to growth between cambial age 12 to 25 years old for each sample.

When the model was fitted to each tree individually the residuals (Figure 3-49) no longer had the same spread with increasing age that was seen when modelled against the global data but, as with the juvenile segment, the residuals may indicate that a linear model is being fitted to a curve. This is not as obvious when the predicted values are plotted against the observed (Figure 3-50) which do not show the same curved pattern as seen in the juvenile section due to the small magnitude of the residuals relative to the observed values.

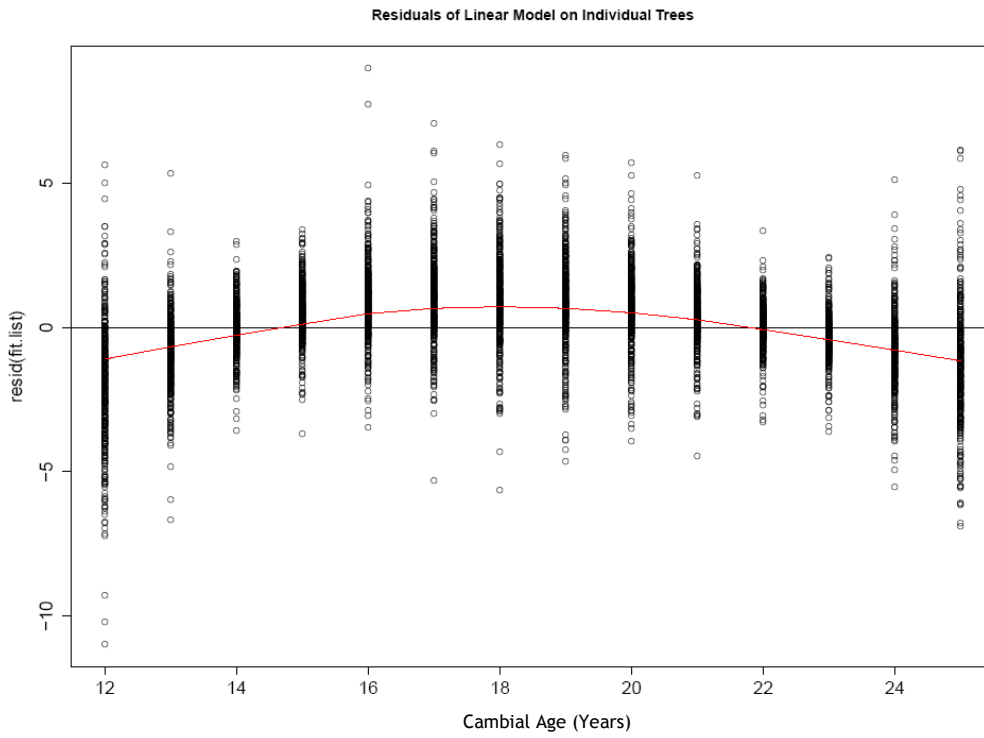


Figure 3-49: Residuals for the mature growth section when linear model is fitted to each tree individually.

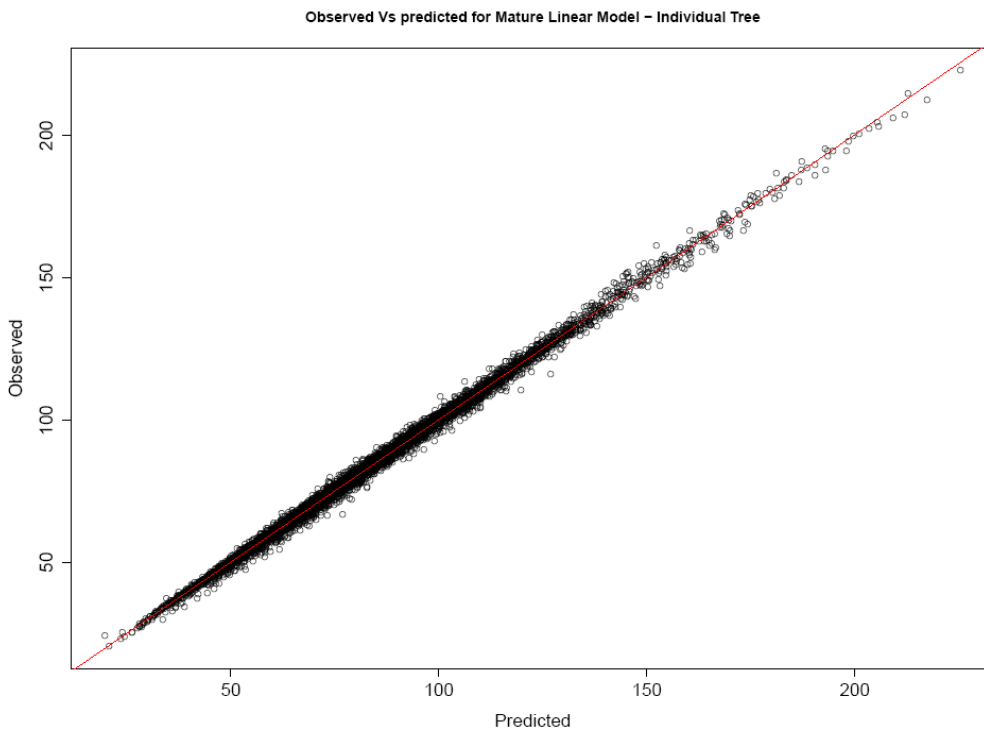


Figure 3-50: Observed Vs predicted for the mature linear model fitted to individual trees, giving an R-squared of 0.99

When the linear model residuals plotted against the observed values for juvenile and mature segments are combined it shows that there may be a discrepancy at the region close to the pith (Figure 3-51) where the model is under predicting. Many trees had 1-3 narrow rings close to the pith which led to a small negative intercept in the juvenile segment, and hence to the residuals shown.

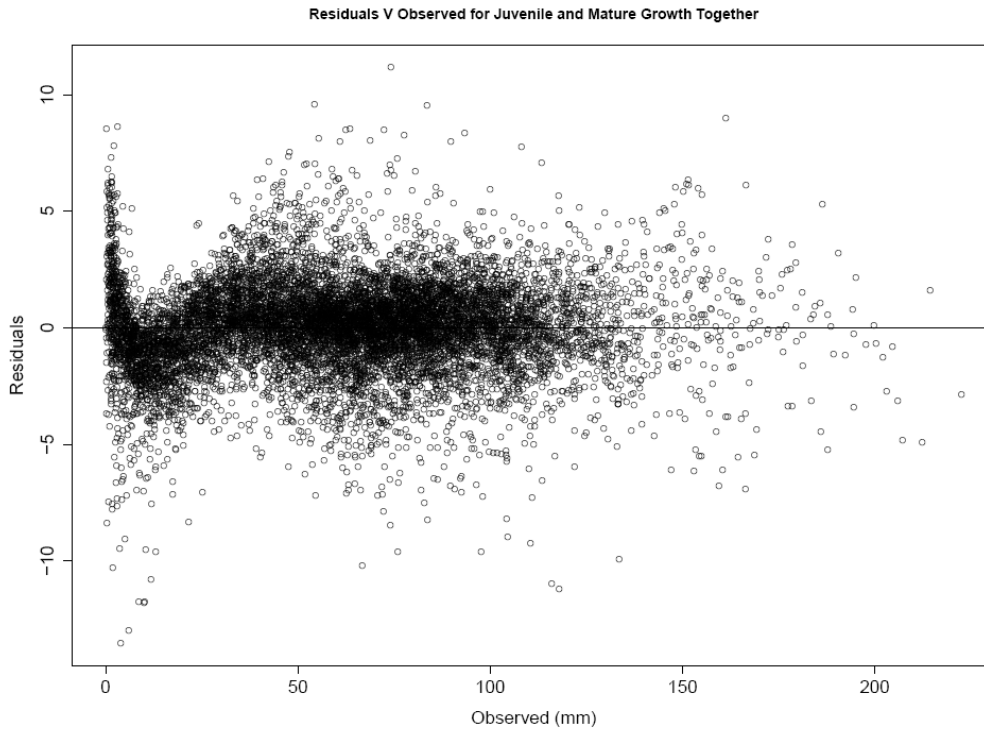


Figure 3-51: Residuals for linear model on the juvenile and mature segments combined

3.4.6 Linear Mixed Effects Models

3.4.6.1 Mixed Effects Model of Juvenile Growth

Due to the unbalanced nature of this data set and to account for the hierarchical experimental design a mixed effects model was used to analyse the variation in growth of both the juvenile and mature growth linear sections. In this analysis site and tree within site were the random effects:

$$Y_{ijk} = \mu + S_i + T_{ij} + \epsilon_{ijk} \quad (\text{Equation 3.19})$$

Where Y_{ijk} is radial growth, μ is the overall mean, S_i is the random effect of site, T_{ij} is the random effect of tree within site and ϵ_{ijk} is the residual error which is attributed to within tree variation.

When the mixed effects model was fitted without fixed effects a variance components analysis showed that approximately 82% of the variation in growth was within tree variation, 7% was between trees in the same site and 10% was between sites. Once age has been taken into account the model predicted an intercept of -3.2mm and a growth rate of 5.9 mm/year with the within tree variation reduced to approximately 24%, just over 44% of the variation being between trees at the same site and approx. 31% being between sites.

However, this is fitted with only the intercept as a random effect and so predicts how each site and tree differs from the intercept. Examination of the residuals show that this may be not quite right (Figure 3-52). In this case a random slope would also be appropriate as this also changes with tree. If the mixed effects model is updated from only having a random intercept to also having a random slope then the residuals, while still not looking quite right are looking better (Figure 3-53). The residuals still indicate that there is a problem of trying to fit a straight line to a curve, although the magnitude of the residuals is very small compared to the fitted values

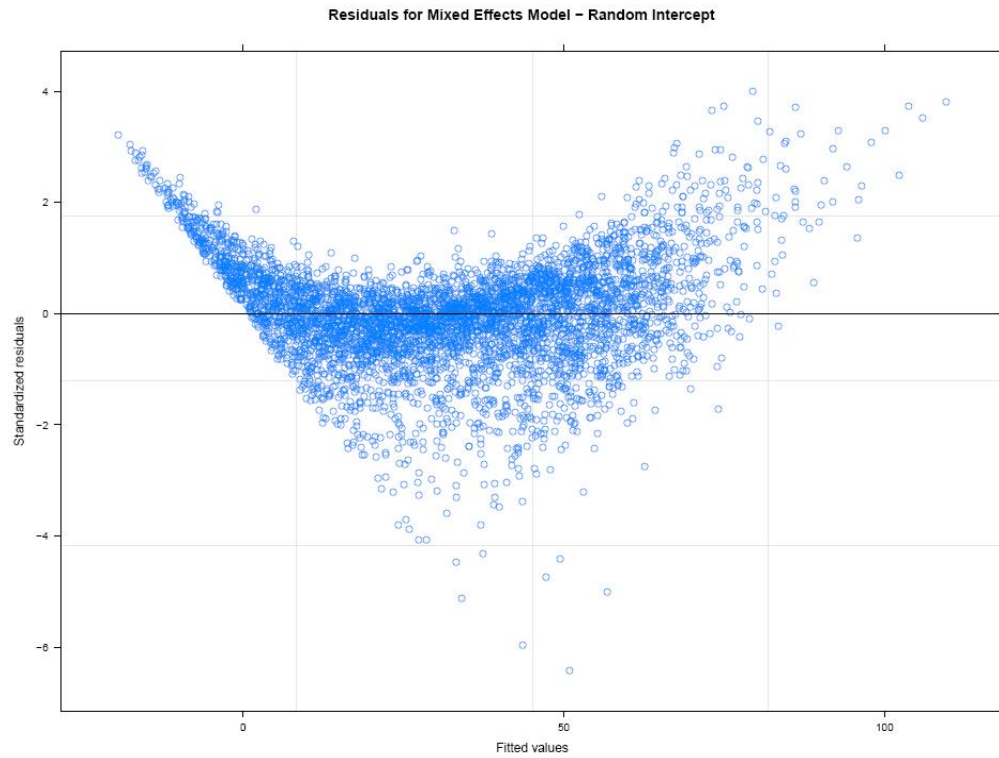


Figure 3-52: Residuals of mixed effects model on the juvenile segment with random intercept only

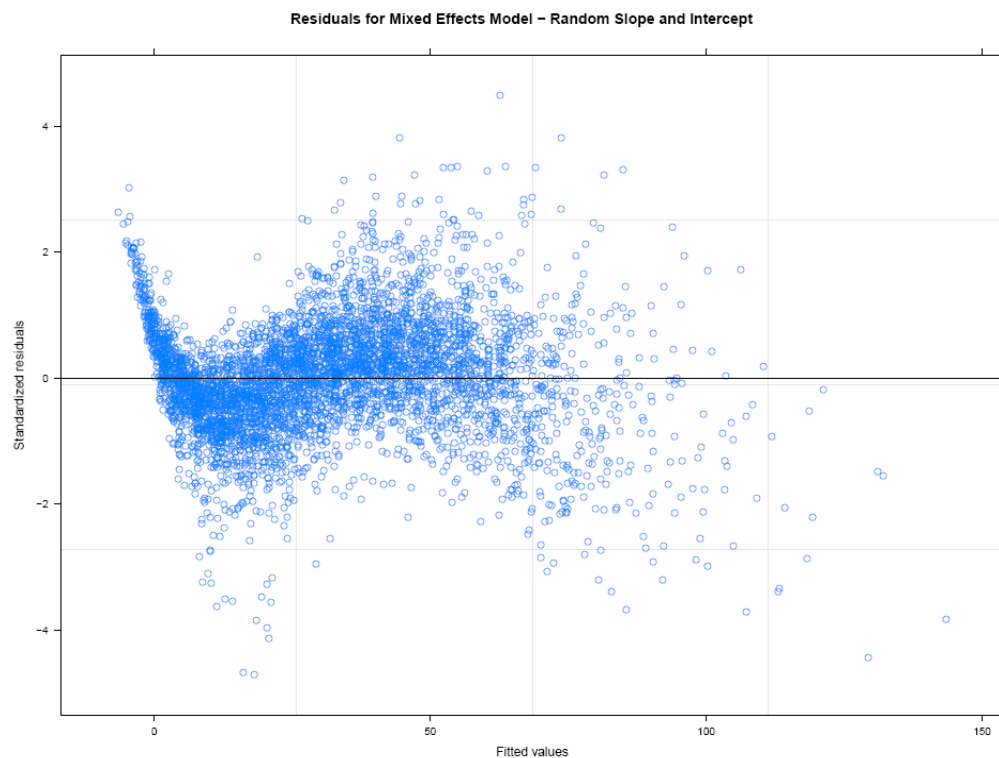


Figure 3-53: Residuals of mixed effects model on the juvenile segment with random intercept and slope

The residuals in (Figure 3-53) may indicate a problem concerning measurement of the first ring but the magnitude of the residuals is very small relative to the

fitted values. When the first ring was removed from the analysis (not shown here) the residual plot remained the same, although this did have the effect of reducing within tree variation to approx 18%.

A log likelihood ratio was carried out on the two models and showed the second model (random slope and intercept) to be a better model, as it has a lower AIC value (25735.28 compared with 32538.77) and the L.Ratio (6811.49) is significant ($p < 0.0001$).

When observed versus the predicted values are plotted for the mixed effects model (Figure 3-54) it indicates that model is predicting very well (R-squared = 0.99) when fitted against individual trees, though there is the same problem as seen before, associated with fitting narrow rings at the pith by the negative juvenile intercept, and a slight curvature of the observed values still appears.

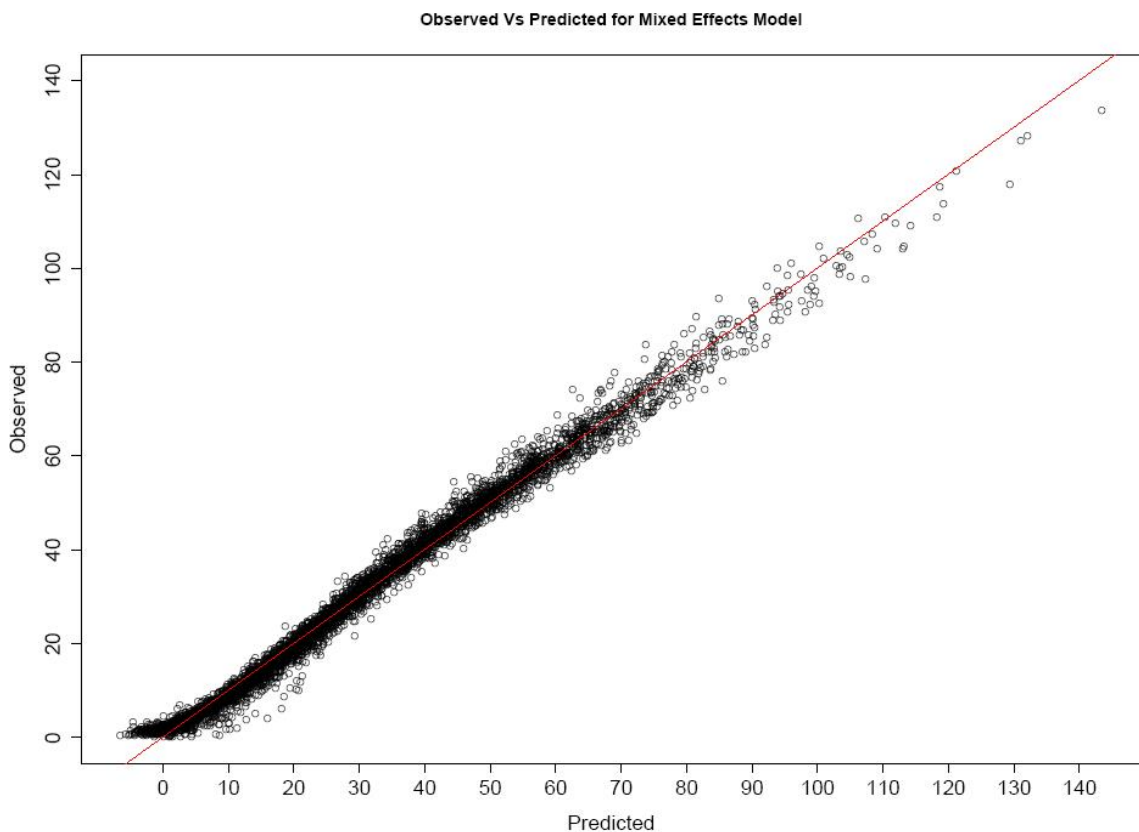


Figure 3-54: The relationship between the predicted values and observed growth values for the mixed effects model on the juvenile segment of growth. The red line represents the line of equality.

3.4.6.2 Mixed Effects Model of Mature Growth

When the mixed effects model was fitted to the whole data set without fixed effects, variance components analysis showed that approximately 24% of the variation is within tree variation, almost 41% being between trees in the same site and approximately 35% of the variation being between sites. Once age has been taken into account then the within tree variation was reduced to just over 5% and most of the variation (51%) was then between trees within the same site. This left almost 44% of the variation being between sites. This is important as the variables being tested, such as northing, easting, elevation or spacing, are based on site data rather than individual tree data.

When the mixed effect model was run with the intercept as the only random effect it gave an intercept of 31.4 mm and a growth rate of 2.9 mm per year. However, due to the large amount of variation seen in the growth this model may also need a random slope (i.e. slope changes with tree).

The residuals for the model which includes only a random intercept are shown in Figure 3-55 and there would seem to be a curved pattern so this may not be quite right. When a random intercept and slope is included in the model the residuals look better (Figure 3-56) indicating that including a random slope would be correct.

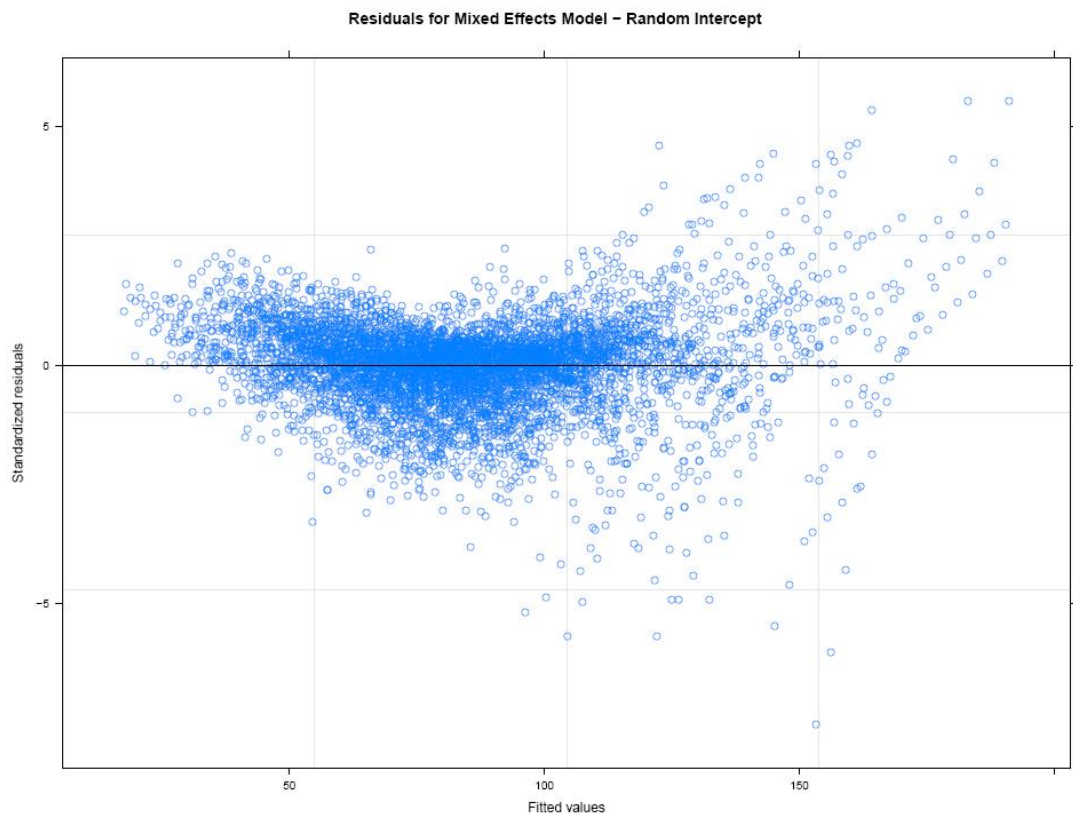


Figure 3-55: Residuals of mixed effects model on the mature growth segment with only random intercept.

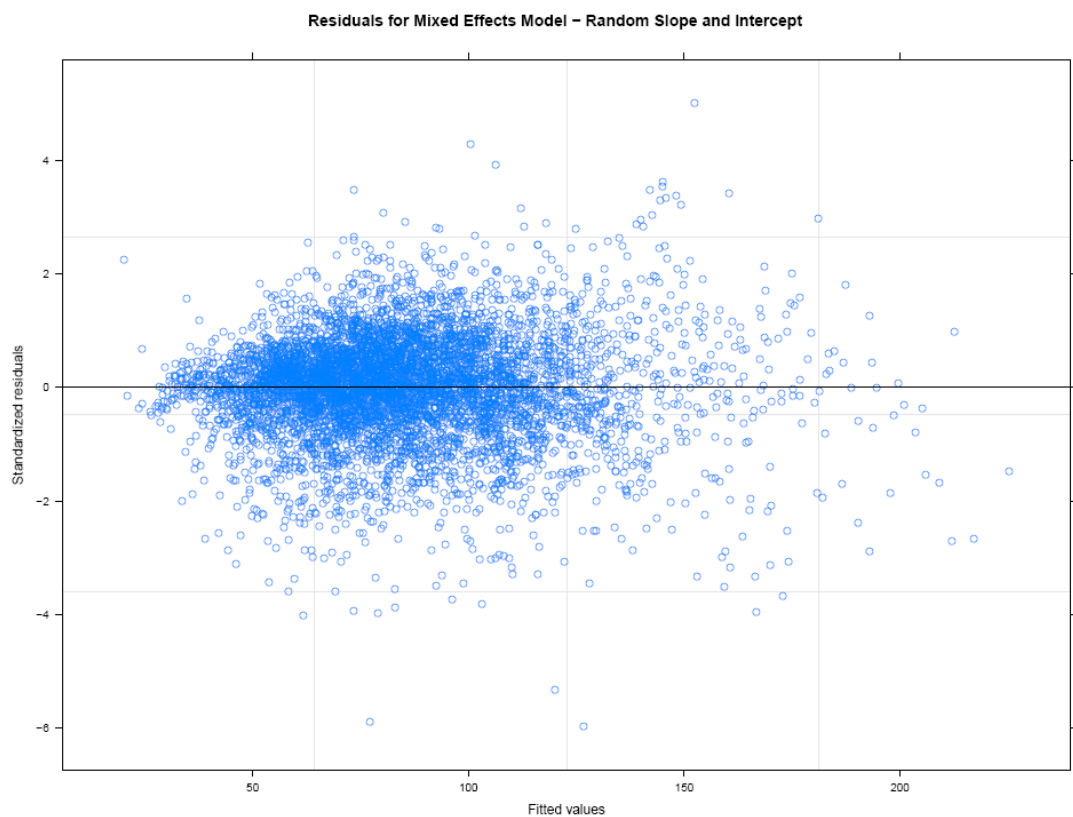


Figure 3-56: Residuals of mixed effects model on the mature growth with random intercept and slope.

The results of log likelihood ratio test of the two models indicates that the second model (including random intercept and slope) is a better model i.e. AIC is lower (29058 compared with 40333) and the L.Ratio of 11283.2 is significant, so in this case adding a random slope produces the best model.

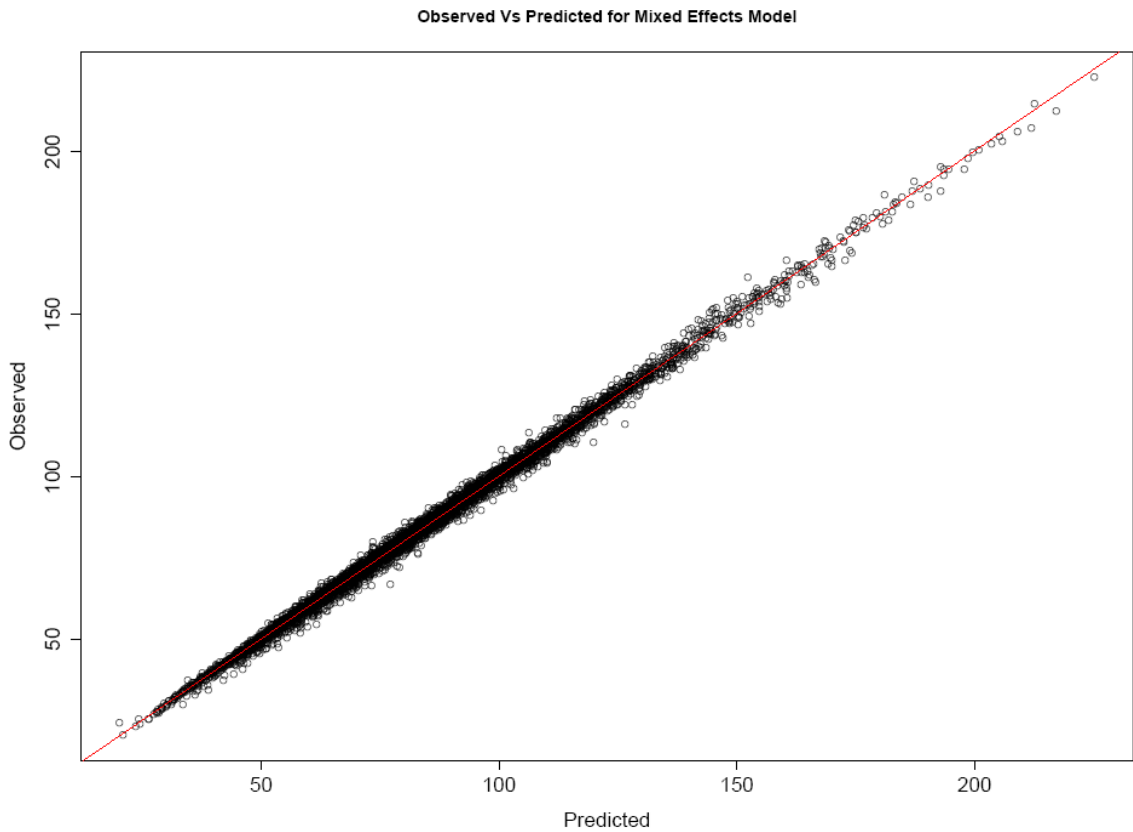


Figure 3-57: Observed Vs Predicted for Mixed Effects Model on the mature segment of growth, showing line of equality (red).

When the observed growth is plotted against that predicted by the model (Figure 3-57) it shows a very good fit ($R\text{-squared} = 0.996$) indicating that when fitted against individual trees the mixed effects model is predicting very well.

3.4.7 Discussion on Growth Models

Observation of the growth data obtained from this experiment indicated that growth could be described as having two different sections. This pattern was implemented in the linear segmented model. Typically there is juvenile phase which is characterised by faster growth, followed by mature phase where there is a visible decrease in the rate of growth. Statistical analysis of growth showed that two distinct phases were indeed present and gave a split point between juvenile and mature wood at a mean of between 11 and 12 years.

Due to the sensitivity of the segmented model to noise it did not always work so well when fitted to individual trees, where it was found to give some extremely low (ring 2) and extremely high (above ring 20) fitted split points, although when examined further some of these extreme points did look to be fitted correctly. When fitted to the global data the segmented model gave a good fit similar to that found in a previous study by (Vihermaa et al., 2014). It should therefore be justifiable to examine juvenile and mature wood using linear mixed effects models on each section separately, that is, one linear model describing growth of the juvenile wood from cambial age 1 to 11 and a separate linear model describing growth from cambial age 12 to 25 years old. Although this model implies that radial growth can be split into two separate segments with a reasonably abrupt change point between the two, this was not always the case and there was usually a more or less gradual change from the juvenile to mature growth segments. This being the case then models which describe juvenile and mature growth together as a curve might fit the data better.

Different forms of curves were looked at in this section and the R-squared values and residual standard errors show them to be relatively similar when fitted to all of the data together. Of the growth models tested, the Hossfeld4 model gave the best fit to the data when fitted to individual trees and the sigmoid form of this model meant it was able to describe growth even at the area close to the pith where most of the other models (including the Exponential and segmented models) had a problem. Although the Hossfeld4 model looked to be the best fit to this data set the parameters are difficult to understand due to the sigmoid nature of the curve and the interaction between the coefficients to describe the rate of growth.

The Exponential model produced a similar R-squared value (0.69) and residual standard error (20 mm) to the Hossfeld4 model when fitted to all of the data and this was also very similar to that of the segmented model. Whilst not as good a fit to individual trees as the Hossfeld4 model, it was found to be a reasonable fit to the data and the effect of each parameter on the curve is easier to understand. However this model looked to have a problem with values near the pith when fitted to individual trees.

The segmented model also looked to be a reasonable fit to the data and although there may also be a problem at the pith with this model, it was a good fit to the mature section of the slope. This model has the advantage of having easy to understand parameters. Analysis of the linear phases of the segmented models using mixed effects analysis showed that most (44%) of the variation in the juvenile growth rate was between trees within the same site with less variation between sites (31%). Similarly in the mature growth phase most of the variation was between trees in the same site (51%) indicating that it may be difficult to determine any site effects on growth and that within site effects may be more important.

All of the other models seemed to have slight problems either with the fit, the number of trees able to be fitted to or the predicted values and residuals. Non-linear residuals were also evident for the linear segmented model and it may suggest that there may be a slight curve to the juvenile segment rather than being straight, which may be a consequence of (a) the split point between the two segments varying between trees and/or (b) fitting a straight line with a negative intercept to the short curved section that results from narrow rings 1-3 (so outside this region the fitted line is curving gently to catch up).

Many of the models tested had problems with predicting values very close to the pith and this may have been due to the growth data not starting from zero. When the data was baseline corrected it made little difference and problems were still seen at the pith with these models. However examination of juvenile and mature growth separately entailed no loss of fit to the experimental data.

3.5 Factors Affecting Growth

As described in Section 3.4 visually there appeared to be two separate segments of growth and segmented analysis showed that growth could indeed be described as having a split point between the two segments with two distinct periods of growth before and after this point. When applied to the full data set this model fitted a value of 11.6 years as the split point between the two segments of juvenile and mature growth. Making use of the split into two segments, this section aims to determine by regression whether the rates of growth of the two segments are affected by latitude, longitude, elevation or spacing, considering these effects as continuous variables.

3.5.1 Regression Analysis

In order to estimate if there is a relationship regression analysis was carried out on the coefficients for the juvenile growth rate and mature growth rate. For the juvenile section latitude, spacing and elevation all came out as significant with latitude and elevation having a negative effect:

$$\text{Juvenile Slope} = 2.18 - 0.000001 * \text{Northing} + 2.47 * \text{Spacing} - 0.00263 * \text{Elevation}$$

When regression analysis was carried out on the mature section of growth only spacing was significant:

$$\text{Mature Slope} = 1.4 + 0.77 * \text{Spacing}$$

However, this does not take into account the nested structure of the data. For this mixed effects models are required which allows the model to vary by tree within site.

3.5.2 Mixed Effects Model Structure

In order to test the significance of treatment, a linear mixed effects (lme) model was used with a nested error structure for the random effects where the nested structure consisted of site and tree within site as shown in Equation 3.20

$$Y_{ijk} = \mu + b_0 + b_1 + b_2 + b_3 + b_4 + S_{ij} + T_{ij} + \epsilon_{ijk} \quad (\text{Equation 3.20})$$

where Y_{ijk} is radial growth, μ is the overall mean, b_0 is cambial age in years, b_1 is northing based on the UK grid reference, b_2 is easting based on the UK grid reference, b_3 is initial spacing at planting in metres, b_4 is the altitude above sea level in metres, S_i is the random effect of site, T_{ij} is the random effect of tree within site and ϵ_{ijk} is the residual error which is attributed to within tree variation.

3.5.3 Factors Affecting Juvenile Growth

A linear mixed effects model was run on the juvenile growth section, i.e. cambial age of 1 to 11 years, with the fixed effects of northing, easting, elevation and spacing as continuous variables (Table 3-8). Spacing was found to have a significant effect on the growth rate ($p=0.001$) and both Spacing and Elevation significantly affected the intercept.

Table 3-8: Result of linear mixed effects model testing the effect of northing, easting, spacing and elevation on the juvenile segment of growth

	numDF	denDF	F-value	p-value
(Intercept)	1	4335	6.8766	0.0088
Age	1	4335	1123.3033	<.0001
Northing	1	41	0.4774	0.4935
Easting	1	41	1.5454	0.2209
Spacing	1	41	4.7437	0.0352
Elevation	1	41	5.8151	0.0205
Age:Northing	1	4335	0.1194	0.7297
Age:Easting	1	4335	1.5162	0.2183
Age:Spacing	1	4335	14.1422	0.0002
Age:Elevation	1	4335	0.4286	0.5127

When the non-significant terms were removed from the equation Spacing remained a significant effect on the growth rate and intercept and elevation became non-significant (Table 3-9).

Table 3-9: Result of linear mixed effects model on juvenile growth with the non-significant terms of northing and easting removed

	numDF	denDF	F-value	p-value
(Intercept)	1	4337	9.0126	0.0027
Age	1	4337	1152.7629	<.0001
Spacing	1	43	6.0844	0.0177
Elevation	1	43	3.7516	0.0593
Age:Spacing	1	4337	15.4020	0.0001
Age:Elevation	1	4337	0.2858	0.5929

When the non-significant terms (i.e. elevation) were removed again this left the model with just cambial age and spacing as the variables. Spacing then had a significant effect on the growth rate but not the intercept (Table 3-10) i.e. its effect was on the rate of growth but not on the starting point.

Table 3-10: Summary of linear mixed effects model on juvenile growth with all non-significant terms removed

	Value	Std.Error	DF	t-value	p-value
(Intercept)	-4.769604	2.486065	4338	-1.9185353	5.510873e-02
Age	0.235773	1.438948	4338	0.1638509	8.698562e-01
Spacing	0.765032	1.255456	44	0.6093660	5.454158e-01
Age:Spacing	2.874140	0.726250	4338	3.9575072	7.694726e-05

If a linear model is set up with cambial age and spacing as the variables the coefficients, in Table 3-11, show that spacing had a positive effect on the rate of growth, equal to 2.95 mm per m spacing per year (Figure 3-58).

Table 3-11: Effect of a linear model on the juvenile growth

	Estimate	Std. Error	t value	Pr(> t)
(Intercept)	-3.25027	0.36538	-8.896	<2e-16 ***
Age	0.06531	0.21527	0.303	0.762
Age:Spacing	2.95319	0.10605	27.846	<2e-16 ***

Signif. codes:	0 '***'	0.001 '**'	0.01 '*'	0.05 '.' 0.1 ' ' 1
Residual standard error: 11.77 on 4771 degrees of freedom				
Multiple R-squared: 0.726, Adjusted R-squared: 0.7259				
F-statistic: 6322 on 2 and 4771 DF, p-value: < 2.2e-16				

The form of the linear model obtained from these data was:

$$RG = 0.06531*x + 2.95319*(x*s) - 3.25027 \quad (\text{Equation 3.21})$$

Where RG = radial growth, x is the cambial age and s is the initial spacing.

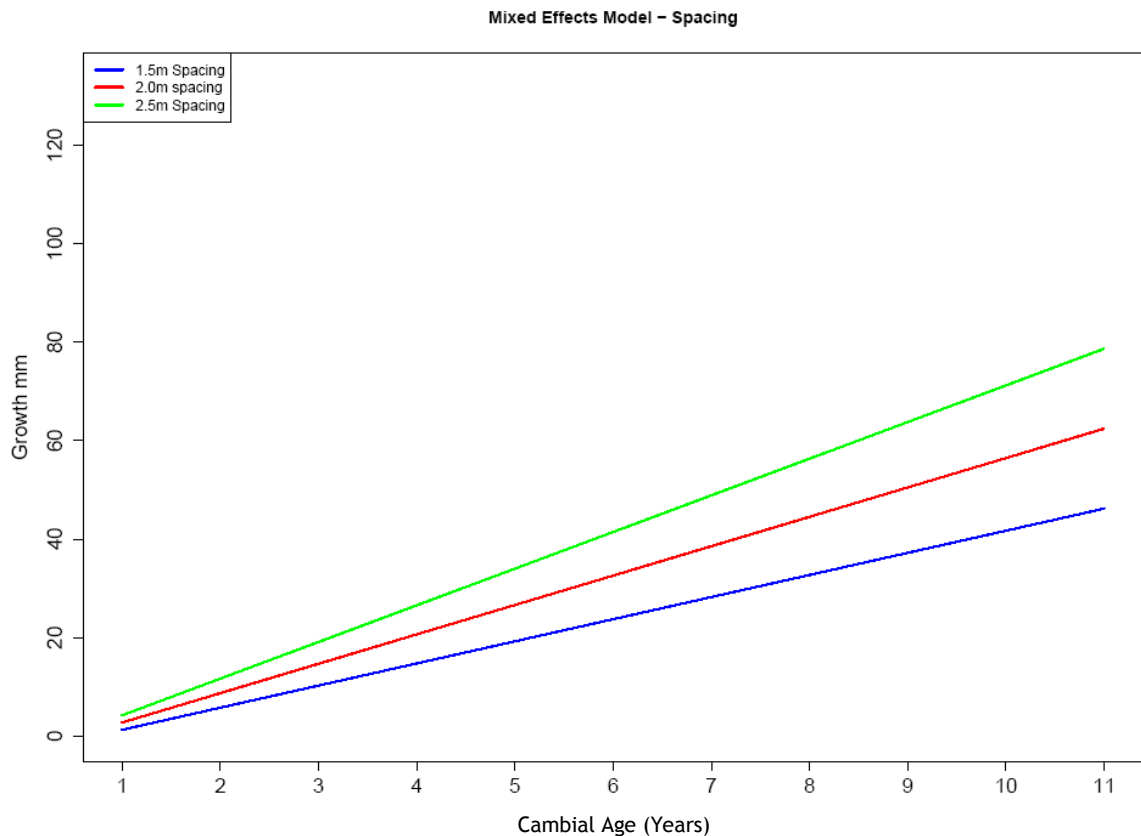


Figure 3-58: Linear model on juvenile growth showing the effect of 1.5m, 2.0m and 2.5m spacing

3.5.3.1 Discussion of factors Affecting Juvenile Wood Growth

Analysis of these data showed that radial growth from cambial age 1 to 11 could be classed as linear and that the initial spacing at which the trees are planted is had significant and positive effect on the rate of growth i.e. as initial spacing is increased then the rate of growth also increases. When spacing was included in the model then the R-squared improved from 0.68 to 0.73. However it is important to note the limitations of this model due to the uneven distribution of spacings, dominated by 2m (208 of 442).

When tested, neither Northing, Easting or Elevation were seen to have a significant effect on the rate of growth suggesting that at this age competition has more of an effect than climate within the climatic range of Great Britain.

3.5.4 Factors Affecting Mature Growth

A linear mixed effects model was run on the mature growth segment i.e. from cambial age 12 to 25 years, with the fixed effects of northing, easting, elevation and spacing as continuous variables (Table 3-12). Spacing was found to have a significant effect on the overall mean radius between years 12 and 25, with all other effects being non-significant (p -values for the interaction are all greater than 0.05).

Table 3-12: ANOVA of lme model testing the effect of northing, easting, spacing and elevation on the mature segment of growth

	numDF	denDF	F-value	p-value
(Intercept)	1	5591	829.2073	<.0001
Age	1	5591	640.1380	<.0001
Northing	1	41	0.0988	0.7548
Easting	1	41	2.2660	0.1399
Spacing	1	41	17.2725	0.0002
Elevation	1	41	0.0794	0.7796
Age:Northing	1	5591	0.0250	0.8744
Age:Easting	1	5591	0.2907	0.5898
Age:Spacing	1	5591	2.2490	0.1338
Age:Elevation	1	5591	0.4524	0.5012

In order to test if spacing was significant, the non-significant terms were removed and this confirmed that spacing had a significant effect on the overall mean radius, due to the earlier effect on (juvenile) growth but had no significant effect on the growth rate during the mature segment (Table 3-13).

Table 3-13: ANOVA of lme model on mature growth with the non-significant terms of northing, easting and elevation removed

	numDF	denDF	F-value	p-value
(Intercept)	1	5594	856.4042	<.0001
Age	1	5594	679.4354	<.0001
Spacing	1	44	19.3883	0.0001
Age:Spacing	1	5594	2.6711	0.1022

As before, the interaction is non-significant and so can be removed from the model. A test of this model shows that on its own spacing still had a significant effect on the intercept (Table 3-14).

Table 3-14: ANOVA of lme model on mature growth with all non-significant terms removed.

	numDF	denDF	F-value	p-value
(Intercept)	1	5595	856.6950	<.0001
Age	1	5595	654.9129	<.0001
Spacing	1	44	19.3904	1e-04

This shows that Spacing has a significant effect on the intercept but not on the growth rate, and none of the other variables are having an effect. This effect on the intercept would be expected as the growth rate of the juvenile wood was affected by spacing therefore would affect the starting point for mature growth. Again it is important to point out the limitations of this analysis due to the lack of replicates at spacing's other than 2m.

Also, the intercepts are different, as we would expect, but the growth rate of the radius stays similar throughout, i.e. if it was high at year 12 then it is likely to be high at year 25. The correlation between radii at different ages can be seen in Figure 3-59 which compares radius at year 12 to radius at the first ring and then at year 25, 30 and 35. This shows that there is a good correlation between the size of the radius at year 12 and later years. This was confirmed by the results of a Pearson correlation test (Table 3-15) which shows correlation of 0.86, 0.81 and 0.78 between radius at year 12 and radius at years 25, 30 and 35 respectively. This observation does not necessarily imply that juvenile and mature growth were correlated, but only that by year 25 juvenile growth still made up a sufficient proportion of the radius to influence the total radius reached. Table 3-15 also shows that there is little correlation between year 1 and later years with a Pearson's correlation of 0.21 between year 1 and year 35 and 0.45 for year 1 and 12.

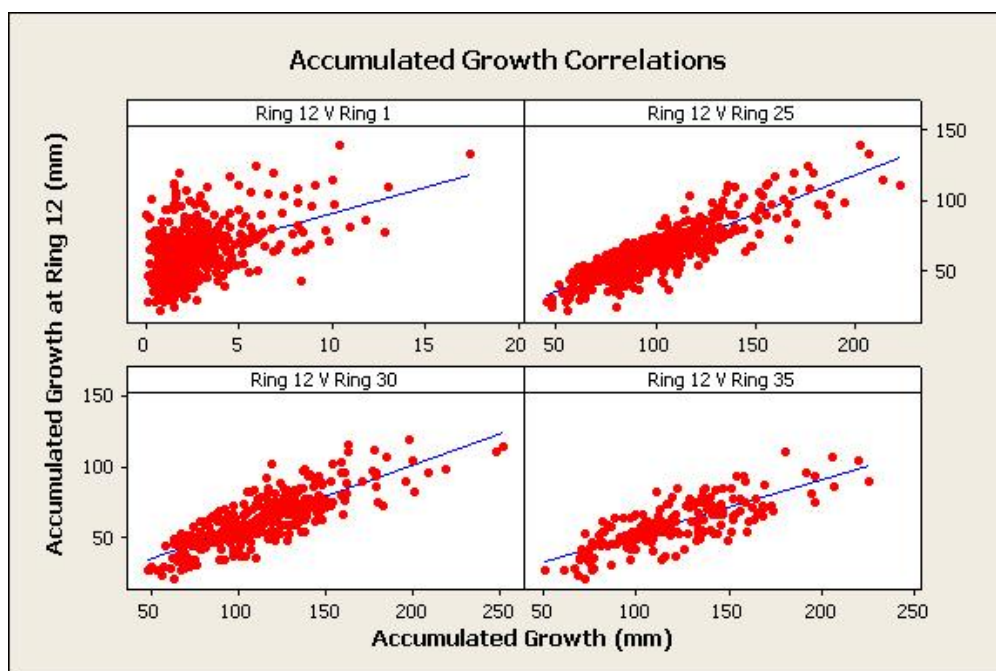


Figure 3-59: Scatterplot showing the correlation between accumulated growth at ring 12 versus accumulated growth at rings 1, 25, 30 and 35.

Table 3-15: Pearson correlation coefficients between growth at ring numbers 1, 12, 25, 30 and 35 which all had significant p -values (<0.0001)

Ring No.	1	12	25	30
12	0.445			
25	0.361	0.863		
30	0.321	0.810	0.985	
35	0.212	0.782	0.955	0.989

Analysis of the linear model shows that when spacing was included in the model the R-squared value increased from 0.19 to 0.31.

3.5.5 Effect on Mature Growth When Spacing is taken into Account

In Section 3.5.3 on juvenile wood growth it was shown that spacing was the dominant factor affecting the rate of growth (i.e. the slope) up to year 12. This therefore would have an effect on the intercept of the mature growth rate, as confirmed by the above models. Because of the dominating effect of spacing it is difficult to see any effect of the environment on growth. Taking this a step further, to investigate whether Northing, Easting and Elevation were having a direct effect the data were separated to include only trees spaced at 2m as this was the group with the largest number of replicates (208 trees out of 442)

3.5.5.1 Effect of latitude, Longitude and Elevation on mature Wood Growth

The same form of linear mixed effects model as Equation 3.20 was used with the spacing term removed as shown in Equation 3.22

$$Y_{ijk} = \mu + b_0 + b_1 + b_2 + b_4 + T_{ij} + T_{ij} + \epsilon_{ijk} \quad (\text{Equation 3.22})$$

where Y_{ijk} is radial growth, μ is the overall mean, b_0 is cambial age in years, b_1 is northing based on the UK grid reference, b_2 is easting based on the UK grid reference, b_4 is the altitude above sea level in metres, S_i is the random effect of site, T_{ij} is the random effect of tree within site and ϵ_{ijk} is the residual error which is attributed to within tree variation.

Analysis of variance on the model shows that easting, northing and elevation (Table 3-16) had no significant effect on the mature growth rate when spacing was equal, with p -values for all effects being greater than 0.05.

Table 3-16: Anova of lme model on mature growth at 2m initial spacing showing no significant effects

	numDF	denDF	F-value	p-value
(Intercept)	1	2610	178.7695	<.0001
Age	1	2610	342.9810	<.0001
Easting	1	18	3.1420	0.0932
Northing	1	18	0.0079	0.9304
Elevation	1	18	0.6803	0.4203
Age:Easting	1	2610	0.1424	0.7060
Age:Northing	1	2610	2.2215	0.1362
Age:Elevation	1	2610	2.2624	0.1327

As shown earlier in Section 3.5.3 spacing had the biggest effect on the intercept of the mature growth rate. This was to be expected as it also had the biggest effect on the rate of the juvenile growth. The intercept coefficients of the mature growth are shown in Figure 3-60 and like the growth rate there is so much variation within each level of northing, easting and elevation that it is very difficult to see any effect.

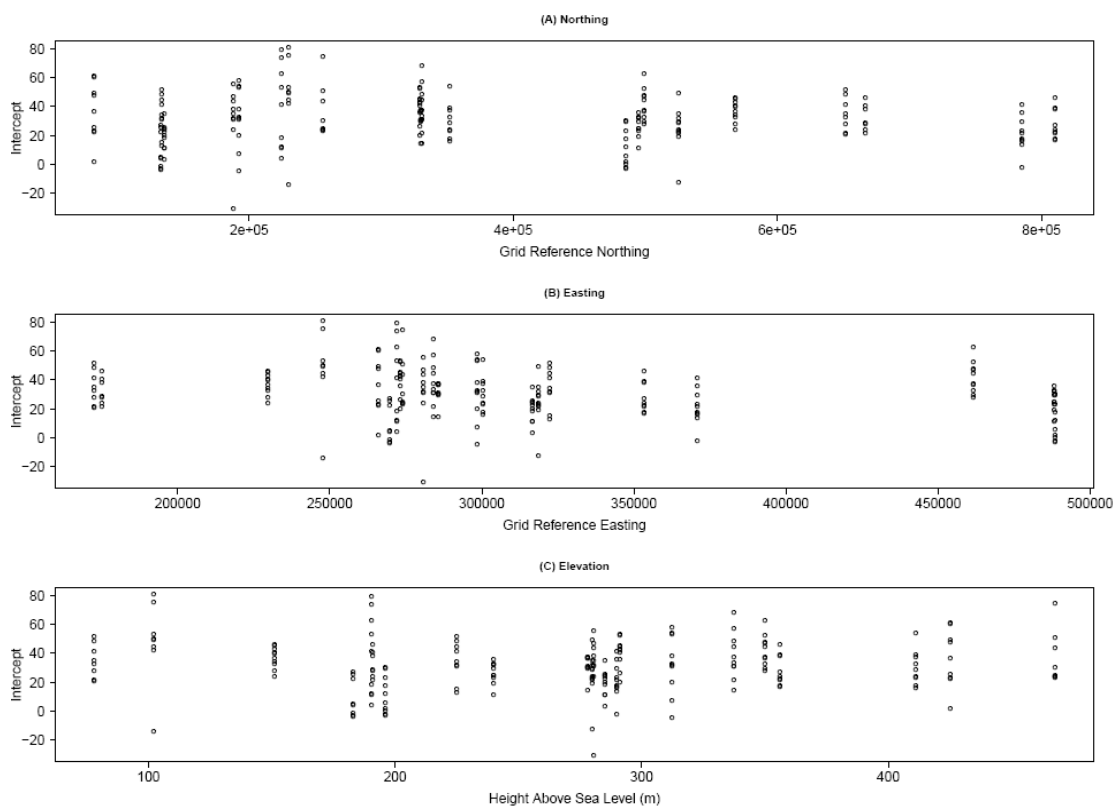


Figure 3-60: The effect of Northing (A), Easting (B) and Elevation (C) on the intercept coefficients when fitted to each tree

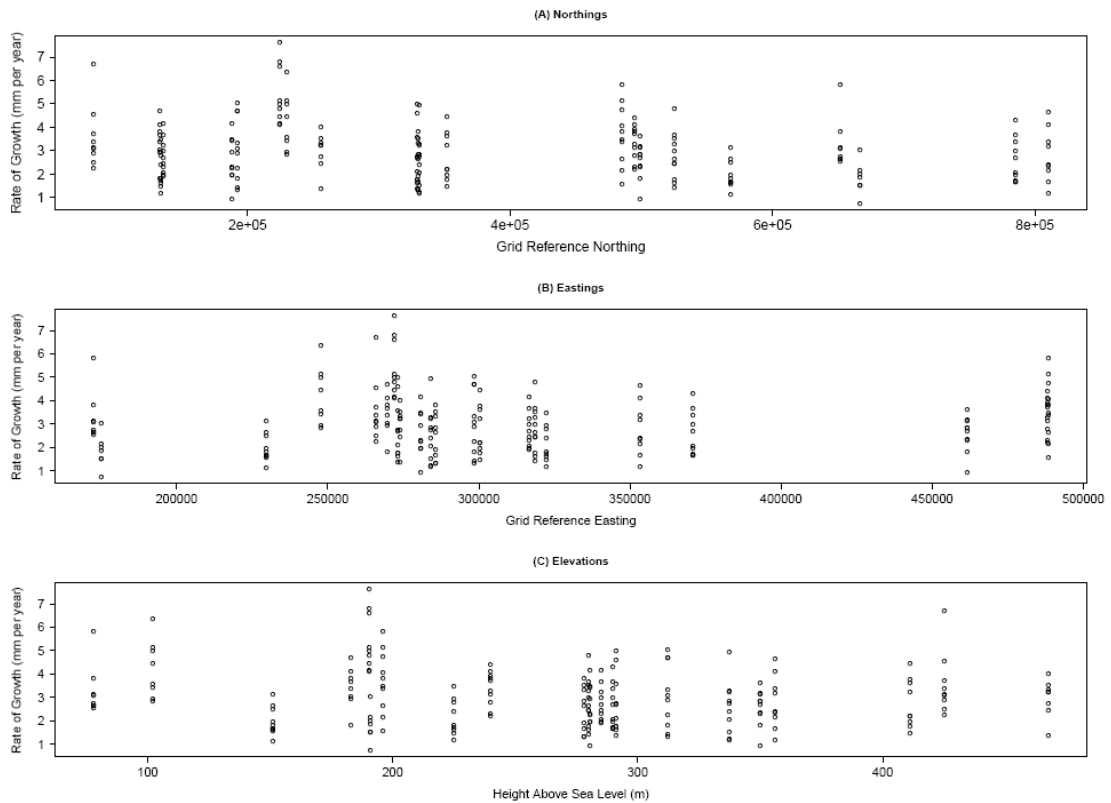


Figure 3-61: The effect of Northing (A), Easting (B) and Elevation (C) on the slope coefficients when fitted to each tree

Figure 3-61 shows visually that there is as much variation within each level of northing, easting and elevation as between the levels which make it very difficult to see any effect of these factors and so it is not surprising that they are not significant in mixed effect model analysis.

3.5.5.2 Effect of Climate on Mature Wood Growth

Section 3.5.5.1 looked at the geographical variables of Northing, Easting and Elevation to see if these had a direct effect on mature growth once spacing had been taken into account, and the analysis showed that this was not the case. It might be suggested that northing, easting and elevation could be used as proxies for temperature and rainfall. Rainfall and temperature variation are not equally distributed throughout the year and northing confounds temperature with day length.

Using ESC data (as described in Chapter 2) this section will now look at climate data specifically to see if they have any effect on mature growth.

Within the ESC data summer rainfall and winter rainfall are shown to be highly correlated at each site (Figure 3-62) and have been combined to give a total annual rainfall. As well as rainfall and accumulated temperature (AT5) other variables looked at include moisture deficit (MD), continentality (Cont), DAMS (a measure of windiness), soil moisture regime (smr) and soil nutrient regime (snr).

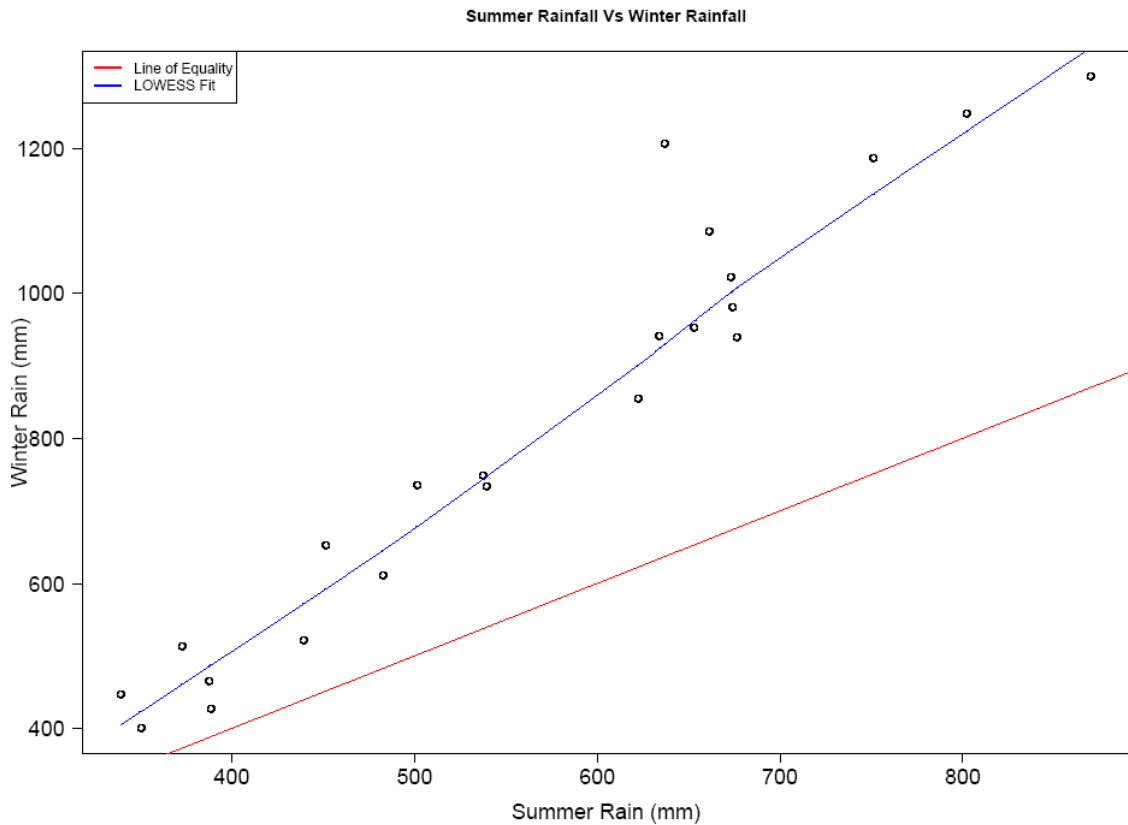


Figure 3-62: Correlation between winter and summer rainfall taken from ESC Data

Using the same form of linear mixed effect model as in the previous sections showed that if all the ESC Data are included in the model (Table 3-17), then there are no climatic effects which are significant. This agrees with the previous section (3.5.5.1) which showed that there is so much variation on tree growth within a site that it is very difficult to see any site effect. As well as this, since most of the variance of the mature segment is in the intercept, it is essentially the effects of climate on juvenile growth that are being tested here.

Table 3-17: Summary of mixed effects model which includes accumulated temperature, Moisture Deficit, Summer rainfall, continentality, DAMS, soil moisture regime and soil nitrogen regime

	Value	Std.Error	DF	t-value	p-value
(Intercept)	21.5027	34.0871	2606	0.6308	0.5282
Age	-3.7851	2.7667	2606	-1.3681	0.1714
AT5	0.0160	0.0203	14	0.7905	0.4424
MD	-0.1364	0.2042	14	-0.6684	0.5147
AnnualRainfal	0.0061	0.0067	14	0.9145	0.3759
Cont	0.8535	1.9492	14	0.4379	0.6681
DAMS	-0.2759	1.3311	14	-0.2073	0.8387
smr	-2.6686	2.1898	14	-1.2187	0.2431
snr	0.9425	3.4057	14	0.2767	0.7860
Age:AT5	-0.0016	0.0016	2606	-1.0026	0.3161
Age:MD	0.0290	0.0166	2606	1.7505	0.0801
Age:AnnualRainfal	0.0009	0.0005	2606	1.6335	0.1024
Age:Cont	0.1021	0.1571	2606	0.6498	0.5158
Age:DAMS	0.1458	0.1078	2606	1.3524	0.1763
Age:smr	0.2898	0.1776	2606	1.6318	0.1028
Age:snr	0.4663	0.2757	2606	1.6913	0.0909

3.5.5.3 Discussion of Mature Growth

As with the juvenile growth, mature growth from ring 12 to 25 was seen to follow a linear pattern and mixed effects models showed that spacing was having a significant positive effect on the overall mean but not on the rate of growth. None of the other variables (Northing, Easting or Elevation) had a significant effect on the growth rate or the overall mean when included in the same model as spacing. When spacing was included in the linear model the R-squared was increased from 0.19 to 0.31 showing that more of the variation is described when spacing is added to the model.

To test if any variables were having an effect once spacing had been accounted for the model was run only on trees at those sites where spacing was 2m. Again this showed that none of the variables of Northing, Easting or Elevation were having a significant effect. A 2010 study on Sitka spruce in Wales (Murphy and Pommerening, 2010) found that using a modified version of the Gompertz function (Gompertz, 1825), soil moisture regime, DAMS and soil nutrient regime had the strongest relationship to growth out of the environmental factors measured though the R-squared values were still not significant. Similarly here, when the ESC climatic data was run in the model no variables were shown as significant.

The models showed that growth rates of the mature segments varied hugely between trees and most of the variation in growth was between trees within the

same sites (51%) which made it difficult to see any difference in growth rates between sites. This shows that the local growing environment and genotype play a huge role in tree growth.

This section has shown that tree growth can be measured in two separate linear segments. The first segment of juvenile growth takes place from the cambial age of 0 to approximately 11 years old and the second segment of mature growth from approximately ring 12 onwards. Models of juvenile growth showed that initial spacing had the biggest effect on the rate of growth and this translated to having the biggest effect on the overall mean of the mature phase. High correlations between the radius at year 12 and in subsequent years suggest that (if there is no thinning) if a tree is larger at cambial age 12 then it is highly likely to be larger at year 25 or 35. Therefore initial spacing at planting is the biggest effect on the amount of growth at later years.

4 Modelling Ring Density of Sitka Spruce

4.1 Introduction

Using the data collected from the sample cores taken as part of the study described in the methods section of Chapter 2, the present chapter describes the variation in density in radial profiles of Sitka spruce across the full latitudinal and longitudinal range in which Sitka spruce grows in Great Britain. The radial trend in density was examined to investigate how this compares with previous studies on Sitka spruce. Various empirical models were examined to investigate which were able to fit to this data set and used to investigate variation in density based on site and climate factors.

4.1.1 Definitions

In this section, unless otherwise stated, when density is discussed it refers to the average ring density measured as kilograms of mass per cubic metre (kg m^{-3}) at 4% moisture content.

Ring number is counted from the pith and is a measure of cambial age in years. For the purposes of this chapter the terms “Ring Number” “Age” and “Cambial Age” are interchangeable.

4.1.2 Outline

The core samples used in this section were taken from 32 sites which covered a range from Sutherland in the north of Scotland down to Devon in the south west of England, as described in the method section of Chapter 2. As well as these, sample cores from a further 15 sites were selected from the original resource evaluation study to cover a larger range of the UK including north east Scotland, south east and south west Scotland and north east England. At each of the 47 sites it was intended to take 10 core samples but due to damage when taking and preparing the cores this number varied between 8 and 11. Added to this, during preparation some samples were found to have knots which would affect the density readings and so these cores were removed. The number of cores per site used in the analysis is shown in Table 4-1.

Table 4-1: The number of samples per site measured for density

Site	23	54	55	63	64	72	80	86	155	226
No.Samples	10	10	9	10	10	10	10	10	10	10
Site	243	278	279	280	281	303	339	461	1211	1251
No.Samples	10	10	10	10	10	9	9	9	9	8
Site	1390	1600	2013	2042	2142	2185	2191	2304	2436	2559
No.Samples	10	9	10	11	8	9	10	9	10	8
Site	2723	2789	3237	3323	4301	5234	5565	5945	6619	6630
No.Samples	11	9	8	10	10	9	9	10	10	10
Site	6874	7643	9004	9008	EXM7	FERN	QUA6			
No.Samples	10	10	10	10	8	10	10			

Each core was split at the pith and analysis was made from pith to bark on the northern side of each core to give a radial profile.

Ring density data was produced using the ITRAX densitometer to measure density in 50 μm steps and by using Windendro (see methods in Chapter 2) software to identify ring boundaries and average the density values by ring.

4.1.3 Aim

The aim of this section is to investigate whether the radial profile of ring density can be modelled using a segmented linear approach and to compare this to other empirical models which describe the variation of density with age within the sampled trees. Existing density models are tested using a more complete dataset than has hitherto been available, so that such models can be used for timber quality modelling across Britain. By fitting a split point and linear models in the juvenile and mature wood phases of density, this section then aims to investigate if site characteristics such as elevation, latitude, longitude and initial spacing have any influence on spruce wood density.

4.2 Radial Variation in Density

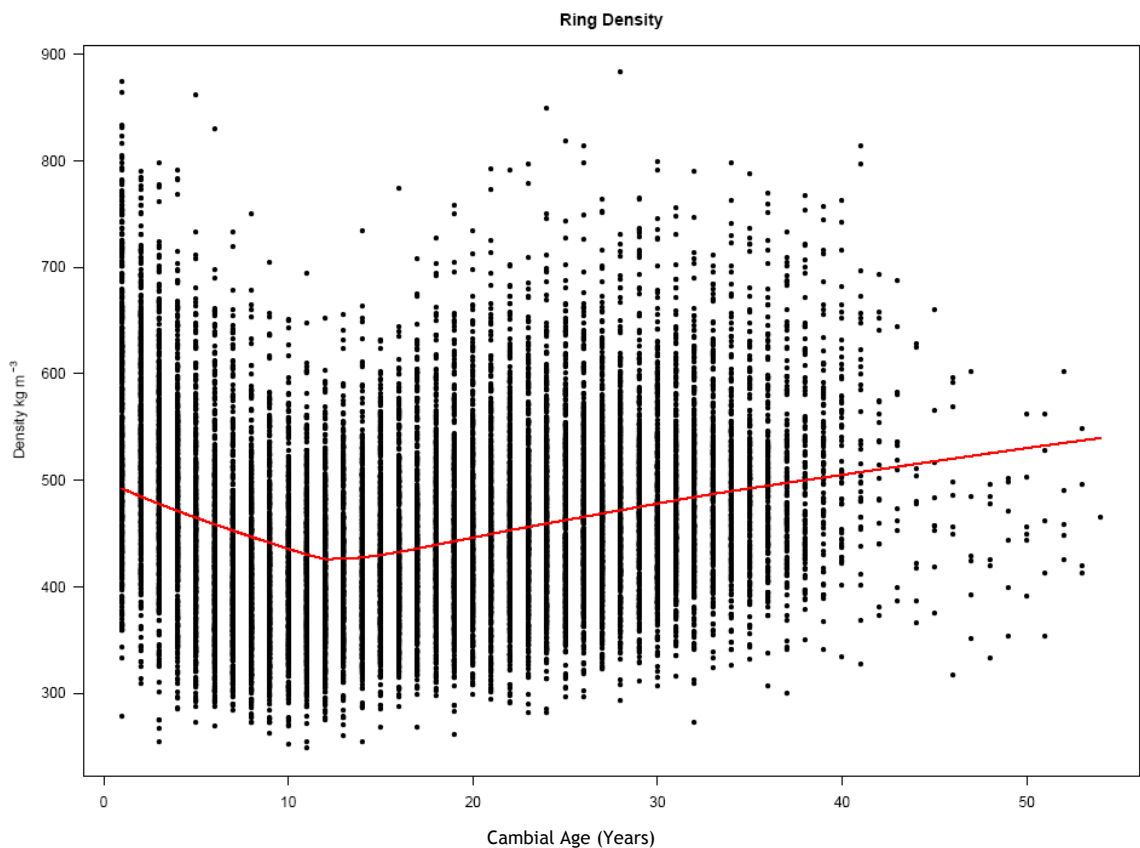


Figure 4-1: Radial profile of mean ring density plotted by cambial age with a LOWESS trend line

The radial profile in density (Figure 4-1) fits the same basic trend as we would expect to see in Sitka spruce (Brazier, 1970). This trend, which is also seen in other spruce species such as Norway spruce (Lindstrom, 1996) and Black spruce (Alteyrac et al., 2006A) as well as Douglas fir (Kennedy, 1995), shows density that is high at the pith (juvenile wood) and decreases for several rings before increasing again in the mature wood. The transition zone between the juvenile and mature phases occurs approximately between rings 7 to 12. This generally conforms to the accepted boundary between the juvenile core and mature wood (Cameron et al., 2005, Brazier and Mobbs, 1993) although the age at which this boundary varies depending on the parameter being measured (Mansfield et al., 2009, Alteyrac et al., 2006B). Although previous studies have shown that the Sitka spruce density profile can be fitted using curved models (Gardiner et al., 2011, Lindstrom, 2000, McLean, 2008) the LOWESS trend line in Figure 4-1 suggests that the trend could perhaps also be described as having two segments

and so it is of interest to investigate whether a simpler linear segmented model could fit the data and how this compares with previous models.

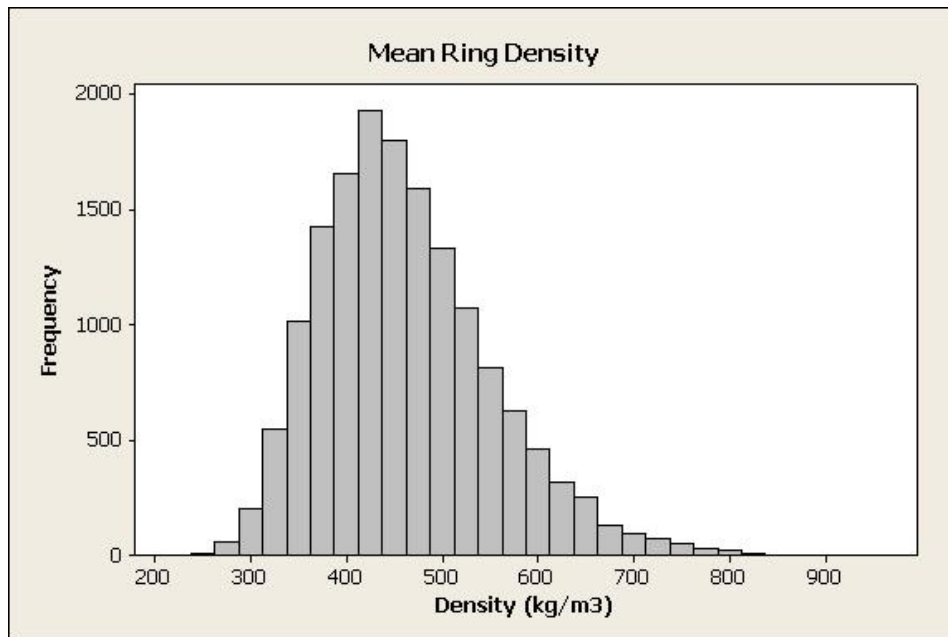


Figure 4-2: Histogram of mean ring density

Investigation by Vihermaa (2010) showed that the method of analysis used in this experiment results in samples with 4% moisture content and the analysis carried out here was based on the 4% moisture content values. The density measured in this data set ranged from a minimum of 248 kg m^{-3} to 883 kg m^{-3} with a mean value of 461 kg m^{-3} which is similar to that found by McLean (2008) (456 kg m^{-3}) and Vihermaa (2010) (447 kg m^{-3}) in previous studies on Sitka spruce using the same method. The overall range is fairly evenly distributed with perhaps a slight skew towards the higher end of the range as shown in Figure 4-2.

Figure 4-3 shows the radial pattern of density when split by the different sites that were sampled. This shows that while most sites follow a similar trend to the overall trend there are differences at certain sites with some, e.g. sites 281 and 6874, having a higher than average density, and others following a slightly different trend. For example whereas sites EXM7, 261 and 1251 have higher density and a steeper decline in the juvenile wood than most other sites, other sites such as 5234 may have more of an increase in the mature wood. This shows that there may be some site factors at work which are influencing the density.

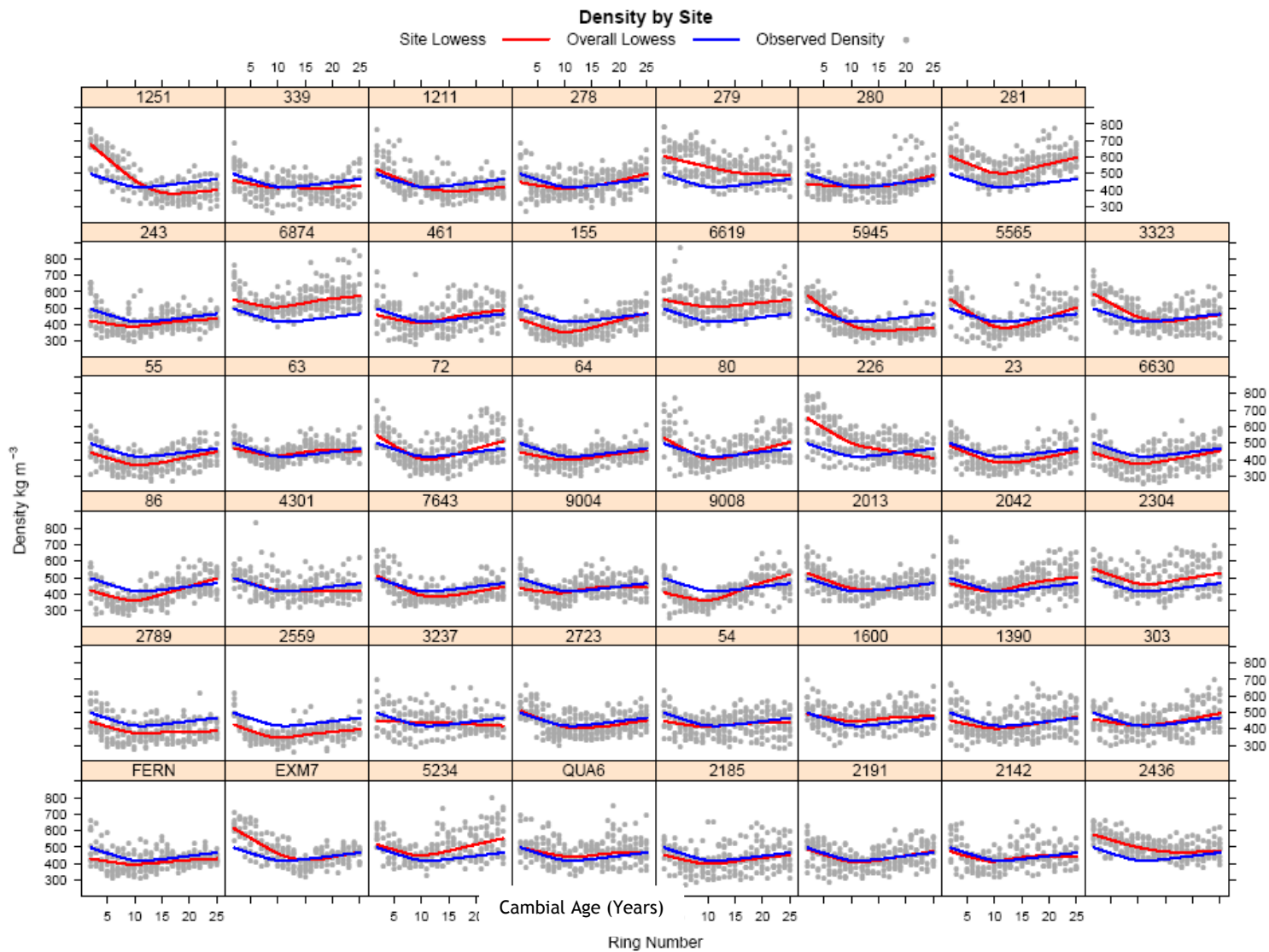


Figure 4-3: Observed density of each tree plotted by site. Showing the LOWESS trend by site (red line) compared to the LOWESS trend for the full data set (blue line)

Table 4-2: The number of samples and sites for each group when measured for density. Northing groups are based on the 100km OS grid square, where 0 is south and 9 is furthest north. Easting is also based on the 100km OS grid square with 1 being west and 4 being east. Spacing is based on the initial spacing in metres and Elevation is grouped in 50 metre increments from 50 to 500 metres above sea level. A total of 47 sites were tested covering a combination of these factors.

Northing Group	0	1	2	3	4	5	6	7	8	9
No.Samples	10	54	46	38	50	99	59	29	26	40
No.Sites	1	6	5	4	5	10	6	3	3	4
Easting Group										
	1	2	3	4						
No.Samples	39	218	154	40						
No.Sites	4	23	16	4						
Spacing Group										
	1.5	1.6	1.7	1.8	1.9	2	2.1	2.4	2.5	
No.Samples	9	18	57	60	20	218	10	20	39	
No.Sites	1	2	6	6	2	23	1	2	4	
Elevation Group										
	1	2	3	4	5	6	7	8	9	
No.Samples	19	47	77	48	79	79	27	38	37	
No.Sites	2	5	8	5	8	8	3	4	4	

In order to visualise how density may be affected by site factors, latitude (Northing), longitude (Easting), spacing and Elevation were grouped as described in Chapter 2. The number of samples and sites per group are shown in Table 4-2 and the spread of density values in each group is plotted in Figure 4-4. The spread of values is large within each group due to the fact that all of the density measurements for each radius are included. However, the overall mean values may give an indication that there may be differences between these groups. This is especially the case with Easting where there seems to be a decrease in mean density from west to east. However to see if there is any real effect the trend in the data will first have to be modelled and then the effect of site or geographical location investigated.

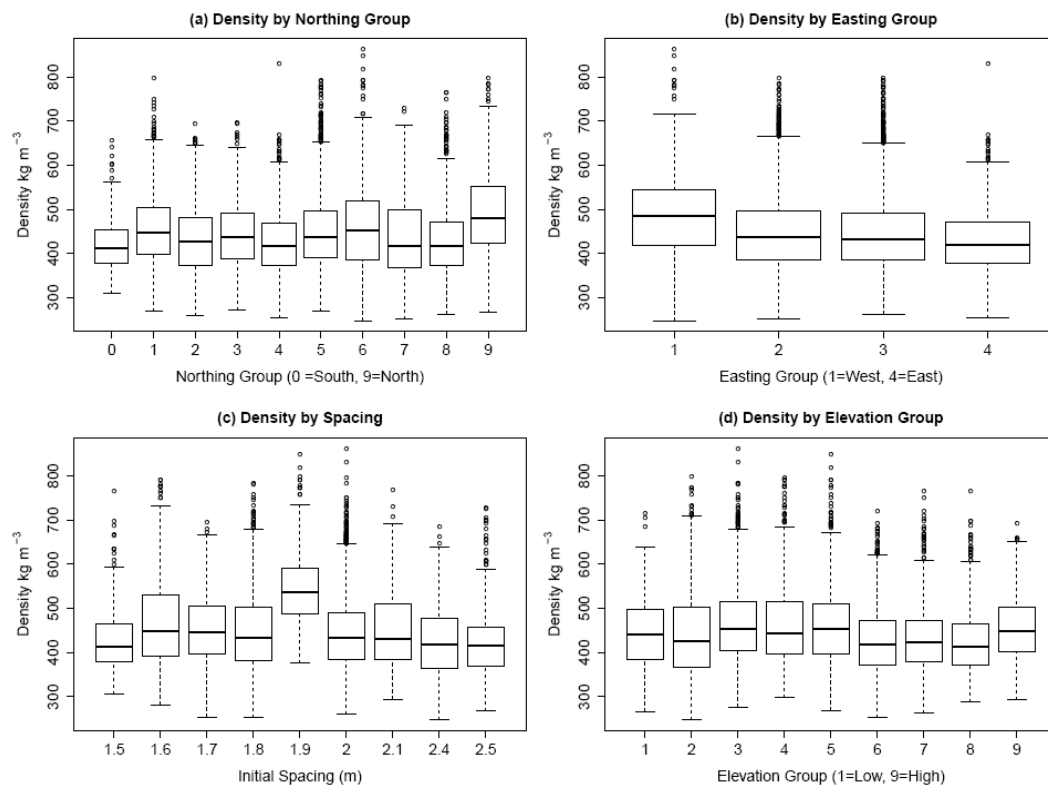


Figure 4-4: Boxplot showing the spread of density when grouped by longitude, latitude, spacing and altitude

4.3 Fitting Models to Ring Density

The aim of this section is to test a selection of published models and to build a final model which can not only be used to investigate the variation in radial density in Sitka spruce throughout its growing range in Great Britain, but also to investigate the effect of site characteristics on the density of the wood.

In order to model ring density a number of statistical models were explored to investigate how well they describe the trend in the data. The forms of these models are shown below. They include a density model for British grown Sitka spruce developed by Gardiner et al. (2011) which was based on earlier models to describe the variation in density of Norway spruce in France (Leban et al., 1997). Also explored was a model derived from Lindstrom (2000) who modelled density in Swedish grown Norway spruce. McLean (2008) found this model to be a good fit to Sitka spruce observed values. However both the Gardiner and Lindstrom models require ring width as a parameter along with ring number so in this study an exponential model based on cambial age alone was explored along with a segmented linear model to investigate how these compare with the previous published models.

1. Segmented Linear Model - Using the segmented package in R (Muggeo, 2008) this model investigates whether there are two separate linear sections to the density radial profile, with a split point between the two sections, using a Davies test (Davies, 1987) for a significant change in gradient. Each linear section follows the form of a linear equation where there is a slope parameter and an intercept parameter. For both the juvenile and mature segments the intercept is interpreted as the value at year 0:

$$\text{Juvenile Phase: } \rho = a_1 * CA + b_1 \quad \text{for } CA \leq \delta \quad (\text{Equation 4.1})$$

$$\text{Mature Phase: } \rho = a_2 * CA + b_2 \quad \text{for } CA > \delta \quad (\text{Equation 4.2})$$

Where ρ is the radial profile of ring density, a_1 and a_2 are the rate of the slope, CA is the cambial age in years (i.e. the ring number from the pith), b_1 and b_2 are the intercept of the respective sections and δ is the break point between the two slopes derived from the segmented analysis.

2. Gardiner3 Model:

$$\rho = c_1(1+c_2*exp^{CA/c_3})(1+c_4*RW) \quad (\text{Equation 4.3})$$

Where ρ is the radial profile of density, CA is cambial age in years, RW is ring width in mm and c_1 , c_2 , c_3 and c_4 are parameters estimated from the data fitted in R using non linear least squares regression (nls function) to find the best fit curve.

3. Lindstrom Model:

$$\rho = d_1*log(RW)+d_2*(1/CA)+d_3 \quad (\text{Equation 4.4})$$

Where ρ is the radial profile of density, CA is cambial age in years, RW is ring width in mm and d_1 , d_2 and d_3 are parameters estimated from the data fitted in R using non-linear least squares regression (nls function) to find the best fit curve.

4. Exponential Model:

$$\rho = \exp^{(z_1/CA)} + z_2 \quad (\text{Equation 4.5})$$

Where CA is the cambial age in years, z_1 the rate value, z_2 is the asymptote parameter estimated from the data and fitted in R using non-linear least squares regression (nls function) to find the best fit curve.

4.3.1 Density Model Parameters

The fitted models are shown against the observed data in Figure 4-5 which shows that visually the exponential model, which is based on age alone, is the worst fitting as it does not pick up the increase in density from approximately ring 7 onwards. This is reflected in it having the lowest R-squared value of the models tested (Table 4-3). Both the Gardiner3 and Lindstrom models show a reasonably good fit to the data with R-squared of 0.44 and 0.48 respectively and similar residual standard errors (64.1 kg m⁻³ and 61.6 kg m⁻³). The R-squared for the segmented model (0.14) was lower than the two published models but higher than the Exponential model. Its residual standard error of 79.2 kg m⁻³ was the highest of the models tested but since this model has easier to understand parameters and uses cambial age alone it may be a useful tool.

Table 4-3: Parameter estimates for the density models along with Standard Errors, residual standard error and R-squared values.

Model Parameter	Estimate	Std Error	Residual Std Error	R-Squared
Segmented -	Split point	7.4 years		
a ₁	-24.9	0.89	79.15	0.14
b ₁	586.9	4.3		
a ₂	3.9	0.17		
b ₂	374.8			
Gardiner3				
c ₁	507.2	1.27	64.08	0.44
c ₂	0.645	0.0171		
c ₃	-3.85	0.142		
c ₄	-0.0412	0.000437		
Lindstrom				
d ₁	-90.0	0.97	61.55	0.48
d ₂	384.57	5.88		
d ₃	514.12	1.31		
Exponential				
z ₁	9.48	0.069	21.78	0.07
z ₂	439.5	0.818		

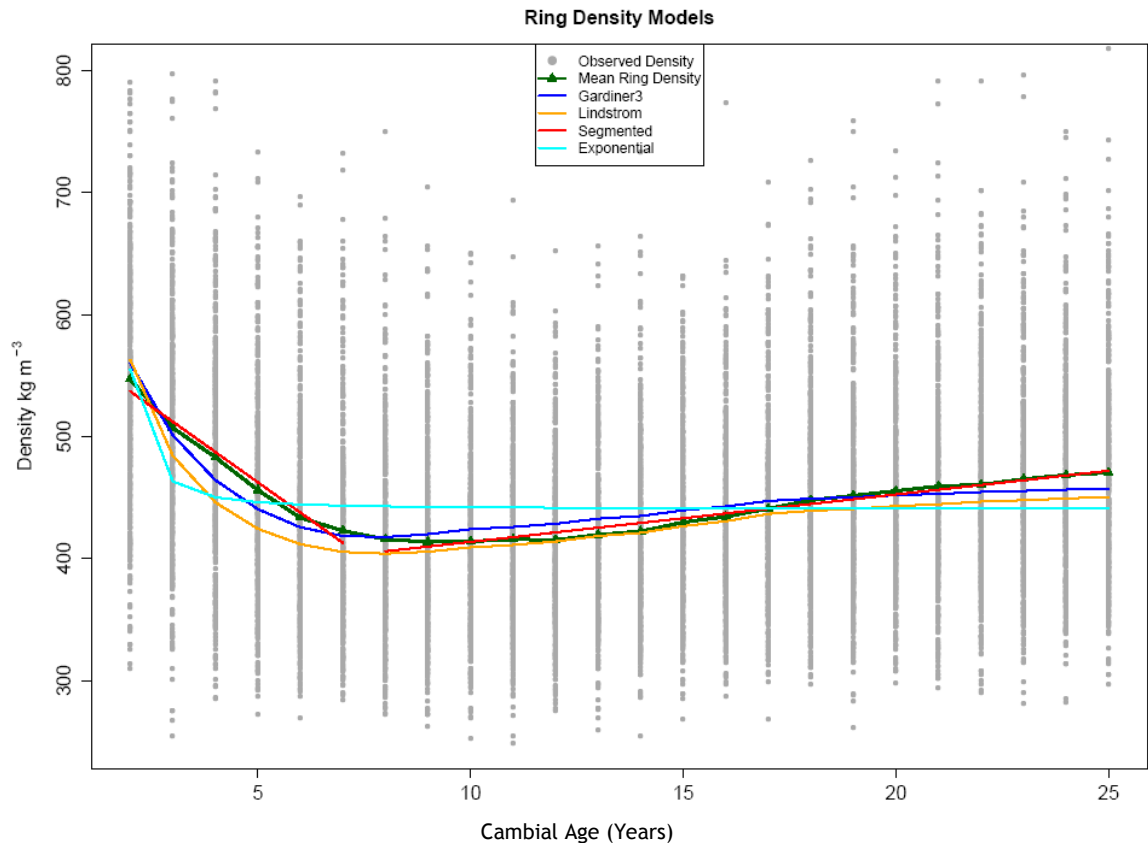


Figure 4-5: The form of the density models plotted along with the mean density for each ring.

As stated previously, the Gardiner and Lindstrom models both require ring width as a parameter, however this may not always be known and so these models of density would also have to include a tree growth model. This has the problem of compounding any errors. In this study ring width is known. Figure 4-6 shows that it is almost a mirror image of the density profile and examination shows that density and ring width are significantly (negatively) correlated (Pearson Correlation Coefficient -0.473). This agrees with previous studies which have shown wider rings to be accompanied by lower ring density (Petty et al., 1990, Gardiner et al., 2011, Kennedy et al., 2013) and may be due to the higher percentage of less dense early wood (Rathgeber et al., 2006) as the amount of latewood is constant irrespective of ring width (Moore, 2011), however the full range of circumstances where this relationship holds has not yet been defined. In this dataset the correlation between density and percent of a ring that is early wood is significant (Pearson Correlation Coefficient -0.362) and shows a similar relationship in both juvenile and mature wood (Figure 4-7).

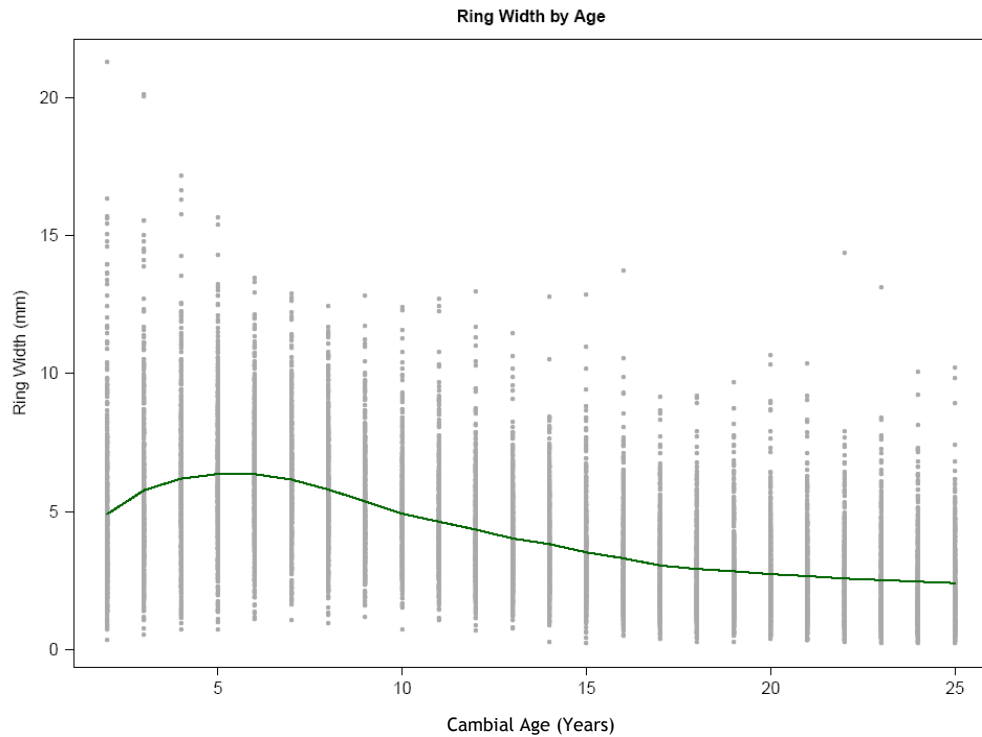


Figure 4-6: Ring width by cambial age (as measured by ring number from the pith) with the mean value for each ring plotted

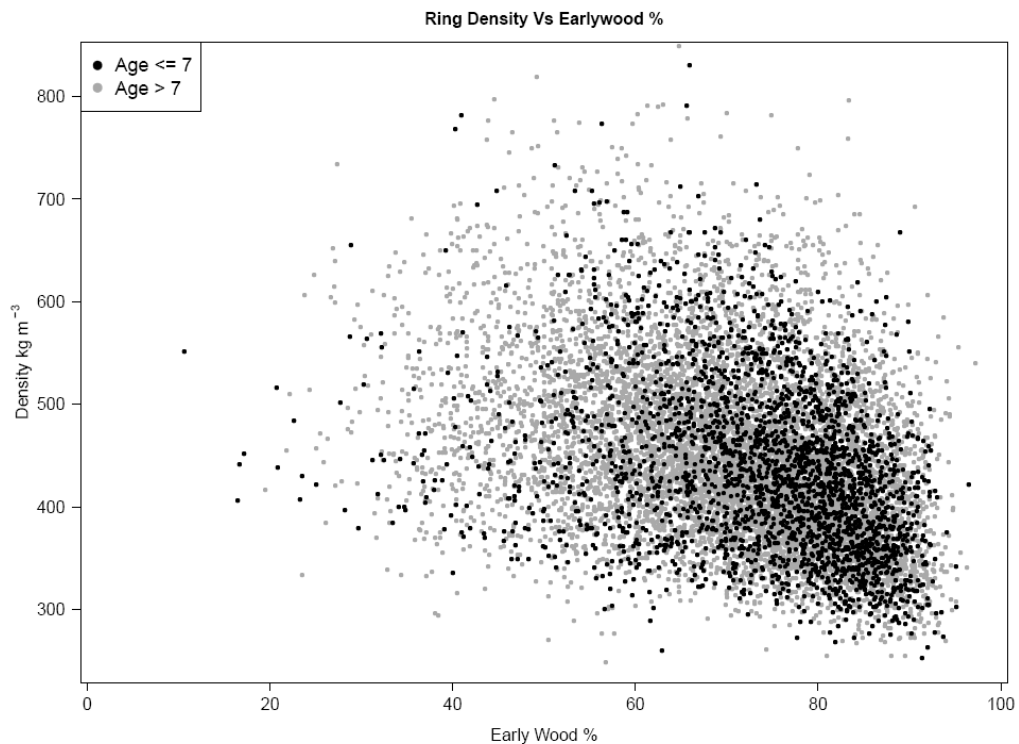


Figure 4-7: The relationship between density and early wood percentage. Pearson correlation coefficient for juvenile wood (i.e. less than or equal to ring 7) is -0.597 and for mature wood (i.e. greater than ring 7) is -0.671. When density is measured there is a clear change point at around cambial age 7 where density starts to increase. Here this is used as the boundary between juvenile and mature wood with regards to density. Although there is an overall

relationship between density and ring width this differs between the juvenile (\leq ring 7) and mature wood ($>$ ring 7) (Figure 4-8) and when these are looked at separately the density has a higher correlation with ring width (Pearson correlation coefficient of -0.597 and -0.671 respectively) than when they are taken together. This changing relationship highlights the difficulty in using ring width as a model parameter and it may be more suitable to use two models; one for below or equal to cambial age 7 and one for over cambial age 7. However for this data set ring width was measured as part of the density analysis so this can be used to parameterize the existing models to investigate which gives the best fit.

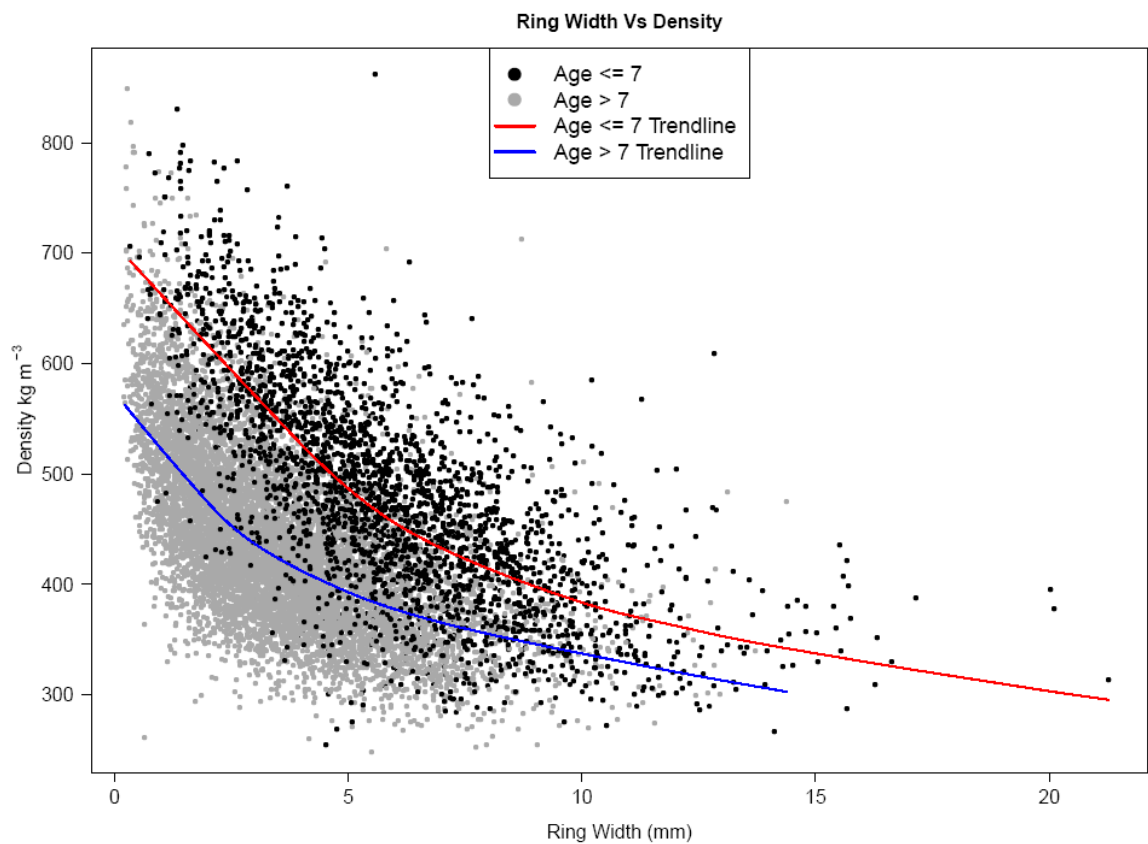


Figure 4-8: Relationship between density and ring width showing these are different between juvenile and mature wood

4.3.2 Gardiner3 Model

Although the fitted lines in Figure 4-5 may indicate that density can be modelled as two separate segments with a specific change point between the two phases,

it is more commonly thought that the change between the juvenile and mature phases is a gradual process so that models which fit a curve to the whole data set may be more appropriate. Therefore as well as looking at juvenile and mature wood as two separate segments this section looks at a selection of different curves, as described in section 4.3, to see which function fits the data the best and how these compare to a segmented linear model.

4.3.2.1 Update to Existing Density Model Parameters

The fit of the Gardiner3 model to the current data set was first investigated using the parameters estimated by Gardiner et al. (2011) These were originally derived from two sites (Clocaenog in North Wales and Kershope in North England). That study also tested two further models (here called Gardiner1 and Gardiner2) from which the final model (Gardiner3) was derived.

The measure of density used by Gardiner et al. (2011) was basic specific gravity which is dry weight/green volume/(density of water at 4⁰ C). In order to compare data the density data measured in this study at 4% moisture content first had to be converted to basic specific gravity using the following equation:

Equation 4.6:

$$SG_B = (SG_m / (1 + MC/100)) / (1 + 0.265 * ((30 - MC) / 30) * SG / (1 + MC/100))$$

Where MC is moisture content percent of the sample, SG_B is basic specific gravity, SG_m is density measured by the ITRAX in kg/m³ divided by 10³ to give specific gravity (ratio of wood density to the density of pure water at 4⁰C) which is dimensionless. The relationship between SG_B and SG_m calculated for this data set is shown in Figure 4-9.

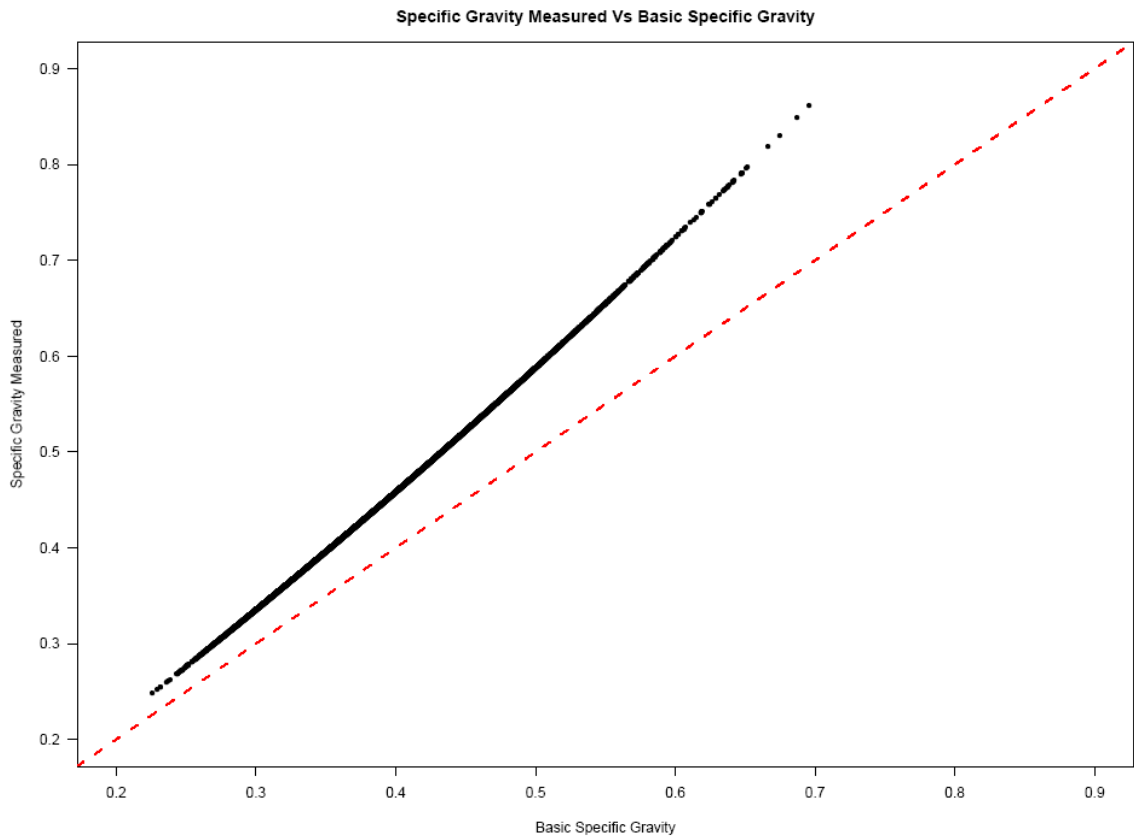


Figure 4-9: Relationship between specific gravity measured as calculated from the ITRAX density data and basic specific gravity. The dashed line shows the line of equality.

Once the data have been converted to basic specific gravity the original parameters described by Gardiner et al. (2011) are plotted against the data in Figure 4-10 using the mean ring width for each ring as the ring width parameter. This shows that the original parameters still a very good fit to this data set and are very closely matched to the parameters derived in this study, especially with the Gardiner3 model. The new parameters which were derived for the three density models using the data collected from 47 sites in this study are shown in Table 4-4 using the same scale as that used in Gardiner et al. (2011).

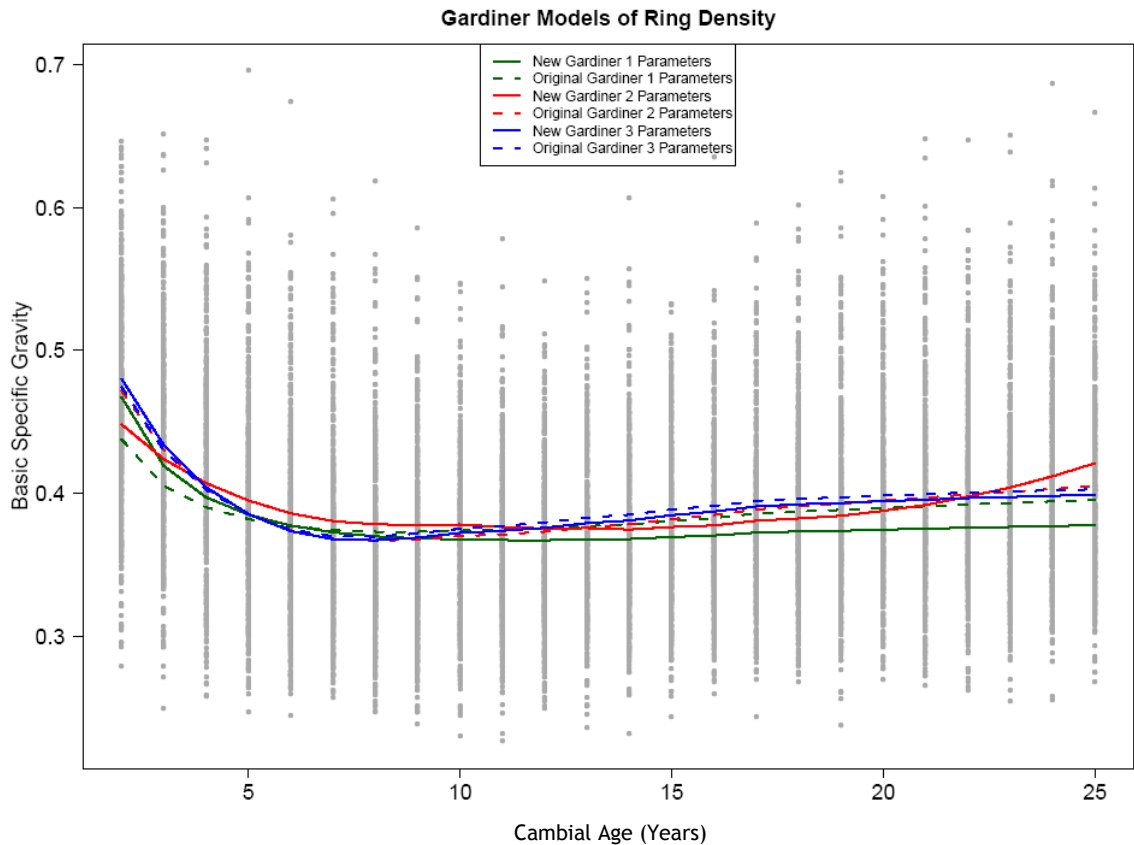


Figure 4-10: Fitted lines for the three models from Gardiner et al. (2011), using the parameters which were derived from the original data and the parameters derived from the data in this study converted at 4% moisture content.

Table 4-4: Parameter estimates for the density models from Gardiner et al. (2011) along with Standard Errors, residual standard error and R-squared values. Where rd is ring density, rn is ring number from the pith, rw is the ring width of each ring and a_i , b_i and c_i are the parameters estimated from the data when converted to basic specific gravity.

Model	Estimate	Std Error	Residual Std Error	R-Squared
Gardiner1:				
$rd = \exp(a_1/rn) * (a_2 + a_3/rw)$				
a_1	0.5982	0.01228	0.05383	0.3607
a_2	0.3252	0.00095		
a_3	0.1049	0.00148		
Gardiner2:				
$rd = b_1 * (1 + b_2 * \exp(rn/b_3)) * (1 + b_4 * rn + b_5 * rw)$				
b_1	0.5344	0.003196	0.05027	0.4365
b_2	0.0262	0.002883		
b_3	6.7633	0.119118		
b_4	-0.0218	0.000528		
b_5	-0.0299	0.000471		
Gardiner3:				
$rd = c_1 * (1 + c_2 * \exp(rn/c_3)) * (1 + c_5 * rw)$				
c_1	0.4385	0.001000	0.05026	0.4374
c_2	0.5748	0.015079		
c_3	-3.9136	0.143626		
c_5	-0.0383	0.000410		

4.3.2.2 Fitting Gardiner3 Model

Although in the previous section density was converted to basic specific gravity, in order to be comparable to previous work done on Sitka spruce in Scotland (McLean, 2008, Vihermaa, 2010) all further analysis was carried out using the density values as measured by the ITRAX densitometer at 4% moisture content in kg m^{-3} .

When the new parameters, estimated from the current data set are used the Gardiner3 model performs reasonably well with an R-squared value of 0.44 although there does seem to be a large spread in the values predicted by the model compared with the observed values and there may be a suggestion that it is over predicting at lower values and under predicting at higher values (Figure 4-11). There also seems to be a discontinuity at the predicted value of approx. 500 kg m^{-3} , although the reasons for this division are unclear. It may represent the predicted density at the upper age limit modelled. The residuals when plotted against cambial age (Figure 4-12) are evenly distributed with no major trend observed though there may be a tendency for the model to under predict around the break in the slope. When the residuals were plotted against the observed values (Figure 4-13) there was a strong trend of over predicting at lower density values and under predicting at higher values. When plotted against ring width (Figure 4-14) there again was a tendency to under predict at higher ring width values though this may be influenced by the lack of data points at higher ring widths.

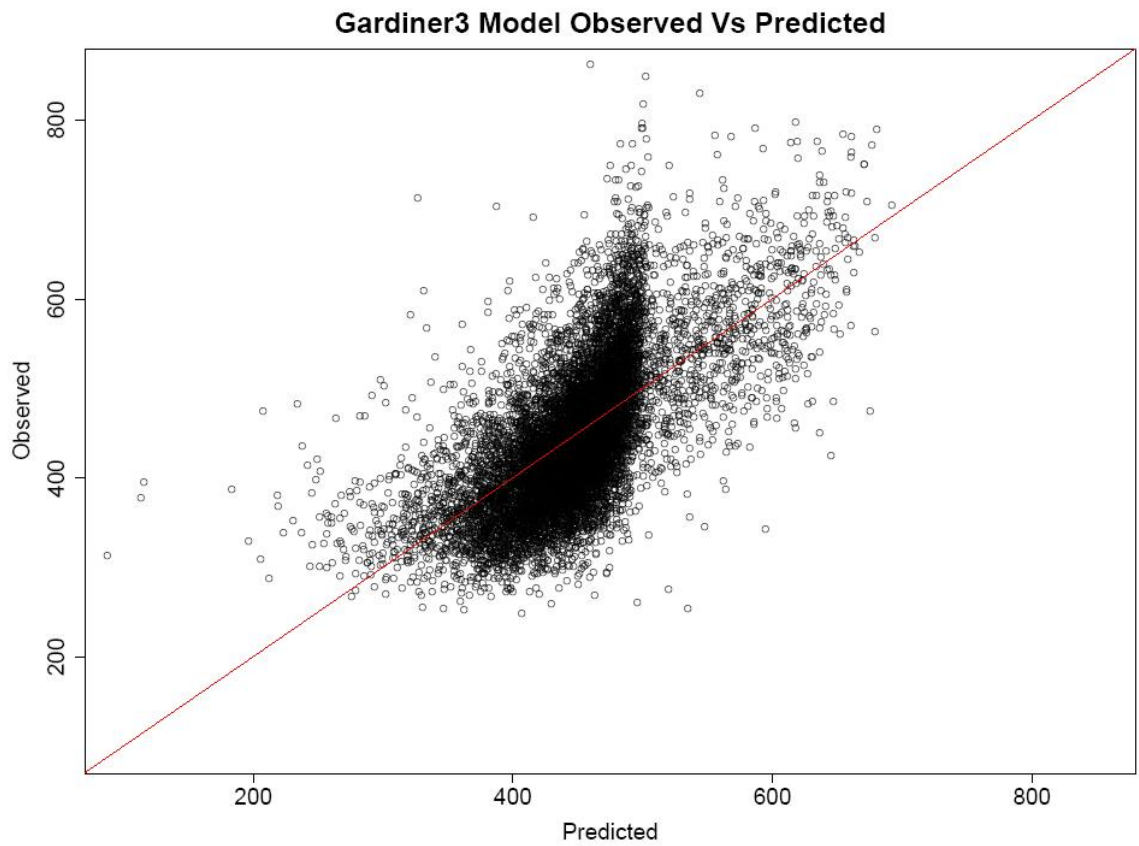


Figure 4-11: Observed Vs Predicted for the Gardiner3 model on all of the density data. Red line shows the line of equality.

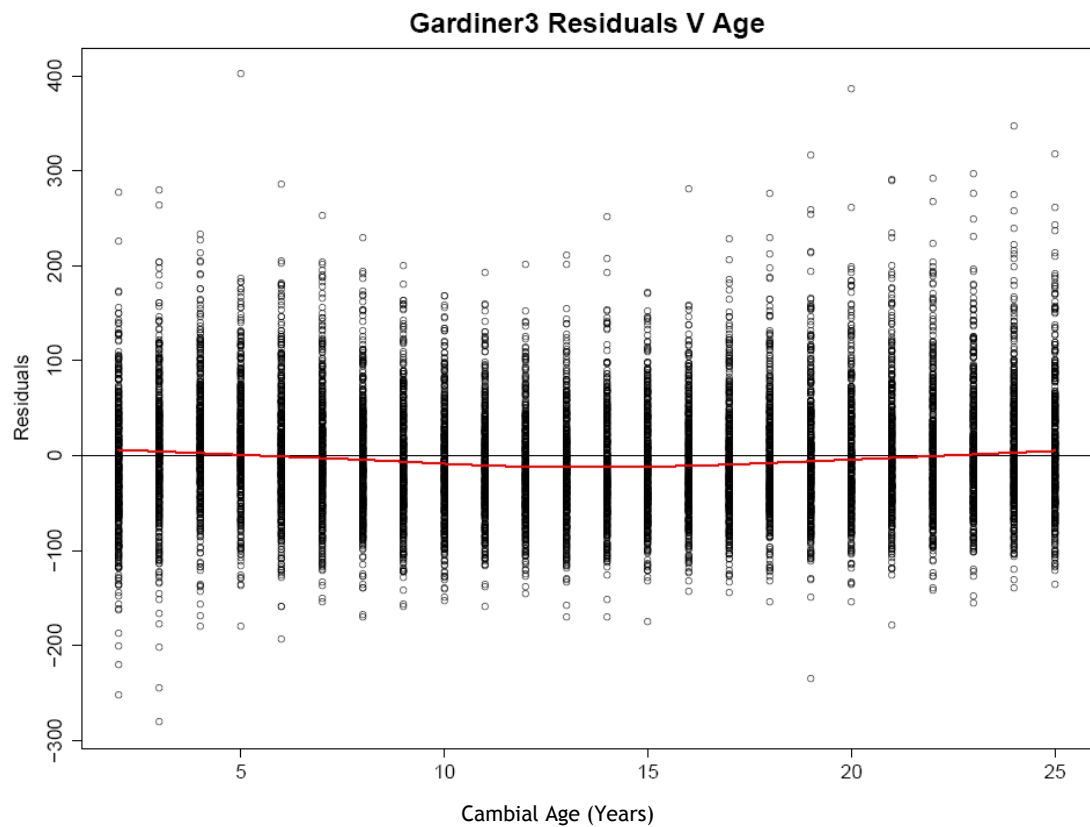


Figure 4-12: Residuals for the Gardiner3 model plotted against cambial age on all of the density data. Red line shows the LOWESS trend line.

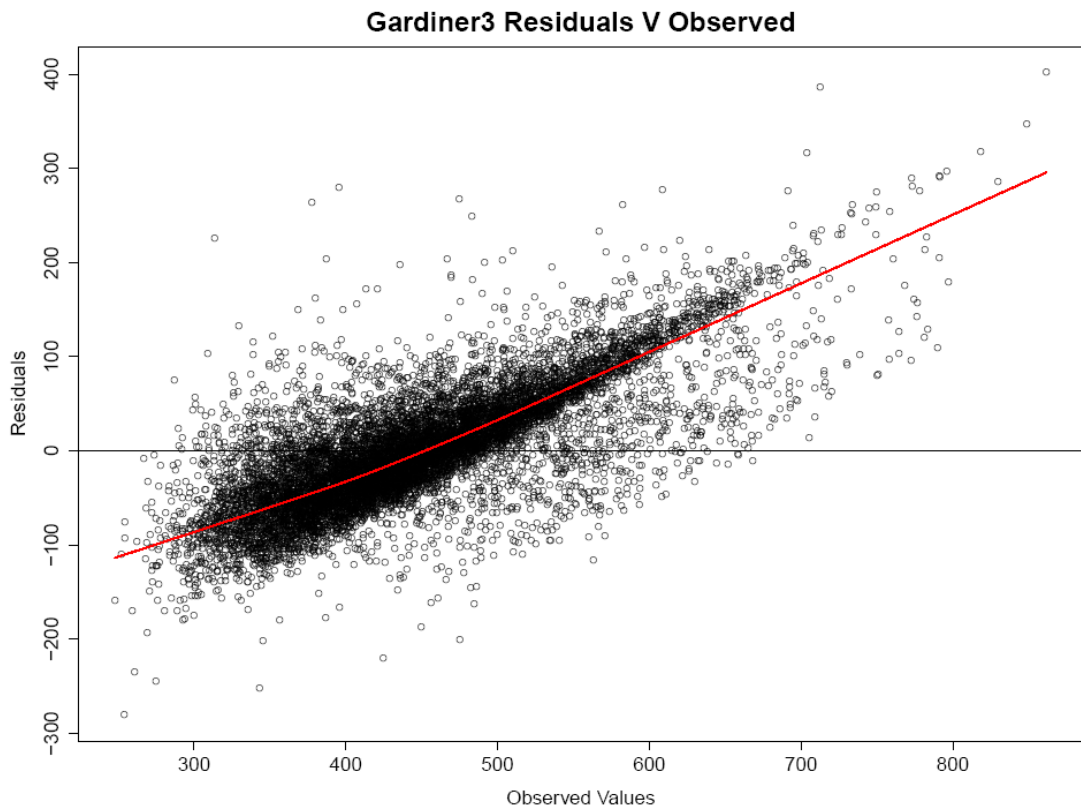


Figure 4-13: Residuals for the Gardiner3 model plotted against observed values on all of the density data. Red line shows the LOWESS trend line.

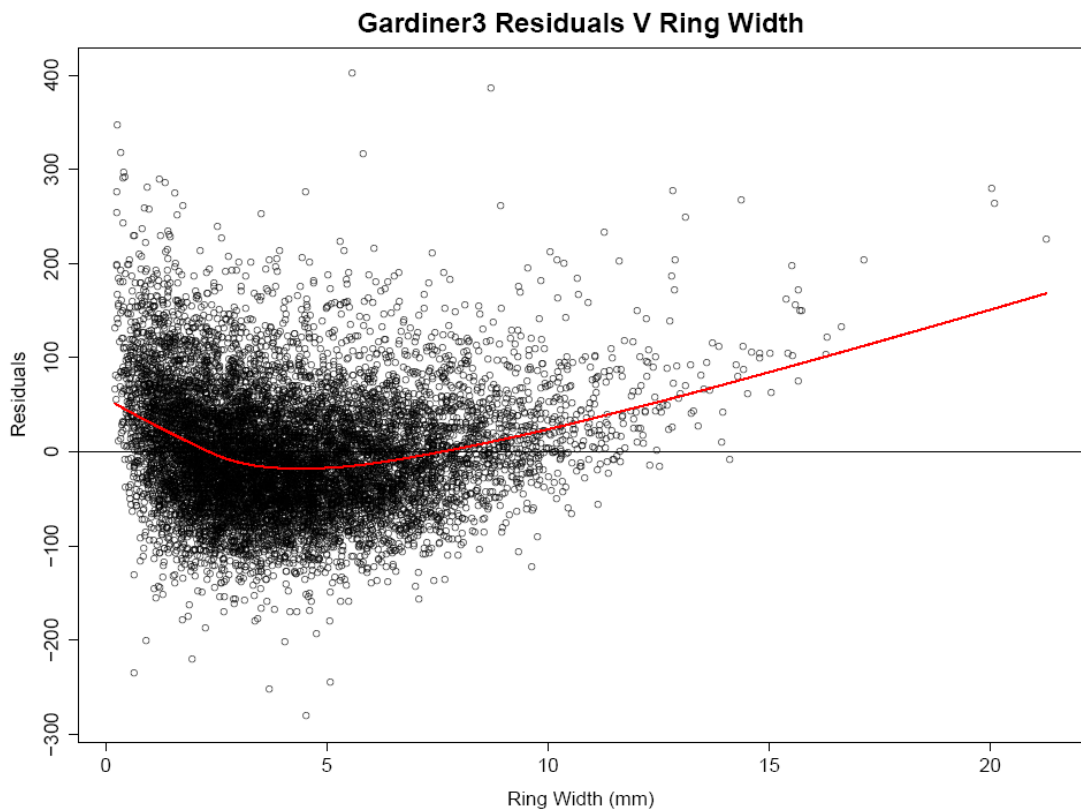


Figure 4-14: Residuals for the Gardiner3 model plotted against ring width on all of the density data. Red line shows the LOWESS trend line.

4.3.3 Lindstrom Model

The Lindstrom model had a slightly higher R-squared (0.48) and slightly lower residual standard error (61.55 kg m^{-3}) than the Gardiner3 model and a plot of the observed density versus those fitted by the model (Figure 4-15) shows that while there may be a more even spread it may still be over predicting at lower values. Plotting the residuals by cambial age (Figure 4-16) shows a relatively even distribution and again there may be a tendency for this model to under predict around the break in the slope. When the residuals were plotted against the observed values (Figure 4-17) there was a strong trend of over predicting at lower density values and under predicting at higher values. When plotted against ring width (Figure 4-18) there again was a tendency to over predict at higher ring width values though again this may be influenced by the lack of data points at higher ring widths.

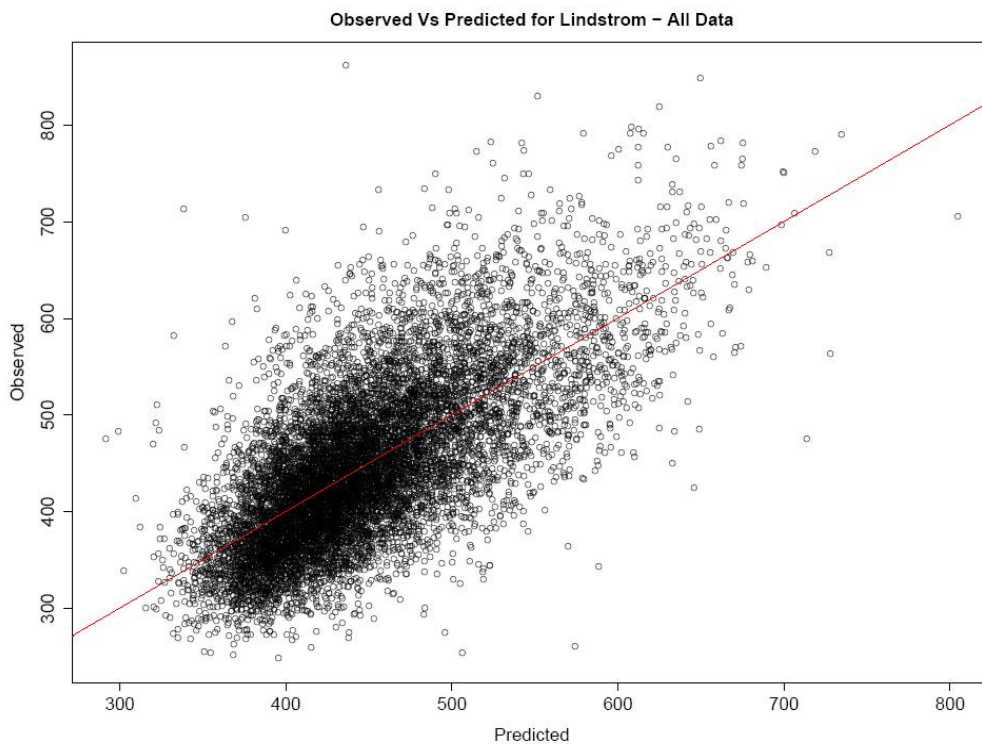


Figure 4-15: Observed Vs Predicted for the Lindstrom model on all of the density data. Red line shows the line of equality.

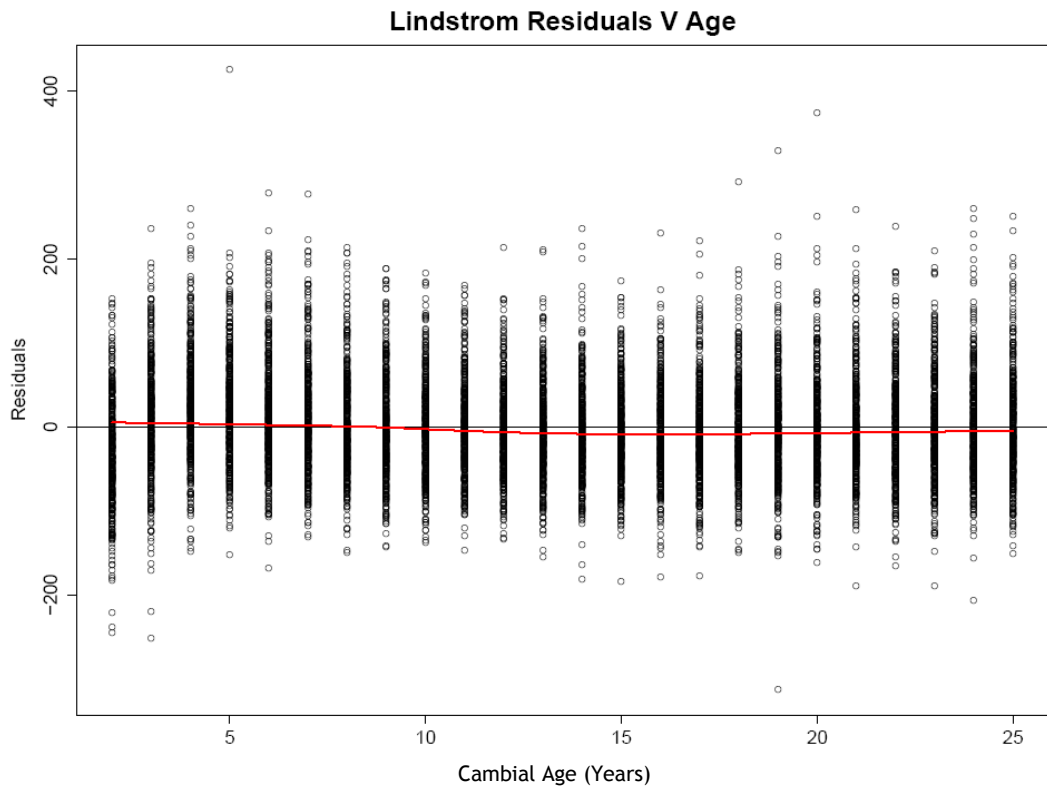


Figure 4-16: Residuals for the Lindstrom model plotted against cambial age on all of the density data. Red line shows the LOWESS trend line.

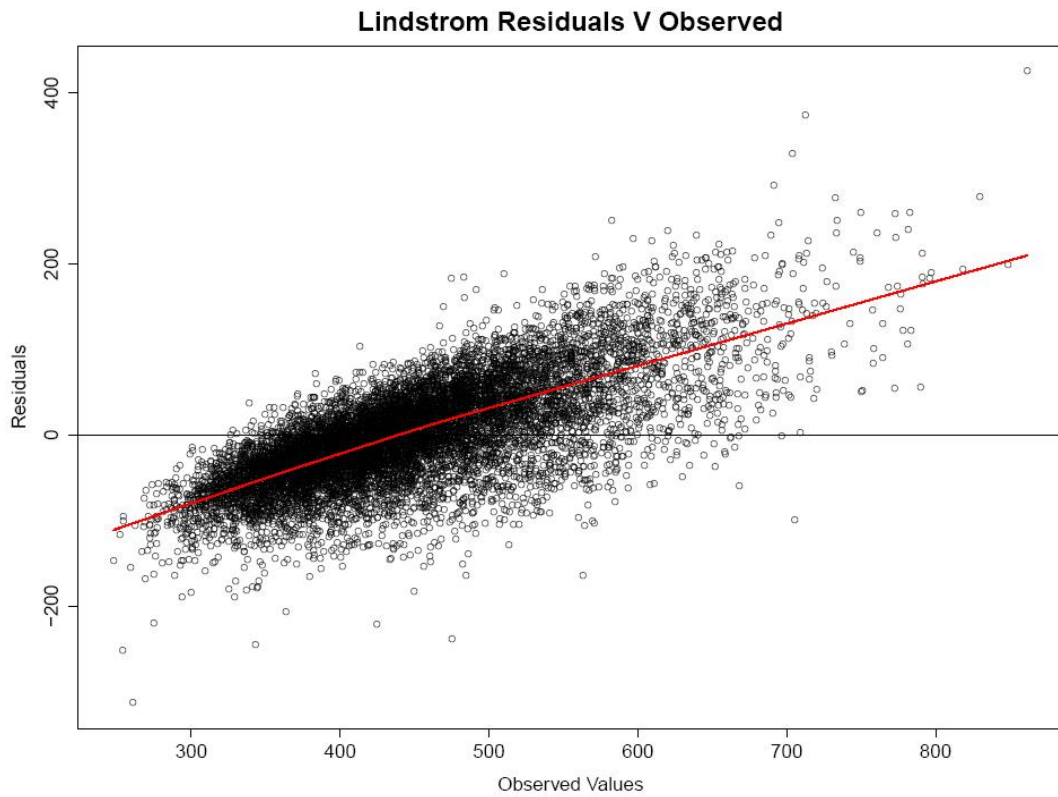


Figure 4-17: Residuals for the Lindstrom model plotted against the observed values on all of the density data. Red line shows the LOWESS trend line.

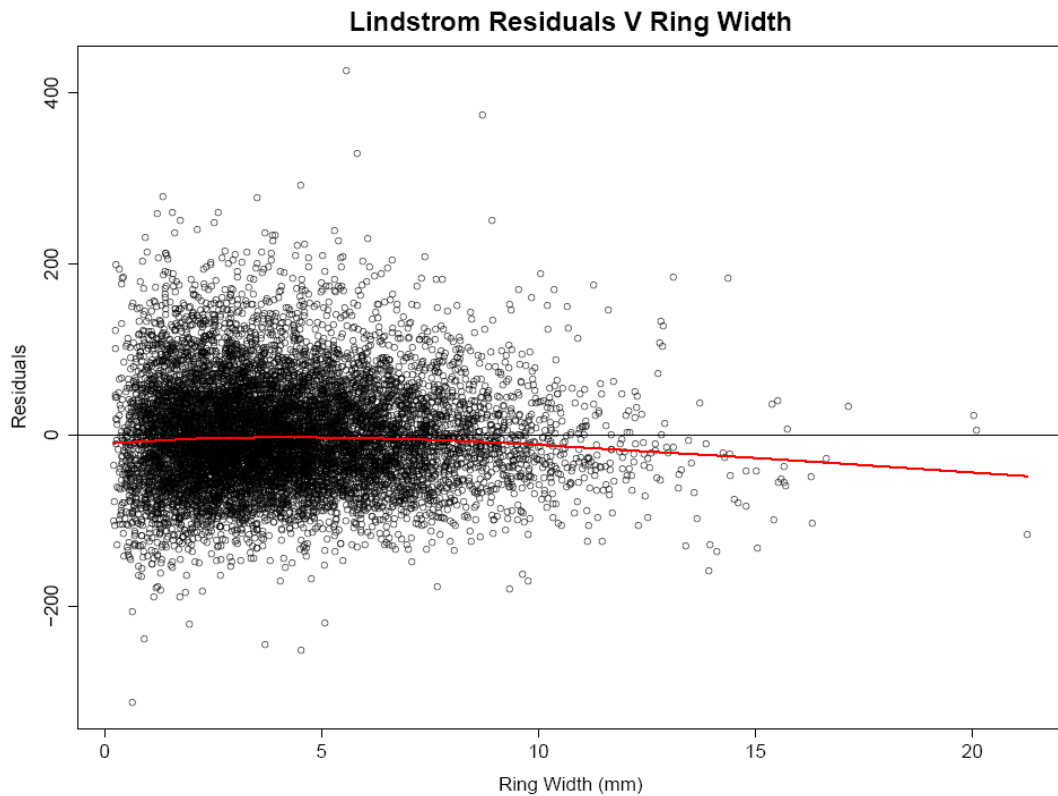


Figure 4-18: Residuals for the Lindstrom model plotted against ring width on all of the density data. Red line shows the LOWESS trend line.

4.3.4 Exponential Model

The exponential model was seen to be the worst fitting of the models tested and analysis showed it had the lowest R-Squared out of those tested (Table 4-3). It also seems to have problems predicting density from cambial age (Figure 4-19) with a division between the prediction for ring number 2 and other rings at the asymptote. Although the residuals (Figure 4-20) are fairly evenly distributed with age the model over predicts between approximately rings 8 and 18, suggesting there may be a problem fitting this model to the data.

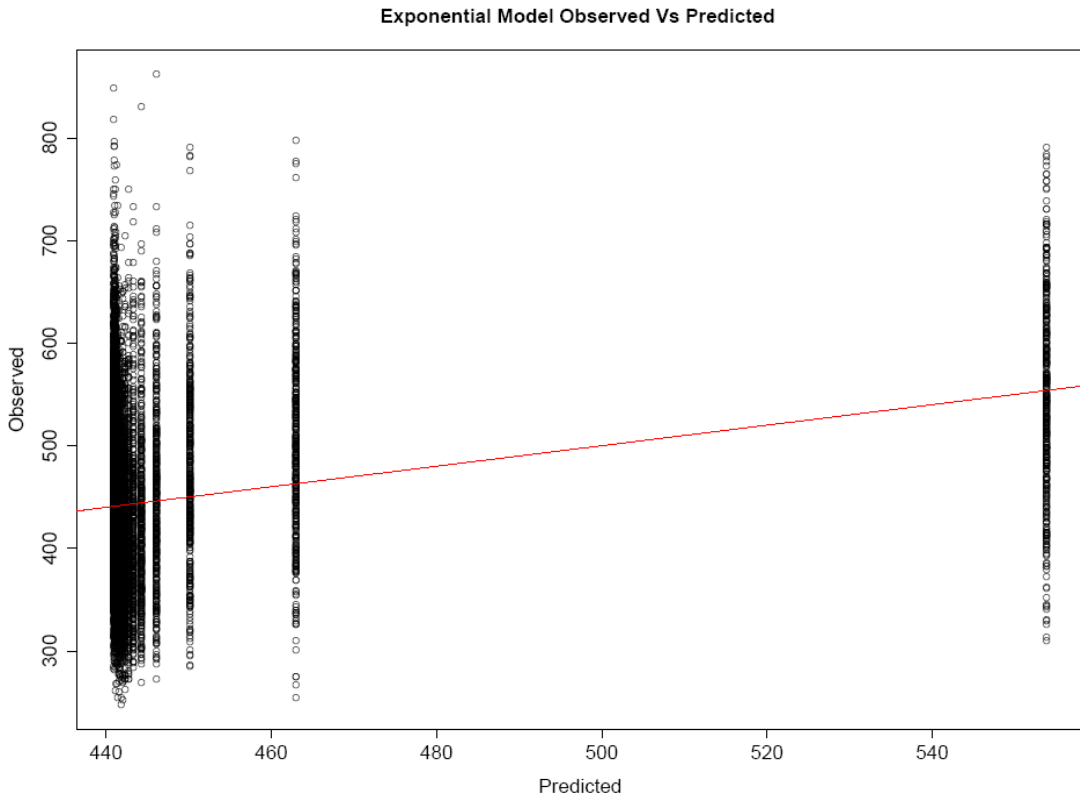


Figure 4-19: Observed Vs Predicted for the Exponential model on all of the density data. Red line shows the line of equality.

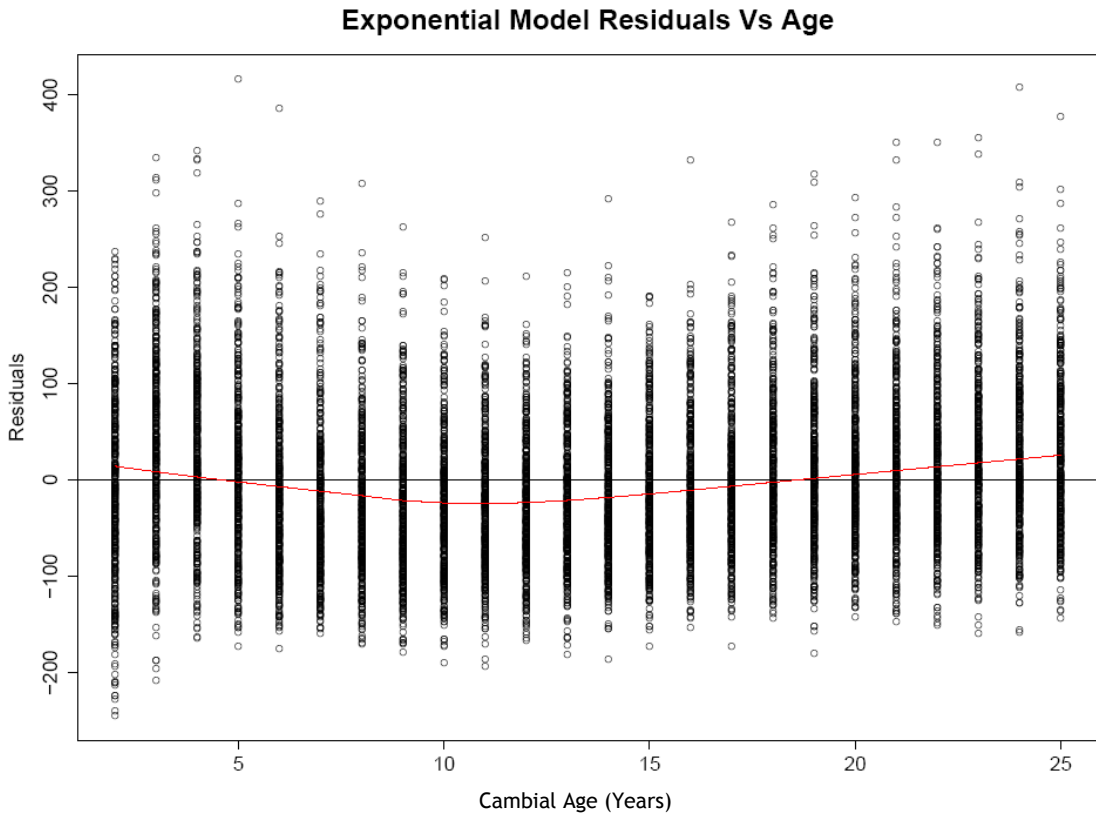


Figure 4-20: Residuals for the Exponential model on all of the density data. Red line shows the LOWESS trend line.

4.3.5 Linear Segmented Model – Split Point between Juvenile and Mature Phase of Density

In order to determine if there are two separate linear segments in the density radial profile a Davies' test was carried out on the entire data set, indicating that there was a significant change in the slope (p -value < 0.0001). Using the Segmented package in R (Muggeo, 2008) a regression model with segmented relationships was used to determine the parameters of the different slope segments (i.e. slope, intercept and split point). The result of this test gave an estimated mean split point between the juvenile and mature segments of the radial profile of density at 7.4 years with a standard error of 0.89 and a residual standard error of 79.15 kg m⁻³.

4.3.5.1 Fitting the Density Profile Split to Individual Trees

A segmented model seems to work well when fitted against the global data and this model can also be fitted against individual trees to give the density rate of change, intercepts and split point for each. When performing the Davies Test for each tree individually the algorithm looks for a significant change in slope. If the Davies Test is not significant then only one slope was calculated for that tree i.e. with no break point, for example sample 1600-22-A in Figure 4-21. This plot also shows the fluctuation in density in each tree and the difficulty faced when trying to fit a split point to each tree.

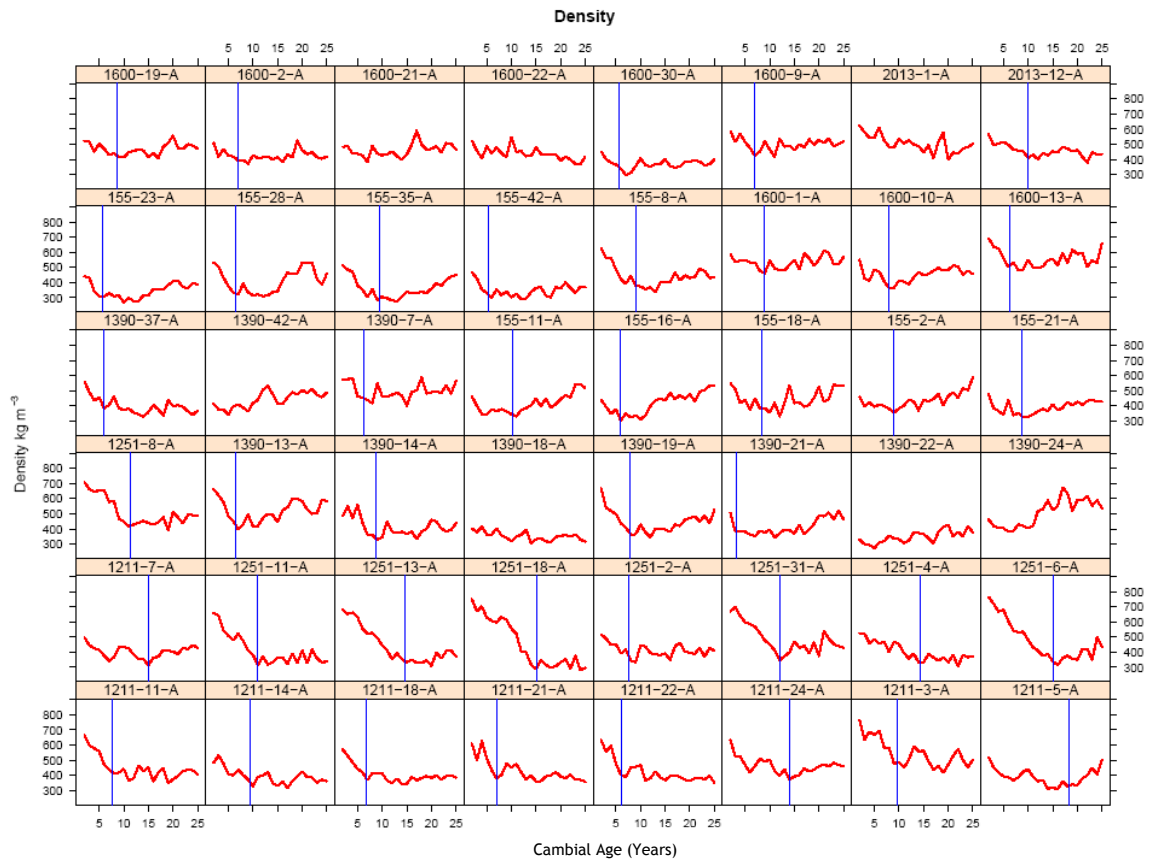


Figure 4-21: Example of the observed density profiles for a selection of trees with the split point fitted by the segmented model

While the two segment model gives a reasonable fit when modelled against the global data, the sensitivity when it is modelled against individual trees produced some very low estimates (<5 years) as well as some high estimates (>20 years) (Figure 4-22) indicating that this method of calculating the split point on individual trees may be too sensitive to local fluctuations in density.

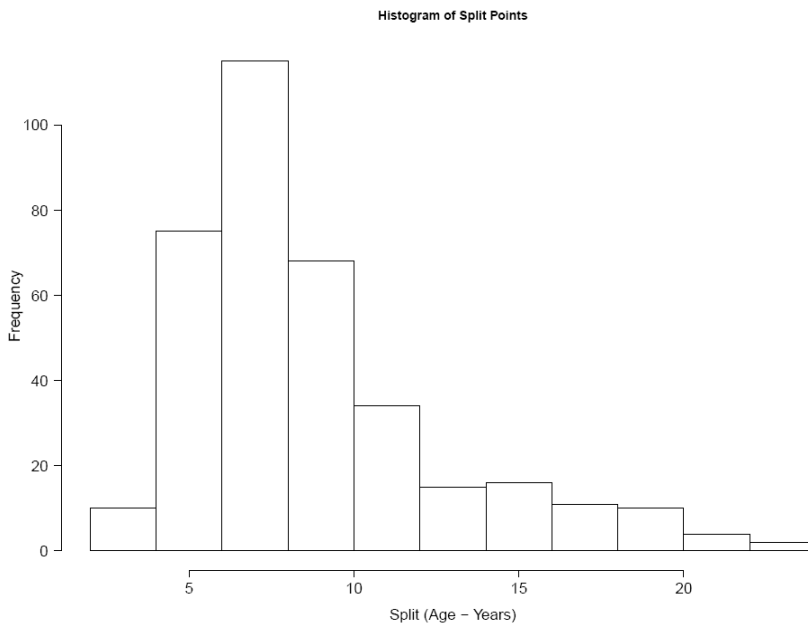


Figure 4-22: Histogram showing the distribution of split points for the density segmented model. The minimum split point was 3.0 years, the maximum was 23.9 years and the mean was 8.7 years.

On this data set the segmented model was unable to fit to 7 (1.5%) of the 451 trees (Figure 4-23). Of the remaining 444 trees the Davies Test found no significant change of slope and therefore no split point in 84 of the trees.

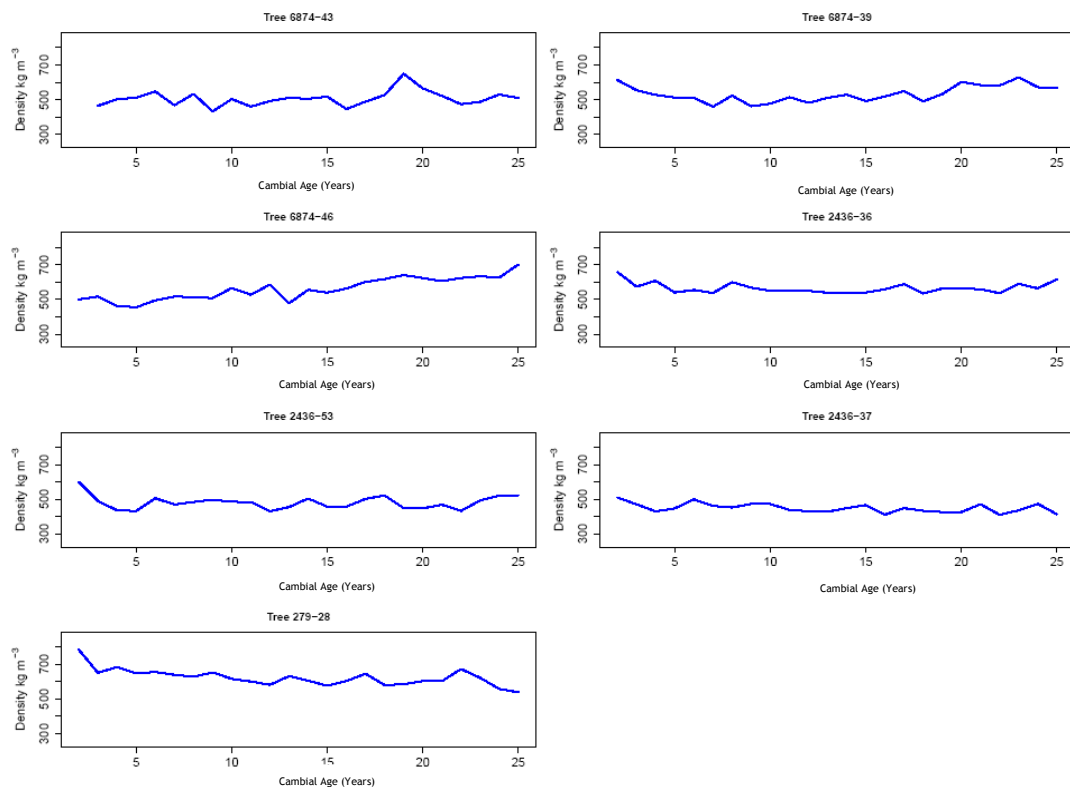


Figure 4-23: The density profile of the 7 trees that the segmented model could not fit

When the observed values are plotted against the predicted values for individual trees (Figure 4-24) there is a relatively good fit and an R-Squared value of 0.83.

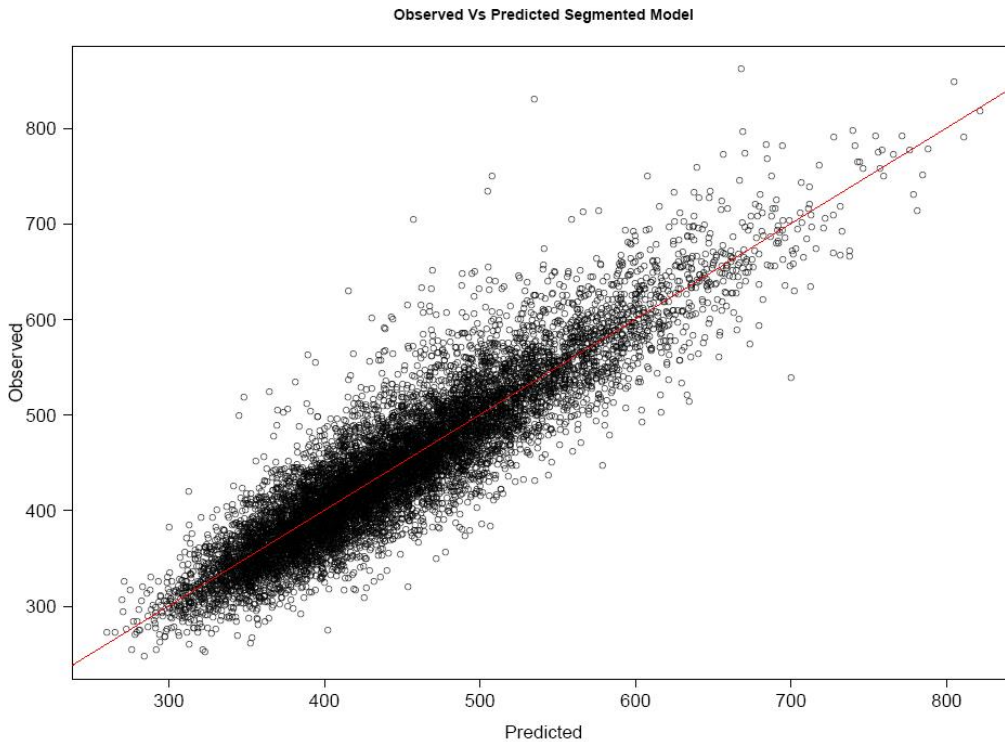


Figure 4-24: Observed Vs Predicted for the density segmented model when fitted to individual trees. R-squared = 0.83

4.3.5.2 Factors Affecting the Split Point

In order to visualise if there is a site or climate effect, the position of the split point fitted to individual trees was compared with the site characteristics and with the climate parameters for each site (Figure 4-25). Analysis showed that the only significant correlation was with rainfall (Pearson correlation coefficient -0.117) with the rest being non-significant. However it is difficult to draw any conclusions from this since the correlation coefficient is so low as well as due to the difficulty of inter correlations. Since a number of the site variables are correlated with the climate variables e.g. elevation with moisture deficit (Pearson correlation coefficient -0.703) and a number of the climate variables are correlated with each other, e.g. accumulated temperature with moisture deficit (Pearson correlation coefficient 0.788), this could cause problems with any regression analysis. As well as this the sensitivity of the segmented model to local changes in the density profile means it is difficult to know if any effect is real or if it is due to the method.

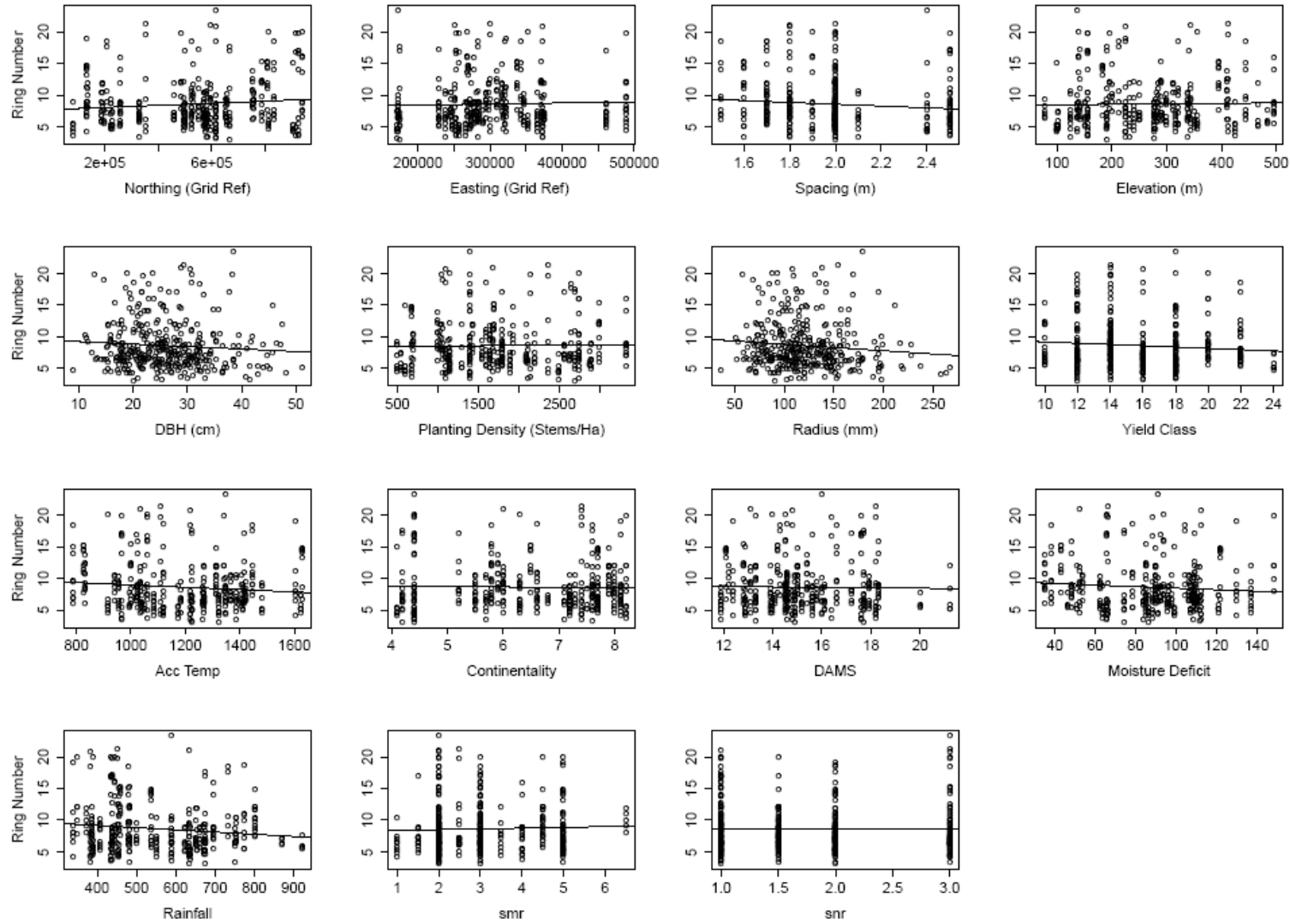


Figure 4-25: The effect of the different variables on the density profile split point, with the black line showing the regression fitted to the data for each. Ring number is measured from the pith.

When the split point is plotted by site (Figure 4-26) the large amount of within site variation can be seen and although there seems to be variation between sites it is difficult to identify the reasons for this variation, which could be due to localised factors within each site. However it would be expected that within an even aged plantation the transition between the juvenile and mature phases of the density profile would be less variable than is seen here and so this is more likely to be due to the sensitivity of the segmented model to small changes in gradient. Not only does this sensitivity, when measured on individual trees, make it difficult to investigate and model any effect on the split point, but also this will lead to a large variation in the slope and intercepts of the different segments. This means that to use the segmented model it may be more appropriate or useful to group the data. For example the split point on the full data set is 7.4 years which could be used as the division between the juvenile and mature phases of the density profile, with each segment before and after this transition having a separate linear model to describe it.

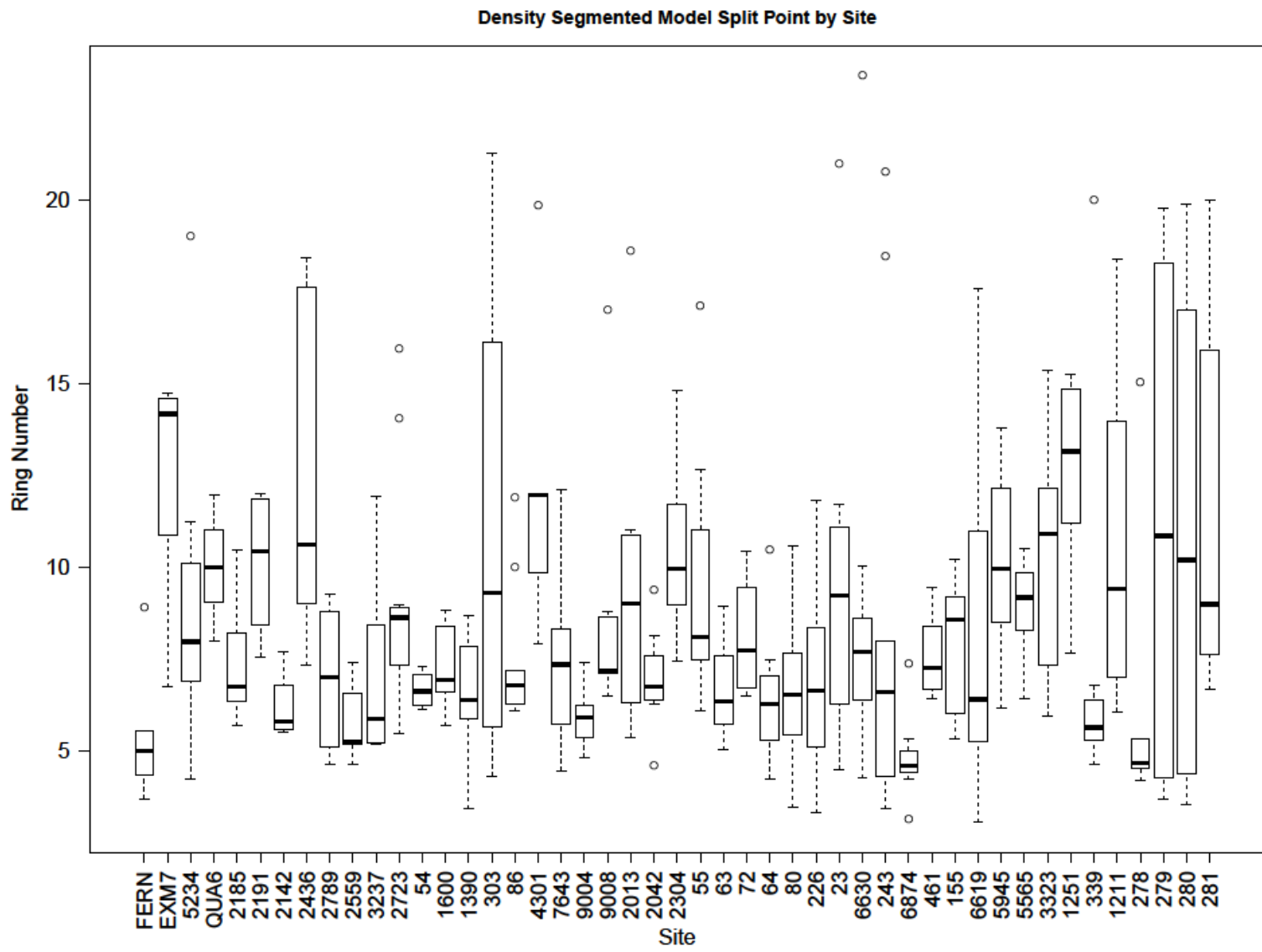


Figure 4-26: The segmented model split plotted by site in order from south (left) to north (right) with ring number measured from the pith.

4.3.6 Density Segmented Model – Juvenile and Mature Segments

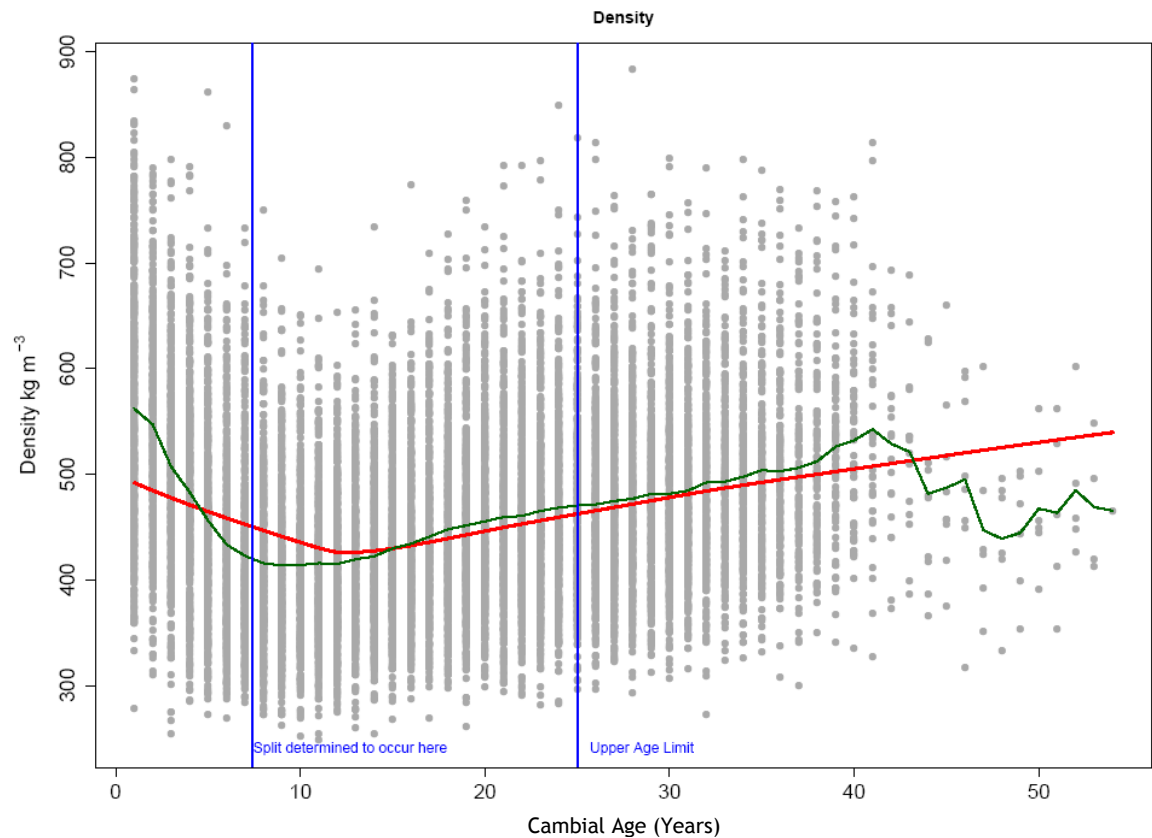


Figure 4-27: Density data showing the mean line (green), the LOWESS trend line (red), the line where the segmented model fitted the split (cambial age 7.4 years) and the upper age limit (25 years) used in this analysis.

As mentioned in 4.3.5, when the segmented model is fitted against the global data it gives us a split between the juvenile and mature segments of the density radial profile at between years 7 and 8, with two separate linear segments: the juvenile section before the split point (cambial age 2 to 7 years) and the mature section (cambial age 8 to 25 years) after the split point (Figure 4-27). Therefore it may be possible to separate the data on either side of this split point and examine the density of the two different segments separately.

When the segments are examined separately for the whole data set density appears linear up until year 7 and also looks relatively linear between year 8 and 25 so it would appear reasonable to continue analysing growth under year 7 and between year 8 and 25 using two separate linear models.

4.4 Factors Affecting the Density Radial Profile

As described in Section 4.3 visually there could be two separate segments in the density profile and segmented analysis showed that density could indeed be described as having a split point between the two segments with two distinct periods before and after this point. When applied to the full data set this model fitted a value of 7.4 years as the split point between the two segments of juvenile and mature density. This section aims to use this split point and two separate linear models to investigate whether the density profile of the two segments are influenced by site effects with the hypothesis being that density variation in the juvenile and mature wood are functions of the site characteristics such as latitude, longitude, elevation or spacing.

4.4.1 Juvenile Density Segment

A linear model was fitted to rings 2 to 7 of the full data set using ordinary least squares regression, performed by the “lm” function in R producing a significant p-value of < 0.0001 , indicating that this segment could be described as linear with a slope of -24.8 kg m^{-3} per year and an intercept of 587 kg m^{-3} . An R-squared value of 0.19 may indicate that while a linear model can be fitted, there is a lot of variation about the slope. The residual plots for the juvenile segment (Figure 4-28) show that the linear model has a relatively even distribution of residuals with cambial age, and the spread of the predicted values is similar throughout the range of observed values (Figure 4-29).

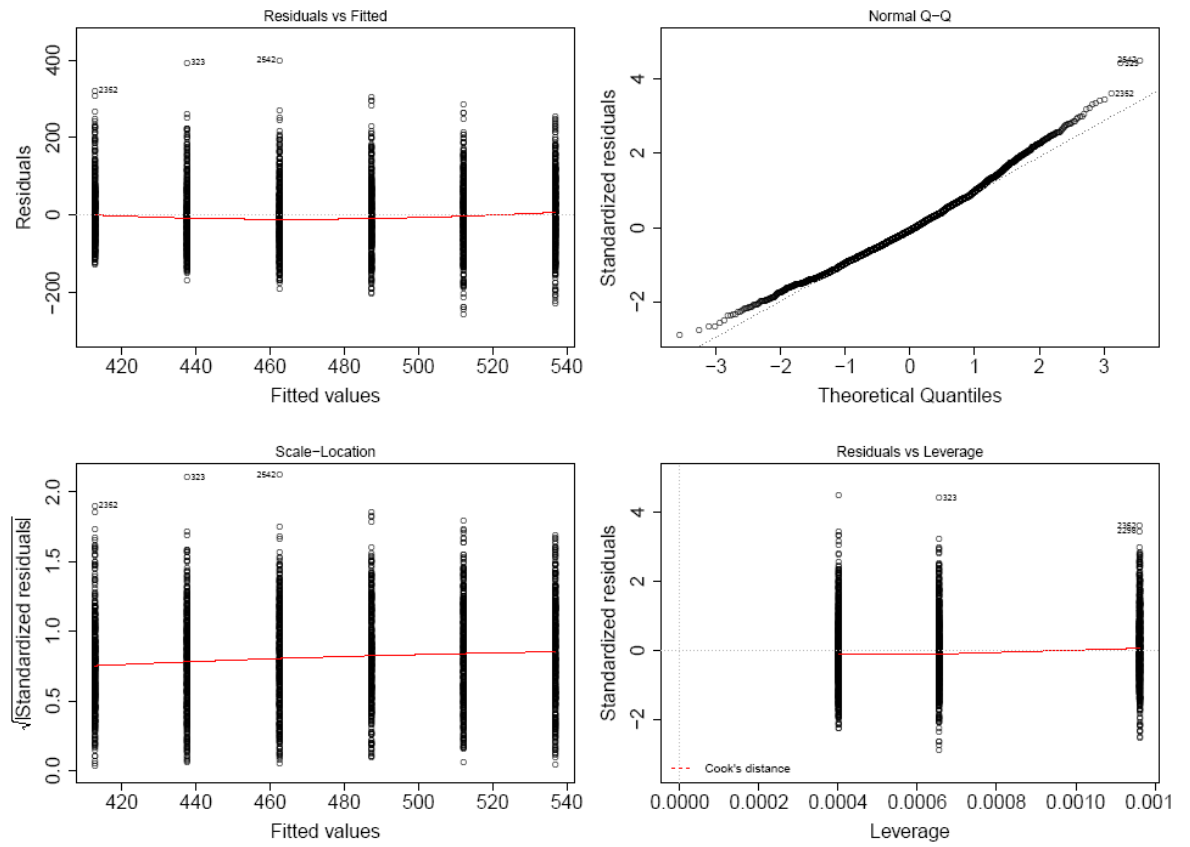


Figure 4-28: Residual plots for the density juvenile segment linear model

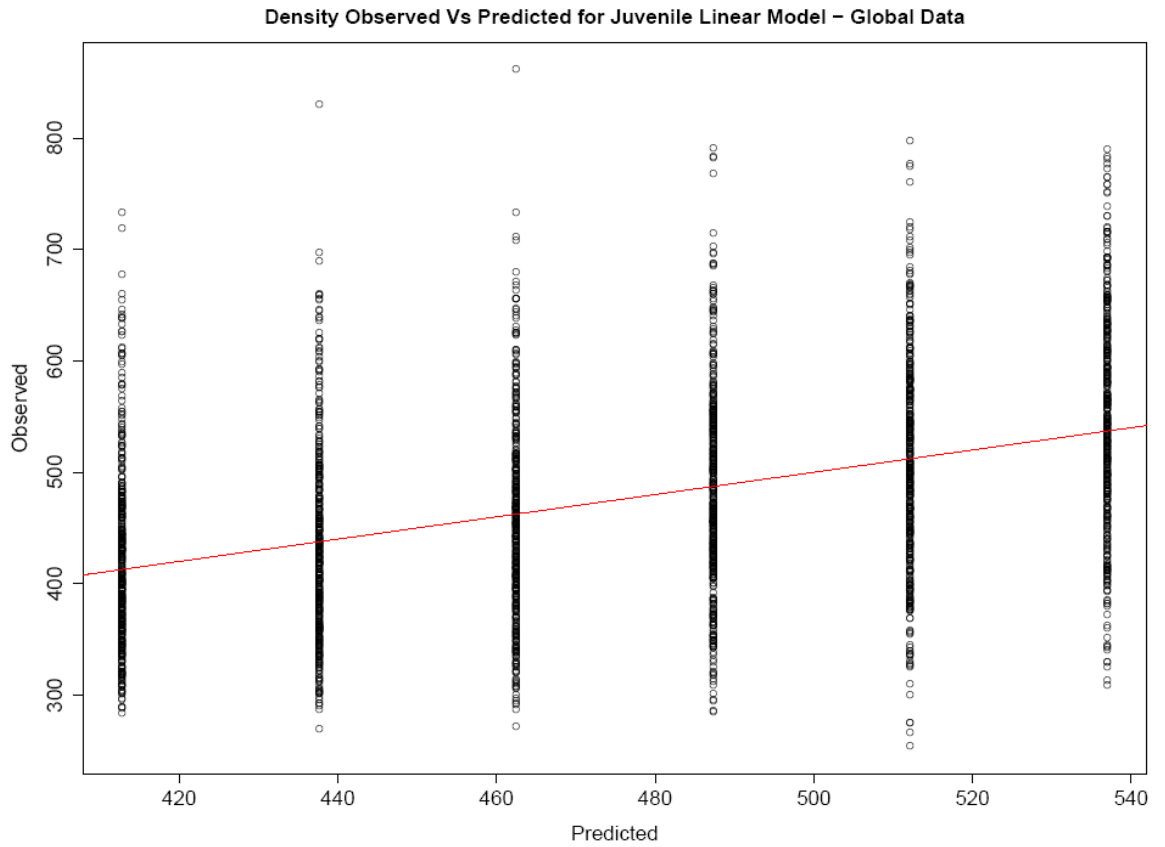


Figure 4-29: Observed versus predicted density values for the juvenile segment linear model. The red line shows the line of equality.

4.4.1.1 Linear Model of Juvenile Density Segment Fitted to Individual Trees

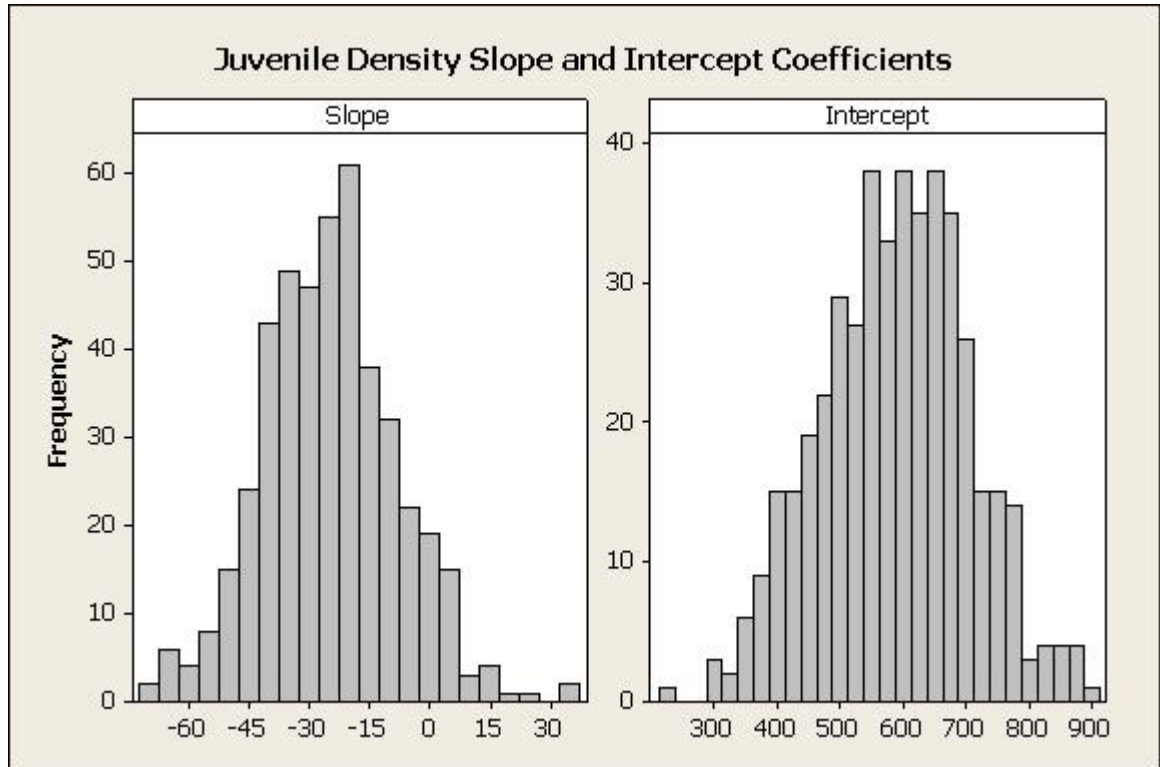


Figure 4-30: Slope and intercept coefficients fitted by the linear model to the density profile up to year 7 for each sample

A linear model fitted to rings 2 to 7 of individual trees shows that there is a lot of variation in both the slope and intercepts (Figure 4-30), although both follow a normal distribution. The slope of this segment ranged from -72 kg m^{-3} per year to 37 kg m^{-3} per year with a mean of -25 kg m^{-3} per year. When modelled against the full dataset the juvenile segment showed a negative slope, as would be expected with Sitka spruce, but when modelled against individual trees 32 of the 444 samples had a positive slope in this phase (Figure 4-31). These samples were investigated and nothing unusual was found, indicating this is just natural variation in the density profiles. This highlights the difficulty in modelling this phase of tree growth in Sitka spruce where there is a variable trend of decreasing density in the first few rings from the pith. The mean intercept for the linear model of the juvenile segment was 586 kg m^{-3} and the intercepts for individual trees ranged from 214 kg m^{-3} to 907 kg m^{-3} .

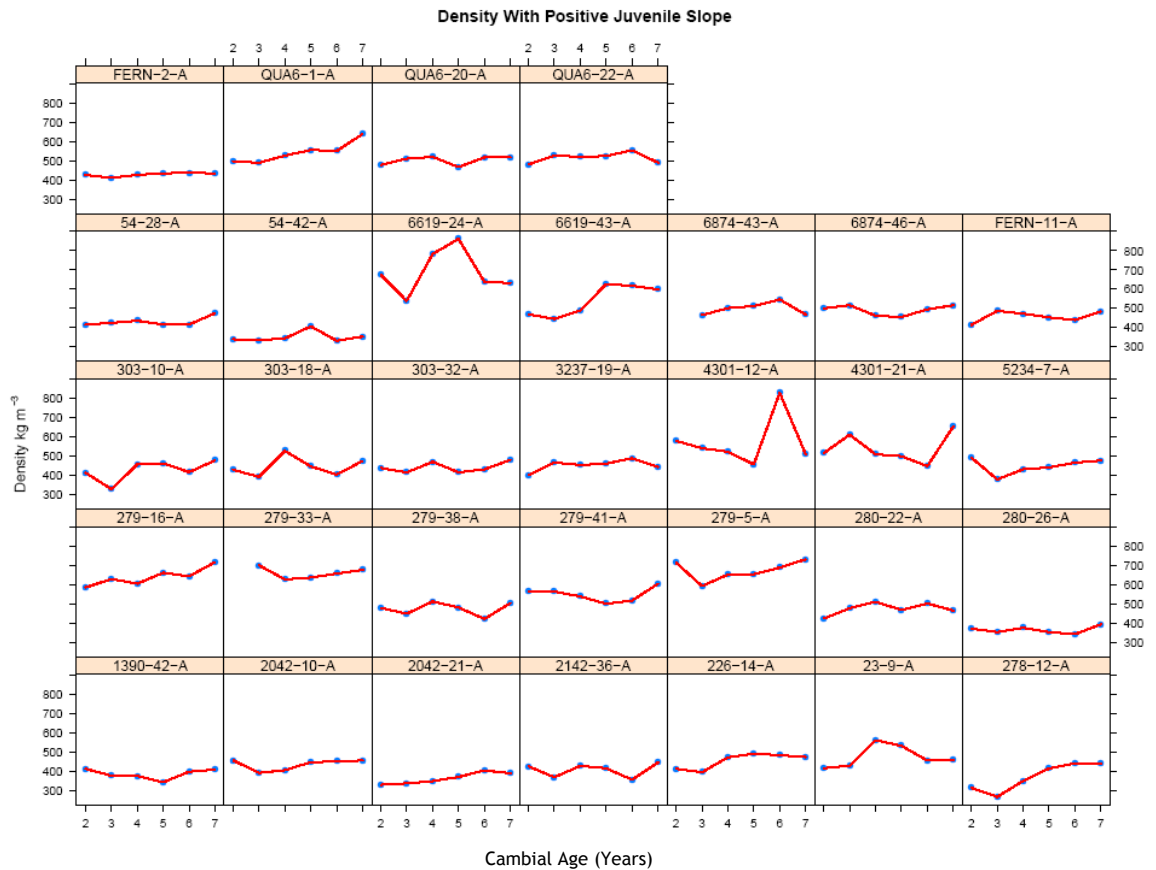


Figure 4-31: The density profiles from rings 2 to 7 of the samples which the linear model predicted a positive slope for density in the juvenile phase.

To test the effectiveness of the model it was fitted against the individual trees. This shows that the residuals have a reasonable fit (Figure 4-32) with a relatively even distribution of residuals with cambial age, though there may be a slight tendency to over predict at lower values and under predict in the middle values. The degree of fit is shown when the observed data are plotted against that predicted by the linear model (Figure 4-33) giving an R-squared of 0.91.

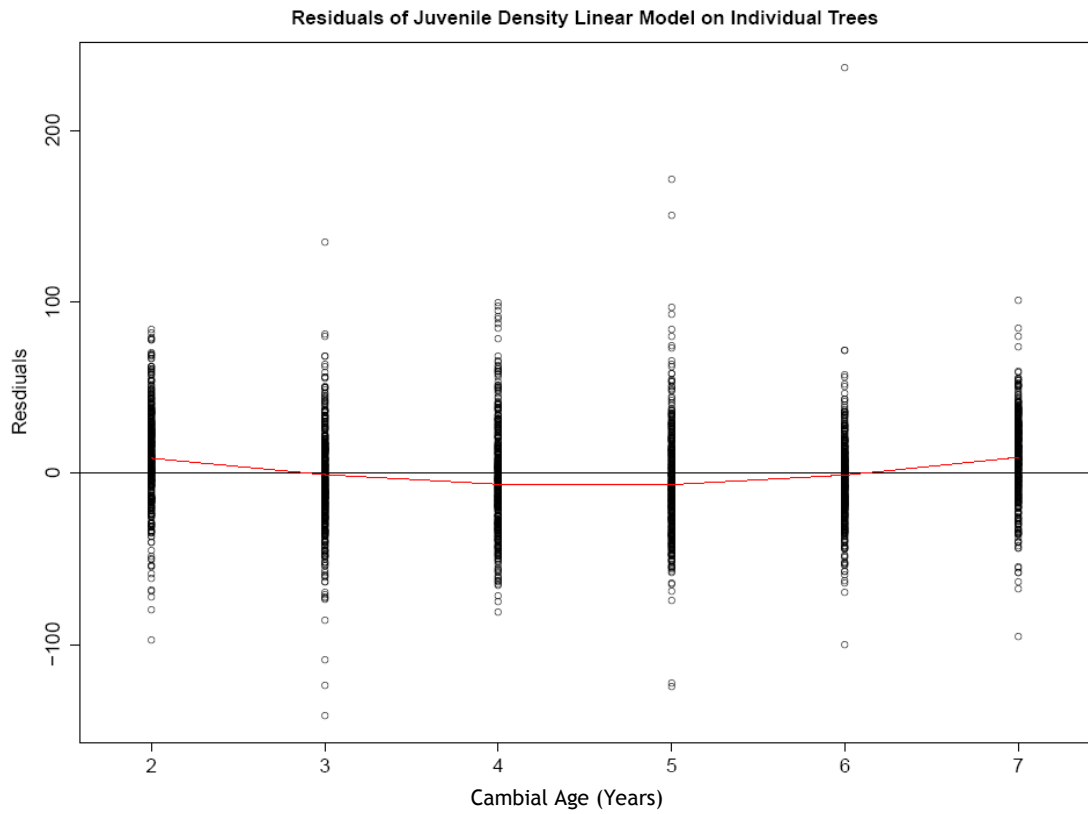


Figure 4-32: Residuals of linear model when fitted to the density profile of the juvenile segment of each tree, with LOWESS trend line (red)

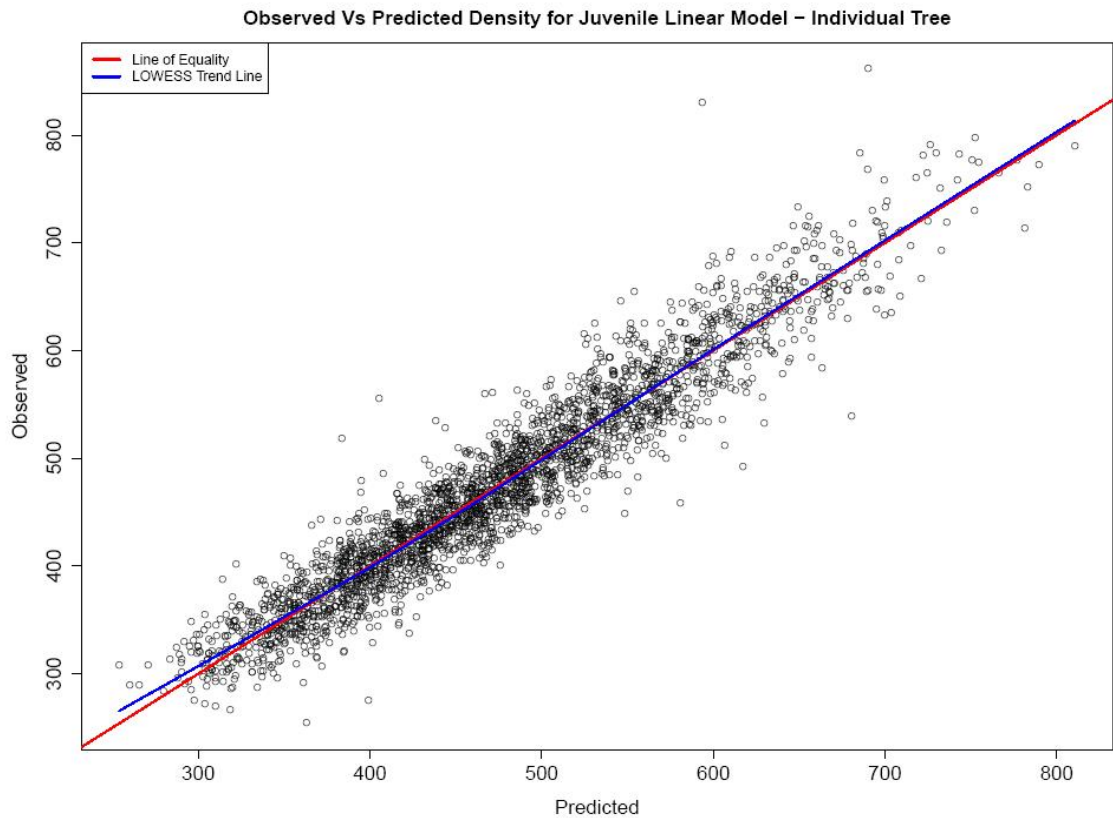


Figure 4-33: Observed Vs predicted for the juvenile density linear model giving an R-Squared of 0.91.

In order to get a visual impression of how the different treatment variables affect the different parameters of the linear model, the coefficients for the two segments (when fitted to individual trees) were plotted against the northing, easting, spacing and elevation groups discussed in Chapter 2.

Although there may be differences in the mean rate at which density in the juvenile segment changes from the pith (Figure 4-34), between northing groups ($p=0.001$ when tested with ANOVA) and between spacing groups ($p=0.04$), visibly there does not seem to be any trend to the differences. There were no significant differences between the easting groups nor between the elevation groups ($p>0.05$).

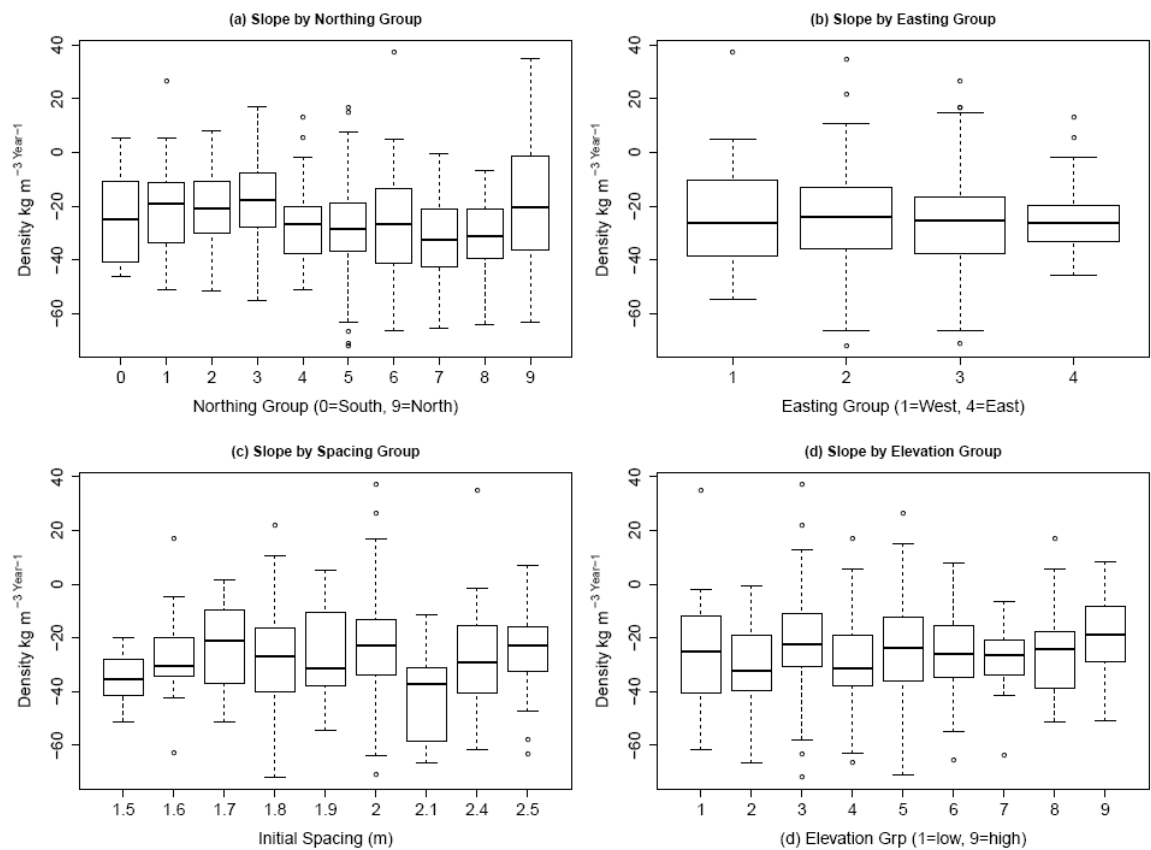


Figure 4-34: The effect of northing, easting, spacing and elevation on the juvenile segment linear model slope coefficient.

The intercept of the juvenile segment of the density profile is shown in Figure 4-35 and would seem to indicate that there are differences between the means for the northing groups ($p<0.0001$) and visually there may be a slight tendency for density to increase with increasing latitude. There may also be an effect of spacing (c) on the mean intercept as analysis of variance shows that

there are significant differences between the groups ($p < 0.0001$) and visually there may be a trend for the mean intercept to decrease with increasing spacing group. As with the slope, there were no significant differences found in the means between the easting groups and the elevation groups ($p > 0.05$ for both).

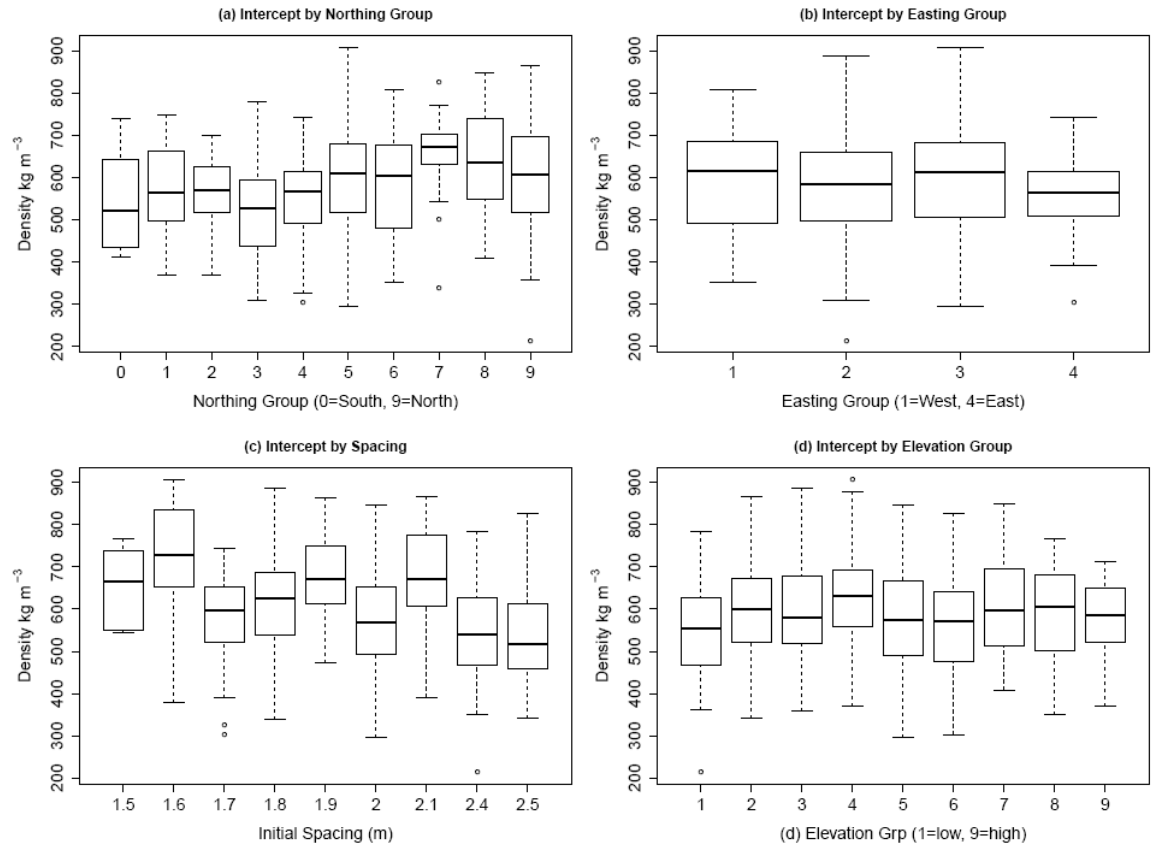


Figure 4-35: The effect of northing, easting, spacing and elevation on the juvenile segment linear model intercept coefficient.

4.4.1.2 Mixed Effects Model of Juvenile Segment of Density Profile

Due to the unbalanced nature of this data set and to account for the hierarchical experimental design a mixed effects model was used to analyse the variation in density across the radial profile of both the juvenile and mature growth linear sections. In this analysis site, and tree within site, were considered as random effects:

$$RD_{ijk} = \mu + S_i + T_{ij} + \epsilon_{ijk} \quad (\text{Equation 4.7})$$

Where RD_{ijk} is the radial profile of density, μ is the overall mean, S_i is the random effect of site, T_{ij} is the random effect of tree within site and ϵ_{ijk} is the residual error which is attributed to within tree variation.

To carry out a variance components analysis the model was fitted without including fixed effects (Equation 4.7) which showed that approximately 43% of the variation was within tree variation, 32% was between trees at the same site and 25% was between sites.

$$RD_{ijk} = \mu + a_0 + S_i + T_{ij} + \epsilon_{ijk} \quad (\text{Equation 4.8})$$

Once the fixed effect of cambial age has been taken into account (Equation 4.8) the within tree variation reduced to 25.5%, just over 44% of the variation being between trees in the same site and 30.5% being between sites. When the fixed effects were included the model predicted an intercept of 587 kg m⁻³ with density decreasing by 25 kg m⁻³ per year. This shows that if the fixed effect of age is included in the model it does a reasonable job of describing within tree variation but, as would be expected, it does not describe between tree variations.

The linear model was first fitted with the intercept as a random effect while slope was fixed, allowing the intercept of each site and tree within site to vary from the mean intercept. Examination of the residuals shows that this approach may be adequate (Figure 4-36). A random slope might also be appropriate as slope also changes with tree. However, if the mixed effects model is updated from having only the intercept as a random term to also having a slope as a random term, then the residuals show a similar amount of variation as when slope is not included (Figure 4-37) indicating that it is perhaps not needed in this case.

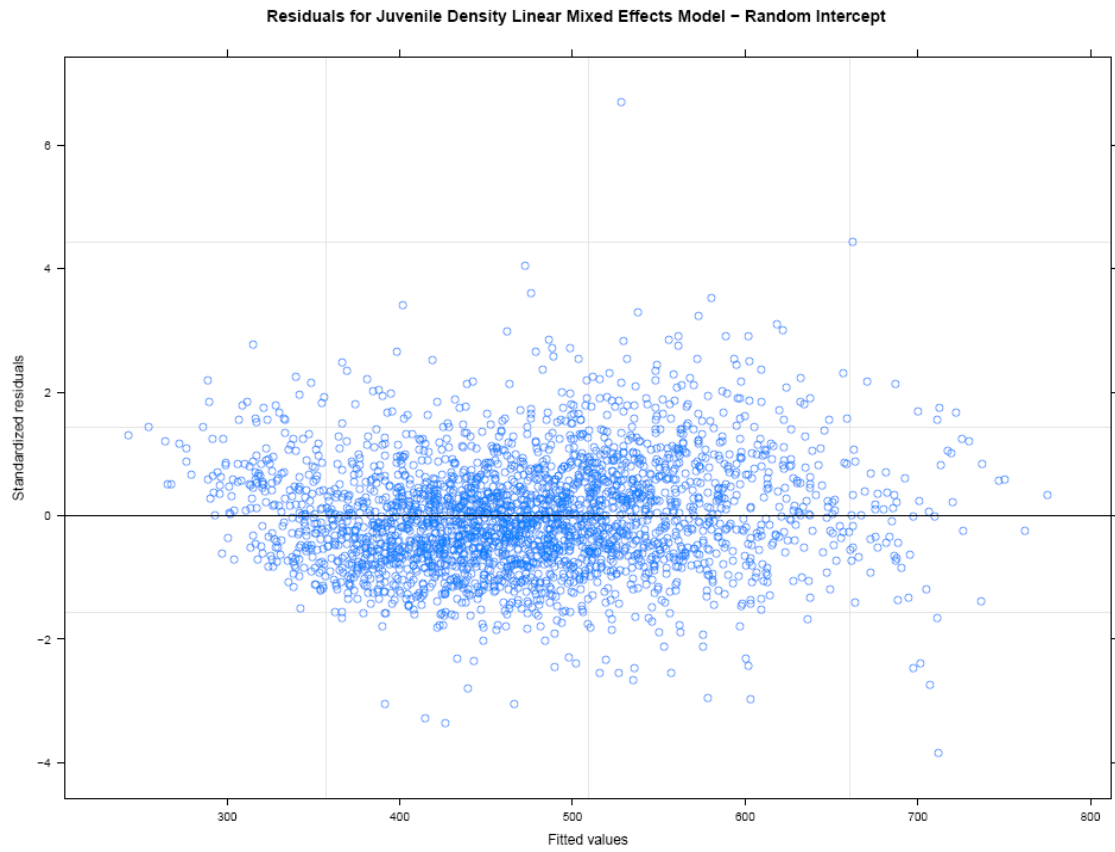


Figure 4-36: Residuals of mixed effects model on juvenile density segment with random intercept only.

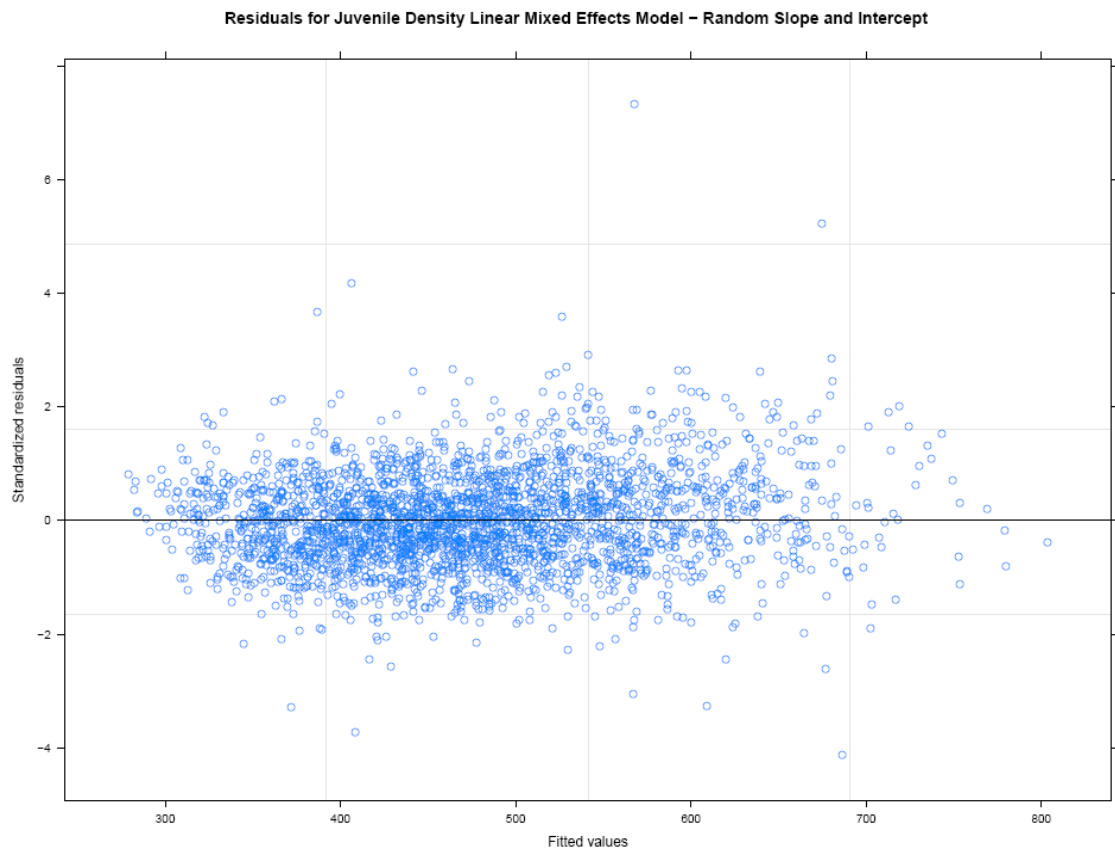


Figure 4-37: Residuals of mixed effects model on density segment with random intercept and slope.

The residuals in Figure 4-36 and Figure 4-37 indicate that the linear mixed effects model is fitting to the juvenile segment with a random scattering of the residuals in both versions. To test the suitability of the model when adding the random effect of slope, Akaike's information criterion (AIC) (Akaike, 1974) was used to compare the suitability of nested models fitted from the same data set and to see whether adding extra parameters to the model would be justified. The model with the lowest AIC value is deemed to be most suitable. The AIC values produced here indicate that the models are very similar. The model which included a random term for both slope and intercept performed slightly better than that which only had the intercept as a random term (the AIC value is very slightly lower (28997 compared to 29466)).

The mixed effects model was then fitted to the juvenile segments of individual trees. Figure 4-38 indicates that model is predicting very well (R-squared = 0.91) when fitted against individual trees although it may over predict at higher values, perhaps due to lack of data points.

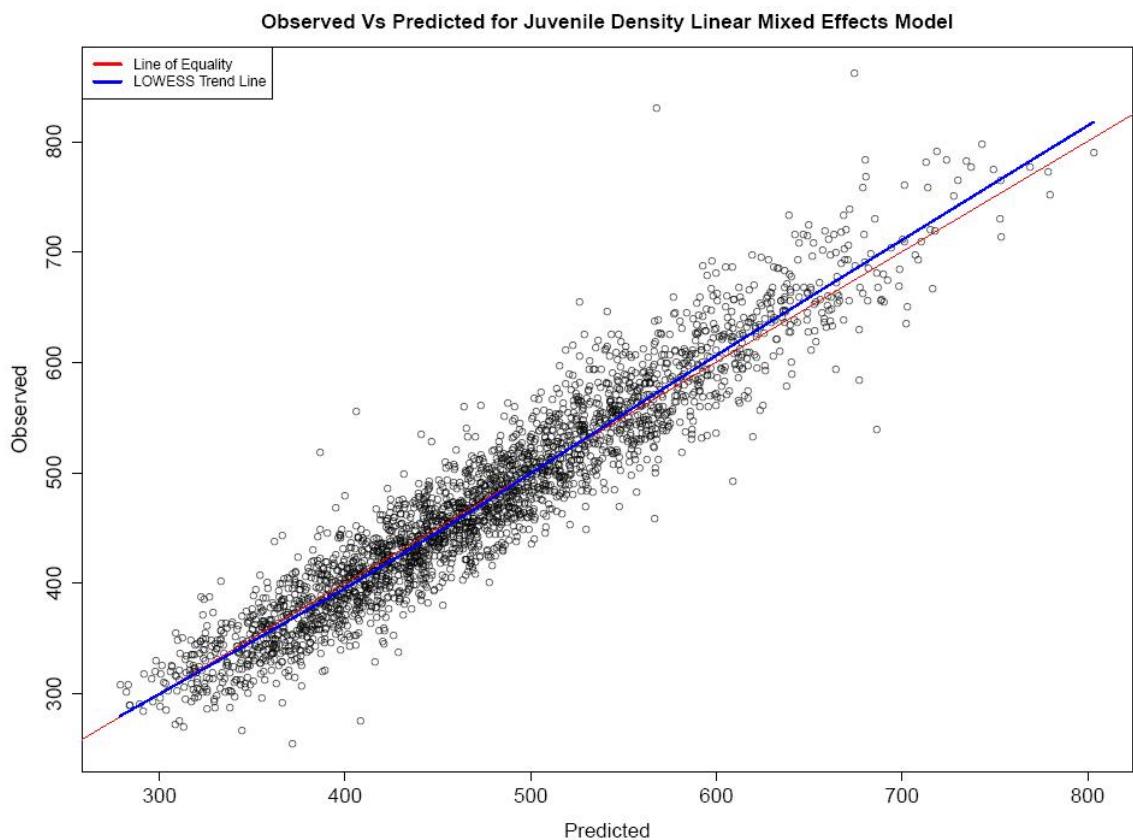


Figure 4-38: The relationship between the observed density and the predicted values for the juvenile density linear mixed effects model giving an R-Squared of 0.91

4.4.2 Mature Segment

Fitting a linear model to the density profiles of rings 8 to 25, for the whole data set, gave a low R-squared of 0.0659, which is a reflection of the large amount of variation in the intercept and the variation in density both between and within each tree. Nevertheless the p -value was less than 0.0001 indicating that a linear model can be fitted to this segment. The residuals for the linear model (Figure 4-39) also show a relatively even spread in magnitude with increasing values.

As with the juvenile phase of density, for the mature segment the model was able to describe the age related trend reasonably well despite a lot of variation between trees in the observed versus predicted growth (Figure 4-40) which tends to increase slightly with increasing values.

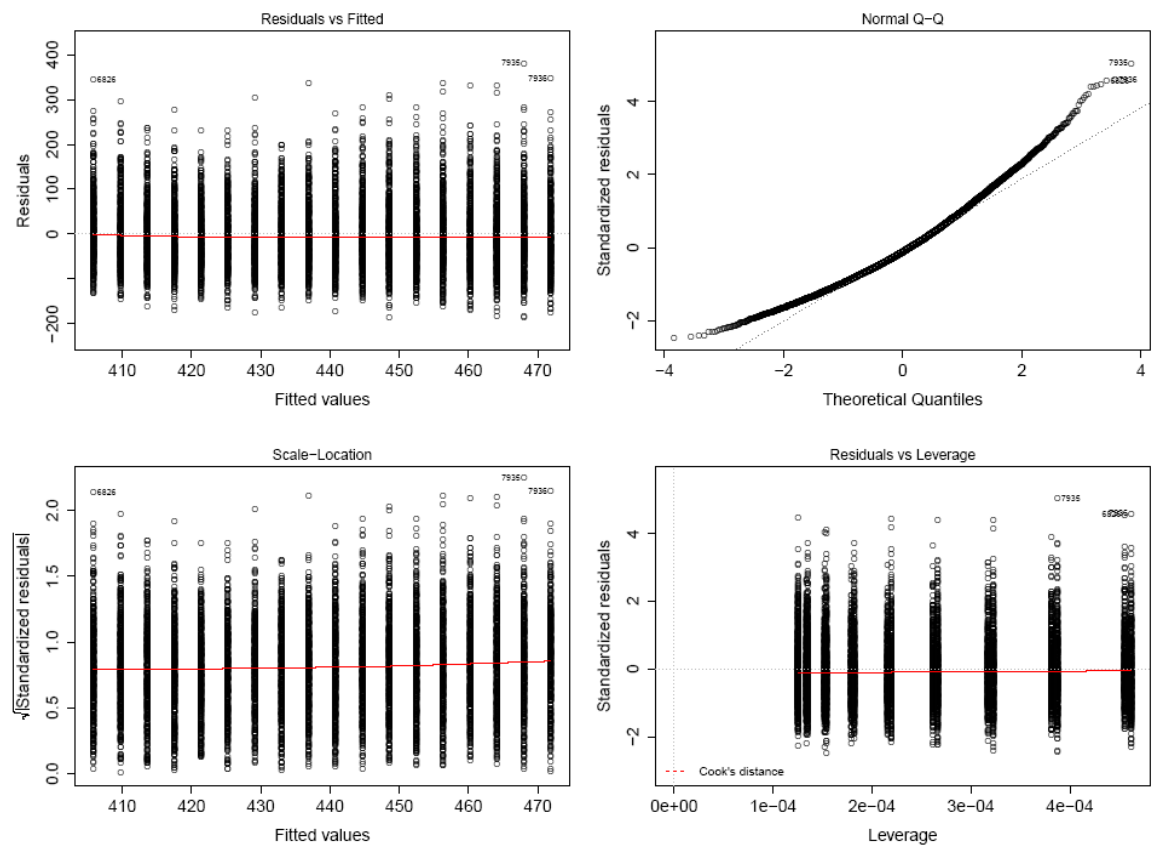


Figure 4-39: Residual plots for the density mature segment linear model

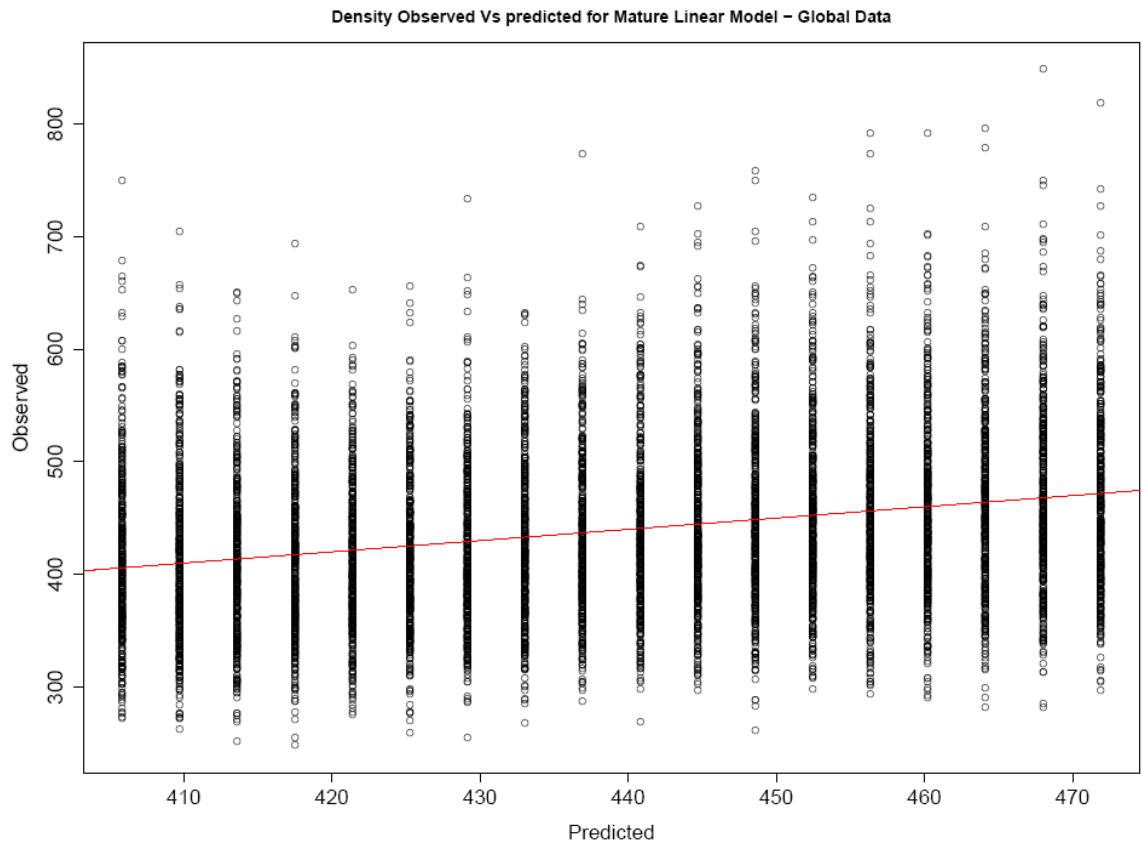


Figure 4-40: Observed versus predicted density values for the mature segment linear model. The red line shows the line of equality.

4.4.2.1 Linear Model of Mature Density Segment Fitted to Individual Trees

When a linear model was fitted to the mature segment of each tree individually the coefficients that were fitted show that there is quite a bit of variation in both the intercept and the rate of change in density. Figure 4-41 shows that the slope, i.e. rate of change in density, fitted by the model varies from -17 kg m^{-3} per year to 22 kg m^{-3} per year with a mean value of 3.9 kg m^{-3} per year indicating that in these data there are samples where the density is increasing towards the bark and others where the density is decreasing. Of the 451 trees tested 96 returned a negative slope, the most extreme of which are shown in Figure 4-42. This could indicate that the split point of 7.4 years may be too early for some trees where the initial decrease in density of the juvenile wood may not have ended by this point. The fitted intercepts for the mature segment linear model varied from approx. 140 kg m^{-3} to 697 kg m^{-3} and have a normal distribution with a mean of 374 kg m^{-3} .

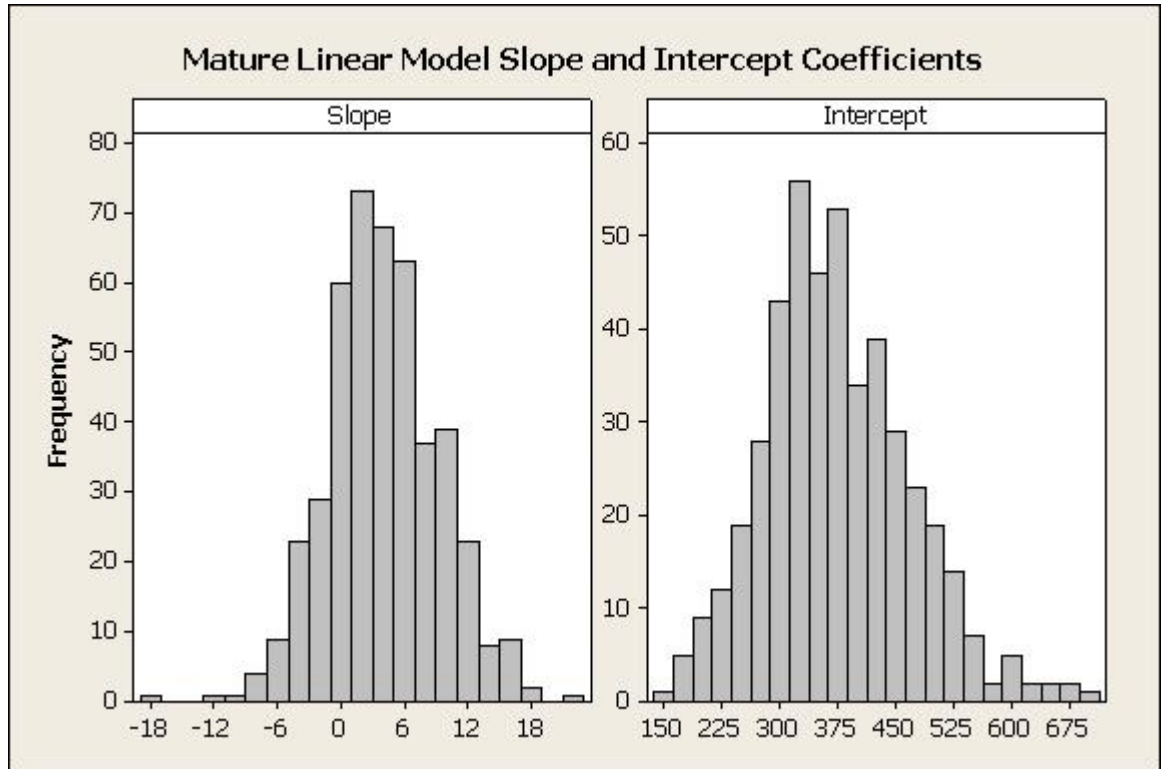


Figure 4-41: Slope and intercept coefficients fitted by the linear model to the density profile of years 8 to 25 for each sample

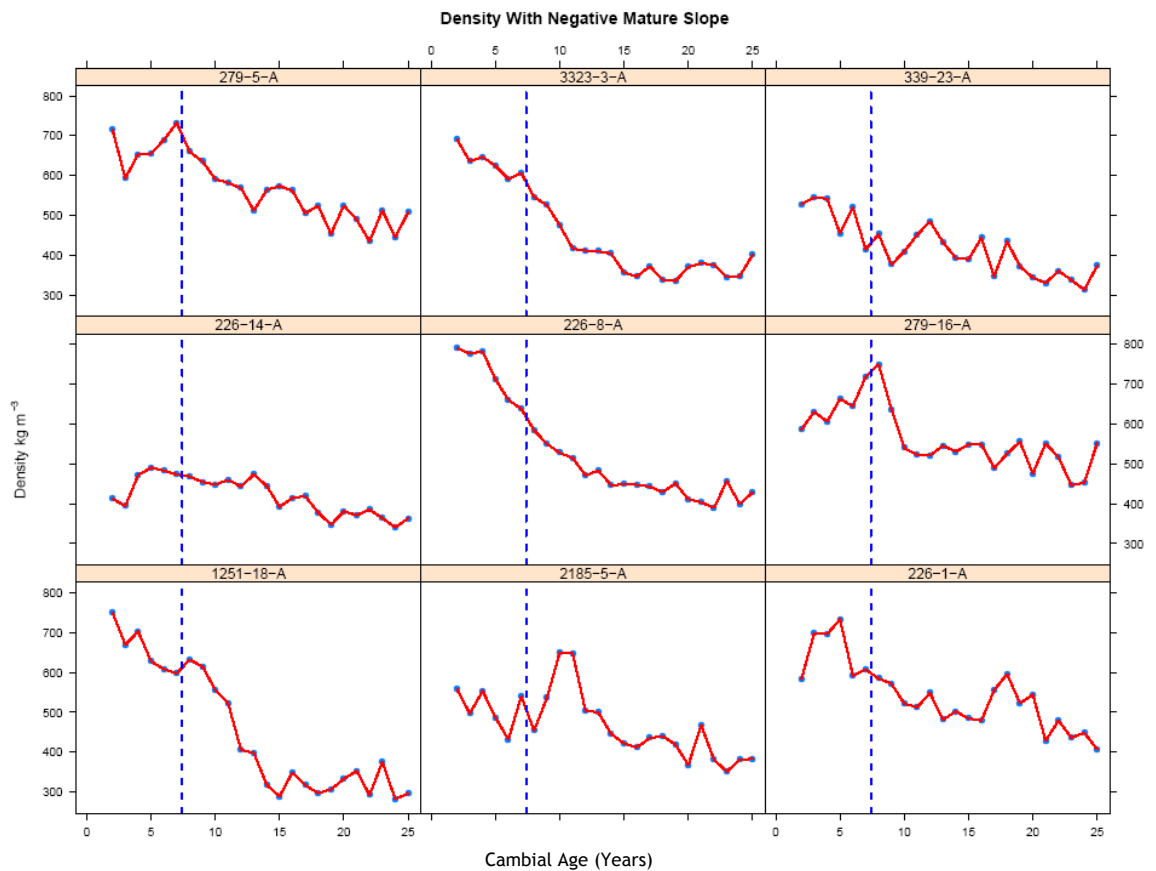


Figure 4-42: The density profiles from year 2 to 25 of the samples which the linear model fitted a negative slope for density in the mature phase. The blue dashed line indicates the split point of 7.4 years showing the cut off between the juvenile and mature phases calculated on the full data set.

When the model was fitted to each tree individually the spread of the residuals (Figure 4-43) look fairly evenly distributed and when the predicted values were plotted against the observed (Figure 4-44) though an R-squared of 0.77 may indicate a large amount of variation in each density profile.

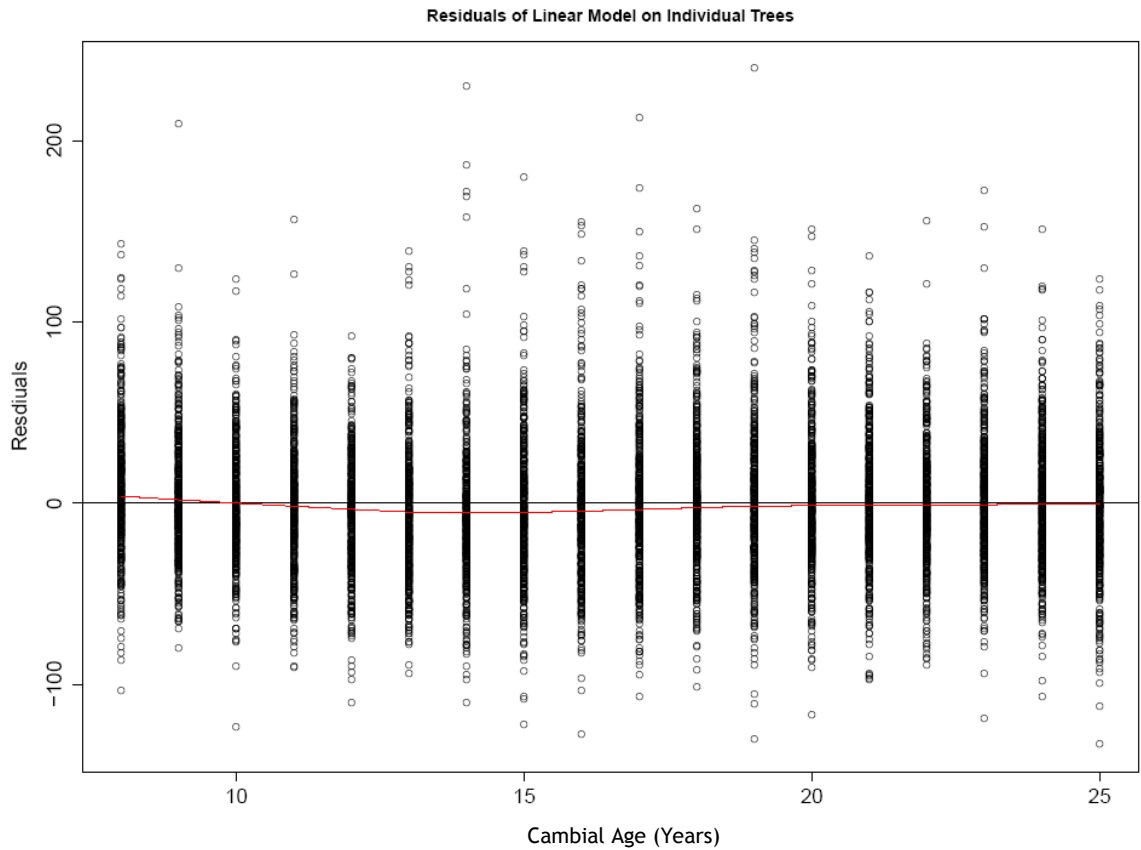


Figure 4-43: Residuals of linear model when fitted to the density profile of the mature segment of each tree, with LOWESS trend line (red)

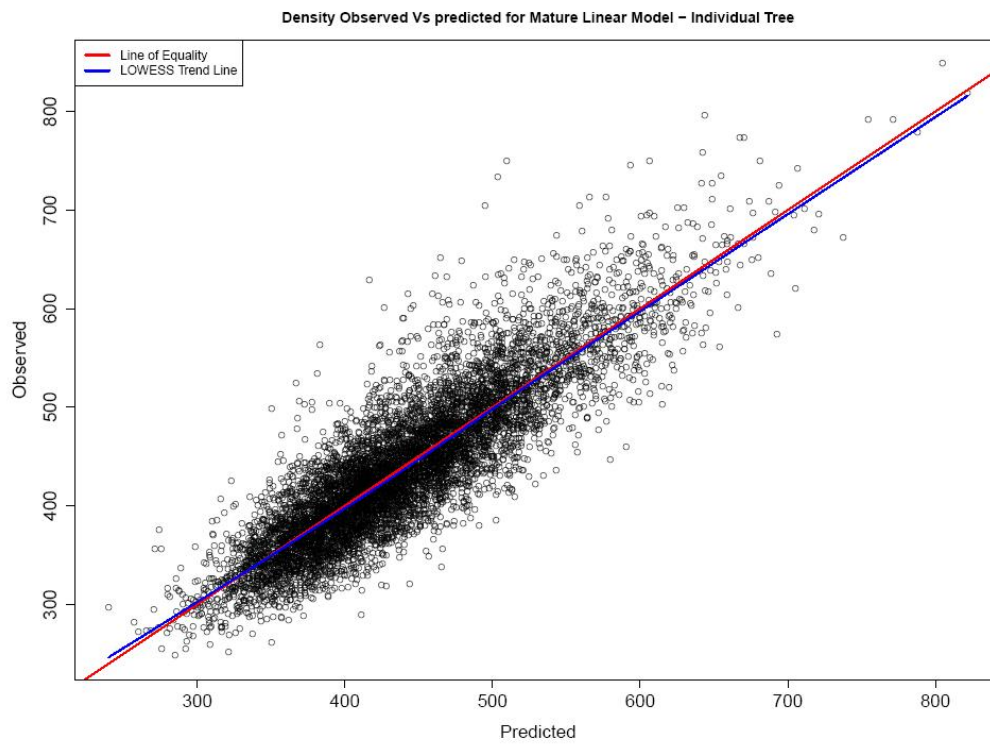


Figure 4-44: Observed Vs predicted for the mature density linear model giving an R-Squared of 0.7675.

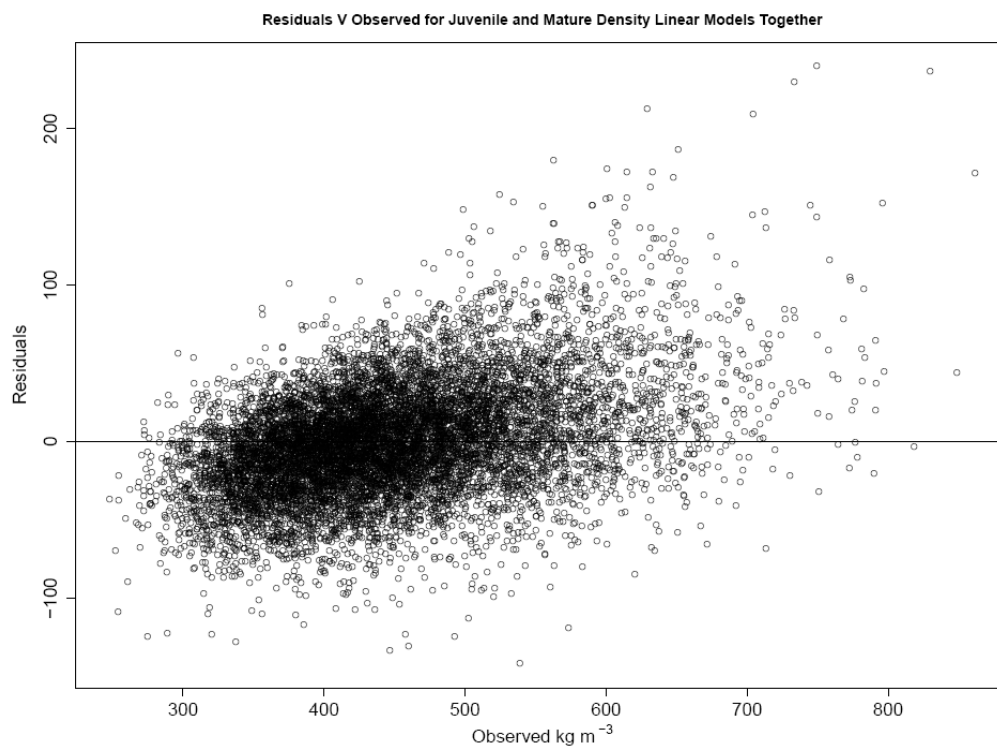


Figure 4-45: Residuals for linear models of the juvenile and mature segments together

As in the previous section on the juvenile phase, in order to get a visual impression of how the different treatment variables affect the different parameters of the linear model; the coefficients for the mature density segment have been plotted by the northing, easting, spacing and elevation groups.

Although there may be differences in the mean slope (Figure 4-46) between the northing groups ($p < 0.0001$ when tested with ANOVA), visibly there does not seem to be any trend to these differences and may be due to Group 8 being lower than the rest. There were no significant differences found between the mean slope coefficients for the easting groups. However, both spacing and elevation groups did have significant differences in slope, which may have a tendency to increase by spacing group and decrease by elevation group.

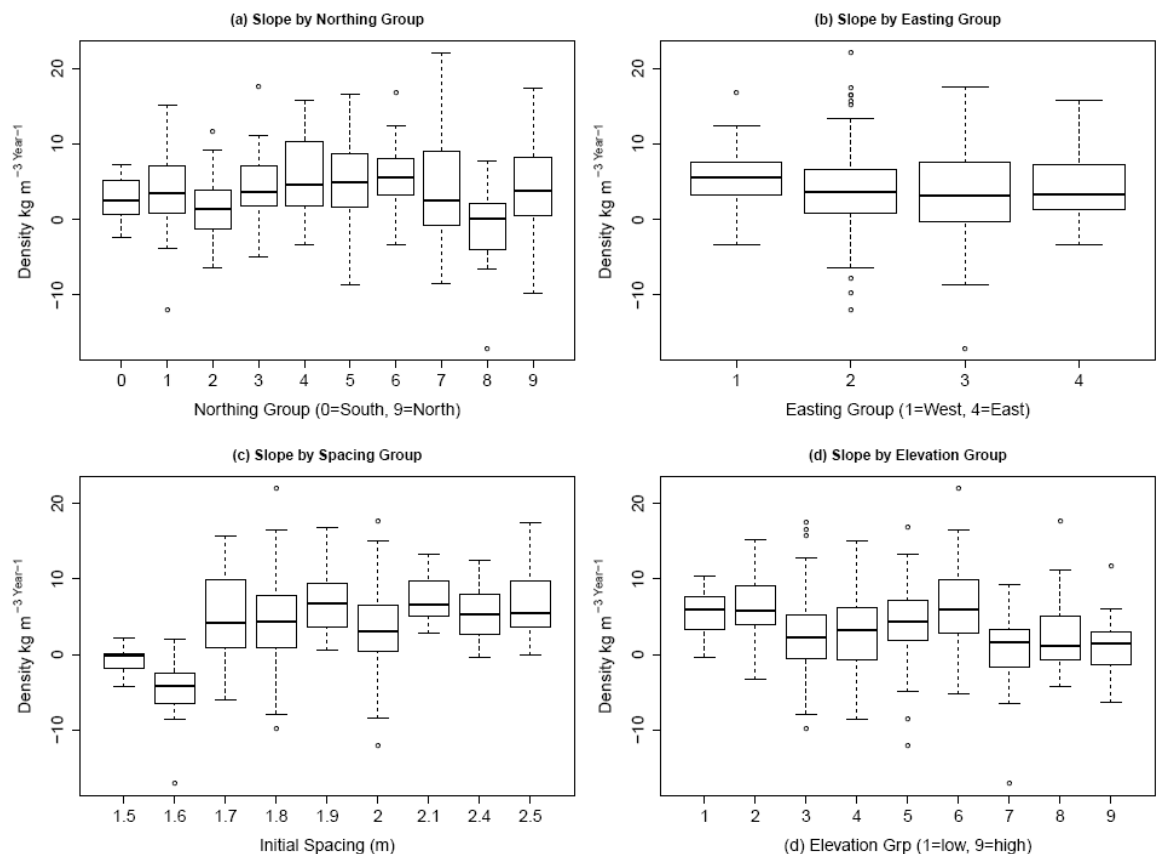


Figure 4-46: The effect of northing, easting, spacing and elevation on the mature segment linear model slope coefficient.

The intercept of the mature segment of density is simply a measure of the density reached at the end of the juvenile phase Figure 4-47 and would seem to show differences between the means of the northing groups ($p < 0.0001$) but it is difficult to see any trend with increasing latitude. There does not look to be any

effect of easting (longitude) on the intercept and analysis of variance shows that there are no significant differences between the easting groups ($p=0.18$).

Statistical analysis using ANOVA showed that there are significant differences between the means of the spacing groups ($p<0.0001$) and also the elevation groups ($p<0.0001$).

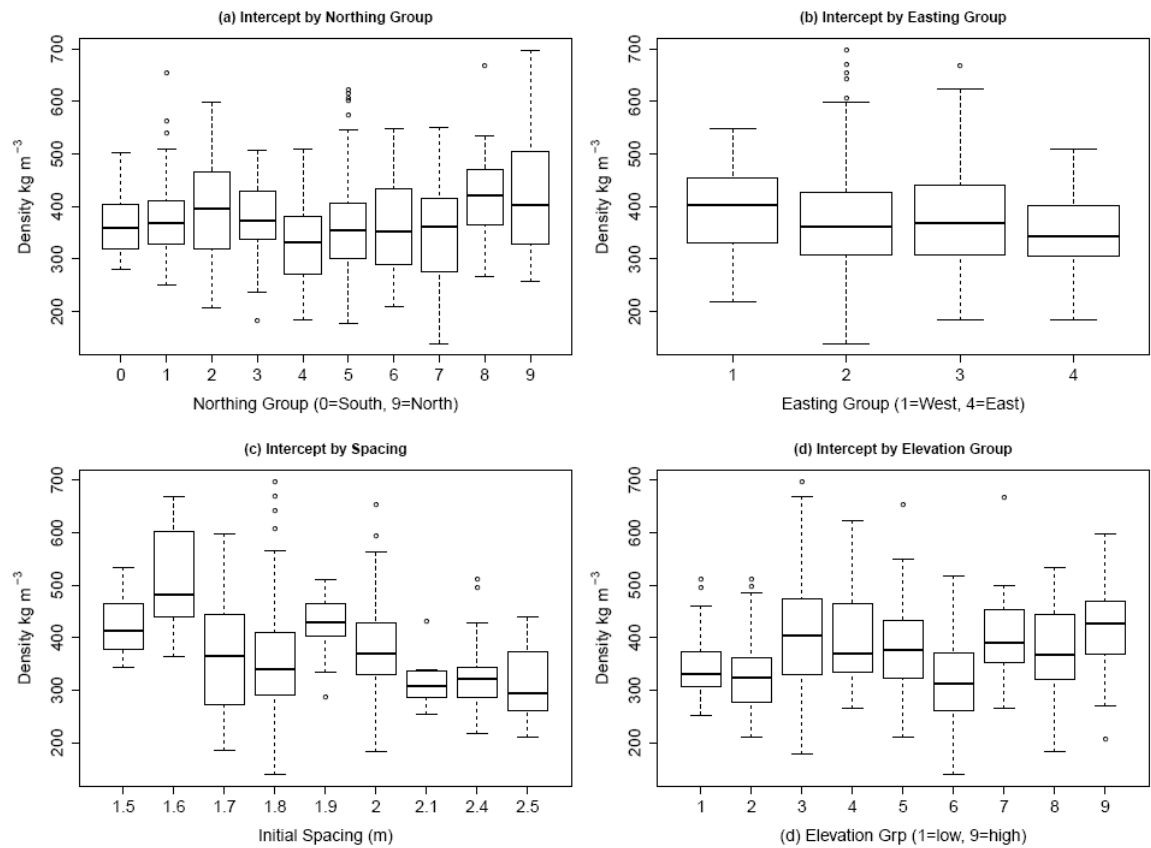


Figure 4-47: The effect of northing, easting, spacing and elevation on the mature segment linear model intercept coefficient.

4.4.2.2 Mixed Effects Model of Mature Segment of Density Profile

The same form of Equations 4.7 and 4.8, shown in the previous section, were used for the analysis of the mature segment of density. When the mixed effects model was fitted without fixed effects (Equation 4.7) a variance components analysis showed that 44% of the variation was within tree variation, 36% was between trees at the same site and 20% was between sites. When the fixed effect of age was taken into account in the model it had very little overall effect. Within tree variation was reduced slightly to 39%, variation between trees in the same site was increased slightly to 39% and now 22% of the variation was between sites.

When the mixed effect model was run with the intercept as the only random effect it gave an intercept of 374 kg m^{-3} and a slope where the density increased by 3.9 kg m^{-3} per year. However, due to the large amount of variation seen in the density this model may also need a random term for the slope (i.e. changing with tree). The residuals for the model which includes only a random term for intercept (Figure 4-48) are fairly randomly distributed though there may be a suggestion of them being grouped in the middle. When a random intercept and slope is included in the model the residuals again look randomly distributed though there may be slightly less variation throughout (Figure 4-49).

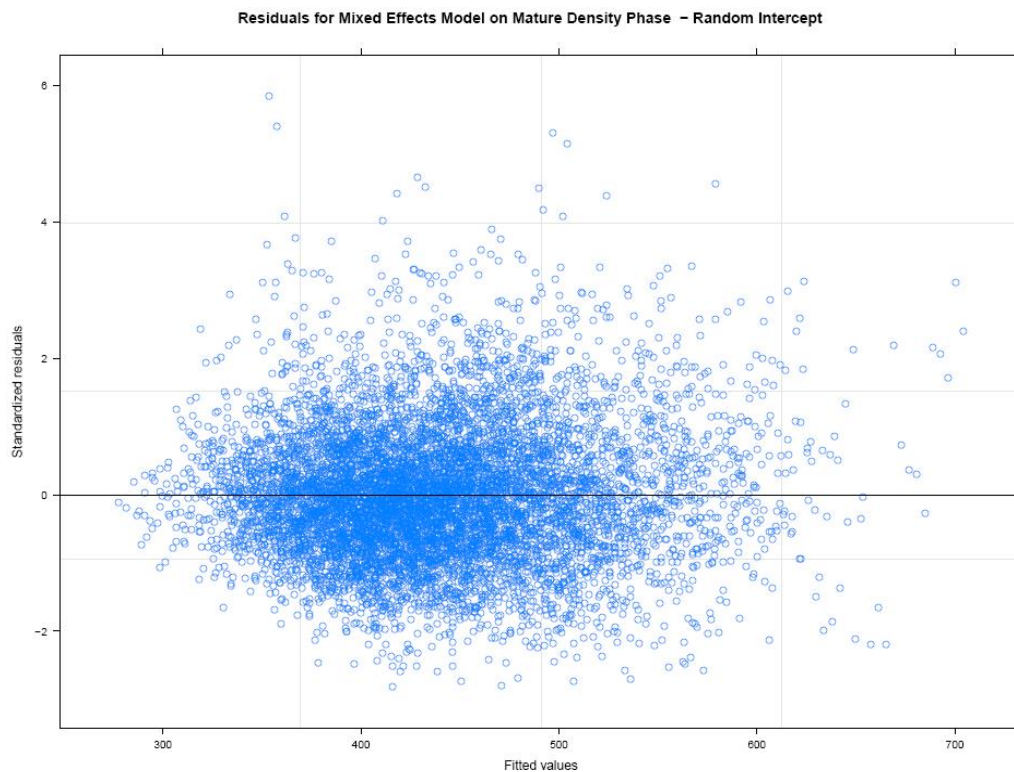


Figure 4-48: Residuals of mixed effects model on density velocity segment with random intercept only.

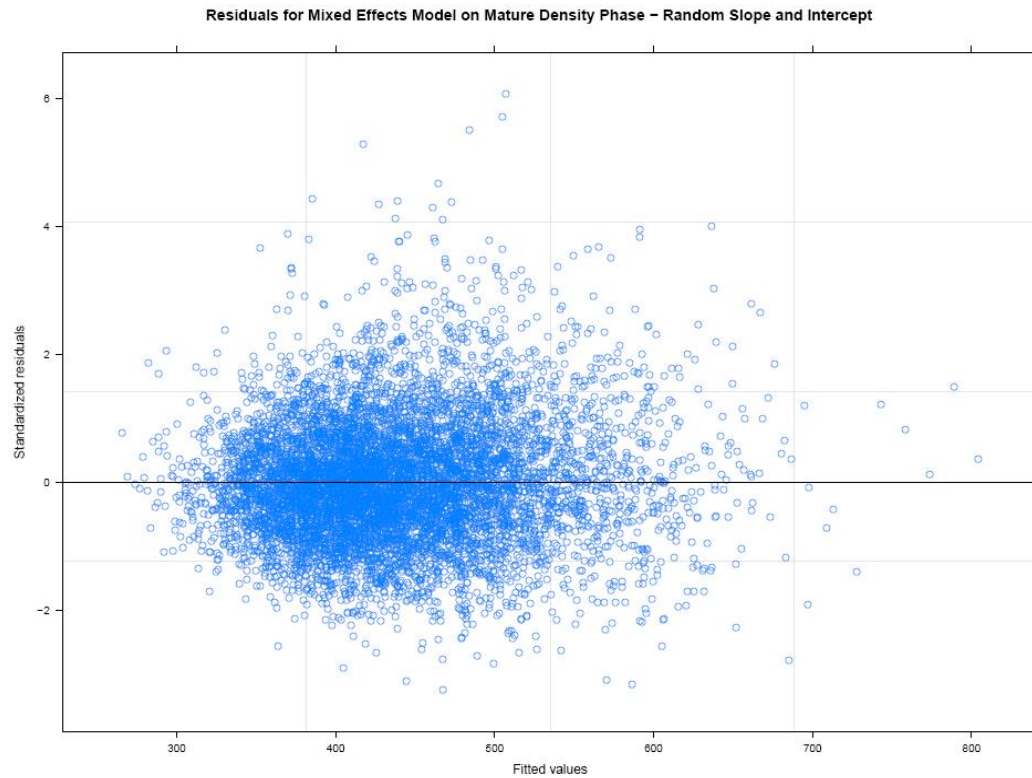


Figure 4-49: Residuals of mixed effects model on mature density segment with random intercept and slope.

The suitability of the model with and without the random effect of slope was again determined using Akaike's information criterion (AIC) i.e the model which only the intercept has a random term compared with the model which both the slope and the intercept have random terms. The results of this test indicate the second model (which includes random terms for slope and intercept) to be slightly better as it has a lower AIC value (84703 compared to 86582).

When the observed density is plotted against that predicted by the model (Figure 4-50) it shows a good fit ($R^2 = 0.77$) indicating that when fitted against individual trees the mixed effects model is predicting reasonably well.

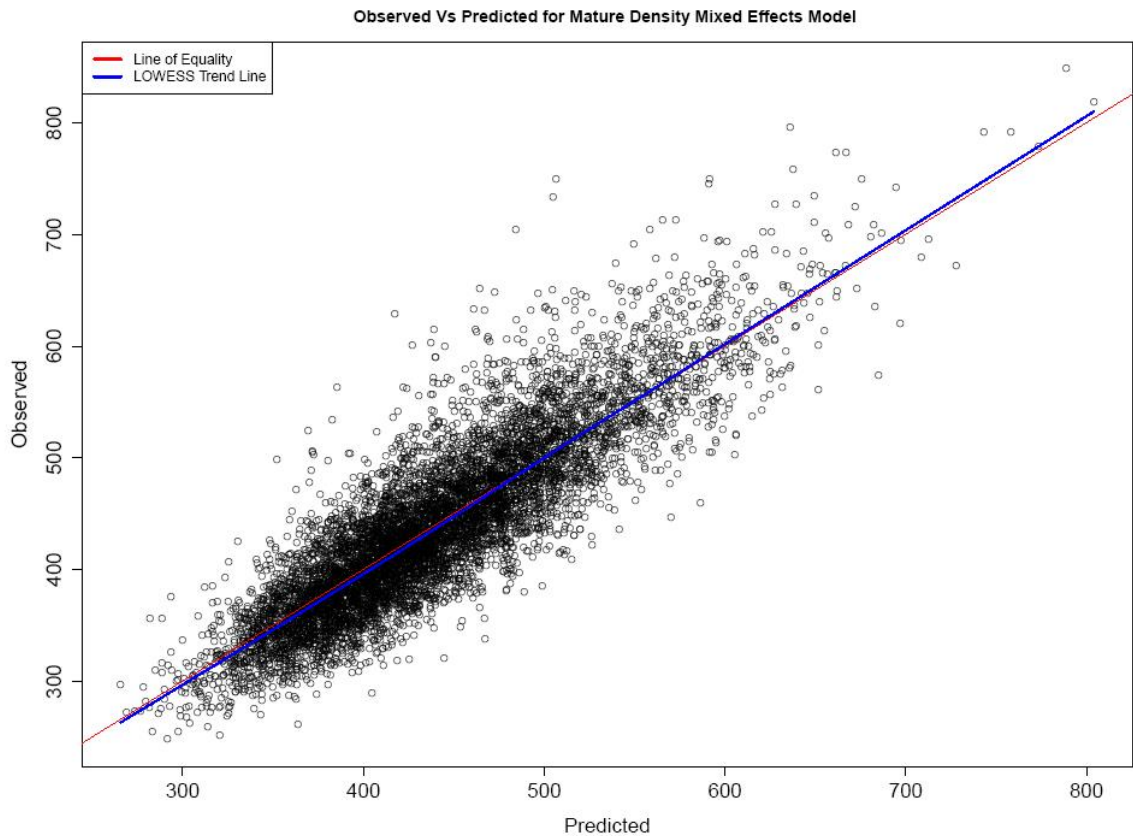


Figure 4-50: The relationship between the observed density and the predicted values for the juvenile density linear mixed effects model giving an R-squared of 0.7647

4.4.3 Mixed Effects Model Structure

In order to test the significance of treatment, a linear mixed effects (LME) model was used with a nested error structure for the random effects where the nested structure consisted of site and tree within site as shown in Equation 4.9:

$$Z_{ijk} = \mu + b_0 + b_1 + b_2 + b_3 + b_4 + S_{ij} + T_{ij} + \epsilon_{ijk} \quad (\text{Equation 4.9})$$

where Z_{ijk} is the radial profile of longitudinal density, μ is the overall mean, b_0 is cambial age in years, b_1 is northing based on the UK grid reference in km, b_2 is easting based on the UK grid reference in km, b_3 is initial spacing at planting in metres, b_4 is the altitude above sea level in metres, S_i is the random effect of site, T_{ij} is the random effect of tree within site and ϵ_{ijk} is the residual error which is not accounted for by age.

4.4.4 Regression Analysis – Juvenile Segment

In order to estimate if there is a relationship regression analysis was carried out on the coefficients for the juvenile and mature segments of density. The rate of change in density in the juvenile section had significant negative correlation with northing (correlation coefficient = -0.121). Easting, spacing and elevation came out as non-significant (Figure 4-51). The intercept for the juvenile segment had a significant positive correlation with northing (correlation coefficient = 0.2) and negative correlation with spacing (correlation coefficient = -0.213). Neither easting nor elevation had a significant correlation with the intercept of the linear model of the juvenile segment (Figure 4-52). However, even though these values are significant, they are still low and describe little of the data.

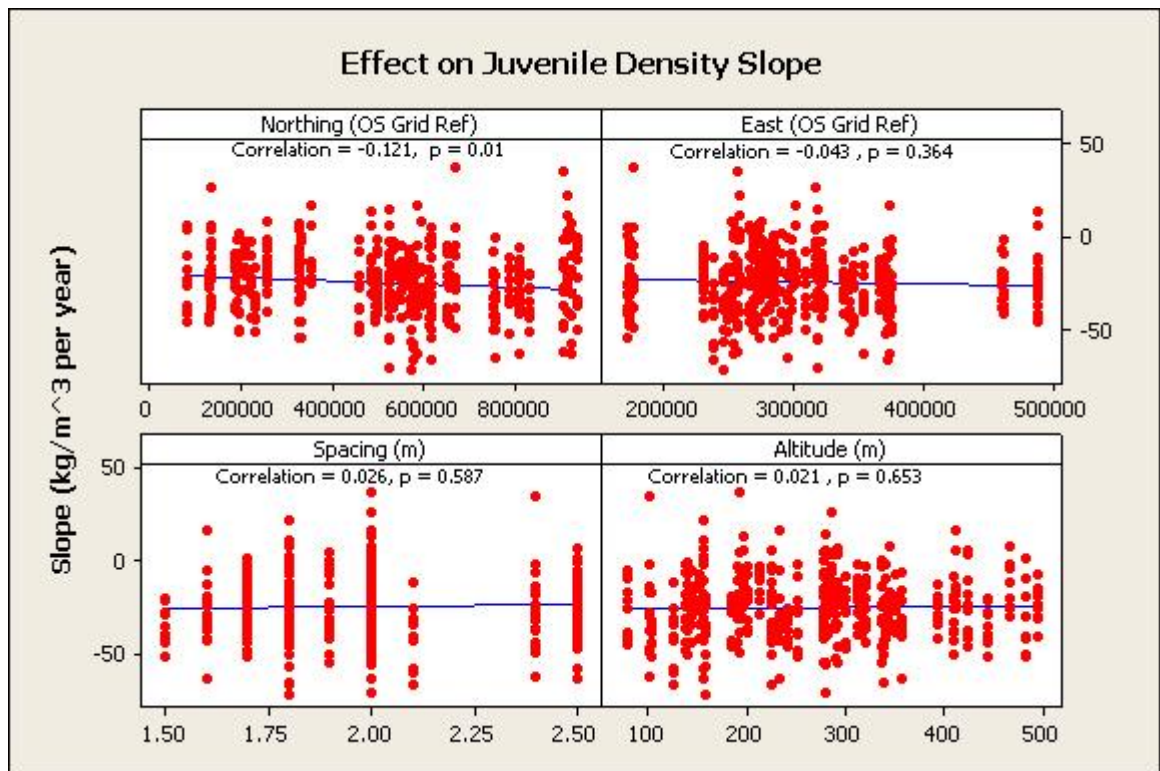


Figure 4-51: Correlation between the linear model slope of the juvenile density segment and northing, easting, spacing and altitude. Only northing was found to have a significant correlation.

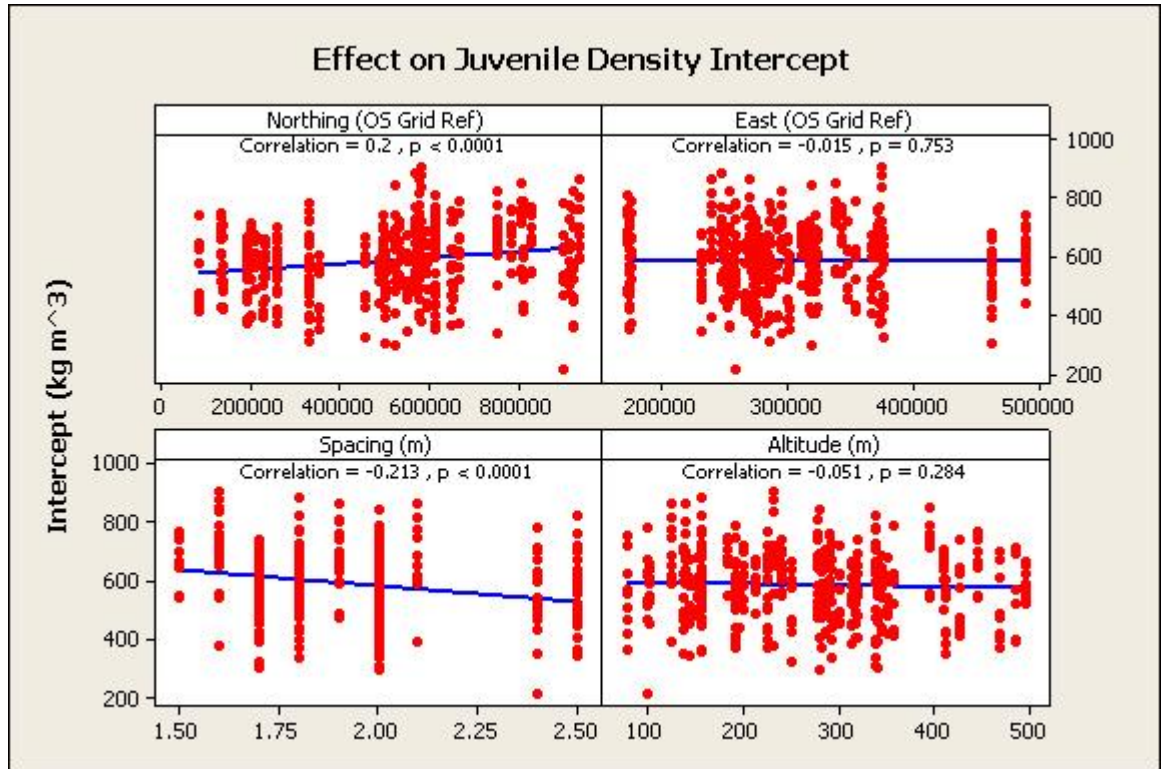


Figure 4-52: Correlation between the linear model intercept of the juvenile density segment and northing, easting, spacing and altitude. Northing and spacing were found to have a significant correlation.

When regression analysis was carried out on the juvenile section the effect of latitude on the slope was significant and both latitude and spacing significantly affected the intercept in accordance with the following equations:

$$\text{Juvenile Slope} = -20.4 - 0.00867 * (\text{Northing} / 1000) \quad \text{Eqn 4.10}$$

$$\text{Juvenile Intercept} = 760 + 0.112 * (\text{Northing} / 1000) - 117 * \text{Spacing} \quad \text{Eqn 4.11}$$

In order to make the parameter estimates for the above equations reasonable the northing value was expressed in kilometres by dividing the value by 1000.

Carrying out regression analysis on these data does not take into account the nested structure of the data. For this mixed effects models are required, which allow the model to vary by tree within site.

4.4.5 Factors Affecting the Juvenile Density Profile

A linear mixed effects model was run on the juvenile density segment, i.e. cambial age of 2 to 7 years, with the fixed effects of northing, easting, elevation and spacing as continuous variables (Table 4-5). Northing and spacing were found to have a significant effect on the intercept (usually interpreted as having an effect on the overall value) but not on the slope; no variables tested significantly affected the slope in the juvenile segment.

Table 4-5: Result of linear mixed effects model testing the effect of northing, easting, spacing and elevation on the juvenile segment of the density profile. Age is cambial age.

	numDF	denDF	F-value	p-value
(Intercept)	1	2249	7073.535	<.0001
Age	1	2249	486.132	<.0001
NorthingKM	1	42	8.637	0.0053
EastingKM	1	42	0.219	0.6423
Spacing	1	42	19.238	0.0001
Elevation	1	42	1.214	0.2768
Age:NorthingKM	1	2249	3.346	0.0675
Age:EastingKM	1	2249	0.400	0.5273
Age:Spacing	1	2249	0.226	0.6342
Age:Elevation	1	2249	0.059	0.8088

When the non-significant terms were removed from the equation Northing and spacing still had a significant effect on the intercept and not the rate (Table 4-6).

Table 4-6: Result of the linear mixed effect model on juvenile density profile with the non-significant interaction terms removed. Age is cambial age.

	numDF	denDF	F-value	p-value
(Intercept)	1	2253	6923.003	<.0001
Age	1	2253	486.239	<.0001
NorthingKM	1	44	8.519	0.0055
Spacing	1	44	17.086	0.0002

A linear model with spacing and northing as the variables shows that northing had a positive effect on the overall mean by 0.07136 kg m⁻³ per km of northing, and spacing had a negative effect on the overall mean by - 104.8 kg m⁻³ per m spacing.

The form of the linear model obtained from these data was:

Equation 4.12:

$$\text{Juvenile Radial Density} = -24.8 \cdot \text{Age} + (0.07136 \cdot \text{Northing} / 1000) - 104.8 \cdot \text{Spacing} + 756$$

4.4.6 Regression Analysis – Mature Segment

The slope coefficient for density in the mature segment (Figure 4-53) had a significant positive correlation with spacing (Pearson correlation coefficient = 0.2) and a significant negative correlation with elevation (Pearson correlation coefficient = -0.126), but no significant correlation with either northing or easting. The intercept for the mature segment (Figure 4-54) had a significant positive correlation with spacing (correlation coefficient = 0.170) but not with northing, easting or elevation. However, even though these correlation coefficients are significant they are extremely low and care should be taken before drawing any conclusions.

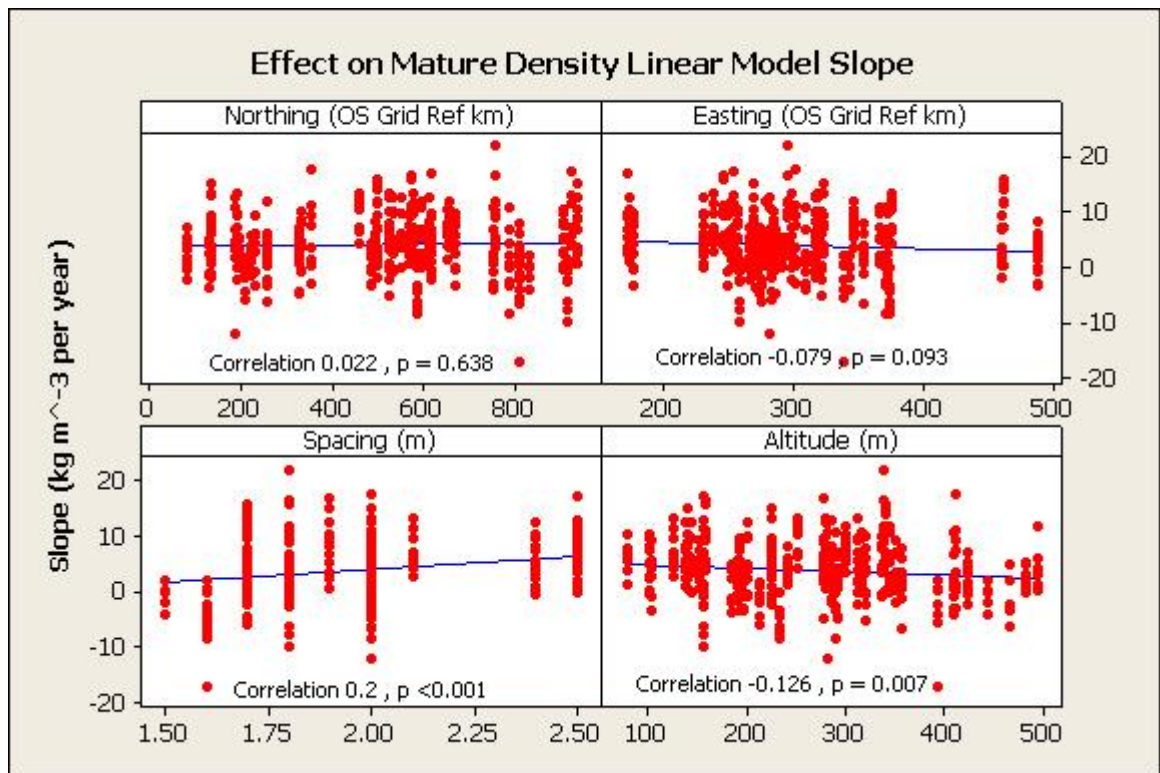


Figure 4-53: Correlation between the linear model slope of the mature density segment and northing, easting, spacing and altitude. Spacing and elevation were found to have a significant correlation.

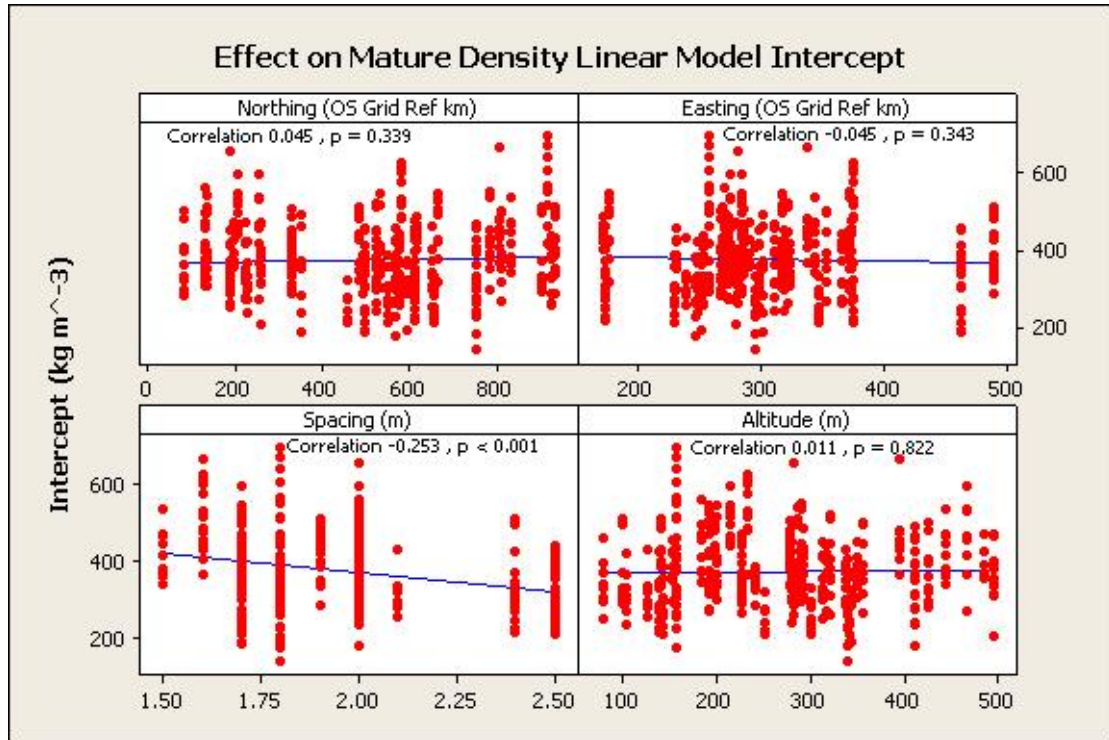


Figure 4-54: Correlation between the linear model intercept of the mature density segment and northing, easting, spacing and altitude. Only spacing was found to have a significant correlation.

When regression analysis was carried out on the mature section of density, only spacing was found to be having a significant effect, on both the slope and intercept in accordance with the following equations:

$$\text{Mature Slope} = -4.73 + 4.40 * \text{Spacing (m)} \quad \text{Equation 4.13}$$

$$\text{Mature Intercept} = 570 - 99.7 * \text{Spacing (m)} \quad \text{Equation 4.14}$$

However, this does not take into account the nested structure of the data. For this mixed effects models are required which allows the model to vary by tree within site.

4.4.7 Factors Affecting the Mature Density Profile

A linear mixed effects model was run on the mature density segment i.e. from cambial age 8 to 25 years, with the fixed effects of northing, easting, elevation and spacing as continuous variables (Table 4-7). None of the variables tested were found to have a significant effect (*p*-values are all greater than 0.05). However spacing is close to being significant at the 5% level on the intercept and slope, as was Northing on the intercept.

Table 4-7: Result of linear mixed effects model testing the effect of northing, easting, spacing and elevation on the mature segment of density.

	numDF	denDF	F-value	p-value
(Intercept)	1	7606	6874.052	<.0001
Age	1	7606	56.771	<.0001
NorthingKM	1	42	3.808	0.0577
EastingKM	1	42	1.116	0.2967
Spacing	1	42	3.772	0.0588
Elevation	1	42	2.110	0.1538
Age:NorthingKM	1	7606	0.677	0.4108
Age:EastingKM	1	7606	0.031	0.8596
Age:Spacing	1	7606	3.722	0.0538
Age:Elevation	1	7606	0.467	0.4944

When the non-significant effects are removed only cambial age is a significant factor (Table 4-8)

Table 4-8: Result of linear mixed effects model on the mature segment of density once the non-significant terms have been removed.

	numDF	denDF	F-value	p-value
(Intercept)	1	7610	5988.592	<.0001
Age	1	7610	55.731	<.0001

A linear model with cambial age as the only significant variable shows that it has a positive effect on the overall mean: by 3.89 kg m⁻³ per year. The form of the linear model for the mature phase of density obtained from this data was:

$$\text{Mature Radial Density} = 374.77 * \text{Cambial Age} + 3.89 \quad \text{Equation 4.15}$$

This shows that whilst latitude and spacing may have an effect on the radial density in the juvenile core, only cambial age is having an effect in the mature wood. Correlations carried out on different ring numbers suggests that density between rings are correlated, and while the correlation decreases with increasing numerical distance between rings the correlations are still significant (Figure 4-55). Correlations are highest between rings which are fully in the juvenile core e.g. rings 2 and 7 (Pearson correlation coefficient = 0.548) or rings fully in the mature wood e.g. rings 12, 20 and 25 with lower correlations between rings which are in the different phases. However, rings 7 and 12 which straddle the transition zone also have a high correlation as they are numerically close to each other.

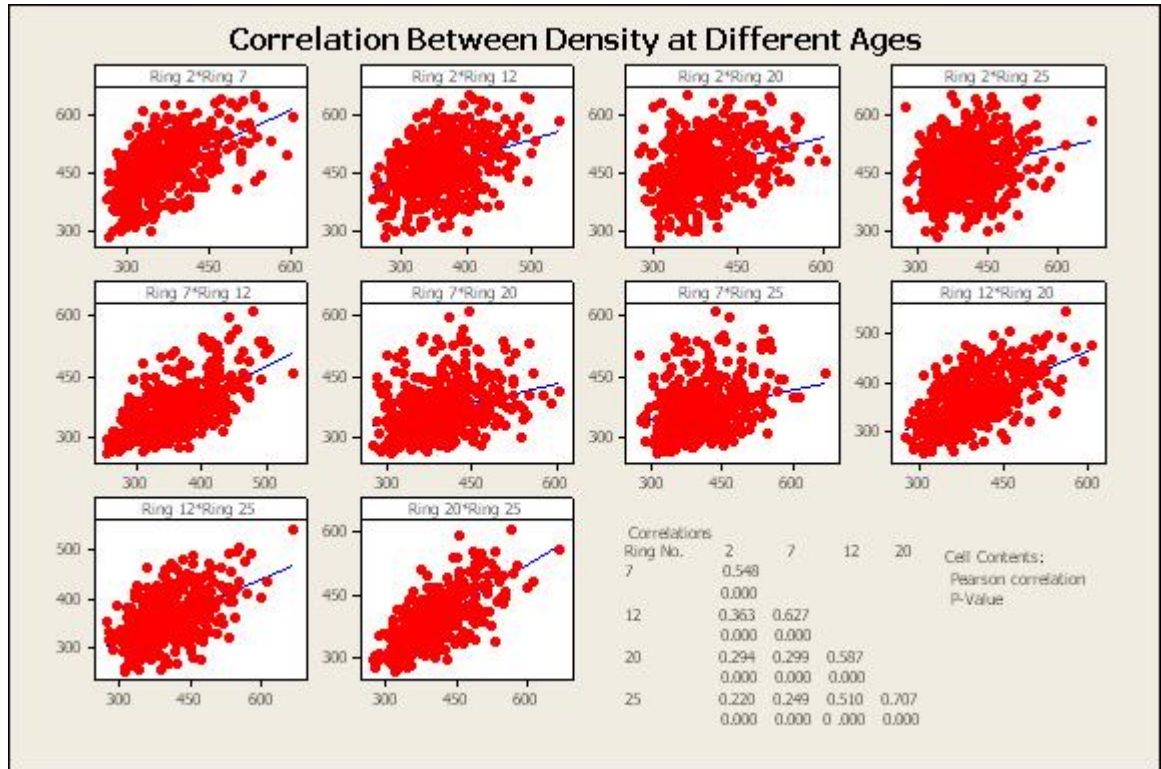


Figure 4-55: Correlation between density measured on different ring numbers where rings are counted from the pith.

4.5 Discussion

4.5.1 Discussion of Density Models

Initial observation of the radial density data obtained from this experiment indicated the data followed the radial trend that would be expected with Sitka spruce (Brazier, 1970) i.e. high wood density at the pith, which decreases outwards for a number of rings reaching a minimum at around ring 7 to 12 before increasing again into the mature wood. In this data set the density measured ranged from 248 kg m^{-3} to 883 kg m^{-3} with a mean of 461 kg m^{-3} which is similar to that found by McLean (2008) and Vihermaa (2010) who found mean values of 456 kg m^{-3} and 447 kg m^{-3} respectively in previous studies on UK grown Sitka spruce.

Examination of the density profiles showed that while there was a lot of variation between trees within sites, there was a suggestion that there were also differences between sites both in the radial trend and in the mean values, although the exact reason for these differences were unclear. Grouping the overall density measurements based on site characteristics such as northing,

easting, spacing and elevation also showed that there could be some differences in overall mean density between the different groups but the differences were very small and it was difficult to determine any trend between groups. An investigation into the effect of altitude on Sitka spruce (Mayhead, 1973) found that the relationship with yield class was not constant throughout Great Britain with considerable variation between and within various regions. This shows the difficulty in drawing conclusions from grouped effects due to the complex interactions (both known and unknown) that often exist.

In order to investigate the radial trend further, this study used a number of published models along with developing a segmented linear model to describe radial density with the aim of identifying which models not only describe the data the best but also which are simple and intuitive to use. Previous studies have shown that there are a number of models which include ring width as an input parameter along with ring number, which can be fitted to the Sitka spruce density profile (Lindstrom, 2000, Gardiner et al., 2011). These models were fitted to this data set along with the two segment linear model, as well as a simple exponential model based only on ring number. As would be expected the exponential model was the poorest fit as it was not able to deal with increasing density in the mature wood. The Gardiner3 and Lindstrom were the best fitting models but this would be expected as these models included ring width which is inversely correlated with ring density (Pearson correlation coefficient -0.473) and accounts for a lot of the variation in density between trees.

Using the segmented model allowed a transition point between juvenile and mature phases of the density profile to be investigated. When fitted to the full data set the split point between juvenile and mature wood was estimated to be between rings 7 and 8 (global mean was 7.4 years). This is similar to that found by Harvald and Olesen (1987) who investigated Sitka spruce in Denmark and found that density decreased from the pith to a minimum at approximately ring 8 to 12 before starting to increase again. When the segmented model was fitted to individual trees, although the overall R^2 value was high (0.83), the sensitivity of the model to local fluctuations meant that there was a great deal of variation in the split points. This problem made it difficult to ascertain if any other factors were having an effect on the split point. For example, plotting the split point by site showed that the trees in some sites had similar transition points

whereas at other sites there was a large spread which may be attributed to random variation between trees, perhaps amplified by dominance. Simplifying the process by fixing the transition point at a constant between rings 7 and 8, allowed the two segments to be examined as two separate linear models and when fitted to individual trees they gave R^2 values of 0.91 and 0.77 for the juvenile and mature segments respectively.

Although the Gardiner³ and Lindstrom models fitted the data well and allowed for a year to year variation around the fitted line, leading to higher R^2 values, the segmented model has simple and intuitive parameters and does not require ring width as an input parameter. Ring width data may not always be available so there is a benefit to having models which are able to predict density from ring number alone.

4.5.2 Discussion of Modelling Factors Affecting Ring Density

While Section 4.3 was concerned with building and testing the models, section 4.4 used these models to explore the effect of different site characteristics on the model parameters. Since the linear models have simple to understand parameters (i.e. a slope and intercept) and does not require ring width as an input parameter these models were used to investigate the site effects.

Analysis of the linear phases of the segmented models using mixed effects analysis showed that most of the variation in juvenile density was between trees at the same site (44%) with 30.5% of the variation being between sites and the remaining 25.5% being within tree variation. In the mature phase within tree variation was 39%, variation between trees in the same site was also 39% and only 22% of the variation was between sites. This within site variation shows the difficulty in trying to investigate effects which are measured at site level and indicates that there are other factors such as micro-site climate effects, for example soil moisture, which may be having an impact on the tree properties.

The initial design of the original resource evaluation study (Moore et al., 2009a) meant that sites were grouped according to a combination of latitude, longitude, spacing and elevation. However within this investigation these site

effects were expressed as continuous variables and were analysed using linear mixed effects models on the linear segmented models for each tree with latitude, longitude, spacing and elevation being fixed effects.

Preliminary analysis of the site effects on the juvenile segment of density indicated that there was a small negative correlation between the rate of change in density and northing. There was also a small but positive correlation between the overall mean and northing and a negative correlation with spacing and this was confirmed by regression analysis. Regression analysis of the mature phase suggested that spacing was the only significant effect on density and had a positive effect on the slope but a negative effect on the mean. However, regression analysis does not take account of the structured nature of the data and so mixed effects models that allow the models to vary by tree within site were used. Mixed effects modelling suggested a positive effect of northing and a negative effect of spacing on the overall mean density in the juvenile section, but not on the rate of change i.e. the mean density of the juvenile segment increases with progress north and decreases with increased spacing. There were no significant site effects on the mature phase of density with cambial age being the only significant effect.

5 Radial Profiles of Longitudinal Acoustic Velocity

5.1 Introduction

This chapter will report on the method and results of an experiment to measure acoustic velocity from pith to bark on the samples taken as part of this resource evaluation study, paralleling the density and ring width measurements performed at The University of Glasgow. This gave the radial profile of longitudinal acoustic velocity on the samples. The velocity at which sound travels through wood is dependent on its modulus of elasticity (MoE), i.e. stiffness, and its density (Evans and Ilic, 2001) provided that the orientation of the grain is parallel to the direction of measurement (Beall, 2002, Suzuki and Sasaki, 1990, Kabir et al., 1997). Therefore, theoretically, given the wood density and the velocity of sound it is possible to determine the MoE of wood (Evans and Ilic, 2001).

The most straightforward way of determining acoustic velocity is by measuring the transit-time of a sound (stress) wave from one point to another, known as time of flight. Most time of flight acoustic devices are designed for longer pieces of timber (>30cm). Devices of this type have been used to measure acoustic velocity on both standing trees (Chauhan and Walker, 2006, Mochan et al., 2009, Auty and Achim, 2008) and logs (Farrell et al., 2012, Tsehaye et al., 2000) and studies have been done on the alternative methods for doing this e.g. (Schimleck et al., 2010, Knowles et al., 2004). These methods have limitations with very short samples. A short term scientific mission (STSM), funded by COST Action FP0802 gave access to a purpose built acoustic scanner, based on time of flight ultrasound, located at the New Zealand School of Forestry, University of Canterbury, making it possible to measure radial sound velocity profiles on tree cores as little as 10 mm thick on samples which radial profiles of density was also measured which had not previously been available for experiments of this kind. Combining these measurements with radial density profiles produced from the same cores would theoretically allow determination of MoE profiles on an annual growth ring basis. The acoustic velocity measurements are useful themselves as an indicator of MFA (Evans and Ilic, 2001).

The objective of this experiment is, by using ultrasonic scanning, to obtain the radial profile of longitudinal acoustic velocity directly from cylindrical increment cores. However this is a new method that has not yet been fully tested on large numbers of samples. Therefore this section also aims to evaluate the potential of this system as a method for obtaining acoustic velocity profiles on increment cores and the problems therein.

Although this section points out certain issues with the method and the quality of the results obtained, empirical models were explored which investigate the variation in longitudinal acoustic velocity across the radial profile of Sitka spruce trees, allowing comparison between juvenile wood and mature wood as well as between trees growing in different silviculture, site and climatic conditions in the UK.

5.2 Materials and Method

Approximately 1000 (Table 5-1) 12mm diameter increment cores were obtained from 32 sites in Scotland, England and Wales as described in Chapter 2, as well as from 69 sites used in a previous resource evaluation study (Moore et al., 2009a) (Figure 5-1).

Table 5-1: Number of sites and cores used in the acoustic velocity measurements

	Previous Sites	Current Sites	Total
No. Sites	69	32	101
No. Cores	681	313	994

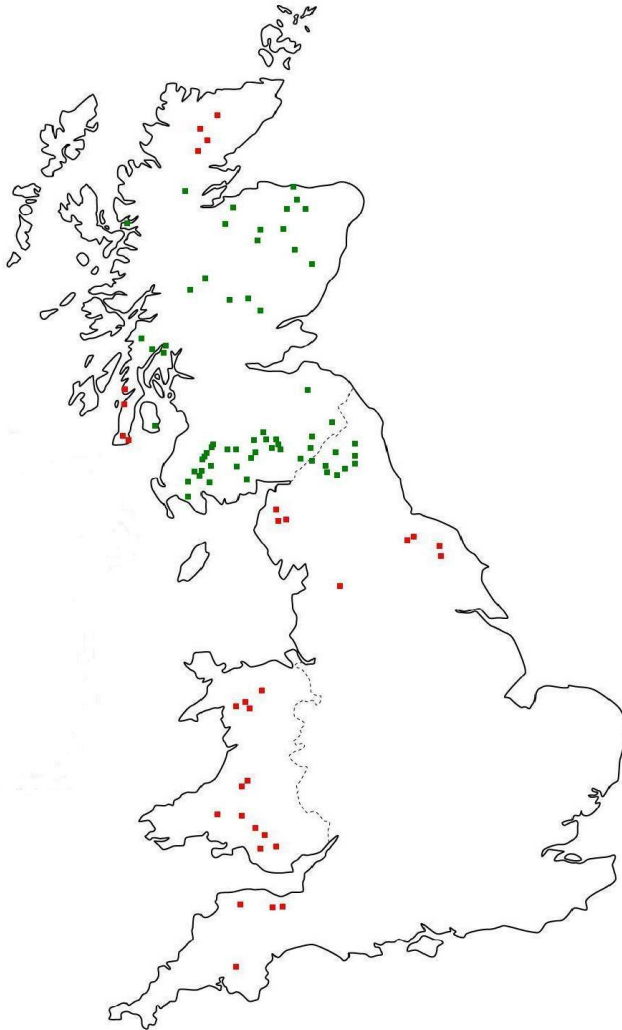


Figure 5-1: Map showing the location of the sites used in this study (red) and the sites from a previous evaluation study (green).

5.2.1 Description of Work

Prior to shipping to New Zealand the Sitka spruce cores were heat treated at 70°C for 8 hours to comply with the strict New Zealand bio security rules. Since temperature (Baechle and Walker, 2006) and moisture content (Kabir et al., 1997, Sakai et al., 1990, Chan et al., 2011, Ilic, 2001b) have been shown to have an effect on acoustic velocity, once in New Zealand the samples were stored at 25°C and 60% humidity for 1 week prior to and up until use to give a moisture content of approximately 12% (Ilic, 2001a).

The acoustic scanner (Figure 5-2) was originally developed for scanning full disks but has been modified to be able to hold and scan increment cores. Initially the cores are marked to show the orientation of the grain as they are placed in the scanner with the grain running vertically. This ensures that the ultrasonic wave

travels in the same direction as the grain giving the fastest path. The cores are held in place by a single pin at one end and a double pin at the other, preventing the core from twisting as it is being measured (Figure 5-3).

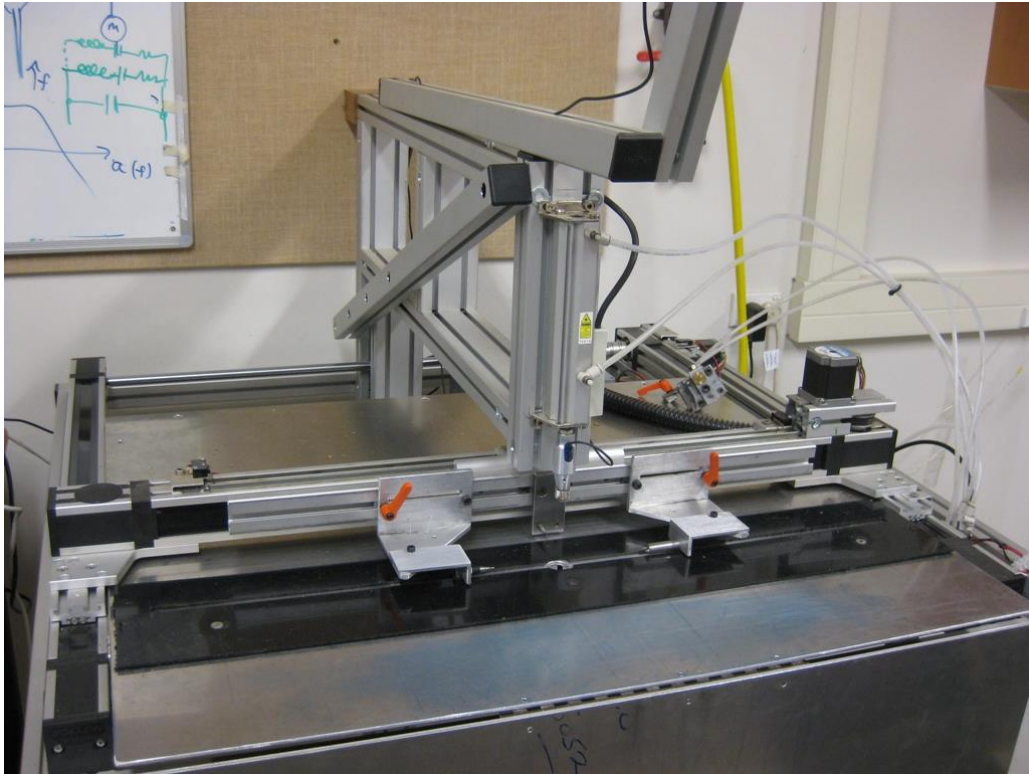


Figure 5-2: Ultrasonic Scanner at University of Canterbury, Christchurch, New Zealand



Figure 5-3: 12mm Sitka spruce increment core clamped into the ultrasonic scanner

The scanner consists of a signal probe and a receiving probe, which, using a system of pneumatics, come together with the core pressed in between. An attached camera and computer allow instructions to be input as to where the measurements should start and stop on the core, the location of the pith and the distance between each measurement (i.e. the resolution). In this case the scan pattern was set to measure every 2mm along the core as shown in Figure 5-4.



Figure 5-4: Computer photographic output showing position of pith (red dot), the start and end points (yellow dots) and scan pattern (blue line)

Once the run is started the instrument automatically moves the sample horizontally. Every 2mm the probes come together, measure the thickness of the sample and a 1.84 kHz sound wave is passed through the core between the probes. The computer program records the distance between the probes and the time the sound wave took to travel that distance giving a velocity output in metres per second for every 2 mm increment (Figure 5-5). In this instrument the head of the probe is 9mm in diameter, so in effect the measurements are an average of a circular area of 9 mm diameter measured every 2 mm with adjacent measurements overlapping.

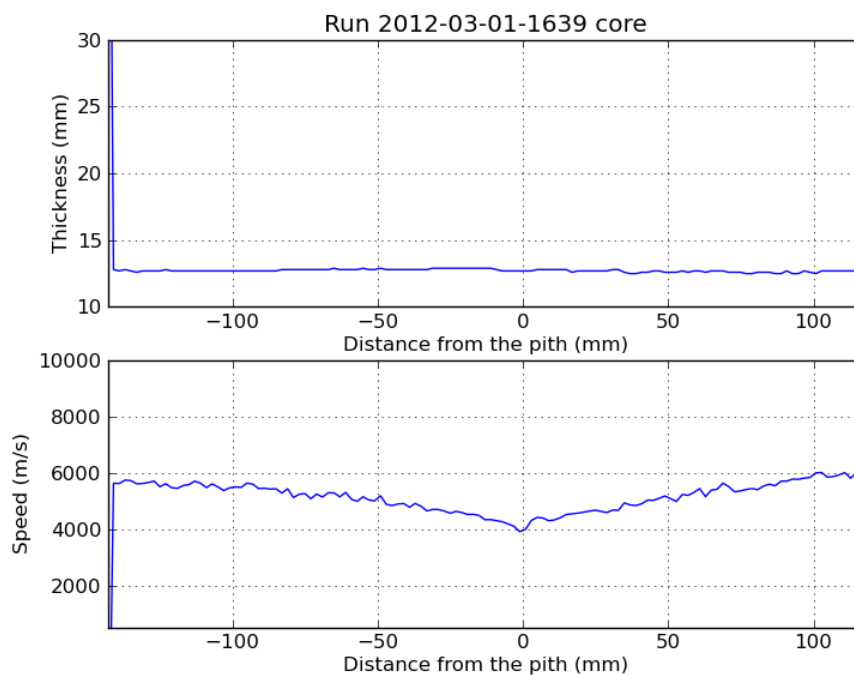


Figure 5-5: Computer output showing the core thickness (top) and the acoustic velocity (bottom) produced by the ultrasonic scanner.

5.3 Method Testing

In total over 1100 analyses were made using this method. Of these approximately 100 were testing the system to investigate how different step sizes would effect the quality of the data, the effect of having the core held at a slight angle so that the grain was not running vertical, and to investigate the effect of sanding the cores, to give a better contact with the probes.

5.3.1 Measurement Resolution

The instrument being used at University of Canterbury is set up so that the step size and therefore the resolution can be manipulated. Due to the number of cores to be measured it was considered whether it would be possible to change the step size to decrease the time spent measuring each core, without compromising the amount and quality of the data. The result of this, shown in Figure 5-6, show that there is little difference between the measurements at 2mm, 3mm and 4mm step sizes. However, it was decided, since density will be measured at a resolution of 50 μm steps, to give as high a resolution and as many data points as possible the acoustic measurements would be continued at 2mm.

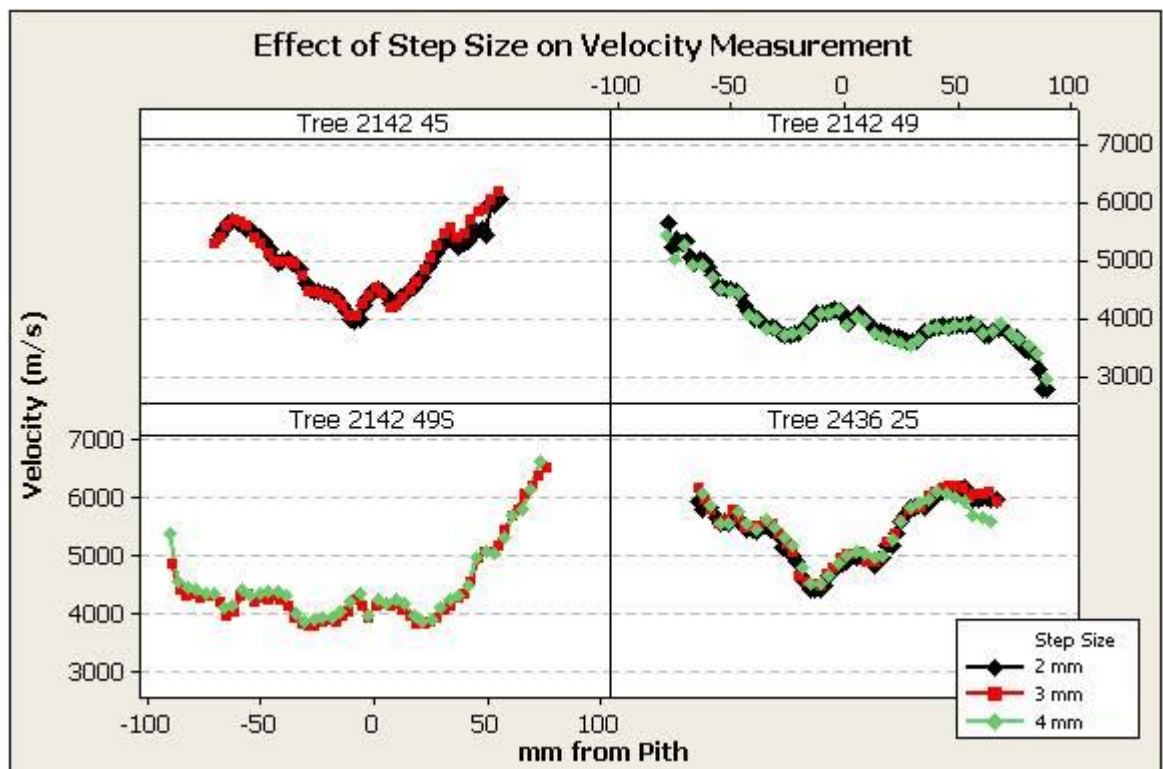


Figure 5-6 - The effect of different step sizes on acoustic velocity. Velocity was measured at 2mm, 3mm, and 4mm to determine if this would have an effect

5.3.2 Effect of Grain Orientation on Acoustic Velocity

Since this system was originally set up to measure discs there are a number of sources of error when trying to measure cores. One of these is the orientation of the grain in the sample.

The stiffness and hence acoustic velocity is strongly dependent on the grain angle (i.e. longitudinal velocity \gg tangential velocity)(Mishiro, 1996, Suzuki and Sasaki, 1990, Bucur and Bohnke, 1994). Therefore as pointed out by Bucur (1983) it is very important that when clamping the core in the instrument it is at the correct orientation with the grain running vertically, thus ensuring that the same measurement is being made on each core. To test the effect of changing the orientation of the grain a selection of cores were scanned with the grain running vertical, and then turned 10° and 20° clockwise and the same anticlockwise (Figure 5-7) being scanned at each step.

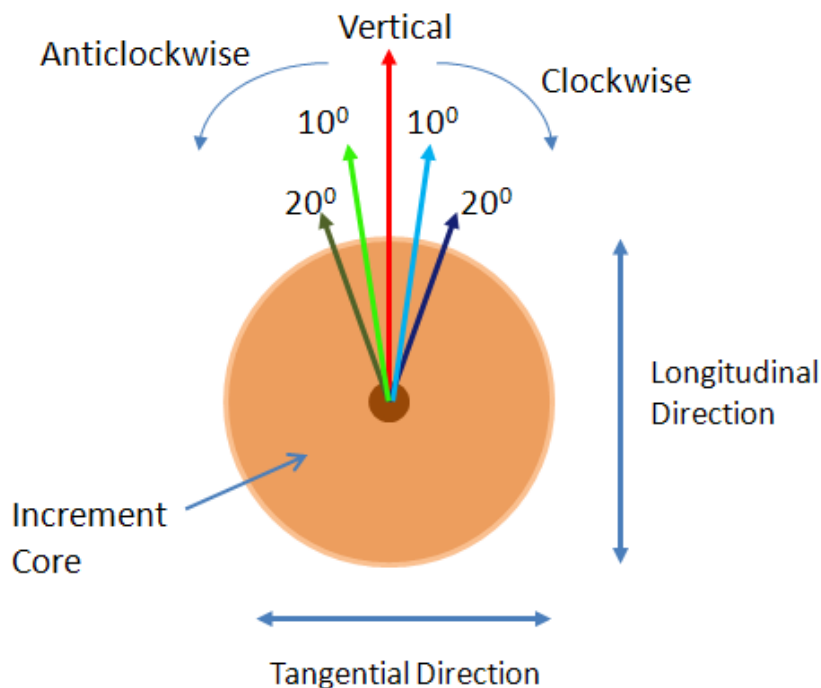


Figure 5-7: Schematic showing the change in grain angle from vertical.

Figure 5-8 shows the effect of turning the core and clearly shows that even a small difference in the orientation of the grain can have a big effect on reducing

the acoustic velocity measurement. When the core is positioned correctly with the grain direction running vertical acoustic velocity was seen to be lowest at, or near the pith, increasing towards the bark. However when the grain was not vertical there not only was an overall reduction in acoustic velocity, the radial trend was for a higher velocity at the pith decreasing towards the bark.

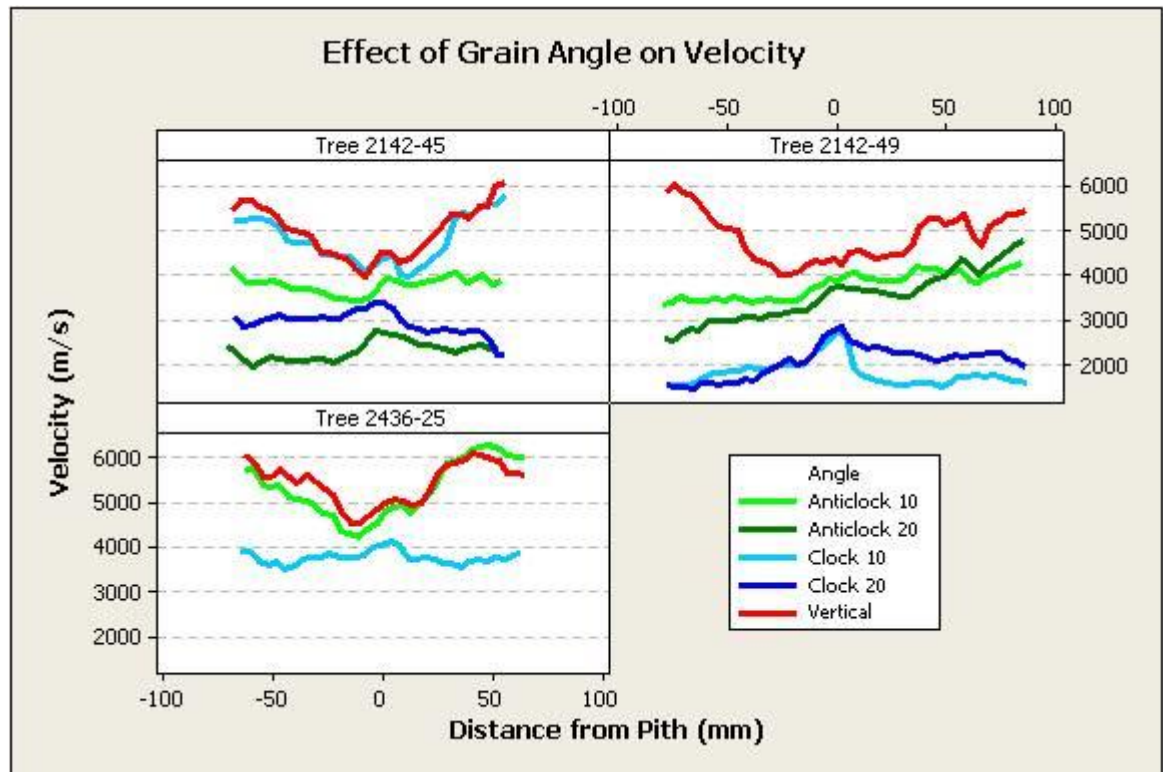


Figure 5-8 - The effect of turning the core by 10° and 20° clockwise and anticlockwise on the acoustic velocity on three separate tree cores

One of the main difficulties found with this method is aligning the cores parallel to the grain. Most of the cores were taken from bark to bark with an attempt made to go through the pith and where possible the bark is left on the core as this helps date the rings when analysed using the ITRAX Densitometer. This means that both ends of the core can be obscured by bark making it very difficult to see the direction of the grain (Figure 5-9). Although every care was taken to ensure that the grain for each sample was completely vertical in some cases this was only able to be done using the direction of the pith or if necessary cutting the cores at the pith to see the direction of the grain. One problem is that this does not take account of any change in grain angle within the core which could be caused by the natural spirality of the grain or the cores twisting or bending when they are drying. If the cores were misaligned within the scanner then this would cause problems with the data as shown in Figure 5-8.



Figure 5-9: Examples of cores taken as part of this study

Another source of error not measured here is the angle between the grain and the axis of the core. The cross sectional view (b) in Figure 5-10 shows the core being taken perfectly perpendicular to the direction of the grain, but it is easy to see how if the core was taken at a slight up or down angle then this would have an effect on the angle of the grain within the core. While every care was taken to ensure the cores were taken perpendicular to the grain the very nature of the shape and direction of growth of trees means that this may not have always been the case. This means that this could be another unknown, but random source of error.

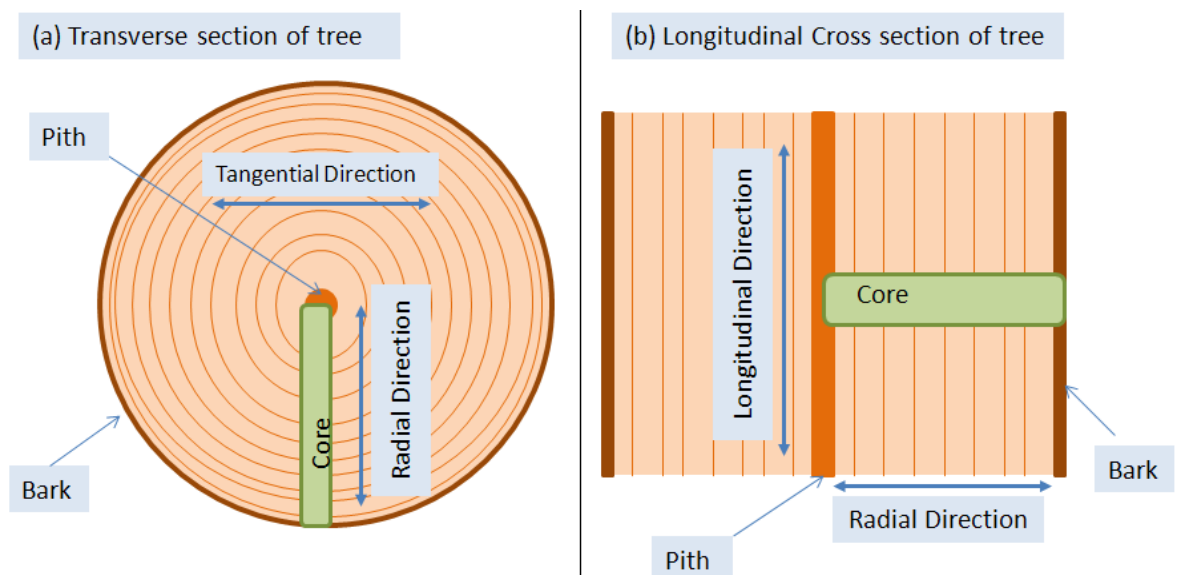


Figure 5-10: Schematic showing direction from which the cores were taken.

5.3.3 Effect of the Physical Condition of the Cores

Another source of error found when using this instrument was the physical condition of the core. The scanner was originally set up to measure the flat surface of a disc and has been adapted to be able to hold and measure cores. However, since the acoustic probe is 9mm in diameter the curved, rough edge of a core could be another source of error. As well as this, the distance that the sound wave has to travel can also have an effect whereby the smaller the measurement distance the larger any error will be.

During the analysis of the cores it was noticed that some of the older cores were in a poor state with rougher surfaces and areas of the surface which were crumbling into powder (Figure 5-11). This may have been caused by degradation in storage or been caused as a result of the corer being blunt.



Figure 5-11: Older cores from the original study showing the rough surface which in some cases has crumbled into powder

When these cores were run through the scanner it was observed that the velocity readings seemed to be more erratic than the cores which were in good condition, and this was put down to the state of the core. To try and counter this any cores which were deemed to be in a poor condition were sanded along the top and bottom to give a smooth surface on the faces that the scanner

probes would be in contact with (Figure 5-12). A total of 551 samples were analysed unsanded (i.e. not sanded) along with 540 sanded cores.



Figure 5-12: Examples showing the rough surface of the core (bottom) and a smoothed surface once sanded (top)

5.3.3.1 Sanded Versus Unsanded Acoustic Velocity Global Data

Overall results of the acoustic velocity measurements showed that while there is a high variability between trees there is a general trend whereby acoustic velocity increases from pith to bark (Figure 5-13). Although this trend was consistent between unsanded and sanded cores, the range of the sanded cores was narrower and at the same time the overall mean was lower.

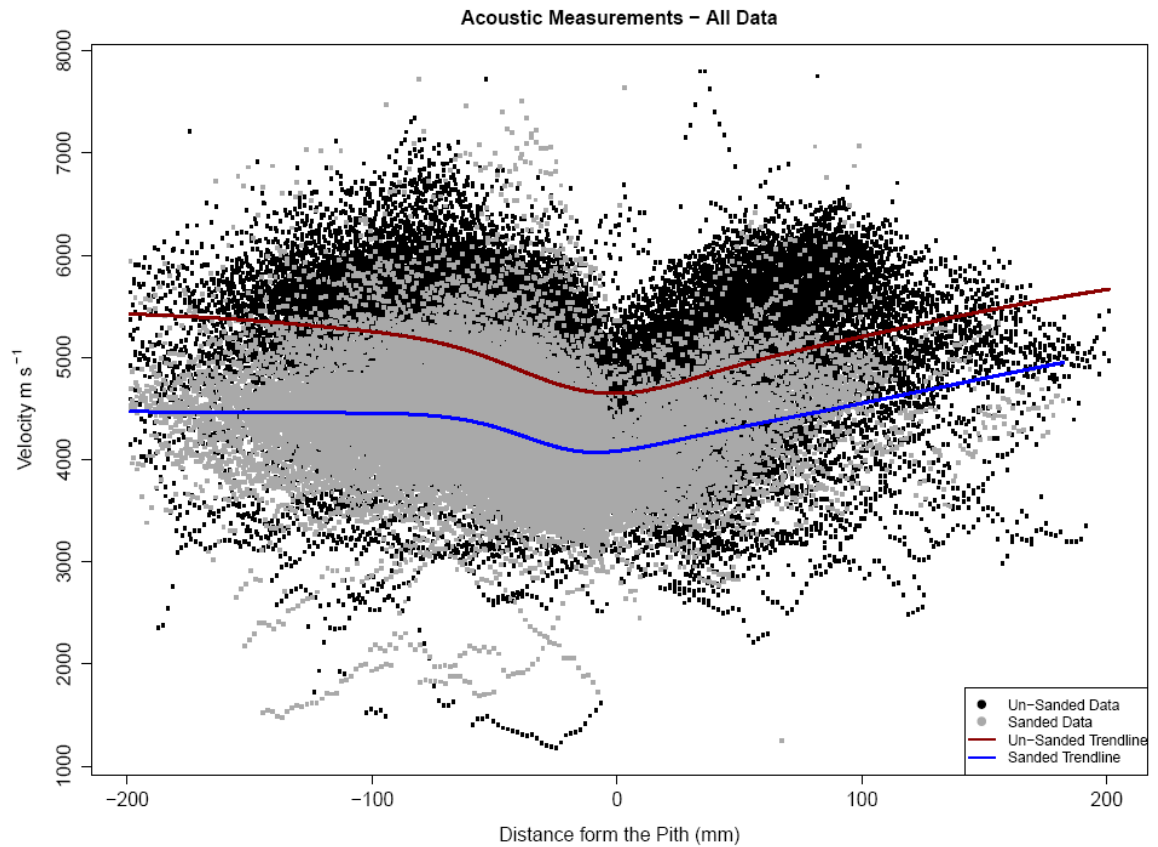


Figure 5-13: Acoustic velocity measurements on the full data set showing a LOWESS trendline for the unsanded and sanded data

5.3.3.2 Sanded Versus Unsanded Cores

In order to investigate if sanding the cores was having an effect, the acoustic velocity of 72 samples was measured on unsanded cores which were then sanded and re-analysed so that a direct comparison of the effect of sanding could be made. As with the global data, when the acoustic velocity measured on the 72 cores is plotted together it follows the same general trend of increasing from pith to bark for both the unsanded and sanded cores (Figure 5-14) and as before the LOWESS trendline for the sanded cores is lower than that for the unsanded cores.

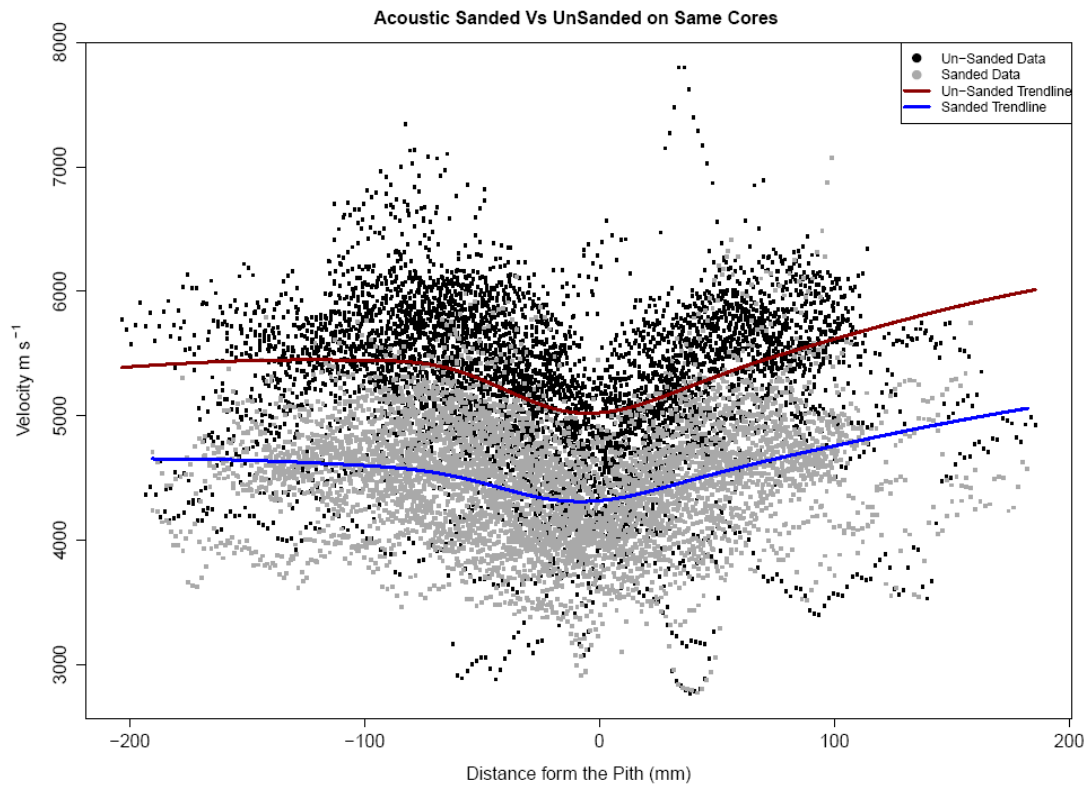


Figure 5-14: Acoustic velocity of the 72 samples where acoustic velocity was measured unsanded and then sanded.

The overall mean acoustic velocity for all 72 cores together is reduced from 5213 m s⁻¹ for the unsanded cores to approximately 4502 m s⁻¹ for the sanded and the overall measurements for the unsanded cores tended to be slightly higher (Figure 5-15).

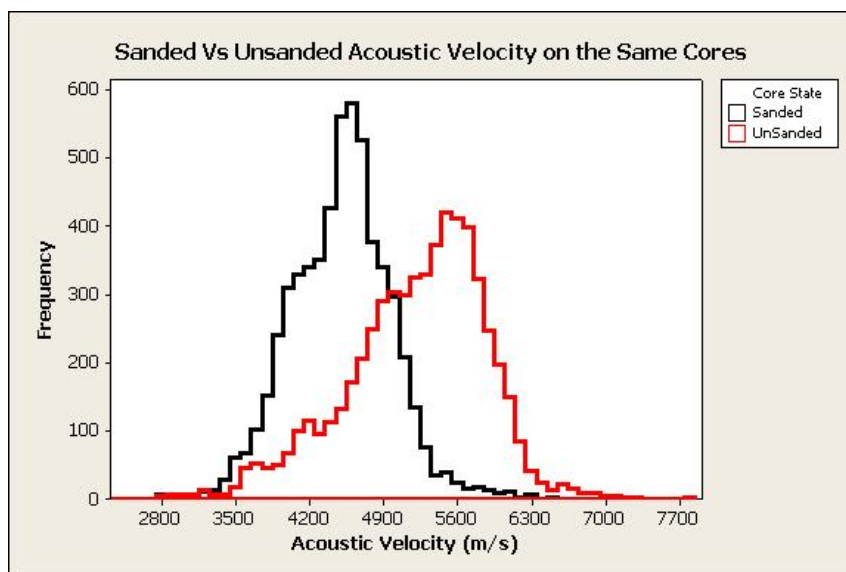


Figure 5-15: Histogram showing the frequency and range of acoustic velocity measurements on the 72 cores which were measured unsanded (red) and then sanded (black).

This would indicate that sanded and unsanded cores can not be directly compared and while in general sanding the cores seemed to have a negative effect on acoustic velocity (Figure 5-16) the magnitude of this effect was not consistent across samples or within sample making it difficult to convert, mathematically, from one to another.

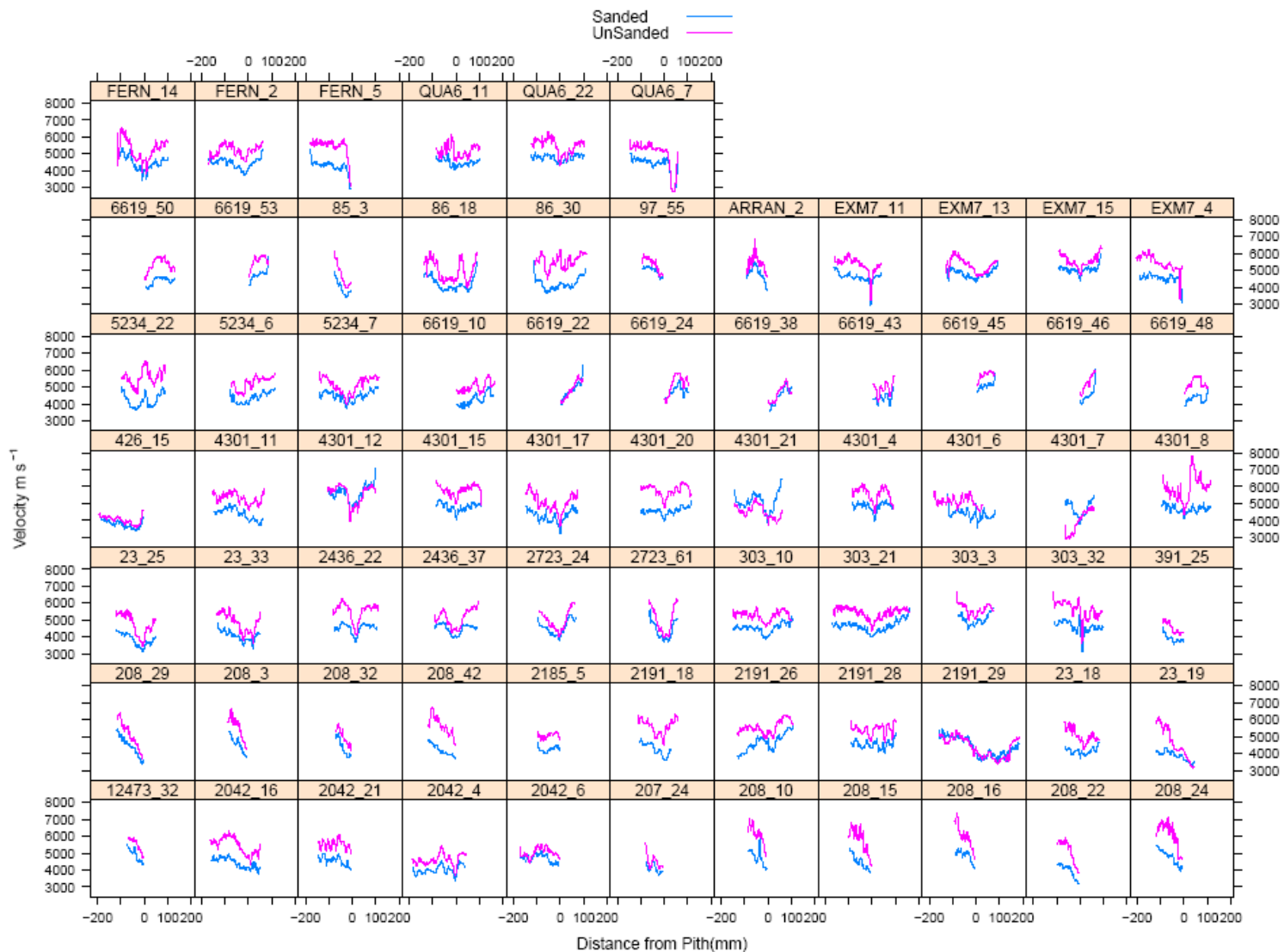


Figure 5-16: Acoustic velocity for the 72 samples which were measured both unsanded and sanded.

When the full subset of sanded v unsanded cores are examined (Figure 5-17), the relationship between measurements on the same core is poor ($R^2 = 0.34$) due to the fact that the relationship between sanded and unsanded varies between (and within) cores. If the intercept and gradient are allowed to vary by sample there is a much better relationship ($R^2 = 0.87$). For a lot of samples there was then a strong linear relationship, but for others there was no relationship (Figure 5-18) therefore this does not allow for a global conversion between one state and the other.

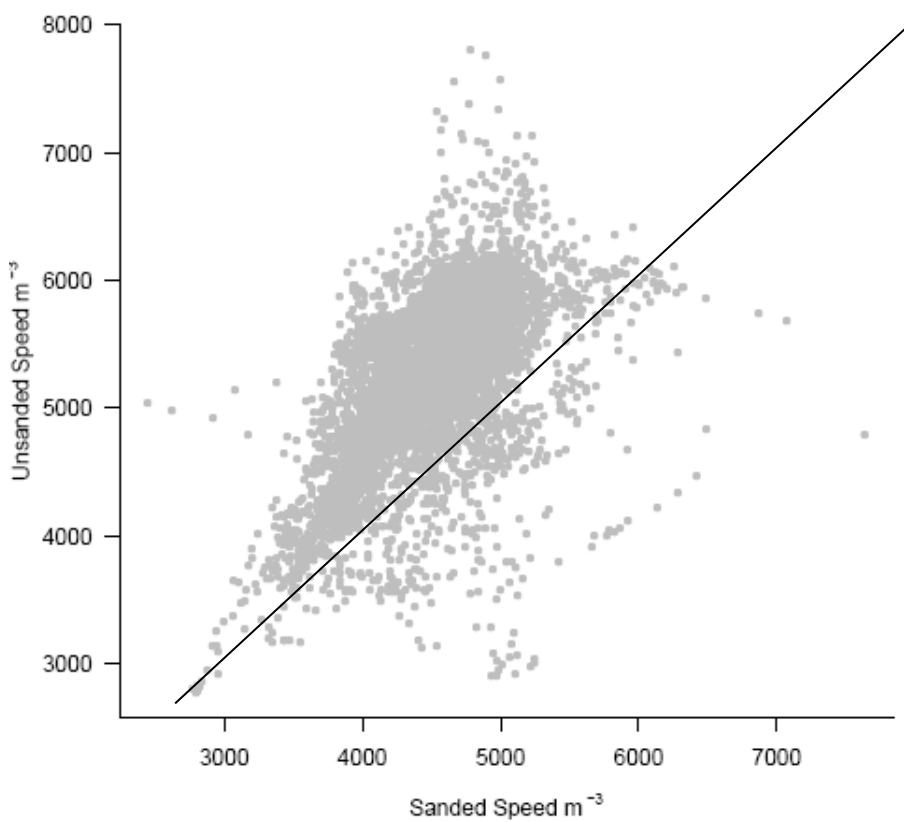


Figure 5-17: Scatterplot of acoustic velocity measured on the same cores unsanded and then sanded. Also shown is the line of equality (black). $R^2 = 0.34$

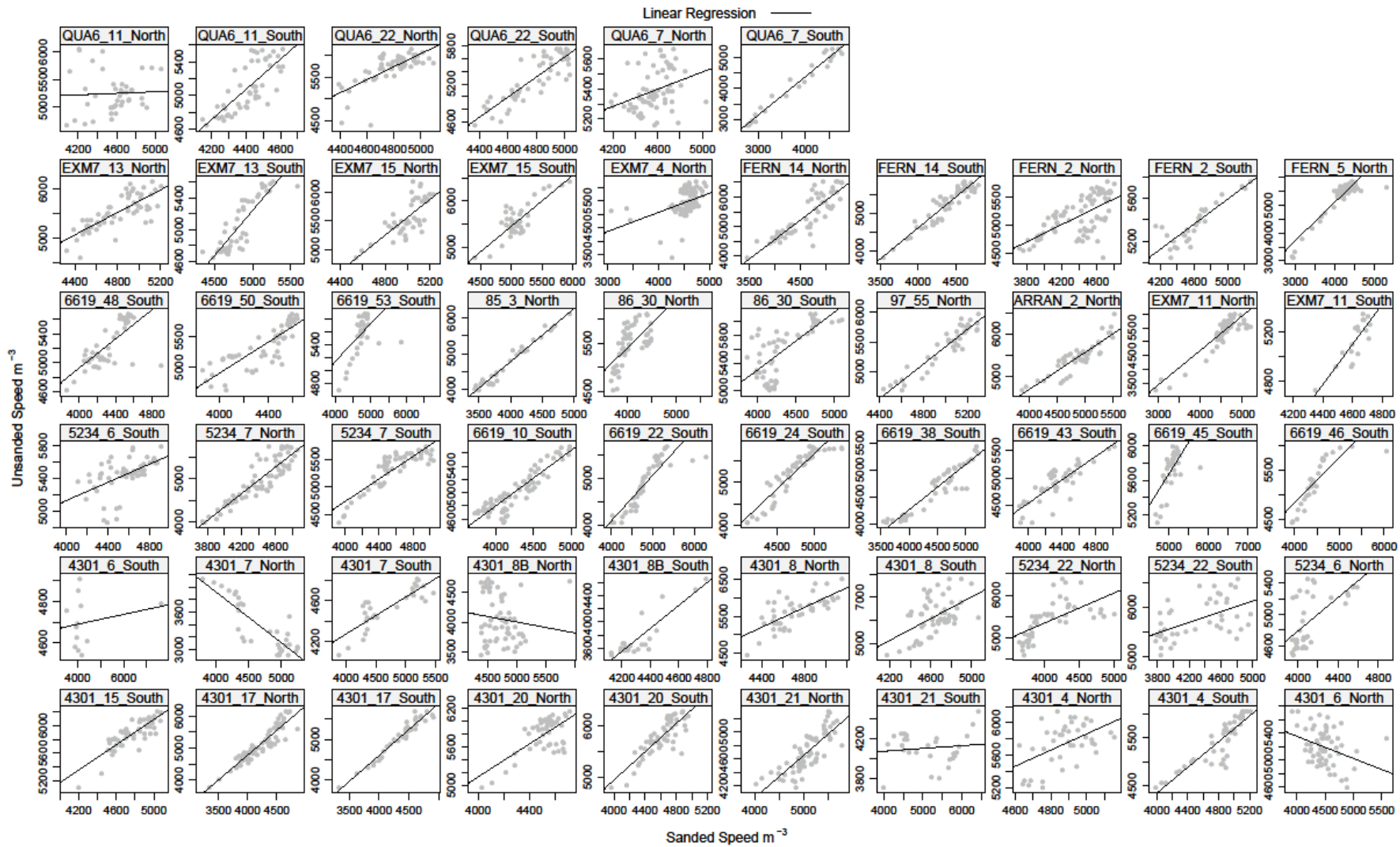


Figure 5-18:
The relationship between unsanded and sanded acoustic velocity on the same cores.

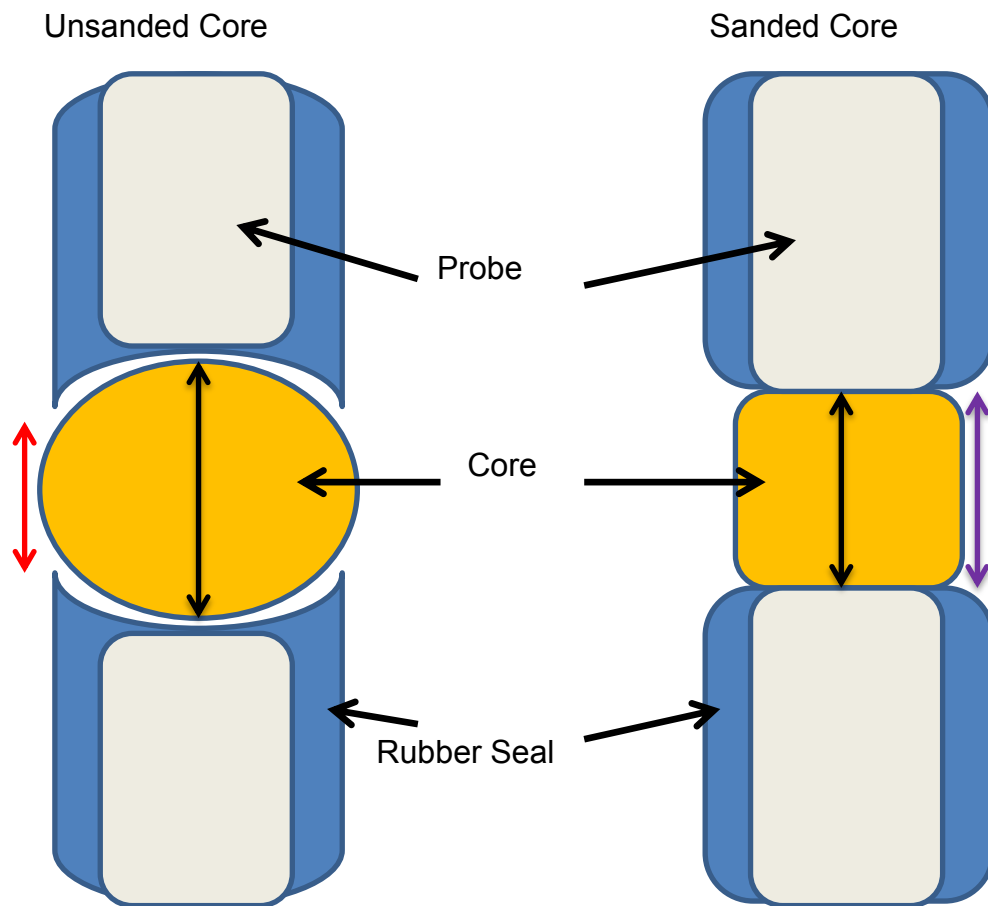


Figure 5-19: Schematic showing how the distance measured could be affected by the shape of the core.

One reason that this may be happening is due to the contact being made between the core and the scanner's probes. Figure 5-19 shows how the probes are held within a rubber seal, as contact is made with the unsanded core the rubber seal would curve round the core slightly. This may have the effect of reducing the distance that the sound wave has to travel although the system still measures the distance as between probes. Conversely, the sanded core has a flat surface where the probe and rubber seal sit flush to the sample which while eliminating this potential error, when the cores were sanded the distance measured would have decreased and as the measured distance gets smaller any error would increase as a proportion of the distance.

The cores were sanded using a large belt sander making it difficult to control the sanding process. The distance measured at each 2mm increment by the scanner ranged from 10.6 mm to 13.5 mm with a mean of approximately 12.6 mm for the unsanded raw cores while the sanded cores ranged from as low as 7.3 mm to 12.8 mm with a mean of 11.3 mm (Figure 5-20).

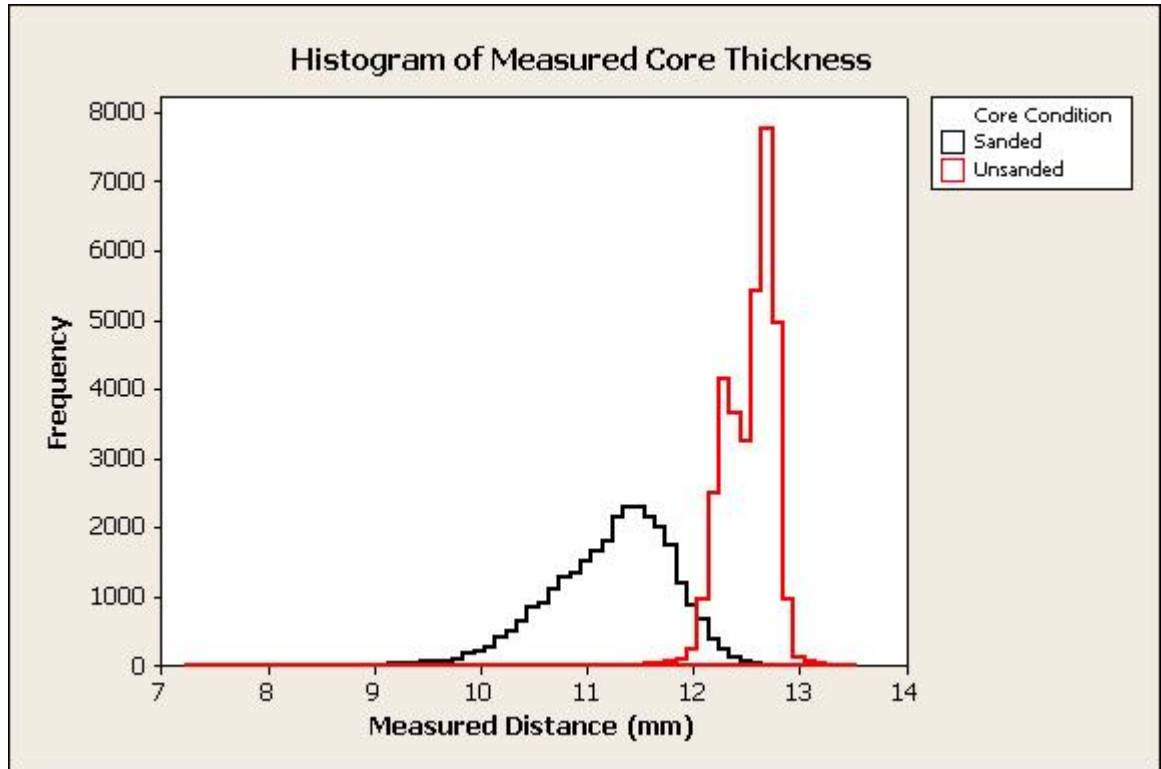


Figure 5-20: The variation in the thickness of the increment cores measured by the acoustic scanner.

There is a significant but small correlation ($p < 0.0001$) between the thickness measured and acoustic velocity for both the unsanded cores (correlation coefficient = 0.087) and the sanded cores (correlation coefficient = 0.277) but these correlations are low and may be due to the number of data points and so it is difficult to draw any conclusions. When the thickness is plotted against acoustic velocity (Figure 5-21) visually there does not look to be a trend due to the distance measured, especially in the unsanded cores, but the slope of the regression lines are similar with the slope of the unsanded cores being 274.4 m s^{-1} per mm and the sanded cores being 260.2 m s^{-1} per mm. However since the average difference between the unsanded and sanded core thickness is approximately 1 mm, the difference in velocity caused by the thickness of the core is not enough to account for the differences seen in the velocity between the two physical states (Figure 5-13).

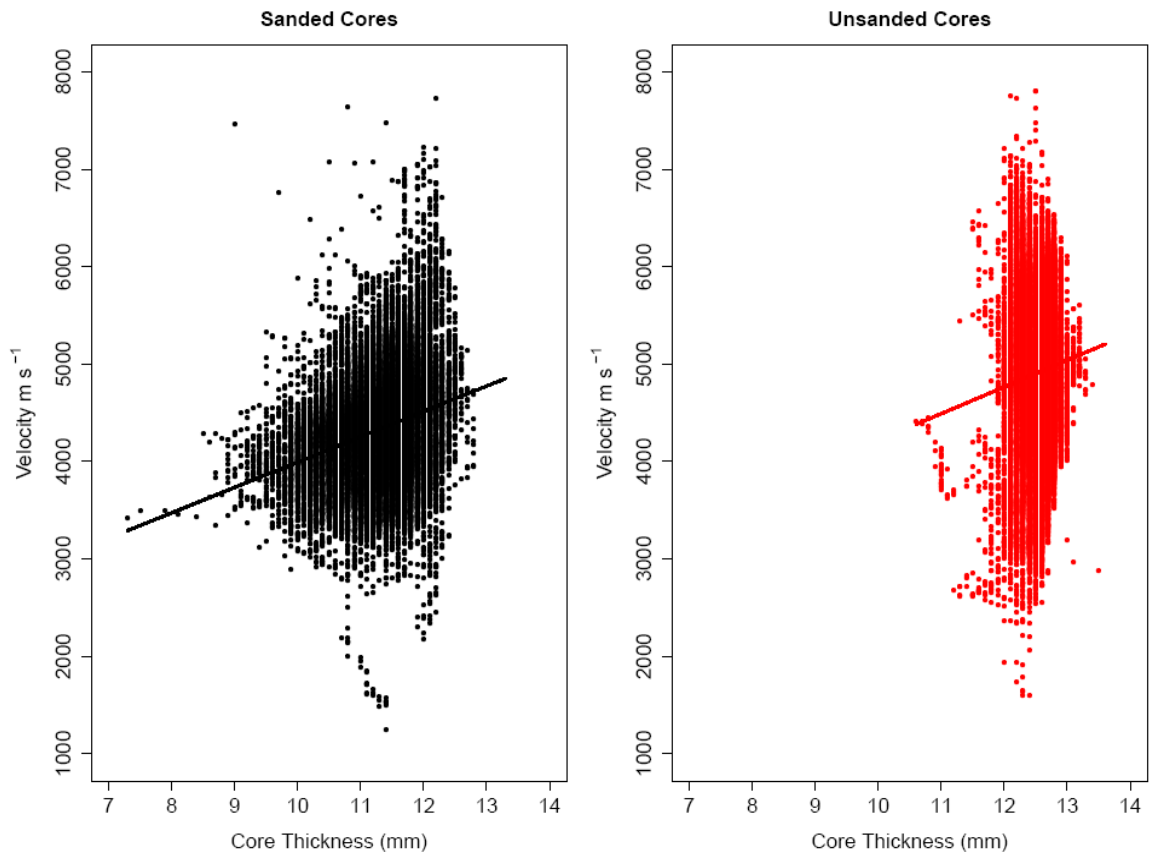


Figure 5-21: Thickness measured by the acoustic scanner for each 2mm increment plotted against the acoustic velocity.

In order to see the direct effect of the reduction in thickness caused by sanding the subset of 72 cores which were analysed both sanded and unsanded were investigated. Analysis shows that the thickness of the unsanded cores ranged from 11.5 mm to 13.1 mm with a mean of 12.6. The thickness of the sanded cores ranged from 10.0 mm to 12.7 mm with a mean thickness of 11.7 mm (Figure 5-22).

For this subset of cores, velocity and the distance measured are significantly correlated (correlation coefficient=0.5, $p < 0.0001$). The average velocity measured on the sanded cores is 4492 m s^{-1} and 5232 m s^{-1} on the unsanded cores making a mean difference of 740 m s^{-1} . When the lines are plotted separately (Figure 5-23) the regression slopes are 125.8 m s^{-1} per mm and 209.4 m s^{-1} per mm for unsanded and sanded cores respectively which suggests that some of the difference between the acoustic velocity can be accounted for by the difference in thickness alone. Conversely it also suggests that there is more than just thickness which is affecting the acoustic velocity.

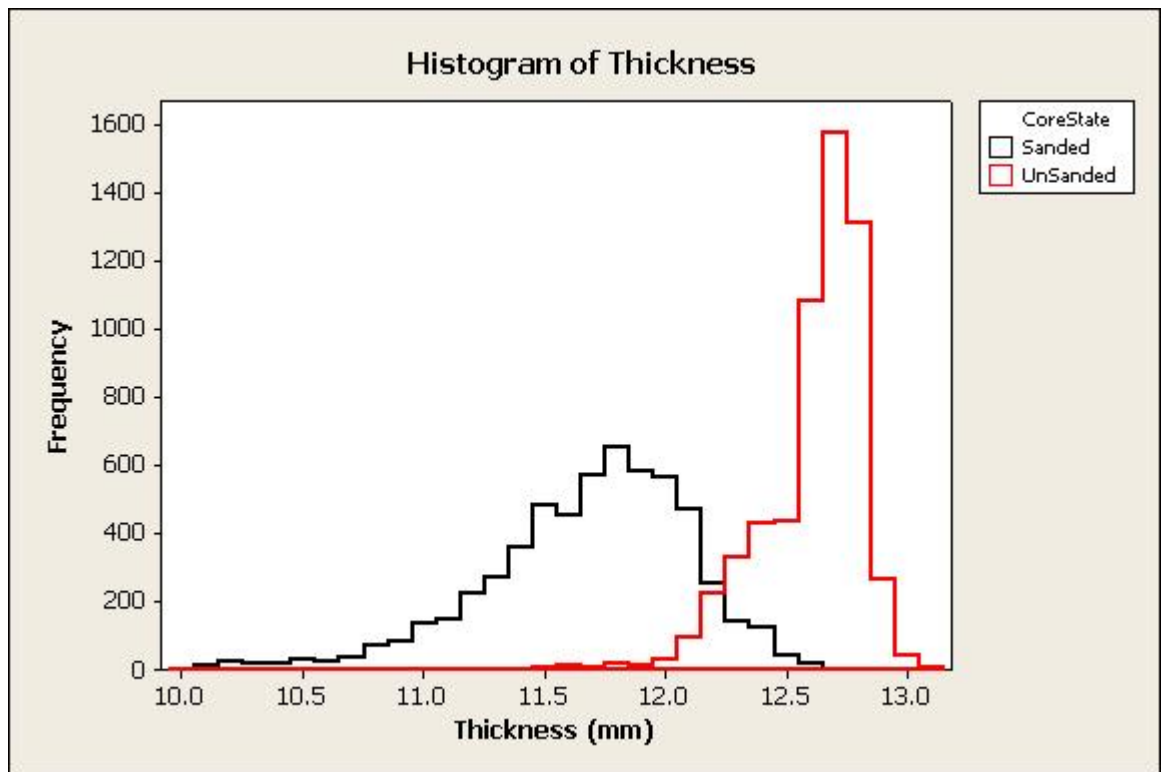


Figure 5-22: The variation in the thickness of the 72 increment cores which were measured by the acoustic scanner both unsanded and sanded.

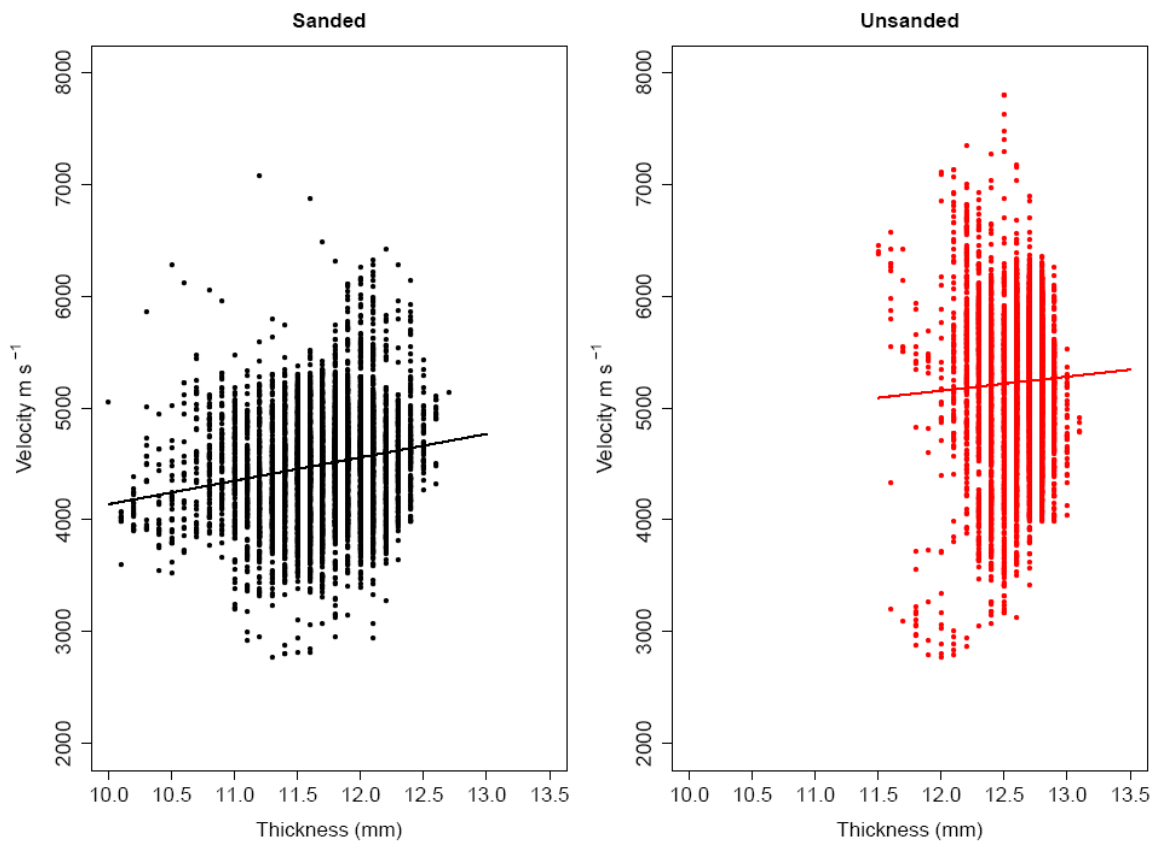


Figure 5-23: Distance measured by the acoustic scanner plotted against the acoustic velocity for the 72 increment cores which were measured by the acoustic scanner both unsanded and sanded.

5.4 Discussion of Method for Measuring Acoustic Velocity on Cores

With a capability of scanning over 100 core samples per day the scanner used in this project provides a quick method for obtaining acoustic velocity measurements, but since the system was originally set up to measure discs there are a number of sources of error when measuring cores.

The mean velocity for the full data set was 4616 m s^{-1} though this includes both sanded and unsanded cores, as well as cores where the grain orientation may not be vertical which would have the effect of reducing the overall mean value. Although the utmost care was taken when positioning the cores within the scanner, subsequent analysis of the form of each profile suggested that a number of them showed the same profile as those where the grain angle was deliberately altered i.e. lower at the bark and increasing towards the pith. These cores were then deemed to be mis-orientated and so were removed along with the sanded cores. The effect of this meant that the mean velocity increased to 5230 m s^{-1} which is slightly lower than that found by Ilic (2003) who reported the velocity on Sitka spruce from Canada at 5770 m s^{-1} . This was measured on small beam samples which were 150 mm in the longitudinal direction and 20 mm radially and it was not stated where in the radius of the tree the samples came from.

The acoustic velocity is strongly dependent on the orientation of the grain and fastest in the longitudinal direction (Bucur and Bohnke, 1994, Bucur, 1983) i.e. the same direction as the grain. As was shown here even a small change in the orientation can have an effect on the velocity. This is consistent with work done on Norway spruce by Niemz et al. (1999) who found that a change in angle of only 10° could reduce velocity by 20%. This investigation showed that the orientation of the grain in an increment core can be extremely difficult to determine in cores especially with the bark intact and that a great deal of care has to be taken when positioning the cores within the scanner.

This system has been used successfully in the past to measure acoustic velocity on Sitka spruce samples (Vihermaa, 2010), but these measurements were on disc samples where the orientation of the grain and the surface finish of the samples

was less of an issue. Tests on the orientation of the core samples showed the radial profile of longitudinal acoustic velocity to follow a general trend of increasing from the pith, if the orientation of the grain was completely vertical; but if this was moved then the shape of the radial profile was altered dramatically to the point where acoustic velocity was seen to decrease from the pith.

The physical condition of the core was also found to be an issue when using this technique. The surface finish of some cores was found to be quite rough and in some cases, especially with the older cores, some degradation had taken place which seemed to be having an effect on the readings. Sanding the “bad” cores to give smooth surface allowed measurements to be made but this change means that no direct comparison between the full dataset can be made. Bucur (1983) also found issues with coupling of the probe to the sample in 5mm diameter cores and used Vaseline as a medium to ensure there was a good bond between the transducer and the wood.

This suggests that if this instrument is to be used in future the cores may need to be in perfect condition on the surface as well as ensuring that the pith is in the core so that the orientation can be adjusted to be perfectly vertical. This issue is known by the University of Canterbury and research is ongoing into a new system involving a smaller probe and rotating the core

6 Modelling Radial Profiles of Longitudinal Acoustic Velocity

6.1 Introduction

Using the data collected from the sample cores described in Chapter 2 this chapter explores the radial profile of longitudinal acoustic velocity in Sitka spruce and how this changes across the full geographical range in which Sitka spruce grows in Great Britain. The radial trend in acoustic velocity was examined to investigate how this matches the known profiles of stiffness and MFA for Sitka and empirical models were created with cambial age as the explanatory variable. These models were then used to investigate whether parameters such as latitude, longitude, altitude and spacing were having an effect.

6.1.1 Definitions

When acoustic velocity is discussed in this section it is referring to the velocity of sound measured in a longitudinal direction (up and down the tree) which was measured in 2mm increments across a radial core (from pith to bark) taken from the tree.

Ring number is counted from the pith and is a measure of cambial age in years. For the purposes of this chapter the terms “Ring Number” “Age” and “Cambial Age” are interchangeable.

6.1.2 Outline

The sample cores were collected as described in Chapter 2. As described in Chapter 5 there were a number of issues relating to the method of analysis of the increment cores. To minimise any discrepancy caused by the physical condition of the cores (i.e. sanded or unsanded), only those cores that were unsanded were used in the modelling analysis.

Since the effect of cambial age was being investigated and acoustic velocity was measured by distance from pith, in order to model acoustic velocity by age the measurements had to be converted from distance from pith to ring number.

This was done using the accumulated ring width measurements for individual samples collected during the density analysis on the ITRAX densitometer (Chapter 2). Acoustic velocity for each sample was designated a ring number as a function of its distance from the pith. A mean value of the acoustic velocity was then assigned to each ring. This had the disadvantage that some rings of less than 2mm had no values assigned.

In order to keep this section comparable with the growth and density modelling sections the ring number had an upper limit of 25 years old.

As discussed in Chapter 5 there were a number of problems associated with measuring acoustic velocity on these cores leading to unreliable results, so at this stage any samples which looked to have had a problem with the acoustic velocity measurement due to the orientation of the core were removed. To do this, the radial profile of acoustic velocity for each core was examined and compared to profiles where the grain orientation was known to be vertical and also compared to profiles that were deliberately misaligned (as described in Section 5.3.2 of Chapter 5). Although there is variation between the profiles of each core the main feature of a properly aligned core is higher acoustic velocity at the bark which decreases towards the pith. Those that were deliberately misaligned showed a profile that was higher at the pith and decreased towards the bark. For the purposes of modelling acoustic velocity the cores which showed a profile where the acoustic velocity was higher at the pith and decreased towards the bark were removed from the analysis.

6.1.3 Aim

The aim of this section is to investigate which empirical models best describe the radial profile of acoustic velocity with age of the sampled trees. These models can then be used as an indication of MFA in these profiles and to investigate any difference in acoustic velocity by altitude, latitude, longitude and initial spacing.

A method for analysing the radial profile of acoustic velocity by these models is presented, but due to the uncertainty in the grain angle it is difficult to

determine where any differences may come from and so any findings would reflect this uncertainty.

6.2 Radial Variation in Acoustic Velocity

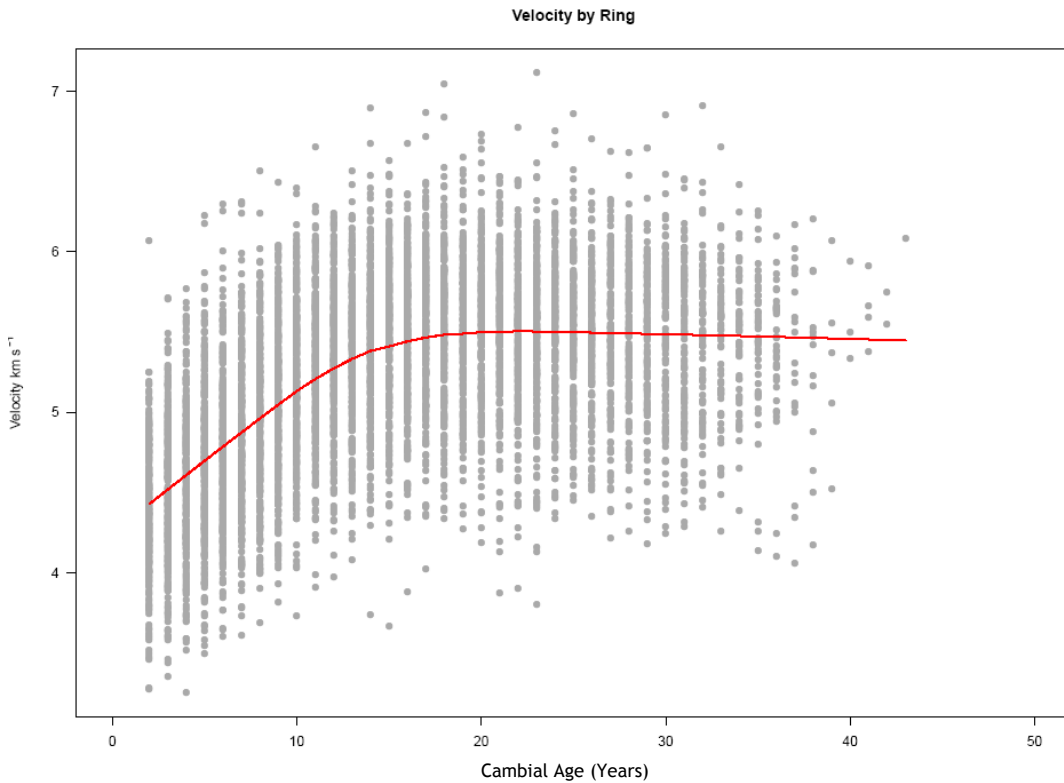


Figure 6-1: Acoustic velocity of all data plotted by ring number with a LOWESS trend line

The radial trend in acoustic velocity could be described as being a curve with an initial increase from the pith to between year 12 and 18 which then levels out to a plateau (Figure 6-1) mirroring the radial pattern of MFA found in Sitka spruce (McLean, 2008). As with radial growth this general trend could be described as conforming to the generally accepted juvenile and mature phases of growth (Cameron et al., 2005, Brazier and Mobbs, 1993, Schaible and Gawn, 1989) and can be linked to radial variation in MFA (Evans and Ilic, 2001).

A total of 279 samples across 37 sites were used in this analysis with the total number of samples per site ranging from 3 to 10 (Table 6-1).

Table 6-1: Number of samples per site.

Site	1390	155	1600	2013	2042	2142	2185	2191	23	2304
No.Samples	9	9	10	5	5	6	7	9	9	7
Site	2436	2559	2723	278	2789	279	280	281	303	3237
No.Samples	9	5	9	3	8	9	6	4	7	6
Site	339	4301	461	5234	54	5945	6619	6630	6874	72
No.Samples	8	8	7	7	10	9	8	9	4	10
Site	7643	86	9004	9008	EXM7	FERN	QUA6			
No.Samples	10	7	9	9	8	6	8			

When each site is looked at separately, even though the acoustic velocity follows the same general trend of increasing from pith to bark (Figure 6-2) within each site there seems to be a large spread in values for each ring between each tree. Although there are differences between sites, especially near the pith, this does not seem to follow any trend in latitude. To be able to visualize how the acoustic velocity is affected by latitude, longitude, spacing and altitude these variables were split into groups as described in the method in Chapter 2. The data were fairly unbalanced due to the problems encountered with the method. The latitude (Northing) groupings run from furthest south (Grp 0) to furthest north (Grp 9), longitude (Easting) runs from west (Grp 1) to east (Grp 4), altitude runs from lowest elevation (Grp 1) to highest elevation (Grp 9) and Spacing is grouped by the measured distance in metres. The number of samples in each of these groupings is shown in Table 6-2.

Table 6-2:: The number of samples and sites per group

Northing Group	0	1	2	3	4	5	6	7	8	9
No. Samples	6	45	37	36	43	36	37	9	8	22
No. Sites	1	6	5	4	5	5	5	1	1	4
Easting Group										
	1	2	3	4						
No. Samples	28	143	72	36						
No. Sites	4	19	10	4						
Altitude Group										
	1	2	3	4	5	6	7	8	9	
No. Samples	10	18	57	33	51	50	17	22	21	
No. Sites	2	3	7	4	7	6	2	3	3	
Spacing (m)										
	1.7	1.8	1.9	2	2.4	2.5				
No. Samples	43	37	8	164	12	15				
No. Sites	6	4	2	21	2	2				

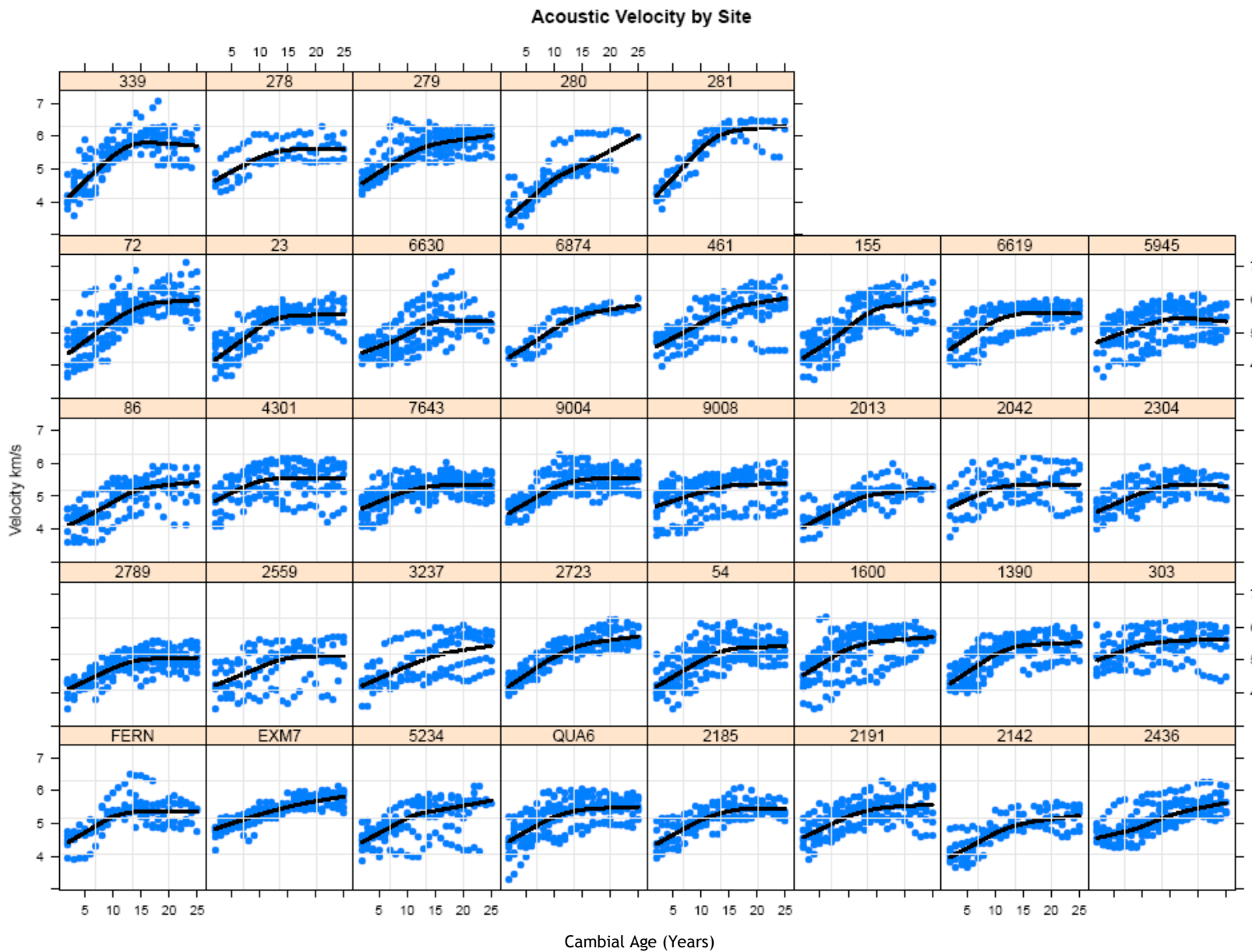


Figure 6-2: Acoustic velocity and LOWESS trend line plotted by site in order from south (bottom left) to north (top right)

6.3 Modulus of Elasticity (MoE)

One of the main quality parameters of Sitka spruce in Britain is its stiffness (also known as Modulus of Elasticity, MOE or Young's modulus) and strength (MacDonald and Hubert, 2002).

The stiffness of wood is dependent on the microfibril angle (MFA) of the S2 cell wall layer and its density (Evans and Ilic, 2001, Cave and Walker, 1994) and relationships have been found between MFA and stiffness in Sitka spruce (Cowdrey and Preston, 1966, McLean et al., 2010) as well as between MFA and acoustic velocity (Koponen et al., 2005), though determination of MFA can often be an expensive process. The speed at which sound travels through a material is related to its stiffness and density therefore given the wood density and the velocity of sound it is possible to predict the stiffness of wood from the following equation:

$${}_d\text{MoE} = \rho V^2 \quad \text{Equation 6.1}$$

Where ${}_d\text{MoE}$ is the dynamic modulus of elasticity, ρ is density in kg/m^3 and V is acoustic velocity in metres per second.

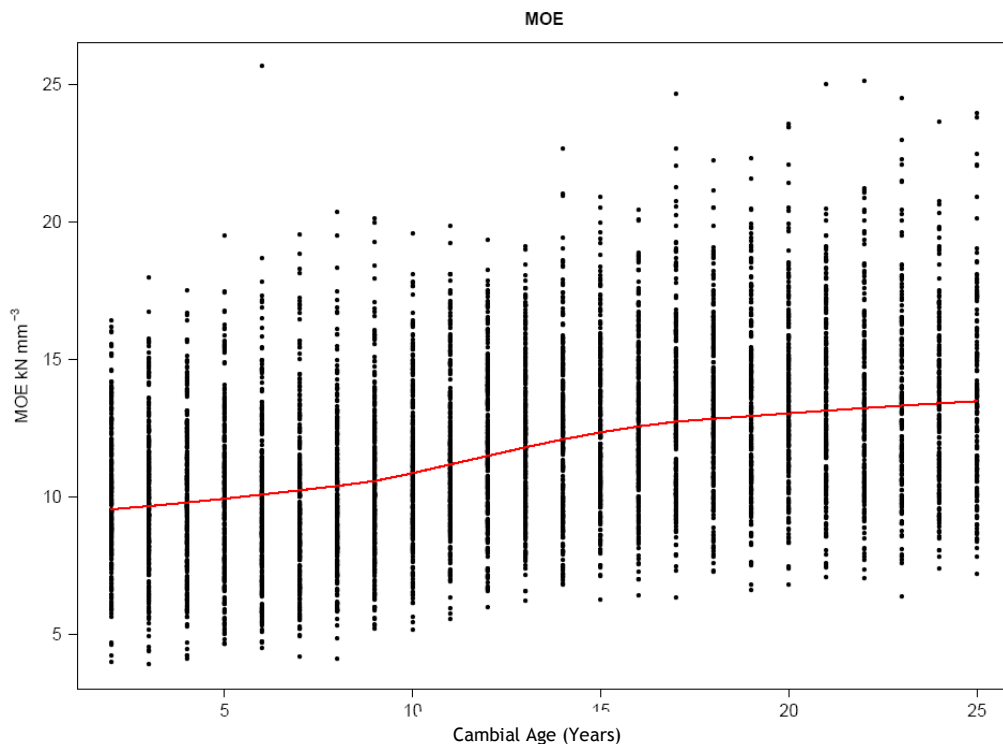


Figure 6-3: Dynamic MoE by ring for the set of data that was measured for acoustic velocity and density.

For this data set, dynamic MoE was calculated on a ring basis from the above equation (6.1) using the mean ring density and mean ring acoustic velocity and the general trend when the data is plotted together is for MoE to increase from the pith (Figure 6-3). However, when individual trees are plotted (Figure 6-4) it shows that for some of the samples the dynamic MoE decreases from the pith for a number of rings before starting to increase. This trend in some of the trees is similar to that found by Vihermaa (2010) using a similar method to calculate dynamic MoE but when McLean et al. (2010) measured static MoE on small defect free samples they were all found to increase from the pith. The discrepancy in the trend seen here may be due to the high density core wood seen in Sitka spruce where density decreases to approximately ring 7 (see Chapter 4) and so it may be that this method of calculating MoE is not suitable for Sitka spruce in the first few rings.

From the calculation of ρ MOE it is therefore possible that the velocity of sound through wood itself is a good predictor of MFA (Koponen et al., 2005) and so is interesting in itself.

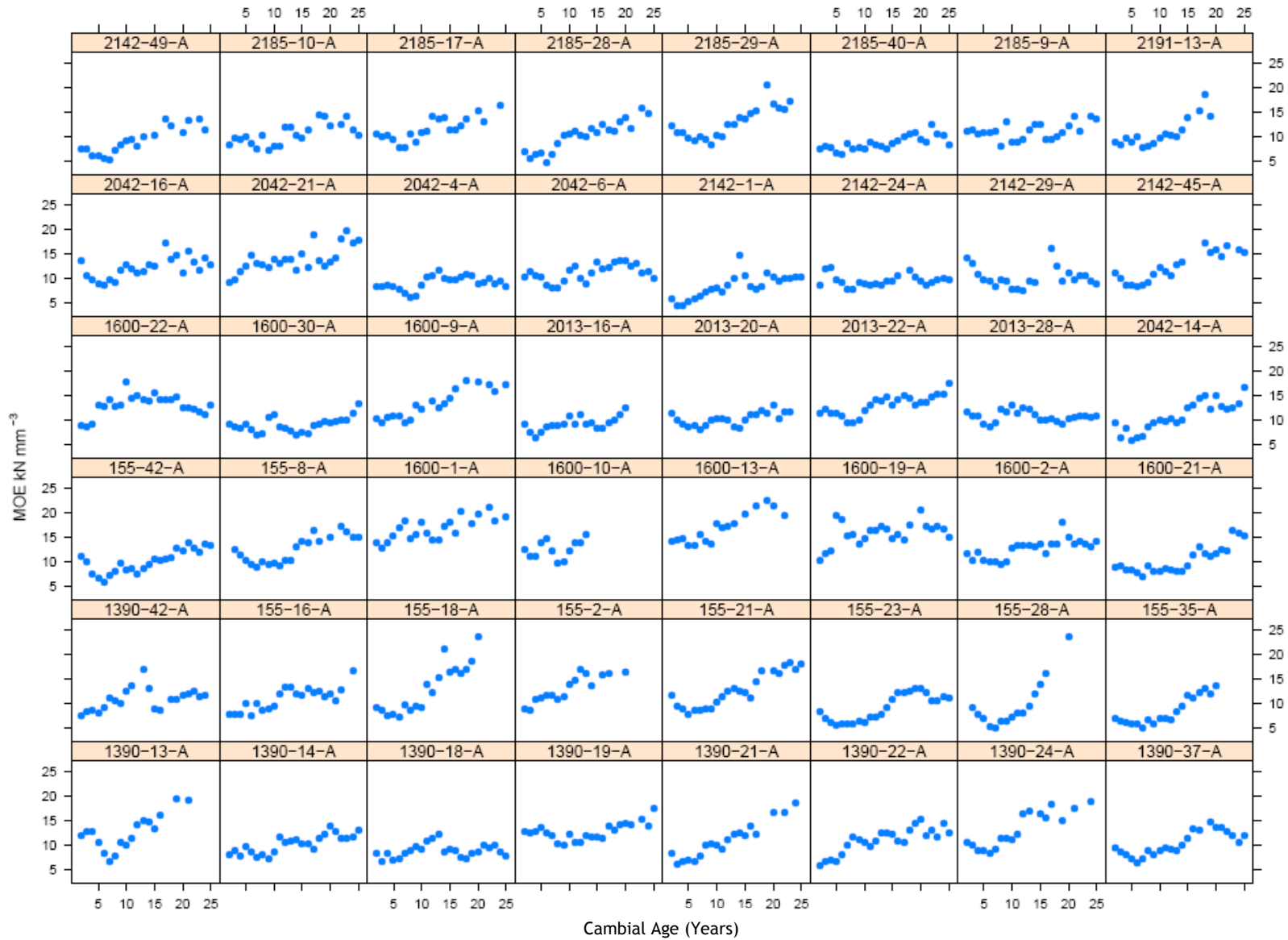


Figure 6-4: Dynamic MoE by ring for a selection of trees

6.4 Fitting Models to Acoustic Velocity

Four statistical models were explored to see how well they described the trend. The form of these models was as follows:

1. Segmented Linear (Seg) Model - Using the segmented package in R (Muggeo, 2008) this model investigates whether there are two separate linear sections to the radial profile of acoustic velocity with a split point between the two sections, using a Davies test (Davies, 1987) to test for a significant change in gradient. Each linear section follows the form of a linear equation:

$$\text{Juvenile Slope: } ACV = m_1x + c_1 \quad x \leq 13 \quad (\text{Equation 6.2})$$

$$\text{Mature Slope: } ACV = m_2x + c_2 \quad x > 13 \quad (\text{Equation 6.3})$$

Where ACV is the radial profile of acoustic velocity, m_1 and m_2 are the slopes, x is the cambial age and c_1 and c_2 are the intercepts of the respective sections. In this model, although it is a parameter of the mature section, c_2 is a measure of the intercept at year zero.

2. Michaelis Menten (MM) Model - based on the Michaelis Menten equation

$$ACV = (a_0 * x) / (a_1 + x) \quad (\text{Equation 6.4})$$

Where ACV is the radial profile of acoustic velocity, x is cambial age, a_0 is the maximum acoustic velocity towards which the observed data tend, and a_1 is a constant estimated from the data which is equal to the age at half of a_0 . This function was fitted in R using non linear least squares regression (nls function) to find the best fit curve.

3. Exponential (Exp) Model - using a variation of an exponential function which can be used to model MFA in Sitka spruce (Jordan et al., 2005) but with a positive rate component:

$$ACV = -b_0 * \exp^{-b_1 * x} + b_2 \quad (\text{Equation 6.5})$$

Where b_0 is the initial value, b_1 is the rate parameter and b_2 is the asymptote parameter estimated from the data and fitted in R using non-linear least squares regression (nls function) to find the best fit curve.

4. Logarithmic (Log) Model

$$ACV = d_0 * \log(x) + d_1 \quad (\text{Equation 6.6})$$

Where d_0 is the gradient, d_1 is the intercept and x is the cambial age and fitted in R using non-linear least squares regression (nls function) to find the best fit curve.

6.5 Comparing Models Fitted to Acoustic Velocity

6.5.1 Model Parameters

Table 6-3: Parameter estimates along with Standard Errors, residual standard error and R-squared value for the four model equations. Also shown is the number of trees and the percent of the total that the model wouldn't fit to.

Parameter	Estimate	Standard Error	Residual Std Error	R-Squared	No. Trees Not Fit	% Total Not Fit
Segmented	Split Point:	13.28 years				
c_1	0.094	0.0023	0.4541	0.3955	4	1.4
m_1	4.222	0.0194				
c_2	0.003	0.0026				
m_2	5.427	0.0491				
Michaelis Menten						
a_0	5.666	0.011	0.2869	0.3454	0	0
a_1	0.806	0.017				
Exponential						
b_0	1.725	0.315	0.2844	0.3858	43	15
b_1	0.131	0.007				
b_2	5.642	0.218				
Logarithmic						
d_0	0.531	0.009	0.2828	0.3751	0	0
d_1	3.932	0.022				

Each of the models was fitted to as many of the samples as possible (global data). The coefficients that were estimated for the four models are presented in Table 6-3 and are plotted along with the LOWESS trend lines of the observed data in Figure 6-5. Of the curved models, visually the Exponential model would

seem to give the best fit and this model was able to explain more of the variation (38.6%) than both the Logarithmic (37.5%) and Michaelis Menten Models (34.5%). The segmented model was able to explain slightly more of the variation (39.6%) and visually this was also a good fit to the data on the juvenile (initial increase) phase and mature (plateau) phase. The residual standard error was the similar for the Exponential (0.28 km/s), Logarithmic (0.28 km/s) and Michaelis Menten (0.29 km/s) models with the segmented model being higher at 0.45 km/s.

Although the Exponential model looked to give a good fit to the data when the models were fitted to individual trees, in the R statistical program (R Core Team, 2013), it was unable to fit to 15% but this may be due to the many profiles which are atypical and may be symptomatic of the grain angle issues described in Chapter 5. Both the Logarithmic and Michaelis Menten models were able to fit to all trees and the segmented model was only unable to fit to 4 samples (1.4% of the total).

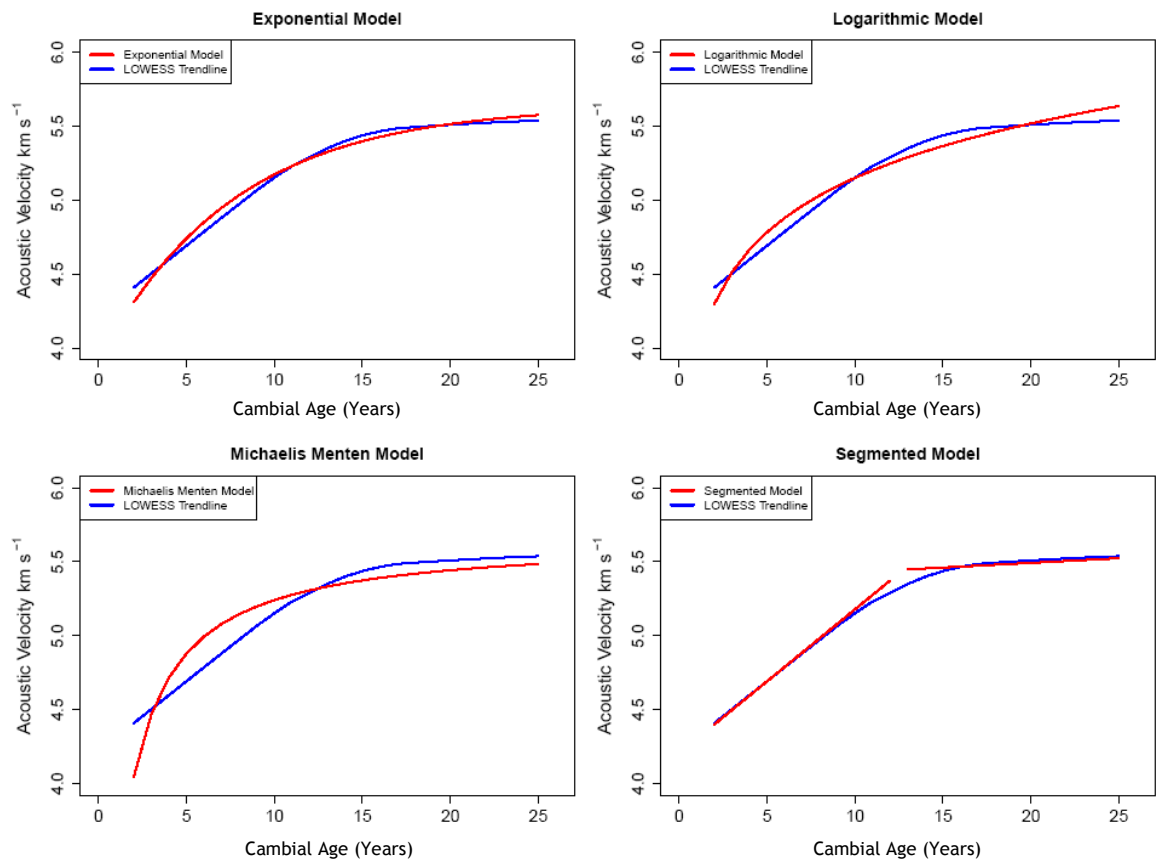


Figure 6-5: The fitted line for each of the statistical models plotted against the LOWESS trend line.

Of the three curved models tested to fit the acoustic velocity data, the Michaelis Menten model had a similar R-squared and residual standard error (Table 6-3) to the other curve models and was also able to fit to all of the trees, however, visually it had the worst fit to the data (Figure 6-5). The Logarithmic model also had a similar R-squared and residual standard error to the other curved models tested (Table 6-3). Visually it looked to have a better fit than the Michaelis Menten model but not quite as good a fit as the Exponential model (Figure 6-5).

Although there is a lot of uncertainty about the where the noise is coming from in the data, the segmented and exponential models would seem to give the best fit and the result of fitting these to the data were examined further to demonstrate the analysis that could have been done.

6.5.2 Segmented Model - Split Point between Juvenile and Mature Phases in Acoustic Velocity

In order to determine if there are two separate linear segments in the acoustic velocity radial profile a Davies' test was carried out, indicating here that there was a significant change in the rate (p -value < 0.0001). Using the Segmented package in R (Muggeo, 2008) a regression model with segmented relationships was used to determine the parameters of the different slope segments (i.e. slope, intercept and split point). The result of this test gave an estimated split point between the juvenile and mature segments of acoustic velocity at 13.28 years with a standard error of 0.26 and residual standard error of 0.45 km/s.

6.5.2.1 Split Point Fitted to Individual Trees

A segmented model seems to work well when fitted against the global data and this model can also be fitted against individual trees to give the acoustic velocity rate, intercepts and split point for each. The Davies Test algorithm for each individual tree looks for a significant change in slope. If the Davies Test is not significant then only one slope was calculated for that tree i.e. with no break point, for example sample 2142-29-A in Figure 6-6. This plot also shows the fluctuation in acoustic velocity within each tree and the difficulty faced when trying to fit a split point to each.

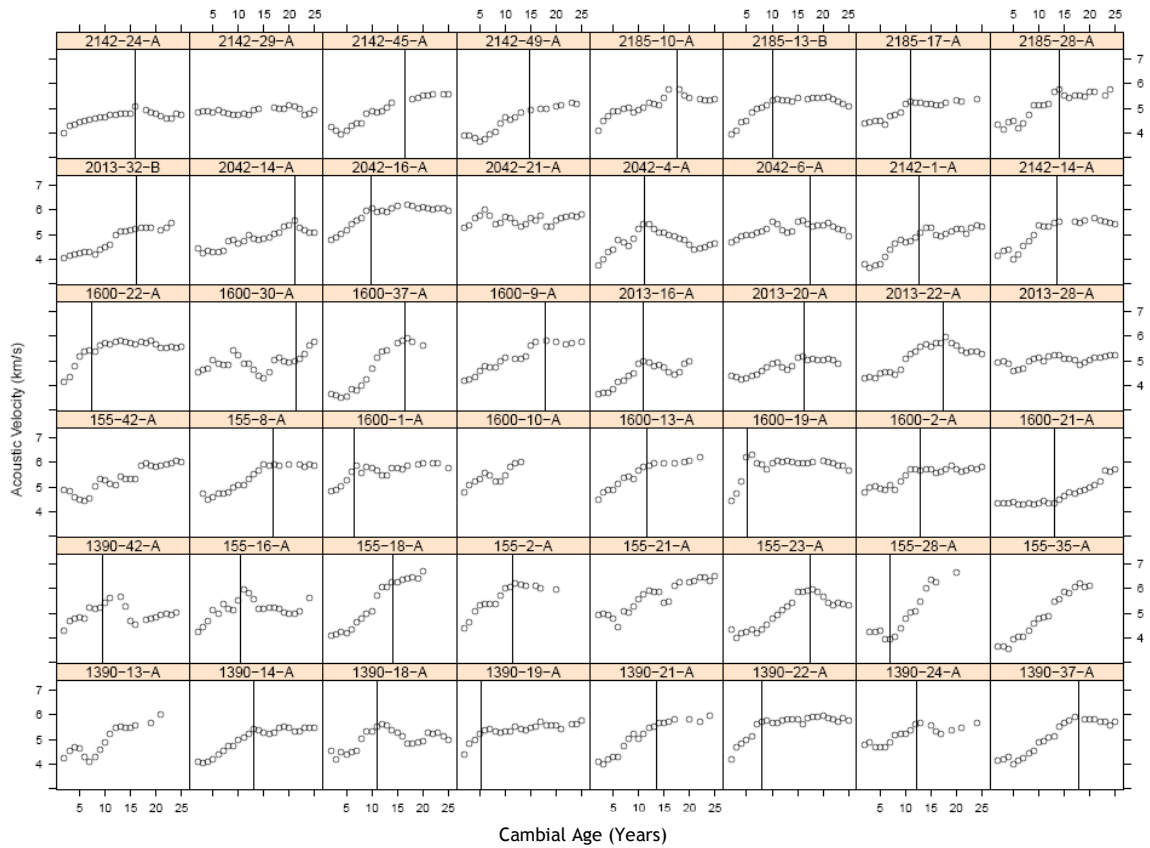


Figure 6-6: Observed acoustic velocity and the split point fitted by the segmented model on a selection of trees

While the two segment model gave a good fit when modelled against the global data, the sensitivity when it is modelled against individual trees produced some very low estimates (<5 years) as well as some high estimates (>20 years) (Figure 6-7) indicating that this method of calculating the split point on individual trees may be sensitive to local fluctuations in acoustic velocity.

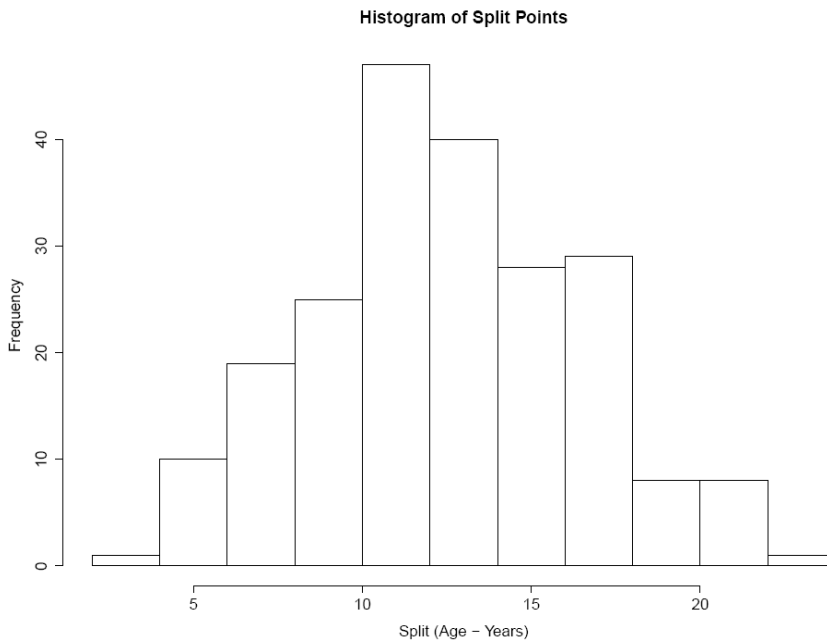


Figure 6-7: Histogram showing the distribution of split points between the two segments fitted by the segmented model.

On this data set the segmented model was unable to fit to 4 of the 279 trees (Figure 6-8). Of the remaining 275 trees the model found no change of gradient and therefore no split point in 59 of the trees (21.5%). A selection of these are shown in Figure 6-9 and again these show the difficulty in fitting any model to these data due to the local fluctuations in acoustic velocity.

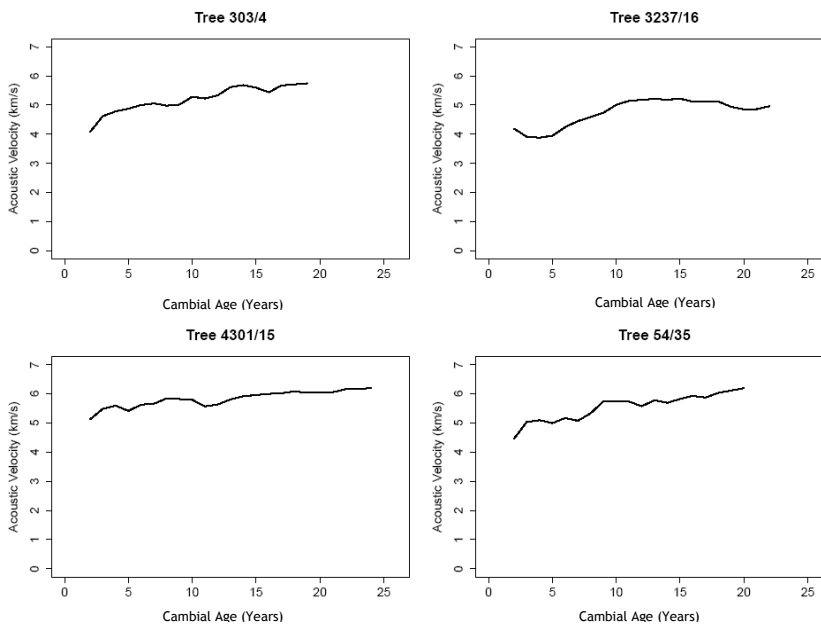


Figure 6-8: Acoustic velocity measurements of the 4 trees that the segmented model couldn't fit to.

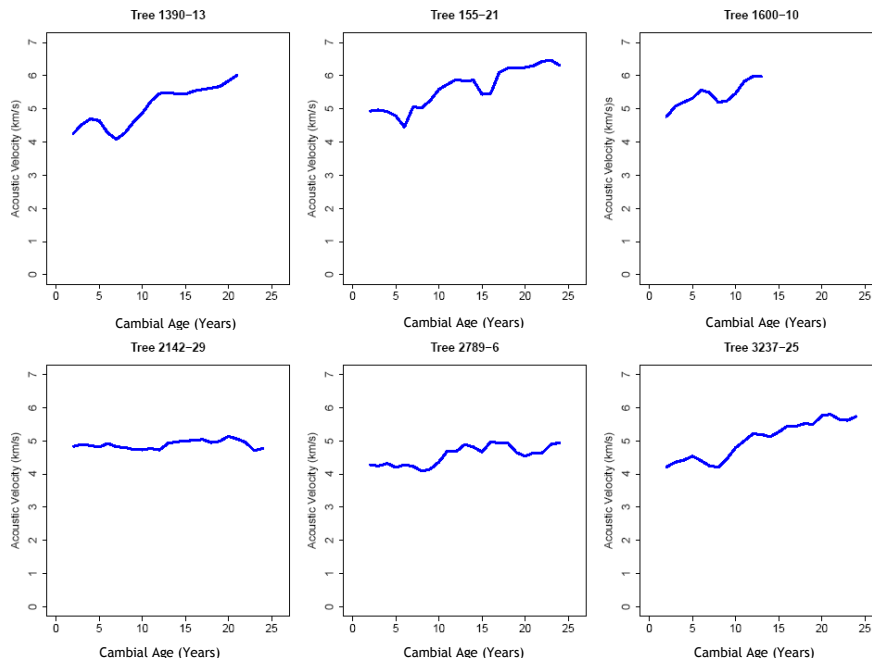


Figure 6-9: Acoustic velocity curves for 6 of the 59 trees that the segmented model couldn't fit a split point.

When the observed values are plotted against the predicted values for individual trees (Figure 6-10) it shows there is a relatively good fit with an R-Squared value of 0.94.

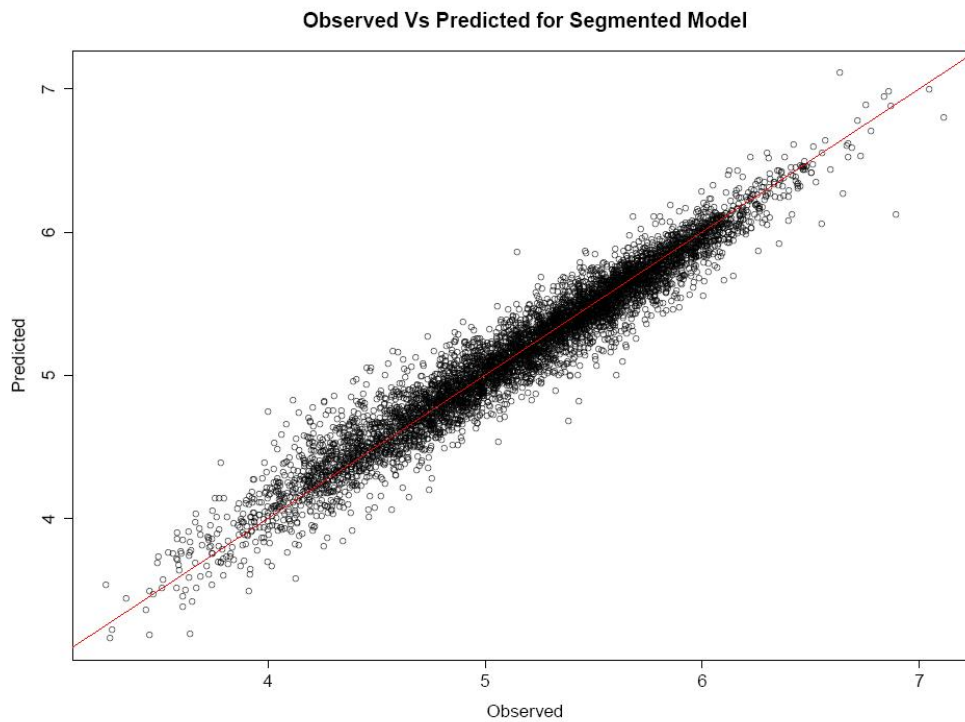


Figure 6-10: Observed Vs predicted for the two segmented model on acoustic velocity when fitted to individual trees. R-squared =0.9389

6.5.2.2 Factors Affecting the Split Point

In order to visualise if there is a treatment effect on the split point, the treatments were arranged into groups as discussed in Chapter 2 and as shown in Figure 6-11. This shows that whilst there were differences in the mean split point between the different groups there does not seem to be any visible trend to these differences. Analysis of variance carried out on the split points showed that there were no significant differences between groups and regression analysis carried out on the individual values returned no significant effect.

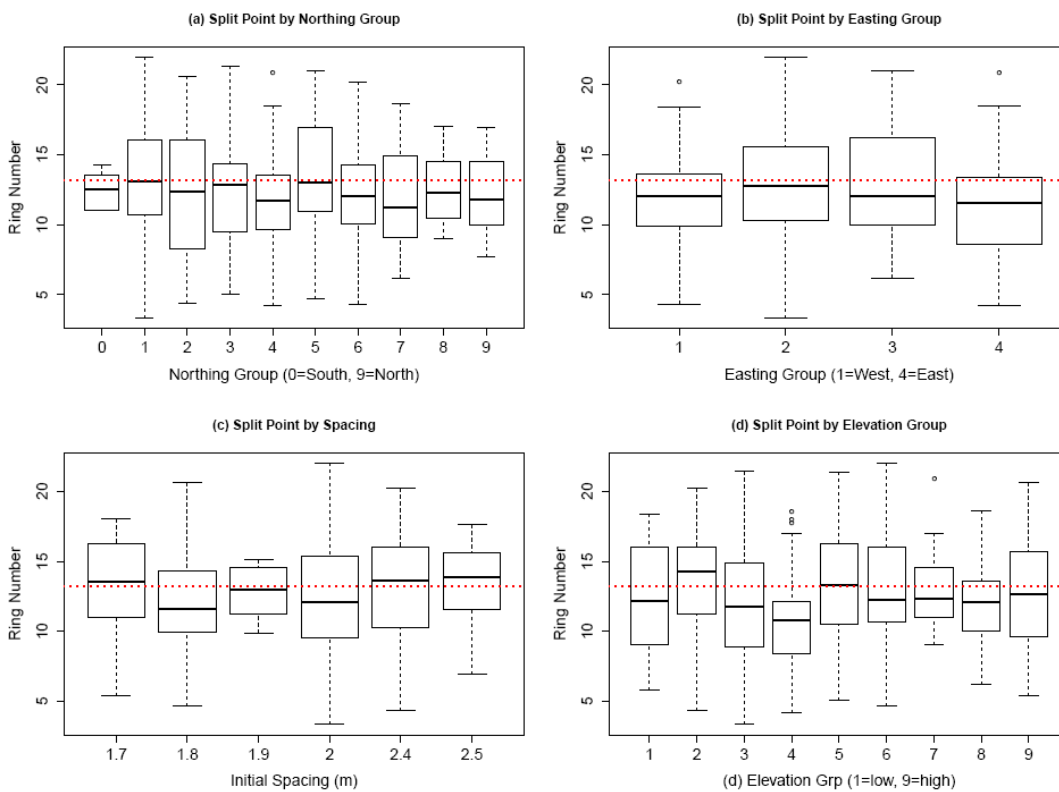


Figure 6-11: Split point between the two phases of the acoustic velocity curve plotted by northing, easting, spacing and elevation groups. Dashed line shows the value (13.3 years) that the model fitted to the global data.

Not only does there appear to be a lot of variation in the split point between sites (Figure 6-12) there is also a large variation within some of the sites with some, e.g. site EXM7, having a within site range as large as the overall range. However, this variation may be due to the sensitivity of the technique to local fluctuations within each radial profile making it difficult to determine what proportion of the variation between trees is due to the method and what is due to actual variation between the samples.

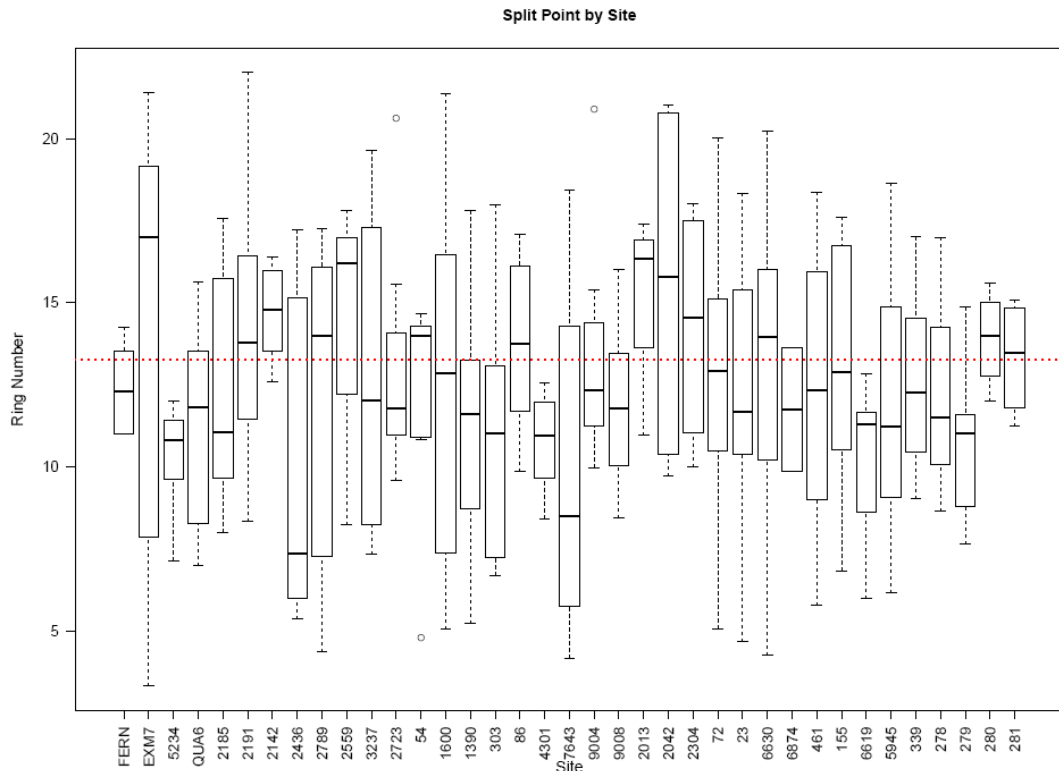


Figure 6-12: The split point between the juvenile and mature phases of acoustic velocity plotted by Site organised from south (left) to north (right). The dashed line shows the value (13.3 years) when modelled against the global data.

6.5.3 Segmented Model – Juvenile and Mature Segments

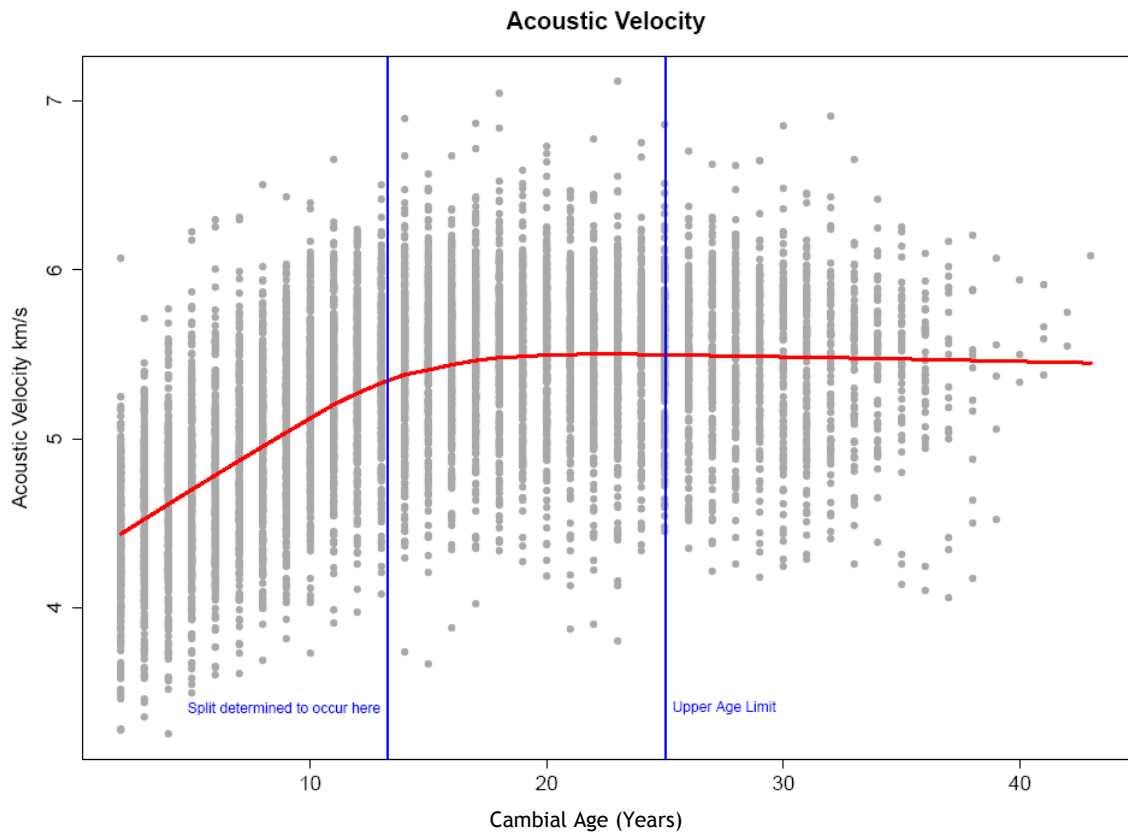
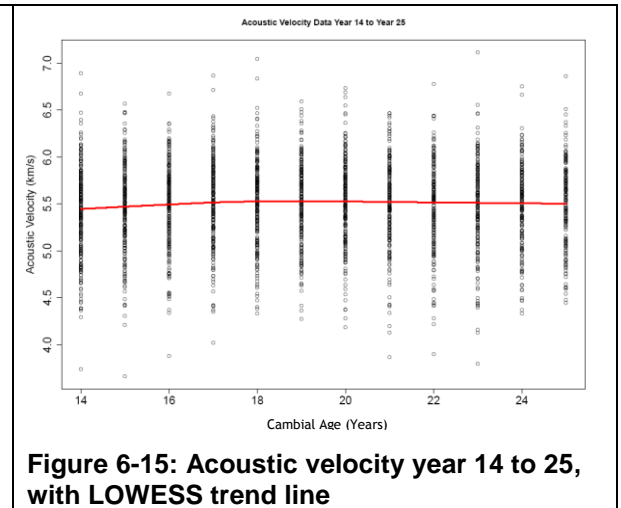
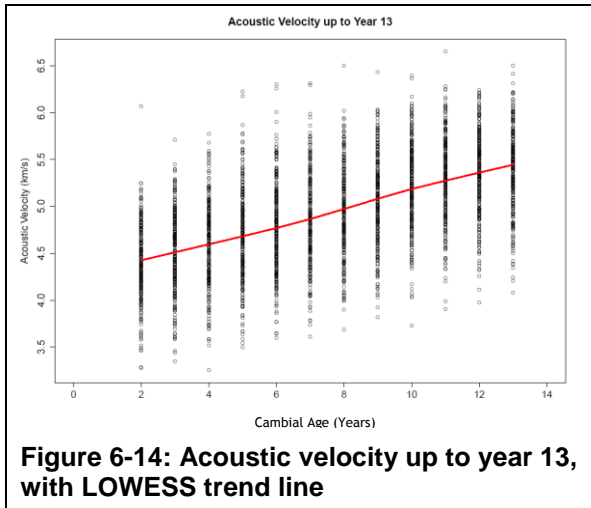


Figure 6-13: Acoustic Velocity data with blue lines showing where the segmented model fitted the split (age 13.2) and the upper limit of ring 25. Also shown is the LOWESS trend line (red line).

When the segmented model is fitted against the global data it gives us a split between the juvenile and mature segments of the radial profile of acoustic velocity of between year 13 and 14 with two separate linear segments: the juvenile section before the split point (cambial age 2 to 13 years) and the mature section (cambial age 14 to 25 years) after the split point (Figure 6-13). Therefore it may be possible to use this split point to examine the radial variation in acoustic velocity of the different segments separately.

When the segments are examined separately acoustic velocity appears linear up until year 13 (Figure 6-14) and also looks relatively linear between year 14 and 25 (Figure 6-15) so it would appear reasonable to continue analysing growth under year 14 and between year 13 and 25 using a linear model. However Figure 6-13 may also suggest that while up to year 13 appears linear the segment after year 14 may become a plateau with no slope in which case a linear model of this segment may not be appropriate as there is no effect of age.



6.5.4 Juvenile Segment of Acoustic Velocity

A linear model was fitted to rings 2 to 13 of all the data using ordinary least squares regression, performed by the “lm” function in R. This produced a significant p-value of < 0.0001 , indicating that this segment is linear with a slope of 0.094 km/s/year and an intercept of 4.22 km/s . An R-squared value of 0.40 may indicate that while this is linear, there is a lot of variation about the slope. The residual plots for the juvenile segment (Figure 6-16) show that the linear model is a reasonable fit with a relatively even distribution of residuals with cambial age.

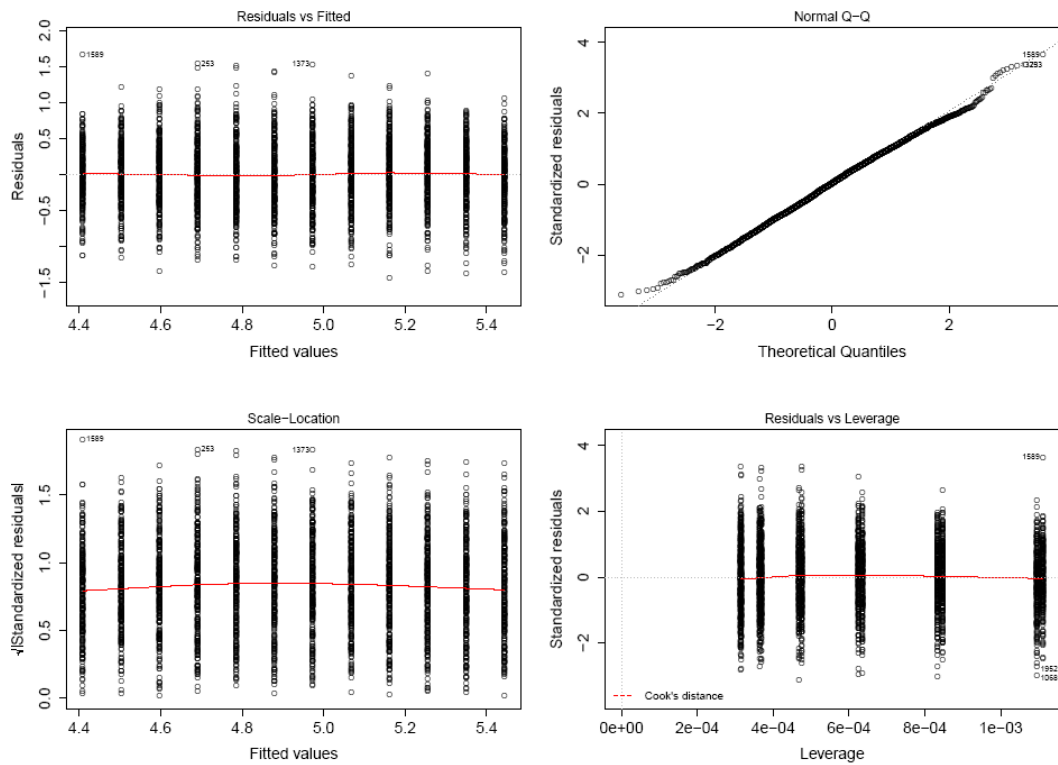


Figure 6-16: Residual plots for the linear model of rings 2 to 13

Although the linear model was able to describe the age related trend in acoustic velocity for the juvenile segment reasonably well there is a lot of variation between trees when the observed values are plotted against those that the model predicts (Figure 6-17).

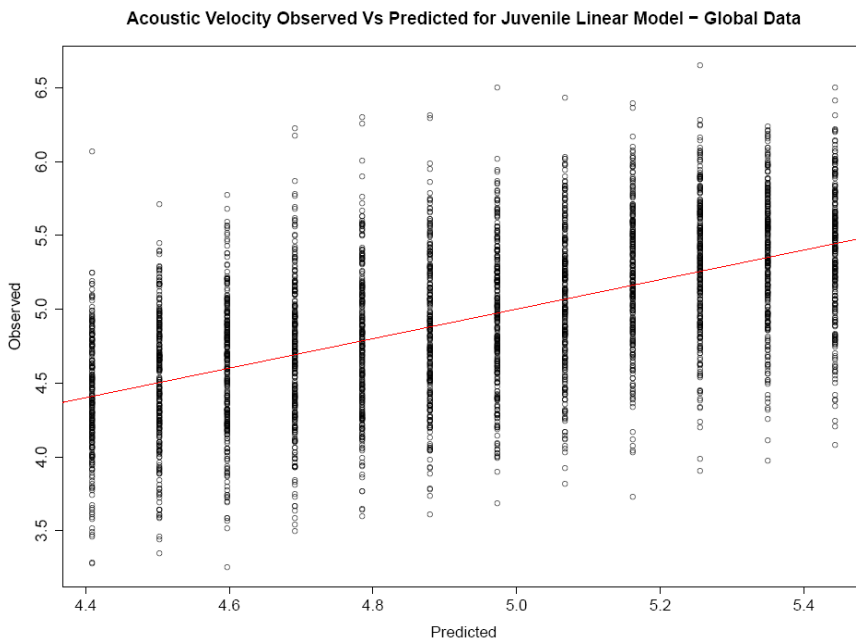


Figure 6-17: Observed Vs Predicted acoustic velocity for the juvenile segment of the linear model. The line of equality is shown in red

6.5.4.1 Linear Model on Juvenile Segment Fitted to Individual Trees

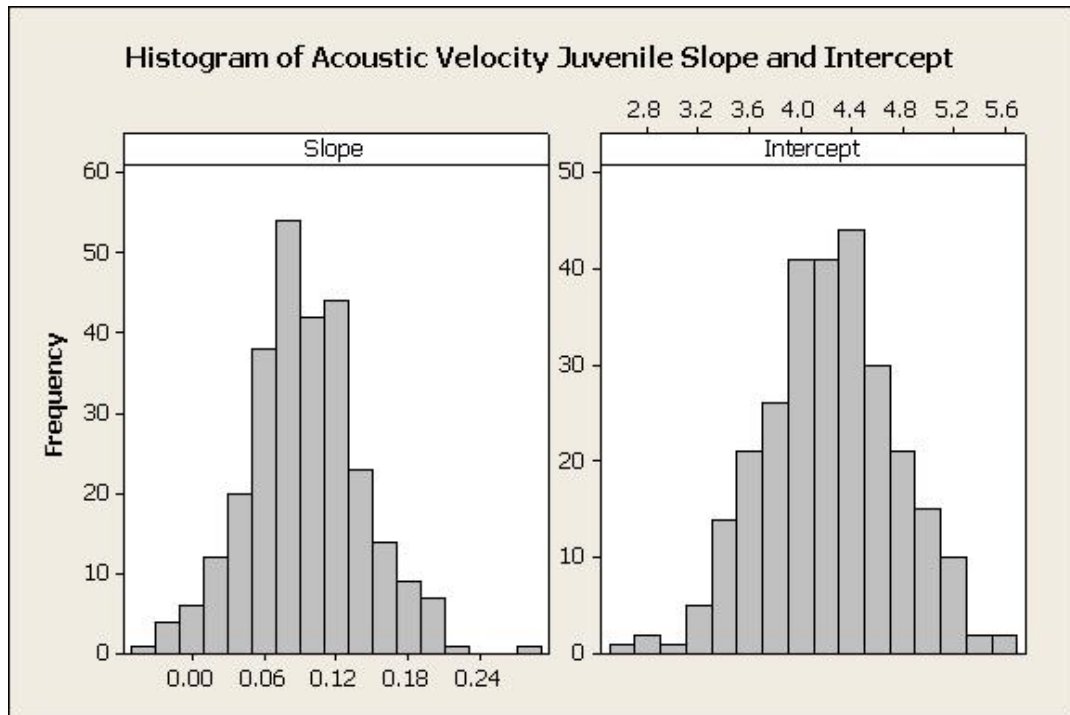


Figure 6-18: Slope and Intercept coefficients fitted by a linear model to the acoustic velocity up to cambial age 13 year for each sample

When a linear model is fitted to the juvenile segment of each tree individually, the coefficients show quite a bit of variation in normal distributions (Figure 6-18) with the slope ranging from just below 0 km/s per year to just under 0.3 km/s per year indicating that acoustic velocity increased with age in the juvenile segment of almost all trees but decreased in a small number (Figure 6-19). The mean intercept for this segment is approximately 4.2 km/s and the range is from approx 2.6km/s to 5.7 km/s.

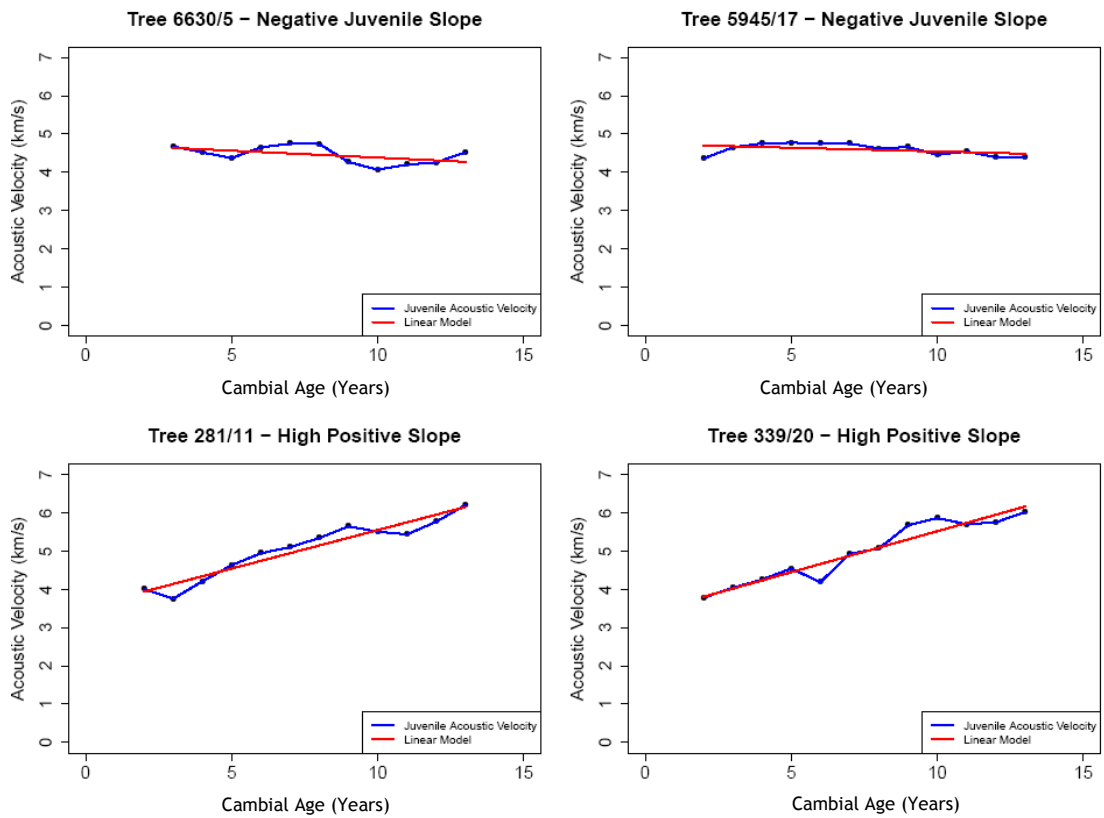


Figure 6-19: Samples with a negative juvenile slope (top row) compared to those with the highest positive slope (bottom row).

The residuals, when taking account of individual trees, have a reasonable fit (Figure 6-20) with a relatively even distribution of residuals with cambial age. This is also shown when the observed data against plotted against the fitted linear model (Figure 6-21) giving an R-squared of 0.91, although there may be a slight curve at the highest and lowest values.

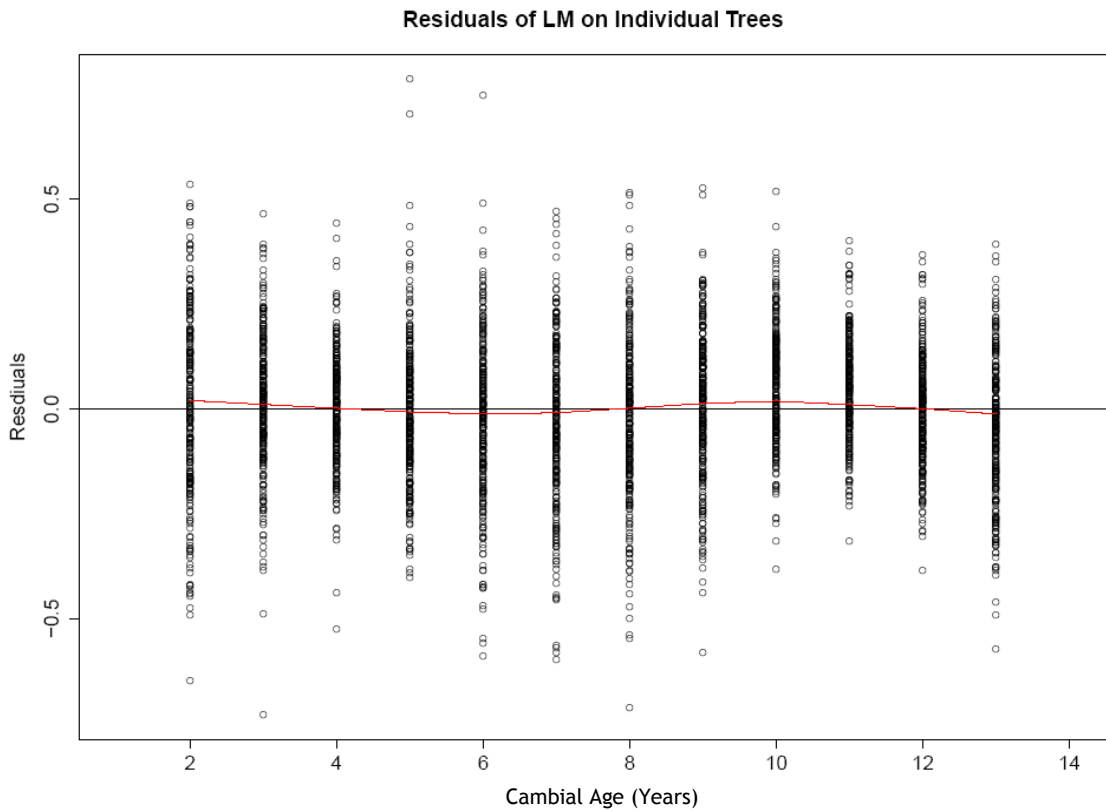


Figure 6-20: Residuals of linear model when fitted to the acoustic velocity of the juvenile segment of each tree, with LOWESS trend line (red)

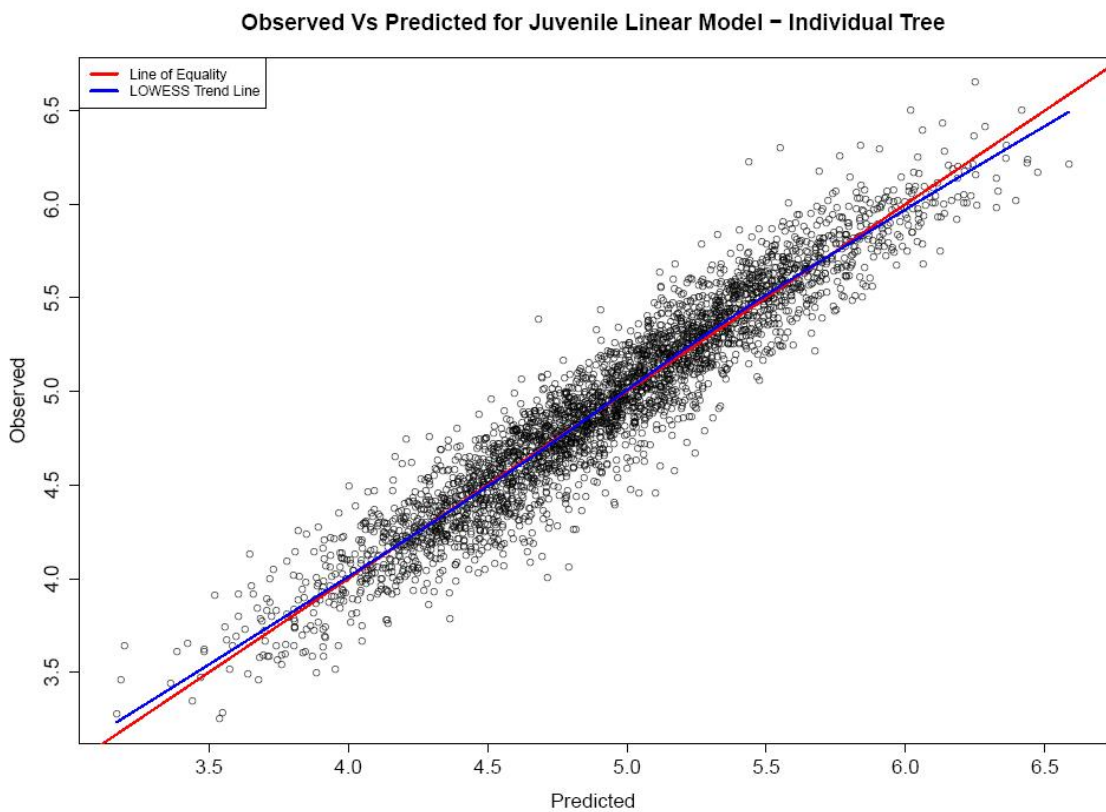


Figure 6-21: Observed Vs predicted for the juvenile linear model giving an R-Squared of 0.91.

In order to get a visual impression of how the different treatment variables affect the different parameters of the linear model, the coefficients for the two segments were plotted by the northing, easting, spacing and elevation groups discussed in Chapter 2.

Although there may be differences in the rate that acoustic velocity is changing from the pith (Figure 6-22) with (a) latitude ($p < 0.0001$ when tested with ANOVA) and (b) longitude ($p = 0.04$), visibly there does not seem to be any trend to the differences. There are also differences between the (c) Spacing groups ($p < 0.0001$), and (d) Elevation groups ($p = 0.001$) but again it is difficult to see any trend in the differences.

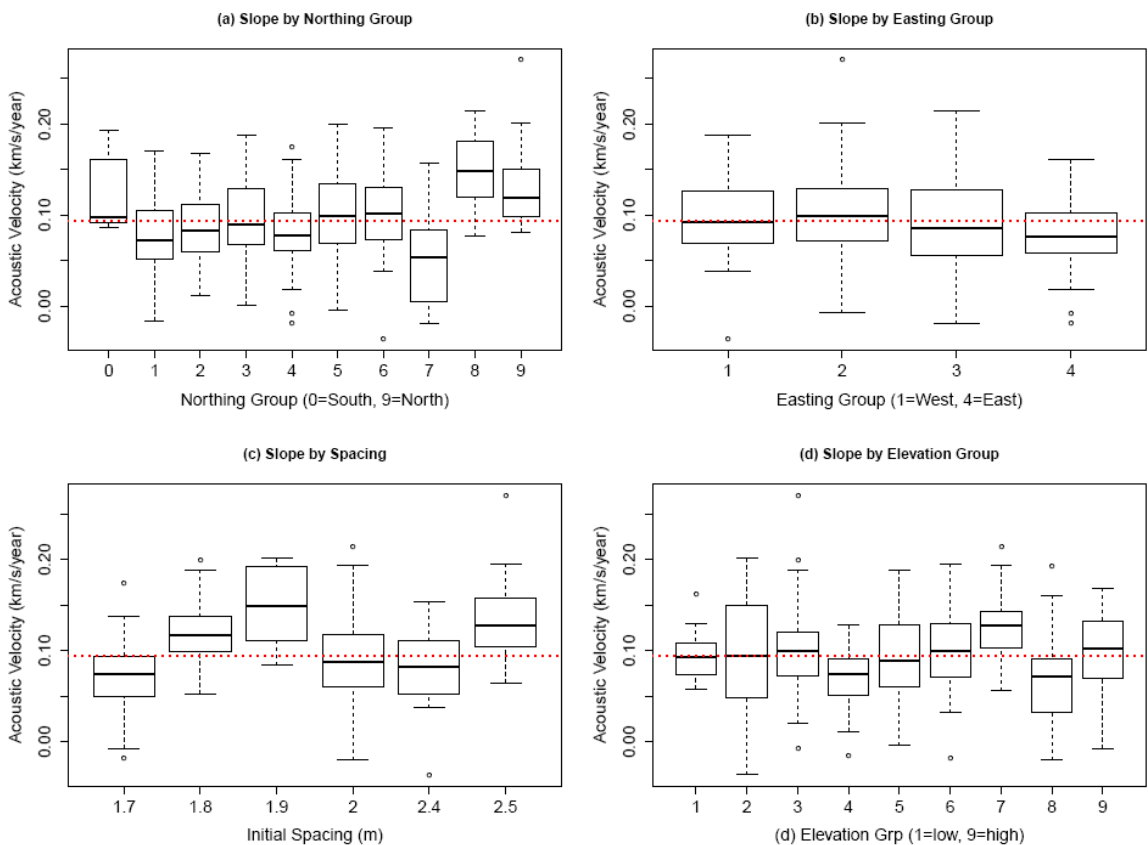


Figure 6-22: Slope coefficients for the juvenile segment of acoustic velocity plotted by northing, easting, spacing and elevation groups. Also shown is the overall mean (red line).

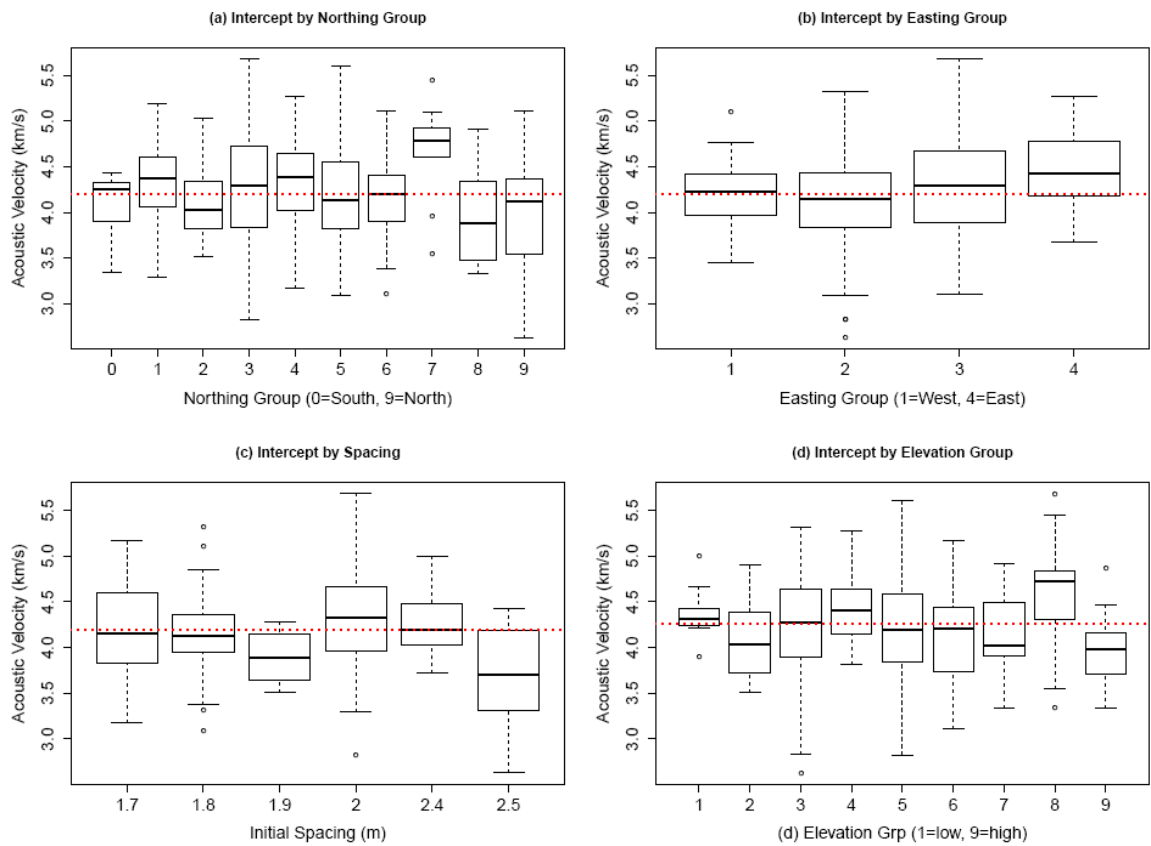


Figure 6-23: Intercept coefficients for the juvenile segment of acoustic velocity plotted by northing, easting, spacing and elevation groups. Also shown is the overall mean (red line).

The intercept of the juvenile segment of acoustic velocity is shown in Figure 6-23. It would seem that there are differences between the Northing groups ($p=0.006$) but again there is no indication of a trend due to latitude (a). There may be a slight positive effect of longitude (b) on the intercept and analysis of variance shows that there are significant differences between the groups ($p=0.003$). Statistical analysis using ANOVA showed that there were differences between the spacing groups ($p<0.0001$) and also elevation groups (d) ($p=0.002$). The unbalanced nature of this data set, with a small number of replicates in some of the groups, and pseudo replication due to trees being treated as individuals rather than as components of sites upon which the data are based are weaknesses in interpreting this data in this way.

6.5.4.2 Mixed Effects Model of Juvenile Segment of Acoustic Velocity

Due to the unbalanced nature of this data set and to account for the hierarchical experimental design a mixed effects model was used to analyse the variation in acoustic velocity across the radial profile of both the juvenile and mature growth linear sections. In this analysis site and tree within site were the random effects:

$$AV_{ijk} = \mu + S_i + T_{ij} + \epsilon_{ijk} \quad (\text{Equation 6.7})$$

where AV_{ijk} is the radial profile of acoustic velocity, μ is the overall mean, S_i is the random effect of site, T_{ij} is the random effect of tree within site and ϵ_{ijk} is the residual error which is attributed to within tree variation.

When the mixed effects model was fitted without fixed effects a variance components analysis showed that approximately 54% of the variation is within tree variation, 36% was between trees at the same site and 10% was between sites. Once age has been taken into account the model predicted an intercept of 4.2 km/s and the acoustic velocity increasing by 0.9 km/s per year with the within tree variation reduced to approximately 28%, just over 58% of the variation being between trees in the same site and 14% being between sites. This shows that if the fixed effect of cambial age is included in the model it does a reasonable job of describing within tree variation but, as would be expected, this does not describe between tree variation. Again it must be noted that there is a lot of uncertainty in the analysis of this data due to the grain orientation problems and this is reflected in the uncertainty of any findings.

The linear model is fitted with the intercept as a random effect while slope is fixed, this allows the intercept of each site and tree within site to vary from the mean intercept and examination of the residuals show that this may be adequate (Figure 6-24). A random slope may also be appropriate as this also changes with tree. However, if the mixed effects model is updated from only having a random intercept to also having a random slope then the residuals show a similar amount of variation as when it is not included (Figure 6-25).

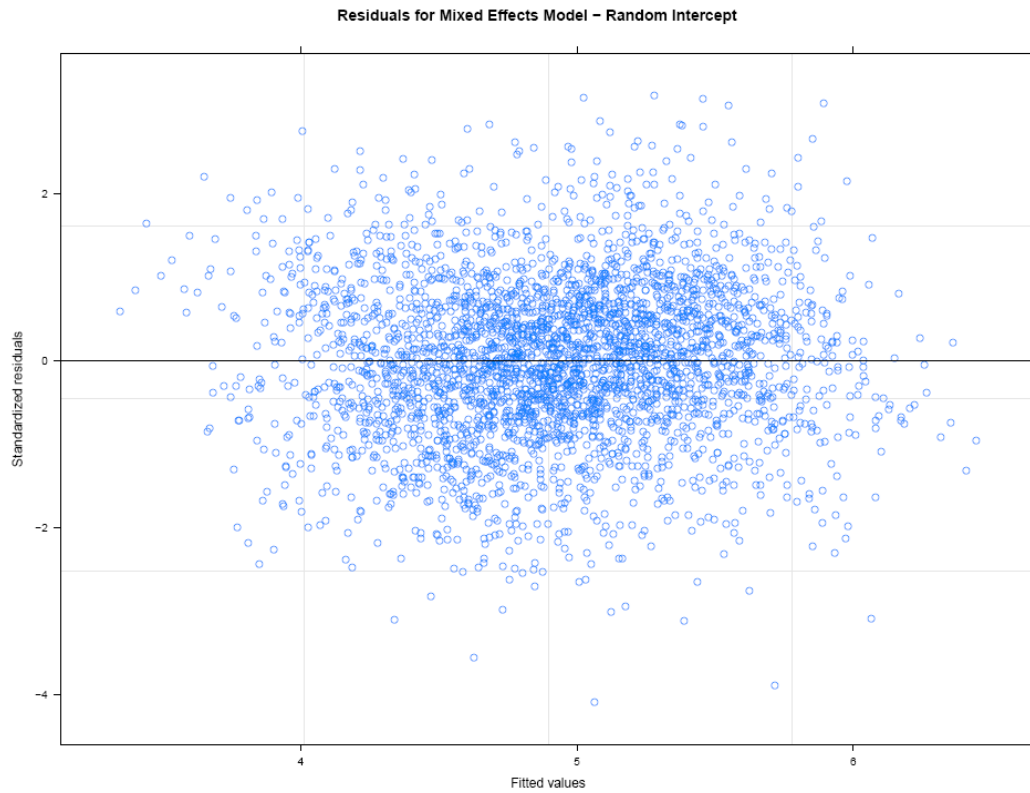


Figure 6-24: Residuals of mixed effects model on juvenile acoustic velocity segment with random intercept only.

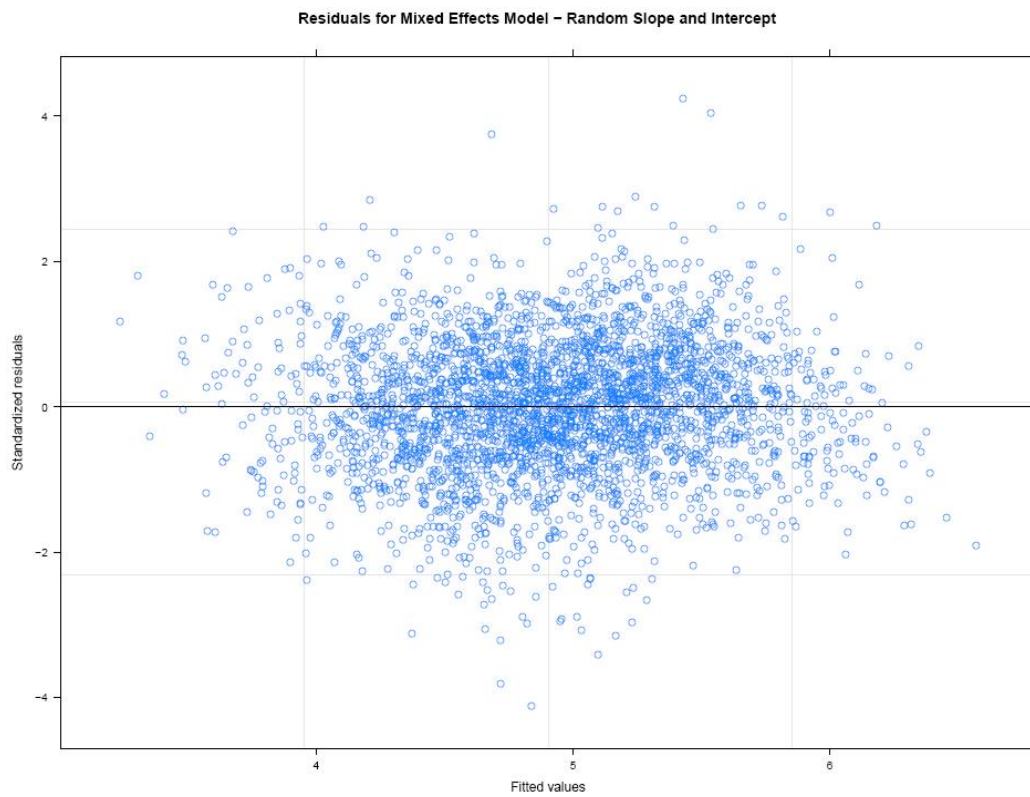


Figure 6-25: Residuals of mixed effects model on juvenile acoustic velocity segment with random intercept and slope.

The residuals in Figure 6-24 and Figure 6-25 indicate that the linear mixed effects model is fitting to juvenile segment quite well with a random scattering of the residuals in both versions. A likelihood ratio carried out in R on the two models and the AIC values produced indicates that the model which included random slope and intercept to be better as the AIC value is lower (17.2 compared with 1020.6).

When observed versus the predicted values are plotted for the mixed effects model (Figure 6-26) it indicates that model is predicting very well (R-squared = 0.91) when fitted against individual trees, though there is same problem as seen before whereby there may be a slight curvature of the values at low and high values due to the lack of data points.

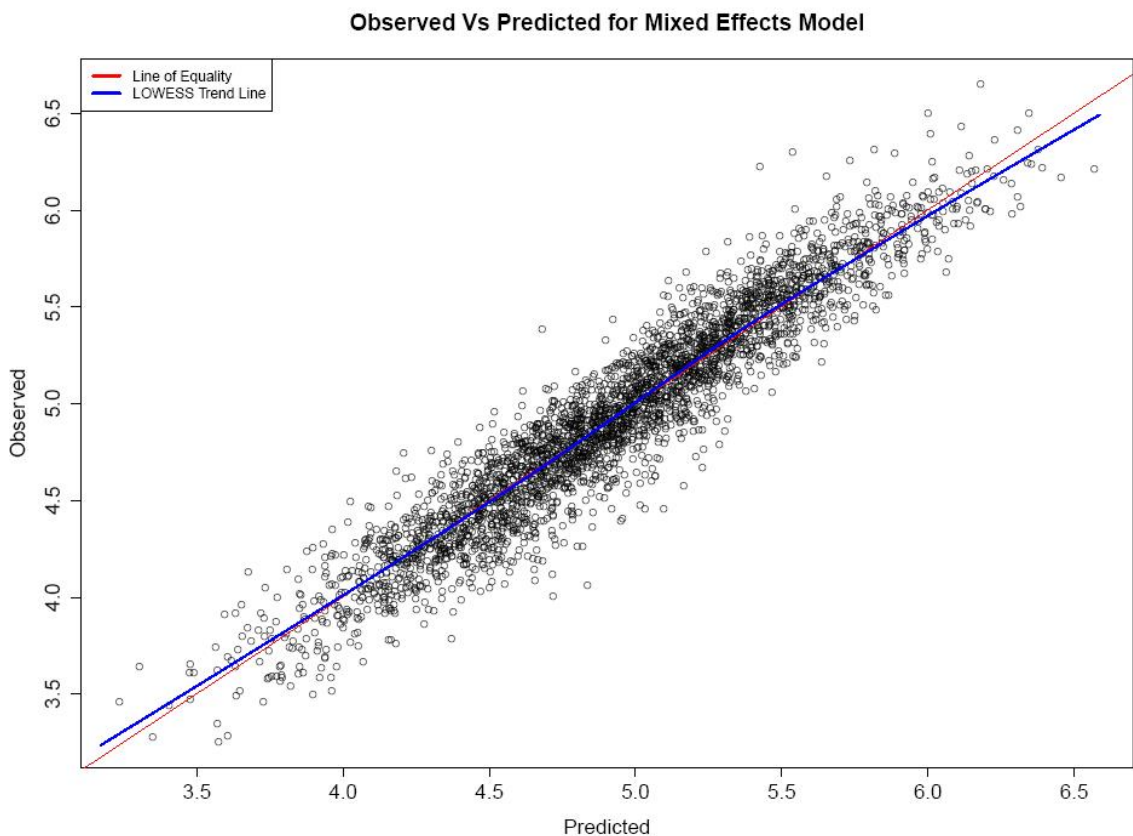


Figure 6-26: Observed Vs predicted for the juvenile mixed effects model giving an R-Squared of 0.91

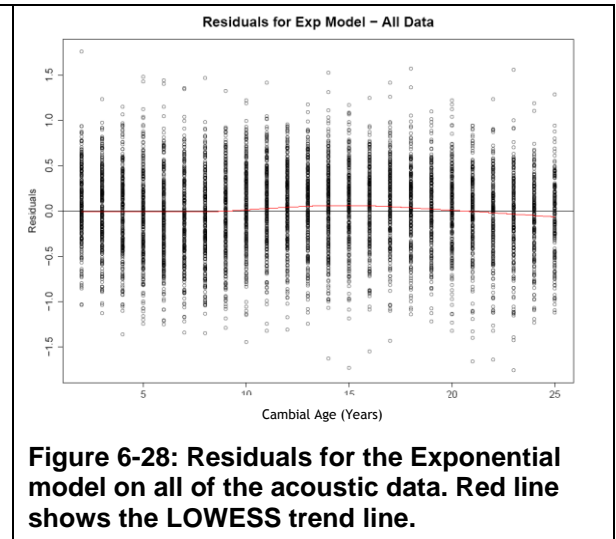
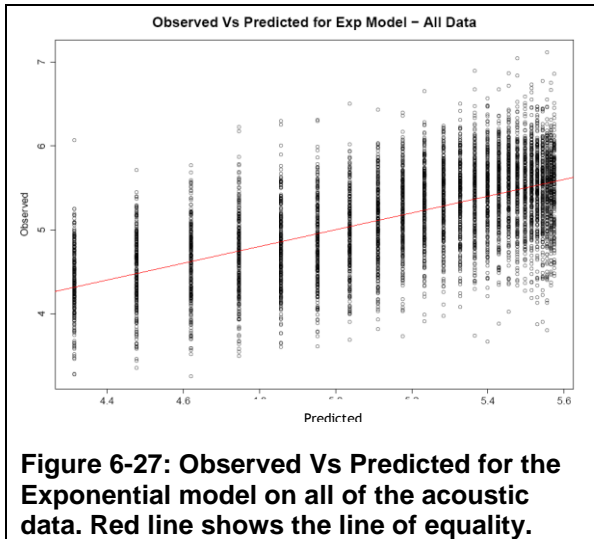
6.5.5 Mature Segment of Acoustic Velocity

Trying to fit a linear model to acoustic velocity of rings 14 to 25 gives an R-squared of 0.0004 and a p -value of 0.146 which is a reflection of the fact that there is a slope of zero in this segment indicating that there is no relationship between acoustic velocity and cambial age in the mature zone. This is not a surprise as this is a mirror of what we would expect the profile of MFA to look like which also reaches a plateau (McLean, 2008). In effect this means that the level of acoustic velocity that the profile reaches (i.e. the intercept of the mature phase) is controlled by the rate in the juvenile phase and therefore any analysis of the mature intercept would only duplicate the juvenile phase analysis. Similarly, any analysis of the mature phase slope would be just looking at noise.

6.5.6 Exponential Model of Acoustic Velocity

Although the segmented analysis may indicate that acoustic velocity can be split into two separate segments with a specific change point between the two phases, it was shown, when looking at the full data set together, that it was difficult to extract a value for the slope of the mature segment, that was significantly different from zero difficult to fit a linear model.

Fitting a LOWESS trend line to this data set (shown in Figure 6-1), indicates there may be a gradual change from juvenile to mature phases of acoustic velocity. This being the case models which describe the juvenile and mature phases together as a curve may fit the data better. Therefore as well as looking at juvenile and mature wood as two separate segments this section looks at a selection of different curves to see which form fits the data the best and how these compare to the segmented model.



The Exponential model was able to predict acoustic velocity from cambial age, describing the age related trend in acoustic velocity reasonably well (Figure 6-27). There is a lot of variation between trees and the spread of the observations tends to stay the same with increasing levels of acoustic velocity. Similarly when the residuals are plotted against cambial age they show a reasonably good fit. The residuals (Figure 6-28) are evenly distributed with cambial age though there may be a slight curve between rings 12 to 19 suggesting the model may have a problem fitting the data around the point where the curve levels off to its asymptote.

6.5.6.1 Exponential model Fitted to Individual Trees

When fitted to individual trees the Exponential model (Figure 6-29) it looks to be predicting reasonably well ($R\text{-squared} = 0.91$) though there may be a slight curve to the data caused by the lack of data in these areas where it may be over predicting at lower values and slightly under predicting at higher values.

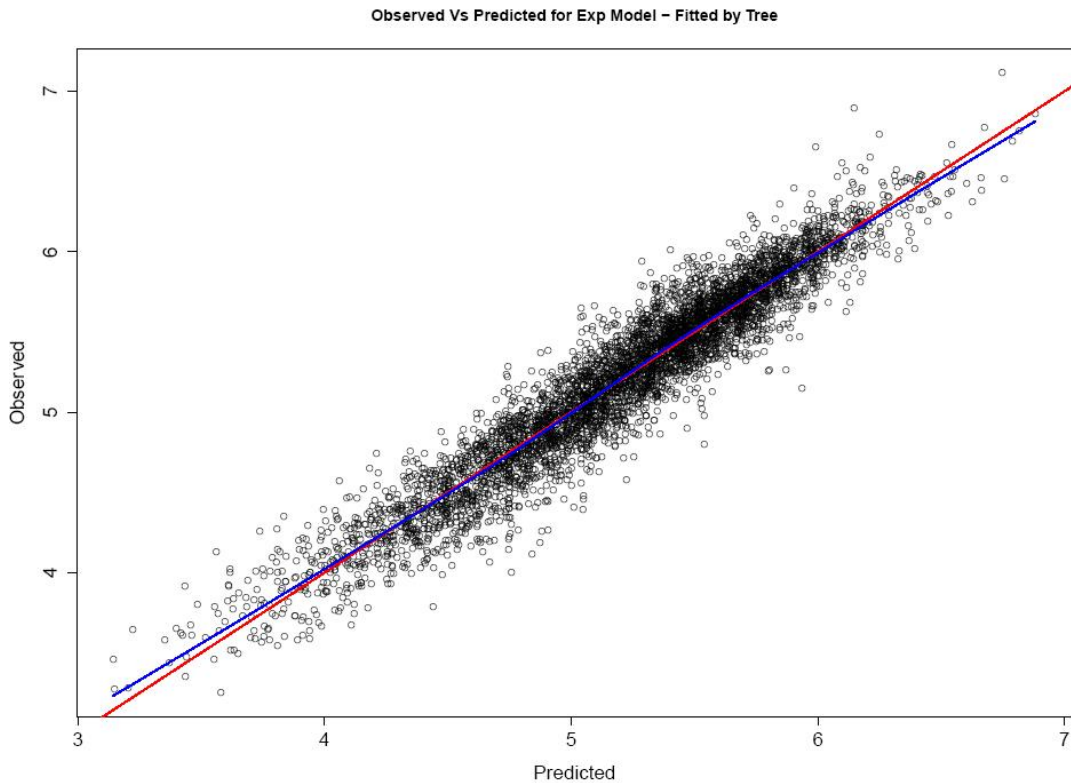


Figure 6-29: Observed vs predicted for exponential model of acoustic velocity when fitted to individual trees. R-Squared = 0.9127.

The residuals for the Exponential model, plotted against cambial age, shows there may be a non-random pattern to the data (Figure 6-30) suggesting that the model is not explaining everything and may be that the observed data lie somewhere between the segmented and exponential models, and this is reflected in the residuals.

When the residuals are plotted against the observed values (Figure 6-31) it again shows a fairly even spread and there may be a slight tendency to increase with increasing acoustic velocity.

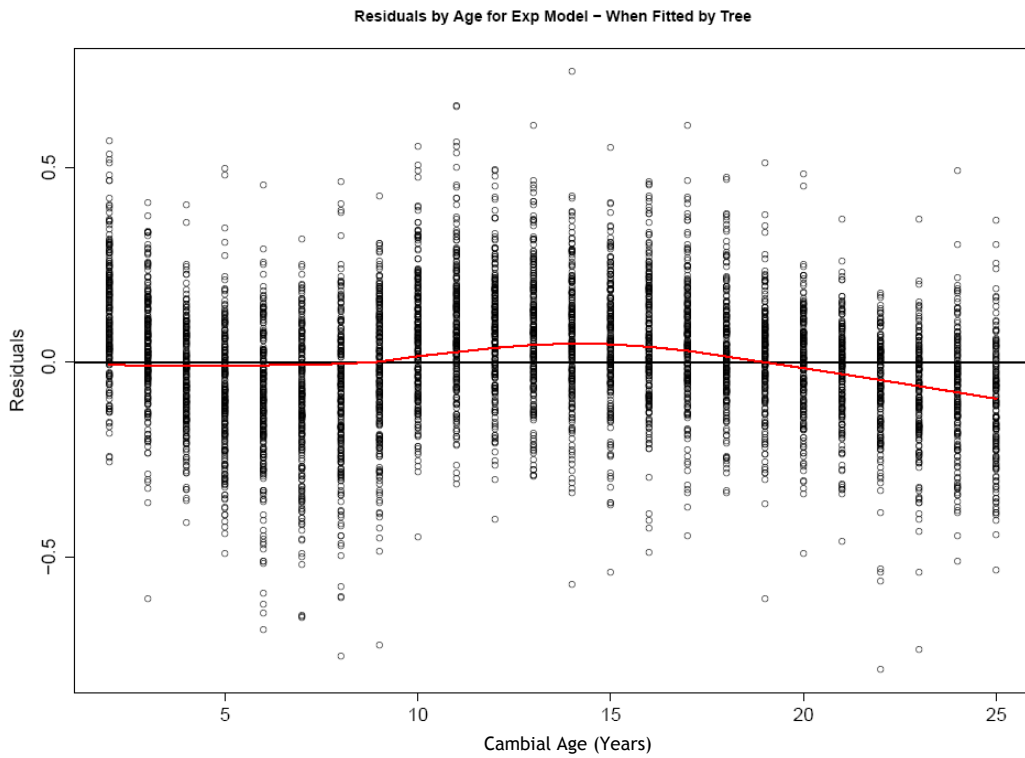


Figure 6-30: Residuals of Exponential model of acoustic velocity when fitted to individual trees, plotted against cambial age.

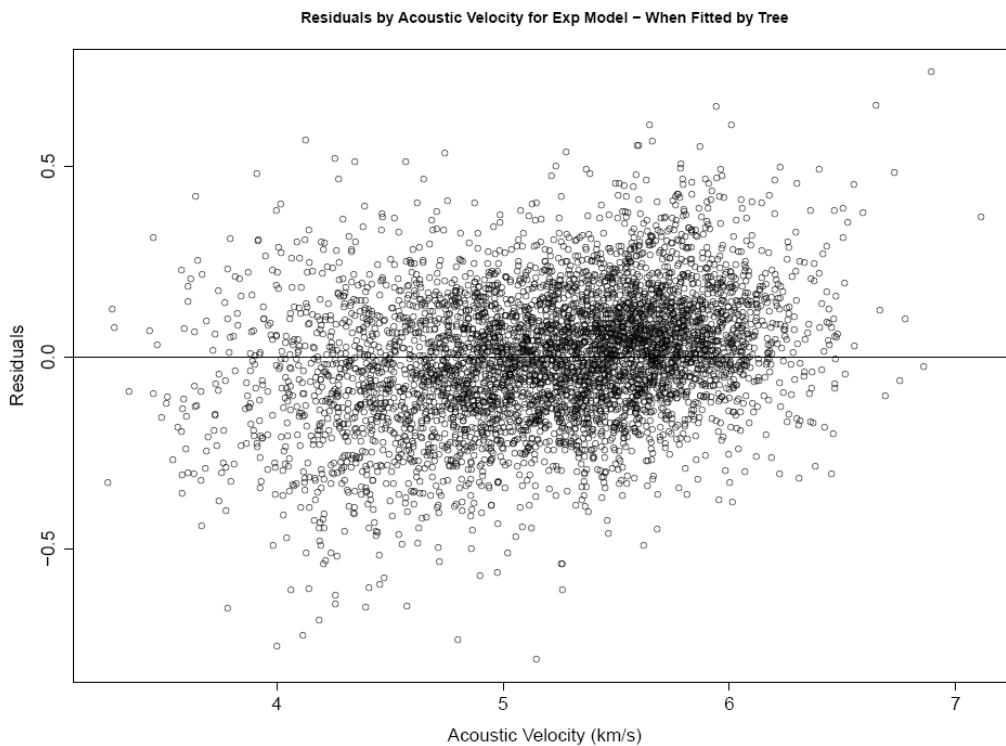


Figure 6-31: Residuals of Exponential model of acoustic velocity when fitted to individual trees, plotted against acoustic velocity.

When the Exponential model was fitted to individual trees it was unable to fit to 43 trees (15%). The radial profile of acoustic velocity for a selection of these is

shown in Figure 6-32 and show the difficulty of trying to fit a model to these samples due to the variation in the acoustic velocity and shape of the radial profiles. Due to the problems with the grain orientation in the method (Chapter 5) it is difficult to tell whether this variation in the profile is due to real variation in acoustic velocity profiles among different samples or if it is due to problems with the grain orientation.

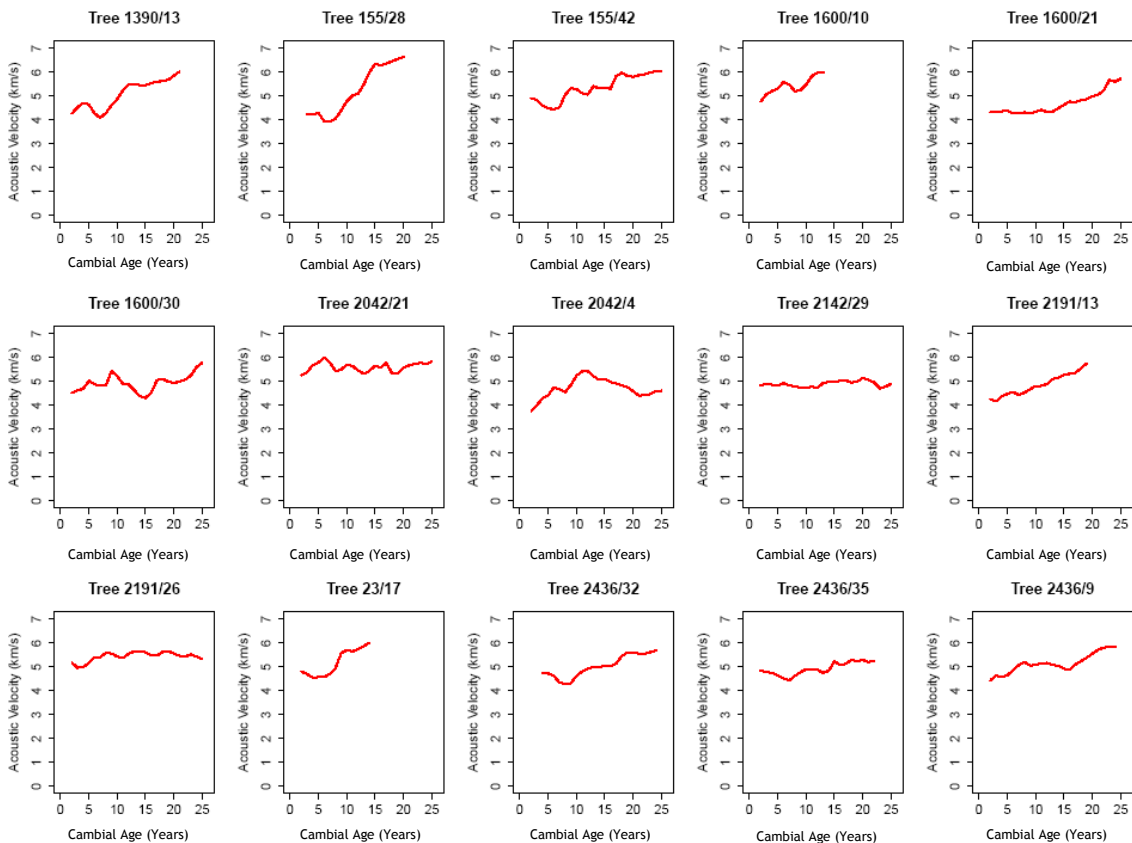


Figure 6-32: Acoustic velocity of 15 of the 43 trees (15% of the total) which the Exponential model couldn't fit.

The Exponential model produced some extremely high figures (relative to the other values) for the coefficients b_0 (initial value), b_1 (rate) and b_2 (asymptote) as shown in the histograms in Figure 6-33. Coefficient b_0 ranges from approximately 0.4 km s^{-1} to a maximum of just over 33 km s^{-1} , with the majority of values falling at the lower end of the scale. Similarly, coefficient b_1 has a minimum of 0.003 km s^{-1} per year and a maximum of 0.9 km s^{-1} per year but again most values fall at the lower end of the scale. Coefficient b_2 ranges from just above 4 km s^{-1} to approximately 36 km s^{-1} again with most values at the lower end of the scale.

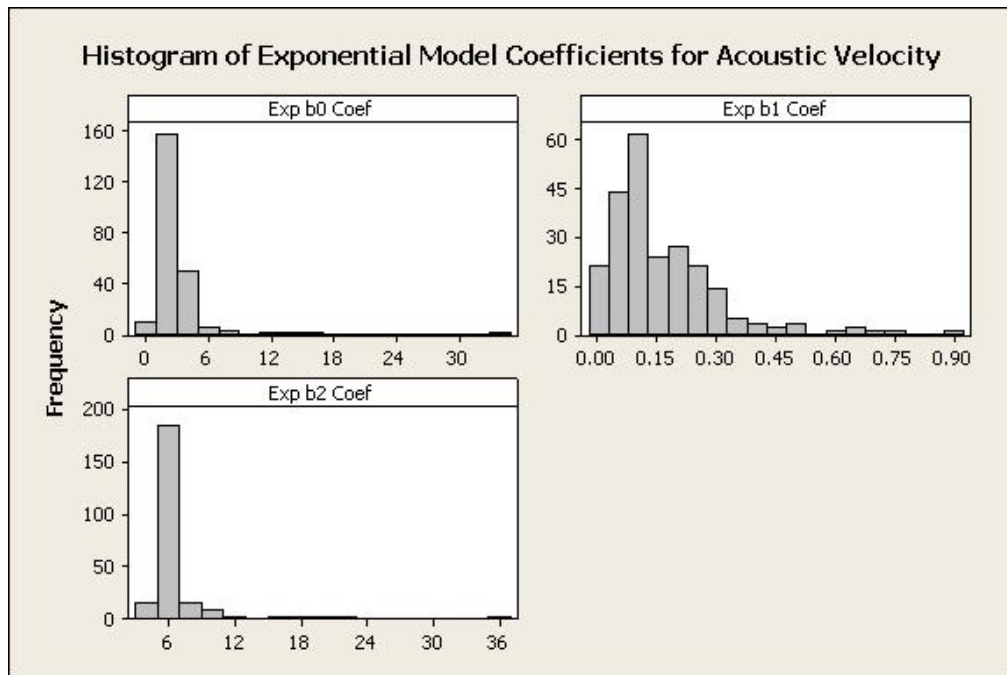


Figure 6-33: Coefficients for the exponential model for acoustic velocity when fitted to individual trees.

When a sample of the most extreme values of each of the coefficients are plotted (Figure 6-34) it shows that these values come as a result of trying to fit an exponential curve to data that may not be curved within this range. The samples which produced the highest b_0 coefficient also produced the highest b_2 coefficient and these two coefficients are highly correlated to each other (correlation coefficient = 0.96) and the same samples also produced the lowest b_1 coefficient (indicating a flat slope) although this shows little correlation with either of the other coefficients.

In this model coefficient b_0 is the starting point, i.e. the intercept, and b_2 is the maximum value so a correlation between these coefficients shows that samples with high acoustic velocity at the pith are likely to have the higher maximum values in later rings within this range. The b_1 coefficient is the rate of change in the slope, with higher values producing a lower rate.

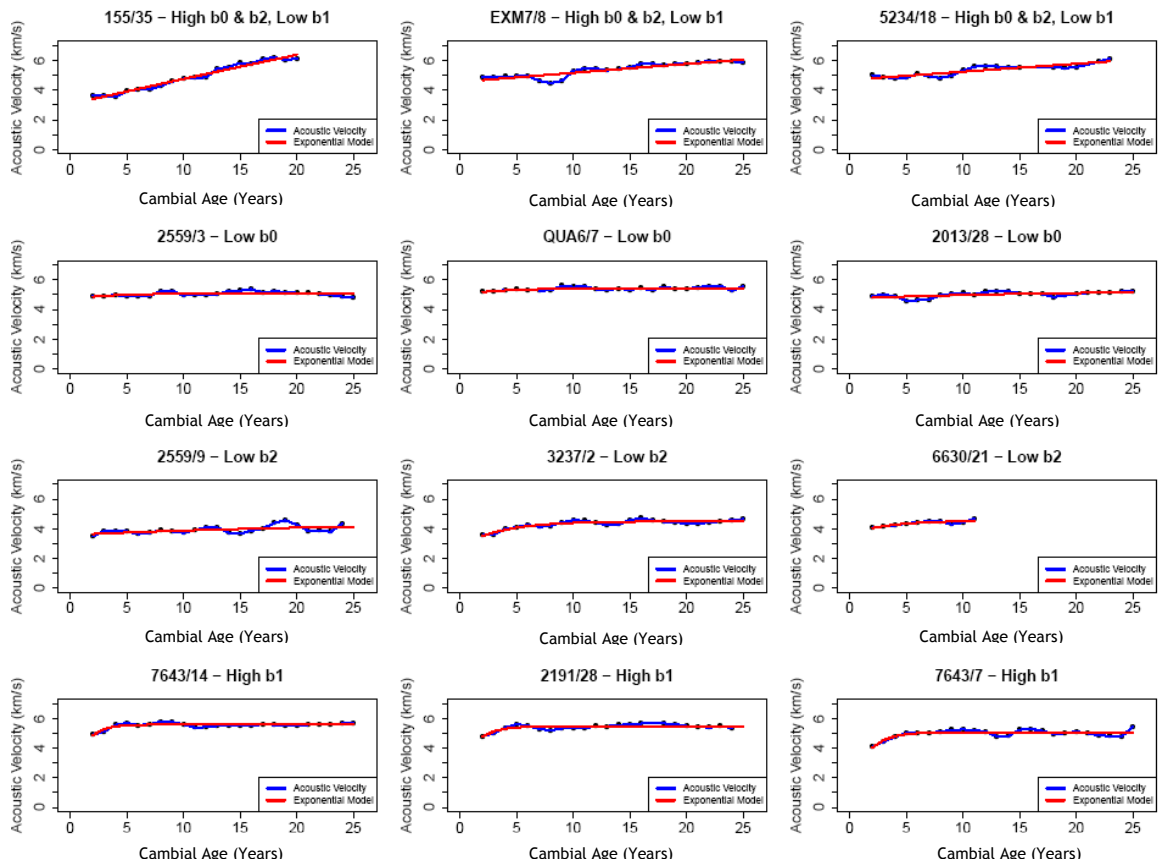


Figure 6-34: Top row shows trees which the Exponential model fitted the highest b_0 and b_2 coefficients. These also correspond to the lowest b_1 coefficients. Also shown are the samples with the lowest b_0 coefficient (2nd top row), the samples with the lowest b_2 coefficients (3rd row) and the samples with the highest b_1 coefficient (bottom row).

Each of these model parameters is involved in producing a fit to the acoustic velocity profile so it is difficult to determine the effect that each site or environmental factor is having on the curve because of some of the extreme values produced. For this reason the coefficients for each treatment were input onto the respective curved model equation and plotted. Figure 6-35 shows the effect of the different treatments, when grouped as categorical variables, on the Exponential model and it looks like longitude (b) may be having an effect with the values at year 25 decreasing in order from west to east. There are also differences in the latitudinal groups (a) with a difference in acoustic velocity at year 25 of just over 0.5 km/s between the highest and lowest groups, with the highest velocity seen at the furthest north groups. It is difficult to see any trend of spacing (c) although there is a large spread of acoustic velocity at year 25 with a difference of approximately 0.7 km/s between the highest and lowest groups. It is also difficult to see any effect of elevation (d) which also shows less of a spread of values at year 25 than the other groups.

It would be difficult to attempt a rigorous statistical treatment of these data due to the problems described previously and also difficult to draw conclusions, except perhaps that exponential functions give fitted coefficients that are linked to one another and vary non-linearly, which makes them difficult to deal with.

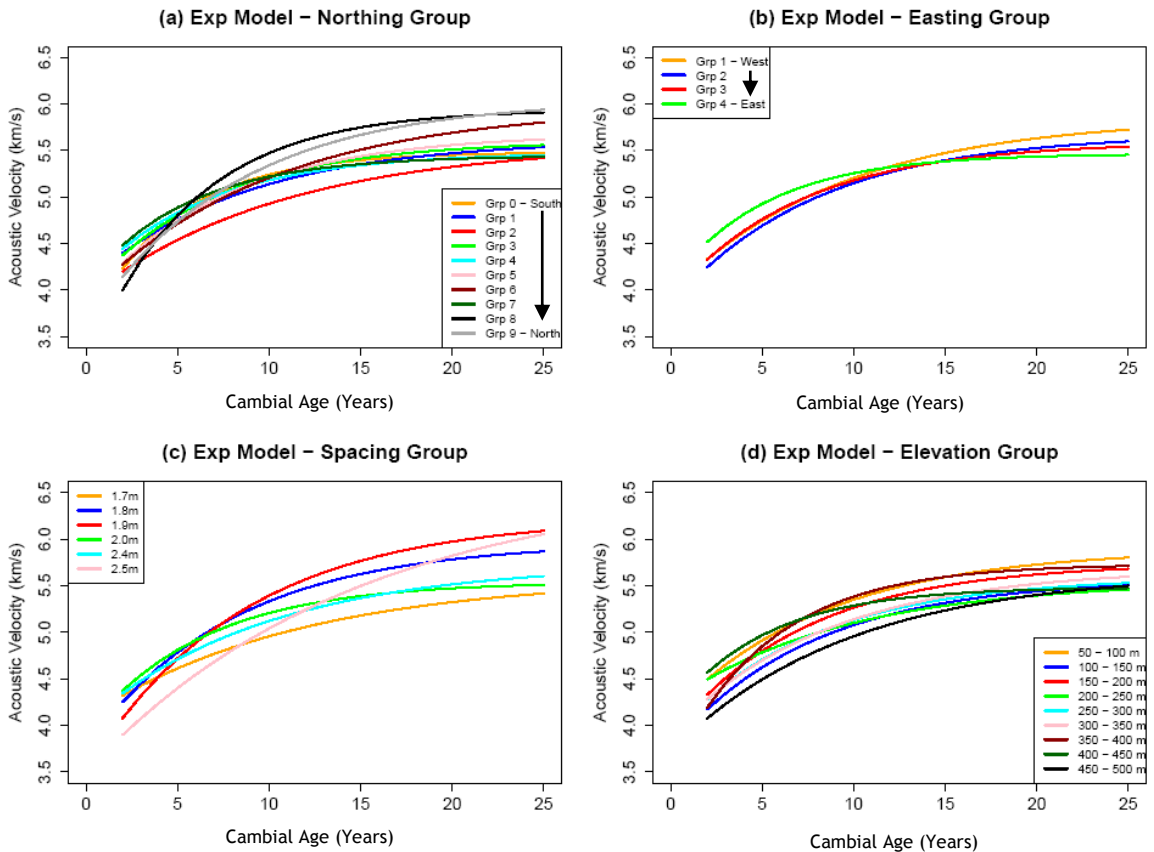


Figure 6-35: Coefficients of the Exponential model plotted by latitude, longitude, spacing and altitude groups.

Although the reliability of these data is questionable, this shows how the acoustic velocity can be modelled and how the model can then be used to determine what is having an effect on it. Because of the large range found in the coefficients when modelled against individual trees the coefficients were also calculated at a site level. When tested no significant correlations were found with the spacing groups or the elevation groups. There was a significant correlation between latitude and the intercept coefficient b_0 (correlation coefficient = 0.41) but not for the rate (b_1) or asymptote (b_2) (Figure 6-36). There was also a correlation between coefficient b_1 and longitude (correlation coefficient = 0.43) though this may be the result of one high value skewing the data (Figure 6-37).

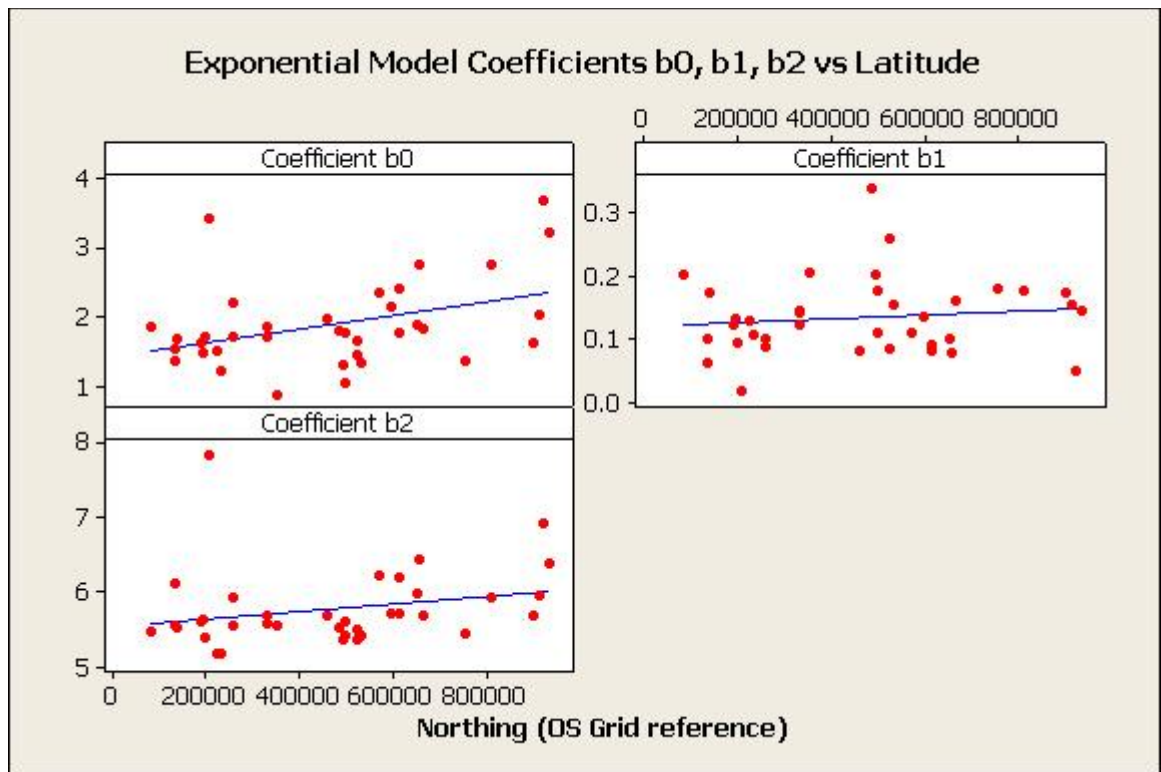


Figure 6-36: Correlation between the Exponential model coefficients, calculated by site, and latitude. Showing a significant correlation between latitude and b_0 , but no significant correlation between either b_1 or b_2 and latitude.

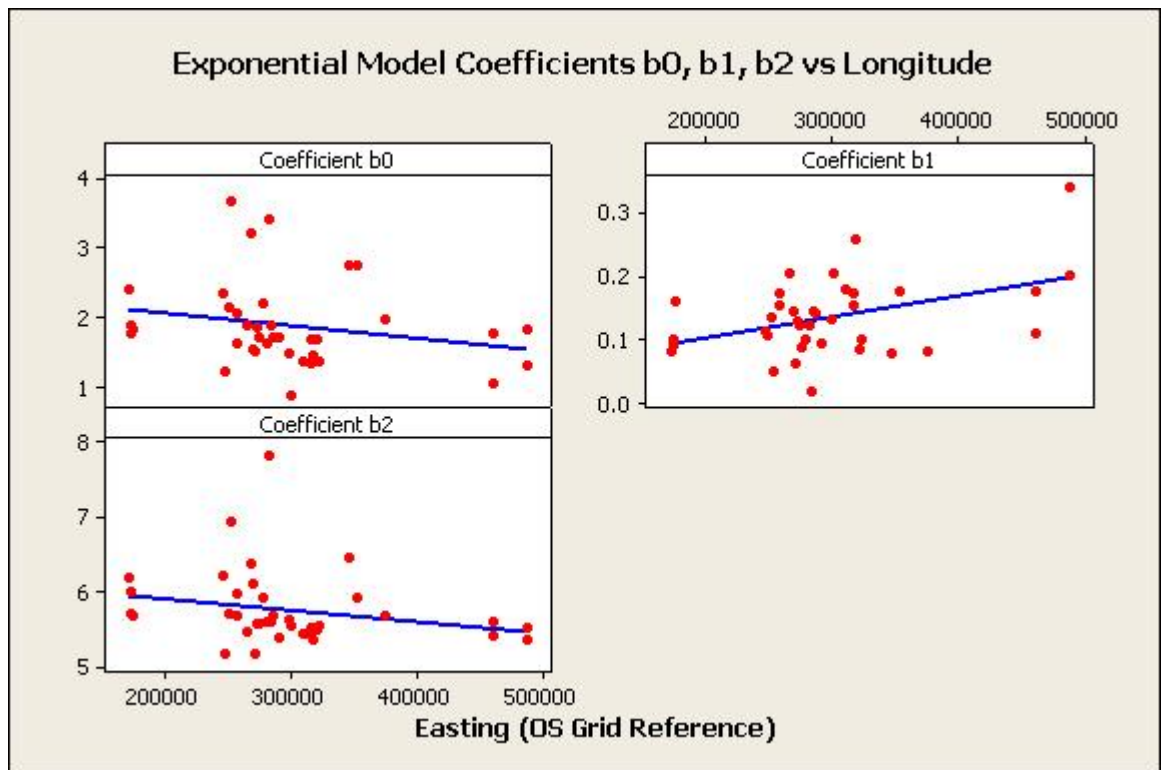


Figure 6-37: Correlation between the Exponential model coefficients, calculated by site, and longitude. Showing a significant correlation between longitude and b_1 , but no significant correlation between either b_0 or b_2 and longitude.

6.6 Discussion of Acoustic Velocity models

McLean (2008) measured static MOE by bending tests on small clear samples of Sitka spruce and found that there is a non-linear increase in MOE with cambial age from the pith similar to that found in other softwood species such as Norway spruce (Koponen et al., 2005). However the samples used by McLean (2008) were small clear batons measuring 20mm in the radial and transverse direction. This means that only one measurement was taken every 20mm in the radial direction and so it is unknown what happens to MOE within those 20mm blocks. Acoustic velocity and density in this study were measured every 2mm from the pith which allowed dynamic MOE to be calculated in much finer resolution and this indicated that dynamic MOE in some samples decreased for the first few rings, before increasing towards the bark. This trend is similar to that found by Vihermaa (2010) who measured acoustic velocity on Sitka spruce discs also in 2 mm increments and found that when dynamic MOE was calculated by tree from the acoustic velocity and density data in some cases it would decrease from the pith in the core wood before increasing after approximately ring 5. This discrepancy between static MOE measured on small clears and the calculated dynamic MOE here would suggest that further research is required in this area to determine the static MOE by bending tests at a finer resolution and to compare that to dynamic MOE calculated from density and acoustic velocity on the same samples.

The initial decrease found in the dynamic MOE is due to Sitka spruce core wood having high density, along with shorter tracheids, at the pith which decreases in the first few rings. The length of tracheids has been found to influence the velocity of sound with it being faster in longer tracheids (Burmeste, 1965). Keunecke et al. (2007) found the velocity of ultrasound was lower in yew than in Norway spruce which they attributed to the shorter tracheids in yew. However, acoustic velocity itself may be a good estimator of micro fibril angle (Lachenburch et al., 2011, Evans and Ilic, 2001) as well as a proxy for cell wall longitudinal stiffness and so it is valuable to measure and model this parameter on its own.

As with the growth data investigated in Chapter 3 observation of the acoustic velocity data indicated that it could be described as having two different

sections. Firstly there is juvenile phase which is characterised by an increase in acoustic velocity which is then followed by mature phase where the acoustic velocity reaches a plateau. Statistical analysis of the radial profile showed that there was evidence that this was the case and gave a split point between the two segments of between 13 and 14 years.

Analysis of the acoustic velocity data showed that when each tree is looked at individually there is a lot of noise within each radial profile making it difficult to distinguish between noise and an actual change in slope. The sensitivity of the segmented model to changes in the slope means that, as a means to define the position of the split point, this method may not work well when fitted to individual trees and this was shown by the range of split points found. When fitted to the global data the segmented model gave a reasonable fit and gave similar split point to that found by (Vihermaa et al., 2014) who measured acoustic velocity on Sitka spruce discs. This suggests that it should be possible to examine juvenile and mature wood using a two segmented model to look at each phase separately with the split between the two segments set between year 13 and 14. However the acoustic velocity in the mature segment had reached a plateau and therefore there is no effect of age on the slope in this phase. Therefore the level of acoustic velocity in the mature phase is dependent only on the juvenile segment.

A linear model was fitted to the juvenile segment and indicated that there is a significant positive linear slope to this phase, although a lot of variation about this was found. R was unable to fit a linear model to the mature phase of acoustic velocity and this is mainly due to the fact that there was no slope and so no effect of age.

As well as this, the first 3 or 4 rings of the mature phase were made up of the deceleration from the increasing juvenile phase to the plateau mature phase and this could suggest that there may be a more gradual change in acoustic velocity rather than the quick change that the segmented model is looking for. This being the case this data may be better suited to models which describe the radial profile as a curve. Different forms of curves were looked at in this section and the R-squared values and residual standard errors show them to be relatively similar when fitted to all of the data together. Of the curve models tested, all

had similar residual standard errors (0.28 to 0.29 km/s) and while both the Michaelis Menten and Logarithmic models could fit to every sample the Exponential couldn't fit to 15%. However the Exponential model gave the best fit to the data when fitted to individual trees (R-squared = 0.39) both visually and by the residuals, with the Michaelis Menten model especially giving a poor fit.

The segmented model looked to be a reasonable fit to the data and though there may be a problem around the area where there is a change in acoustic velocity, the R-squared was the highest of the models tested (although as was the residual standard errors) and it was able to fit to almost 99% of the trees.

Analysis of the linear phases of the segmented models using mixed effects analysis showed that most (58%) of the variation in the juvenile profile of acoustic velocity was between trees within the same site and a large proportion of the variation being within tree variation (28%) with less variation between sites (14%). Similarly in the mature phase most of the variation was also between trees in the same site (69%) indicating that it may be difficult to determine any site effects on the acoustic velocity and that within site effects may be more important.

All of the other models seemed to have slight problems either with the fit, the number of trees able to fit to or with the predicted values and residuals. This was also the case when plotted for the linear segmented model and it may be as a result of the variation in the acoustic velocity profile of each sample and this may be a consequence of the problems encountered with the method as discussed earlier in the chapter. The next stage in this process would be to analyse the juvenile portion of the profile using a linear mixed effects model or the whole profile using non-linear mixed effect to investigate any site factors that are having an influence on acoustic velocity, however analysis shows that there a lot of within site variation and since there is uncertainty with this data as to whether the variation is real or caused by the method it is difficult to discern what is noise and what is actual acoustic velocity and so to take it further would be flawed.

7 Within Season Variation in Tree Radial Expansion

There have been various studies which investigated the influence that the environment has on tree growth, focussing on productive conifers in the UK with some focus on Sitka spruce. Studies have investigated the growth response of trees to silvicultural practices such as weed control and fertiliser (McIntosh, 1981) and how this response can be modelled (Snowdon, 2002) to estimate the long term effects. Further studies have examined the gross response using CO₂ exchange to measure the productivity of a forest (Clement et al., 2003) and how this can be modelled to assess the impact of the environment on this exchange (Clement et al., 2012). Wang et al. (1991) investigated photosynthetically active radiation (PAR) and how this could be related to biomass production and Beauchamp et al. (2013) were able to relate the timing of seasonal growth to sap flux. However, although these studies are able to relate the growth response to these factors they are limited as a method of measuring tree growth and how it responds to changes in the environment. Feliksik and Wilczynski (2008) reported on the effect of climate on Sitka spruce in Poland and found a positive correlation between winter and early spring temperature and growth and a negative correlation between early summer temperature and growth. The same study also found that winter frost and dry summers are the main limiting factors for growth, and increased growth depended on high precipitation not only during the growing season but also during the latter stages of the previous year. Feliksik and Wilczynski (2009) reported a further study that suggested that the coastal area of the Baltic Sea low temperature was the main limiting factor for growth of Sitka spruce. In a different study, which used micro-cores to measure the relationship between growth and climate in Black spruce and Balsam fir, it was found that precipitation and humidity can influence the cell area and diameter in earlywood, but had less of an influence on latewood (Krause et al., 2010). Summer droughts and so low soil moisture due to high summer temperatures were the most important factors in limiting radial growth in a study into Norway spruce in Russia (Aakala and Kuuluvainen, 2011).

To investigate the effect of seasonal climate on the radial expansion of trees this study utilised a long term experimental site at Griffin Forest near Aberfeldy, in Scotland, which has been used in previous studies (Beauchamp, 2011,

Wingate, 2003, Vihermaa, 2010), as well as a new control site which was established in Harwood Forest in the North East of England. At these sites, radial expansion was measured using point dendrometers, which record any change in the diameter of the tree (Drew and Downes, 2009, Irvine and Grace, 1997). Additional supporting meteorological climatic measurements of air temperature, relative humidity, and soil moisture were recorded at both Griffin and Harwood, with Met Office weather data obtained for Aberfeldy from a local Met-Office weather station at Dull. These climate variables were then compared to the radial expansion measurements to investigate the interactive effects on temporal growth dynamics and the timing of radial expansion events such as when radial expansion start/ends, when latewood growth starts, daily fluctuations in radial expansion and annual variation in radial expansion. Various studies have shown that while dendrometers can give measurements of stem size, they can be of limited value for measuring the timing of growth and the 'type' of wood being produced (Baucker et al., 1998, Makinen et al., 2003, Turcotte et al., 2009) due to water movement causing a natural shrinkage and swelling of the stem giving a false impression of when growth starts in the spring (Turcotte et al., 2009) and when it ends in the autumn (Makinen et al., 2003). 5°C is widely accepted as a threshold for the thermal growing season (Sarvas, 1972), and photosynthetic production can occur in spruce any time that temperature is above 5°C (Jarvis and Leverenz, 1982), although during the winter this may produce stored carbohydrate reserves rather than growth (Collakova et al., 2013, Dauwe et al., 2012). The aim of this study was to take radial expansion measurements at a high temporal resolution at the Griffin site by dendrometers to determine the variation in radial expansion, and therefore growth, at a within site level and to investigate the influence of the local climate on growth through comparison with simultaneous investigations at Harwood.

Although growth may be controlled by a number of factors there is doubt as to which responses are more closely controlled by genotype and day length and what is controlled by climate. By taking radial expansion measurements at very fine time resolution (at two minute intervals) along with background meteorological data this study investigated and reports on how changing daily and seasonal conditions can effect growth.

7.1 Griffin Site

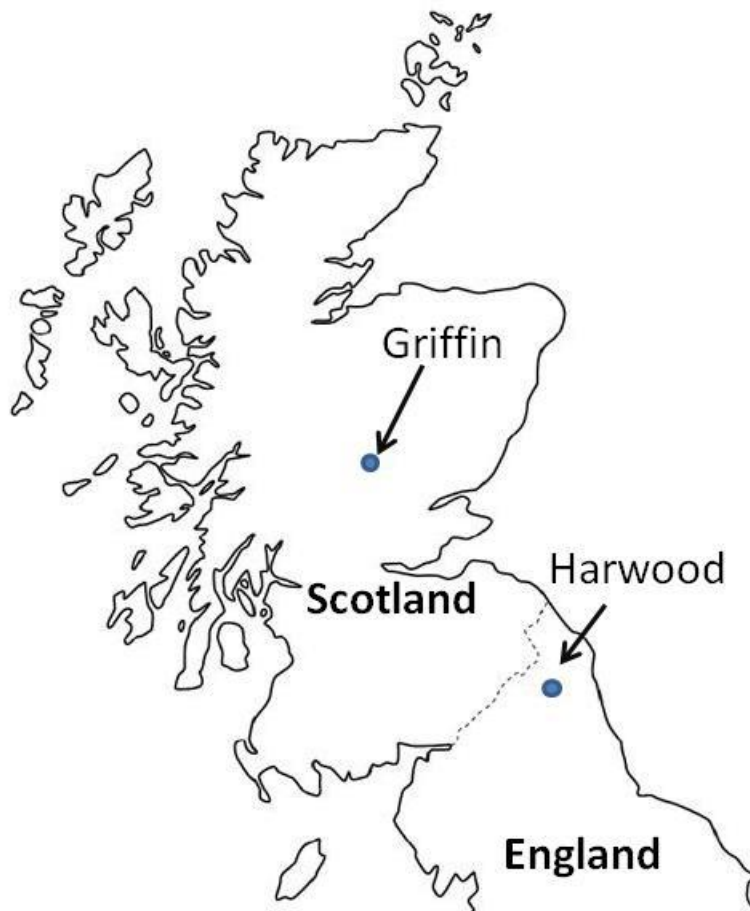


Figure 7-1: Map of Scotland and Northern England showing locations of the Griffin and Harwood sites.

The study investigated the radial expansion of trees at two location: Griffin Forest near Aberfeldy in Perthshire, Scotland (grid reference NN 289809 747485) (Figure 7-1) and Harwood Forest (in Northumberland in the North East of England, grid reference NY 398510 591340). The Griffin site was chosen as this forest has previously been used for long term monitoring by previous PhD studies from the University of Edinburgh (Wingate, 2003, Beauchamp, 2011) and the University of Glasgow (Vihermaa, 2010), and also had other studies being undertaken concurrently within this experimental forest. This investigation's primary focus was to build on work done in of these previous studies, especially those reported by Vihermaa (2010), to provide high-resolution data and improved understanding of the triggers for radial expansion of Sitka spruce.

Griffin Forest site is an even-aged plantation of Queen Charlotte Islands provenance Sitka spruce that was planted in 1981 on an area that was previously moorland with soil at the site being peaty gley and peaty podsoles. It is situated at an elevation of 340m, has an average temperature of 8.2°C and a mean annual precipitation of 1200mm (Wingate, 2003). The forest was planted at 2200 trees per hectare (Wingate, 2003) and has since been thinned, with every 5th row being removed (Vihermaa, 2010).

7.1.1 Tree Selection

Table 7-1: Tree and dendrometer (LVDT) number, diameter at breast height (DBH) and height of the trees selected at Griffin forest in April 2008 (Vihermaa, 2010) and the DBH of the same trees measured in July 2012 towards the end of the current experiment.

Tree Number	LVDT Number	DBH (cm) April 2008	DBH (cm) July 2012	Height (m) April 2008
08	3	30.4	35.5	18.8
15	4	28.0	32.8	18.7
43	2	27.6	34.4	17.9
48	1	36.7	44.3	20.6
66	5	26.0	28.3	15.7

Within the Griffin site, the radial expansion of 5 trees was monitored. The initial selection and set up of these trees was carried out by Vihermaa, (2010), during 2008, by randomly selecting 5 dominant trees within a sampling plot. The details of the 5 trees are shown in Table 7-1. The diameter at breast height (DBH) was measured at the beginning of the experiment (April 2008) and again towards the end of the experiment (July 2012) using a DBH tape, which calculates the DBH from the circumference, providing an independent check on the dendrometer measurements. Figure 7-2 shows a detailed schematic site diagram of the Griffin site. At the site a gentle 5° slope is downhill from left to right and also from top to bottom giving an overall diagonal from the top left to the bottom right of Figure 7-2. There is a small stream at the western side of the plot which is also the lowest point. Thinning has taken place at this site and the positions of trees which have been cut down are marked on the schematic site diagram (with yellow dots). This shows that two full rows of trees have been removed adjacent to trees 48, 43 and 8. The positions of all the other trees in the plot provide an indication of the competition for the experimental trees.

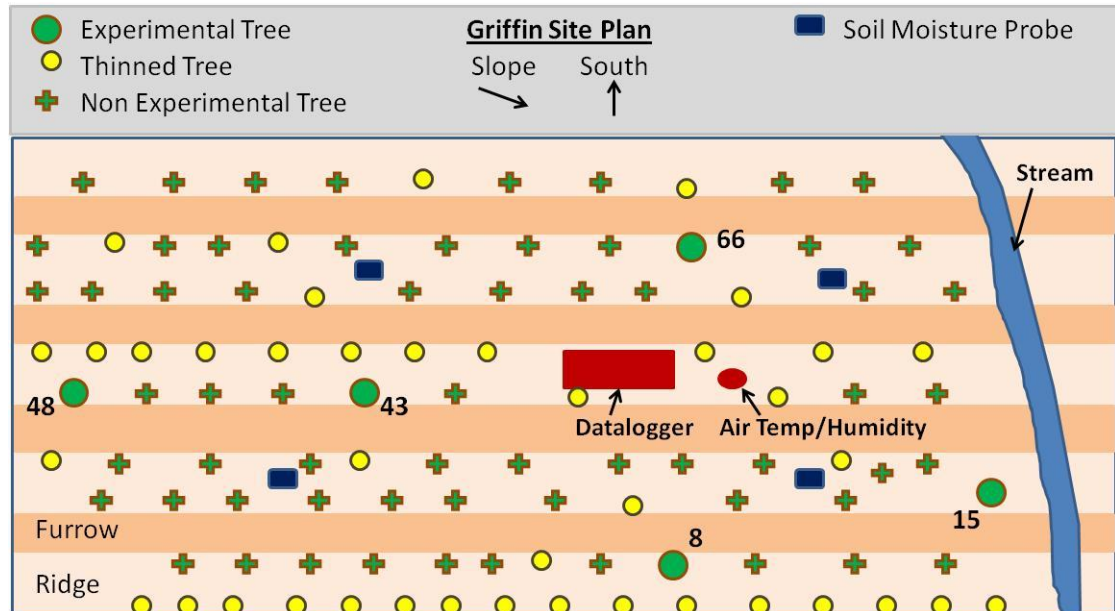


Figure 7-2: Plan of the experimental site within Griffin Forest. Showing the position of the trees used within the experiment along with the position of the other trees and where trees have been thinned. This plan is an approximation and not to scale.

7.1.2 Methods

At the Griffin site radial expansion was measured using point dendrometers, consisting of LVDT (Linear Variable Displacement Transducer) probes which, by using the change in an applied voltage, record variations in the tree diameter at very fine time resolutions (2 minute intervals). The LVDT probes were held in place on the northern side of the tree by two stainless steel beams which are insulated by Styrofoam and attached to each other at 90° . One beam is attached to the eastern face of the tree with a screw and the LVDT is attached to the other beam enabling measurements to be made on the northern face (Figure 7-3). A spirit level attached to the second beam adjacent to the LVDT ensures that the LVDT is positioned correctly after any adjustment and any movement can be detected (Figure 7-4). To measure changes in temperature between the tree wood and the steel beams two thermistor temperature sensors were used. One was attached to the steel beam beneath the insulation and the other was inserted into a small hole drilled into the tree. The data were collected using a Campbell Scientific CR23X datalogger, powered by two 12v car batteries, which collected growth data from the LVDT at 2 minute intervals and averaged to 15 minutes. As well as tree growth measurements, background meteorological data at the site was also recorded including air temperature ($^{\circ}\text{C}$) and relative humidity (%) using a Campbell Scientific CS215 probe placed at 1.3

m above the ground, and soil moisture using TDR (Time Domain Reflectometry) probes (which measure the time taken for an electromagnetic wave to travel between needles embedded in the soil and then expressed as percent moisture) at 4 points within the experimental plot, logged every 15 minutes (Figure 7-2).

Site visits took place every two weeks during the growing season and three weeks during the winter. During the visits the data was downloaded using the Campbell Scientific Loggernet computer program to a laptop computer and during the growing season the LDVT were readjusted to take account of any radial expansion that had taken place.

During site visits two small micro-cores (1.5 mm in diameter) were taken from each tree, using a Trephor Microcorer. Though not described within this study it is intended that in the future these micro-cores can be used to determine the type of cells being produced at specific times which could be compared to the dendrometer data to give a detailed pattern of wood growth throughout the year.



Figure 7-3: Picture of an LVDT dendrometer and insulated steel beam supports measuring tree growth on Tree 8 at Griffin Forest.



Figure 7-4: Picture of an LVDT dendrometer and spirit level attached to Tree 8 at Griffin Forest.

7.1.3 Results

7.1.3.1 Griffin Climate

While there are significant correlations between the measurements of soil moisture where all four probes follow the same trend (Pearson Correlation coefficients range from 0.95 to 0.99 between the four probes) there are differences in the absolute values measured ($p < 0.0001$) when tested with ANOVA. The 5 year profile of the soil moisture probes is shown in Figure 7-5. Since the soil moisture of all four probes fluctuate at the same time the effect of changing soil moisture can still be compared to the growth to see if there is a connection. To do this the mean value for the 4 probes was used.

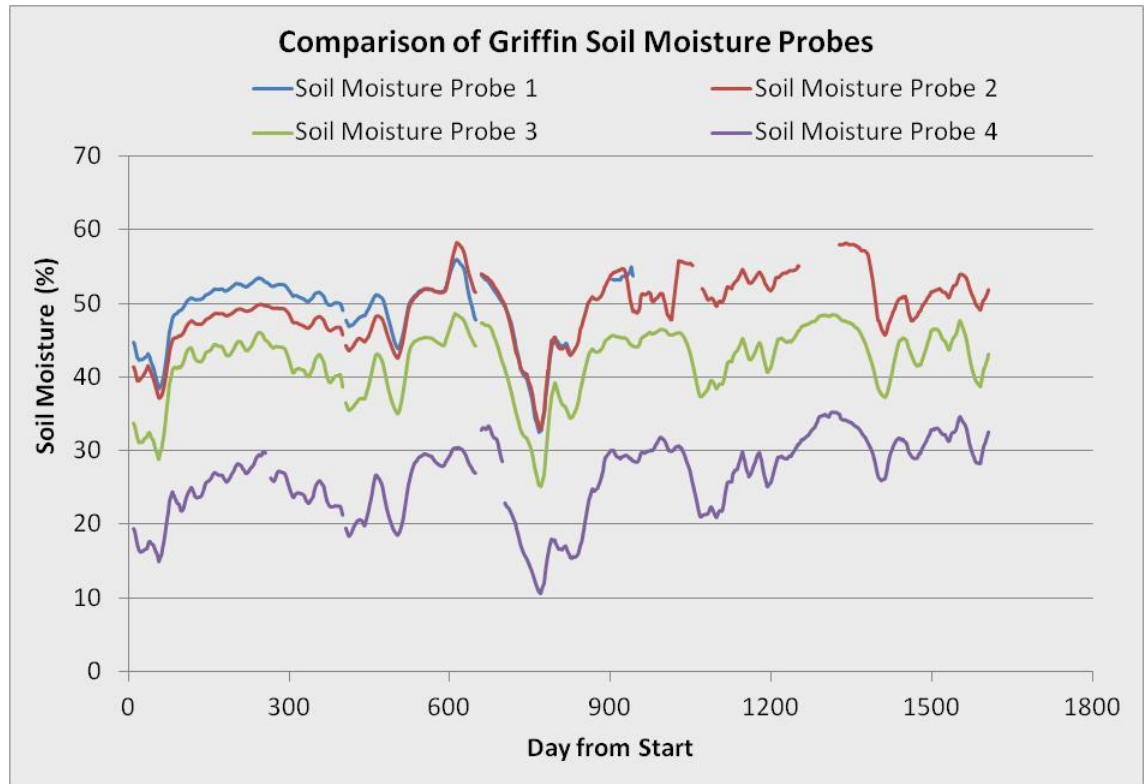


Figure 7-5: Comparison of soil moisture probes showing how the soil moisture can change over a short distance on one site.

As well as the measurements being taken at the Griffin site weather station data was also obtained from the Aberfeldy Dull Met Office weather station. This is approximately 8 km from the Griffin site (grid ref: NN 281964 749289) at a height of 100 metres. Comparison of the weather station data to that measured at Griffin shows that there is quite a strong agreement between rainfall events and soil moisture as shown in the 2010 example in Figure 7-6 and this was similar across all the years measured. Figure 7-6 also gives an indication of how quickly soil moisture is depleted after rainfall events, especially during the growing season (approx. days 90 to 270) with only sustained rain resulting in increased soil moisture over longer periods.

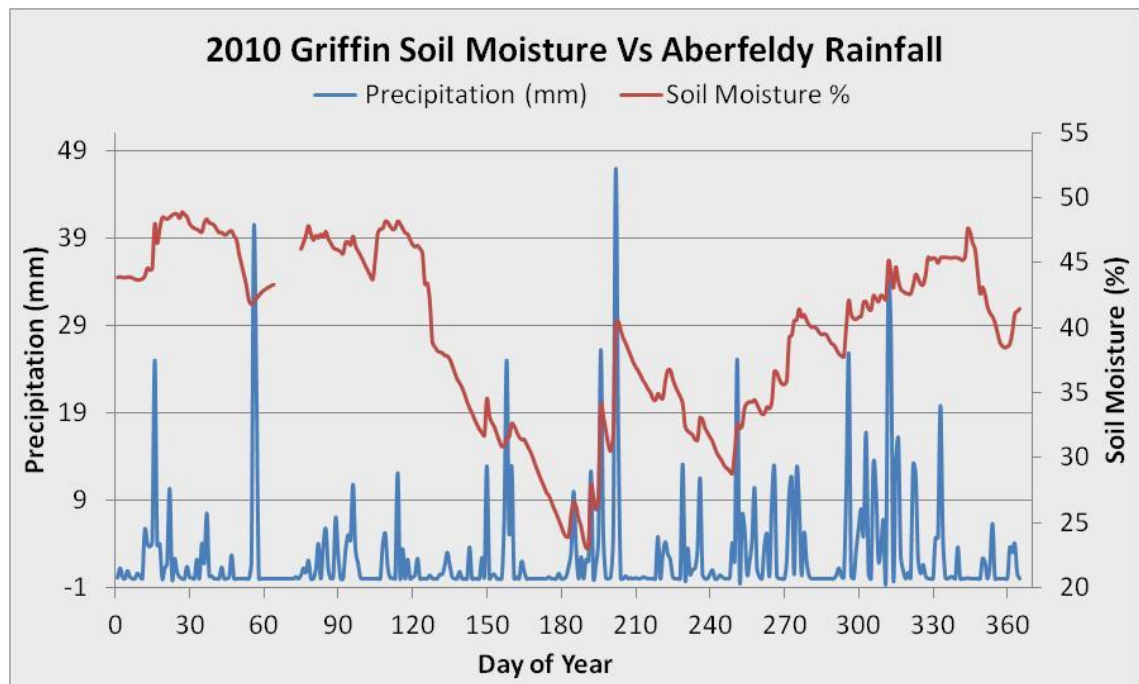


Figure 7-6: Comparison of soil moisture measured at Griffin site during 2010 with rainfall measured at Aberfeldy, Dull weather station.

The temperature measured at Griffin shows a very similar pattern to that measured at the weather station in Aberfeldy where the minimum daily temperature follows an almost exact pattern and scale (Figure 7-7) and the two measurements were found to be highly correlated (Pearson correlation coefficient 0.918). Although the mean daily temperatures measured in Aberfeldy are consistently higher and the range is larger than those at the Griffin site they both follow a very similar pattern with the peaks and troughs occurring at the same time (Figure 7-8) and again both were found to be highly correlated (Pearson correlation coefficient 0.935). The larger range found in the temperatures measured at Aberfeldy weather station indicates that the temperature within the forest does not fluctuate as much as those out in the open but may be more indicative of the type of fluctuation in temperature which could be expected in the canopy of the trees. The examples shown in Figure 7-7 and Figure 7-8 are for 2010 but the pattern was similar across all years measured.

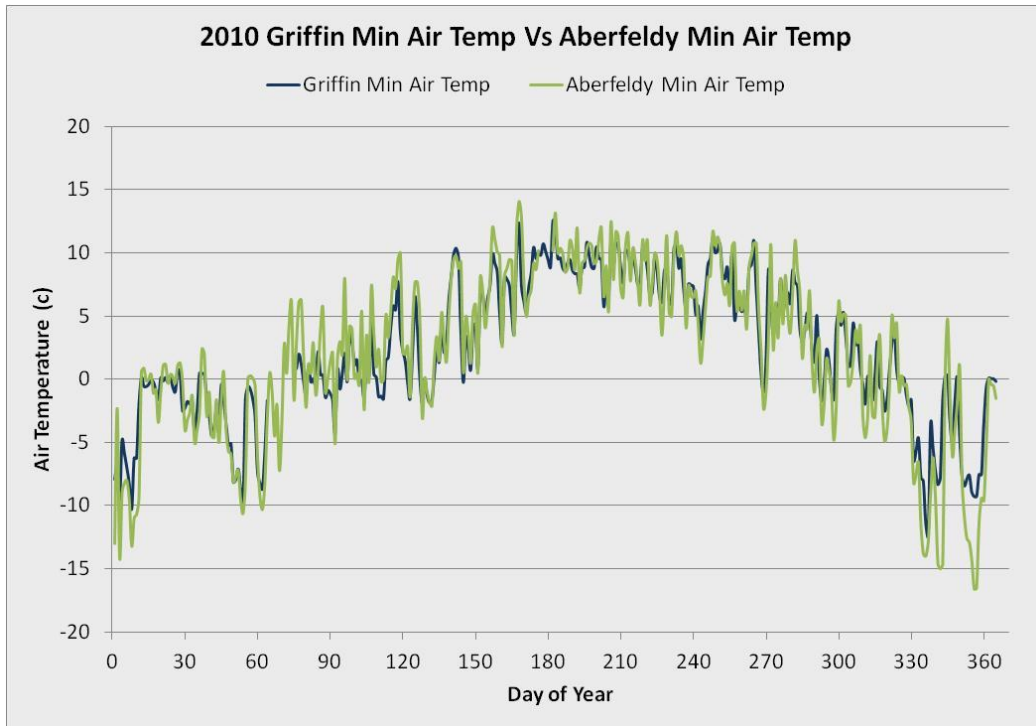


Figure 7-7: Comparison of minimum daily temperature measured at Griffin site during 2010 with that measured at Aberfeldy Dull weather station.

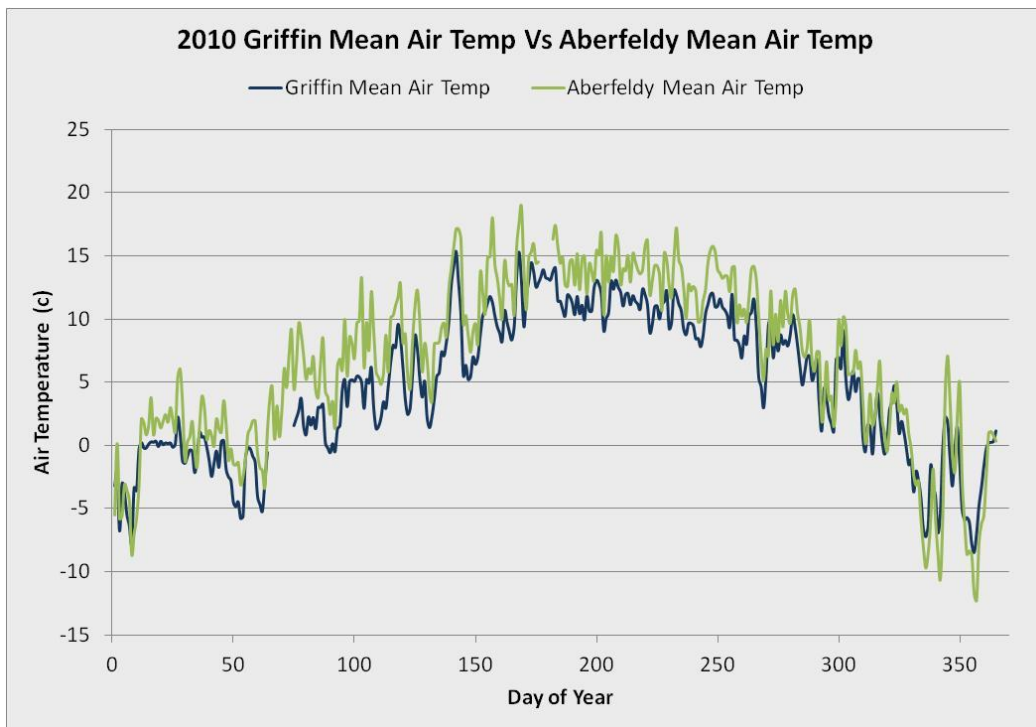


Figure 7-8: Comparison of mean daily temperature measured at Griffin site during 2010 with that measured at Aberfeldy Dull weather station.

To be able to visually compare the data the daily temperature data were smoothed (by taking a 30-day moving average) and there were some differences between years found in mean temperature measured at Griffin site (Figure 7-9). This is especially true during the winter periods which saw two extremely cold winters (2009-2010 and 2010-2011) and is also evident in early spring. The summer temperatures are similar throughout as are the autumn temperatures when temperature begins to decrease again.

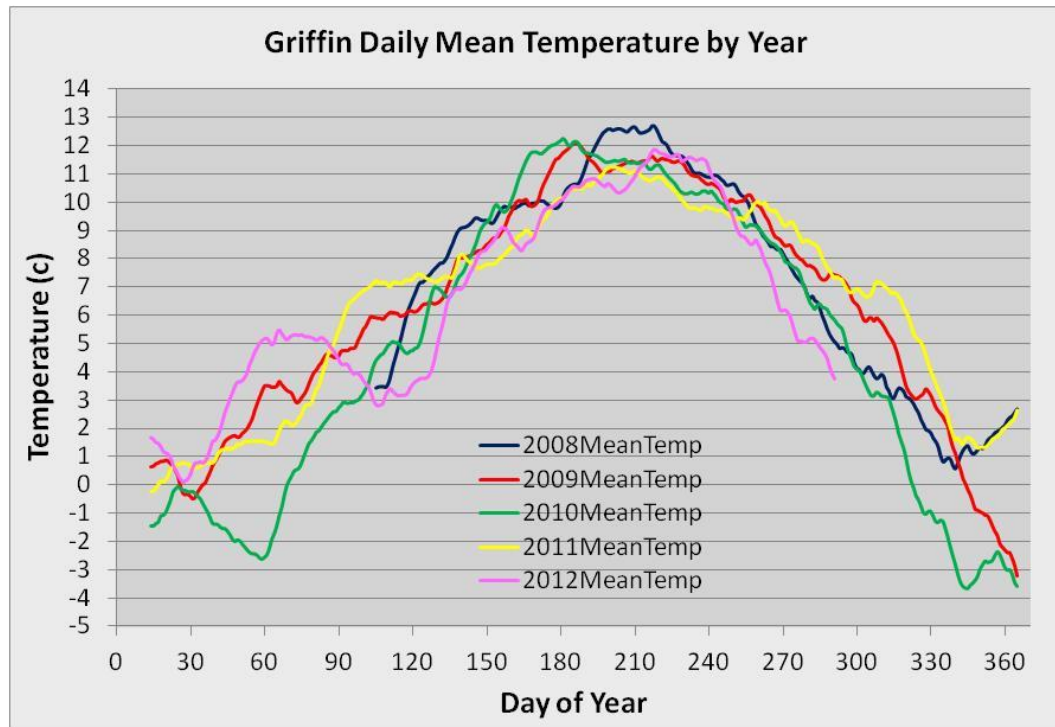


Figure 7-9: Comparison of daily mean air temperature by year measured at the Griffin site

To be able to compare soil moisture across years (Figure 7-10) the data were also smoothed using a 30-day moving average. Differences in soil moisture between the years are apparent with 2008 and 2010 notably drier years and 2012 being a wetter year. Apart from 2012 the other years show a tendency for the summer months to be the period of lowest soil moisture, while the winter periods show similar levels of soil moisture between the years.

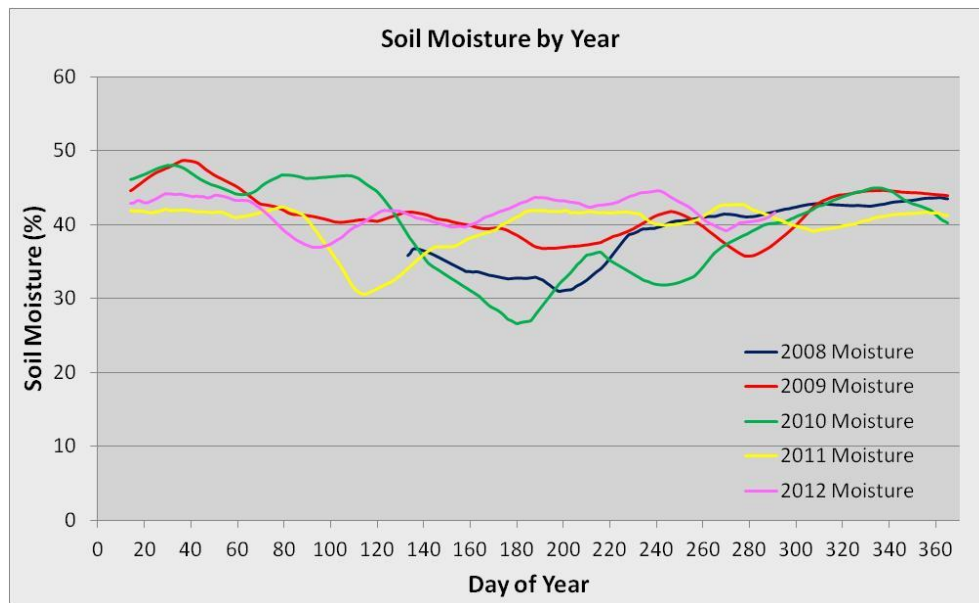


Figure 7-10: Comparison of the daily mean soil moisture by year measured at the Griffin site

7.1.3.2 Variation in Radial Expansion

At the Griffin site radial expansion of the tree stem starts each year around the beginning of April and ends in mid-September and as expected this period corresponds to the time when temperatures start to increase in spring and carries on until temperatures start to drop again in autumn (Figure 7-11). This period also corresponds to the drier summer period when relative humidity and soil moisture are low and less water is available to the trees. The timing of radial increment is similar in trees 43 and 48 (red and black line respectively) and the magnitude of radial expansion is similar until the final two growing periods (2011 and 2012). Radial expansion is slightly less in tree 15 (blue line) and through the first 4 years and in 2012 there was a malfunction of the dendrometer for this tree resulting in no radial expansion measured. Tree 66 (grey line) shows very little response over the whole time period and examination of the site shows that this tree is no longer one of the dominant trees in the area. Tree 8 (green line) initially showed a large increase but wildly fluctuating results can be seen since the summer of 2010 into 2011 and these are put down to problems with the data-logging cabling at the site.

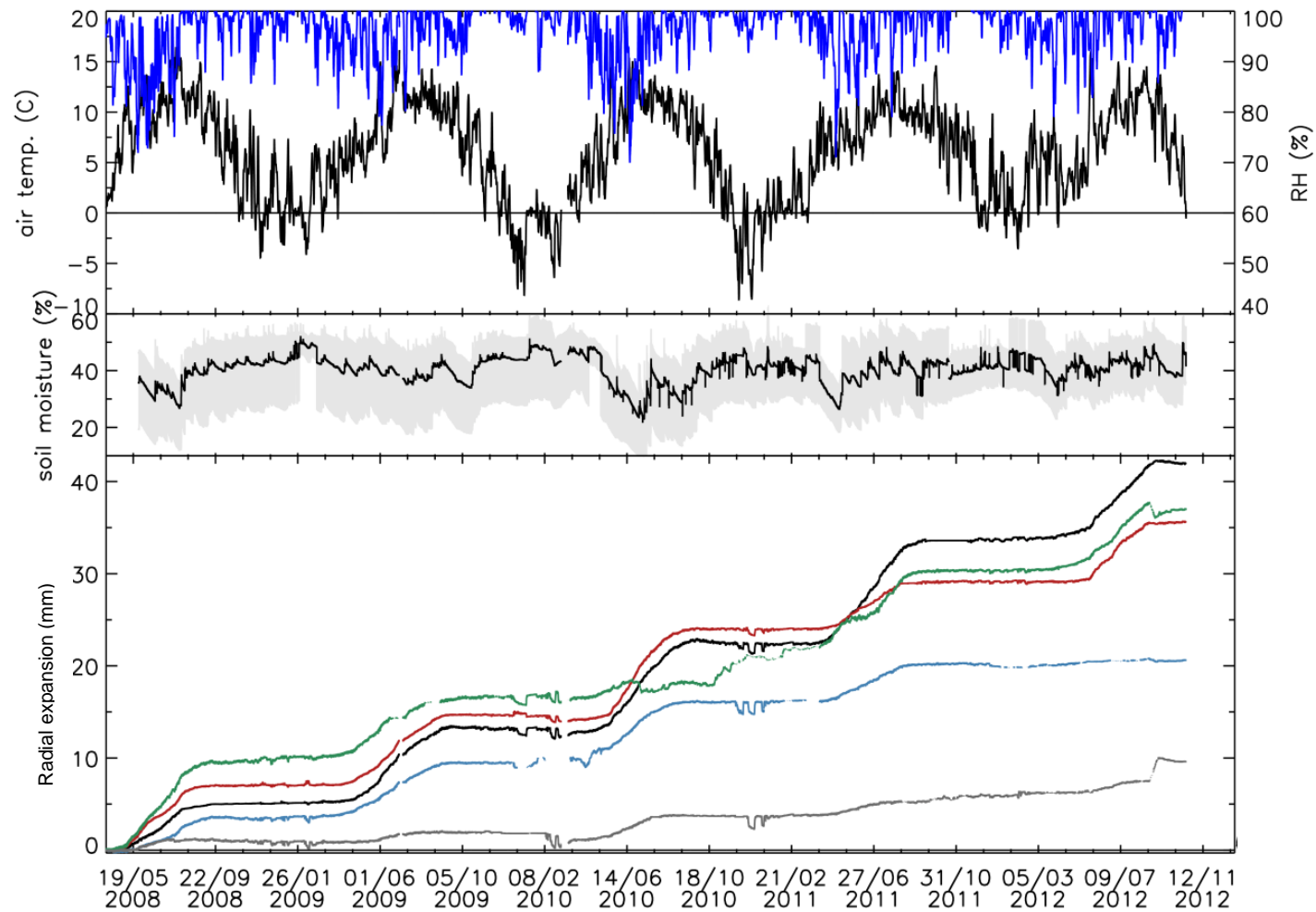


Figure 7-11: Griffin site measurements from June 2008 to October 2012. The top panel of the graph shows air temperature (°C, black) and relative humidity (% , blue), soil moisture (%) is shown in the middle and radial expansion of the five trees, as measured by LVDT dendrometers in the bottom panel.

The results shown in Figure 7-11 also show large decreases in stem size on all trees during the winter of 2009/2010 and then again in 2010/2011. Closer inspection of the measurements at this time reveals that the dips in readings occur at the same time as extreme cold periods (e.g. Figure 7-12). The reasons for this dip are unclear but similar effects have also been seen in other studies (Winget and Kozlowski, 1964, Zweifel et al., 2000, Devine and Harrington, 2010) and it has been proposed that this phenomenon may reflect changes in the bark water content as water moves inwards due to a water potential gradient developing as water freezes in the outer section of the tree? (Zweifel et al., 2000). Low temperatures around this time also caused the power source to fail leading to a short term loss of data.

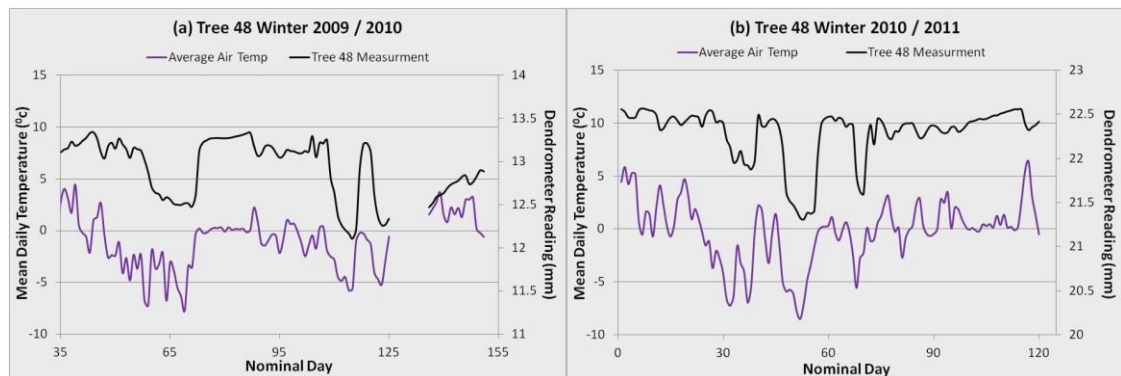


Figure 7-12: Measurements for tree 48 during the winter of (a) 2009/2010 and (b) 2010/2011 showing a big dip in readings corresponding to extreme cold events.

Table 7-2: Comparison between manual DBH measurements and the radial expansion measurements taken by the dendrometers

Griffin Tree No.	Growth by DBH (Diameter cm)	Expansion by Dendrometers (Radius cm)
48	7.6	4.0
43	6.8	3.4
8	5.1	3.6
15	4.8	2.1
66	2.3	0.7

DBH measurements were taken at the beginning of the experiment and also towards the end of the experiments (as shown earlier in Table 7-1) and these can be used to confirm the dendrometer readings for each tree. The difference between the beginning and end DBH measurements are shown in Table 7-2 along with the overall measurement of radial expansion calculated from the dendrometer data. From this it can be seen that both methods give similar

results though there were differences. Tree 48 would appear to have the most radial expansion, with agreement by both assessment methods, with an increase in DBH of 7.6 cm and radius of 4.0 cm. Whilst tree 43 has the second most radial expansion by DBH (6.8 cm) the radial increment (3.4 cm) is slightly smaller than that for tree 08 (3.6 cm) and this anomaly is likely to be due to the equipment failure on tree 08 during 2010. Tree 15 shows slightly higher growth by DBH than dendrometer (4.8 cm compared with 2.1 cm) but again this may reflect a period of equipment failure in 2012. Tree 66 shows the least radial expansion by both methods with the dendrometer readings slightly smaller than the DBH readings. Figure 7-11 provides clear evidence that whilst there are similarities in the timing of commencement and cessation of radial expansion there are clear differences between individual trees in the amount of radial expansion that takes place each year. This intra-site variability highlights the difficulty in measuring and predicting growth with a site factor such as climatological data when micro site factors, genetics and other within site factors clearly have influence. In order to compare the radial expansion of each tree the values for each year were standardised by subtracting the baseline value which had the effect of zeroing the starting point of radial expansion each year. Figure 7-13 attempts to show this by plotting the amount of radial expansion by each tree for each year. As mentioned previously the 2010 season for tree 8 (blue) can be ignored since this was an equipment malfunction. As well as this there were problems with equipment for tree 15 at the beginning of 2010 and in 2012.

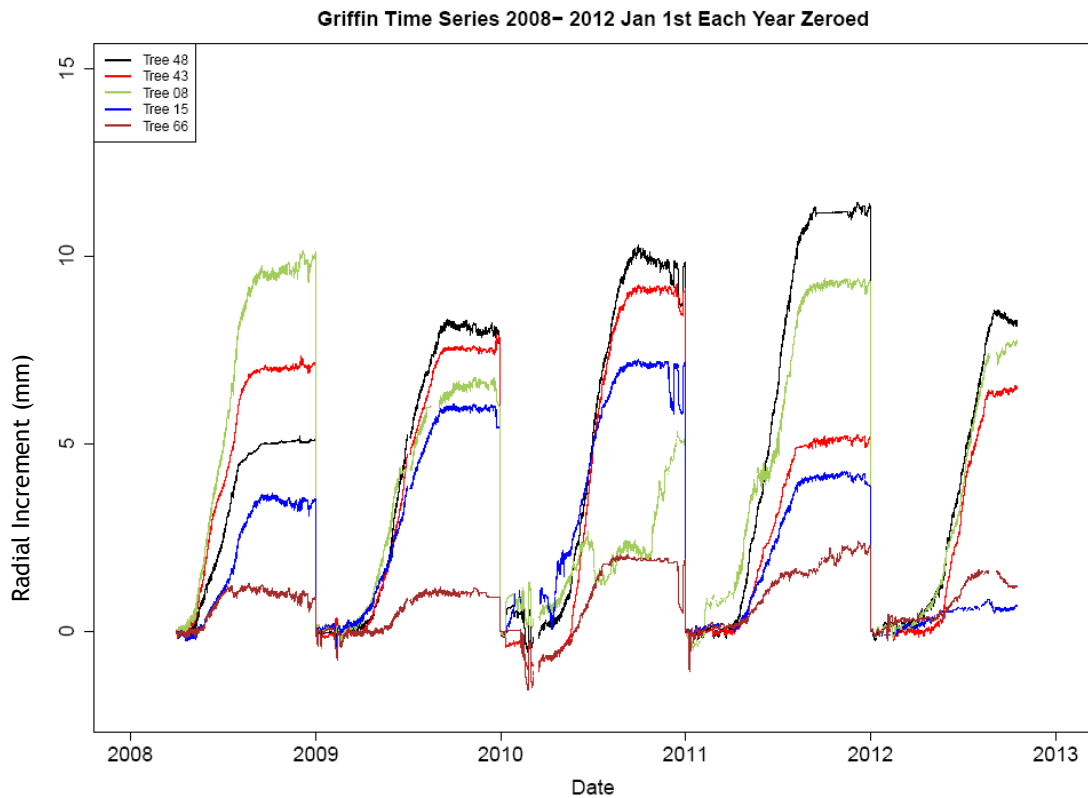


Figure 7-13: Comparison by year of the radial expansion curves of the 5 trees at Griffin when radial expansion is reset to zero each year

Figure 7-13 shows that tree 48 has the highest radial expansion most years and tends to increase each year for the first 4 years, with a radial increment of approximately 5mm in 2008 increasing to approximately 11.4 mm in 2011, and then a drop in 2012. Although at a different magnitude, trees 43, 15 and 66 show a similar pattern to tree 48 in the first 3 years with an increase in the amount of radial expansion each year. However trees 43 and 15 then show less radial expansion in 2011 than they did in previous years and then a slight increase again in 2012. Tree 8 shows the most radial expansion in the first year but less in the second year before increasing again in 2011. However problems developed with the cable connecting the logger to the dendrometer means that measurements at the end of 2009, through 2010 and the beginning of 2011 can be discounted. Tree 66 shows the least radial expansion out of all the trees and in fact shows very little expansion overall in any of the years measured. The amount of radial expansion shown by each tree for each year is shown in Table 7-3. This shows that although there are some similarities in the yearly trends, and also some differences, each tree also has a different magnitude of radial expansion.

Table 7-3: Amount of radial expansion achieved by each tree each year measured by point dendrometers.

Max Radial Expansion by Year (mm)					
Tree	2008	2009	2010	2011	2012
48	5.0	8.3	10.3	11.4	8.6
43	7.1	7.9	9.25	5.2	6.5
8	9.7	6.8	n/a	9.4	7.8
15	3.7	6.1	7.3	4.3	n/a
66	1.2	1.2	2.0	2.4	1.6

7.1.3.3 Temperature and Soil Moisture Effect on Radial Expansion

In order to investigate the effect of temperature and soil moisture on tree radial expansion the maximum daily dendrometer value was used to give an integrated daily radial expansion curve. In order to determine a radial expansion trend the noise seen with the raw data was removed using 30 day moving average. The first derivative of radial expansion with respect to day (*i.e.* daily radial expansion rate) was calculated by subtracting each daily value on the smoothed curve from the following daily value on the same curve to give a radial expansion rate for each day. An example of this is shown in Figure 7-14 for tree 48 during the growing period of 2011.

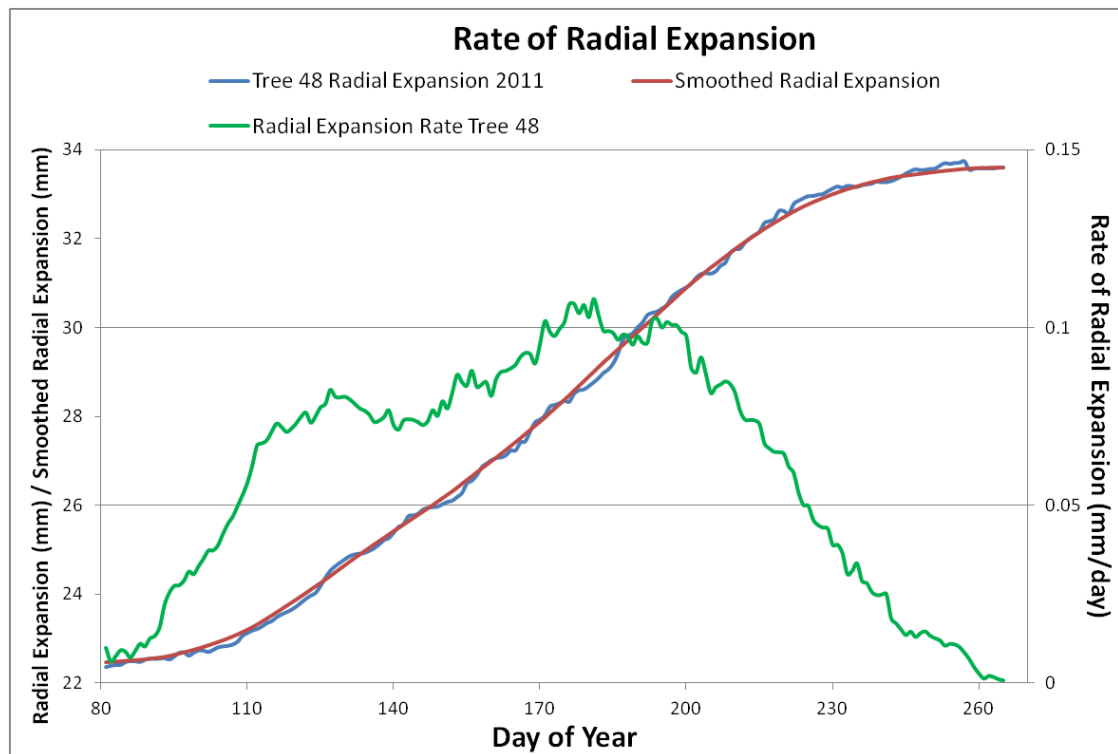


Figure 7-14: Example of calculating the radial expansion rate for tree 48 during the growing season of 2011. The rate value was calculated by subtracting each daily value from the following daily value.

The main points of interest from this experiment are to investigate when radial expansion starts and ends each year, the amount of radial expansion each year as well as when growth switches from early to late wood and what are the climatic controls of this process and transition. By plotting soil moisture and air temperature against the daily radial expansion rate patterns starts to emerge. In this series tree 48 is used as the main example and this is looked at for each year followed by the four other trees for the same year. The soil moisture and temperature readings were done on a site basis so are the same for each year across the different tree graphs.

In general there does seem to be more instrumental noise in the winter months which could indicate freeze-thaw impacts on the outer layers of the tree during extreme cold weather events or could be evapotranspirational demand when the soil-plant-atmosphere continuum is perturbed by lack of soil water availability (due to frozen soil) but this reduces as the trees start to expand.

Although there are slight differences in the trees the radial expansion of each tree is characterised by distinct periods during the growing season similar to that seen in Figure 7-14. This includes a period of slow expansion of the stem during

early spring followed by a period of rapid expansion. The expansion rate then peaks and is followed by a period where the rate of radial expansion slows, which may be linked to the tree switching from earlywood growth to latewood growth characterised by smaller cells with denser walls.

Figure 7-15 shows the measurements for tree 48 in 2008. Although measurements did not commence until April of that year they coincided with the start of the growing season. Distinct periods of radial expansion can be observed and how these can be related to the climate variables, which are consistent across most of the trees and can be described in the following steps:

1. When the mean temperature is above approximately 3°C a period of slow expansion of the trunk begins. This temperature may also correspond to minimum temperatures rising above 0 °C.
2. Once the mean temperature is consistently above 5°C there is a rapid increase in the expansion rate.
3. As summer progresses and temperatures reach a peak the radial expansion rate starts to decrease.
4. Radial expansion stops as temperatures are decreasing in the autumn but before the mean temperature reaches 5°C.

The same basic features of points 1 - 4 above can be seen in the four other trees during the same year (Figure 7-16) although tree 66, which had very little radial expansion, has a different timing for the decrease in rate and cessation of active radial expansion.

Another feature which appears in the rate of radial expansion of some trees is a plateau or hump in the radial expansion rate during the growing season e.g. trees 43 and 8 in 2008 (Figure 7-16) which would suggest that in these trees the rate of radial expansion slows and then speeds up again.

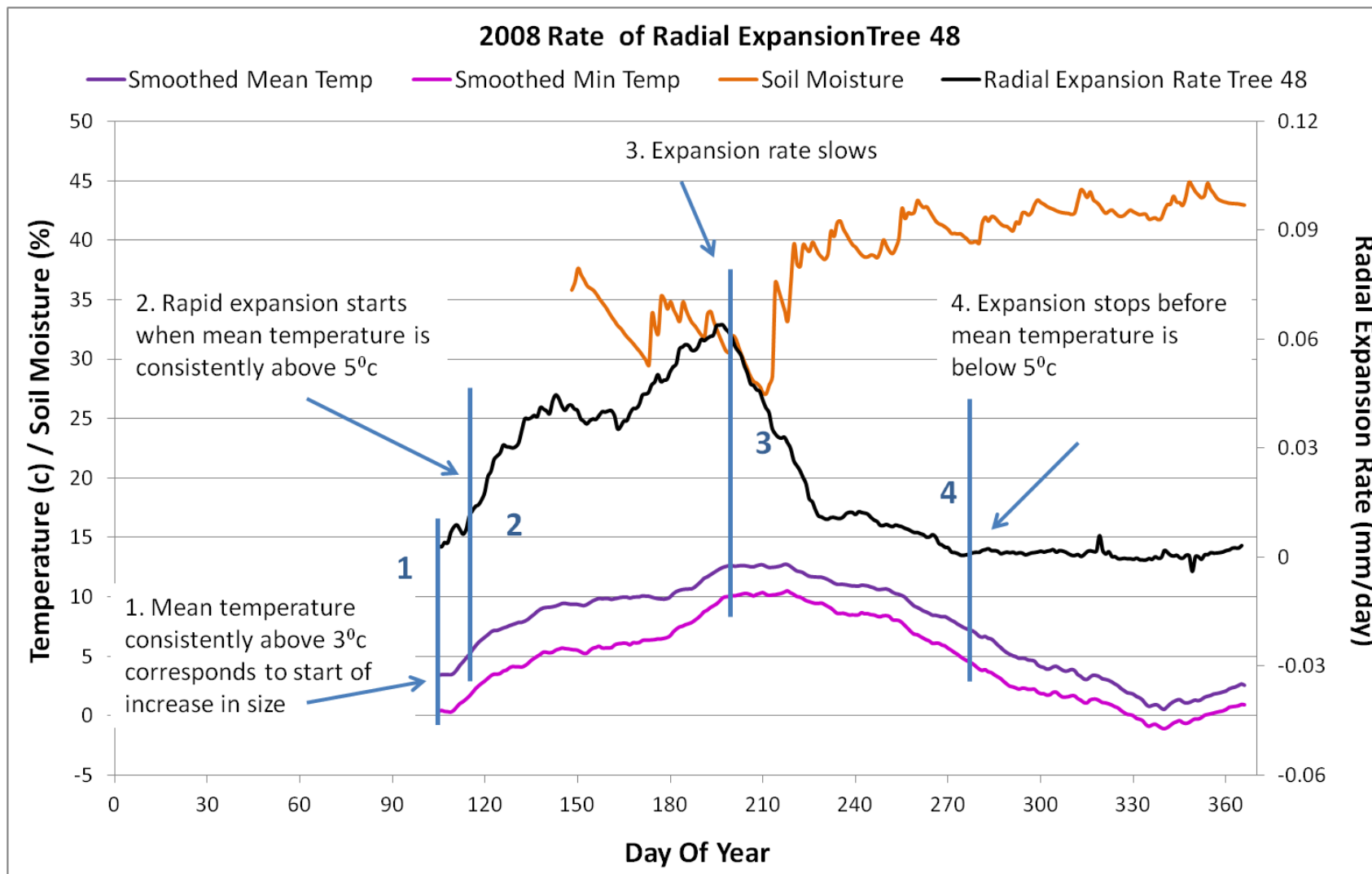


Figure 7-15: The effect of soil moisture and temperature on the rate of expansion of Tree 48 at Griffin during 2008.

The rate of radial expansion of tree 48 during 2008 is shown in Figure 7-15. Mean temperature rose above 5°C on day 115 (15th April) and this corresponds to an increase in the radial expansion rate of the tree. The expansion rate slows from approximately day 143 (23th May) until day 163 (June 12th) forming a “hump” before rising again until day 197 (16th July). Following this the expansion rate decreases sharply until radial expansion stops on day 270 (27th Sept). Towards the end of the year mean temperature drops below 5°C around day 292 (19th Oct). Soil moisture measurements commenced on day 148 (27th May) and was followed by a period of decreasing soil moisture during late summer (corresponding to the slowing of the rate of radial expansion) before rising again in autumn. The first drop in soil moisture seems to have little effect on the radial expansion rate which continues to rise. The second dip in soil moisture (approximately day 180 to 220), however, corresponds to the period of highest radial expansion rate which for tree 48 starts to decline as soil moisture reaches approximately 30%.

The radial expansion rate during 2008 of trees 43, 8, 15 and 66 are shown in Figure 7-16 below. While the temperature and soil moisture measurements are the same as in Figure 7-15 there are differences in the radial expansion rate of the individual trees. Trees 43 and 8 show similar initial increases in radial expansion rate but tree 15 has a much slower rate. All three trees show a levelling of the radial expansion rate, as seen for tree 48 before, at around day 145 before rising again at approximately day 185. The radial expansion rate of trees 43, 8 and 15 all start to decrease in summer at around day 200 and have all stopped expanding by day 270 similar to tree 48. Tree 66 shows a different pattern to the other trees. Radial expansion starts later, has a much slower rate and stops expanding before the other trees with radial expansion finished by about day 190. Similar to that seen in tree 48 Figure 7-16 shows the same dip in soil moisture around day 180 to 220, which corresponds to the period of highest radial expansion rate for all trees except tree 66. The radial expansion rate of trees 43, 8 and 15 all start to decline as soil moisture reduces to 30%.

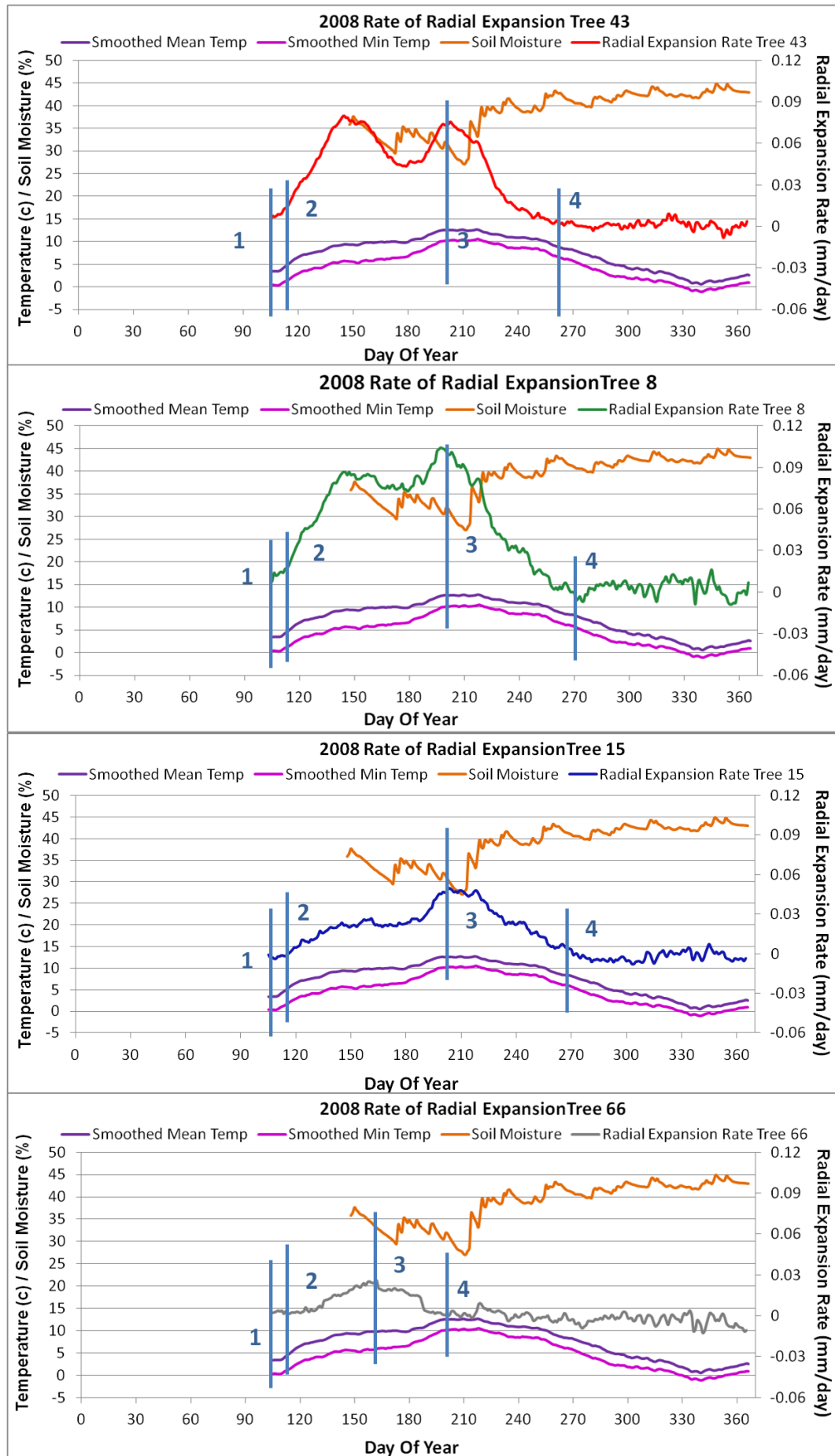


Figure 7-16: The effect of soil moisture and temperature on the radial expansion rate of Trees 43, 8, 15 and 66 at Griffin during 2008.

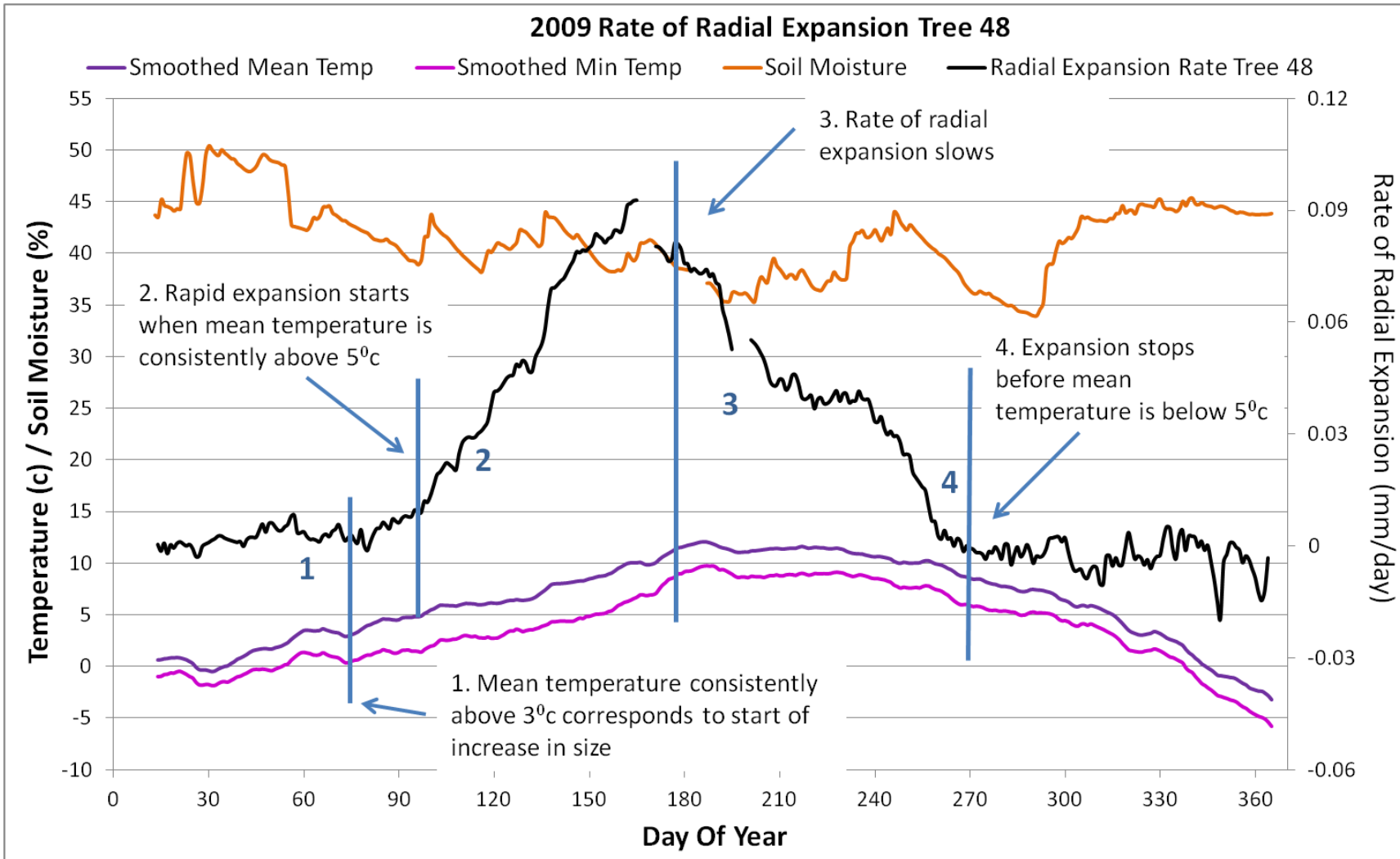


Figure 7-17: The effect of soil moisture and temperature on the radial expansion rate of Tree 48 at Griffin during 2009.

The radial expansion rate of tree 48 during 2009 is shown in Figure 7-17. The rate of radial expansion first starts to increase around day 82 (23rd March). Mean temperature rose above 5°C on day 98 (8th April) which corresponds to a period of increased radial expansion rate. The rate of radial expansion continues to increase until approximately day 165 (14th June) when a loss of power meant no measurements were taken until day 171 when radial expansion rate had already started to decrease. This also corresponds to a period of decreasing soil moisture. Radial expansion stops on for tree 48 on approximately day 269 (26th Sept).

The radial expansion rate during 2009 of trees 43, 8, 15 and 66 are shown in Figure 7-18 below. The initial increase in the radial expansion rate for trees 43, 8 and 15 starts at around day 79 (20th March) followed by a slight increase in the rate at around day 94 (4th April). As in Figure 7-17 a loss of power at around day 165 makes it difficult to determine when the peak radial expansion rate was reached and when it started to decline and at approximately day 150 problems occurred with the cable of tree 8 causing problems with the readings. As before, tree 66 shows very little increase in the radial expansion rate, which starts after and finishes before the other trees.

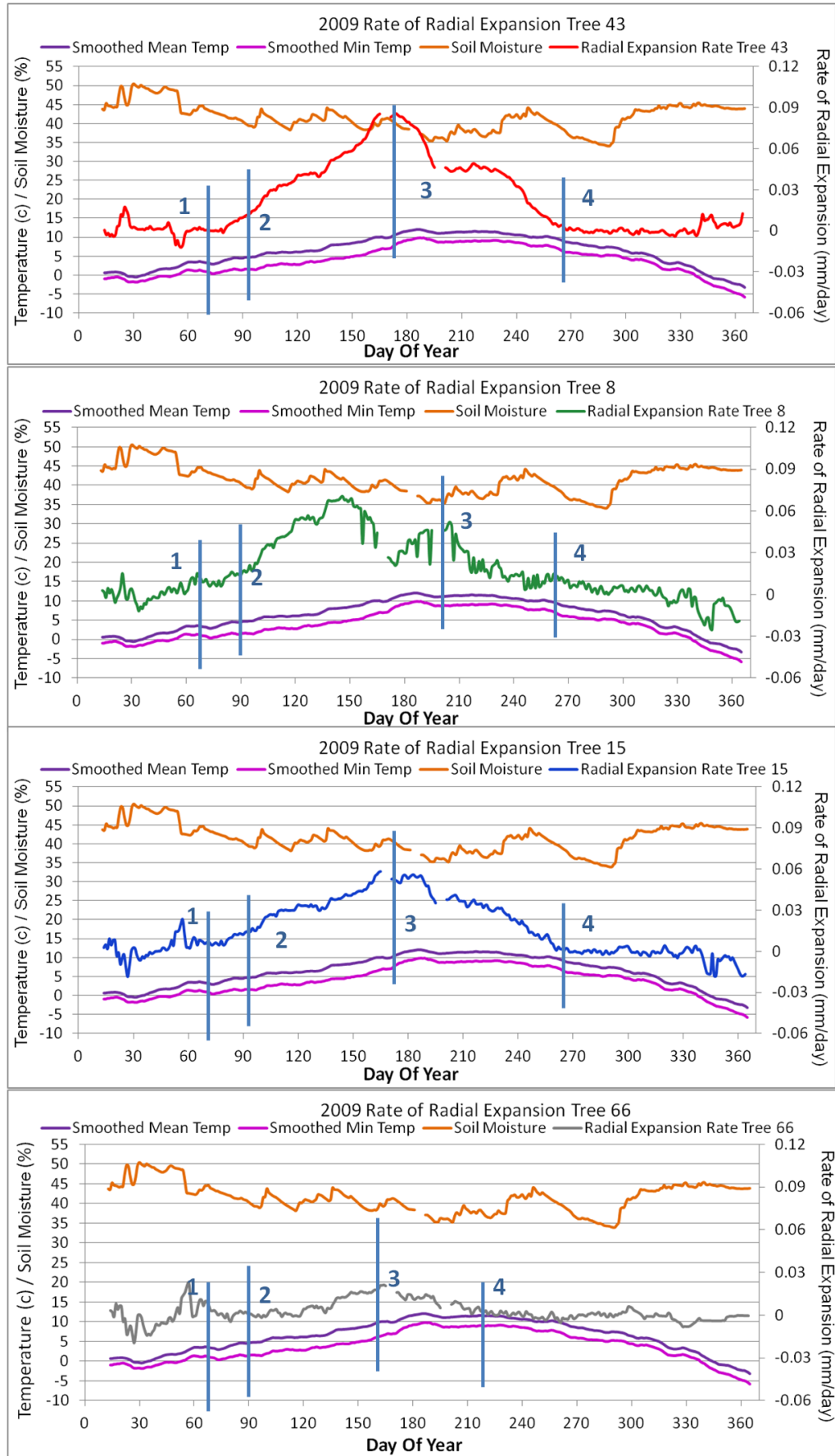


Figure 7-18: The effect of soil moisture and temperature on the rate of radial expansion of Trees 43, 8, 15 and 66 at Griffin during 2009.

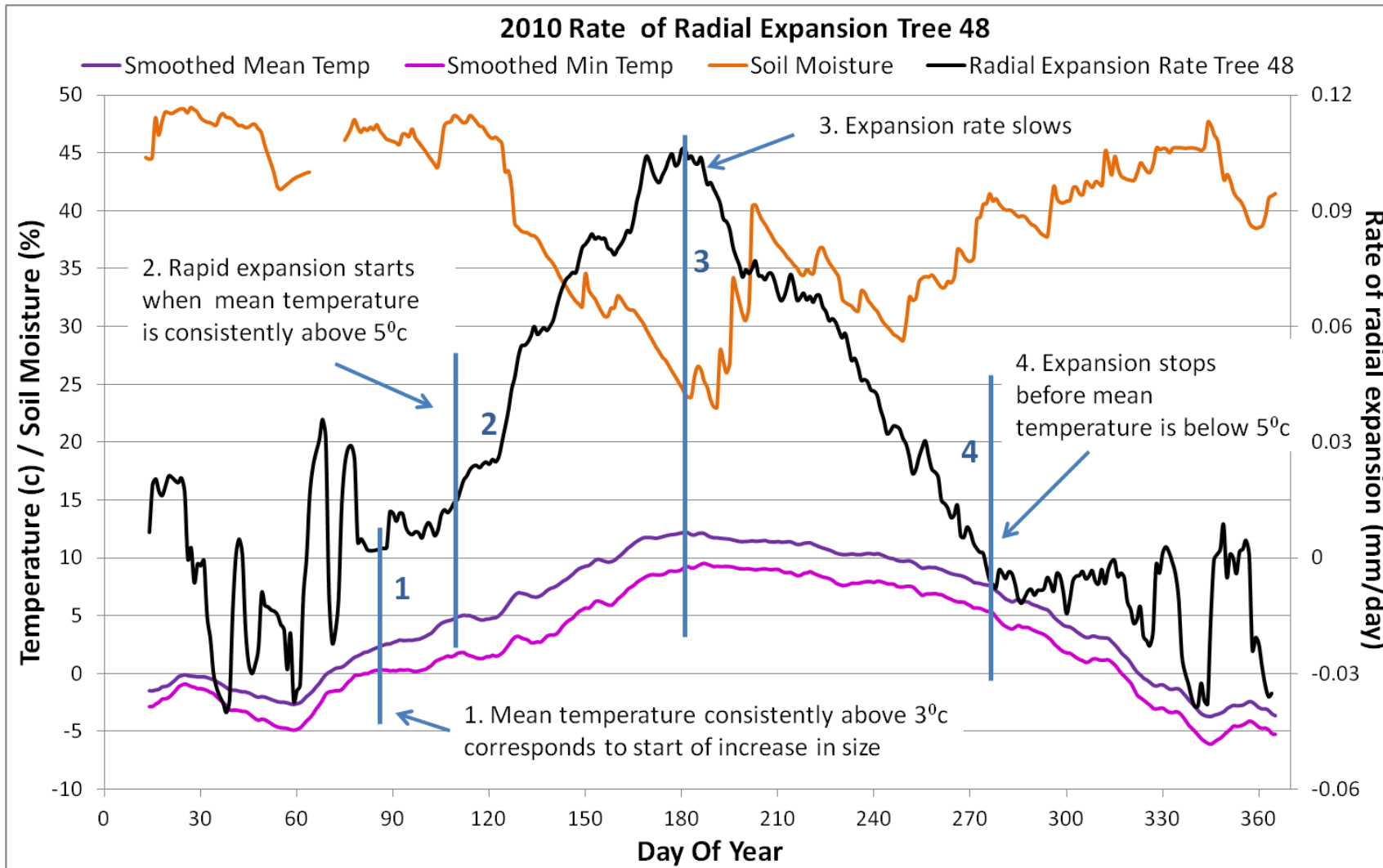


Figure 7-19: The effect of soil moisture and temperature on the radial expansion rate of Tree 48 at Griffin during 2010.

Prior to the growing season starting in 2010 there was a sustained period of extremely cold weather which caused large fluctuations in the size of the tree stems and this is reflected in the radial expansion rate of tree 48 at the beginning of the year shown in Figure 7-19. After the cold period slow expansion starts at around day 90 (31st March) and starts to increase more rapidly at day 103 (13th April) around the same time which mean temperature rose above 5°C. The radial expansion rate continues to increase until approximately day 181 (30th June) when it starts to decrease again and radial expansion stops around day 274. During the growing season of 2010 there was a marked decrease in soil moisture corresponding to the period of highest radial expansion rate and also corresponds to the time when the radial expansion rate starts to decline. When soil moisture decreases to 30% there seems to be a corresponding dip in radial expansion rate in tree 48, although there is a slight recovery after this before radial expansion rate starts to decline towards the end of the growing season.

Since there were problems with the equipment during 2010 on tree 8 the measurements are not shown along with the other trees in Figure 7-20. In this, following a similar trend to tree 48, tree 43 starts to slowly expand at around day 88 (29th March) before radial expansion rate increases rapidly at around day 122 (2nd May). Radial expansion rate peaks at day 165 (14th June) and stops at day 269 (26th September). Tree 15 starts a period of rapid expansion around day 90 (31st March) which peaks at day 116 (26th April) followed by a sudden drop in the radial expansion rate until about day 126 (6th May). The rate then increases again and peaks at day 169 (18th June) before decreasing and radial expansion stops around day 268 (25th September). Although tree 66 starts to increase at around the same day as the other trees the rate of radial expansion is much slower starts to decrease earlier in the year (day 185) and radial expansion stops earlier in the year (approximately day 240). Similar to tree 48, when soil moisture decreases to 30% the radial expansion rate of trees 43 and 15 starts to decline, but unlike tree 48 they continue to decline until radial expansion stops at the end of the season. This is the same effect as seen earlier in 2008.

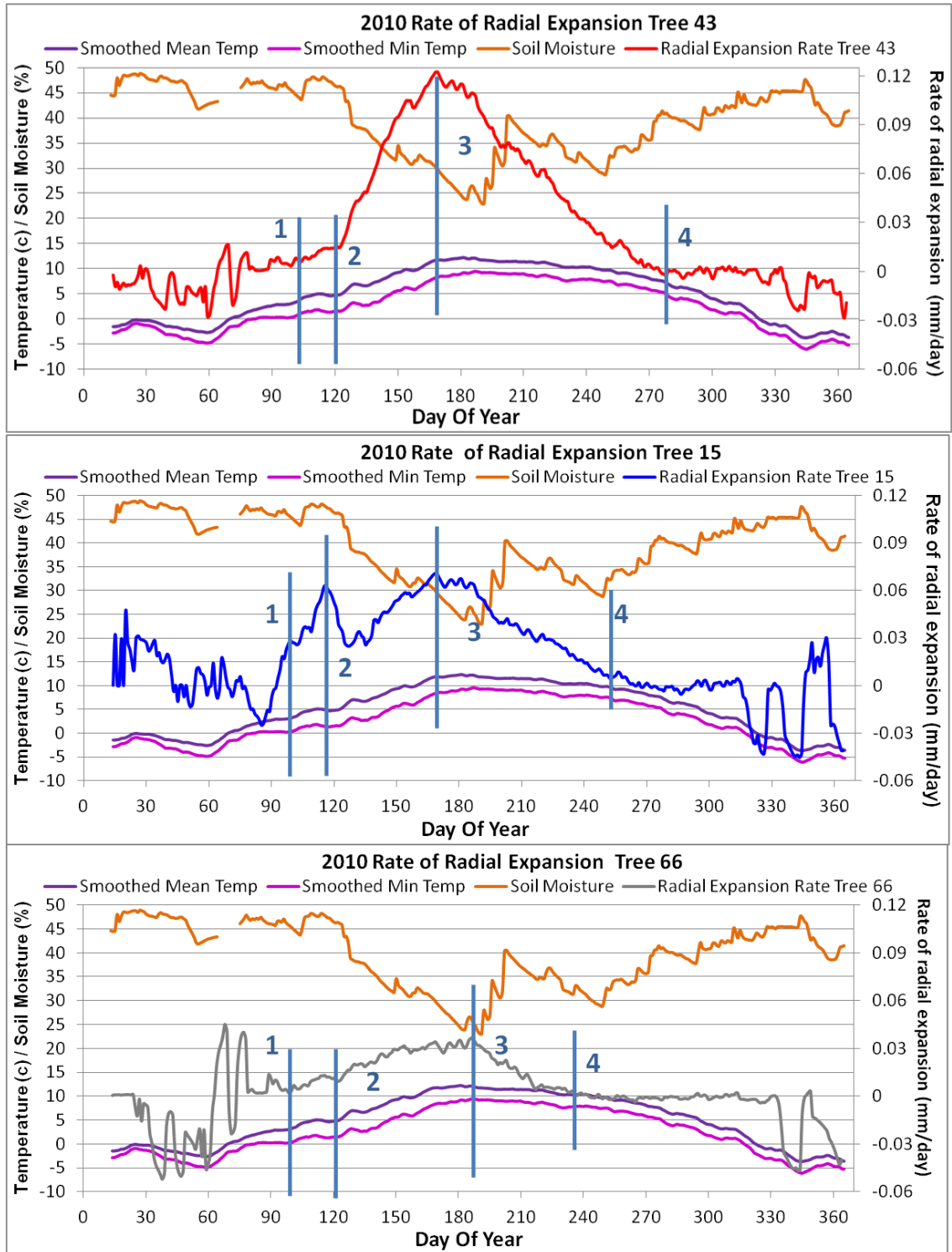


Figure 7-20: The effect of soil moisture and temperature on the rate of radial expansion of Trees 43, 15 and 66 at Griffin during 2010.

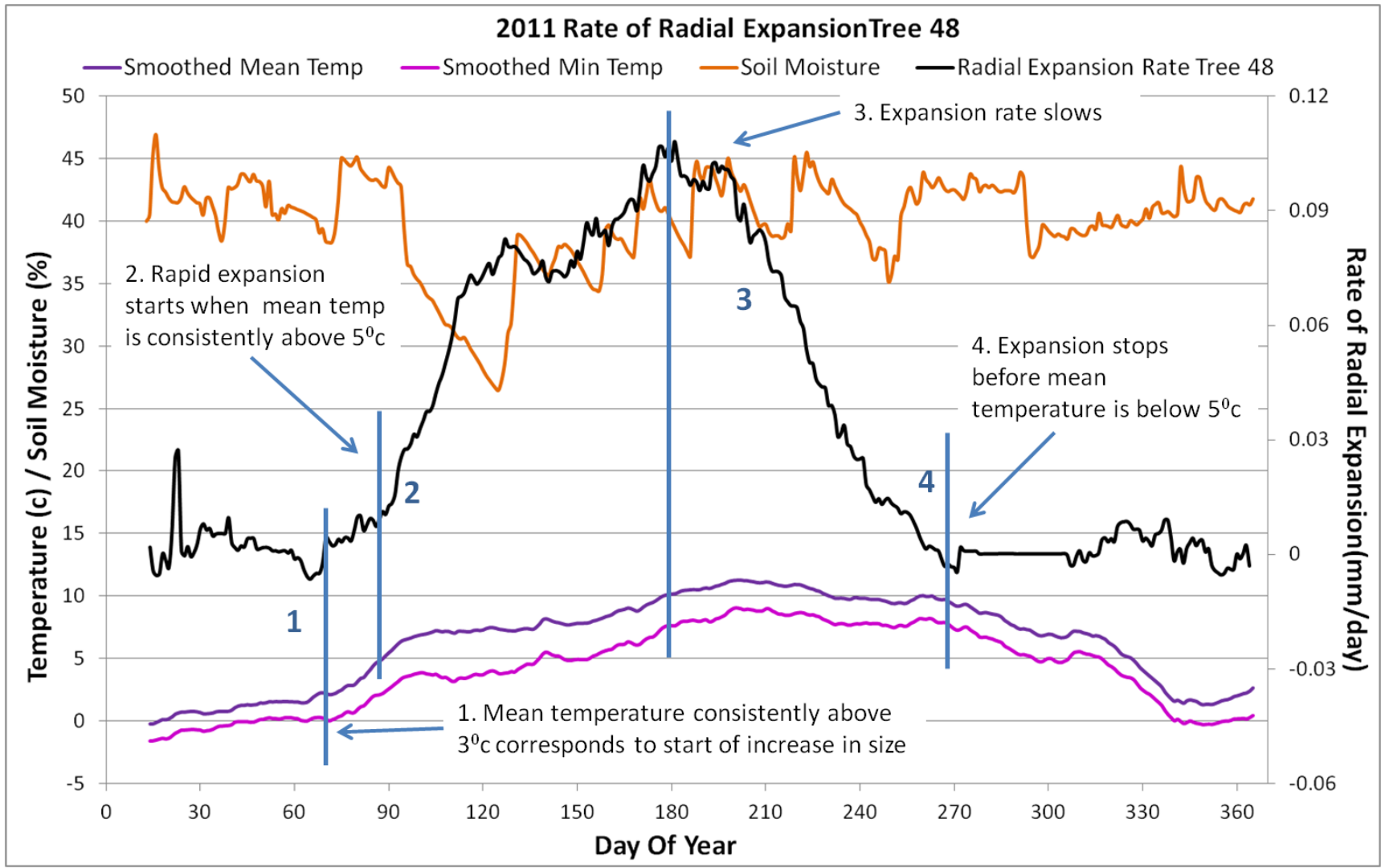


Figure 7-21: The effect of soil moisture and temperature on the radial expansion rate of Tree 48 at Griffin during 2011

The rate of radial expansion of tree 48 during 2011 is shown in Figure 7-21. The stem starts to expand on day 70 (11th March) before radial expansion rate increases rapidly on day 88 (29th March) corresponding to the same day that mean temperature rose above 5°C. The radial expansion rate slows slightly from approximately day 127 (7th May) to 146 (26th May) before rising again and peaking around day 181 (30th June). Following this the radial expansion rate decreases sharply until radial expansion stops on day 265 (22nd Sept). Towards the end of the year mean temperature drops below 5°C around day 325 (21st Nov). Although relatively high for the remainder of the year, soil moisture decreases early in the growing season which corresponds to the time when a decrease in radial expansion rate is seen, around day 127.

Problems continued with the equipment on tree 8 during 2011 and Figure 7-22 shows the radial expansion rate for trees 43, 15 and 66 during 2011. The radial expansion rate for tree 43 and 15 are lower than seen in previous years leading to lower radial expansion in these trees. Expansion starts for all three trees around the same time around day 70 (11th March) and there are increases in the radial expansion rate around day 90 (31st March). Tree 43 radial expansion rate peaks around day 140 (20th May) then slows slightly and remains relatively constant until decreasing again in late summer (day 203 - 22nd July) and stopping around day 260 (17th Sept). The radial expansion rate for tree 15 also peaks and reaches a plateau between days 125 to 199 (5th May to 18th July) before decreasing and stops expanding around day 249 (6th Sept).

Although tree 66 starts to increase at around the same day as the other trees the rate of radial expansion is much slower starts to decrease earlier in the year (approx. day 163 - 12th June) and radial expansion stops earlier in the year (approximately day 240 - 28th Aug).

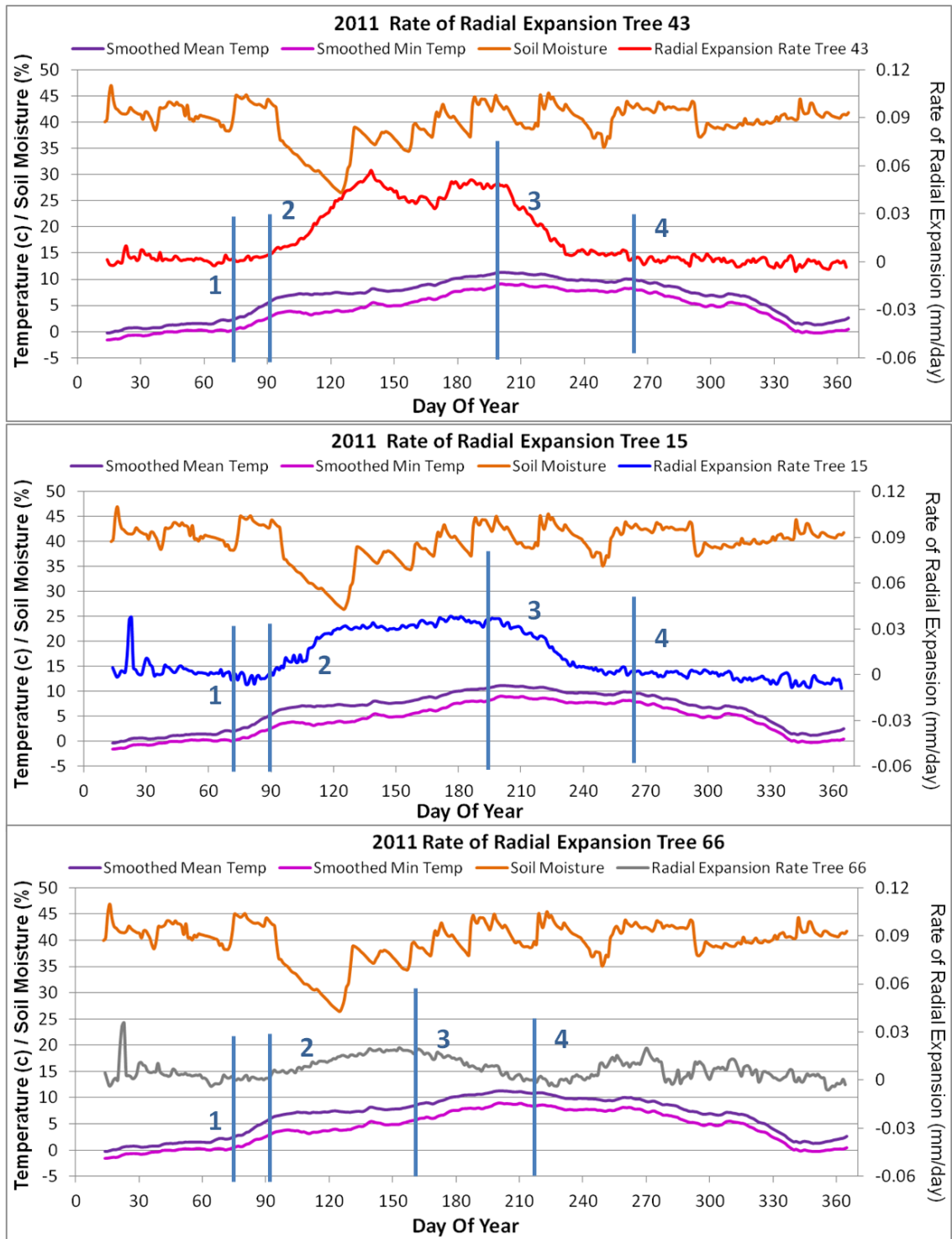


Figure 7-22: The effect of soil moisture and temperature on the radial expansion rate of Trees 43, 15 and 66 at Griffin during 2011.

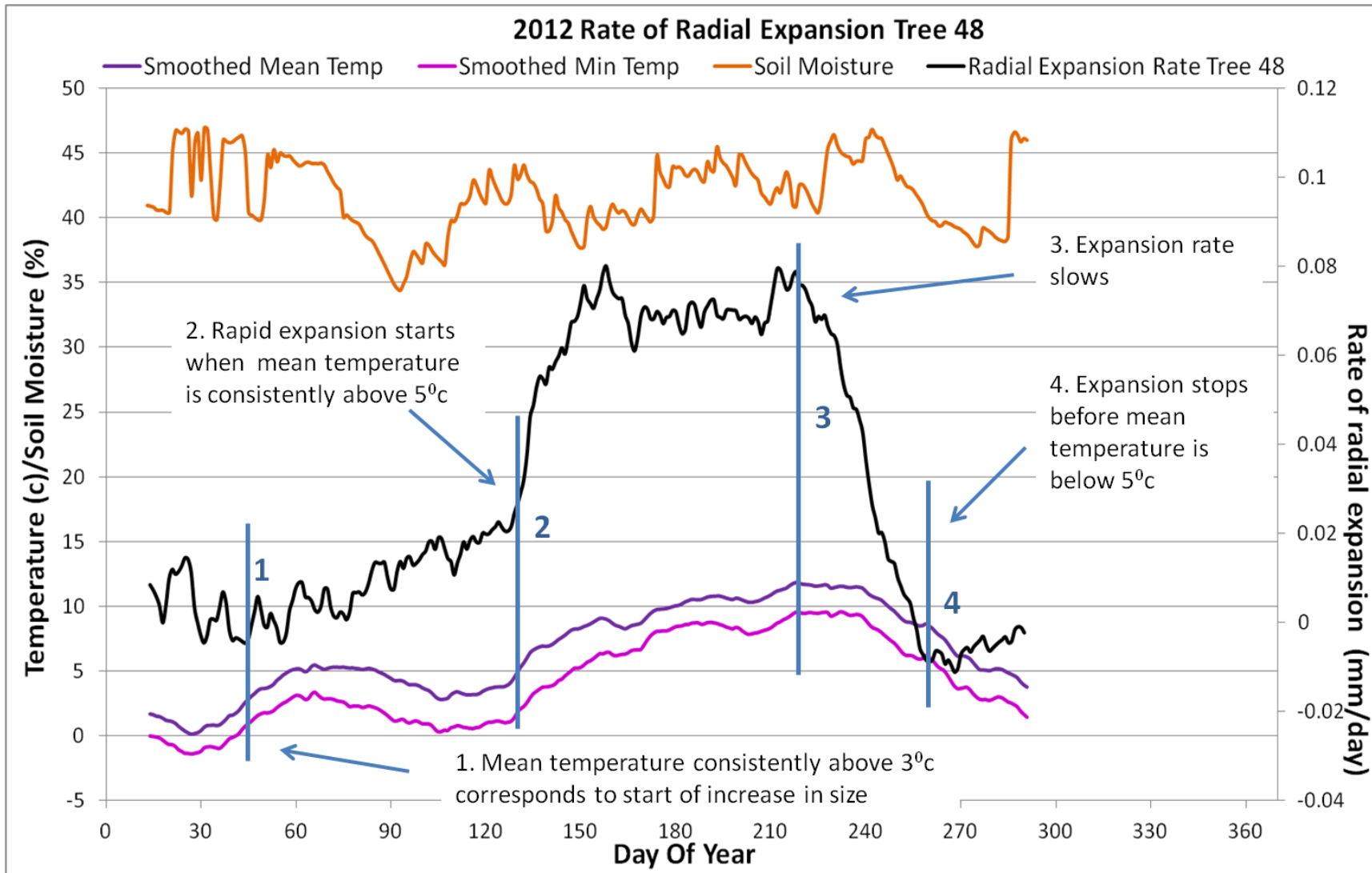


Figure 7-23: The effect of soil moisture and temperature on the radial expansion rate of Tree 48 at Griffin during 2012.

The beginning of 2012 shows a slightly different pattern of temperature than the previous years. Not only was the preceding winter period milder there was a period of increasing temperature early in the year before temperatures dropped again. This resulted in mean temperatures being above 3°C consistently from mid February although temperatures were not consistently above 5°C until the beginning of May. Figure 7-23 shows that this resulted in a much longer period of slow increment gain, from approximately day 75 (16th March) to day 128 (8th May), before the period of rapid radial expansion when mean temperatures eventually rose above 5°C. The radial expansion rate for tree 48 peaked then continued at a steady rate from day 157 (6th Jun) before starting to slow down after day 218 (7th August). However the time when tree 48 stopped expanding was similar to that seen in previous years (day 255 - 13th Sept) leading to a shorter growing season and to the decrease in the amount of radial expansion seen on the tree.

This same effect can be seen in the radial expansion of trees 43 and 15 during 2012 shown in Figure 7-24. Both have a longer period of slow expansion at the beginning of the season which lasts through the dip in temperature until mean temperature consistently rises above 5°C on at day 130 (10th May). Both trees start to slow down around day 190 (9th July) and growth stops around day 250 (7th Sept) which is similar to that seen in previous years. As seen in previous years, tree 66 has a much slower radial expansion rate than the other trees, although in 2012 the increase in radial expansion rate, decline in radial expansion rate and the date that radial expansion stops occur at a similar time to the other trees investigated.

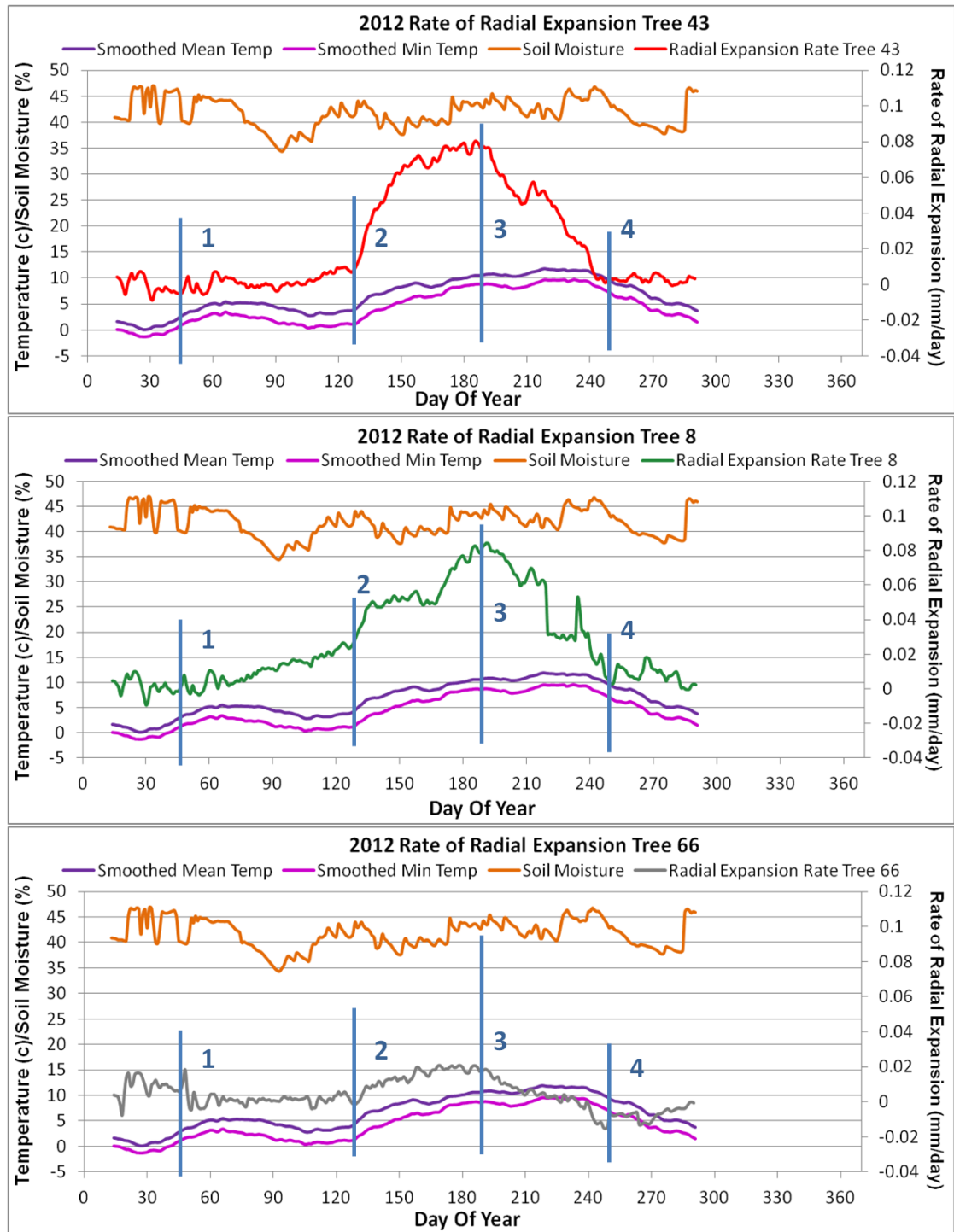


Figure 7-24: The effect of soil moisture and temperature on the radial expansion rate of Trees 43, 8, and 66 at Griffin during 2012.

The day of the year when trees start expanding are plotted against the day of the year that the mean temperature is consistently above 5°C in Figure 7-25. This shows that trees start to expand at a similar time to each other which coincide with when temperatures rise above 5°C each year. Since this is different for each of the years investigated it suggests that the main driver for the start of the growing season is temperatures rising above 5°C.

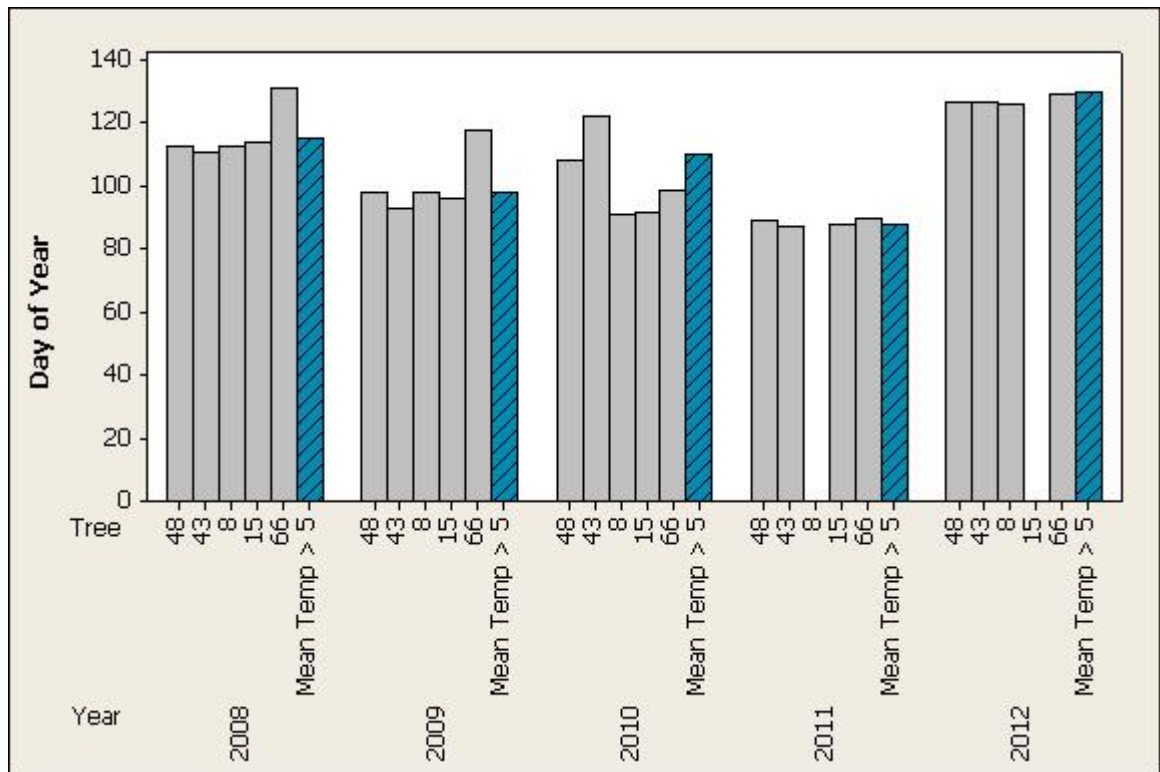


Figure 7-25: Shows the day of the year that the radial expansion rate starts to rapidly increase along with when temperature is greater than 5°C

At Griffin the day the mean air temperatures reach 3°C was also plotted for each year against the day that the trees showed a slow increase in size (Figure 7-26) and again there are not only similarities as to when this occurs between trees but also occurs at a similar time to minimum temperatures rising above 3°C.

The day that radial expansion stops was also plotted for each tree (Figure 7-27) showing that it not only occurs at a similar time for each tree but also occurs at a similar time each year and this is before the mean temperature drops below 5°C.

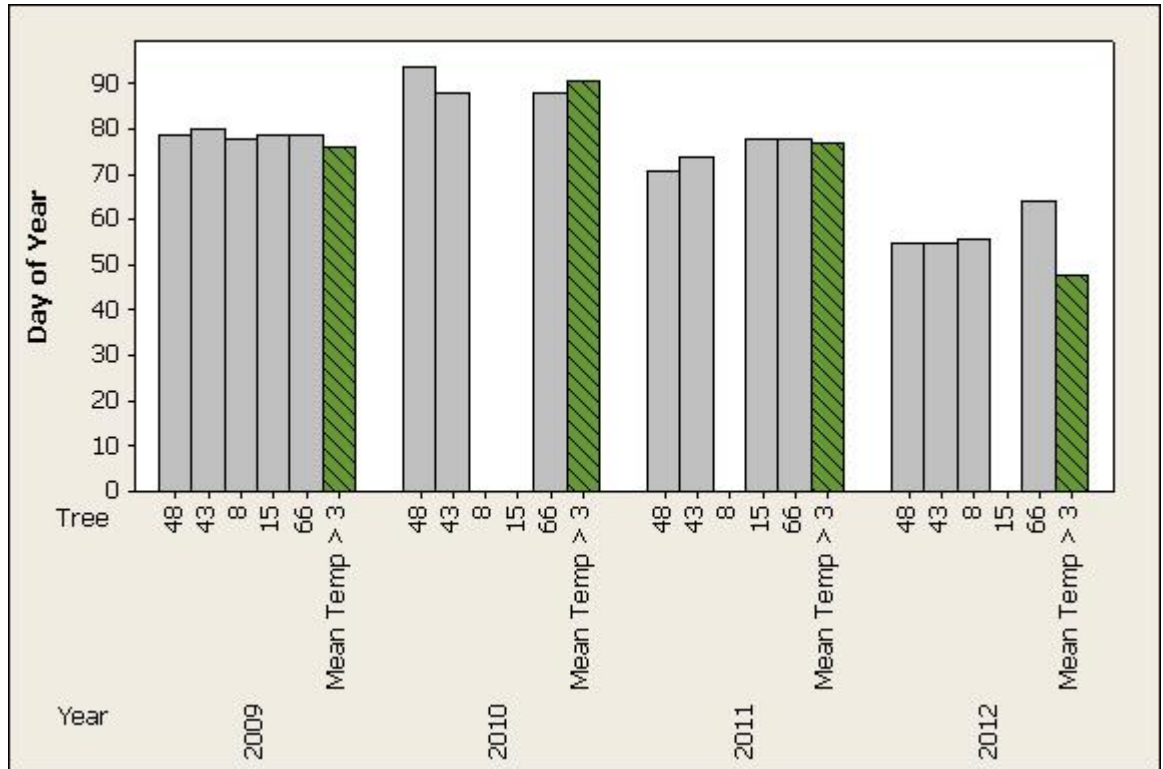


Figure 7-26: Shows the day of the year that the slow expansion of the trees starts and when the mean temperature is greater than 3°C

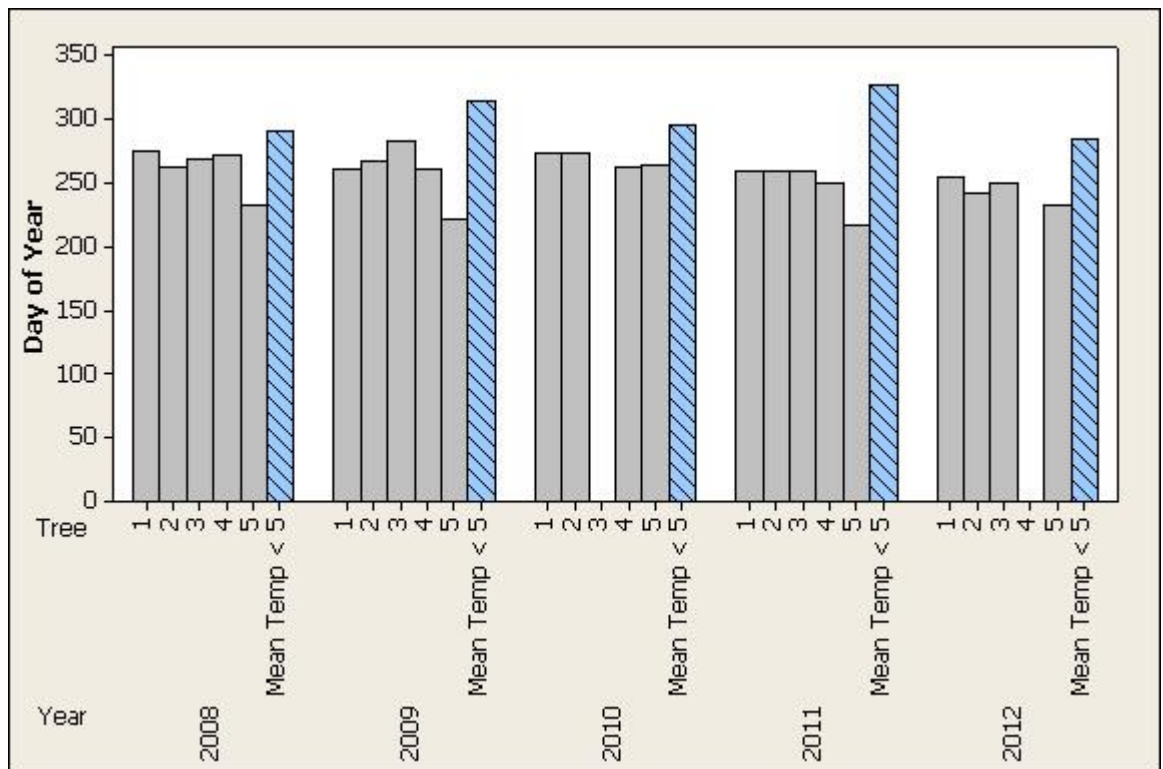


Figure 7-27: Shows the day of the year that the radial expansion stops along with the days that the mean temperature is consistently below 5°C.

Although there are some differences between years in the timing of when the radial expansion rate starts to decrease it is similar between the different trees each year (Figure 7-28).

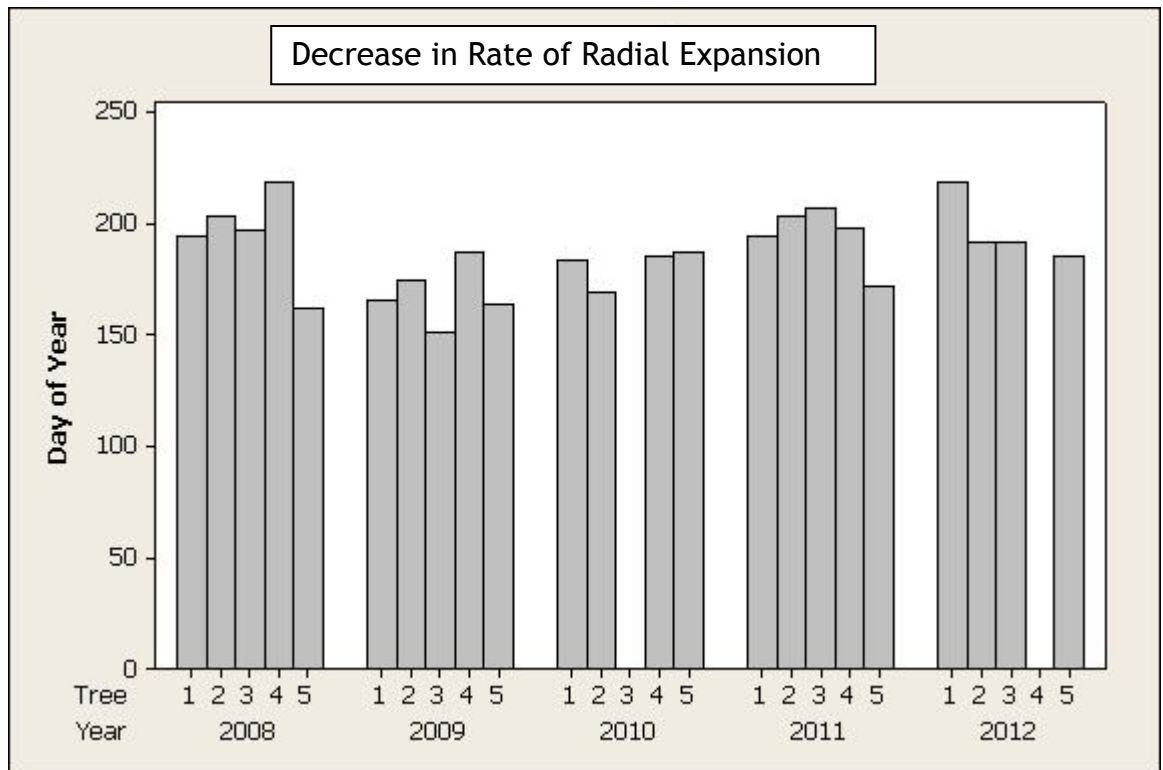


Figure 7-28: Shows the day of each year that the radial expansion rate of the trees at Griffin starts to decrease.

7.1.3.4 Soil Moisture and Precipitation Effect on Maximum Daily Expansion

In order to investigate the effect of soil moisture further, the radial expansion data for the period when radial expansion was taking place was detrended by subtracting the smoothed 30 day moving average value from the maximum daily radial expansion value. This allowed the daily maximum value to be plotted without the influence of the radial expansion trend. An example of how this was done is shown for tree 48 in 2011 is shown in Figure 7-29.

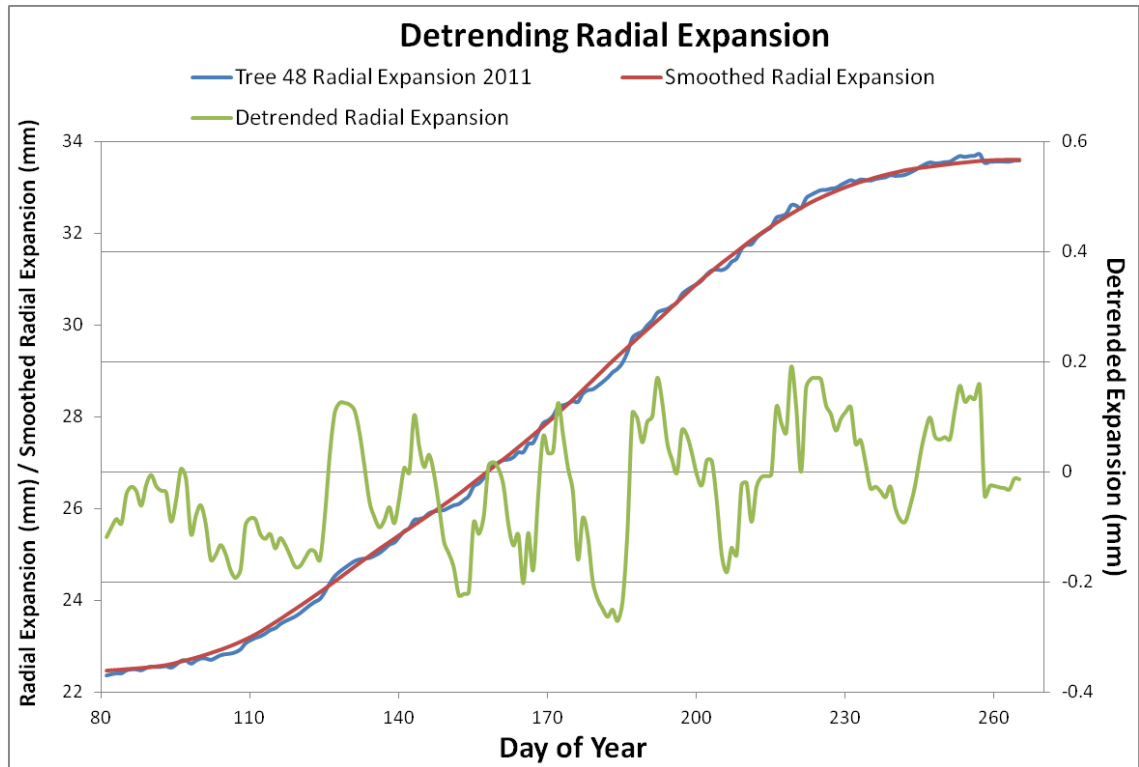


Figure 7-29: Example of detrending the radial expansion curve for tree 48 in during the growing season of 2011. The detrended value was calculated by subtracting the 30 day moving average smoothed radial expansion value from the radial expansion value for the same day.

Once the maximum daily expansion of the stem has been detrended in this way a comparison was made to soil moisture for the period of radial expansion of each tree for each year. The daily changes in the maximum stem size appear to coincide with changes in soil moisture with a lot of the peaks in both (though not all) occurring at the same time. Examples of this for each tree each year are shown in Figure 7-30 to Figure 7-39.

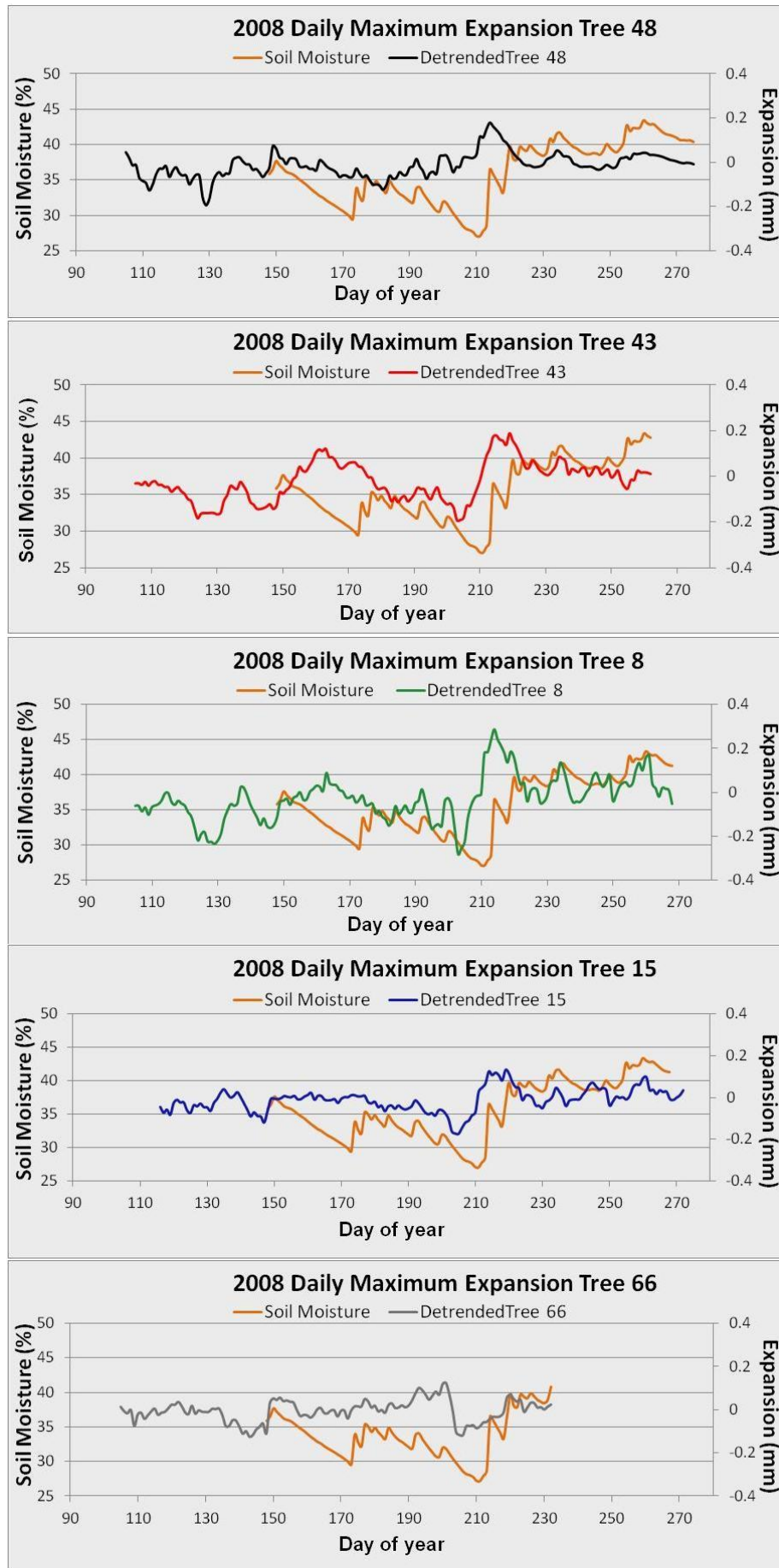


Figure 7-30: The detrended maximum daily expansion measured for each tree plotted against the mean daily soil moisture value for the period where growth was occurring during 2008.

During the growing season of 2008 (Figure 7-30), the maximum daily expansion of each tree is closely aligned, with peaks occurring at the same time (although to different magnitudes). There are two periods where soil moisture declines (from approximately day 150 to 175 and from day 200 to 210). The first of these dips during the season leads to little effect on the maximum daily expansion in tree 43, 15 and 66, but trees 43 and 8 show an increase during this period. For the second dry period, later in the season, most trees show a dip in the maximum expansion as the soil moisture reaches a level of 30%. This is followed by an increase which starts prior to the recovery of soil moisture. At the end of the growing period there is a time where soil moisture and the expansion look to be linked (from approximately day 220 to day 270).

In some years soil moisture is seen to decline during the period when radial expansion rate starts to decline although may be connection is unclear (Section 7.1.3.3). However, since low soil moisture could be caused by tree uptake or lack of rain during the summer soil moisture for 2008 was plotted against rainfall for the same period (Figure 7-31) and shows that the drop in moisture seen at approximately day 210 may have been due to a period of low rainfall which would be compounded by the fact that this is also a period of high water uptake by the tree. Periods of low rainfall outside the growing season do not show this same drop in soil moisture e.g. days 320 to 340 in Figure 7-31.

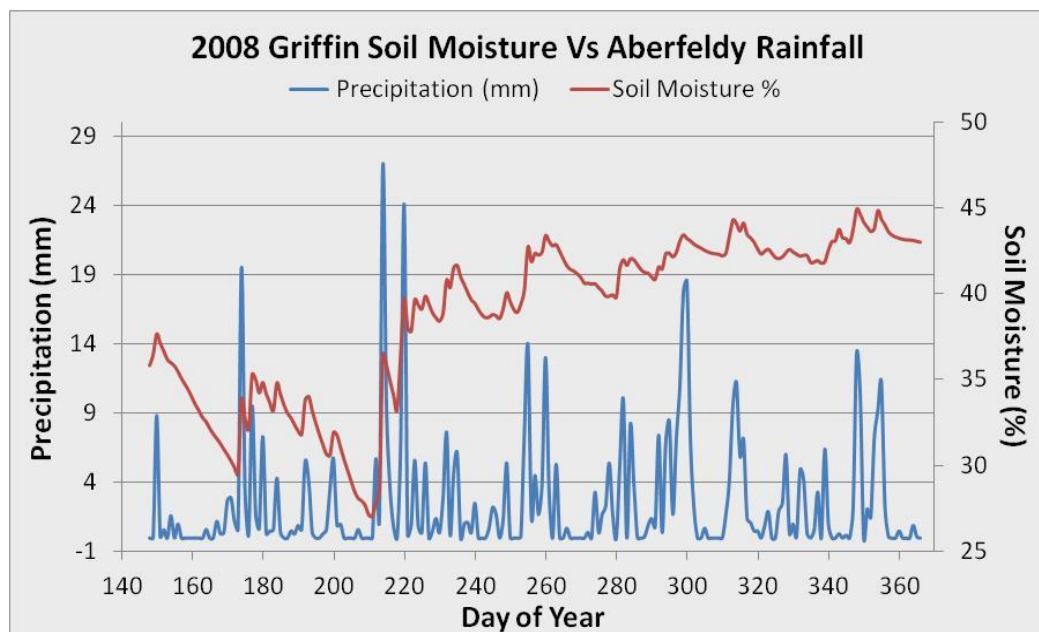


Figure 7-31: Soil moisture measured at Griffin plotted against rainfall at Aberfeldy for year 2008. A period of low soil moisture at approximately day 210 corresponds to a period relatively low rainfall.

By superimposing the rainfall data on to the maximum daily expansion data it shows that the peaks in daily expansion occur at similar times in each tree and these often correspond closely to rainfall events (Figure 7-32)

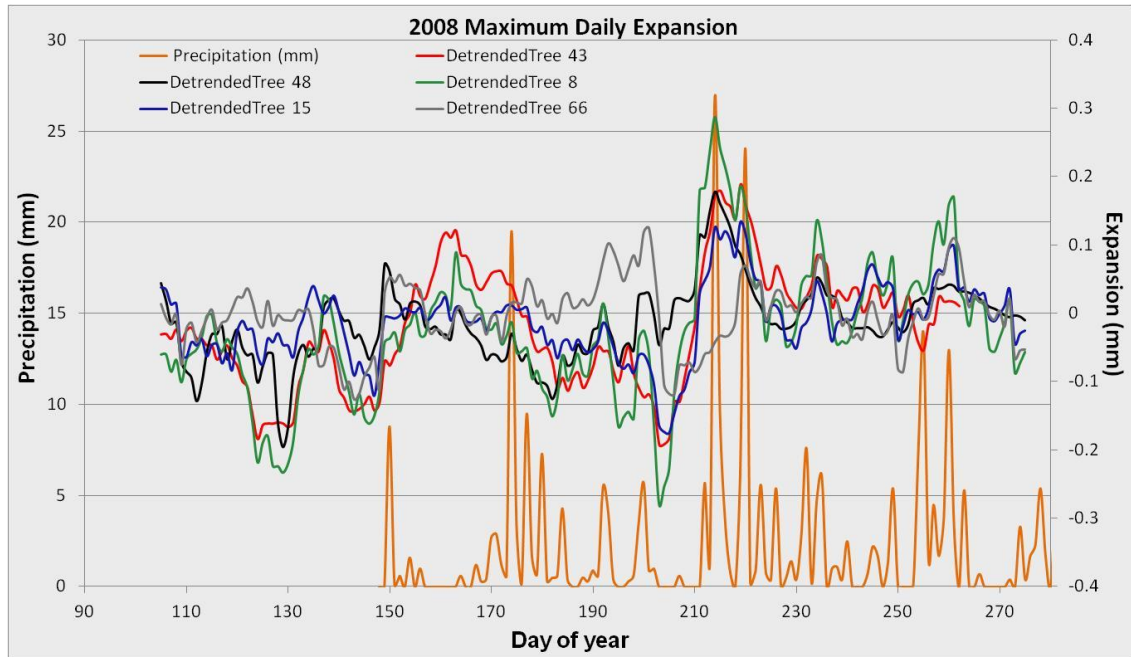


Figure 7-32: Rainfall measured at Aberfeldy weather station compared to the maximum daily expansion of trees for the same period during 2008.

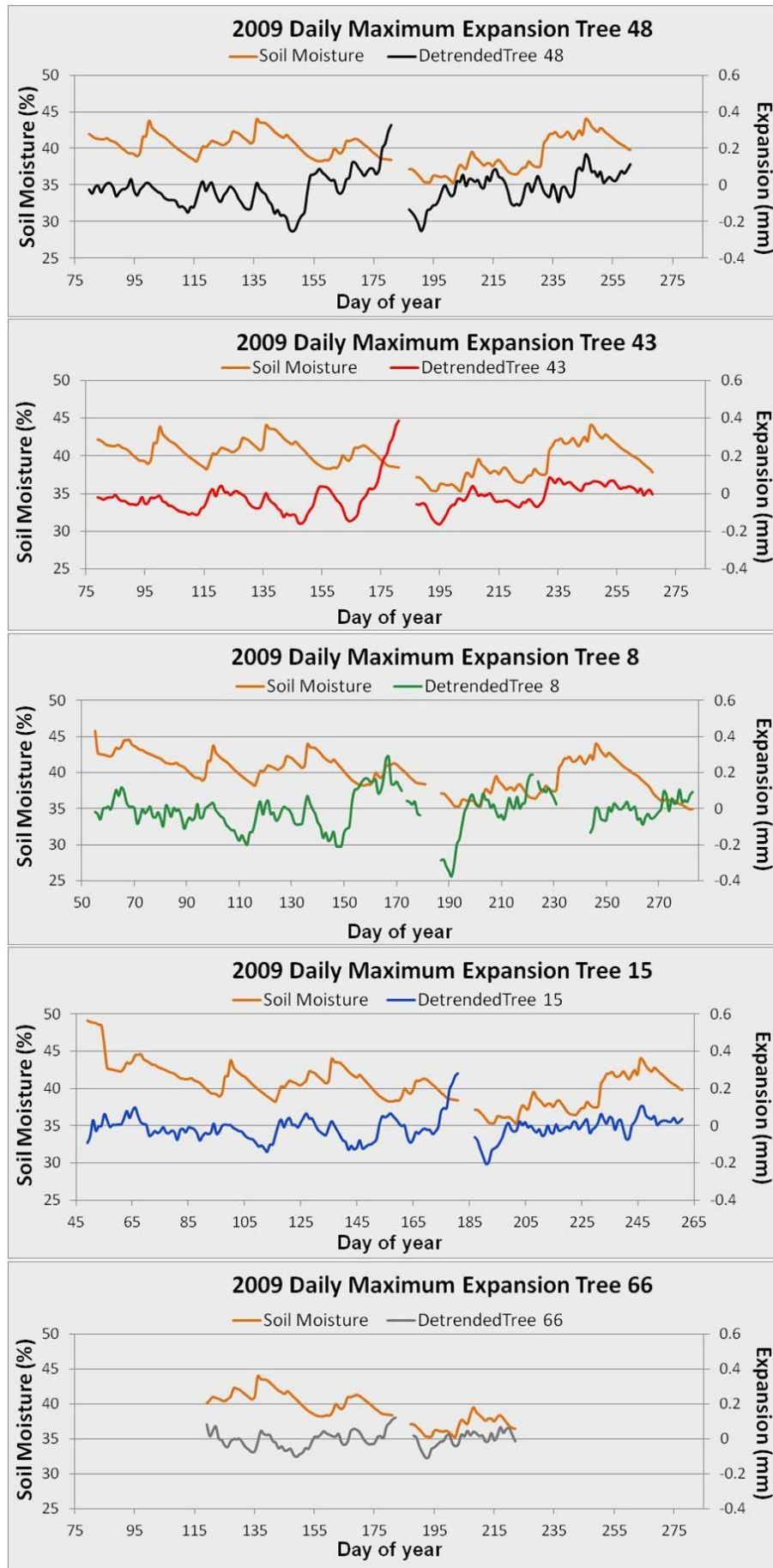


Figure 7-33: The detrended maximum daily expansion measured for each tree plotted against the mean daily soil moisture value for 2009.

Figure 7-33 shows there are no clear impact as moisture does not reach a sub optimal level. However peaks in soil moisture do, again, appear to correspond to peaks in the maximum daily expansion of the trunk. When the maximum daily expansion is plotted against rainfall (Figure 7-34), it shows again that many of the peaks in daily expansion correspond to rainfall events.

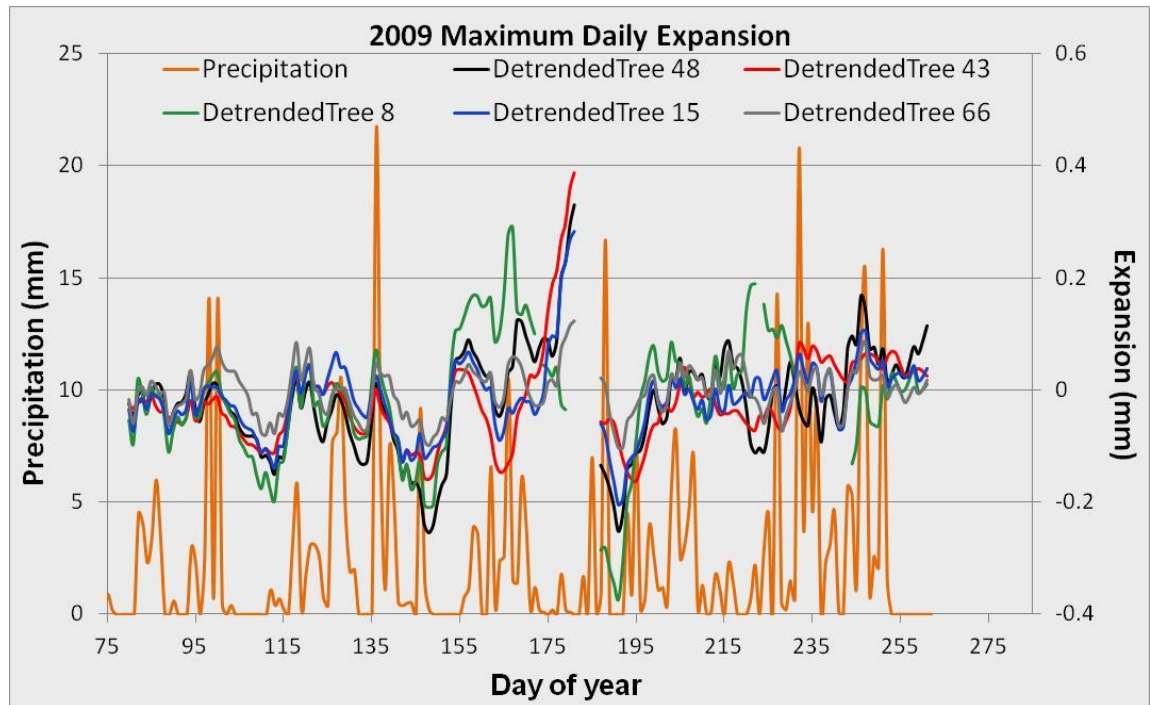


Figure 7-34: Rainfall measured at Aberfeldy weather station compared to the maximum daily expansion of trees for the same period during 2009.

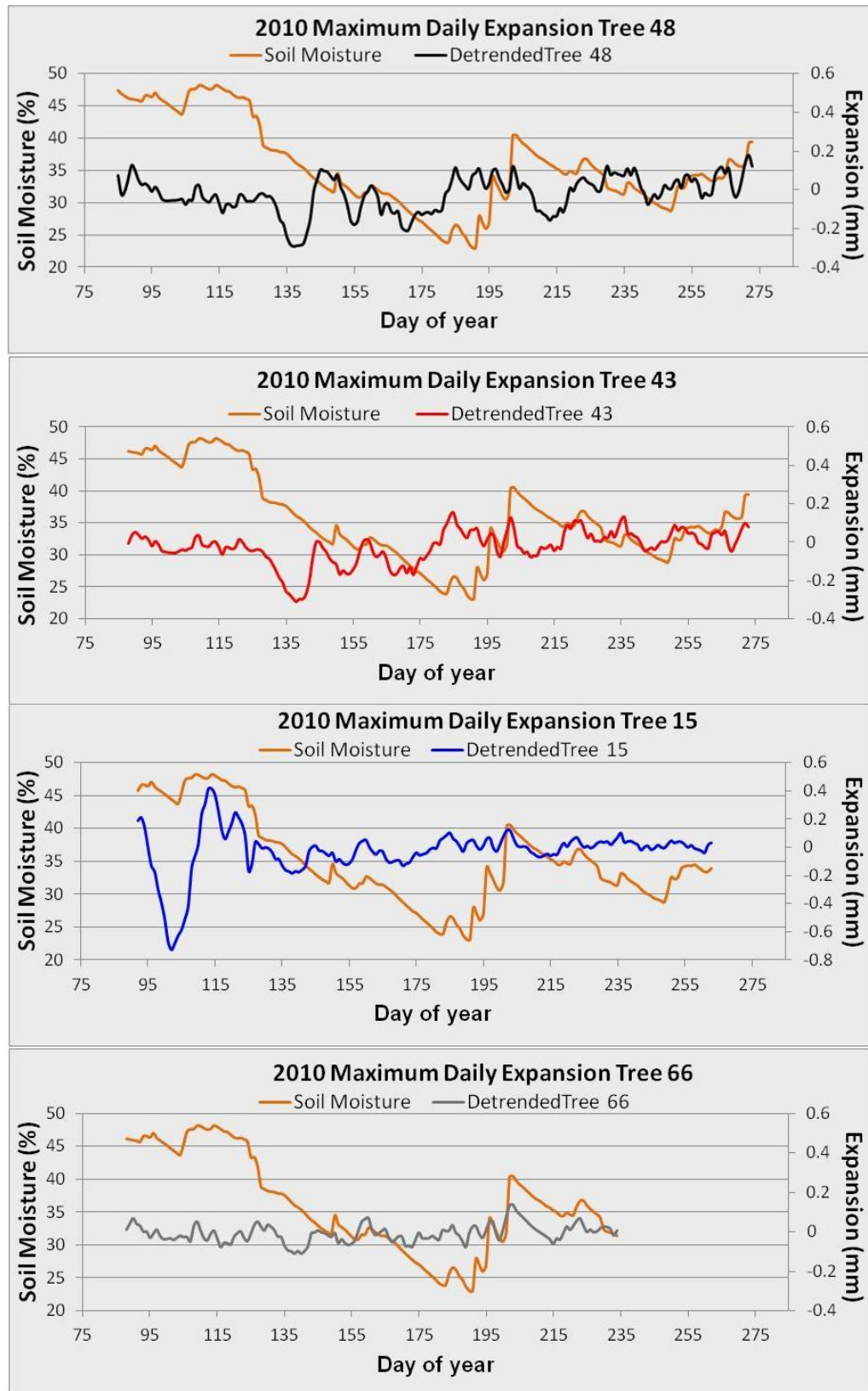


Figure 7-35: The detrended daily maximum expansion measured for each tree plotted against the mean daily soil moisture value for 2010.

2010 saw the largest dip in soil moisture seen in any of the years investigated at Griffin, however this does not seem to have an effect on the overall amount of radial expansion as this was one of the most productive years, as shown earlier

(Figure 7-13), and also does not seem to have had an impact on the daily expansion which, although there were fluctuations remained relatively consistent throughout (Figure 7-35). There does, however, seem to be another signal at approximately day 135 where there is a consistent dip across all trees. Although the reason for this dip is unclear it may coincide with a period of low precipitation (Figure 7-36).

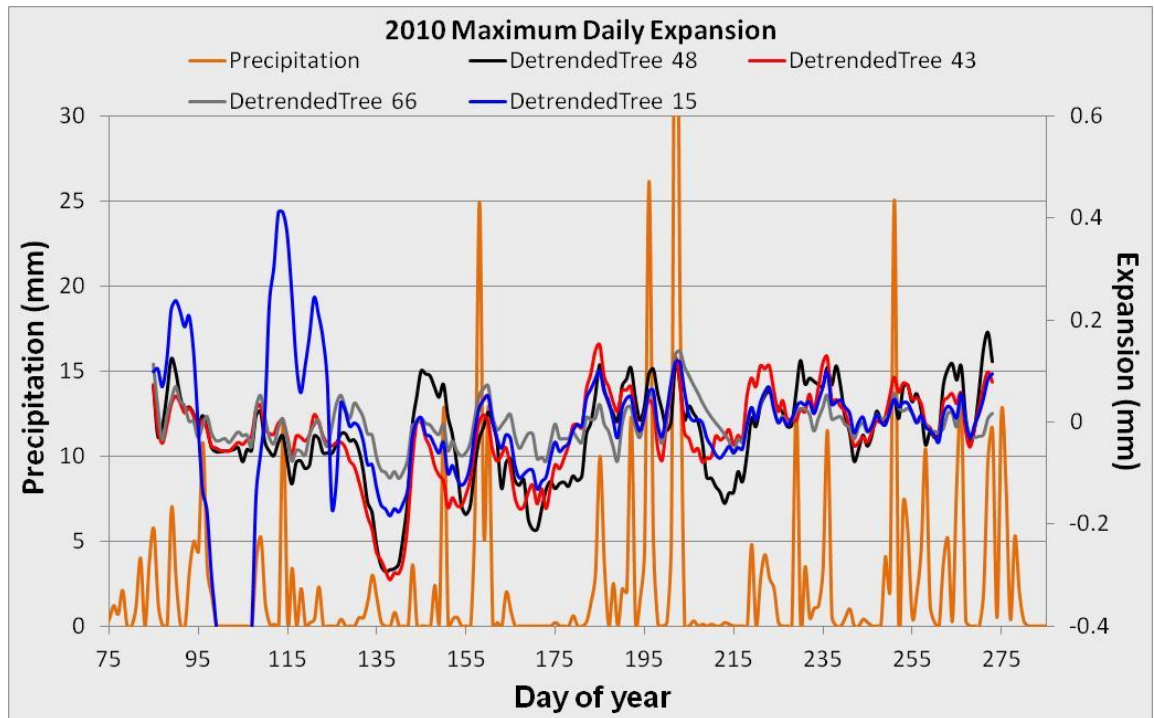


Figure 7-36: Rainfall measured at Aberfeldy weather station compared to the maximum daily expansion of trees for the same period during 2010.

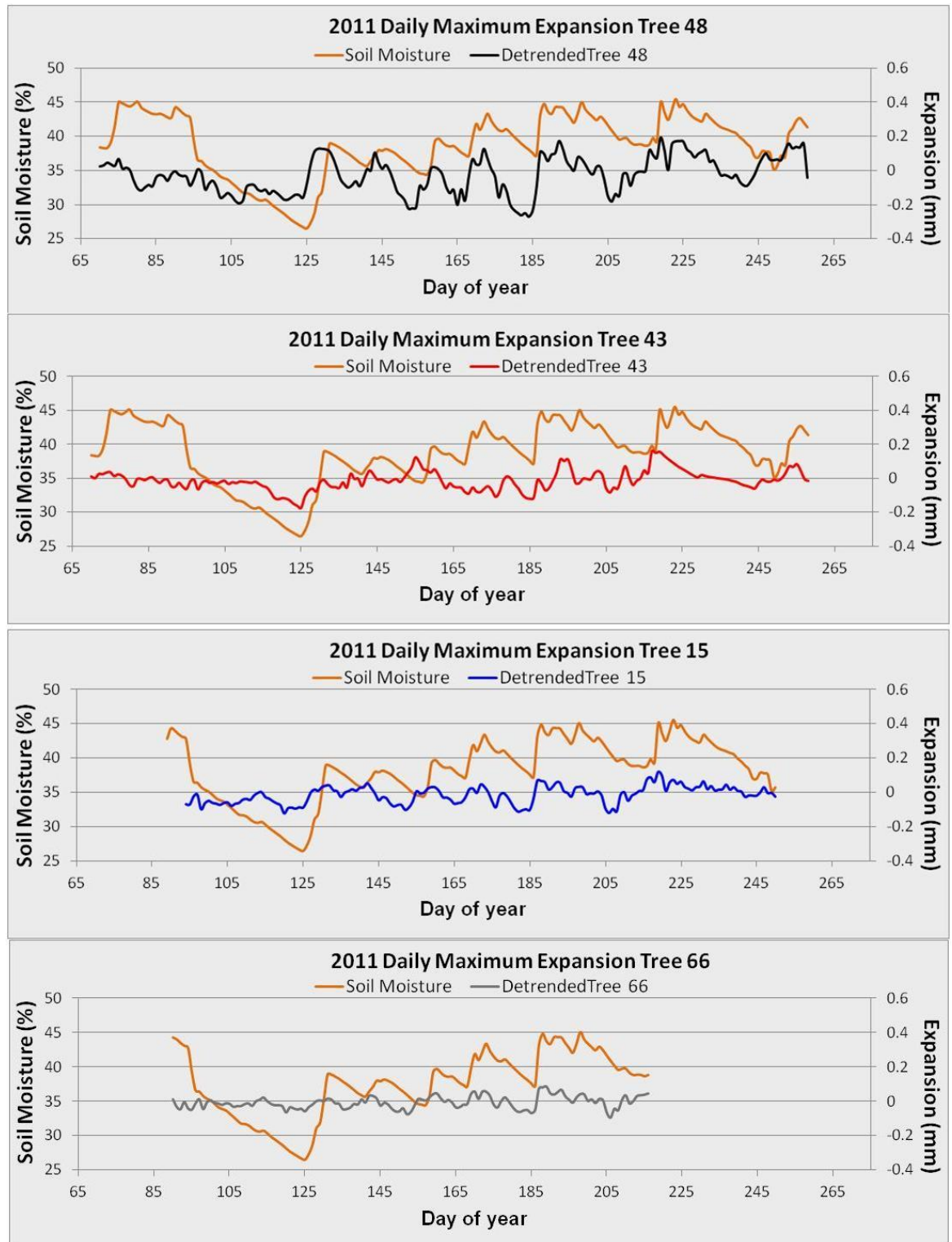


Figure 7-37: The detrended daily maximum expansion measured for each tree plotted against the mean daily soil moisture value for 2011.

There appears to be a clear linkage between the maximum daily expansion and soil moisture during 2011 from approximately day 130 onwards (Figure 7-37) which is consistent across all trees measured and this is also translated into a link with rainfall events (Figure 7-38) which seem to be higher and more consistent than the other years investigated.

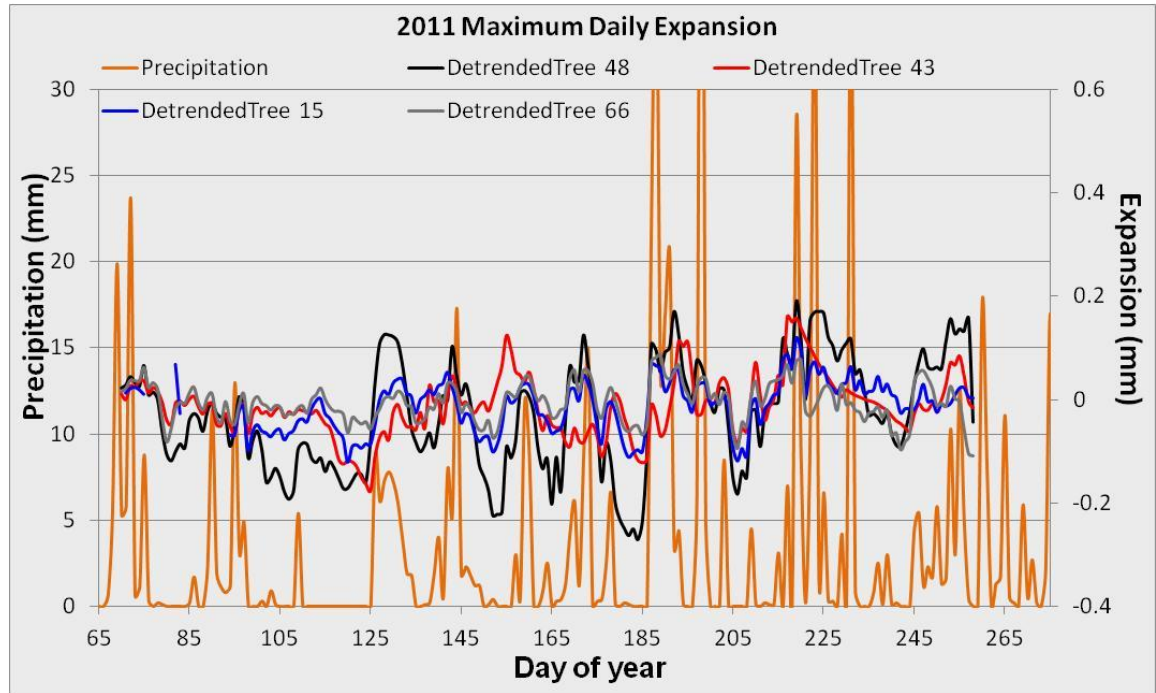


Figure 7-38: Rainfall measured at Aberfeldy weather station compared to the maximum daily expansion of trees for the same period during 2011.

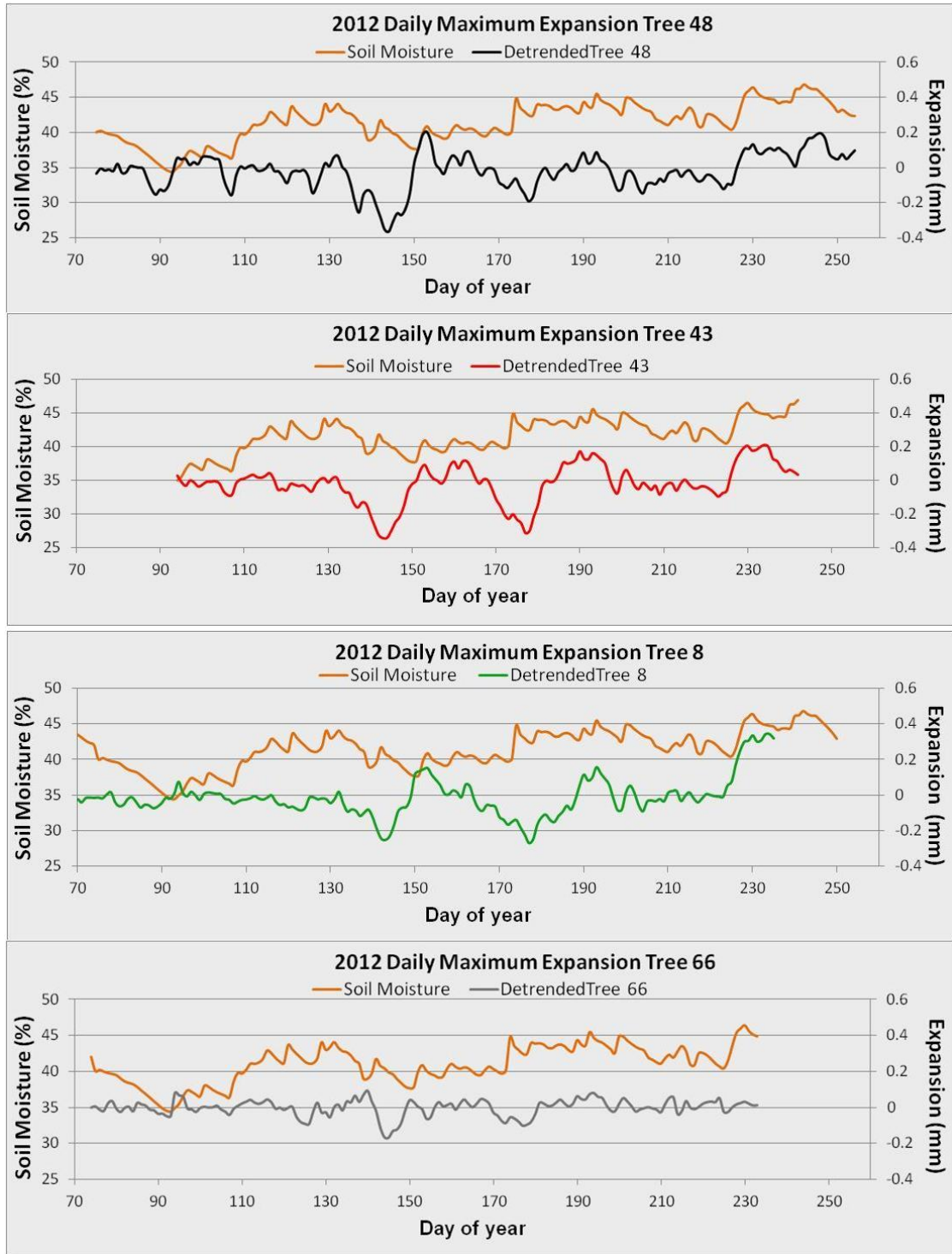


Figure 7-39: The detrended daily maximum expansion measured for each tree plotted against the mean daily soil moisture value for 2012.

Figure 7-39 shows a dip in the daily expansion around day 145 and again on approximately day 175 consistently across all trees although this does not seem to be connected to soil moisture. When plotted against rainfall (Figure 7-40) the first dip corresponds to a period of low rainfall, consistent with previous years. However for the dip around day 175 corresponds to a period of relatively high rainfall.

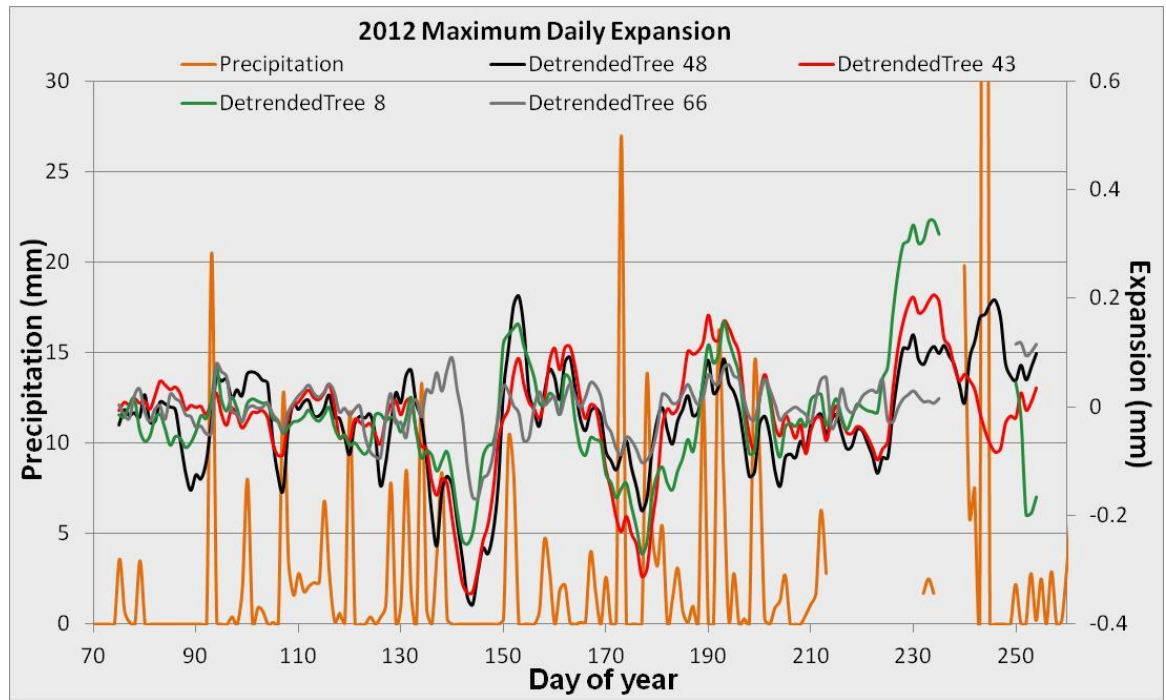


Figure 7-40: Rainfall measured at Aberfeldy weather station compared to the maximum daily expansion of trees for the same period during 2012.

7.2 : Harwood Site

Since Griffin site was already set up at the beginning of this study, it was decided that a new “control” site would be set up using the same measurements so that any variability between the sites could be evaluated.

7.2.1 Site Selection

The second site used was at Harwood Forest in Northumberland in the North East of England (NY 398510 591340) (Figure 7-1). Harwood was chosen as it has previously been used for a number of studies by The University of Edinburgh (Zerva and Mencuccini, 2005, Mojeremane et al., 2010, Ball et al., 2007). Harwood is a plantation dominated by different aged Queen Charlotte Islands provenance Sitka spruce that was first established in the 1930s with further planting in the 1950s and 1980s (Mojeremane et al., 2010). It is planted on an area that was previously upland rough pasture with soil at the site being peaty gley. The sample site within this forest consists of approx. 30-year-old trees and is situated at an elevation of 309m. The average temperature is 7.6 °C and a mean annual precipitation of 950 mm (Zerva and Mencuccini, 2005). The site characteristics of Griffin compared with Harwood site are shown in Table 7-4.

Table 7-4: Comparison of characteristics of Griffin and Harwood sites

Site	Griffin	Harwood
Age (Years)	30	27
Soil Type	Peaty gley / podsols	Peaty gley
Trees Ha ⁻¹	2200	1600
Average Tree Height (m)	18.3	22.48
Average DBH (cm)	29.7	36.26
Elevation (m)	340	309
Mean Annual Temperature (°C)	8.2	7.6
Mean annual Precipitation (mm)	1200	950

Within the site chosen there was currently no research being undertaken and therefore a new sample area had to be set up, although as a result of the previous studies there was mains electricity. The electricity connected to a shed was able to be used to ensure that the batteries from which the instruments and loggers run were constantly recharged negating the loss of power problems experienced at Griffin.

7.2.2 Tree Selection

Tree selection was done during April 2010 by plotting a rectangular area (20m x 50m) within the forest of approximately 100 trees (total number of trees in the area discounting dead trees was 92). Within this plot the trees were numbered from 1 to 92 and the diameter at breast height (DBH) of all the trees measured. The trees were then divided into quartiles dependant on the DBH and 5 trees from the dominant quartile (i.e. largest DBH) which had no major physical defects were randomly selected to be used for dendrometer measurements. Dominant trees are selected so that the effect of competition from other trees is minimised. Details of the 5 trees selected are shown in Table 7-5.

Table 7-5: Number, diameter at breast height (DBH) and height of the trees selected at Harwood forest in April 2010

Tree Number	LVDT Number	DBH (cm)	Height (m)
19	1	36.5	23.1
1	2	38.3	22.8
41	3	34.3	25.0
28	4	41.0	21.0
14	5	31.2	20.5

7.2.3 Method

The Harwood site was set-up to run a series of measurements similar to those recorded at Griffin including radial expansion of the trees, tree wood and metal beam temperatures, soil moisture, air temperature, relative humidity.

Whilst the Griffin site was already set-up before the current study started and measurements have been taken since 2008 (Vihermaa, 2010), the Harwood site looked to replicate the set up of Griffin, but since it was a new experiment all of the equipment had to be sourced, built, programmed and installed from the beginning. A full list of equipment used can be found in Appendix 1.

Tree radial expansion was measured using Linear Variable Displacement Transducer (LVDT) probes (one per tree), fixed to the tree using stainless steel beams, which are then insulated with Styrofoam. Since there are differences in the thermal expansion of wood compared to the steel beams this has to be taken into account as it could have an effect on the measurements being taken

(Sevanto et al., 2005a). In order to calculate the difference in thermal expansion, the temperature of each is measured using one thermistor temperature sensor attached to the steel beam and another inserted a small hole drilled in the tree. The measurements can then be corrected using the linear thermal expansion co-efficient for wet wood and that for the steel beam (Sevanto et al., 2005a, Vihermaa, 2010). Using this method Vihermaa (2010) reported that there was no effect due to no difference between the expansion of the wood and the steel beam.

Soil moisture was measured using 3 ThetaProbe ML2x soil moisture sensors placed within the plot area at a depth of 30 cm. Sap flow was measured using Dynamax, Inc. TDP30 Thermal Dissipation Sap Velocity Probe. Each tree had two probes, one placed on the north side of the trunk and the other on the south side. Each probe consists of two probes (one of which is electrically heated) inserted into the trunk and measures sap flow by heat dissipation in the sapwood which increases with sap flow (Granier, 1985). However, there was a problem getting the logger systems to work in the initial stages which was found to be caused by the sap flow sensors drawing too much power. It was therefore decided to discontinue the sap flow measurements so that radial expansion measurements could be obtained.

Harwood tree radial expansion was measured and logged every two minutes, with the data then being averaged to every 15 minutes once downloaded. Temperature, humidity and soil moisture was measured and logged every 15 minutes. The site was visited every two weeks during the growing season to download data from the dataloggers, reset the dendrometers and also to take microcores as described for Griffin.

Whereas the Griffin site had one datalogger to cover the measurements of all five trees, at Harwood there were four Campbell CR1000 data loggers (Appendix 2 shows an example schematic for logger 1 and 2), which were placed to record data from no more than two trees each. The original design and initial programming of the loggers was put together with the help of Dr. Kevin Scott of Meteometrics Ltd. A schematic drawing of the Harwood site is shown in Figure 7-41 and each datalogger was set up as follows:

- **Logger 1** (Trees 1 and 41): 2 dendrometers, 4 thermistors, 4 sap flow sensors, and 1 soil moisture. Total 11 channels. (See Appendix 2)
- **Logger 2** (Trees 14 and 28): 2 dendrometers, 4 thermistors, 4 sap flow sensors, and 1 soil moisture. Total 11 channels. (See Appendix 2)
- **Logger 3** (Tree 19): 1 dendrometer, 2 thermistors, 2 sap flow sensors, 1 soil moisture, 1 temperature and 1 humidity. Total 8 channels.
- **Logger 4** (Tower): 1 temperature, 1 humidity, 1 rainfall, 1 PAR (photosynthetic active radiation), 1 wind speed (counter) and 1 wind direction. Total 6 channels.

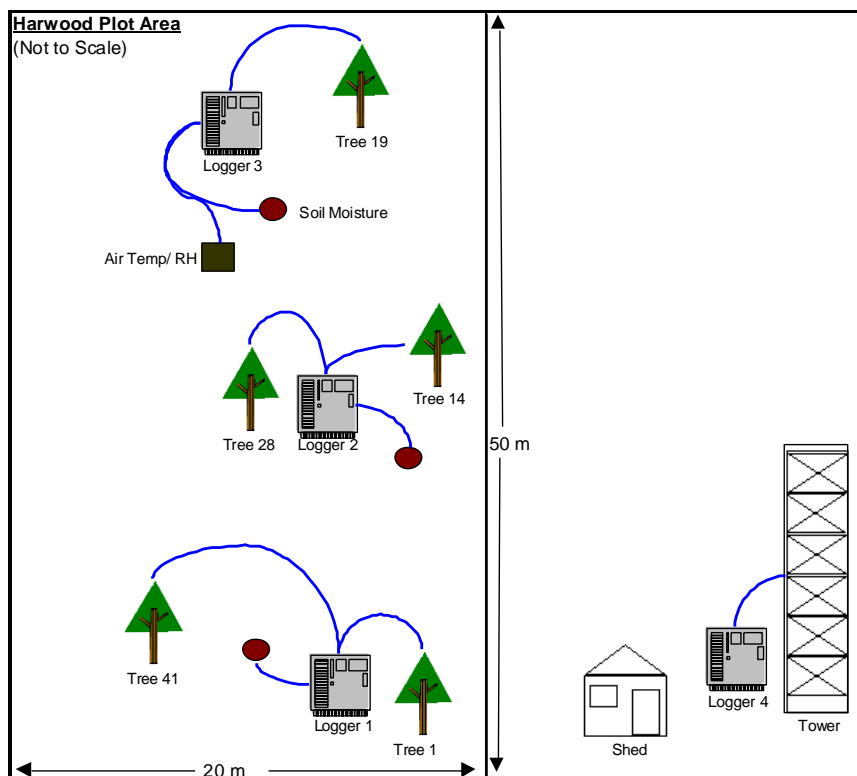


Figure 7-41: Schematic of Harwood field site showing position of trees, tower, soil moisture probes and air temperature/ relative humidity probes and the associated dataloggers.

7.2.4 Results

Results were obtained from the Harwood site from the beginning February 2012 until the middle October 2012 when the growing season had ended.

7.2.4.1 Site Climate Comparison

Harwood forest in Northumberland has a similar climate to Griffin forest in Perthshire. During this study the air temperature was monitored at both locations and a comparison of these are shown in Figure 7-42. Temperatures at both of the sites are extremely well matched especially in the first half of the year where it is difficult to see any difference. In the second half of the year there is a slight difference in the range of temperatures with Harwood getting slightly higher temperatures, but the highs and lows of the temperature profiles occur simultaneously.

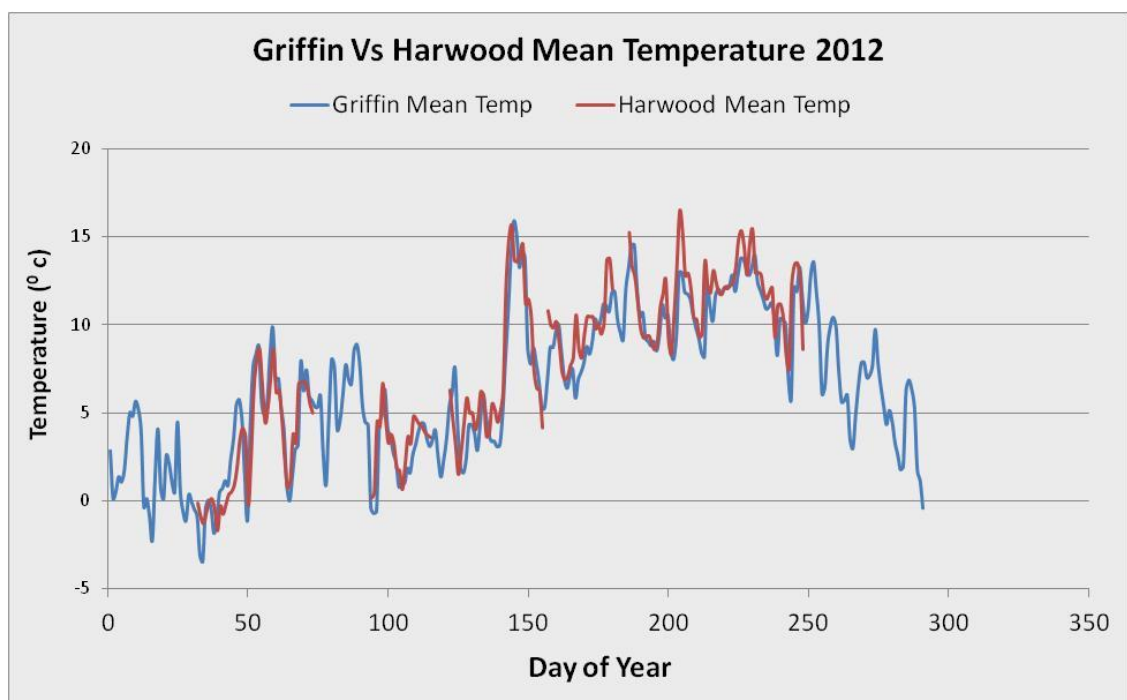


Figure 7-42: Comparison of temperatures measured at Griffin and Harwood during 2012.

Soil moisture was also measured at both sites which show a similar overall level of soil moisture with Harwood being slightly higher (Figure 7-43). Some of the peaks in soil moisture occur at the same time, but this is not as clear as seen with temperature.

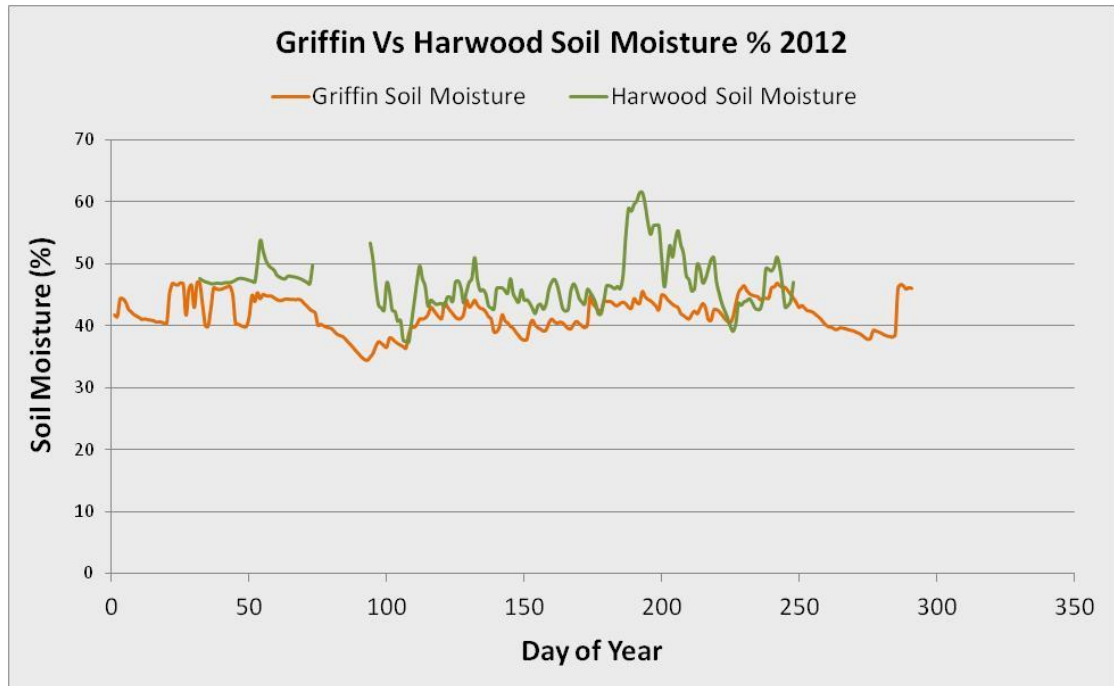


Figure 7-43: Comparison of soil moisture measured at Griffin and Harwood during 2012.

7.2.4.2 Growth at Harwood

Problems with the dendrometer for tree 1 meant that, although it was measuring growth it wasn't doing so correctly until a new replacement dendrometer was installed at the end of July. Therefore the results for tree 1 before this point can be ignored.

At the Harwood site radial expansion of the tree stem starts each year around the beginning of April and ends at the beginning of September (Figure 7-44). As with Griffin this period corresponds to the time when temperatures start to increase in spring and carries on until temperatures start to drop again in autumn.

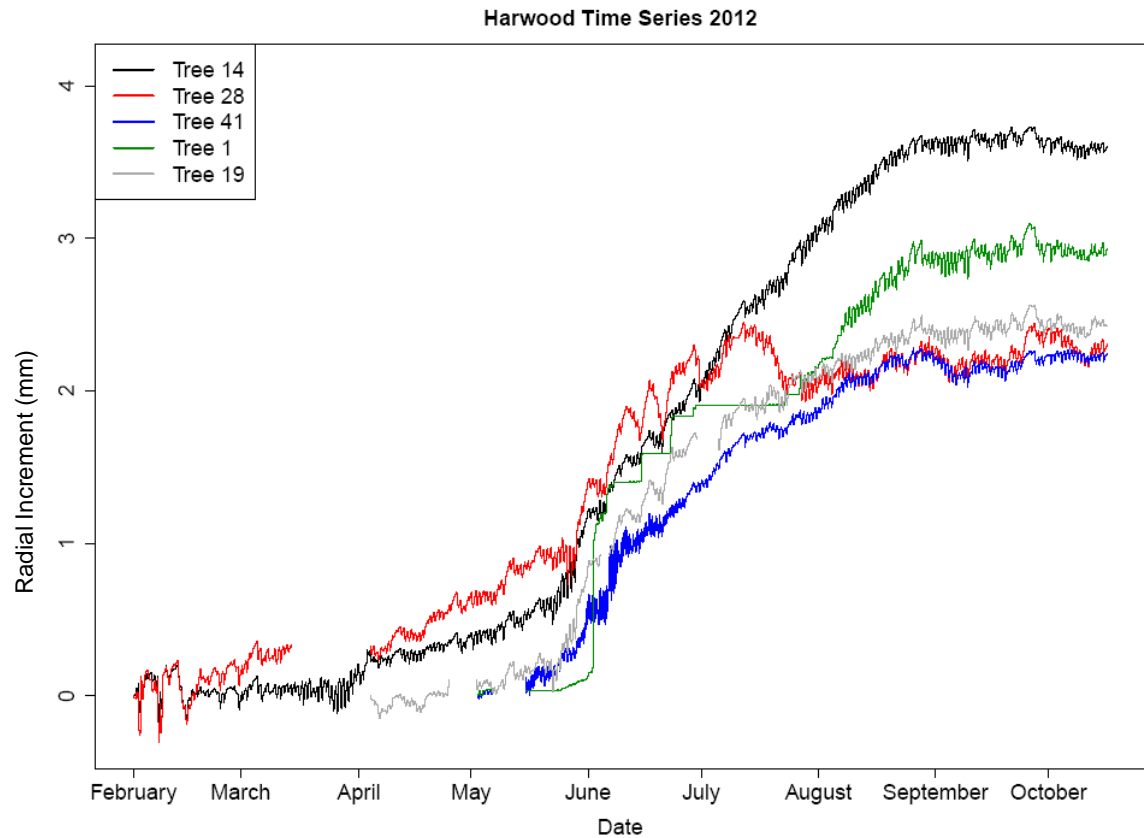


Figure 7-44: Harwood site radial expansion measurements from February 2012 showing radial growth of the five trees, as measured by LVDT dendrometers.

The period of expansion for Griffin and Harwood were also found to be very similar for 2012. On average trees started expanding at Griffin on day 127 of the year (7th May) and at Harwood on day 128. Similarly at Griffin radial expansion stopped on average at day of year 245 (2nd September) while at Harwood radial expansion stopped on average at day 243. A full list of days when radial expansion starts and stops is shown in Table 7-6.

Table 7-6: Comparison between Griffin and Harwood sites of the days when radial expansion started and stopped.

Griffin vs Harwood radial expansion Period 2012						
Griffin Tree	Start Day of Year	Stop Day of Year	Harwood Tree	Start Day of Year	Stop Day of Year	
48	127	254	14	127	258	
43	127	242	28	130	189	
8	126	250	1		266	
15			41	125	235	
66	129	233	19	131	266	
Average	127	245	Average	128	243	

Although Table 7-6 shows that the date when radial expansion starts and stops is very similar between the two sites measured, the overall radial expansion during 2012 was found to be higher at Griffin. The amount of radial expansion measured at Griffin during 2012 varied from almost 2 mm to almost 9 mm with an average radial expansion of 6.4 mm. The radial expansion between the Harwood trees was more similar ranging from 2.3 mm to 3.7 mm and an average of 2.7 mm (Table 7-7).

Table 7-7: Comparison between Griffin and Harwood sites of total radial expansion for each tree during 2012

Griffin vs Harwood Total radial expansion 2012			
Griffin Tree	Expansion (mm)	Harwood Tree	Expansion (mm)
48	8.82	14	3.67
43	6.81	28	2.44
8	7.97	1	
15		41	2.27
66	1.98	19	2.49
Average	6.40	Average	2.72

The same distinct periods of radial expansion that were seen at Griffin can also be seen at Harwood. The radial expansion rate for tree 14 at Harwood can be seen in Figure 7-45 which shows that early in the season when mean temperatures start to increase there is a slow expansion in the stem (1). Once temperatures are consistently above 5⁰C there is a rapid increase in the radial expansion rate (2) from around day 129 (9th May) which speaks at approximately day 160 (9th June) before decreasing again in late summer (3). Similar to Griffin radial expansion stops at around day 260 (17th Sept) (4) before temperatures drop below 5⁰C.

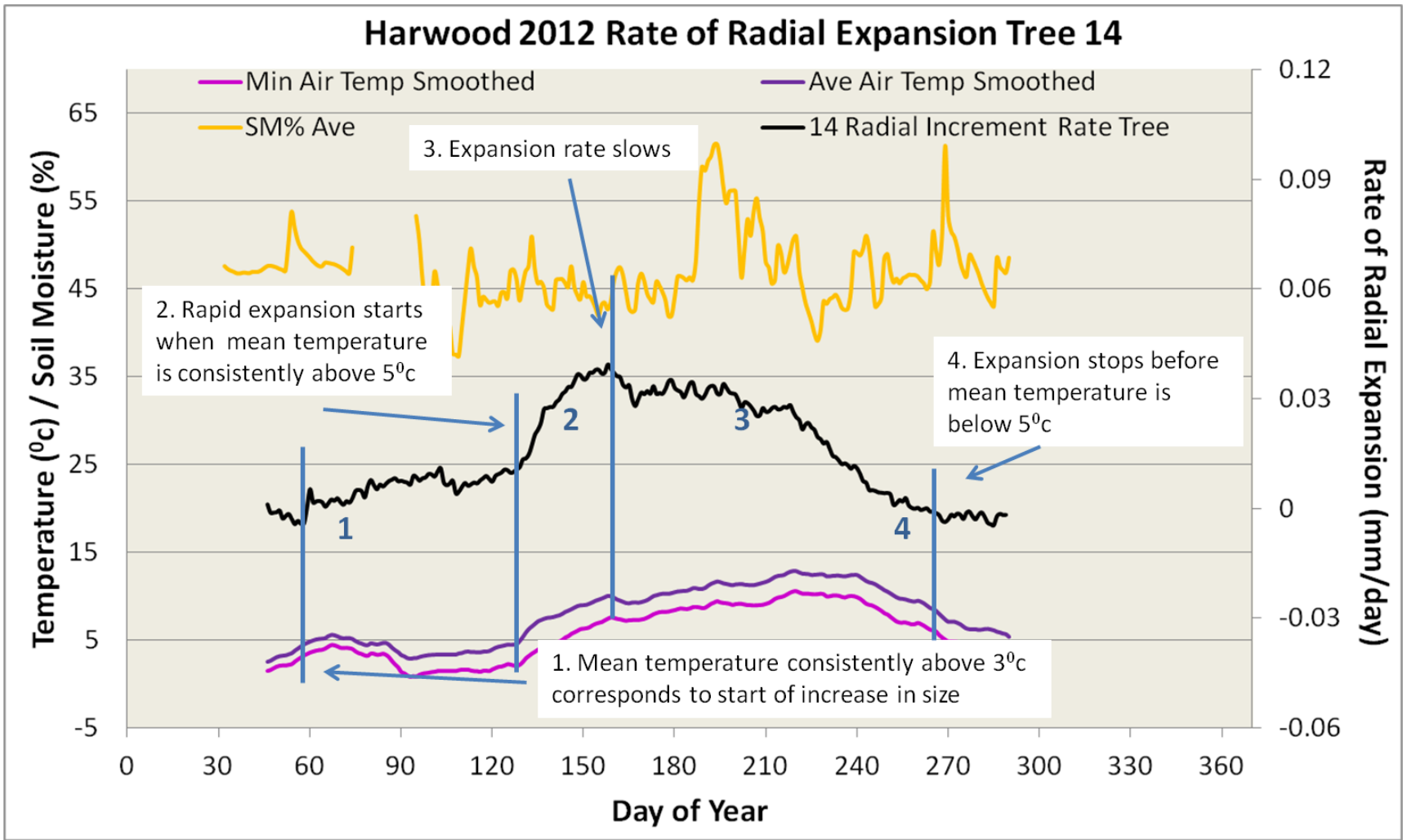


Figure 7-45: The effect of soil moisture and temperature on the radial expansion rate of Tree 48 at Harwood during 2012.

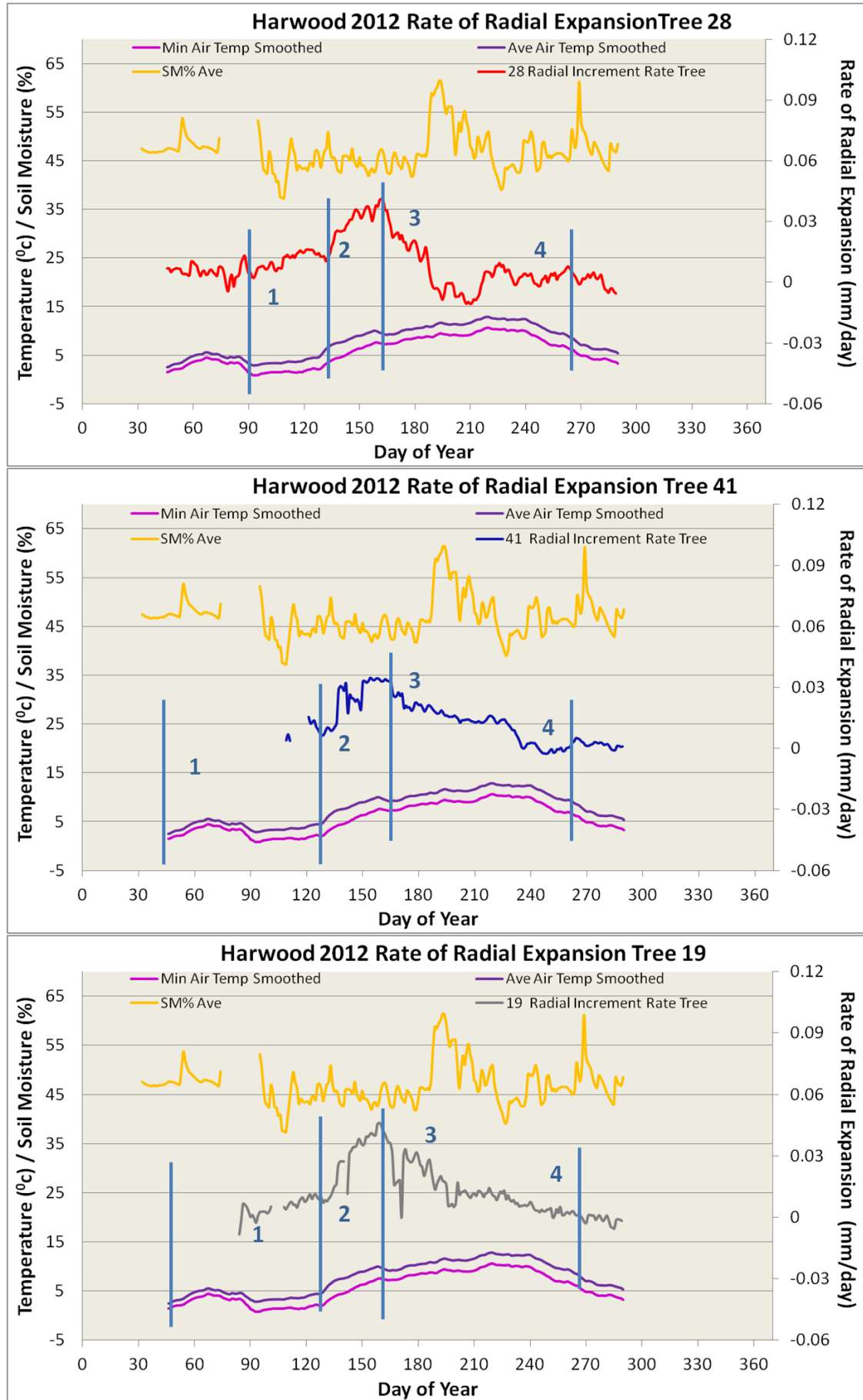


Figure 7-46: The effect of soil moisture and temperature on the radial expansion rate of Trees 28, 41, and 19 at Harwood during 2012.

The effects seen in Figure 7-45 can also be seen in the other trees at Harwood (Figure 7-46). In this, trees 28 and 19 show a period of slow expansion at the early part of the growing season, followed by a more rapid radial expansion rate starting at approximately day 130 (10th May). This period of rapid radial expansion rate can also be seen in tree 41 though data for earlier in the season is missing. The radial expansion rate of all three trees shown starts to decline around day 160 to 165 although this would seem to be a more gradual decrease in the rate than that seen at Griffin. Radial expansion seems to stop for tree 28 at around day 190 and also tree 41 around day 244. However, both of these trees then appear to show a slight increase in the radial expansion rate after this time which may correspond to a period of increased soil moisture.

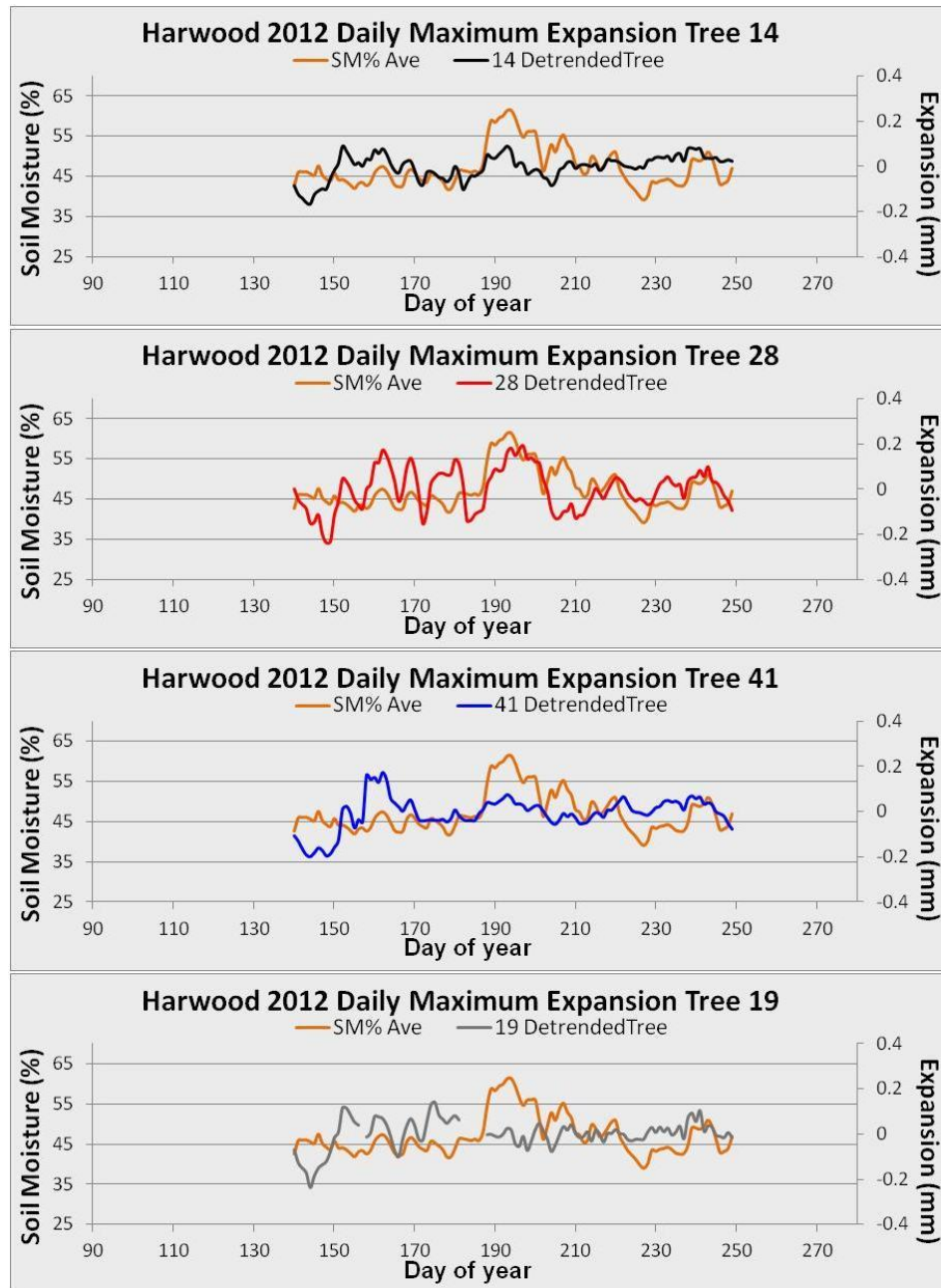


Figure 7-47: The detrended daily maximum expansion measured for each tree at Harwood plotted against the mean daily soil moisture value for 2012.

As described with the Griffin growth data, the daily maximum radial expansion was detrended to allow a comparison to be made with soil moisture for the growth period. Like Griffin, the daily changes in the maximum stem size appear to coincide with changes in soil moisture with a lot of the peaks in both (though not all) occurring at the same time (Figure 7-47). This is especially true with trees 14 and 28 which appear to follow similar patterns to the soil moisture measurements. Soil moisture was higher at Harwood than at Griffin and this was maintained throughout the growing season and this would be unlikely to limit tree growth.

7.3 Variation in Stem Width - Diurnal / Seasonal Changes / Amplitude

As well as the seasonal trend in stem expansion there is also a daily trend with fluctuations of shrinking and swelling caused by water movement within the stem (Devine and Harrington, 2010, Abe and Nakai, 1999, Downes et al., 1999, Makinen et al., 2003, Turcotte et al., 2009, Irvine and Grace, 1997). It has been suggested that these daily fluctuations are a result of high transpiration rates during the day when absorption of water through the roots cannot supply enough water to the stem resulting in water being drawn from tissue causing the stem to shrink, and then swell again at night when the stem re-saturates with water (Herzog et al., 1995). A study by Duchesne and Houle (2011) found that stem diameter expansion occurred on rainy days when solar radiation was low and humidity was high whereas on dry periods with high solar radiation and low humidity the stem diameter decreased. Herzog et al. (1995) described the daily fluctuations in 5 phases: 1. Nightly re-saturation of the stem with water, there is no sap flow, 2. Delay between the increase in the flow and the shrinking of the stem, 3. The stem shrinks rapidly and the flow increases, 4. Delay between the maximum in the flow and the minimum in the radius, 5. Decrease in flow and radius increases. A later study then reduced to three distinct phases: 1.contraction, 2.swelling, and 3.stem radius increase; which cycle in approx 24 hrs (Downes et al., 1999) (see Figure 7-48). This three step daily stem cycle approach has been used by various studies for growth and climate analysis on various tree species (Downes et al., 1999, Deslauriers et al., 2003, Deslauriers et al., 2007, Turcotte et al., 2009).

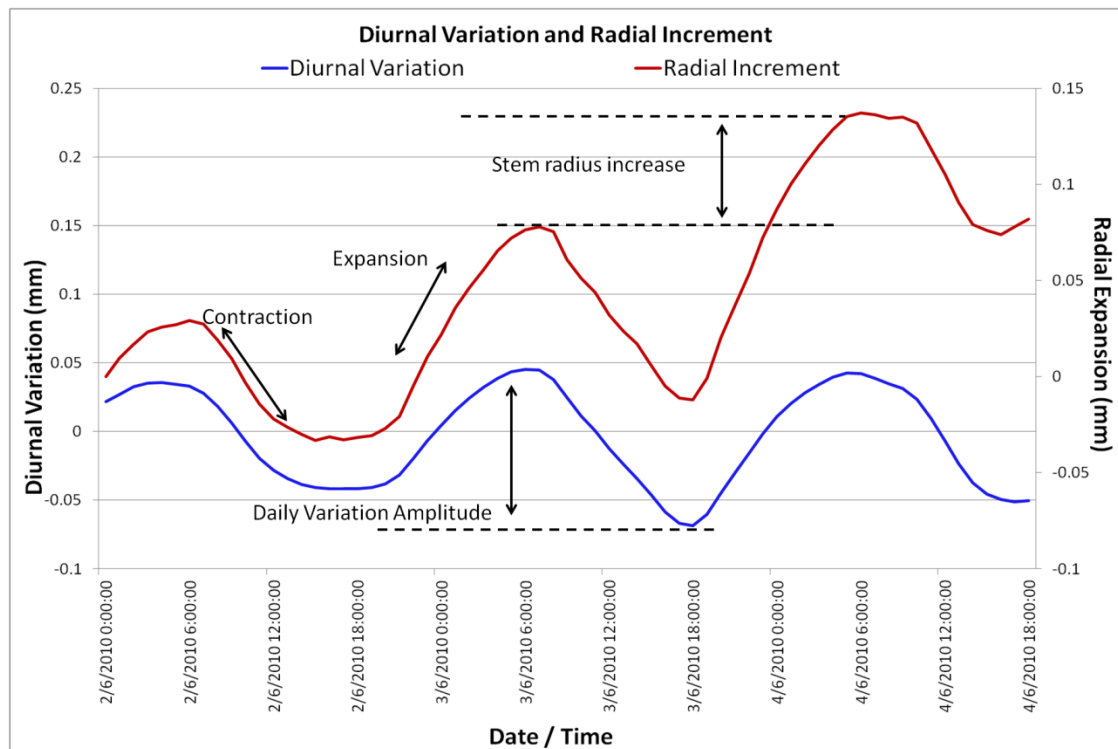


Figure 7-48: The daily expansion and contraction of the tree trunk along with the radial increment (red). Here the radial expansion curve has also been detrended (blue) to take account of the seasonal increase in size allowing the amplitude of the diurnal variation to be measured.

7.3.1 Analysis

The dendrometer measurements taken at Griffin (discussed in section 7.1.2) give data on the annual increment of the radius of the trees being measured (as shown in Figure 7-11 but if looked at in more detail the measurements also give data on the daily fluctuations in the radius due to shrinking and swelling of the stem. In order to look at the diurnal shrinking and swelling in more detail and the amplitude of these changes the data must first be detrended to take out the natural seasonal variation.

In order to remove the trend of increasing radial expansion the best fit linear line was calculated over a 2-day period using the “Trend” function in Excel. Next, to remove noise, a 60 point (2 hourly) moving average was taken.

The amplitude of the diurnal change was calculated for each day between a maximum in the morning (when the stem is at its largest) and a minimum in the afternoon (when the stem has shrunk to its smallest).

7.3.2 Results

Tree measurements at Griffin are recorded every two minutes giving information on stem radius at a very fine time resolution that has been ongoing with data available since 2008. Figure 7-49 shows a small portion of the data recorded over a twelve-day period in May/June 2010 showing an example of the radial expansion curves compared to the detrended data for the same period. The data collected at Griffin during the summer shows the natural trend as described by (Downes et al., 1999), where there is a daily cycle of shrinking, swelling and radial increase (Figure 7-49). This shows the difficulty in comparing diurnal changes and radial expansion between trees as each has a different starting point and a slightly different slope. Once the data have been detrended it is easier to see how each tree not only follows a similar pattern, but also have similar amplitudes each day. At Griffin the trees reach a peak in size each day at about 6 am and at a minimum size in the evening at about 6pm.

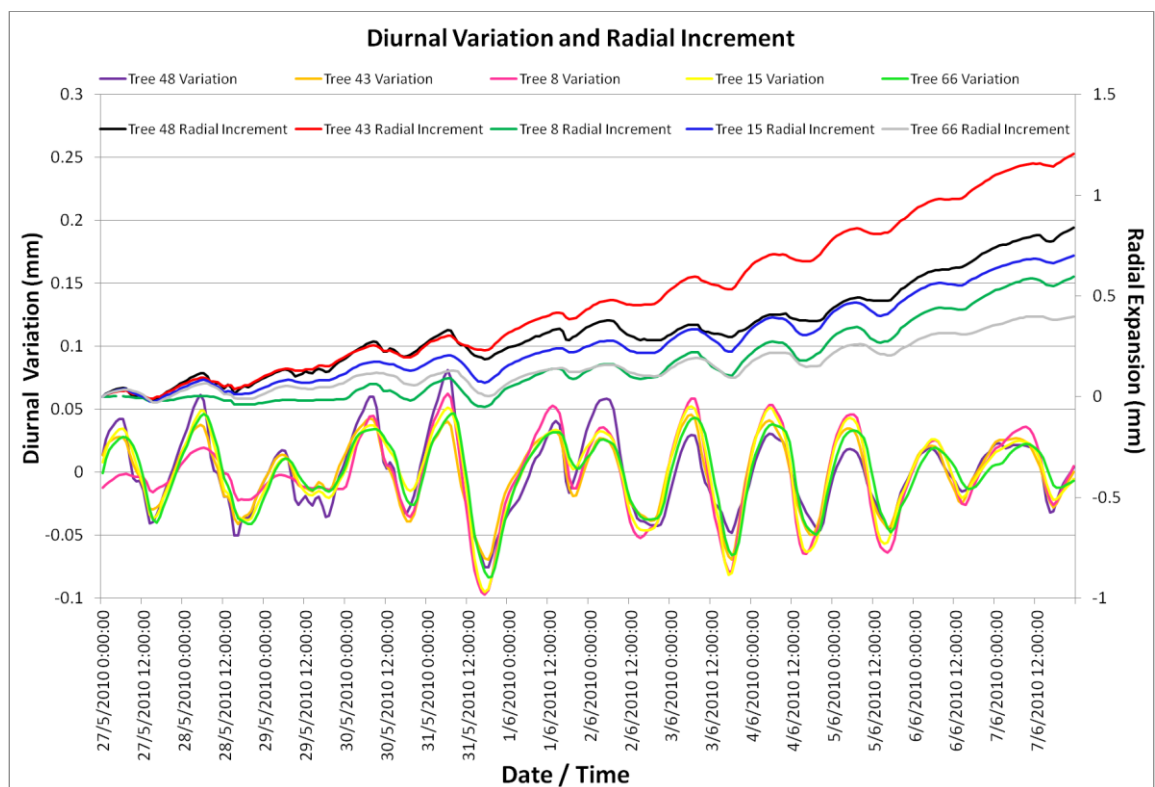


Figure 7-49: Dendrometer data collected from Griffin in June 2010 showing the raw data (a) showing the upward trend and the detrended data (b) showing the daily variation in readings and so the diurnal variation in stem width

The diurnal variation data has been plotted for three separate months during the measurements to give an example of the effect of soil moisture and air temperature on the diurnal variation. Figure 7-50 shows an example from the summer of 2009 and although soil moisture is relatively steady during this period there were two slight rises which could correspond to changes in the diurnal amplitude. However this period also corresponds to changes in the normal temperature pattern for this period making it unclear the amplitude of shrinkage and swelling change as a result of temperature or soil moisture, or as a combination of these factors.

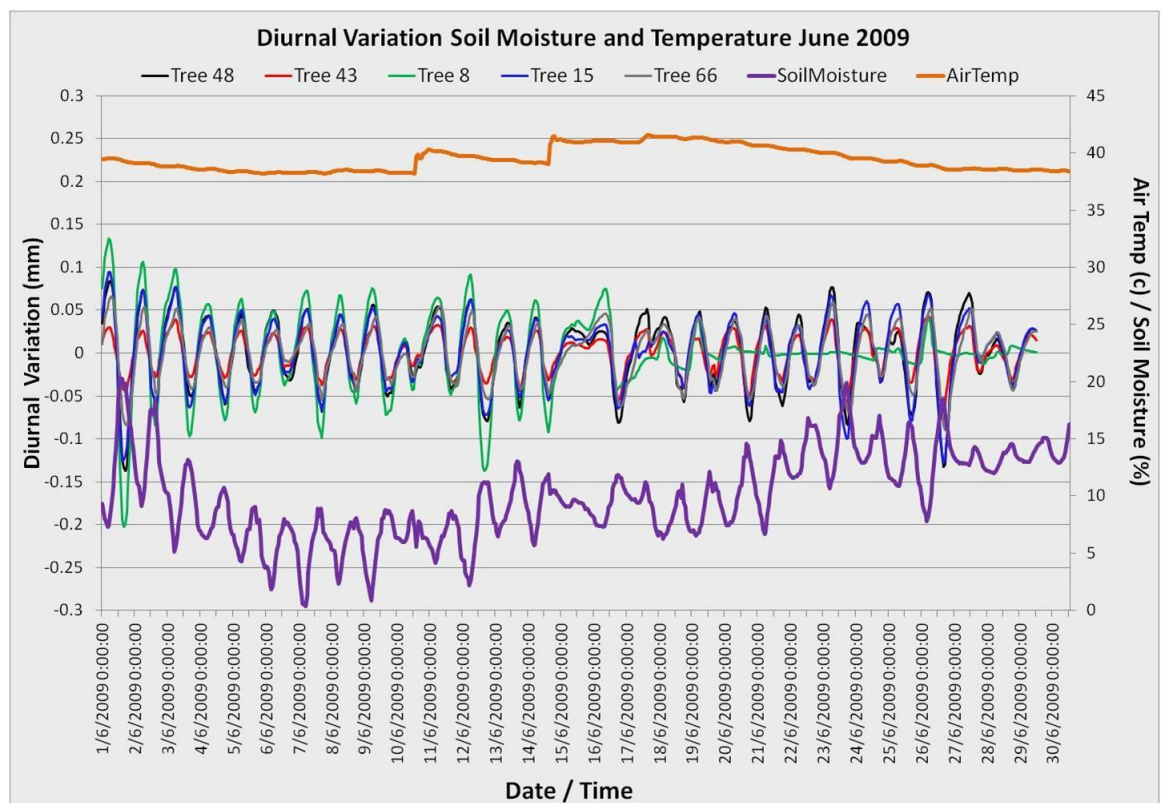


Figure 7-50: Air temperature, soil moisture and detrended radial expansion logged at Griffin in June 2009.

Figure 7-51 shows the diurnal variation from a period in July and August 2010. During this period there were larger changes in soil moisture which may have an effect on the regular pattern of daily swelling and shrinking. For example on approx 15th and 22nd July when there was an increase in soil moisture the amount of shrinkage was reduced.

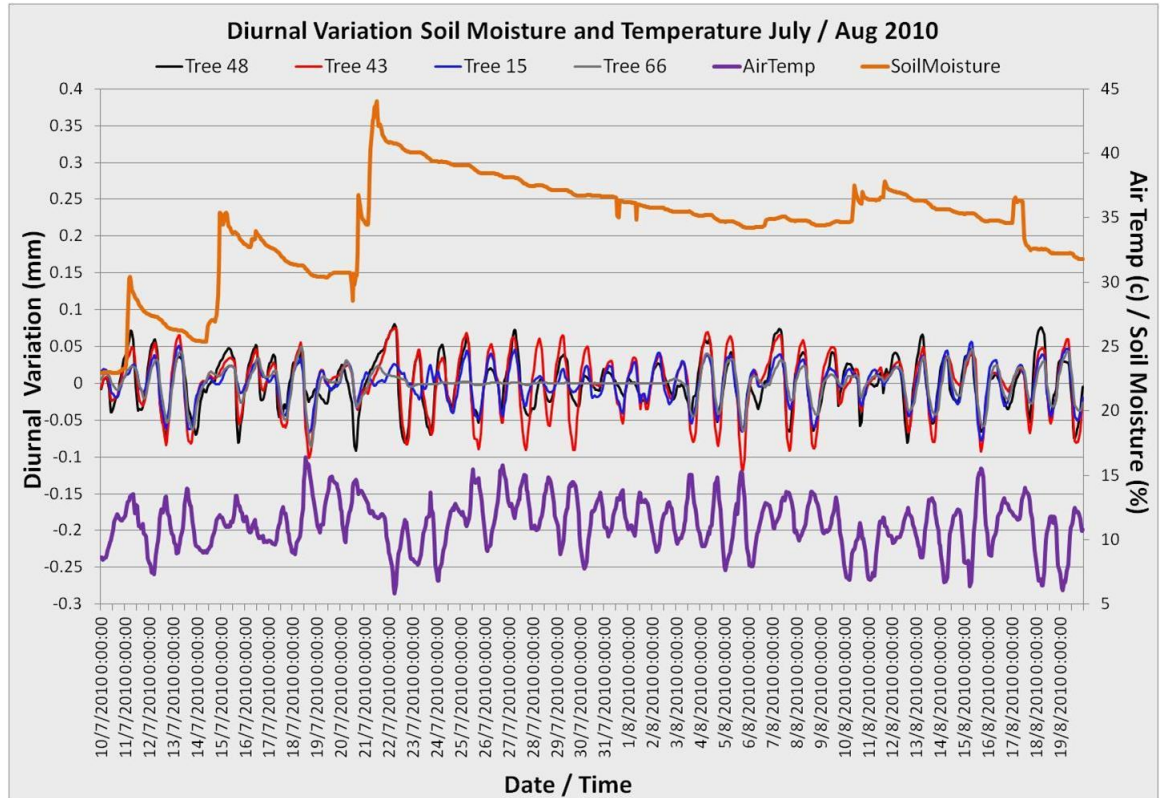


Figure 7-51: Air temperature, soil moisture and detrended radial expansion logged at Griffin in July and August 2010

This same pattern seen in Figure 7-51 is repeated in Figure 7-52, that is that times of increased soil moisture seem to coincide with periods of irregular diurnal changes in the stem size. As with the previous examples this often occurs at the same time as the daily temperature patterns become irregular. There may also be a suggestion from all three graphs (Figure 7-50, Figure 7-51 and Figure 7-52) that some days where shrinkage is at a maximum corresponds to days when high temperatures were recorded.

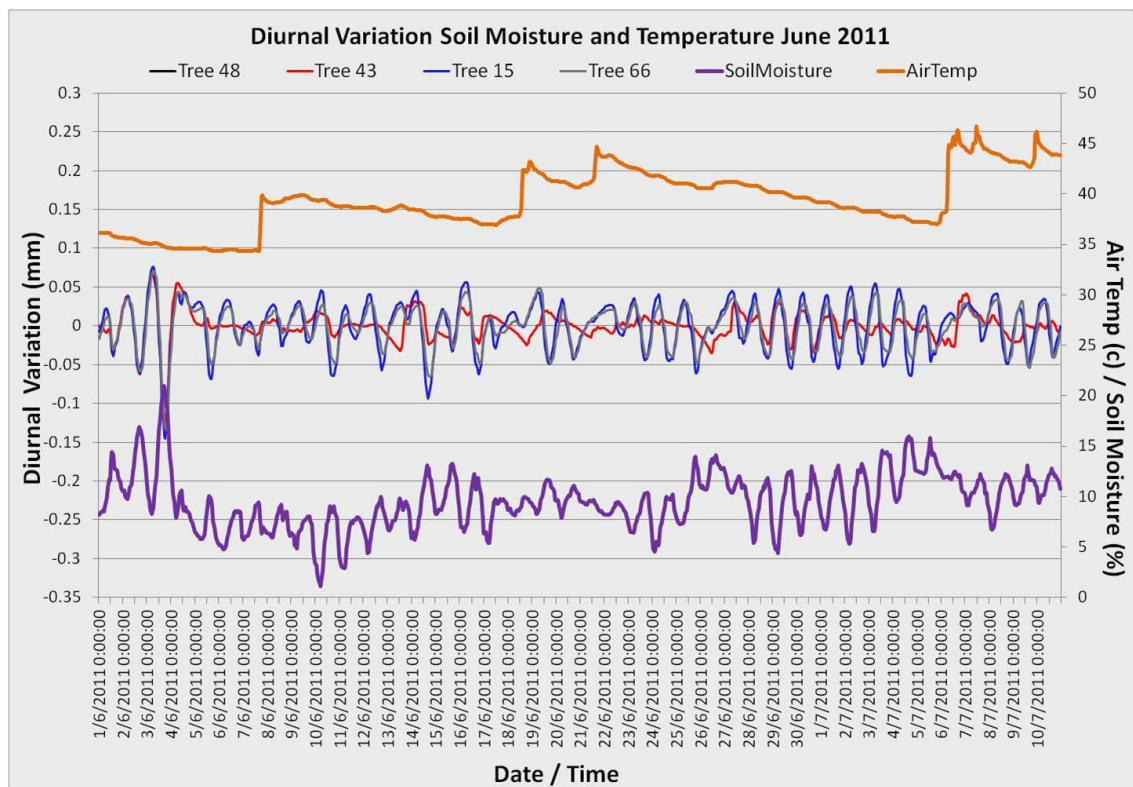


Figure 7-52: Air temperature, soil moisture and detrended radial expansion logged at Griffin in June and July 2011.

Whilst Figure 7-50, Figure 7-51 and Figure 7-52 show diurnal changes over a relatively short time period during the growing seasons Figure 7-53 shows a similar timescale but during the winter. This shows that there is still a diurnal variation in the stem size even though no growth is taking place. Although the trees are following similar pattern to each other during the winter the variation does not show the same regular pattern as during the summer.

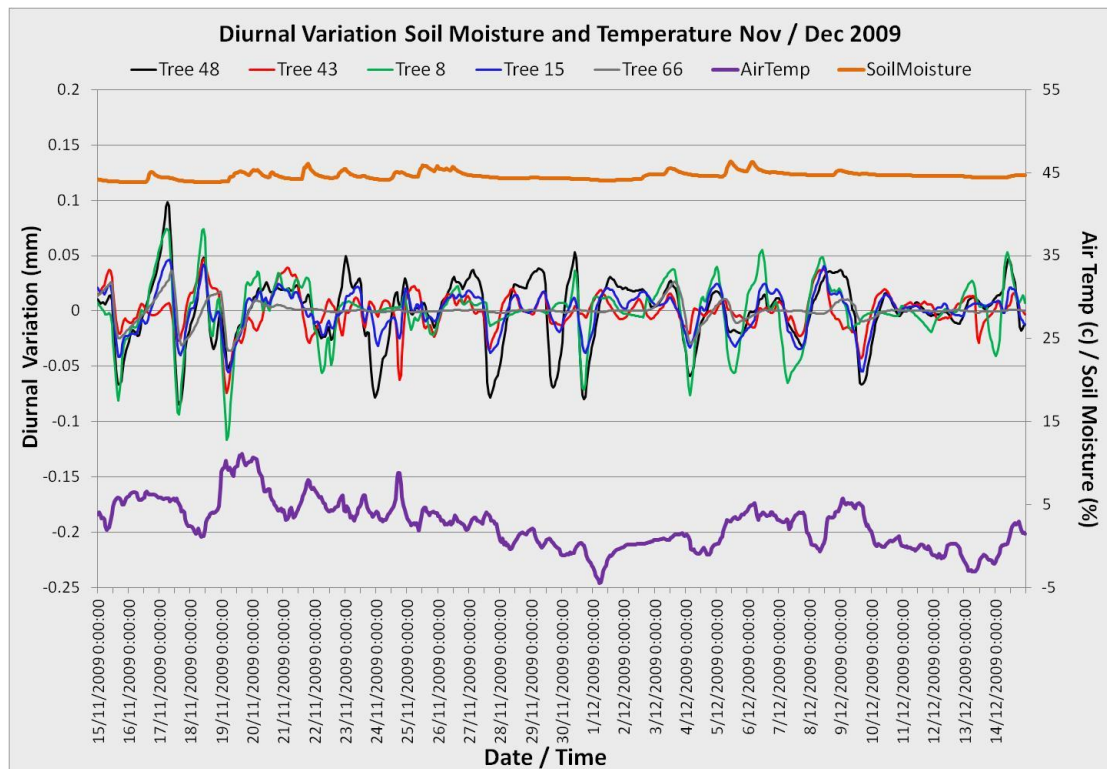


Figure 7-53: Air temperature, soil moisture and detrended radial expansion logged at Griffin in November and December 2009.

Figure 7-54 shows the daily amplitude in stem size for the Griffin trees over the whole time period that data is available, from April 2008 to October 2012. Although there are high values seen in the winter periods this is explained by the shrinkage of the trees due to extreme cold conditions experienced at this time (as shown in Figure 7-12), which has also been noted in previous studies (Devine and Harrington, 2010, Zweifel and Hasler, 2000). The variation in the amplitude is relatively synchronised in all trees and shows there may be some indication that the amplitude is smaller in winter periods and largest during the summer.

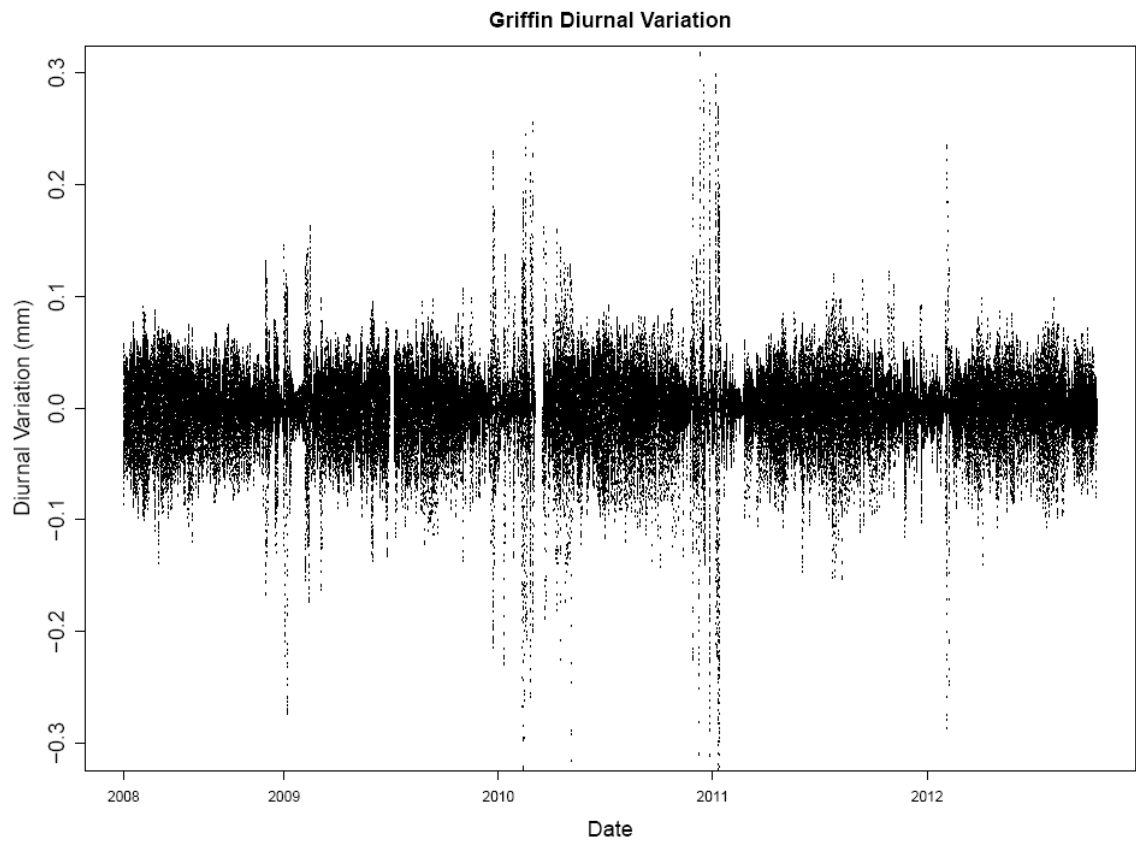


Figure 7-54: The amplitude of the daily changes in radius of the trees at Griffin site from April 2008 to October 2012.

7.4 Discussion on Tree Growth at Griffin and Harwood

Growth measurements at Griffin have been collected along with meteorological data since 2008 with the data being used in previous studies into the effect of site and climate on the growth of Sitka spruce (Vihermaa, 2010). This study aimed to build on this previous work by the collection of further measurements at Griffin site in the hope that a relatively long timeline of data over a number of seasons can yield more information on the effect that climate has on Sitka spruce. Along with the Griffin site measurements, a new experimental site was established at Harwood forest in Northumberland allowing growth for 2012 at the two sites to be compared. Although only one season of growth data was measured at Harwood it showed that although there were a lot of similarities in when growth started and stopped during the year the amount of growth varied within the sites but overall was lower at Harwood. The reasons for this are unclear as temperatures were very similar at both sites and soil moisture was slightly higher at Harwood but could be caused by the age of the crop, nutrient limitation or waterlogging at the site. At the Griffin site the growth in radius measured by dendrometers was compared with the change in DBH manually measured at the beginning and end of the experiment. Although there were slight differences between the two measurements this would be expected due to the different method used and both gave similar values.

Analysis of tree growth at the Griffin site has shown that there is a lot of variation in the amount of growth measured between different trees. From this experiment it is difficult to ascertain the reason for these differences since detailed soil moisture and temperature readings were not made for each tree. However, soil moisture was measured at four different points within the site and these showed there was variation in soil moisture throughout the site. If this was extrapolated to the whole site then it is easy to see that different trees have different amounts of soil moisture available and this could have an effect on growth. Of the trees measured in this experiment, tree 66 had by far the least amount of growth and this may have been due to the management of this site. Thinning is known to have an impact on tree growth (Savill and Sandels, 1983, Deans and Milne, 1999, MacDonald and Hubert, 2002) and this may be a factor here. The trees which showed the most growth each year (48, 43 and 8) were all adjacent to a row where thinning had taken place and this may contribute to the

higher growth rate. Although some thinning had taken place near tree 66 there was still a lot of competition from other trees and this resulted in tree 66 no longer being a dominant tree. Tree 66 not only shows a slower growth rate, but also stops growing earlier in the season than the other trees and this may be due root competition for soil water and shading effects as this tree had become subdominant and therefore subject to crown competition for available incoming net solar radiation. Wang and Jarvis (1990) found that the total area of leaves and spatial distribution in the crown were the most important factors for radiation absorbance and photosynthesis. By becoming subdominant the sub-canopy position of tree 66 could mean that the majority of its photosynthate is captured only when the sun is high in the sky (midsummer) and during the central part of the day which could lead to lower growth rates and a shorter growing season.

Previous studies on other species in other countries have shown that the timing of the beginning of growth can vary between years (Deslauriers et al., 2003) and that temperature is the main factor determining when growth starts (Turcotte et al., 2009, Rossi et al., 2007, Rossi et al., 2008). In the current study at the beginning of each growing season there is a point where the mean temperature is consistently above 3⁰C, which in most cases also corresponds to minimum temperatures rising above 0⁰C. From the measurements made here this point coincides with a gradual increase in the stem size which could be related to spring rehydration which has been seen to occur before radial growth occurs in Black spruce in Canada (Turcotte et al., 2009). In a 2008 study comparing different methods of analysing wood formation (pinning, microcores and dendrometers) in Norway spruce and Scots pine in Finland, Makinen et al. (2008) found that dendrometers showed an increase in stem radius earlier in spring when no wood formation was detected by either microcores or by pinning. A study by Vihermaa (2010), which compared dendrometer readings with microcores taken in 2008 for the same five trees at Griffin used in this experiment, also found that dendrometers detected an increase in stem size earlier in spring than growth was detected by analysing microcores. Investigating Norway spruce growing in southern Finland using microcores Kalliokoski et al. (2012) found that tracheid formation did not occur until several weeks after mean air temperature had been above 5⁰C. In the Vihermaa (2010) study

dendrometers detected an increase in stem size at the end of April while growth was not detected in the microcores until the second half of May. This coincides with the period of rapid expansion seen in the stems in this study suggesting that the expansion seen in early spring may be due to reasons other than growth and is likely to reflect the onset of active evapotranspiration with enhanced hydraulic conductivity from the soil to leaf to support the onset of photosynthetic carbon gain.

In this study, this period of rapid expansion coincides with the mean daily temperature rising above 5⁰C. Rossi et al. (2007) found that growth of larch, Stone pine and Norway spruce in northern Italy occurred when air temperature was above 5.6⁰C to 8.5⁰C suggesting there was a thermal limit to wood formation. This was also seen in Scots pine in Austria by Swidrak et al. (2011) who found that there was an air temperature threshold of 5-6⁰C for the start of xylem growth and also that air temperature rather than precipitation was the trigger for growth. By artificially heating localized areas of the stem of Norway spruce trees Gricar et al. (2006) were able to initiate cambial divisions earlier than that for a control tree with no heating which again suggests that temperature is the main driver for the onset of growth in spring. The onset of radial growth of the stem of the tree must be predicated by the fixing of CO₂ in the needles, with the possibility that there may be some complex carbohydrate storage (starch or acylglycerols or sacchharides) (Dauwe et al., 2012, Collakova et al., 2013) which gene regulations onset by temperature (Joosen et al., 2006) may bring 'out of store', therefore the likelihood is that cambial division onset by heating is accessing these stored compounds.

Table 7-8: The number of days during the preceding winter that the mean temperature was below 5⁰C before the growing season at Griffin started.

Growing Season	2008	2009	2010	2011	2012
No. Days Previous Winter < 5 ⁰ C (Chill Days)	NA	173	173	158	140

It has been suggested that bud burst in Sitka spruce is subject to a high chilling requirement (i.e. the period preceding the growing season having 140 days less than 5⁰C) (Cannell and Smith, 1983, Murray et al., 1989). In this study the mean temperature for the winters preceding the growing seasons of 2009, 2010 and

2011 all exceeded this requirement (Table 7-8) and growth started immediately when the temperature rose above 5°C. However, the chill period preceding the growing season of 2012 initially did not meet this requirement as there was an early increase in temperature to approx 5°C after only 96 days. There was then a period of mild temperatures with mean temperatures stabilising around the 5°C mark for approximately 30 days before temperatures dropped below 5°C again. There was then a second period of “chill days” lasting 44 days before mean daily temperature rose above (and stayed above) 5°C. Growth for this period did not fully start until the mean temperatures rose above 5°C for the second time which coincided with exactly 140 chill days. The lack of growth from the trees after only 96 days may suggest that there is some evidence for the chilling requirement in Sitka spruce meaning though this is difficult to confirm here with only one investigated year coming close to this requirement. Cannell and Smith (1986) suggested that an increase in temperature could lead to earlier budburst at the beginning of the growing season, which in turn could increase the risk of frost damage if the temperatures were to decrease again. In the one year that this happened in this study (2012) the evidence suggested that with regards to growth, the trees were able to cope with a drop in temperature in spring time after an initial warmer period. After an initial increase in stem size (maybe due to rehydration) growth was effectively put on hold until the temperature had increased again. However this did lead to a year with low growth rates.

Antonova and Stasova (1993) suggested that water stress can determine the end of growth by affecting the wood production. In this study, throughout 2008 there are two periods where soil moisture decreased significantly. The second of these dry periods (approx. day 180 to 220 of Figure 7-15 and Figure 7-16) corresponds to the period of highest growth rate (with the exception of tree 66) which peaks around day 200. However once soil moisture reaches what could be described as the sub-optimal level of 30% (personal statement M.Perks) the growth rate of the trees starts to decline as the trees switch to producing latewood. There was a similar dry period during 2010 in which the 30% soil moisture was reached (Figure 7-19 and Figure 7-20) and although it happens slightly earlier (approx. day 150 to 200) it corresponds to the time when growth rate is at its peak in all of the trees (with the exception of tree 66). This may suggest that 30% soil moisture is a threshold below which growth of Sitka spruce starts to decline and

the slight differences between trees may be due to slight differences in soil moisture throughout the site due to competition from other trees. In two of the years where soil moisture did not decline to the same extent (2011 and 2012) the peak in growth rate was extended for a longer period of time and the decrease in growth rate happened later in the season.

The effect of these dips in soil moisture, during 2008 and 2010 on the daily expansion of the stems can be seen in Figure 7-30 and Figure 7-35 and shows that the daily expansion is at its lowest during the early part of the dry spell, but seems to increase before the recovery of soil moisture. This may reflect the localised relief of tension in water availability at the needle (rather than the soil) with local increase able to provide carbon substrate before whole-tree hydraulic architecture is 'functioning' which was also noted in Scots pine which were subjected to drought conditions (Perks et al., 2002), and could be as a result of rainfall events which occur prior to soil water replenishment (Figure 7-6). This may provide some evidence that the tree is accessing water successfully during the summer period until soil moisture reaches a threshold of 30%, but when favourable conditions return there is an increase in the maximum daily expansion and while this is getting to the time of year which is not peak photosynthetic period Sitka is able to thrive on diffuse radiation (Dengel et al., 2009).

Another feature which appears in the growth rate of some trees is a plateau or hump in the growth rate during the growing season between the initial rapid growth period at the beginning of the which would suggest that the rate of growth slows and then speeds up again and this may be due to a localised dry period for these trees however more soil moisture sensors positioned around each tree would be required to test this.

Figure 7-14 showed that at Griffin the average daily growth is consistent across the season although further analysis showed that there were periods of maximum expansion i.e. from the start of the season into May and then again from day 180-190, with the second period being relatively consistent across years and the second short period is also reflected in Harwood around day 210. Rossi et al. (2006) found that maximum growth in conifers occurred around the time of year when day light hours are at a maximum and not necessarily the

warmest time. Again this is consistent with the findings here where the maximum growth rate was relatively consistent over the years occurring in June/July which corresponds to the days with the longest hours of daylight and although this corresponds to the time when temperature is at its highest and relatively constant, ultimately, growth is driven by photosynthetic carbon capture and not by temperature. Denne and Smith (1971) suggested a decrease in the growth rate corresponds to the decrease in daylight as the trees switch from producing large cells (earlywood) to producing cells with thicker walls (latewood). Figure 7-55 shows an example of the daylight hours throughout the year for Edinburgh in Scotland. Day 172 i.e. June 21st is the day with the most amount of daylight each year and the average day each year when the growth rate started to decrease varied between from day 168 in 2009 to day 196 in 2012, which suggests that even though the longest day occurs at the same time each year, the change in growth is not quite as consistent

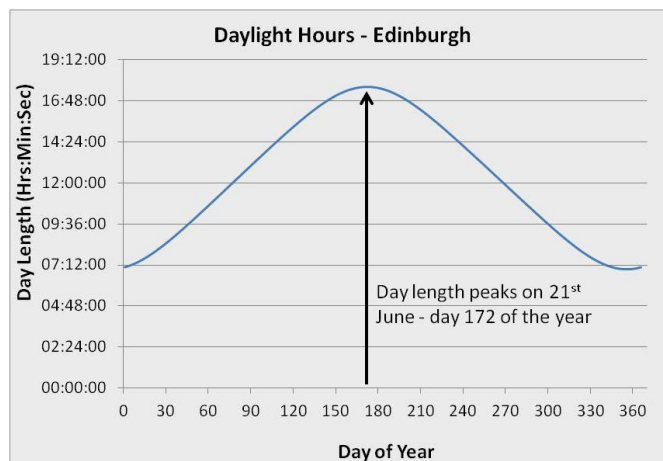


Figure 7-55: The daily hours of daylight changes throughout the year, peaking at approximately 17.5 hours on 21st June.

This study also found that the trees stop growing before temperatures dipped below 5⁰C suggesting again that temperature is not the controlling factor for the end of growth. A 2006 study into Scots pine found that dormancy in autumn occurred due to a combination of light availability and temperature where the initial phase of dormancy were in response to a decrease in day length and the second phase due to low temperatures (Joosen et al., 2006) and other studies have shown that this may be genetically controlled (Olsen, 2010, Gonzalez et al., 2012). To avoid damage when temperatures drop in the winter months the trees must have finished growth and secondary wall lignification before winter

starts. This may suggest that trees would only take advantage of a longer growing season if the growing season is longer at the beginning of the season rather than the end.

As shown by the measurements taken at Griffin Figure 7-11 there is a seasonal trend in the growth, with a steep increase during the summer period and levelling out during the winter. However, this is not just a case of growth causing an increase in width as shrinking and swelling can occur due to changes in water relations within the stem (Kozlowski and Winget, 1964) as well as other environmental factors including air temperature, humidity, soil moisture and precipitation (Deslauriers et al., 2003, Downes et al., 1999). This means that within the increasing trend being measured there is a seasonal trend where stems can shrink during summer, when there is little water available, and swell in autumn when there is more precipitation. This effect can mask the onset of growth as trees start to take up water again in the spring (Kozlowski and Winget, 1964, Turcotte et al., 2009) and also mask the end of growth as trees rehydrate in the autumn (Makinen et al., 2003).

Investigating Scots pine in Russia, Antonova and Stasova (1993) found that temperature was the main influence on xylem division and expansion in May to June and that precipitation had a bigger influence later in the season (July - August). Michelot et al. (2012) found that different species responded differently to precipitation and temperature at different times of year e.g. beech growth was positively correlated with May to July precipitation and Scots pine growth was sensitive to low soil moisture. A study on Balsam fir in Canada (Deslauriers and Morin, 2005) suggested that air temperature had a bigger influence on growth during the earlywood phase of growth. However a study by Oberhuber and Gruber (2010) found that radial increments during the growing season in Scots pine were related to precipitation and humidity and not to soil moisture and air temperature. In this study, although temperature seems to have an effect on the overall trend of when growth starts the short term changes in daily growth may be influenced by soil moisture (conversely soil moisture may depend on growth as the growing trees take up more water). Similarly Bouriaud et al. (2005) studying Norway spruce found that fluctuations in climate and soil moisture were related to short term variations in growth. At Griffin site, although soil moisture dropped during the summer months it never dropped

below 25% and was only close to this level for short periods before it rained again. This suggests that moisture at Griffin is not a limiting factor. However there was some correlation between increased growth and increased soil moisture which may be as a result of increased water uptake swelling the stem.

It has been seen in previous studies that daily shrinking and swelling of a tree stem cannot only be greater than, but also mask any growth that is taking place (Kozlowski and Winget, 1964, Oberhuber and Gruber, 2010). Care has to be taken when using dendrometers to ensure that any increase in stem diameter being measured is due to growth and not due to swelling and shrinking (Devine and Harrington, 2010). Vihermaa (2010) found that stem expansion, measured by dendrometers on the same 5 trees as used in this experiment, started earlier in the season than growth measured by analysis of cells on microcores suggesting that there was some pre growth expansion in Sitka spruce early in spring. By using mathematical operations to smooth the data over extended periods (e.g. 30 days) and to show the rate of growth throughout the year this study was able to indicate that there were distinct periods of growth during the year which could correspond to the periods of rehydration in early spring, rapid growth of early wood in early summer and a period of slower growth of latewood later in the summer.

As well as the diurnal variation, seasonal changes in stem width also have been seen and these may also be affected variations in climate. The start and end of the growing season may be hidden when water movement can give a false impression of when growth starts in the spring (Turcotte et al., 2009) and when it ends in the autumn (Makinen et al., 2003). The study by Turcotte et al. (2009) was able to divide the year into three distinct phases of winter shrinkage, spring rehydration and summer transpiration and showed that the expansion of the stem during rehydration after winter can easily be confused with the start of growth, which is also confirmed in other studies (Makinen et al., 2008), and that climatic variables such as temperature is a major limiting factor to growth initiation. Makinen et al. (2003) showed that while changes in the radius measured by dendrometers were affected by changes in temperature and precipitation, the timing of the changes differed from actual xylem formation which again was put down to rehydration of the stem.

Previous studies on different tree species have shown a correlation between changes in daily stem radius with temperature and precipitation (Makinen et al., 2003), precipitation and relative humidity, but not temperature or soil moisture (Oberhuber and Gruber, 2010) and vapour pressure deficit and soil moisture (Sevanto et al., 2005b). It has also been noted that during extended dry periods there may be net stem shrinkage even though growth is taking place (Kozlowski and Winget, 1964). The same study also saw that diurnal shrinkage was smaller in spring, when there was more soil moisture and less transpiration, and greater at the end of summer when there is less soil moisture with differences also being noted between cloudy humid days and clear dry days. Herzog et al. (1995) suggested that the stems shrunk during the day and swell at night time and this trend was shown with the Griffin trees which followed a regular pattern where the trees peaked at the maximum size at approximately 0600 hrs and were at their minimum size at around 1800 hrs. It also showed that stem radius increase was only seen on the Griffin trees between approximately midnight and 0600 hrs once the previous maximum stem size had been passed. This same pattern was found in Canadian Balsam fir by Deslauriers et al. (2003), which peaked at around 0800 to 0900 hrs and were at a minimum at around 1600 to 1700 hrs. The same study showed that the increment phase of the daily variation started at approximately 0000 hrs to 0200 hrs.

The trees investigated at Griffin showed similar amounts of daily shrinking and swelling and these tended to be higher in the summer and lower in the winter though this is masked by large changes (relative to the normal daily changes) in stem size during extreme cold periods. Swelling and shrinking took place during the winter when no growth was taking place although the pattern was a lot less regular than during the summer and this may be due to soil water availability due to low temperatures, i.e. frozen water in the soil surface layers. There may have been a suggestion that the daily shrinking and swelling of the stem is related to soil moisture as there were fluctuations in the diurnal swelling and shrinking pattern when soil moisture increased, however, this also corresponded to periods when fluctuations in the normal daily temperature trend were seen. Within the time period of this study there were no extended periods of low soil moisture to examine the effect that this may have which may imply that moisture is not a limiting factor at this site.

8 Discussion

The formation of the Forestry Commission after World War 1 led to significant afforestation, with Sitka spruce as the main species due to its ability to grow on a wide range of sites including upland areas with poor soils (Moore, 2011). However, rapid growth of Sitka can have consequences on the quality of wood produced, with faster growth associated with less dense wood. This coupled with rotation times of 30 to 40 years means that the less dense juvenile wood makes up a larger percent of the tree when processed. This can lead to wood of poorer quality being produced (Brazier, 1970). With the current focus on climate change in Britain there is a worry that any change could have an adverse effect on the quantity and quality of wood being produced. This study aimed to investigate how projected climate change in Britain could affect the growth and quality of wood being produced by Sitka spruce trees. This was done by looking at Sitka spruce in the full latitudinal range at which it grows in Britain to investigate if there are any site or climate effects. This study also investigated the within site variation in growth to see how Sitka spruce is affected at a more local level and to examine how changes in local climate at sub-annual timescales can affect growth. This section aims to discuss and summarize the findings of these investigations.

8.1 Discussion of Method

8.1.1 Resource Evaluation Study

As part of this investigation sample cores were collected from sites across the full latitudinal range of Sitka spruce plantations in Great Britain, to be examined for radial wood density, radial growth and the radial profile of acoustic velocity. Sound travels through wood at a velocity that is dependent on its modulus of elasticity (MoE), i.e. stiffness, and its density so theoretically, given the wood density and the velocity of sound it is possible to determine the MoE of wood (Evans and Ilic, 2001). One of the main contributors to the stiffness of wood is the angle of the winding cellulose microfibril helix (MFA) within the S2 layer of the secondary cell wall (Barnett and Bonham, 2004). Wood secondary cell walls are made up of three layers (S1, S2 and S3) (Bailey and Kerr, 1935) with the S2 layer being by far the thickest and therefore dominating the MFA in the cell wall

(Barnett and Bonham, 2004). In Sitka spruce MFA is initially higher at the pith and declines to around rings 6 to 9 before becoming more stable in the mature wood (Phillips, 1941). As MFA drops the cell wall becomes stiffer. Various studies have shown a relationship between wood stiffness and MFA in Sitka spruce (Cowdrey and Preston, 1966) and other species such as radiata pine (Cave, 1968, Walker and Butterfield, 1996). Although MFA is one of the main criteria for defining wood quality (MacDonald and Hubert, 2002) within this experiment MFA measurements were not feasible due to the expense of using the Silviscan instrument. However since acoustic velocity is a measure of stiffness this can also be used as an indirect measure of the MFA (Evans and Ilic, 2001). The experiments carried out by Vihermaa (2010) were among the first lab-scale measurements of acoustic velocity, but required samples 10 cm in axial length. Within the current study, there was a unique opportunity to take this concept further by making acoustic measurements on increment cores themselves using a facility available in Christchurch, NZ. Calculation of stiffness from acoustic velocity requires density measurements, which had not previously been available to the Christchurch group. By making use of the increment cores, this study was able to measure acoustic velocity and density on the same pieces of wood.

As part of a previous resource evaluation study, Vihermaa (2010) had collected cores for examination in a similar way, however the narrow geographical range of that experiment made it difficult to draw conclusions from comparisons between sites. A problem also arose because the southern half of the core was being used which, when taking the cores in a north to south direction, would often (though not always) leave the bark and a few rings attached to the tree when the increment corer exited on the south side (Vihermaa, 2010). In this study this problem was overcome by ensuring that all cores were taken north to south and the north half (bark to pith) of the core was used in the analysis. It was also often the case in the field that if damage occurred then a fresh core would be taken. In this way it was ensured that the bark was left intact on every core. This however does not alleviate the problem of the surface finish of the core (a problem when measuring acoustic velocity on the full core), breakages of the core, or other factors such as knots which are unknown until later when the core is analysed. The surface finish of the core depends on the sharpness of the corer tool being used. This is not an issue for density analysis using the ITRAX

densitometer as 2 mm sample strips, with extremely smooth surface finish, were milled from the middle of the cores. The original plan for these cores included the measurement of density and ring width only. However the opportunity arose to examine the cores for acoustic velocity and the surface finish of the core could then become an issue as the acoustic probes coupled with varying effectiveness to the core (see section 8.1.2 below). Knots were also a problem as these might not be seen in the field when the core was taken and it was only during the preparation that they were noticed. In this way 31 cores had to be discarded from the analysis. One further problem with using cores for analysis is the skill involved in managing to take the core so that it goes through the pith. Often the pith may not be exactly central in the tree so in some cases the pith was missed. This made numbering of rings more difficult and time consuming as each sample that had no pith had to be examined individually to ensure that the rings had been counted correctly.

As well as being cost effective, taking radial increment cores from trees is a quick and non-destructive (Wunder et al., 2011) way of obtaining samples and thus acoustic testing of cores proved to be a very useful tool for the type of analysis carried out in this study. However, care must be taken when taking and preparing the cores as it is difficult to avoid any defects during the analysis.

An ITRAX densitometer was used to analyse density and growth (by accumulated ring width). The method for this system was developed by McLean (2008) and refined by Vihermaa (2010) and comparison between these studies and the current investigation showed that the overall mean density was very similar for all three.

8.1.2 Acoustic Velocity Method

As part of this study, funding was secured from COST Action FP0802 for a short term scientific mission to The University of Canterbury in Christchurch New Zealand to investigate a system whereby the radial profile of longitudinal acoustic velocity could be measured directly from increment cores. The hope for this part of the experiment was to combine the acoustic velocity measurements with density measurements made on the same cores to give a radial profile of MOE and to consider if this changed throughout Britain. Previous trials had been

carried out on radiata pine in the Christchurch laboratory but the method could not be fully evaluated until comparable density measurements were available for the same material, as was the case here. However, there were a number of problems associated with the method which meant that much of the data were deemed to be unreliable. The two main issues found with this method were the orientation of the grain and the surface finish of the core. The grain orientation is important as the fastest path is in the same direction as the grain (Bucur, 1983, Bucur and Bohnke, 1994) and as shown here any deviation from this can have an effect on the measurement. Identifying the grain direction on increment cores can be a difficult task, especially if the bark is intact at both ends of the core. As well as this, grain angle within a core can vary from ring to ring, or even within a ring. This makes it difficult to know if any variation in the measurement (both within a tree and between trees) is due to actual variation in acoustic velocity or if it is due to the way that it is being measured. This problem is something that the School of Forestry in The University of Canterbury were aware of and at the time of writing they are working on a new system to try and counter this problem.

The second issue encountered with this method was to do with the surface condition of the core. Some of the older cores used in this study had rough surfaces and this seemed to cause problems with coupling with the acoustic velocity probes. This led to what seemed like more erratic readings than seen with cores that were in good condition. To counteract this, the offending cores were sanded to smooth the surfaces along which the measurements were taken, but examination of cores which were measured unsanded, then sanded and measured again showed that the sanding treatment had the effect of changing the result. There was also no universal conversion factor between the two states; in most cases the sanded cores had slower acoustic velocity measurements but this was not always the case and the magnitude of the difference varied between and even within each core. In this experiment, approximately half of the cores were measured without being sanded and the other half were measured after sanding but since no conversion procedure was available this meant that these two sets of measurements were not comparable.

8.2 Discussion of Tree Growth and Wood Properties

The growth rate of wood is known to affect wood properties such as density whereby wider rings tend to have low density (Petty et al., 1990, Herman et al., 1998). It is possible to model the age related trends of these properties. There have been a number of models used to describe radial growth of trees, many of which have been modified from studies in other organisms. A number of these were described by Zeide (1993). There are also models that describe radial variation in the density of trees and a number of these, which have previously been used to describe the radial trend in density of spruce (Lindstrom, 2000, Gardiner et al., 2011), were explored in this study. Spruce wood along with other species such as Douglas fir (Kennedy, 1995) have densities that decreases in the first few rings from the pith before increasing again towards a plateau in the mature wood (Gardiner et al., 2011). On the other hand the rate of radial growth has a tendency to have two to three years of slow growth at the pith, occurring during establishment, which is then followed by faster growth in the juvenile phase before the rate slows in the mature wood. Both radial growth and radial density were modelled in this study and the age related trends found here conform to these generally accepted trends.

Within this study a number of published growth models were explored with the aim of describing how age related trends are affected by site, management and location. Published density models were also explored and the parameters of these models updated to reflect the outcome of this investigation where a much larger data set than was previously available was used. Whilst the published models tend to describe the change in the radial trend of both growth and density as gradual (i.e. a curve) it was seen here that this trend may be able to be described as two separate phases with a defined split point between the two. With this in mind two-segment linear models were used to describe the radial trend in both density and growth separately to compare how these fared against the published models. The segmented models had the advantage that they had simple, intuitive parameters (i.e. a slope and intercept) and it was easy to understand how a change in these parameters changed the form of the relationship.

8.2.1 Radial Growth

Visual examination of the growth trend showed what could be described as a two stage pattern with wider rings in the faster juvenile growth period up to approximately year 10 to 20, followed by a slower growth rate in the mature wood, in a similar pattern to that described for Sitka spruce previously (McLean, 2008, Moore, 2011). To describe the growth trend 16 statistical models were compared, of which 14 were able to describe the trend reasonably well, with each model explaining approximately 69% of the variation and residual standard errors of 20.1 mm to 20.3 mm reflecting the scatter in the data. When the residuals were examined, the models which fitted a sigmoid function were able to describe the data slightly better, especially at the pith, as they are able to cope with the slight reverse curve in the first 2 to 3 years when growth is slower. Of these the Hossfeld4 model was deemed to be the best fit. However, because these models are describing a sigmoid shaped curve they are also more complicated with parameters which interact to describe the curve. Simpler models which described the trend as a smooth curve were also tested and an Exponential model was found to be the best of these. Although this was found to give reasonable fits it had problems describing growth at the pith, but had the advantage of having simple to understand parameters.

The two-segment linear model also had slight problems at the pith due to the slower growth in the first couple of years after establishment, which appeared in the model as a small negative intercept at ring zero. However, this model fitted as well as most of the other models and because of its simplicity was used to predict the effect of site and geographical effects.

Although there was a lot of variation between individual trees, when fitted against the full data set the segmented model predicted that the transition between the juvenile and mature phases of growth occurred between years 11 and 12. This concurs with the generally accepted juvenile and mature phases of growth in Sitka spruce (Cameron et al., 2005, Brazier and Mobbs, 1993, Schaible and Gawn, 1989). The cambial age that this transition occurs may be linked to canopy closure which typically occurs between cambial ages 10 to 12 years depending on the initial spacing (Kilpatrick et al., 1981, Savill and Sandels, 1983). Plotting the transition points by site showed that there was a lot of

variation between different sites, as well as within site variation. While some of the sites had a small range of transition points as would be expected if the timing of the transition was fully dependent on canopy closure (which would occur at approximately the same time for each tree at the same site) other sites had a large range in ages where the transition occurred. The variation between sites did not translate to any systematic variation when the transition age was looked at by the different site effects, suggesting that the amount of juvenile wood that a tree produces is not controlled by geographical location.

To investigate the effect of site factors on growth the juvenile and mature phases of growth of each tree were separated at 11.6 years and linear mixed effects models were used to analyse the fitted coefficients of the linear segments separately. In the juvenile phase the fixed effects of longitude, latitude, elevation and initial spacing as continuous variables were included in the mixed effects model and when the non-significant effects were left out only spacing was found to be significant with 3mm of additional ring width per metre of spacing per year. Including spacing in the model increased the R-squared value from 0.68 to 0.73.

The same fixed effects were included in the mixed effects model on the mature phase of growth (i.e. cambial age 12 to 25 years) and none were found to be significant on the rate of growth, although spacing had a significant effect on the overall mean. This would be expected as the rate of growth of the juvenile segment and the mean of the mature segment are linked so any effect on one has an effect on the other. It was also found that the radius of the trees at 12 years old was positively correlated with the radius of the same tree in later years suggesting that the management of a site during planting will have a big effect on the radial growth in later years.

The effect that initial spacing has on radial growth is well documented with increased growth being due to less competition for sunlight, water and nutrients (MacDonald and Hubert, 2002). However wider spacing can affect other properties such as the number and size of knots (Brazier, 1977) and may have a negative effect on the straightness of the stem (Brazier and Mobbs, 1993). Brazier et al. (1985) suggested that spacings of more than 2m would have a detrimental effect on wood quality and this was also found in a later study

(Brazier and Mobbs, 1993) which stated that spacing should not exceed 2m. This became the standard spacing regime promoted by the Forestry Commission and widely used throughout Britain (MacDonald and Hubert, 2002).

Because of this practice most of the sites used in this study (22 of 47) had 2 m spacing. Therefore these sites were analysed separately to investigate if longitude, latitude or elevation was having an effect on growth when the spacing was the same. However when tested using mixed effects models none of these effects were significant. Similarly when using ESC climate data directly again no effects were significant.

ESC data showed that there were differences between sites in accumulated temperature and moisture deficit according to latitude, longitude and elevation. However this was not translated into differences in tree growth within the geographical range over which Sitka has been commonly planted in GB. There did not seem to be any different effect on trees growing in southern England compared to those growing in northern Scotland, which covers the full UK range of accumulated temperature, suggesting that Sitka spruce is comfortable growing in the full range of temperatures in the UK. It may also mean that day length is unimportant over this range of latitudes, although there is a question of whether latitude would have been taken into account in the choice of seed provenance for any of the sites. The same applies to the east and west sites measured which again showed no difference. Elevation, over the range covered, was also seen to be having no significant effect on either juvenile or mature growth. This analysis may also show that there is so much within site variation that it is very difficult to see any environmental effects since these environmental effects are measured at a site level.

8.2.2 Radial Density

Traditionally density is seen as one of the most important and widely used factors to describe wood quality (MacDonald and Hubert, 2002) as although MFA may be a better guide to quality (due to its association with stiffness) it has been in general harder to measure and is still (via Silviscan) a very expensive measurement. In this study the pith to bark radial profile of density was measured on approximately 450 trees from 47 different sites across the full

latitudinal range of Great Britain. The resulting data were used to evaluate existing density models, to explore how these fitted a much more representative national data set than has previously been available and to update the existing model parameters to reflect this. These models were then also compared with a segmented linear model that not only has parameters that are simple to understand, but also does not require ring width as an input and so may be a valuable analytical tool in circumstances, such as in timber processing, where ring width data are not available.

In this investigation the overall mean radial density was similar to that found for Sitka spruce at a site in Kershope in North England (McLean, 2008) and at two Scottish sites (Vihermaa, 2010). The radial profile found here fitted the normal radial trend that would be expected with Sitka spruce (Brazier, 1970) i.e. density was high near the pith with a sharp decline in the first few rings to a minimum within the juvenile wood before increasing again towards the bark. Qualitatively this agrees with the profiles described in previous investigations (Bryan and Pearson, 1955, Brazier, 1967, Petty et al., 1990). This is a similar pattern to density found in other spruce species (e.g. Norway spruce (Lindstrom, 1996) and Black spruce (Alteyrac et al., 2006A, Alteyrac et al., 2006B) and can also be found in some other conifer species for example Douglas fir (Kennedy, 1995). Increasing density in mature wood has been linked to a higher latewood proportion (Jyske et al., 2008) and is due to smaller cells with thicker walls (Rathgeber et al., 2006). However the trend in the juvenile wood has always made it difficult to model density in Sitka spruce as the processes which cause the high density in the mature wood (i.e. smaller tracheids with thicker cell walls (Mitchell and Denne, 1997)) are thought to be different from those controlling density nearer the pith, where high density is associated with high microfibril angle and rapid radial change in grain angle (Moore, 2011) and this is one reason why density may be an unsatisfactory indicator of timber quality in spruces. Previous studies have shown that the radial density profile of Sitka spruce can be fitted using curvilinear models that include ring width as an input parameter along with ring number (Lindstrom, 2002, Gardiner et al., 2011) and these models were investigated as part of this study along with a simple exponential model that was based only on ring number and a two-segment linear model which also did not require ring width. The sites used by Gardiner et al.

(2011) showed a similar radial pattern and similar values to that found here and the coefficients of the models developed in that study were re-parameterized to reflect the much larger dataset used in this study.

Ring width is a measure of the growth rate during the year represented by the ring, and including this can increase the effectiveness of the model. The overall ring density is governed by the amount of less dense earlywood since the amount of latewood is roughly constant irrespective of ring width (Moore, 2011) and wider rings are associated with a decrease in density. If ring width is known then there is good reason to use it within a model. However, if ring width is not known then including it in the model would add an unnecessary step of having to model ring width, which can lead to propagation of error by adding steps in the analysis. For this reason, even though the models that include ring width give a better fit to the data, and although it may be argued that the change between the juvenile and mature phases of density is gradual rather than an abrupt change, a simple model such as the segmented linear model which uses just cambial age instead of both cambial age and growth is also a very useful tool.

Fitting the two-segment linear model to the full data set indicated a transition point between the juvenile and mature phases at a cambial age of 7.4 years although when this was fitted to individual trees it was found to be extremely variable, due to the sensitivity of the model to local fluctuations. This variation in the split point of individual trees also made it difficult to determine if any site effects were having an influence on the transition between the juvenile and mature phases, and no significant effects were found. This suggests that the age when density changes from the juvenile to mature phase is not governed by overall site factors but may be governed by more local factors.

In order to simplify the fitting process, the transition point was assumed to be constant at between years 7 and 8 and the two phases were analysed using separate linear models. This allowed site effects to be investigated on each of the phases individually. This analysis showed that much of the variation in density was within tree variation. Fitting models to the radial profile of density was made difficult by this variability and this is illustrated by the low R-squared values. There was also a large amount of variation in density between trees within the same site which makes it difficult to see the effect of site

characteristics, a point which was also made by Zobel and Buijtenen (1989) and which may indicate that more localised site effects impact on density. Genetics also play a large part in controlling wood properties (McLean, 2008, Kennedy et al., 2013). A study investigating the effect of genetics (Moore et al., 2009b) also found that the main sources of variation in density were within trees and between trees of the same treatment. This was put down to the fact that the trees were not clonal but highly diverse genetically. The trees used in this study are most likely grown from seed of Queen Charlotte Islands (Canada) origin collected from wild populations so that a large amount of between tree variation would be expected (Moore et al., 2009a).

Using mixed effects models on the two segments separately indicated that in the juvenile segment mean density increased with increasing latitude but decreased with increasing spacing. Therefore higher density near the pith was most pronounced at more northern sites with close spacings and may be associated with slow establishment (Brazier, 1970). However unlike in the mature wood where high density might indicate better wood quality, high density at the pith is associated with high microfibril angle and a rapid change in grain angle (Moore, 2011) and therefore does not indicate high quality wood.

In the mature segment there were no significant site effects, with cambial age being the only significant factor. Although a link was found between northing and the density of the juvenile wood, there was none found in the mature wood. Since temperature and northing are linked it suggests that the temperature range found within Great Britain is not having an effect on the density of mature wood. In fact in some cases trees grown in the south of England were found to have similar density to those grown in northern Scotland under very different climates.

This shows that the latitude of the samples and silviculture may have an effect on the overall level of density but the initial decrease found in the juvenile wood of Sitka spruce was independent of any of these site effects. Once the trees have reached the mature phase mixed effects models indicated that there were no significant site effects on the density, although spacing was close to being significant at the 5% level. Investigating Sitka spruce and Norway spruce planted in southern Scotland, Petty et al. (1990) found little difference in

density at two different spacings (0.9m and 2.4m). In this study cambial age was found to be the only factor having a significant effect on density in the mature phase whereby density increased by 3.9 kg m^{-3} per year.

8.2.3 Radial Profile of Longitudinal Acoustic Velocity

This study also investigated the radial trend in longitudinal acoustic velocity. While there were problems associated with the method, models to describe the radial trend were also explored. As with growth and density, acoustic velocity was seen to follow a two stage pattern and so was investigated using both curved models and a linear segmented model. However due to uncertainty introduced by the surface finish of the cores and by the grain orientation, it was decided that to use the model to describe variation due to other factors would be wrong, since the variation might be coming from the measurement method itself.

The radial trend in acoustic velocity shows a minimum at the pith with an initial sharp increase until approximately cambial age 10 to 20 years, where the rate of change slows and the acoustic velocity levels off towards the bark. As in the previous sections, this trend could be described as a two stage process although the transition between the two phases may be seen to be more gradual than with either growth or density. However, a segmented linear model fitted the data as well as the curvilinear models and indicated an overall transition point at between cambial ages 13 and 14 years, which is similar to that found in a previous study which measured acoustic velocity of Sitka spruce disks (Vihermaa 2010).

Although this indicates that it is possible to model acoustic velocity using both curvilinear and segmented linear models, the use of these models was taken no further in this study due to the complications that arose with the method and led to the unreliability of the data.

8.2.4 Comparing Growth and Wood Properties

This study indicated that there is an inverse relationship between ring width and radial density (Pearson correlation coefficient -0.473) (Figure 4-8) agreeing with previous studies which have suggested that faster growth is associated with low

density (Petty et al., 1990, Kennedy et al., 2013). The Pearson correlation coefficient between ring width and density in the juvenile wood up to ring 7 was -0.671 compared with -0.597 in the wood from ring 8 onwards. This suggests that the relationship is slightly different in the juvenile core than in the mature wood and the full range of conditions where the relationship holds is not fully understood. Caution is required because both correlations are likely to be affected by slope and scatter as well as the nature of the underlying relationship.

The coefficients from the linear models also allowed comparisons to be made between juvenile and mature segments. For example a correlation was found (Pearson correlation coefficient -0.549, $p = 0.001$) between density modelled at the pith (i.e. juvenile density intercept) and the small negative growth intercept (Figure 8-1). This small negative intercept corresponds to slow growth of the stem during the first 2 to 3 years after it has reached breast height, where the cores were taken, and the high density near the pith therefore appears connected with delayed establishment (Brazier, 1970), or more precisely with slow radial growth after the tree reaches breast height. Also a correlation was found (Pearson correlation coefficient -0.517, $p = 0.001$) between the intercept of the mature phases of density and growth (Figure 8-2), which may imply that around the 7 to 12 year old cambial age period the density of wood being formed is less in the bigger trees

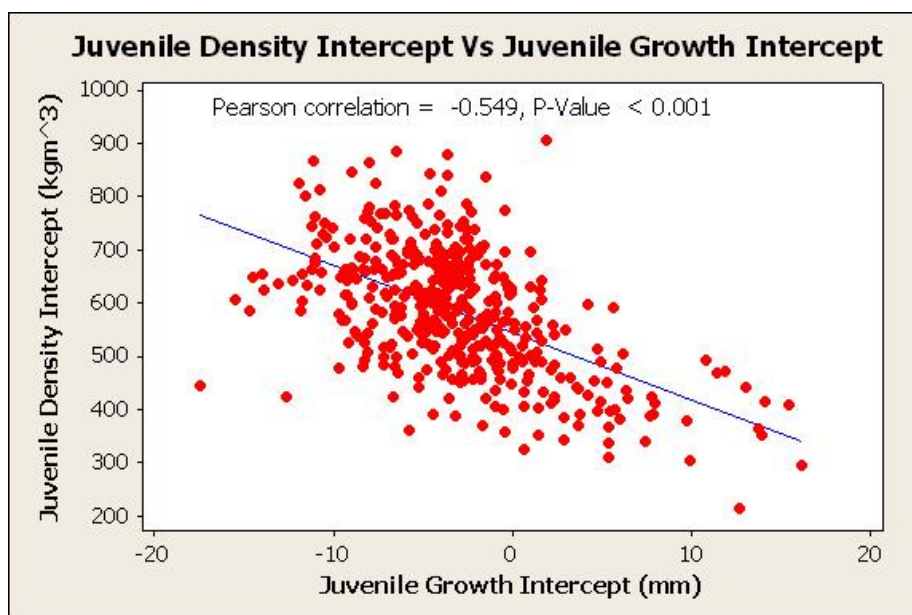


Figure 8-1: Correlation between the intercept coefficient of the juvenile linear models of growth and density

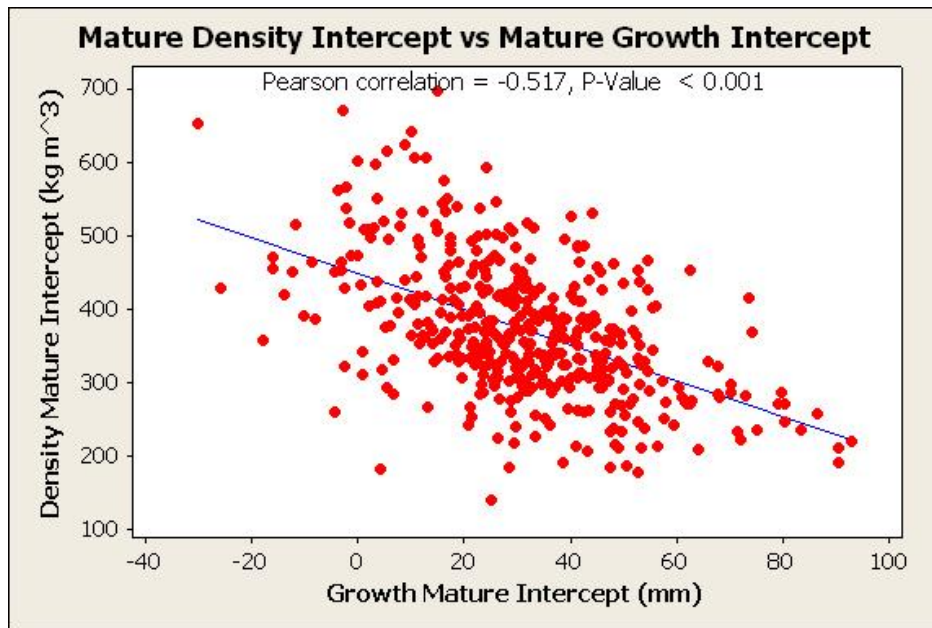


Figure 8-2: Correlation between the intercept coefficient of the mature linear models of growth and density

Correlations were also seen when both density and growth were examined individually across the age range of the trees. For example, density of ring 2 was correlated with density of ring 7 and also less so with rings 20 and 25. Similarly, growth rate was correlated between rings across the same age range. For both growth rate and density, correlations were highest between rings within either juvenile or mature wood and lower between rings in the different phases. For example high correlations were found between density at cambial age 12 and density at cambial age 25 (Pearson correlation coefficient 0.510) and also between growth rate at cambial age 12 and growth rate at cambial age 25 (Pearson correlation coefficient 0.863). This suggests that the juvenile stage of tree growth is very important in determining the properties of the mature wood, whether due to the establishment of dominance or for other reasons such as genes for density expressed throughout both growth phases.

8.2.4.1 Transition from Juvenile to Mature Wood

As discussed previously, transitions between juvenile and mature phases were evident in ring width, density and acoustic velocity data and although these could also be described as gradual, fitting a segmented model to the data allowed a transition point to be predicted. When fitted to the full data set the linear segmented model predicted a different transition point depending on the

property being measured. The split point for density was between 7 and 8 years, for growth it was between 11 and 12 years and for acoustic velocity it was between 13 and 14 years (Figure 8-3). This agrees with previous studies indicating that the boundary varies depending on the parameter being measured (Mansfield et al., 2009, Alteyrac et al., 2006B) and with estimates that the boundary between the juvenile core and mature wood occurs at about ring 7 to 12 (Brazier and Mobbs, 1993, Cameron et al., 2005).

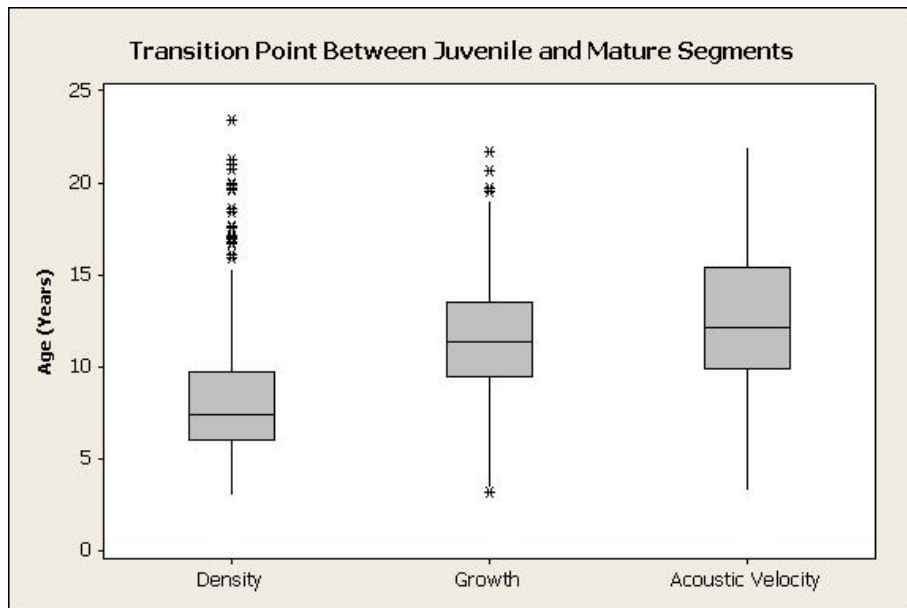


Figure 8-3: The transition point between the juvenile and mature phases when fitted by density, growth and acoustic velocity

However the transition points that the linear segmented models predicted for density and growth had a very small but significant correlation (Pearson correlation coefficient 0.168 $P= 0.002$) as seen in Figure 8-4, indicating that there may be a weak connection between the transition from juvenile to mature phases of these two properties although since it is so small it is difficult to draw any conclusion. Acoustic velocity showed no such correlation with either density or growth and although the transition points for growth rate and acoustic velocity are not significantly different, the fact that they are uncorrelated may suggest that it is not a single process which controls them. Conversely the transition points for density and growth are quite a bit apart, but there is this weak correlation between them.

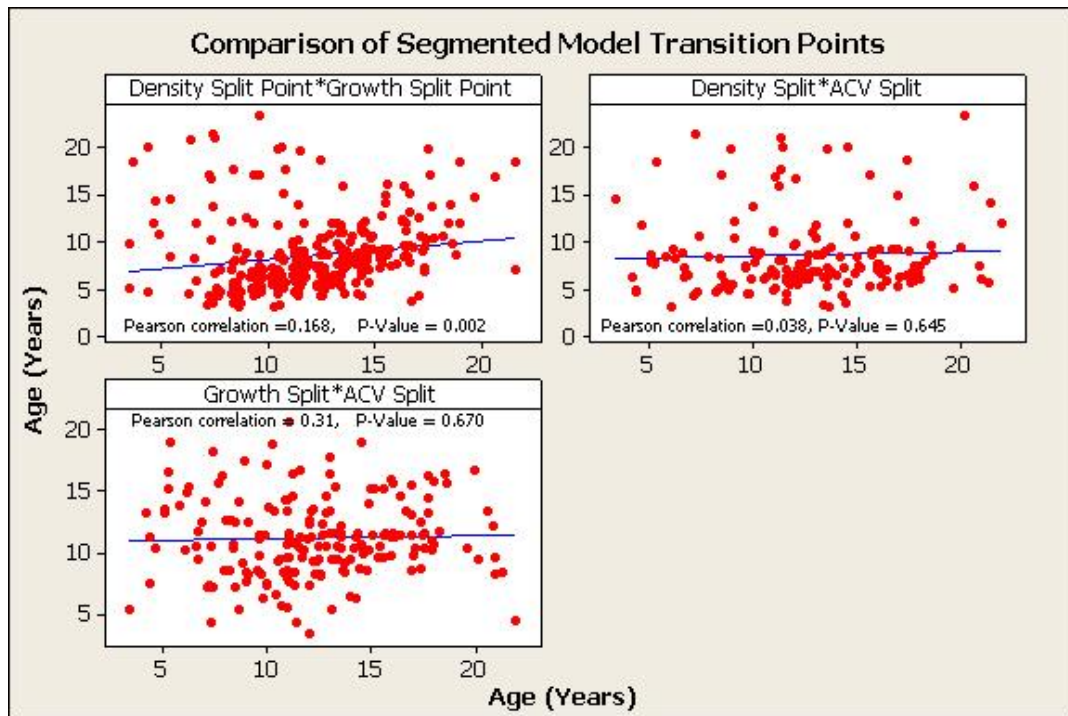


Figure 8-4: Relationship in the transition points between juvenile and mature phases when modelled by density, growth and acoustic velocity.

Although this may seem to indicate that separate physiological processes are at work, care must be taken before any conclusions are drawn from differences between the mean transition points, since the transitions between the two phases in the radial profiles of these properties are curvilinear, which may not be accurately fitted by the abrupt change of the segmented linear model. For example, the break in the slope of the growth model coincides well with the apparent midpoint in the transition of the growth rate, but the break in slope of the density model is at a lower ring number than the minimum of the mean density curve which is also not a close match to the LOWESS trend line (which changes slope at around ring 12 to 13).

8.3 Discussion on Seasonal Variation in Tree Growth

In this study most of the variation in all three properties modelled was between trees at the same site. This shows the difficulty in trying to predict the effect that a site factor can have when there are many within site factors that seemingly have an influence. To investigate the within site variation and the influence that climate has on growth at a fine time scale, two sites were used and at each site 5 trees were measured continuously for growth using LVDT point dendrometers.

The data used in this study were initiated in 2008 as part of a long term project at Griffin Forest near Aberfeldy in Perthshire, Scotland, with measurements during 2008 and 2009 being taken and used as part of a previous PhD study (Vihermaa, 2010) and continued as part of this study. The second site was a new site established at Harwood Forest in Northumberland, northern England.

It was seen that there were differences in growth between the trees within a site. Although not measured specifically for each tree, soil moisture was shown to vary within the site and this could have a more local effect on tree growth. Competition for sunlight would also have an effect on growth and at the Griffin site it was noticeable that the tree with the least amount of growth was no longer a dominant tree and was also not next to a row that had been thinned, so this tree may only have been getting enough sunlight at certain times of day and year. However the effect of thinning (or lack of it) applies equally to competition for water, and it is difficult to distinguish between competition for light and competition for water without data on crown dimensions.

The yearly pattern of growth followed the usual pattern that would be expected for Sitka spruce during the yearly growing season. That is, initial radial expansion of the tree started in spring around the end of March, followed by a period of rapid expansion through spring and into early summer as the trees produced large earlywood cells, peaking around mid summer. After this the growth rate started to decrease as the tree switched from producing earlywood to latewood, characterised by smaller cells with thicker cell walls. Growth stopped around mid to late September. There then followed a period of dormancy where no growth occurred during the winter period.

The onset of growth in spring was found to be influenced by mean temperature rising above 5°C although some radial expansion occurred before this when mean temperatures rose consistently above about 3°C (which coincided with minimum temperatures rising above 0°C). Similarly Vihermaa (2010) found that radial expansion occurred prior to growth starting when dendrometer readings were compared to actual cell production on microcores. Sitka spruce may be subject to a high chilling requirement whereby bud burst will not occur until after 140 days of temperatures below 5°C during the preceding winter (Cannell and Smith, 1986), and this may have been the case here as growth started as soon as

temperatures rose above 5°C in years where this requirement was met. In the one year where this requirement was not met there was a delay in the onset of growth when temperature initially rose above the 5°C threshold. Temperatures then dropped again in early spring fulfilling the requirement for 140 days below 5°C and growth started once the temperature rose again. Since it is thought that this chilling requirement is an adaptation to stop frost damage if bud burst was to occur too early in spring (Cannell and Smith, 1986) then in this case, when there was a late drop in temperatures, the mechanism worked. However, it is difficult to draw overall conclusions from this since only 4 years of data for the previous winters was measured, of which only one winter did not meet the chilling requirement.

The decrease in growth rate is assumed to be when production switches from early to latewood and is thought to be connected to a decrease in day length (Denne and Smith, 1971, Rossi et al., 2006) and although the switch was seen here occurring around the same time as maximum daylight hours, there were some differences between years in the date when it occurred. A decrease in soil moisture was found to affect the growth rate if a dry period occurred at the period of peak growth rate. Soil moisture falling below 30% coincided with the peak growth rate in two of the years measured and on both occasions the growth rate started to decline as this threshold was met and continued to decline for the remainder of the growing season even when soil moisture recovered. In two years where soil moisture did not fall below this 30% threshold the peak in growth rate continued for a longer period until later in the growing season before starting to decline. This suggests that the amount of moisture available will have an influence not only on the amount of growth but also on the type of growth that takes place. If seasons with less available moisture lead to an earlier switch from early to latewood then this would lead to an increase in the latewood proportion of the ring and therefore to increased average ring density. The date of final cessation of growth was relatively constant in each year and occurred before temperature fell below 5 C, (except tree 66) suggesting that this was controlled by day length. Therefore since the length of the growing season is the same, any decrease in growth rate would correspond to a decrease in growth. Seasons with abundant moisture may lead to an increased proportion of earlywood which in turn would lead to less dense wood. This ties in with the

good performance of density models that included a term for ring width as well as terms for ring number.

8.4 How will projected climate affect Sitka spruce

According to climate change projections, temperatures in Britain are set to rise throughout and this should be accompanied by drier summers and wetter winters (UKCP09, 2009a). However since this is projecting into the future there is huge uncertainty. Projections used in this study for specific sites indicated that accumulated temperatures are set to rise throughout the country but that there may be an east west split with regards to moisture. That is, the west is projected to get wetter and the east drier. Sitka spruce enjoys a wet climate (Cannell, 1984, Moore, 2011) and for this reason Sitka spruce plantations in the east of Britain are already limited to more northern and upland areas.

With the east projected to become drier during the summer this will limit the locations suitable for Sitka further. This study found no effect of longitude on growth or density and this may be due to the fact that the sites where Sitka is grown in the east are those in which soils are suitable for growth. However, the moisture deficit for the eastern sites used in this study is projected to increase leading to drier soil conditions. This study investigated growth at very fine time resolution and found that if water was limited during the height of the growing season then this could trigger a decrease in the growth rate. This would potentially lead to denser wood as the latewood percentage would be increased. However the adverse effect of this is that there would be less radial growth. Conversely an increase in moisture leads to increase in early wood growth but the amount of latewood stays the same, so although there will be an increase in the wood produced this will be accompanied by a decrease in density.

In general the productivity (i.e. general yield class) of forests in northern Britain has increased substantially over the past three to four decades and this is attributed to a combination of elevated CO₂ levels and improved nutrient status (Cannell et al., 1998). From the inverse correlation between growth rate and density observed in this study this change in productivity may be expected to have reduced wood density. However we can not be certain without having observed the effects of these environmental variables directly and potentially

future changes in management (e.g. spacing) could be enough to offset any such effect.

Temperature projections suggest that there will be an increase in accumulated temperatures throughout the latitudinal range of Britain (Figure 2-16), with future temperatures in the north projected to increase until they are similar to those found in the south today. This study found no difference in the amount of growth between trees growing in the south of Wales and England compared with those in the north of Scotland, with silviculture having a bigger influence on the growth rate. However there was an effect of latitude on wood density with density of the juvenile core increasing in a northward direction and there was also a correlation between the density at the end of the juvenile core and in the mature wood. This may suggest that density of wood could be adversely affected if temperatures in the north were to increase and at the same time moisture deficit decreased.

Increasing temperature can affect tree growth in a number of ways. It can have an effect on moisture availability by increasing evapotranspiration and it can have an effect on the length of the growing season. This study found no reason to disagree with previous studies suggesting that Sitka spruce has a winter chill requirement of 140 days of temperatures below 5°C before bud burst will occur. At the Griffin site where growth was measured, the chilling requirement was easily met on most years and so growth occurred as soon as temperatures rose above a 5°C threshold. However if winter temperatures rise then this requirement may not be met, leading to a delay in the onset of growth as was seen at Griffin. This led to a shorter growing season and therefore less growth for Sitka of a given provenance. This study also found no indication that Sitka spruce, of the provenances currently planted, would be able to take advantage of an extension to the growing season in autumn. Growth rate decreased and growth stopped at roughly the same time every year and this was always before temperatures dropped below 5°C. It has been suggested that the termination of growth at the end of the season is triggered by the amount of daylight hours and if this is the case and is genetically controlled then the trees will not take advantage of a longer growing season.

8.5 Conclusion

Several models used to describe growth were tested within this study, the best of which were able to describe about 69% of the variation. Of these, a segmented linear model fitted no better than the other models tested but met other intended criteria i.e. simplicity, intuitive parameters and reversibility whereby it can be expressed as distance from pith.

Due to the negative correlation between growth rate and density, including ring width as a variable along with ring number improved the prediction capabilities of the density models. Linear segmented models were able to predict density from ring number alone and this provides a powerful tool. In practice ring width may not always be available and so there is a need for models which can predict density from ring number alone. The reversibility of the linear segmented growth model permits the linear segmented model for density to be expressed in terms of distance from pith rather than ring number and in that form it may be of more interest for timber processing.

Although a great deal of variation between sites in both growth and density was observed, most of the variation was between trees in the same site. Initial spacing was found to be the only significant effect on growth and then only by having a positive effect on the growth rate of the juvenile wood. This had a knock on effect on the mature wood as trees were larger by the time they reached the end of the juvenile phase, and tended to stay larger throughout the mature phase. The latitude, longitude and altitude that the trees were growing at were found to have no significant effect on growth. Both spacing and latitude were found to be having a significant effect on the mean density of the juvenile wood with spacing having a negative effect and density a positive effect. In the mature wood, cambial age was found to be the only significant effect. This suggests that within the geographical range over which Sitka spruce is grown in Britain, climate is not yet a limiting factor, with site management, especially around the time of planting, having a bigger influence.

Examination of seasonal variation in growth found that the start of growth is associated with mean temperature rising above 5°C and that during the growing season the expansion of the stem can be affected by soil moisture. Competition

within a site can greatly influence trees growth and again forest management can have a big effect on competition for both soil moisture and sunlight. Soil moisture deficit was seen to influence the growth rate with 30% soil moisture seeming to be a threshold below which the growth rate is affected especially at the time of peak growth. The cessation of growth was similar in date throughout the years measured and happened before temperatures dropped below 5°C. This suggests that it is not temperature controlled and may indicate that if potential growing seasons are extended due to a changing climate then trees such as Sitka spruce may not take advantage of it.

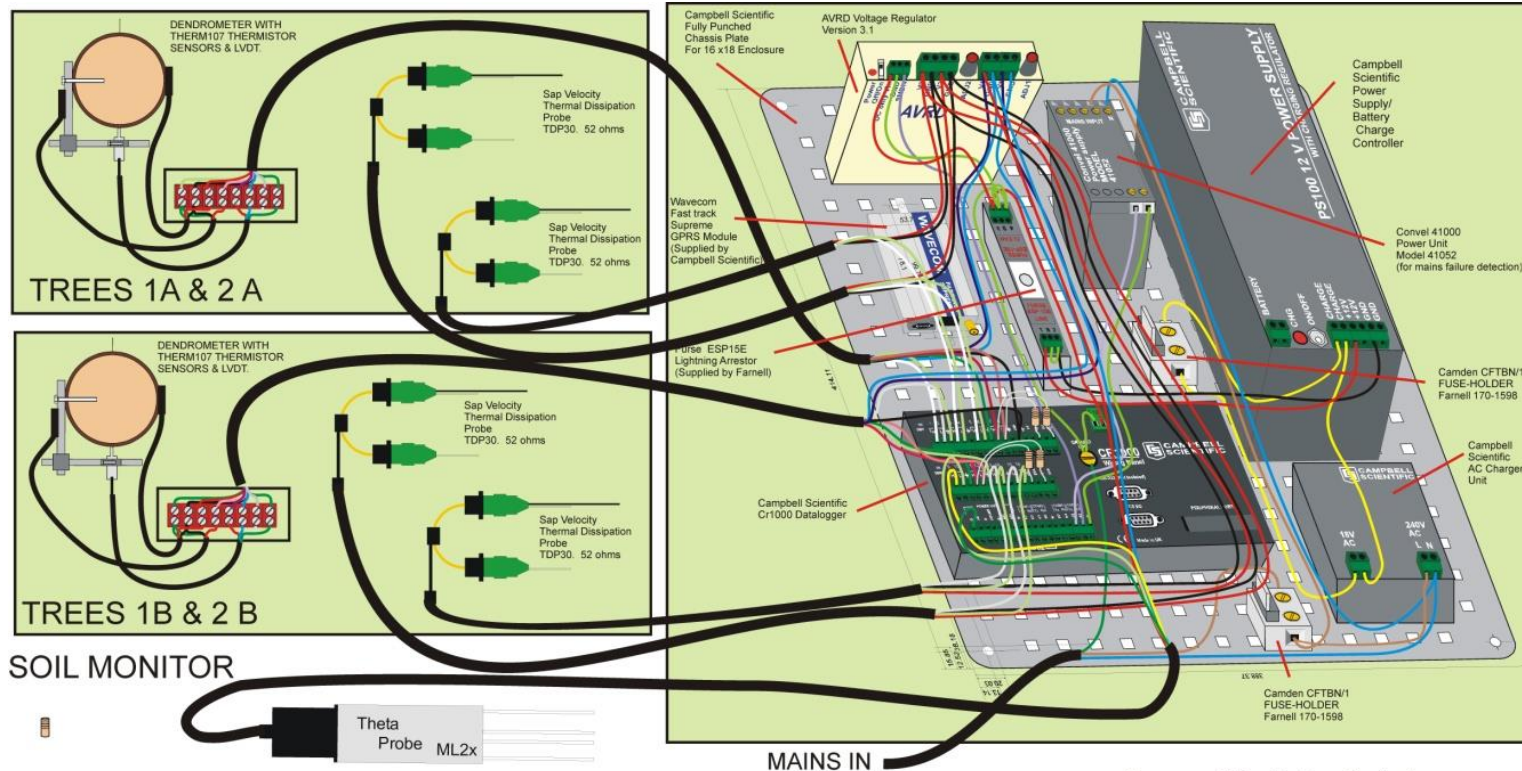
Appendices

Appendix1: List of equipment used at the Harwood site:

Item	Model/Serial No.	Qty	Supplier/Location
12V power supply	PS100	4	Campbell Scientific
AC-AC adaptor/charger unit	AC-ADAPT2	4	Campbell Scientific
5V power supply unit (for mains failure detection)	Convel 41000 Model 41052	4	Farnell
Thermistor	Therm107	12	Campbell Scientific
Lightning arrester/surge protector	Furse ESP 15E	4	RS Stock No. 456-8162
Terminal block/fuse holder	Camden CFTBN-1	10	Farnell order code 3882792
AVRD voltage regulator	Version 3.1	4	Dynamax
Resistors (pull-up type for dendrometers)	1K, 0.1% tolerance	?	
Resistors (pull-up type for dendrometers)	249K, 0.1%	?	
Resistors (pull-up type for rain gauge and anemometer)	MULTICOMP MF50 1K5	?	Farnell order code 9339990
Cable glands	Bulgin BE123461	?	Farnell order code 1701598
Datalogger	Cr1000	4	Metrometrics(x1)/ NRS (x3)
Sap flow sensor	TDP30	10	AH
Soil moisture sensor	ThetaProbe ML2x	3	AH
Rain gauge		1	AH
PAR Sensor		?	NRS
Temperature probe		1	AH
Humidity probe		1	AH
Anemometer		1	NRS
Wind vane		1	NRS

AH = Alice Holt, NRS = Northern Research Station

Appendix 2: Schematic plan of loggers 1 and 2



WIRING NOTES:

(A) CABLES: Wiring of power carrying conductors should be in 24x0.2 flexible cable. Eg Farnell 117-2965. Available in various colours.

(B) Stripped ends should be fitted with crimped bootlace ferrules before fitting to terminal strips.

(C) Cabled Glends: Butyl type BE 1234611 (Farnell 170-1598) is suggested. It provides sealing to ip67.

(D) FUSEHOODERS & FUSES: The design has fuses placed in the mains supply and in the 18 volt output from the Campbell Scientific AC adapter. The battery pack is fitted with an internal 3amp thermal fuse. Fuseholder is Camden CFTBN1 (Farnell 388-2782). The fuses are 20mm x5mm 2amp & 500mA slow blow. (Farnell 114-9646 & 114-9651).

(E) CABLE TIES: The drawing shows the wiring spread for maximum visibility. On completion, the wiring should be bundled and secured with cable ties. (Eg Farnell 136-9999)

(F) CABLE ALLOWANCE FOR BATTERY REPLACEMENT: Some cable allowance should be allowed when wiring the battery/charger module as it has to be lifted some distance above the base plate to change the battery. Battery life under float charge conditions is typically 5 years.

(G) Pull-up resistors: For optimum precision, the manufacturers of the TH107 Thermistor probes used on the dendrometers recommend that the precision 1K resistor, wired between the signal lead and ground, be placed at the datalogger end of the cable, especially if long cables are used. Belden cable 8761 or 8451 is recommended for such extensions. The resistors are shown mounted at the datalogger in the wiring diagram. In the case of the rain gauge and the anemometer counters, again pull-up resistors are necessary and are shown in the appropriate diagrams. These latter resistors are 1.5K and Farnell 933-9990 are suitable.

(H) POWER OUT DETECTION: To provide the software in the CR1000 datalogger with notice of a mains power failure, a small 5v power supply is connected to main supply with its 5v output connected to the C7 digital input on the datalogger. This enables the software to respond to a mains failure, by logging and timing it, by executing power saving procedures, and by sending an alarm message.

(I) GROUNDING: In general, sensors should not share ground cores. Each ground should be brought back to the datalogger independently. Also, cables should not be grounded at both ends, and earth loops should be avoided within the datalogger enclosure.

MAIN COMPONENTS LIST

Ref	quantity	Ref Name	Manufacturer/Supplier
U14	4	AC-ADAPT2	Campbell Scientific
U13	4	AVRD	Dynamax
BATT1	4	BPS4E-LA	Campbell Scientific
L29	4	CONVEL41052	Farnell
U1	4	CR1000	Campbell Scientific
L30	4	ESP15E	Furse
FS1	8	FUSE	Farnell
U15	2	HMP45C	Campbell Scientific
L34	5	LVDTensor	RS Components
L12	2	ML2X	Delta T
L27	1	NRC4DH4200P	NOR Systems
L26	1	PAR	Farnell
R	12	R	Farnell
L28	1	RANGAUGE	Dynamax
U2	10	TDP3APROBE	Campbell Scientific
U2	4	Enclosures 16/18	Campbell Scientific
L2	1	GPRS module	Wavecom

CR1000 DATALOGGING SYSTEM: POWER AUDIT

COMPONENT	Avg	Max	No	Total Avg	Total Max
CR1000 SYSTEM	27.9	27.4	4	110.4	109.4
Wavecom F S GSM	300	2500	1	300	2500
LVDT OC	13	13	4	52	52
CONVEL41052	1	0	0	0	0
BPS4E-LA	0	0	4	0	0
CR1000	4	4	2	8	8
ESP15E	0	0	0	0	0
HMP45C	20	20	1	20	20
ML2X	0	0	1	0	0
NRC4DH4200P	0	0	1	0	0
PAR	200	200	5	1000	1000
TDP3APROBE	0	0	10	0	0
TH107	0	0	10	0	0
TOTAL for 4 units				1484.4	3684.4

PROJECTED BATTERY LIFE

BATTERY TYPE	AH	LIFE HRS (AVG)	LIFE HRS (MAX)
BPS4E-LA	0	10	7.5
BPS4E-LA	24	64	38

Harwood Monitoring Project

DATA LOGGER 1 & 2 WIRING DIAGRAM

METEORMETRICS LTD Kirklands, Craigend Road, Stow, Galashiels, Selkirkshire, TD12RJ 0131 208 9402 www.meteormetrics.com

DRAWING: DATALOGGER 1&2 WIRING DIAGRAM

Forestry Commission NRS Harwood Monitoring Project DATE: 09/11/10

CONTACT: Kevin Scott: drkfs@AOL.com 0771 969 7799 Copyright Meteormetrics Ltd, all rights reserved.

List of References

- AAKALA, T. & KUULUVAINEN, T. 2011. Summer droughts depress radial growth of *Picea abies* in pristine taiga of the Arkhanglesk province, northwestern Russia. *Dendrochronologia*, 29, 67-75.
- ABE, H. & NAKAI, T. 1999. Effect of the water status within a tree on tracheid morphogenesis in *Cryptomeria japonica* D-Don. *Trees-Structure and Function*, 14, 124-129.
- AKAIKE, H. 1974. New look at statistical-model identification. *Ieee Transactions on Automatic Control*, AC19, 716-723.
- ALLISON, S. M., PROE, M. F. & MATTHEWS, K. B. 1994. The prediction and distribution of general yield classes of Sitka spruce in Scotland by empirical-analysis of site factors using a geographic information-system. *Canadian Journal of Forest Research-Revue Canadienne De Recherche Forestiere*, 24, 2166-2171.
- ALTERYRAC, J., CLOUTIER, A., UNG, C. H. & ZHANG, S. Y. 2006A. Mechanical properties in relation to selected wood characteristics of black spruce. *Wood and Fiber Science*, 38, 229-237.
- ALTERYRAC, J., CLOUTIER, A. & ZHANG, S. Y. 2006B. Characterization of juvenile wood to mature wood transition age in Black spruce (*Picea mariana* (Mill.) BSP) at different stand densities and sampling heights. *Wood Science and Technology*, 40, 124-138.
- ANTONOVA, G. F. & STASOVA, V. V. 1993. Effects of environmental-factors on wood formation in Scots pine stems. *Trees-Structure and Function*, 7, 214-219.
- AUTY, D. & ACHIM, A. 2008. The relationship between standing tree acoustic assessment and timber quality in Scots pine and the practical implications for assessing timber quality from naturally regenerated stands. *Forestry*, 81, 475-487.
- BAECHLE, H. & WALKER, J. 2006. The influence of temperature on the velocity of sound in green pine wood. *Holz Als Roh-Und Werkstoff*, 64, 429-430.
- BAILEY, I. W. & KERR, T. 1935. The visible structure of the secondary wall and its significance in physical and chemical investigations of tracheary cells and fibers. *Jour Arnold Arboretum*, 16, 273-300.
- BALL, T., SMITH, K. A. & MONCRIEFF, J. B. 2007. Effect of stand age on greenhouse gas fluxes from a Sitka spruce [*Picea sitchensis* (Bong.) Carr.] chronosequence on a peaty gley soil. *Global Change Biology*, 13, 2128-2142.
- BARNETT, J. R. & BONHAM, V. A. 2004. Cellulose microfibril angle in the cell wall of wood fibres. *Biological Reviews*, 79, 461-472.
- BAUCKER, E., BUES, C. T. & VOGEL, M. 1998. Radial growth dynamics of spruce (*Picea abies*) measured by micro-cores. *Iawa Journal*, 19, 301-309.
- BEALL, F. C. 2002. Overview of the use of ultrasonic technologies in research on wood properties. *Wood Science and Technology*, 36, 197-212.
- BEAUCHAMP, K. 2011. *The biology of heartwood formation in Sitka spruce and Scots pine*. PhD, University of Edinburgh.
- BEAUCHAMP, K., MENCUCCINI, M., PERKS, M. & GARDINER, B. 2013. The regulation of sapwood area, water transport and heartwood formation in Sitka spruce. *Plant Ecology & Diversity*, 6, 45-56.
- BEGUM, S., NAKABA, S., YAMAGISHI, Y., YAMANE, K., ISLAM, A., ORIBE, Y., KO, J.-H., JIN, H.-O. & FUNADA, R. 2012. A rapid decrease in temperature

- induces latewood formation in artificially reactivated cambium of conifer stems. *Annals of Botany*, 110, 875-885.
- BERGES, L., NEPVEU, G. & FRANCO, A. 2008. Effects of ecological factors on radial growth and wood density components of sessile oak (*Quercus petraea* Liebl.) in Northern France. *Forest Ecology and Management*, 255, 567-579.
- BERGSTEN, U., LINDEBERG, J., RINDBY, A. & EVANS, R. 2001. Batch measurements of wood density on intact or prepared drill cores using x-ray microdensitometry. *Wood Science and Technology*, 35, 435-452.
- BOURIAUD, O., LEBAN, J. M., BERT, D. & DELEUZE, C. 2005. Intra-annual variations in climate influence growth and wood density of Norway spruce. *Tree Physiology*, 25, 651-660.
- BRAZIER, J. D. 1967. Timber improvement .1. A study of variation in wood characteristics in young Sitka spruce. *Forestry*, 40, 117-&.
- BRAZIER, J. D. 1970. Timber improvement .2. Effect of vigour on young-growth Sitka spruce. *Forestry*, 43, 135-&.
- BRAZIER, J. D. 1977. Effect of forest practices on quality of harvested crop. *Forestry*, 50, 49-66.
- BRAZIER, J. D., HANDS, R. & SEAL, D. T. 1985. Structural wood yields from Sitka spruce: the effect of planting spacing. *Forestry and British Timber*, 14, 34-37.
- BRAZIER, J. D. & MOBBS, I. D. 1993. The influence of planting distance on structural wood yields of unthinned Sitka spruce. *Forestry*, 66, 333-352.
- BROADMEADOW, M. S. J. (ed.) 2002a. *Climate change: impacts on UK forests*, Edinburgh: Forestry Commission
- BROADMEADOW, M. S. J. (ed.) 2002b. *Climate change: impacts on UK forests. Bulletin 125*, Edinburgh: Forestry Commission.
- BROWN, S., BOORMAN, P. & MURPHY, J. 2009. *Interpretation for use of surface wind speed projections from the 11-member Met Office Regional Climate Model ensemble* [Online]. Retrieved 21/04/2010, http://ukclimateprojections.defra.gov.uk/images/stories/Tech_notes/UK_CP09_wind_technote.pdf.
- BRYAN, J. & PEARSON, F. G. O. 1955. The quality of Sitka spruce grown in Great Britain. *Empire Forest Rev*, 34, 144-153.
- BUCUR, V. 1983. An ultrasonic method for measuring the elastic-constants of wood increment cores bored from living trees. *Ultrasonics*, 21, 116-126.
- BUCUR, V. & BOHNKE, I. 1994. Factors affecting ultrasonic measurements in solid wood. *Ultrasonics*, 32, 385-390.
- BURLEY, J. 1966. Genetic variation in seedling development of Sitka spruce *Picea sitchensis* (bong) carr. *Forestry*, 39, 68-&.
- BURMESTE, A. 1965. Relationship between sound velocity and morphological physical and mechanical properties of wood. *Holz Als Roh-Und Werkstoff*, 23, 227-&.
- CAMERON, A. D. 2002. Importance of early selective thinning in the development of long-term stand stability and improved log quality: a review. *Forestry*, 75, 25-35.
- CAMERON, A. D., LEE, S. J., LIVINGSTON, A. K. & PETTY, J. A. 2005. Influence of selective breeding on the development of juvenile wood in Sitka spruce. *Canadian Journal of Forest Research-Revue Canadienne De Recherche Forestiere*, 35, 2951-2960.
- CANNELL, M. G. R. 1984. Sitka spruce. *Biologist*, 31, 255-261.
- CANNELL, M. G. R. & SMITH, R. I. 1983. Thermal time, chill days and prediction of budburst in *Picea sitchensis*. *Journal of Applied Ecology*, 20, 951-963.

- CANNELL, M. G. R. & SMITH, R. I. 1986. Climatic warming, spring budburst and frost damage on trees. *Journal of Applied Ecology*, 23, 177-191.
- CANNELL, M. G. R., THORNLEY, J. H. M., MOBBS, D. C. & FRIEND, A. D. 1998. UK conifer forests may be growing faster in response to increased N deposition, atmospheric CO₂ and temperature. *Forestry*, 71, 277-296.
- CARON-DECLOQUEMENT, A. 2010. *Extractives from Sitka Spruce*. PhD, University of Glasgow.
- CAVE, I. D. 1968. Anisotropic elasticity of plant cell wall. *Wood Science and Technology*, 2, 268-&.
- CAVE, I. D. & WALKER, J. C. F. 1994. Stiffness of wood in fast-grown plantation softwoods - the influence of microfibril angle. *Forest Products Journal*, 44, 43-48.
- CHAN, J. M., WALKER, J. C. & RAYMOND, C. A. 2011. Effects of moisture content and temperature on acoustic velocity and dynamic MOE of radiata pine sapwood boards. *Wood Science and Technology*, 45, 609-626.
- CHAUHAN, S. S. & WALKER, J. C. F. 2006. Variations in acoustic velocity and density with age, and their interrelationships in radiata pine. *Forest Ecology and Management*, 229, 388-394.
- CHERUBINI, P., SCHWEINGRUBER, F. H. & FORSTER, T. 1997. Morphology and ecological significance of intra-annual radial cracks in living conifers. *Trees-Structure and Function*, 11, 216-222.
- CLEMENT, R., MONCRIEFF, J. B. & JARVIS, P. G. 2003. Net carbon productivity of sitka spruce forest in Scotland. *Scottish Forestry*, 57, 5-10.
- CLEMENT, R. J., JARVIS, P. G. & MONCRIEFF, J. B. 2012. Carbon dioxide exchange of a Sitka spruce plantation in Scotland over five years. *Agricultural and Forest Meteorology*, 153, 106-123.
- COLLAKOVA, E., KLUMAS, C., SUREN, H., MYERS, E., HEATH, L. S., HOLLIDAY, J. A. & GRENE, R. 2013. Evidence for extensive heterotrophic metabolism, antioxidant action, and associated regulatory events during winter hardening in Sitka spruce. *Bmc Plant Biology*, 13.
- COWDREY, D. R. & PRESTON, R. D. 1966. Elasticity and microfibrillar angle in wood of Sitka spruce. *Proceedings of the Royal Society Series B-Biological Sciences*, 166, 245-&.
- DAUWE, R., HOLLIDAY, J. A., AITKEN, S. N. & MANSFIELD, S. D. 2012. Metabolic dynamics during autumn cold acclimation within and among populations of Sitka spruce (*Picea sitchensis*). *New Phytologist*, 194, 192-205.
- DAVIES, R. B. 1987. Hypothesis-testing when a nuisance parameter is present only under the alternative. *Biometrika*, 74, 33-43.
- DEANS, J. D. & MILNE, R. 1999. Effects of respacing on young Sitka spruce crops. *Forestry*, 72, 47-57.
- DENGEL, S., AEBY, D. & GRACE, J. 2009. A relationship between galactic cosmic radiation and tree rings. *New Phytologist*, 184, 545-551.
- DENNE, M. P. & SMITH, C. J. 1971. Daylength effects on growth, tracheid development, and photosynthesis in seedlings of *Picea sitchensis* and *Pinus sylvestris*. *Journal of Experimental Botany*, 22, 347-&.
- DESLAURIERS, A. & MORIN, H. 2005. Intra-annual tracheid production in balsam fir stems and the effect of meteorological variables. *Trees-Structure and Function*, 19, 402-408.
- DESLAURIERS, A., MORIN, H., URBINATI, C. & CARRER, M. 2003. Daily weather response of balsam fir (*Abies balsamea* (L.) Mill.) stem radius increment from dendrometer analysis in the boreal forests of Quebec (Canada). *Trees-Structure and Function*, 17, 477-484.

- DESLAURIERS, A., ROSSI, S. & ANFODILLO, T. 2007. Dendrometer and intra-annual tree growth: What kind of information can be inferred? *Dendrochronologia*, 25, 113-124.
- DEVINE, W. D. & HARRINGTON, C. A. 2010. Factors affecting diurnal stem contraction in young Douglas-fir. *Agricultural and Forest Meteorology*, 151, 414-419.
- DOWNES, G., BEADLE, C. & WORLEDGE, D. 1999. Daily stem growth patterns in irrigated Eucalyptus globulus and E-nitens in relation to climate. *Trees-Structure and Function*, 14, 102-111.
- DREW, D. M. & DOWNES, G. M. 2009. The use of precision dendrometers in research on daily stem size and wood property variation: A review. *Dendrochronologia*, 27, 159-U7.
- DUCHESNE, L. & HOULE, D. 2011. Modelling day-to-day stem diameter variation and annual growth of balsam fir (*Abies balsamea* (L.) Mill.) from daily climate. *Forest Ecology and Management*, 262, 863-872.
- DUTILLEUL, P., HERMAN, M. & AVELLA-SHAW, T. 1998. Growth rate effects on correlations among ring width, wood density, and mean tracheid length in Norway spruce (*Picea abies*). *Canadian Journal of Forest Research-Revue Canadienne De Recherche Forestiere*, 28, 56-68.
- EVANS, R. & ILIC, J. 2001. Rapid prediction of wood stiffness from microfibril, angle and density. *Forest Products Journal*, 51, 53-57.
- FARRELL, R., INNES, T. C. & HARWOOD, C. E. 2012. Sorting Eucalyptus nitens plantation logs using acoustic wave velocity. *Australian Forestry*, 75, 22-30.
- FELIKSIK, E. & WILCZYNSKI, S. 2008. Tree-ring chronology as a source of information on susceptibility of Sitka spruce to climatic conditions of Pomerania (northern Poland). *Geochronometria*, 30, 79-82.
- FONWEBAN, J., MAVROU, I., GARDINER, B. & MACDONALD, E. 2013. Modelling the effect of spacing and site exposure on spiral grain angle on Sitka spruce (*Picea sitchensis* (Bong.) Carr.) in Northern Britain. *Forestry*, 86, 331-342.
- FORD, E. D., ROBARDS, A. W. & PINEY, M. D. 1978. Influence of environmental-factors on cell production and differentiation in early wood of *Picea sitchensis*. *Annals of Botany*, 42, 683-&.
- FORESTRY_COMMISSION 2011. Standing Timber Volume for Coniferous Trees in Britain. *National Forest Inventory Report*. Edinburgh: Forestry Commission.
- GARDINER, B., LEBAN, J.-M., AUTY, D. & SIMPSON, H. 2011. Models for predicting wood density of British-grown Sitka spruce. *Forestry*, 84, 119-132.
- GINDL, W., GRABNER, M. & WIMMER, R. 2001. Effects of altitude on tracheid differentiation and lignification of Norway spruce. *Canadian Journal of Botany-Revue Canadienne De Botanique*, 79, 815-821.
- GOMPERTZ, B. 1825. On the Nature of the Function Expressive of the Law of Human Mortality, and on a New Mode of Determining the Value of Life Contingencies. *Philosophical Transactions of the Royal Society of London*, 115, 513-585.
- GONZALEZ, L. M. G., EL KAYAL, W., JU, C. J. T., ALLEN, C. C. G., KING-JONES, S. & COOKE, J. E. K. 2012. Integrated transcriptomic and proteomic profiling of white spruce stems during the transition from active growth to dormancy. *Plant Cell and Environment*, 35, 682-701.

- GRABNER, M., CHERUBINI, P., ROZENBERG, P. & HANNRUP, B. 2006. Summer drought and low earlywood density induce intra-annual radial cracks in conifers. *Scandinavian Journal of Forest Research*, 21, 151-157.
- GRANIER, A. 1985. A new method of sap flow measurement in tree stems. *Annales Des Sciences Forestieres*, 42, 193-200.
- GREEN, S., HENDRY, S. J. & REDFERN, D. B. 2008. Drought damage to pole-stage Sitka spruce and other conifers in north-east Scotland. *Scottish Forestry*, 62, 10-18.
- GREEN, S. & RAY, D. 2009. Potential impacts of drought and disease on forestry in Scotland. *Forestry Commission Research Note 4*.
- GRICAR, J., ZUPANCIC, M., CUFAR, K., KOCH, G., SCHMITT, U. & OVEN, P. 2006. Effect of local heating and cooling on cambial activity and cell differentiation in the stem of Norway spruce (*Picea abies*). *Annals of Botany*, 97, 943-951.
- GUILLEY, E., HERVE, J. C. & NEPVEU, G. 2004. The influence of site quality, silviculture and region on wood density mixed model in *Quercus petraea* Liebl. *Forest Ecology and Management*, 189, 111-121.
- HARVALD, C. & OLESEN, P. O. 1987. The Variation of the Basic Density within the Juvenile Wood of Sitka Spruce (*Picea sitchensis*). *Scandinavian Journal of Forest Research*, 2, 525-537.
- HENDRY, S. J. 2009. Drought crack & drought damage in conifers. Forest Research, NRS.
- HERMAN, M., DUTILLEUL, P. & AVELLA-SHAW, T. 1998. Growth rate effects on temporal trajectories of ring width, wood density, and mean tracheid length in Norway spruce (*Picea abies* (L.) Karst.). *Wood and Fiber Science*, 30, 6-17.
- HERZOG, K. M., HASLER, R. & THUM, R. 1995. Diurnal changes in the radius of a sub-alpine Norway spruce stem - their relation to the sap flow and their use to estimate transpiration. *Trees-Structure and Function*, 10, 94-101.
- HOLLIDAY, J. A., RITLAND, K. & AITKEN, S. N. 2010. Widespread, ecologically relevant genetic markers developed from association mapping of climate-related traits in Sitka spruce (*Picea sitchensis*). *New Phytologist*, 188, 501-514.
- HULME, M., JENKINS, G. J., LU, X., TURNPENNY, J. R., MITCHELL, T. D., JONES, R. G., LOWE, J., MURPHY, J. M., HASSELL, D., BOORMAN, P., MCDONALD, R. & HILL, S. 2002. *Climate Change Scenarios for the United Kingdom: The UKCIP02 Scientific Report* [Online]. Retrieved 20/04/2010, http://www.ukcip.org.uk/index.php?id=353&option=com_content&task=view.
- ILIC, J. 2001a. Relationship among the dynamic and static elastic properties of air-dry *Eucalyptus delegatensis* R. Baker. *Holz Als Roh-Und Werkstoff*, 59, 169-175.
- ILIC, J. 2001b. Variation of the dynamic elastic modulus and wave velocity in the fibre direction with other properties during the drying of *Eucalyptus regnans* F. Muell. *Wood Science and Technology*, 35, 157-166.
- ILIC, J. 2003. Dynamic MOE of 55 species using small wood beams. *Holz Als Roh-Und Werkstoff*, 61, 167-172.
- IRVINE, J. & GRACE, J. 1997. Continuous measurements of water tensions in the xylem of trees based on the elastic properties of wood. *Planta*, 202, 455-461.
- JARVIS, N. J., MULLINS, C. E. & MACLEOD, D. A. 1983. The Prediction of Evapo-Transpiration and Growth of Sitka Spruce from Meteorological Records. *Annales Geophysicae*, 1, 335-343.

- JARVIS, P. G. & LEVERENZ, J. W. 1982. Productivity of Temperate, Deciduous and Evergreen Forests. In: O.L.LANGE, O. L., NOBEL, P. S., OSMOND, C. B. & ZIEGLER, H. (eds.) *Physiological Plant Ecology, IV. Encyclopedia of Plant Physiology. New Series*. Berlin: Springer
- JENKINS, G. J., MURPHY, J., SEXTON, D. & LOWE, J. 2009a. *UK Climate Projections: Briefing Report* [Online]. Retrieved 21/04/2010, <http://ukclimateprojections.defra.gov.uk/content/view/826/519/>.
- JENKINS, G. J., PERRY, M. & PRIOR, J. 2009b. *The climate of the UK and recent trends* [Online]. Revised Edition. Retrieved 21/04/2010, <http://ukclimateprojections.defra.gov.uk/content/view/816/9/>.
- JONES, P., HARPHAM, C., KILSBY, C., GLENIS, V. & BURTON, A. 2009. *UK Climate Projections science report: Projections of future daily climate for the UK from the Weather Generator* [Online]. Accessed 27/04/2010 http://ukclimateprojections.defra.gov.uk/images/stories/UKCP09_WGenerator.pdf.
- JOOSEN, R. V. L., LAMMERS, M., BALK, P. A., BRONNUM, P., KONINGS, M. C. J. M., PERKS, M., STATTIN, E., VAN WORDRAGEN, M. F. & VAN DER GEEST, A. H. M. 2006. Correlating gene expression to physiological parameters and environmental conditions during cold acclimation of *Pinus sylvestris*, identification of molecular markers using cDNA microarrays. *Tree Physiology*, 26, 1297-1313.
- JORDAN, L., DANIELS, R. F., CLARK, A. & HE, R. 2005. Multilevel nonlinear mixed-effects models for the modeling of earlywood and latewood microfibril angle. *Forest Science*, 51, 357-371.
- JYSKE, T., MAEKINEN, H. & SARANPAEAE, P. 2008. Wood density within Norway spruce stems. *Silva Fennica*, 42, 439-455.
- KABIR, M. F., SIDEK, H. A. A., DAUD, W. M. & KHALID, K. 1997. Effect of moisture content and grain angle on the ultrasonic properties of rubber wood. *Holzforschung*, 51, 263-267.
- KALLIOKOSKI, T., REZA, M., JYSKE, T., MAKINEN, H. & NOJD, P. 2012. Intra-annual tracheid formation of Norway spruce provenances in southern Finland. *Trees-Structure and Function*, 26, 543-555.
- KAPPELLER, S., LEXER, M. J., GEBUREK, T., HIEBL, J. & SCHUELER, S. 2012. Intraspecific variation in climate response of Norway spruce in the eastern Alpine range: Selecting appropriate provenances for future climate. *Forest Ecology and Management*, 271, 46-57.
- KENNEDY, R. W. 1995. Coniferous wood quality in the future - concerns and strategies. *Wood Science and Technology*, 29, 321-338.
- KENNEDY, S. G., CAMERON, A. D. & LEE, S. J. 2013. Genetic relationships between wood quality traits and diameter growth of juvenile core wood in Sitka spruce. *Canadian Journal of Forest Research-Revue Canadienne De Recherche Forestiere*, 43, 1-6.
- KERHOULAS, L. P. & KANE, J. M. 2012. Sensitivity of ring growth and carbon allocation to climatic variation vary within ponderosa pine trees. *Tree Physiology*, 32, 14-23.
- KEUNECKE, D., SONDEREGGER, W., PERETEANU, K., LUETHI, T. & NIEMZ, P. 2007. Determination of Young's and shear moduli of common yew and Norway spruce by means of ultrasonic waves. *Wood Science and Technology*, 41, 309-327.
- KILPATRICK, D. J., SANDERSON, J. M. & SAVILL, P. S. 1981. The influence of 5 early respacing treatments on the growth of Sitka spruce. *Forestry*, 54, 17-29.

- KNOWLES, R. L., HANSEN, L. W., WEDDING, A. & DOWNES, G. 2004. Evaluation of non-destructive methods for assessing stiffness of Douglas fir trees. *New Zealand Journal of Forestry Science*, 34, 87-101.
- KOPONEN, T., KARPPINEN, T., HEEGGSTROM, E., SARANPAA, P. & SERIMAA, R. 2005. The stiffness modulus in Norway spruce as a function of year ring. *Holzforschung*, 59, 451-455.
- KOSTIAINEN, K., KAAKINEN, S., SARANPAA, P., SIGURDSSON, B. D., LUNDQVIST, S. O., LINDER, S. & VAPAAVUORI, E. 2009. Stem wood properties of mature Norway spruce after 3 years of continuous exposure to elevated [CO₂] and temperature. *Global Change Biology*, 15, 368-379.
- KOZLOWSKI, T. T. & WINGET, C. H. 1964. Diurnal and seasonal variation in radii of tree stems. *Ecology*, 45, 149.
- KRAUSE, C., ROSSI, S., THIBEAULT-MARTEL, M. & PLOURDE, P. Y. 2010. Relationships of climate and cell features in stems and roots of black spruce and balsam fir. *Annals of Forest Science*, 67, 402p1-402p7.
- LACHENBURCH, B., MOORE, J. R. & EVANS, R. 2011. Radial variation in wood structure and function in woody plants, and hypotheses for its occurrence. In: MEINZER, F. C., LACHENBRUCH, B. & DAWSON, T. E. (eds.) *Size- and age-related changes in tree structure and function*. Springer.
- LEBAN, J. M., DAQUITAINE, R., HOULLIER, F. & SAINT-ANDRE, L. 1997. Linking models for tree growth and wood quality in Norway spruce *Picea abies*. Part I: Validation of predictions for sawn boards properties, ring width, wood density and knottiness. *IUFRO WP 55.01-04. Proceedings, second workshop: Connection between silviculture and wood quality through modelling approaches and simulation software, Berg-en-Dal, Kruger National Park, South Africa, August 26-31, 1996.*, 220-228.
- LEE, S. J. 1999. Improving the timber quality of Sitka spruce through selection and breeding. *Forestry*, 72, 123-133.
- LEE, S. J. & CONNOLLY, T. 2010. Finalizing the selection of parents for the Sitka spruce (*Picea sitchensis* (Bong.) Carr) breeding population in Britain using Mixed Model Analysis. *Forestry*, 83, 423-431.
- LINDSTROM, H. 1996. Basic density in Norway spruce .3. Development from pith outwards. *Wood and Fiber Science*, 28, 391-405.
- LINDSTROM, H. 2000. Intra-tree models of basic density in Norway spruce as an input to simulation software. *Silva Fennica*, 34, 411-421.
- LINDSTROM, H. 2002. Intra-tree models of juvenile wood in Norway spruce as an input to simulation software. *Silva Fennica*, 36, 521-534.
- LUPI, C., MORIN, H., DESLAURIERS, A. & ROSSI, S. 2010. Xylem phenology and wood production: resolving the chicken-or-egg dilemma. *Plant Cell and Environment*, 33, 1721-1730.
- LUPI, C., MORIN, H., DESLAURIERS, A. & ROSSI, S. 2012. Xylogenesis in black spruce: does soil temperature matter? *Tree Physiology*, 32, 74-82.
- MACDONALD, E., GARDINER, B. & MASON, W. 2010. The effects of transformation of even-aged stands to continuous cover forestry on conifer log quality and wood properties in the UK. *Forestry*, 83, 1-16.
- MACDONALD, E. & HUBERT, J. 2002. A review of the effects of silviculture on timber quality of Sitka spruce. *Forestry*, 75, 107-138.
- MACDONALD, E., MOCHAN, S. & CONNOLLY, T. 2000. Protocol for stem straightness assessment in Sitka spruce. *Information Note - Forestry Commission*.
- MACDONALD, J. A. B. 1979 Norway or Sitka spruce? *Forestry* 40, 129-138.

- MAKINEN, H., JAAKKOLA, T., PIISPANEN, R. & SARANPAA, P. 2007. Predicting wood and tracheid properties of Norway spruce. *Forest Ecology and Management*, 241, 175-188.
- MAKINEN, H., NOJD, P., KAHLE, H. P., NEUMANN, U., TVEITE, B., MIELIKAINEN, K., ROHLE, H. & SPIECKER, H. 2002. Radial growth variation of Norway spruce (*Picea abies* (L.) Karst.) across latitudinal and altitudinal gradients in central and northern Europe. *Forest Ecology and Management*, 171, 243-259.
- MAKINEN, H., NOJD, P. & SARANPAA, P. 2003. Seasonal changes in stem radius and production of new tracheids in Norway spruce. *Tree Physiology*, 23, 959-968.
- MAKINEN, H., SEO, J. W., NOJD, P., SCHMITT, U. & JALKANEN, R. 2008. Seasonal dynamics of wood formation: a comparison between pinning, microcoring and dendrometer measurements. *European Journal of Forest Research*, 127, 235-245.
- MANSFIELD, S. D., PARISH, R., DI LUCCA, C. M., GOUDIE, J., KANG, K.-Y. & OTT, P. 2009. Revisiting the transition between juvenile and mature wood: a comparison of fibre length, microfibril angle and relative wood density in lodgepole pine. *Holzforschung*, 63, 449-456.
- MAYHEAD, G. J. 1973. The effect of altitude above sea level on the yield class of Sitka spruce. *Scottish Forestry*, 27, 231-237.
- MCINTOSH, R. 1981. Fertilizer treatment of Sitka spruce *Picea sitchensis* in the establishment phase in upland Britain UK. *Scottish Forestry*, 35, 3-13.
- MCLANE, S. C., DANIELS, L. D. & AITKEN, S. N. 2011. Climate impacts on lodgepole pine (*Pinus contorta*) radial growth in a provenance experiment. *Forest Ecology and Management*, 262, 115-123.
- MCLEAN, J. P. 2008. *Wood properties of four genotypes of Sitka spruce*. Ph.D Ph.D, University of Glasgow.
- MCLEAN, J. P. 2012. Sitka spruce Benchmark Project - Interim Report. Edinburgh: SIRT Network.
- MCLEAN, J. P., EVANS, R. & MOORE, J. R. 2010. Predicting the longitudinal modulus of elasticity of Sitka spruce from cellulose orientation and abundance. *Holzforschung*, 64, 495-500.
- MERIAN, P. & LEBOURGEOIS, F. 2011. Size-mediated climate-growth relationships in temperate forests: A multi-species analysis. *Forest Ecology and Management*, 261, 1382-1391.
- METHLEY, J. 1995. Mensuration. *Report on Forest Research*. Forestry Commission, HMSO, London.
- MICHELOT, A., BREDA, N., DAMESIN, C. & DUFRENE, E. 2012. Differing growth responses to climatic variations and soil water deficits of *Fagus sylvatica*, *Quercus petraea* and *Pinus sylvestris* in a temperate forest. *Forest Ecology and Management*, 265, 161-171.
- MIMURA, M. & AITKEN, S. N. 2007. Adaptive gradients and isolation-by-distance with postglacial migration in *Picea sitchensis*. *Heredity*, 99, 224-232.
- MIMURA, M. & AITKEN, S. N. 2010. Local adaptation at the range peripheries of Sitka spruce. *Journal of Evolutionary Biology*, 23, 249-258.
- MISHIRO, A. 1996. Effects of grain and ring angles on ultrasonic velocity in wood. *Mokuzai Gakkaishi*, 42, 211-215.
- MITCHELL, M. D. & DENNE, M. P. 1997. Variation in density of *Picea sitchensis* in relation to within-tree trends in tracheid diameter and wall thickness. *Forestry*, 70, 47-60.
- MOCHAN, S., MOORE, J. & CONNOLLY, T. 2009. Using acoustic tools in forestry and the wood supply chain. *Forestry Commission Technical Note*, FCTN018.

- MOJEREMANE, W., REES, R. M. & MENCUCCINI, M. 2010. Effects of site preparation for afforestation on methane fluxes at Harwood Forest, NE England. *Biogeochemistry*, 97, 89-107.
- MOORE, J. 2011. Wood properties and uses of Sitka spruce in Britain. *Research Report - Forestry Commission, UK*.
- MOORE, J. R., LYON, A. J. & LEHNEKE, S. 2012. Effects of rotation length on the grade recovery and wood properties of Sitka spruce structural timber grown in Great Britain. *Annals of Forest Science*, 69, 353-362.
- MOORE, J. R., LYON, A. J., SEARLES, G. J. & VIHERRMAA, L. E. 2009a. The Effects of Site and Stand Factors on the Tree and Wood Quality of Sitka Spruce Growing in the United Kingdom. *Silva Fennica*, 43, 383-396.
- MOORE, J. R., MOCHAN, S. J., BRUCHERT, F., HAPCA, A. I., RIDLEY-ELLIS, D. J., GARDINER, B. A. & LEE, S. J. 2009b. Effects of genetics on the wood properties of Sitka spruce growing in the UK: bending strength and stiffness of structural timber. *Forestry*, 82, 491-501.
- MUGGEO, V. M. R. 2008. Segmented: an R package to fit regression models with broken-line relationships. *R News* 8/1, 20-25.
- MURPHY, J., SEXTON, D., JENKINS, G., BOORMAN, P., BOOTH, B., BROWN, K., CLARK, R., COLLINS, M., HARRIS, G., KENDON, L. & CENTRE, M. O. H. 2009a. *UK Climate Projections Science Report: Climate Change Projections* [Online]. Available: <http://ukclimateprojections.defra.gov.uk/content/view/824/517/> [Accessed 21/04/2010].
- MURPHY, J., SEXTON, D., JENKINS, G. J., BOORMAN, P., BOOTH, B., BROWN, K., CLARK, R., COLLINS, M., HARRIS, G. & KENDON, L. 2009b. *UK Climate Projections Science Report: Climate Change Projections* [Online]. Retrieved 21/04/2010, <http://ukclimateprojections.defra.gov.uk/content/view/824/517/>.
- MURPHY, S. T. & POMMERENING, A. 2010. Modelling the Growth of Sitka Spruce (*Picea sitchensis* (BONG.) CARR.) in Wales using WENK'S Model Approach. *Allgemeine Forst Und Jagdzeitung*, 181, 35-43.
- MURRAY, M. B., CANNELL, M. G. R. & SMITH, R. I. 1989. Date of budburst of 15 tree species in Britain following climatic warming. *Journal of Applied Ecology*, 26, 693-700.
- NAKICENOVIC, N. & SWART, R. (eds.) 2000. *Special Report on Emissions Scenarios. A Special Report of Working Group III of the Intergovernmental Panel on Climate Change*, Cambridge, UK and New York: Cambridge University Press.
- NIEMZ, P., KUCERA, L. J. & BERNATOWICZ, G. 1999. Studies on the effect of grain angle on the propagation velocity of soundwaves in wood. *Holz Als Roh-Und Werkstoff*, 57, 225-225.
- NIKOLAEV, A. N., ISAEV, A. P. & FEDOROV, P. P. 2011. Radial increment of larch and pine in central Yakutia as dependent on climate change over the past 120 years. *Russian Journal of Ecology*, 42, 263-269.
- OBERHUBER, W. & GRUBER, A. 2010. Climatic influences on intra-annual stem radial increment of *Pinus sylvestris* (L.) exposed to drought. *Trees-Structure and Function*, 24, 887-898.
- OLIVAR, J., BOGINO, S., SPIECKER, H. & BRAVO, F. 2012. Climate impact on growth dynamic and intra-annual density fluctuations in Aleppo pine (*Pinus halepensis*) trees of different crown classes. *Dendrochronologia*, 30, 35-47.
- OLSEN, J. E. 2010. Light and temperature sensing and signaling in induction of bud dormancy in woody plants. *Plant Molecular Biology*, 73, 37-47.

- PARK, Y.-I. D. & SPIECKER, H. 2005. Variations in the tree-ring structure of Norway spruce (*Picea abies*) under contrasting climates. *Dendrochronologia*, 23, 93-104.
- PELTOLA, H., KELLOMÄKI, S. & VÄISÄNEN, H. 1999. Model computations of the impact of climatic change on the windthrow risk of trees. *Climatic Change*, 41, 17-36.
- PERKS, M. P., IRVINE, J. & GRACE, J. 2002. Canopy stomatal conductance and xylem sap abscisic acid (ABA) in mature Scots pine during a gradually imposed drought. *Tree Physiology*, 22, 877-883.
- PETTY, J. A., MACMILLAN, D. C. & STEWARD, C. M. 1990. Variation of density and growth ring width in stems of Sitka and Norway spruce. *Forestry*, 63, 39-49.
- PHILLIPS, E. W. J. 1941. The inclination of the fibrils in the cell wall and its relation to the compression strength of timber. *Empire Forestry Journal*, 20, 74-8.
- PROE, M. F., ALLISON, S. M. & MATTHEWS, K. B. 1996. Assessment of the impact of climate change on the growth of Sitka spruce in Scotland. *Canadian Journal of Forest Research-Revue Canadienne De Recherche Forestiere*, 26, 1914-1921.
- PYATT, G., RAY, D. & FLETCHER, J. 2001. An Ecological Site Classification for Forestry In Great Britain. *Forestry Commission Bulletin 124*.
- R_CORE_TEAM 2013. R: A Language and Environment for Statistical Computing. Vienna, Austria: R Foundation for Statistical Computing.
- RATHGEBER, C. B. K., DECOUX, V. & LEBAN, J.-M. 2006. Linking intra-tree-ring wood density variations and tracheid anatomical characteristics in Douglas fir (*Pseudotsuga menziesii* (Mirb.) Franco). *Annals of Forest Science*, 63, 699-706.
- RAY, D. 2008a. Impacts of climate change on forestry in Scotland - a synopsis of spatial modelling research. *Forestry Commission Reserach Note*, FCRN 101.
- RAY, D. 2008b. Impacts of climate change on forestry in Scotland - a synopsis of spatial modelling research. *Forestry Commission Reserach Note*, FCRN 101.
- RAY, D. 2008c. Impacts of climate change on forestry in Wales. *Forestry Commission Reserach Note*, FCRN301.
- RAY, D., WAINHOUSE, D., WEBBER, J. & GARDINER, B. 2008. Impacts of climate change on forests and forestry in Scotland. Forest Research, Forestry Commission.
- READ, D. J., FREER-SMITH, P. H., MORISON, J. I. L., HANLEY, N., WEST, C. C. & SNOWDON, P. (eds.) 2009. *Combating climate change - a role for UK forests. An assessment of the potential of the UK's trees and woodlands to mitigate and adapt to climate change*, Edinburgh: The Stationery Office.
- ROSSI, S., DESLAURIERS, A., ANFODILLO, T. & CARRARO, V. 2007. Evidence of threshold temperatures for xylogenesis in conifers at high altitudes. *Oecologia*, 152, 1-12.
- ROSSI, S., DESLAURIERS, A., ANFODILLO, T., MORIN, H., SARACINO, A., MOTTA, R. & BORGHETTI, M. 2006. Conifers in cold environments synchronize maximum growth rate of tree-ring formation with day length. *New Phytologist*, 170, 301-310.
- ROSSI, S., DESLAURIERS, A., GRICAR, J., SEO, J.-W., RATHGEBER, C. B. K., ANFODILLO, T., MORIN, H., LEVANIC, T., OVEN, P. & JALKANEN, R. 2008.

- Critical temperatures for xylogenesis in conifers of cold climates. *Global Ecology and Biogeography*, 17, 696-707.
- SAKAI, H., MINAMISAWA, A. & TAKAGI, K. 1990. Effect of moisture-content on ultrasonic velocity and attenuation in woods. *Ultrasonics*, 28, 382-385.
- SARANPAA, P. 1994. Wood Density and Growth. In: BARNETT, J. R. & JERONIMIDIS, G. (eds.) *Wood Quality and its Biological Basis*. Oxford: Blackwell Publishing Ltd.
- SARVAS, R. 1972. Investigations on the annual cycle of development of forest trees. Active period. *Metsantutkimuslaitoksen Julkaisuja*, 76, 110 pp.-110 pp.
- SAVILL, P. S. & SANDELS, A. J. 1983. The influence of early respacing on the wood density of Sitka spruce. *Forestry*, 56, 109-116.
- SCHAIBLE, R. & GAWN, L. J. 1989. Variation in timber strength of fast grown unthinned Sitka spruce in Northern Ireland. *Irish Forestry*, 46, 43-50.
- SCHIMLECK, L. R., MORA, C. R., PETER, G. F. & EVANS, R. 2010. Alternative methods for nondestructively determining modulus of elasticity in young trees. *Iawa Journal*, 31, 161-167.
- SEVANTO, S., HOLTTA, T., HIRSIKKO, A., VESALA, T. & NIKINMAA, E. 2005a. Determination of thermal expansion of green wood and the accuracy of tree stem diameter variation measurements. *Boreal Environment Research*, 10, 437-445.
- SEVANTO, S., HOLTTA, T., MARKKANEN, T., PERAMAKI, M., NIKINMAA, E. & VESALA, T. 2005b. Relationships between diurnal xylem diameter variation and environmental factors in Scots pine. *Boreal Environment Research*, 10, 447-458.
- SHERWOOD, S. C., BONY, S. & DUFRESNE, J. L. 2014. Spread in model climate sensitivity traced to atmospheric convective mixing. *Nature*, 505, 37-42.
- SNOWDON, P. 2002. Modeling Type 1 and Type 2 growth responses in plantations after application of fertilizer or other silvicultural treatments. *Forest Ecology and Management*, 163, 229-244.
- SOHN, J. A., KOHLER, M., GESSLER, A. & BAUHUS, J. 2012. Interactions of thinning and stem height on the drought response of radial stem growth and isotopic composition of Norway spruce (*Picea abies*). *Tree Physiology*, 32, 1199-1213.
- STRIMBECK, G. R. & KJELLEN, T. D. 2010. First frost: Effects of single and repeated freezing events on acclimation in *Picea abies* and other boreal and temperate conifers. *Forest Ecology and Management*, 259, 1530-1535.
- SUZUKI, H. & SASAKI, E. 1990. Effect of grain angle on the ultrasonic velocity of wood. *Mokuzai Gakkaishi*, 36, 103-107.
- SWIDRAK, I., GRUBER, A., KOFLER, W. & OBERHUBER, W. 2011. Effects of environmental conditions on onset of xylem growth in *Pinus sylvestris* under drought. *Tree Physiology*, 31, 483-493.
- TAEGER, S., ZANG, C., LIESEBACH, M., SCHNECK, V. & MENZEL, A. 2013. Impact of climate and drought events on the growth of Scots pine (*Pinus sylvestris* L.) provenances. *Forest Ecology and Management*, 307, 30-42.
- TSEHAYE, A., BUCHANAN, A. H. & WALKER, J. C. F. 2000. Sorting of logs using acoustics. *Wood Science and Technology*, 34, 337-344.
- TURCOTTE, A., MORIN, H., KRAUSE, C., DESLAURIERS, A. & THIBEAULT-MARTEL, M. 2009. The timing of spring rehydration and its relation with the onset of wood formation in black spruce. *Agricultural and Forest Meteorology*, 149, 1403-1409.
- UK METEOROLOGICAL OFFICE 2012. UK Meteorological Office. Met Office Integrated Data Archive System (MIDAS) Land and Marine Surface Stations

- Data (1853-current), [Internet]. NCAS British Atmospheric Data Centre, 2012, Available from http://badc.nerc.ac.uk/view/badc.nerc.ac.uk__ATOM__dataent_ukmo-midas
- UKCP09. 2009a. *UK Climate Projections* [Online]. Available: <http://ukclimateprojections.defra.gov.uk/> [Accessed 21/04/2010].
- UKCP09. 2009b. *UK Climate Projections* [Online]. <http://ukclimateprojections.defra.gov.uk/>.
- VIHERMAA, L., MCLEAN, J. P., CHAUHAN, S. S., ALTANER, C. M., JARVIS, M. C. & GARDINER, B. 2014. Using segmented linear models to analyse the radial variation in Sitka spruce. *Annals of Forest Science - In Preparation*.
- VIHERMAA, L. 2010. *Influence of site factors and climate on timber properties of Sitka spruce (Picea sitchensis (Bong.) Carr.)*. PhD, University of Glasgow.
- VITASSE, Y., FRANCOIS, C., DELPIERRE, N., DUFRENE, E., KREMER, A., CHUINE, I. & DELZON, S. 2011. Assessing the effects of climate change on the phenology of European temperate trees. *Agricultural and Forest Meteorology*, 151, 969-980.
- WALKER, J. C. F. & BUTTERFIELD, B. G. 1996. The importance of microfibril angle for the processing industries. *New Zealand Forestry*, 40, 34-40.
- WANG, Y. P. & JARVIS, P. G. 1990. Influence of crown structural-properties on par absorption, photosynthesis, and transpiration in Sitka spruce - application of a model (MAESTRO). *Tree Physiology*, 7, 297-316.
- WANG, Y. P., JARVIS, P. G. & TAYLOR, C. M. A. 1991. Par absorption and its relation to aboveground dry-matter production of Sitka spruce. *Journal of Applied Ecology*, 28, 547-560.
- WARING, R. H. 2000. A process model analysis of environmental limitations on the growth of Sitka spruce plantations in Great Britain. *Forestry*, 73, 65-79.
- WIMMER, R. & GRABNER, M. 2000. A comparison of tree-ring features in Picea abies as correlated with climate. *Iawa Journal*, 21, 403-416.
- WINGATE, L. 2003. *The Contribution of photosynthesis and respiration on the net ecosystem exchange and net ¹³C discrimination of a Sitka spruce plantation*. PhD, University of Edinburgh.
- WINGET, C. H. & KOZLOWSKI, T. T. 1964. Winter shrinkage in stems of forest trees. *Jour Forest*, 62, 335-337.
- WORRELL, R. & MALCOLM, D. C. 1990a. Productivity of Sitka spruce in northern Britain .1. The effects of elevation and climate. *Forestry*, 63, 105-118.
- WORRELL, R. & MALCOLM, D. C. 1990b. Productivity of Sitka spruce in northern Britain .2. Prediction from site factors. *Forestry*, 63, 119-128.
- WU, S. H., JANSSON, P.-E. & KOLARI, P. 2012. The role of air and soil temperature in the seasonality of photosynthesis and transpiration in a boreal Scots pine ecosystem. *Agricultural and Forest Meteorology*, 156, 85-103.
- WUNDER, J., REINEKING, B., HILLGARTER, F.-W., BIGLER, C. & BUGMANN, H. 2011. Long-term effects of increment coring on Norway spruce mortality. *Canadian Journal of Forest Research-Revue Canadienne De Recherche Forestiere*, 41, 2326-2336.
- ZANG, C., PRETZSCH, H. & ROTHE, A. 2012. Size-dependent responses to summer drought in Scots pine, Norway spruce and common oak. *Trees-Structure and Function*, 26, 557-569.
- ZEIDE, B. 1993. Analysis of growth equations. *Forest Science*, 39, 594-616.

- ZERVA, A. & MENCUCCINI, M. 2005. Short-term effects of clearfelling on soil CO₂, CH₄, and N₂O fluxes in a Sitka spruce plantation. *Soil Biology & Biochemistry*, 37, 2025-2036.
- ZOBEL, B. J. & BUIJTENEN, J. P. V. 1989. *Wood variation: its causes and control*, Berlin Germany, Springer-Verlag.
- ZWEIFEL, R. & HASLER, R. 2000. Frost-induced reversible shrinkage of bark of mature subalpine conifers. *Agricultural and Forest Meteorology*, 102, 213-222.
- ZWEIFEL, R., ITEM, H. & HASLER, R. 2000. Stem radius changes and their relation to stored water in stems of young Norway spruce trees. *Trees-Structure and Function*, 15, 50-57.